POLYMER CHEMISTRY

The Basic Concepts

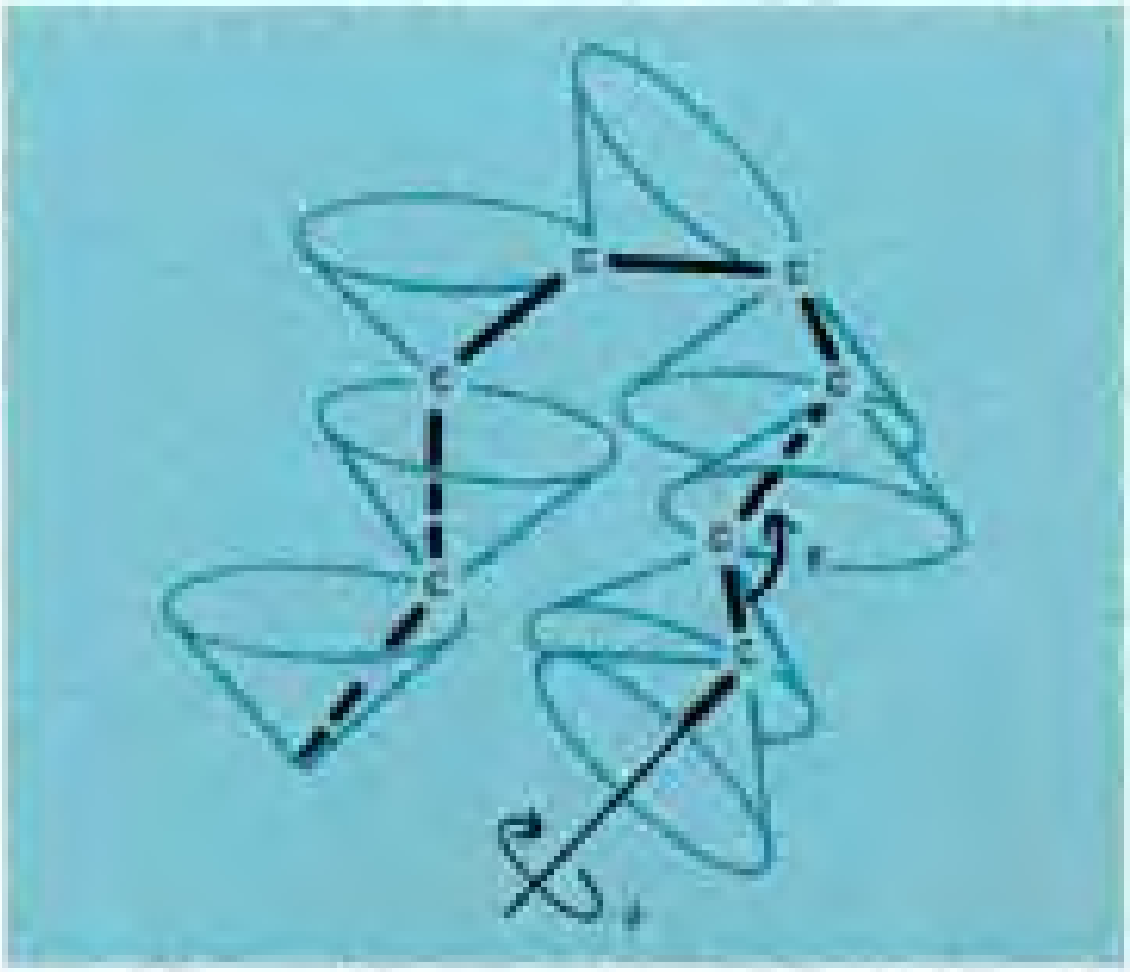

PAUL C. HIEMENZ

Polymer Chemistry

The Basic Concepts

Paul C. Hiemenz

California State Polytechnic University
Pomona, California

MARCEL DEKKER, INC. NEW YORK • BASEL • HONG KONG

"The Dance Of The Solids" by John Updike
Copyright © 1968 by John Updike
Reprinted from *Midpoint and Other Poems* by John Updike, by permission of
Alfred A. Knopf, Inc., New York

"When The Nylons Bloom Again" by George Marion, Jr. and Fats Waller
Copyright © 1943 by Joy Music, Inc.
Copyright renewed. Controlled in the U.S.A. by Chappell & Co., Inc. and Advanced Music Corp. (Intersong Music & Warner Bros. Music, Publishers.)
International copyright secured
ALL RIGHTS RESERVED Used by permission

"I Remember" by Stephen Sondheim
Copyright © 1966 by Burthen Music Co., Inc.
All rights administered by Chappell & Co., Inc.
International copyright secured
ALL RIGHTS RESERVED Used by permission

"Come Back To Me" by Alan Jay Lerner and Burton Lane
Copyright © 1965 by Alan Jay Lerner and Burton Lane
Chappel & Co., Inc., owner of publication and allied rights throughout the world
International copyright secured
ALL RIGHTS RESERVED Used by permission

Library of Congress Cataloging in Publication Data

Hiemenz, Paul C., [dste]

Polymer chemistry.

Includes index.
1. Polymers and polymerization. I. Title.
QD381.H52 1984 547.7 83-25207
ISBN 0-8247-7082-X

COPYRIGHT © 1984 by MARCEL DEKKER, INC. ALL RIGHTS RESERVED

Neither this book nor any part may be reproduced or transmitted in any form or by any means, electronic or mechanical, including photocopying, microfilming, and recording, or by any information storage and retrieval system, without permission in writing from the publisher.

MARCEL DEKKER, INC.
270 Madison Avenue, New York, New York 10016

Current printing (last digit):
10 9 8 7

PRINTED IN THE UNITED STATES OF AMERICA

PREFACE

Physical chemistry has been defined as that branch of science that is fundamental, molecular, and interesting. I have tried to write a polymer textbook that could be described this way also. To the extent that one subscribes to the former definition and that I have succeeded in the latter objective, then the approach of this book is physical chemical. As a textbook, it is intended for students who have completed courses in physical and organic chemistry. These are the prerequisites which define the level of the book; no special background in physics or mathematics beyond what is required for physical chemistry is assumed. Since chemistry majors generally study physical chemistry in the third year of the undergraduate curriculum, this book can serve as the text for a senior-level undergraduate or a beginning graduate-level course. Although I use chemistry courses and chemistry curricula to describe the level of this book, students majoring in engineering, materials science, physics, and various specialties in the biological sciences will also find numerous topics of interest contained herein.

Terms like "fundamental," "molecular," and "interesting" have different meanings for different people. Let me explain how they apply to the presentation of polymer chemistry in this text.

The words "basic concepts" in the title define what I mean by "fundamental." This is the primary emphasis in this presentation. Practical applications of polymers are cited frequently—after all, it is these applications that make polymers such an important class of chemicals—but in overall content, the stress is on fundamental principles. "Foundational" might be another way to describe this. I have not attempted to cover all aspects of polymer science, but the topics that have been discussed lay the foundstion—built on the bedrock of organic and physical chemistry—from which virtually all aspects of the subject are developed. There is an enormous literature in polymer science; this book is intended to bridge the gap between the typical undergraduate background in polymers—which frequently amounts to little more than occasional "relevant" examples in other courses—and the professional literature on the subject.

Accordingly, the book assumes essentially no prior knowledge of polymers, and extends far enough to provide a usable level of understanding.

"Molecular" describes the perspective of the chemist, and it is this aspect of polymeric materials that I try to keep in view throughout the book. An engineering text might emphasize processing behavior; a physics text, continuum mechanics; a biochemistry text, physiological function. All of these are perfectly valid points of view, but they are not the approach of this book. It is polymer molecules—their structure, energetics, dynamics, and reactions—that are the primary emphasis throughout most of the book. Statistics is the type of mathematics that is natural to a discussion of molecules. Students are familiar with the statistical nature of, say, the kinetic molecular theory of gases. Similar methods are applied to other assemblies of molecules, or in the case of polymers, to the assembly of repeat units that comprise a single polymer molecule. Although we frequently use statistical arguments, these are developed quite thoroughly and do not assume any more background in this subject than is ordinarily found among students in a physical chemistry course.

The most subjective of the words which (I hope) describe this book is "interesting." The fascinating behavior of polymers themselves, the clever experiments of laboratory researchers, and the elegant work of the theoreticians add up to an interesting total. I have tried to tell about these topics with clarity and enthusiasm, and in such a way as to make them intelligible to students. I can only hope that the reader agrees with my assessment of what is interesting.

This book was written with the student in mind. Even though "student" encompasses persons with a wide range of backgrounds, interests, and objectives; these are different than the corresponding experiences and needs of researchers. The following features have been included to assist the student:

1. Over 50 solved example problems are sprinkled throughout the book.

2. Exercises are included at the end of each chapter which are based on data from the original literature.

3. Concise reviews of pertinent aspects of thermodynamics, kinetics, spectrophotometry, etc. are presented prior to developing applications of these topics to polymers.

4. Theoretical models and mathematical derivations are developed in enough detail to be comprehensible to the student reader. Only rarely do I "pull results out of a hat," and I scrupulously avoid saying "it is obvious that . . . "

5. Generous cross-referencing and a judicious amount of repetition have been included to help unify a book which spans quite a wide range of topics.

6. SI units have been used fairly consistently throughout, and attention is paid to the matter of units whenever these become more than routine in complexity.

The book is divided into three parts of three chapters each, after an introductory chapter which contains information that is used throughout the book.

In principle, the three parts can be taken up in any order without too much interruption in continuity. Within each of the parts there is more carryover from chapter to chapter, so rearranging the sequence of topics within a given part is less convenient. The book contains more material than can be covered in an ordinary course. Chapter 1 plus two of the three parts contain about the right amount of material for one term. In classroom testing the material, I allowed the class to decide—while we worked on Chapter 1—which two of the other parts they wished to cover; this worked very well.

Material from Chapter 1 is cited throughout the book, particularly the discussion of statistics. In this connection, it might be noted that statistical arguments are developed in less detail further along in the book as written. This is one of the drawbacks of rearranging the order in which the topics are covered. Chapters 2 through 4 are concerned with the mechanical properties of bulk polymers, properties which are primarily responsible for the great practical importance of polymers. Engineering students are likely to have both a larger interest and a greater familiarity with these topics. Chapers 5 through 7 are concerned with the preparation and properties of several broad classes of polymers. These topics are closer to the interests of chemistry majors. Chapters 8 through 10 deal with the solution properties of polymers. Since many of the techniques described have been applied to biopolymers, these chapters will have more appeal to students of biochemistry and molecular biology.

Let me conclude by acknowledging the contributions of those who helped me with the preparation of this book. I wish to thank Marilyn Steinle for expertly typing the manuscript. My appreciation also goes to Carol Truett who skillfully transformed my (very) rough sketches into effective illustrations. Lastly, my thanks to Ron Manwill for preparing the index and helping me with the proofreading. Finally, let me acknowledge that some errors and/or obscurities will surely elude my efforts to eliminate them. I would appreciate reports about these from readers so that these mistakes can eventually be eliminated.

PAUL C. HIEMENZ

CONTENTS

Preface iii

1 1
The Chains and Averages of Polymers: An Overview

1.1
Introduction

1.2
How Big is Big?

1.3
Linear and Branched Polymers and Homopolymers and Copolymers

1.4
Addition, Condensation, and Natural Polymers

1.5
Polymer Nomenclature

1.6
Positional, Stereo, and Geometrical Isomerism

1.7
Molecular Weight by End Group Analysis

1.8
Molecular Weight Averages

1.9
The Binomial Distribution and the Random Walk

1.10
Size Parameters for Random Coils

1.11
Application to Polymer Chains

1.12
Preview of Things to Come

Bulk Polymers and their Mechanical Behavior

2 75
The Viscous State

2.1
Introduction

2.2
The Coefficient of Viscosity

2.3
Measuring Viscosity: Concentric Cylinder Viscometers

2.4
The Power Law for Pseudoplastic Liquids

2.5
A Model for Flow in Liquids

2.6
Flow As a Rate Process

2.7
The Effect of Shearing Forces

2.8
Testing the Eyring Equation

2.9
The Molecular Weight Dependence of Viscosity: Experimental Aspects

2.10
A Theory for Viscosity in the Absence of Entanglements

2.11
The Segmental Friction Factor

2.12
Dealing with Entanglements: The Bueche Theory

2.13
The Reptation Model

CONTENTS

Preface iii

1 1
The Chains and Averages of Polymers: An Overview

1.1
Introduction

1.2
How Big is Big?

1.3
Linear and Branched Polymers and Homopolymers and Copolymers

1.4
Addition, Condensation, and Natural Polymers

1.5
Polymer Nomenclature

1.6
Positional, Stereo, and Geometrical Isomerism

1.7
Molecular Weight by End Group Analysis

1.8
Molecular Weight Averages

1.9
The Binomial Distribution and the Random Walk

1.10
Size Parameters for Random Coils

1.11
Application to Polymer Chains

1.12
Preview of Things to Come

Bulk Polymers and their Mechanical Behavior

2 75
The Viscous State

2.1
Introduction

2.2
The Coefficient of Viscosity

2.3
Measuring Viscosity: Concentric Cylinder Viscometers

2.4
The Power Law for Pseudoplastic Liquids

2.5
A Model for Flow in Liquids

2.6
Flow As a Rate Process

2.7
The Effect of Shearing Forces

2.8
Testing the Eyring Equation

2.9
The Molecular Weight Dependence of Viscosity: Experimental Aspects

2.10
A Theory for Viscosity in the Absence of Entanglements

2.11
The Segmental Friction Factor

2.12
Dealing with Entanglements: The Bueche Theory

2.13
The Reptation Model

2.14
The Effects of Branching

3 133
The Elastic and Viscoelastic States

3.1
Introduction

3.2
Elastic Deformation

3.3
Thermodynamics and Elasticity

3.4
Entropy Elasticity

3.5
Experimental Behavior of Elastomers

3.6
The Shear Modulus and the Compliances

3.7
The Maxwell Model: Stress Relaxation

3.8
Understanding the Modulus: Molecules and Models

3.9
The Voigt Model: Creep

3.10
Dynamic Viscoelasticity

3.11
The Dynamic Components: Measurement and Interpretation

3.12
A Molecular Theory for Viscoelasticity: The Rouse Model

4 199
The Glassy and Crystalline States

4.1
Introduction

4.2
The Glass and Melting Transitions

4.3
The Thermodynamics of Crystallization: Round I

4.4
The Thermodynamics of Melting: Round II

4.5
The Kinetics of Crystallization: The Avrami Equation

4.6
The Kinetics of Crystallization: Experimental Aspects

4.7
Levels of Structure: Crystal Morphology

4.8
Thermodynamics and the Glass Transition

4.9
Free Volume

4.10
Time-Temperature Equivalency

4.11
Polymer Processing Technology

4.12
Preview of Things to Come

Some Important Classes Of Polymers And Polymerization Reactions

5 273
Condensation or Step-Growth Polymerization

5.1
Introduction

5.2
Condensation Polymers: One Step at a Time

5.3
Kinetics of Step-Growth Polymerization

5.4
Distribution of Molecular Sizes

5.5
Polyesters

5.6
Polyamides

5.7
Stoichiometric Imbalance

5.8
Branching and Crosslinking

5.9
Some Cross-linked Step-Growth Polymers

5.10
Rings 'n Things

5.11
More Rings

6 345
Addition or Chain-Growth Polymerization

6.1
Introduction

6.2
Chain-Growth and Step-Growth Polymerizations: Some Comparisons

6.3
Initiation

6.4
Termination

6.5
Propagation

6.6
Radical Lifetime

6.7
Distribution of Molecular Weights

6.8
Chain Transfer

6.9
Techniques of Polymerization: Emulsion Polymerization

6.10
Anionic Polymerization

6.11
Cationic Polymerization

7 423
Polymers with Microstructure: Copolymers and Stereoregular Polymers

7.1
Introduction

7.2
Copolymer Composition

7.3
Reactivity Ratios

7.4
Resonance and Reactivity

7.5
The Price-Alfrey Equation

7.6
A Closer Look at Microstructure

7.7
Copolymer Composition and Microstructure: Experimental Aspects

7.8
Applications of Copolymers

7.9
Stereoregular Polymers

7.10
A Statistical Description of Stereoregularity

7.11
Measuring Stereoregularity by Nuclear Magnetic Resonance

7.12
Ziegler-Natta Catalysts

7.13
Preview of Things to Come

Some Properties of Polymer Solutions and their Relation to Polymer Characterization

8 505
The Thermodynamics of Polymer Solutions

8.1
Introduction

8.2
Classical and Statistical Thermodynamics

8.3
The Flory-Huggins Theory: The Entropy of Mixing

8.4
The Flory-Huggins Theory: The Enthalpy of Mixing

8.5
Cohesive Energy Density

8.6
Phase Separation

8.7
Polymer Fractionation

8.8
Osmotic Pressure

8.9
Molecular Weight by Osmometry

8.10
Excluded Volume

8.11
The Flory-Krigbaum Theory

8.12
Theta Conditions

8.13
Osmotic Pressure of Charged Polymers

9 583
Frictional Properties of Polymers in Solution

9.1
Introduction

9.2
Viscous Forces on Rigid Spheres

9.3
The Intrinsic Viscosity of Rigid Molecules

9.4
The Poiseuille Equation and Capillary Viscometers

9.5
The Mark-Houwink Equation

9.6
To Drain or Not to Drain?

9.7
The Coil Expansion Factor

9.8
The Diffusion Coefficient and the Friction Factor

9.9
The Diffusion Coefficient: Experimental Aspects

9.10
Sedimentation Velocity and Sedimentation Equilibrium

9.11
Gel Permeation Chromatography

10 659
Light Scattering by Polymer Solutions

10.1
Introduction

10.2
The Intensity of Scattered Light and Turbidity

10.3
Electric Fields and Their Interaction with Matter

10.4
Light Scattering by an Isolated Molecule

10.5
Rayleigh Scattering

10.6
Fluctuations and Rayleigh Scattering

10.7
Light Scattering by Solutions

10.8
Experimental Aspects of Light Scattering

10.9
Optical Interference

10.10
The Radius of Gyration

10.11
Zimm Plots

10.12
Appendix: Electrical Units

Index to Tables 723

Subject Index 725

1

The Chains and the Averages of Polymers

An Overview

The *polymers*, those giant molecules,
Like starch and polyoxymethylene,
Flesh out, as protein serfs and plastic fools,
The kingdom with life's stuff

The Dance of the Solids, by John Updike

1.1 Introduction

Science tends to be plagued by clichés which make invidious comparisons of its efforts: "they can cure such and such a dreaded disease, but they cannot do anything about the common cold" or "we know more about the surface of the moon than the bottom of the sea." If such comparisons were popular in the 1920s, the saying might have been, "we know more about the structure of the atom than about those messy, sticky substances called polymers." Indeed, Millikan's determination of the electron's charge, Rutherford's idea of the nuclear atom, and Bohr's model of the hydrogen atom were all well-known concepts before the notion of truly covalent macromolecules was accepted. This was the case in spite of the great importance of polymers to human life and activities. Our bodies, like all forms of life, depend on polymer molecules: carbohydrates, proteins, nucleic acids, and so on. From the earliest times, polymeric materials have been employed to satisfy human needs: wood; hide; natural resins and gums; and fibers like cotton, wool, silk, and so forth.

Attempts to characterize polymeric substances had been made, of course, and high molecular weights were indicated, even if they were not too accurate. Early workers tended to be more suspicious of the interpretation of the colligative properties of polymeric solutions than to accept the possibility of high molecular weight compounds. Faraday had already arrived at C_5H_8 as the empirical formula of rubber in 1826, and isoprene was identified as the product

resulting from the destructive distillation of rubber in 1860. The idea that a natural polymer such as rubber somehow "contained" isoprene emerged, but the nature of its involvement was more elusive.

During the early years of this century, organic chemists were enjoying success in determining the structures of ordinary-sized organic molecules, and this probably contributed to their reluctance to look beyond structures of convenient size. Physical chemists were interested in intermolecular forces at this period, and the idea that polymers were the result of some sort of association between low molecular weight constituent molecules prevailed for a long while.

Staudinger is generally credited as being the father of modern polymer chemistry, although a foreshadowing of his ideas can be traced through older literature. In 1920 Staudinger proposed the chain formulas we accept today, maintaining that structures are held together by covalent bonds which are equivalent in every way to those in low molecular weight compounds. There was a decade of controversy before these ideas began to experience widespread acceptance. Staudinger was awarded the Nobel Prize in 1953 for his work with polymers.

By the 1930s, Carothers began synthesizing polymers using well-established reactions of organic chemistry such as esterification and amidation. His products were not limited to single ester or amide linkages, however, but contained many such groups: They were *poly*esters and *poly*amides. Physical chemists also got in on the act. Kuhn and Guth and Mark† were soon applying statistics and crystallography to describe the multitude of forms a long-chain molecule could assume.

Our purpose in this introduction is not to trace the history of polymer chemistry beyond the sketchy version above, instead, the objective is to introduce the concept of polymer chains which is the cornerstone of all polymer chemistry. In the next few sections we shall introduce some of the categories of chains, some of the reactions that produce them, and some aspects of isomerism which multiply their possibilities. A common feature of all of the synthetic polymerization reactions is the random nature of the polymerization steps. Likewise, the twists and turns the molecule can undergo along the backbone of the chain produce shapes which are only describable as averages. As a consequence of these considerations, another important part of this chapter is an introduction to some of the statistical concepts which also play a central role in polymer chemistry.

† No enterprise as rich as polymer science has only one "father." Herman Mark is one of those to whom the title could readily be applied. An interesting interview with Professor Mark appears in the *Journal of Chemical Education*, 56:83 (1979).

1.2 How Big Is Big?

The term *polymer* is derived from the Greek words *poly* and *meros*, meaning many parts. We noted in the last section that the existence of these parts was acknowledged before the nature of the interaction which held them together was known. Today we realize that ordinary covalent bonds are the intramolecular forces which keep the polymer molecule intact. In addition, the usual type of intermolecular forces—hydrogen bonds, dipole-dipole interactions, and London forces—hold assemblies of these molecules together in the bulk state. The only thing that is remarkable about these molecules is their size, but that feature is remarkable indeed.

One of the first things we must consider is what we mean when we talk about the size of a polymer molecule. Ordinarily, the molecular weight is meant, although a closely related concept, called the degree of polymerization, may also be used in this context. A variety of experimental techniques are available for determining the molecular weight of a polymer. We shall discuss one such method in Sec. 1.7 and defer most of the rest to Part III of this book, which is concerned with the properties of polymer solutions. The expression *molecular weight* should almost always be modified by the word *average*. This, too, is something we shall take up presently. For now, we assume that a polymer molecule has a molecular weight M, which can be anywhere in the range 10^3–10^7 or more in magnitude. We shall omit units when we write molecular weights in this book, but the student is advised to attach the units g mol^{-1} or amu $molecule^{-1}$ to these quantities when they appear in problem calculations.

Since polymer molecules are made up of chains of repeating units, after the chain itself comes the repeat unit as a structural element of importance. Many polymer molecules are produced by covalently bonding together only one or two types of repeating units. These units are the parts from which chains are generated; as a class of compounds they are called monomers. Throughout this book, we shall designate the molecular weight of a repeat unit M_0.

The degree of polymerization of a polymer is simply the number of repeat units in a molecule. The degree of polymerization n is given by the ratio of the molecular weight of the polymer to the molecular weight of the repeat unit:

$$n = \frac{M}{M_0} \tag{1.1}$$

One type of polymerization reaction is the addition reaction in which successive repeat units add on to the chain. No other product molecules are formed, so the weight of the monomer and that of the repeat unit are identical in this case. A second category of polymerization reaction is the condensation reaction, in which one or two small molecules like water or HCl are eliminated for each chain linkage formed. In this case the molecular weight of the monomer and the

repeat unit are somewhat different. For example, suppose an acid (subscript A) reacts with an alcohol (subscript B) to produce an ester linkage and a water molecule. The molecular weight of the ester—the repeat unit if an entire chain is built up this way—differs from the combined weight of the reactants by twice the molecular weight of the water; therefore

$$n = \frac{M}{M_0} = \frac{M}{M_A + M_B - 2M_{H_2O}} \tag{1.2}$$

The end units in a polymer chain are different from the units that are attached on both sides to other repeat units. The end units are attached to the chain on one side only; the valence which would continue the chain if this were not the end must be capped off in some other way. We see this situation in the *n*-alkanes: Each end of the chain is a methyl group and the middle parts are methylene groups. Of course, the terminal group does not have to be a hydrogen as in the alkanes; indeed, it is generally something different. Our interest in end groups is concerned with the question of what effect they introduce into the evaluation of n through Eq. (1.2). The following example examines this through some numerical calculations.

Example 1.1

As a polymer prototype consider an *n*-alkane molecule consisting of n methylenes and 2 methyl groups. How serious an error is made in M for different n's if the difference in molecular weight between methyl and methylene groups is ignored?

Solution

The effect of different end groups on M can be seen by comparing the true molecular weight with an approximate molecular weight, calculated on the basis of a formula $(CH_2)_{n+2}$. These M's and the percentage difference between them are listed here for several values of n:

n	M_{true}	$M_{approx.}$	Percent difference
1	44	42	4.5
5	100	98	2.0
10	170	168	1.2
50	730	728	0.3
100	1,430	1,428	0.14
500	7,030	7,028	0.028
1000	14,030	14,028	0.014

Although the difference is almost 5% for propane, it is closer to 0.1% for the case of n = 100, which is about the threshold for polymers. The precise values of these numbers will be different, depending on the specific repeat units and end groups present. For example, if M_0 = 100 and M_{end} = 80, the difference is 0.39% in a calculation like those above for n = 100.

•

The example shows that the contribution of the ends becomes progressively less important as the number of repeat units in a structure increases. By the time polymeric molecular sizes are reached, the error associated with failure to distinguish between segments at the end and those within the chain is generally less than experimental error. In Sec. 1.7 we shall consider a method for polymer molecular weight determination which is based on chemical analysis for the end groups in a polymer. A corollary of the present discussion is that the method of end group analysis is applicable only in the case of relatively low molecular weight polymers.

Not all polymers are built up from bonding together a single kind of repeating unit. At the other extreme, protein molecules are polyamides in which n amino acid repeat units are bonded together. Although we might still call n the degree of polymerization in this case, it is less useful, since an amino acid unit might be any one of some 20-odd molecules that are found in proteins. In this case the molecular weight itself, rather than the degree of polymerization, is generally used to describe the molecule. When the actual content of individual amino acids is known, it is their sequence that is of special interest to biochemists and molecular biologists.

We began this section with an inquiry into how to define the size of a polymer molecule. In addition to the molecular weight or the degree of polymerization, some linear dimension which characterizes the molecule could also be used for this purpose. For purposes of orientation, let us again consider a hydrocarbon molecule stretched out to its full length but without any bond distortion. There are several features to note about this situation:

1. The tetrahedral geometry of the bonding at the carbon atoms has bond angles of 109.5°.
2. The equilibrium bond length between adjacent singly bonded carbon atoms is 0.154 nm or 1.54 Å.
3. Because of the possibility of rotation around carbon-carbon bonds, a molecule possessing many such bonds will undergo many twists and turns along the chain.
4. The fully extended molecular length is not representative of the spatial extension that a molecule actually displays. The latter is sensitive to environmental factors, however, so the extended length is convenient for our present purposes to provide an idea of the spatial size of polymer molecules.

A fully extended hydrocarbon molecule will have the familiar zigzag profile

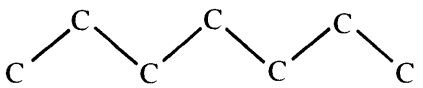

in which the hydrogens extend in front of and in back of the plane containing the carbons, also making an angle of 109.5° between them at the carbon atoms. The chain may be pictured as a row of triangles resting corner to corner. The length of the row equals the product of the number of triangles and the length of the base of each. Although it takes three carbons to define one of these triangles, one of these atoms is common to two triangles; therefore the number of triangles is the same as the number of *pairs* of carbon atoms, except where this breaks down at the ends of the molecule. If the chain is sufficiently long, this end effect is inconsequential. The law of cosines can be used to calculate the length of the base of each of these triangles: $[2(0.154)^2(1 - \cos 109.5°)]^{1/2} = 0.252$ nm. If the repeat unit of the molecule contributes two carbon atoms to the backbone of the polymer—this is the case for vinyl polymers—the extended chain length is given by n(0.252) nm. For a polymer with $n = 10^4$, this corresponds to 2.52 μm. Objects which actually display linear dimensions of this magnitude can be seen in an ordinary microscope, provided that they have suitable optical properties to contrast with their surroundings. Note that the distance between every other carbon atom we have used here is also the distance between the substituents on these carbons for the fully extended chains.

We shall see in Sec. 1.10 that, because of all the twists a molecule undergoes, the actual end-to-end distance of the jumbled molecule increases as $n^{1/2}$. With the same repeat distance calculated above, but the square root dependence on n, the actual end-to-end distance of the coiled chain with $n = 10^4$ is closer to $(10^4)^{1/2}$ 0.252 nm = 25 nm. If we picture one end of this jumbled chain at the origin of a coordinate system, the other end might be anywhere on the surface of a sphere whose radius is given by this end-to-end distance. This spherical geometry comes about because the random bends occurring along the chain length can take the end of the chain anywhere in a spherical domain whose radius depends on the chain length (as $n^{1/2}$).

The above discussion points out the difficulty associated with using the linear dimensions of a molecule as a measure of its size: It is not the molecule alone that determines its dimensions, but also the shape in which it exists. Linear arrangements of the sort described above exist in polymer crystals, at least for some distance, although not over the full length of the chain. We shall take up the structure of polymer crystals in Chap. 4. In the solution and bulk states, many polymers exist in the coiled form we have also described. Still other structures are important, notably the helix, which we shall discuss in Sec. 1.11. The overall shape assumed by a polymer molecule is greatly affected

by the molecule's environment. The shape of a molecule in solution plays a role in determining many properties of polymer solutions. From a study of these solutions, some conclusions can be drawn regarding the shape of the molecule in that environment. The discussion of polymer solutions is taken up in Part III.

Figure 1.1 is a rather remarkable photograph which shows individual polystyrene molecules as spherical blobs having average diameters of about 20 nm. The picture is an electron micrograph in which a 10^{-4}% solution of polystyrene was deposited on a suitable substrate, the solvent evaporated, and the contrast enhanced by shadow casting. There is a brief discussion of both electron microscopy and shadowing in Sec. 4.7. Several points should be noted in connection with Fig. 1.1:

1. The circular cross section of the polymer blobs does not prove that the polymer existed in solution as a tangled coil (although this is the case). The shape displayed by the particles in the photograph is probably due in part to surface tension occurring during the drying of the sample.
2. Since the preparation of the specimen began with such a dilute solution, there seems to be little doubt that the particles are individual polymer molecules rather than clusters thereof. The diameters of the blobs are of the right order of magnitude for random structures, although this comparison must be used cautiously in view of item (1).
3. The fact that the dimensions of the various blobs is not identical should not surprise us. Again, we acknowledge that this may be an artifact arising from sample preparation. At the same time, however, we recall that the nature of polymerization reactions is such that a range of molecular weights is obtained. Accordingly, we expect a range of linear dimensions as well.

We conclude this section by questioning whether there is a minimum molecular weight or linear dimension that must be met for a molecule to qualify as a polymer. Although a dimer is a molecule for which $n = 2$, no one would consider it a polymer. The term *oligomer* has been coined to designate molecules for which $n < 10$. If they require a special name, apparently the latter are not full-fledged polymers either. At least as a first approximation, we shall take the attitude that there is ordinarily no discontinuity in behavior with respect to some observed property as we progress through a homologous series of compounds with different n values. At one end of the series we may be dealing with a simple low molecular weight compound, and at the other end with a material that is unquestionably polymeric. The molecular weight and chain length increase monotonically through this series, and a variety of other properties smoothly increase also. This point of view emphasizes a continuity with familiar facts concerning the properties of low molecular weight compounds. There are some properties, on the other hand, which follow so closely from the chain structure of polymers that the property is simply not observed until a certain

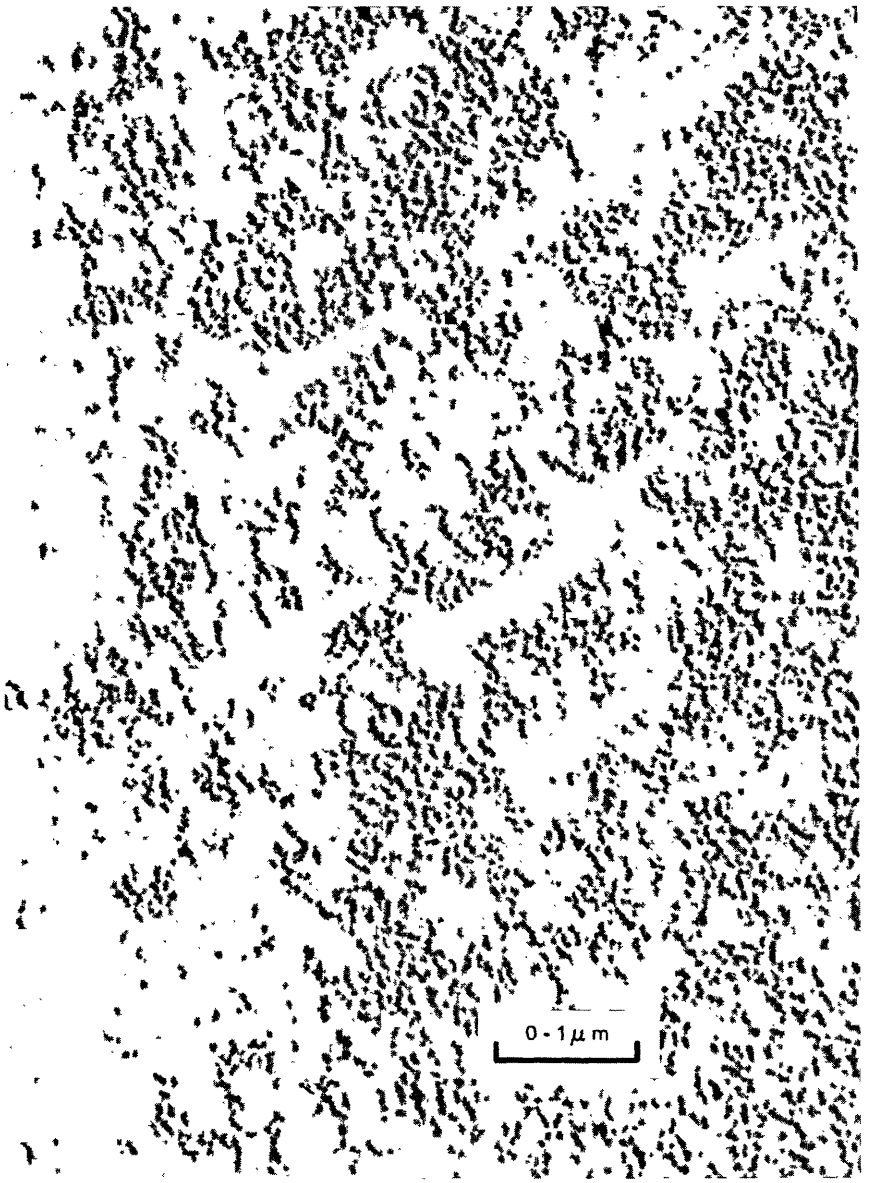

Figure 1.1 Individual polystyrene molecules as seen in an electron microscope. "Tails" are the result of shadow casting, which is used to enhance the visibility of the particles. [From M. J. Richardson, *Proc. Royal Soc.* 279A:50 (1964).]

critical molecular size has been reached. This critical size is often designated by a threshold molecular weight. The elastic behavior of rubber and several other so-called mechanical properties fall into this latter category. In theoretical developments, large values of n are often assumed to justify neglecting end effects, using certain statistical methods and other mathematical approximations. With these ideas in mind, M = 1000 is a convenient round number for designating a compound to be a polymer, although it should be clear that this cutoff is arbitrary.

1.3 Linear and Branched Polymers, Homopolymers, and Copolymers

The preceding section was based on the implicit assumption that polymer chains are linear. In evaluating both the degree of polymerization and the extended chain length, we assumed that the chain had only two ends. While linear polymers are important, they are not the only type of molecules possible. Branched and cross-linked molecules are also important. When we speak of a branched polymer, we refer to the presence of additional polymeric chains issuing from the backbone of a linear molecule. Substituent groups such as methyl or phenyl groups on the repeat units are not considered branches. Branching is generally introduced into a molecule by intentionally adding some monomer with the capability of serving as a branch. Consider the formation of a polyester. The presence of difunctional acids and difunctional alcohols allows the polymer chain to grow. These difunctional molecules are incorporated into the chain with ester linkages at both ends of each. Trifunctional acids or alcohols, on the other hand, produce a linear molecule by reacting two of their functional groups. If the third reacts and the resulting chain continues to grow, a branch has been introduced into the original chain. Adventitious branching sometimes occurs as a result of an atom being abstracted from the original linear molecule, with chain growth occurring from the resulting active site. Molecules with this kind of accidental branching are generally still called linear, although the presence of significant branching has profound effects on some properties of the polymer, most notably the tendency to undergo crystallization.

The amount of branching introduced into a polymer is an additional variable that must be specified for the molecule to be fully characterized. When only a slight degree of branching is present, the concentration of junction points is sufficiently low that these may be simply related to the number of chain ends. For example, two separate linear molecules have a total of four ends. If the end of one of these linear molecules attaches itself to the middle of the other to form a T, the resulting molecule has three ends. It is easy to generalize this result. If a molecule has ν branches, it has $\nu + 2$ chain ends if the branching is relatively low. Branched molecules are sometimes described as either combs or

stars. In the former, branch chains emanate from along the length of a common backbone; in the latter, all branches radiate from a central junction.

If the concentration of junction points is high enough, even branches will contain branches. Eventually a point is reached at which the amount of branching is so extensive that the polymer molecule becomes a giant three-dimensional network. When this condition is achieved, the molecule is said to be cross-linked. In this case, an entire macroscopic object may be considered to consist of essentially one molecule. The forces which give cohesiveness to such a body are covalent bonds, not intermolecular forces. Accordingly, the mechanical behavior of cross-linked bodies is much different from those without cross-linking.

Just as it is not necessary for polymer chains to be linear, it is also not necessary for all repeat units to be the same. We have already mentioned molecules like proteins where a wide variety of different repeat units are present. Among synthetic polymers, those in which a single kind of repeat unit are involved are called homopolymers, and those containing more than one kind of repeat unit are copolymers. Note that these definitions are based on the repeat unit, not the monomer. An ordinary polyester is not a copolymer, even though two different monomers, acids and alcohols, are its monomers. By contrast, copolymers result when different monomers bond together in the same way to produce a chain in which each kind of monomer retains its respective substituents in the polymer molecule. The unmodified term *copolymer* is generally used to designate the case where two different repeat units are involved. Where three kinds of repeat units are present, the system is called a terpolymer; where there are more than three, the system is called a multicomponent copolymer. The copolymers we discuss in this book will be primarily two-component molecules. We shall discuss copolymers in Chap. 7, so the present remarks are simply for purposes of orientation.

The moment we admit the possibility of having more than one kind of repeat unit, we require additional variables to describe the polymer. First, we must know how many kinds of repeat units are present and what they are. This is analogous to knowing what components are present in a solution, although the similarity ends there, since the repeat units in a polymer are bonded together and not merely mixed. To describe the copolymer quantitatively, the relative amounts of the different kinds of repeat units must be specified. Thus the empirical formula of a copolymer may be written A_xB_y, where A and B signify the individual repeat units and x and y indicate the relative number of each. From a knowledge of the molecular weight of the polymer, the molecular weights of A and B, and the values of x and y, it is possible to calculate the number of each kind of monomer unit in the copolymer. The sum of these values gives the degree of polymerization of the copolymer. Note that we generally do not call n_A and n_B the degrees of polymerization of the individual units. The inadvisability of the latter will become evident presently. The following example illustrates some of the ways of describing a copolymer.

Example 1.2

A terpolymer is prepared from vinyl monomers A, B, and C; the molecular weights of the repeat units are 104, 184, and 128, respectively. A particular polymerization procedure yields a product with the empirical formula $A_{3.55}B_{2.20}C_{1.00}$. The authors† of this research state that the terpolymer has "an average unit weight of 134" and "the average molecular weight per angstrom of 53.5." Verify these values.

Solution

The empirical formula gives the relative amounts of A, B, and C in the terpolymer. The total molecular weight of this empirical formula unit is given by adding the molecular weight contributions of A, B, and C: 3.55(104) + 2.20(184) + 1.00(128) = 902 amu per empirical formula unit. The total number of chain repeat units possessing this total weight is 3.55 + 2.20 + 1.00 = 6.75 repeat units per empirical formula unit. The ratio of the total molecular weight to the total number of repeat units gives the average molecular weight per repeat unit:

$$\frac{902}{6.75} = 134 \text{ amu per repeat unit}$$

Since the monomers are specified to be vinyl monomers, each contributes two carbon atoms to the polymer backbone, with the associated extended length of 0.252 nm per repeat unit. Therefore the total extended length of the empirical formula unit is

$$6.75(0.252\text{ nm}) = 1.70\text{ nm} = 17.0\text{ Å}$$

The ratio of the total weight to the total extended length of the empirical formula unit gives the average molecular weight per length of chain:

$$\frac{902}{17} = 53 \text{ amu per Å}$$

Note that the average weight per repeat unit could be used to evaluate the overall degree of polymerization of this terpolymer. For example, if the molecular weight were 43,000, the corresponding degree of polymerization would be

$$\frac{43{,}000 \text{ amu molecule}^{-1}}{134 \text{ amu (repeat unit)}^{-1}} = 321 \text{ repeat units per molecule}$$

•

† A. Ravve and J. T. Khamis, *Addition and Condensation Polymerization Processes*, Advances in Chemistry Series, Vol. 91, American Chemical Society Publications, Washington, D.C., 1969.

With copolymers, it is not sufficient merely to describe the empirical formula to characterize the molecule. Another question that can be asked concerns the distribution of the different kinds of repeat units in the molecule. Starting from monomers A and B, the following distribution patterns are obtained in linear polymers:

1. Random. The A–B sequence is governed strictly by chance, subject only to the relative abundances of repeat units. For equal proportions of A and B we have:

   –AAABABAABBABBB–

2. Alternation. A regular pattern of alternating repeat units:

   –ABABABABABAB–

3. Block. A long, uninterrupted sequence of each monomer is the pattern:

   –AAAAAAAAAAAAAABBBBBBBBBBBBBBBAAAAAAAAA–

If a copolymer is branched with different repeat units occurring in the branches and the backbone, we have the following:

4. Graft. This segregation is accomplished by first homopolymerizing the backbone. This is dissolved in the second monomer, with sites along the original chain becoming the origin of the comonomer side-chain growth:

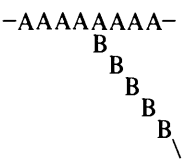

In a cross-linked polymer, the junction units are different kinds of monomers than the chain repeat units, so these molecules might be considered to be still another comonomer. While the chemical reactions which yield such cross-linked substances are copolymerizations, the products are described as cross-linked rather than as copolymers. In this instance, the behavior due to cross-linking takes precedence over the presence of an additional type of monomer in the structure.

It is apparent from items (1)–(3) above that linear copolymers—even those with the same proportions of different kinds of repeat units—can be very different in structure and properties. In classifying a copolymer as random, alternating, or block, it should be realized that we are describing the average character of the molecule; accidental variations from the basic patterns may be present. In Chap. 7 we shall see how an experimental investigation of the sequence of repeat units in a copolymer is a valuable tool for understanding copolymerization reactions. This type of information along with other details of structure are collectively known as the microstructure of a polymer.

1.4 Addition, Condensation, and Natural Polymers

In the last section we examined some of the categories into which polymers can be classified. Various aspects of molecular structure were used as the basis for classification in that section. Next we shall consider the chemical reactions that produce the molecules as a basis for classification. The objective of this discussion is simply to provide some orientation and to introduce some typical polymers. For this purpose a number of polymers may be classified as either addition or condensation polymers. Each of these classes of polymers are discussed in detail in Part II of this book, specifically Chaps. 5 and 6 for condensation and addition, respectively. Even though these categories are based on the reactions which produce the polymers, it should not be inferred that only two types of polymerization reactions exist. We have to start somewhere, and these two important categories are the usual place to begin.

These two categories of polymer can be developed along several lines. For example, in addition-type polymers the following applies:

1. The repeat unit in the polymer and the monomer have the same composition, although, of course, the bonding is different in each.
2. The mechanism of these reactions places addition polymerizations in the kinetic category of chain reactions, with either free radicals or ionic groups responsible for propagating the chain reaction.
3. The product molecules usually have a carbon chain backbone, with pendant substituent groups

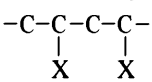

in condensation-type polymers:

4. The polymer repeat unit arises from reacting together two different functional groups which usually originate on different monomers. In this case the repeat unit is different from either of the monomers. In addition, small molecules are often eliminated during the condensation reaction. Note the words *usual* and *often* in the previous statements; exceptions to both statements are easily found.
5. The mechanistic aspect of these reactions is summarized by saying that the reactions occur in steps. Thus the formation of an ester linkage is not essentially different between two small molecules or in a polyester.
6. The product molecules have the functional groups formed by the condensation reactions interspersed regularly along the backbone of the polymer molecule:

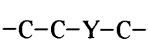

Next let us consider a few specific examples of these classes of polymers.

The addition polymerization of a vinyl monomer $CH_2=CHX$ involves three distinctly different steps. First, the reactive center must be initiated by a suitable reaction to produce a free radical or an anion or cation reaction site. Next, this reactive entity adds consecutive monomer units to propagate the polymer chain. Finally, the active site is capped off, terminating the polymer formation. If one assumes that the polymer produced is truly a high molecular weight substance, the lack of uniformity at the two ends of the chain—arising in one case from the initiation, and in the other from the termination—can be neglected. Accordingly, the overall reaction can be written

$$n CH_2=CHX \longrightarrow \{CH_2-CHX\}_n \qquad (1.A)$$

Again we emphasize that end effects are ignored in writing reaction (1.A). These effects as well as the conditions of the reaction and other pertinent information will be discussed when these reactions are considered in Chap. 6. Table 1.1 is a list of several important addition polymers, showing the polymerization reaction in the manner of reaction (1.A). Also included in Table 1.1 are the molecular weights of the repeat units and the common names of the polymers. The former will prove helpful in many of the problems in this book; the latter will be discussed in the next section. Poly(ethylene oxide) and poly(ϵ-caprolactam) have been included in this list as examples of the hazards associated with classification schemes. They resemble addition polymers because the molecular weight of the repeat unit and that of the monomer are the same; they resemble condensation polymers because of the heteroatom chain backbone. The reaction mechanism, which might serve as arbiter in this case, can be either chain or step, depending on the reaction conditions! These last reactions are examples of ring-opening polymerizations, still another category of classification.

The requirements for formation of condensation polymers are twofold: The monomers must possess functional groups capable of reacting to form the linkage and they ordinarily require more than one reactive group to generate a chain structure. The functional groups can be distributed such that two difunctional monomers with different functional groups react or a single monomer reacts which is difunctional with one group of each kind. In the latter case especially, but also with condensation polymerization in general, the tendency to form cyclic products from intramolecular reactions may compete with the formation of polymer. This possibility is discussed in Sec. 5.10. Condensation polymerizations are especially sensitive to impurities. The presence of monofunctional reagents introduces the possibility of a reaction product forming which would not be capable of further growth. If the functionality is greater than 2, on the other hand, branching becomes possible. Both of these modifications dramatically alter the product compared to a high molecular weight linear product. When reagents of functionality less than or greater than 2 are added in carefully measured and controlled amounts, the size and geometry of product

Table 1.1 Reactions by Which Several Important Addition Polymers are Produced[a]

Monomer and M_0 (g mol^{-1})		Polymer repeat unit and name(s)
1. $nCH_2{=}CH_2$	$\longrightarrow$	$\{CH_2{-}CH_2\}_n$
(M_0 = 28.0)		polyethylene
2. $nCH_2{=}CH$	$\longrightarrow$	$\{CH_2{-}CH\}_n$
C_6H_5		C_6H_5
(M_0 = 104)		polystyrene
3. $nCH_2{=}CHCl$	$\longrightarrow$	$\{CH_2{-}CHCl\}_n$
(M_0 = 62.5)		poly(vinyl chloride), "vinyl"
4. $nCH_2{=}CH$	$\longrightarrow$	$\{CH_2{-}CH\}_n$
CN		CN
(M_0 = 53.9)		polyacrylonitrile, "acrylic"
5. $nCH_2{=}CCl_2$	$\longrightarrow$	$\{CH_2{-}CCl_2\}_n$
(M_0 = 97.0)		poly(vinylidene chloride)
CH_3		CH_3
6. $nCH_2{=}C$	$\longrightarrow$	$\{CH_2{-}C\}_n$
$O{=}C{-}O{-}CH_3$		$O{=}C{-}O{-}CH_3$
(M_0 = 100)		poly(methyl methacrylate), Plexiglas, lucite
CH_3		CH_3
7. $nCH_2{=}C$	$\longrightarrow$	$\{CH_2{-}C\}_n$
CH_3		CH_3
(M_0 = 56.0)		polyisobutylene
8. $nCF_2{=}CF_2$	$\longrightarrow$	$\{CF_2{-}CF_2\}_n$
(M_0 = 100)		polytetrafluoroethylene, Teflon
9. $nCH_2{-}CH_2$ (O bridge)	$\longrightarrow$	$\{CH_2{-}CH_2{-}O\}_n$
(M_0 = 44.0)		poly(ethylene oxide), carbowax
10. $nC{-}(CH_2)_5{-}N$ (O, H)	$\longrightarrow$	$\{(CH_2)_5{-}C{-}N\}_n$
(M_0 = 113)		poly(ϵ-caprolactam), nylon-6

[a] Molecular weights of repeat units and common names of the products are included for future reference. Reactions 9 and 10 are ring-opening polymerizations and are discussed in Sec. 5.10.

molecules can be manipulated. When such reactants enter as impurities, the undesired results can be disasterous! Marvel† has remarked that more money has been wasted in polymer research by the use of impure monomers than in any other manner.

Table 1.2 lists several examples of condensation reactions and products. Since the reacting monomers can contain different numbers of carbon atoms between functional groups, there are quite a lot of variations possible among these basic reaction types.

The inclusion of poly(dimethyl siloxane) in Table 1.2 serves as a reminder that polymers need not be organic compounds. The physical properties of inorganic polymers follow from the chain structure of these molecules, and the concepts developed in this volume apply to them and to organic polymers equally well. For example, poly(dimethyl siloxane) shows a very low viscosity compared to other polymers of comparable degree of polymerization. We shall see in Chap. 2 that this is traceable to its high chain flexibility, which, in turn, is due to the high concentration of chain backbone atoms with no substituents. We shall not examine the classes and preparations of the various types of inorganic polymers in this text. References in inorganic chemistry should be consulted for this information.

We conclude this section with a short discussion of naturally occurring polymers. Since these are of biological origin, they are also called biopolymers. Although our attention in this volume is primarily directed toward synthetic polymers, it should be recognized that biopolymers, like inorganic polymers, have physical properties which follow directly from the chain structure of their molecules. The synthesis by and contribution to living organisms by these biopolymers is the subject matter of other disciplines, such as biochemistry and molecular biology. The reader who desires information on this aspect of these naturally occurring polymers should consult references in these other disciplines.

As examples of natural polymers, we consider polysaccharides, proteins, and nucleic acids. Another important natural polymer, polyisoprene, will be considered in Sec. 1.6.

Polysaccharides are macromolecules which make up a large part of the bulk of the vegetable kingdom. Cellulose and starch are, respectively, the first and second most abundant organic compounds in plants. The former is present in leaves and grasses; the latter in fruits, stems, and roots. Because of their abundance in nature and because of contemporary interest in renewable resources, there is a great deal of interest in these compounds. Both cellulose and starch are hydrolyzed by acids to D-glucose, the repeat unit in both polymer chains.

† Carl S. Marvel, another pioneer in polymer chemistry, reminisces about the early days of polymer chemistry in the United States in the *Journal of Chemical Education*, 58:535 (1981).

Table 1.2 Reactions by Which Several Important Condenstation Polymers are Produced[a]

1. Polyester

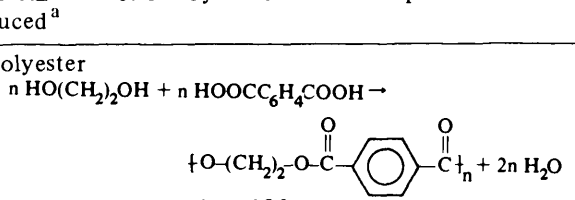

$M_0 = 192$

poly(ethylene terephthalate), Terylene, Dacron, Mylar

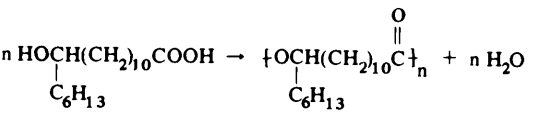

$M_0 = 282$

poly(12-hydroxystearic acid)

2. Polyamide

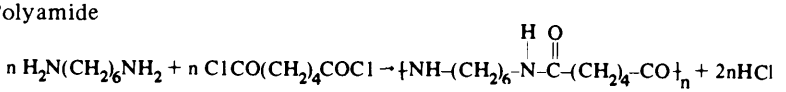

$M_0 = 226$

poly(hexamethylene adipamide), nylon 6,6

3. Polyurethane

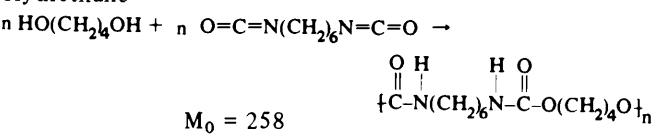

$M_0 = 258$

poly(tetramethylene hexamethylene urethane), spandex, Perlon U

4. Polycarbonate

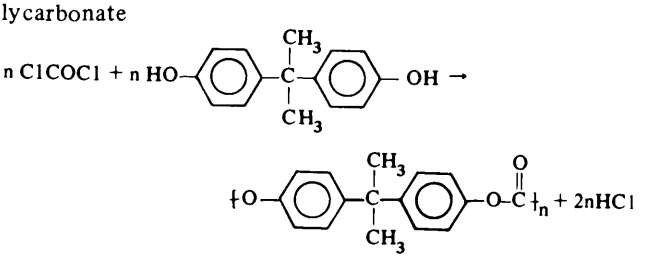

$M_0 = 244$

poly(4,4-isopropylidenediphyenylene carbonate), bisphenol A polycarbonate, lexan

5. Inorganic

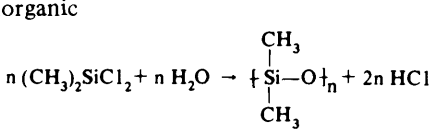

$M_0 = 74.0$

poly(dimethyl siloxane)

[a] Molecular weights of repeat units and common names of the products are included for future reference.

The configuration of the glucoside linkage is different in the two, however. Structures [I] and [II], respectively, illustrate that the linkage is a β-acetal–hydrolyzable to an equitorial hydroxide–in cellulose, and an α-acetal–hydrolyzable to an axial hydroxide–in amylose, a starch:

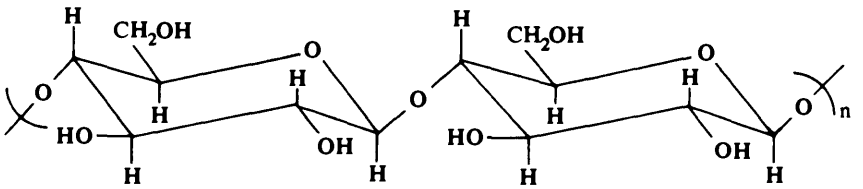

[I]

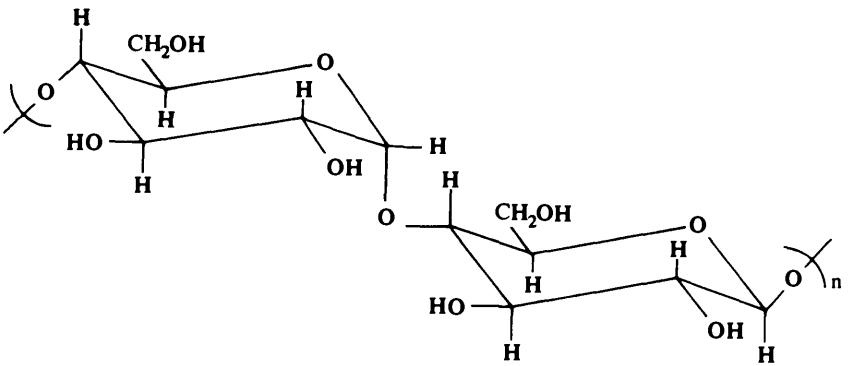

[II]

Amylopectin and glycogen are saccharides similar to amylose, except with branched chains.

The cellulose molecule contains three hydroxyl groups which can react and leave the chain backbone intact. These alcohol groups can be esterified with acetic anhydride to form cellulose acetate. This polymer is spun into the fiber acetate rayon. Similarly, the alcohol groups in cellulose react with CS_2 in the presence of strong base to produce cellulose xanthates. When extruded into fibers, this material is called viscose rayon, and when extruded into sheets, cellophane. In both the acetate and xanthate formation, some chain degradation also occurs, so the resulting polymer chains are shorter than those in the starting cellulose.

As noted above, proteins are polyamides in which α-amino acids make up the repeat units, as shown by structure [III]:

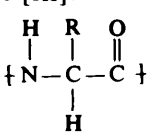

[III]

These molecules are also called polypeptides, especially in cases where $M \lesssim 10{,}000$. The various amino acids differ in R groups. The nature of R, the name, and the abbreviation used to represent some of the more common amino acids are listed in Table 1.3. In proline (Pro) and hydroxyproline (Hyp), the nitrogen and the α-carbon are part of the five-atom pyrrolidine ring. Since some of the amino acids carry substituent carboxyl or amino groups, protein molecules are charged in aqueous solutions, and hence migrate in electric fields. This is the basis of electrophoresis as a means of separating and identifying proteins.

It is conventional to speak of three levels of structure in protein molecules:

1. Primary structure refers to the sequence of amino acids in the polyamide chain.
2. Secondary structure refers to the shape of the molecule as a whole, particularly to those aspects of structure which are stabilized by intramolecular hydrogen bonds.
3. Tertiary structure also refers to the overall shape of a molecule, especially to structures stabilized by disulfide bridges (cystine) formed by the oxidation of cysteine mercapto groups.

Hydrogen bonding stabilizes some protein molecules in helical forms, and disulfide cross-links stabilize some protein molecules in globular forms. We shall consider helical structures in Sec. 1.11 and shall learn more about ellipsoidal globular proteins in the chapters concerned with the solution properties of polymers, especially Chap. 9. Both secondary and tertiary levels of structure are also influenced by the distribution of polar and nonpolar amino acid molecules relative to the aqueous environment of the protein molecules. Nonpolar amino acids are designated in Table 1.3.

The three levels of structure listed above are also useful categories for describing nonprotein polymers. Thus details of the microstructure of a chain is a description of the primary structure. The overall shape assumed by an individual molecule as a result of the rotation around individual bonds is the secondary structure. Structures that are locked in by chemical cross-links are tertiary structures.

Examples of the effects and modification of the higher-order levels of structure in proteins are found in the following systems:

1. Collagen is the protein of connective tissues and skin. In living organisms, the molecules are wound around one another to form a three-strand helix stabilized by hydrogen bonding. When boiled in water, the collagen dissolves and forms gelatin, apparently establishing a new hydrogen bond equilibrium with the solvent. This last solution sets up to form the familiar gel when cooled, a result of shifting the hydrogen bond equilibrium.
2. Keratin is the protein of hair and wool. These proteins are insoluble because of the disulfide cross-linking between cystine units. Permanent waving of

Table 1.3 Name, Abbreviation, and R Group for Some Common Amino Acids

Name	Abbreviation	R group
Alanine[a]	Ala	$-CH_3$
Arginine	Arg	$-CH_2CH_2CH_2NHC(=NH)NH_2$
Aspartic acid	Asp	$-CH_2COOH$
Cysteine	Cys	$-CH_2SH$
Glutamic acid	Glu	$-CH_2CH_2COOH$
Glycine	Gly	$-H$
Histidine	His	
Isoleucine[a]	Ile	$-CH(CH_3)CH_2CH_3$
Leucine[a]	Leu	$-CH_2CH(CH_3)_2$
Lysine	Lys	$-CH_2CH_2CH_2CH_2NH_2$
Methionine[a]	Met	$-CH_2CH_2SCH_3$
Phenylalanine[a]	Phe	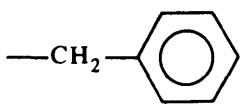
Serine	Ser	$-CH_2OH$
Threonine	Thr	$-CHOHCH_3$
Tryptophan[a]	Trp	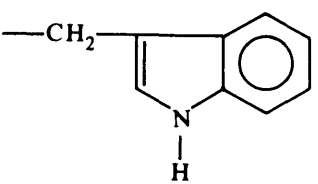
Tyrosine	Tyr	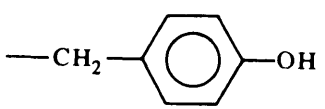
Valine[a]	Val	$-CH(CH_3)_2$

[a] Nonpolar R groups.

hair involves the rupture of these bonds, reshaping of the hair fibers, and the reformation of cross-links which hold the chains in the new positions relative to each other. We shall see in Chap. 3 how such cross-linked networks are restored to their original shape when subjected to distorting forces.

3. The globular proteins albumin in eggs and fibrinogen in blood are converted to insoluble forms by modification of their higher-order structure. The process is called denaturation and occurs, in the systems mentioned, with the cooking of eggs and the clotting of blood.

Ribonucleic acid (RNA) and deoxyribonucleic acid (DNA) are polymers in which the repeat units are substituted polyesters. The esters are formed between the hydrogens of phosphoric acid and the hydroxyl groups of a sugar, D-ribose in the case of RNA and D-2-deoxyribose in the case of DNA. The sugar rings in DNA carry four different kinds of substituents: adenine and guanine, which are purines, and thymine and cytosine, which are pyramidines. The familiar double-helix structure of the DNA molecule is stabilized by hydrogen bonding between pairs of substituent base groups. The replication of these molecules, the template model of their functioning, and their role in protein synthesis and the genetic code make the study of these polymers among the most exciting and actively researched areas in all science. A single paragraph scarcely does justice to the fundamental importance, brilliant research, and extensive body of knowledge centered around these materials. As for inorganic polymers, however, we refer the reader who seeks more information about these substances to texts in biochemistry or molecular biology.

1.5 Polymer Nomenclature

Considering that a simple compound like C_2H_5OH is variously known as ethanol, ethyl alcohol, grain alcohol, or simply alcohol, it is not too surprising that the vastly more complicated polymer molecules are also often known by a variety of different names. The International Union of Pure and Applied Chemistry (IUPAC) has recommended a system of nomenclature based on the structure of the monomer or repeat unit. A semisystematic set of trivial names is also in widespread usage; these latter names seem even more resistant to replacement than is the case with low molecular weight compounds. Synthetic polymers of commercial importance are often widely known by trade names which seem to have more to do with marketing considerations than with scientific communication. Polymers of biological origin are often described in terms of some aspect of their function, preparation, or characterization.

If a polymer is formed from a single monomer, as in addition and ring-opening polymerizations, it is named by attaching the prefix *poly* to the name

of the monomer. In the IUPAC system, the monomer is named according to the IUPAC recommendations for organic chemistry, and the name of the monomer is set off from the prefix by enclosing the former in parentheses. Variations of this basic system often substitute a common name for the IUPAC name in designating the monomer. Whether or not parentheses are used in the latter case is influenced by the complexity of the monomer name; they become more important as the number of words in the monomer name increases. The polymer $\text{-}(CH_2\text{-}CHCl)\text{-}_n$ is called poly(1-chloroethylene) according to the IUPAC system; it is more commonly called poly(vinyl chloride) or polyvinyl chloride. Acronyms are not particularly helpful but are an almost irresistible aspect of polymer terminology, as evidenced by the initials PVC, which are so widely used to describe the polymer just named. The trio of names—poly(1-hydroxyethylene), poly(vinyl alcohol), and polyvinyl alcohol—emphasizes that the polymer need not actually be formed from the reaction of the monomer named; this polymer is formed by the hydrolysis of poly(1-acetoxyethylene), otherwise known as poly(vinyl acetate). These same alternatives are used in naming polymers formed by ring-opening reactions; for example, poly(6-aminohexanoic acid), poly(6-aminocaproic acid) and poly(ϵ-caprolactam) are all more or less acceptable names for the same polymer.

Those polymers which are the condensation product of two different monomers are named by applying the preceding rules to the repeat unit. For example, the polyester formed by the condensation of ethylene glycol and terephthalic acid is called poly(oxyethylene oxyterphthaloyl) according to the IUPAC system, as well as poly(ethylene terephthalate) or polyethylene terephthalate.

The polyamides poly(hexamethylene sebacamide) and poly(hexamethylene adipamide) are also widely known as nylon-6,10 and nylon-6,6, respectively. The numbers following the word *nylon* indicate the number of carbon atoms in the diamine and dicarboxylic acid, in that order. On the basis of this same system, poly(ϵ-caprolactam) is also known as nylon-6.

Most of the polymers in Tables 1.1 and 1.2 are listed with more than one name. Also listed are some of the patented trade names by which these substances—or materials which are mostly of the indicated structure—are sold commercially.

Some commercially important cross-linked polymers go virtually without names. These are heavily and randomly cross-linked polymers which are insoluble and infusible and therefore widely used in the manufacture of such molded items as automobile and household appliance parts. These materials are called resins and, at best, are named by specifying the monomers which go into their production. Often even this information is sketchy. Examples of this situation are provided by phenol-formaldehyde and urea-formaldehyde resins, for which typical structures are given by structures [IV] and [V], respectively:

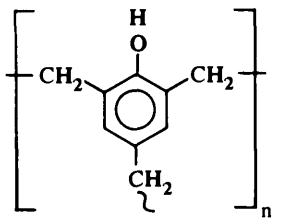

[IV]

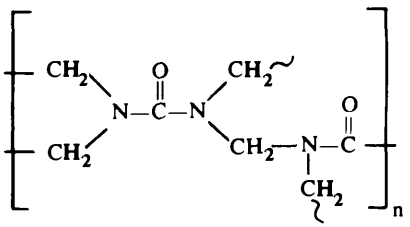

[V]

1.6 Positional, Stereo, and Geometrical Isomerism

In this section we shall consider three types of isomerism which are encountered in polymers. These are positional isomerism, stereo isomerism, and geometrical isomerism. We shall focus attention on synthetic polymers and shall, for the most part, be concerned with these types of isomerism occurring singly, rather than in combination. The synthetic and analytical aspects of stereo isomerism will be considered in Chap. 7. Our present concern is merely to introduce the possibilities of these isomers and some of the vocabulary associated with them.

Positional isomerism is conveniently illustrated by considering the polymerization of a vinyl monomer. In such a reaction, the adding monomer may become attached to the growing chain in either of two orientations:

$$\sim CH_2{-}CHX + CH_2{=}CHX \longrightarrow \begin{cases} \sim CH_2{-}CHX{-}CH_2{-}CHX & [VI] \\ \sim CH_2{-}CHX{-}CHX{-}CH_2 & [VII] \end{cases} \qquad (1.B)$$

Structures [VI] and [VII], respectively, are said to arise from head-to-tail or head-to-head orientations. In this terminology, the substituted carbon is defined to be the head of the molecule, and the methylene is the tail. Tail-to-tail linking is also possible. The term *orienticity* is also used to describe positional isomerism.

For most vinyl polymers, head-to-tail addition is the dominant mode of addition. Variations from this generalization become more common for polymerizations which are carried out at higher temperatures. Head-to-head addition is also somewhat more abundant in the case of halogenated monomers such as vinyl chloride. The preponderance of head-to-tail additions is understood to arise from a combination of resonance and steric effects. In many cases the ionic or free-radical reaction center occurs at the substituted carbon due to the possibility of resonance stabilization or electron delocalization through the substituent group. Head-to-tail attachment is also sterically favored, since the substituent groups on successive repeat units are separated by a methylene

carbon. At higher temperatures of polymerization, larger amounts of available thermal energy make the less-favored states more accessible. In vinyl fluoride, no resonance stabilization is possible and steric effects are minimal. This monomer adds primarily in the head-to-tail orientation at low temperatures and tends toward a random combination of both at higher temperatures. The styrene radical, by contrast, enjoys a large amount of resonance stabilization in the bulky phenyl group and polymerizes almost exclusively in the head-to-tail mode. The following example illustrates how chemical methods can be used to measure the relative amounts of the two positional isomers in a polymer sample.

Example 1.3

1,2-Glycol bonds are cleaved by reaction with periodate; hence poly(vinyl alcohol) chains are broken at the site of head-to-head links in the polymer. The fraction of head-to-head linkages in poly(vinyl alcohol) may be determined by measuring the molecular weight before (subscript b) and after (subscript a) cleavage with periodate according to the following formula: Fraction = $44(1/M_a - 1/M_b)$. Derive this expression and calculate the value for the fraction in the case of $M_b = 10^5$ and $M_a = 10^3$.

Solution

Begin by recognizing that a molecule containing x of the head-to-head links will be cleaved into x + 1 molecules upon reaction. Hence if N is the number of polymer molecules in a sample of mass w, the following relations apply before and after cleavage: $N_a = (x + 1)N_b$ or $w/M_a = (x + 1)(w/M_b)$. Solving for x and dividing the latter by the total number of linkages in the original polymer gives the desired ratio. The total number of links in the mass w of polymer is w/n_bM_0. Therefore the ratio is $x/n_b = M_0\,(1/M_a - 1/M_b)$. For polyvinyl alcohol M_0 is 44, so the desired formula has been obtained. For the specific data given, $x/n_b = 44(10^{-3} - 10^{-5}) = 0.044$, or about 4% of the additions is in the less favorable orientation. We shall see presently that the molecular weight of a polymer is an average which is different, depending on the method used for its determination. The present example used molecular weights as a means for counting the number of molecules present. Hence the sort of average molecular weight used should also be one which is based on counting.†

•

†A physical chemistry laboratory experiment based on this principle is found in D. P. Shoemaker, C. W. Garland, J. I. Steinfels, and J. W. Nibler, *Experiments in Physical Chemistry*, 4th ed., McGraw-Hill, New York, 1981.

The second type of isomerism we discuss in this section is stereo isomerism. Again we consider the number of ways a singly substituted vinyl monomer can add to a growing polymer chain:

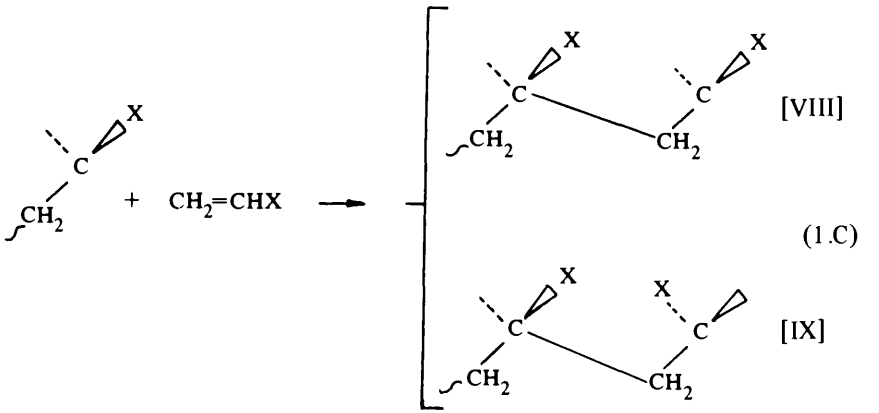

Structures [VIII] and [IX] are not equivalent; they would not superimpose if the extended chains were overlaid. The difference has to do with the stereochemical configuration at the asymmetric carbon atom. Note that the asymmetry is more accurately described as pseudoasymmetry, since two sections of chain are bonded to these centers. Except near chain ends, which we ignore for high polymers, these chains provide local symmetry in the neighborhood of the carbon under consideration. The designations D and L or R and S are used to distinguish these structures, even though true asymmetry is absent.

We use the word *configuration* to describe the way the two isomers produced by reaction (1.C) differ. It is only by breaking bonds, moving substituents, and reforming new bonds that the two structures can be interconverted. This state of affairs is most readily seen when the molecules are drawn as fully extended chains and then examining the side of the chain on which substituents lie. The configurations are not altered if rotation is allowed to occur around the various bonds of the backbone to change the shape of the molecule to a jumbled coil. We shall use the term *conformations* to describe the latter possibilities for different molecular shapes. The configuration is not influenced by conformational changes, but the stability of different conformations may be affected by differences in configuration. We shall return to these effects in Sec. 1.11.

In the absence of any external influence such as a catalyst which is biased in favor of one configuration over the other, we might expect structures [VIII] and [IX] to occur at random with equal probability as if the configuration at each successive addition were determined by the toss of a coin. Such, indeed, is the ordinary case. However, in the early 1950s, stereospecific catalysts were discovered; Ziegler and Natta received the Nobel Prize for this discovery in 1963.

Following the advent of these catalysts, polymers with a remarkable degree of stereoregularity have been formed. These have had such a striking impact on polymer science that a large part of Chap. 7 is devoted to a discussion of their preparation and characterization. For now, only the terminology involved in their description concerns us. Three different situations can be distinguished along a chain containing pseudoasymmetric carbons:

1. Isotactic. All substituents lie on the same side of the extended chain. Alternatively, the stereoconfiguration at the asymmetric centers is the same, say, –DDDDDDDDD–.
2. Syndiotactic. Substituents on the fully extended chain lie on alternating sides of the backbone. This alternation of configuration can be represented as –DLDLDLDLDLDL–.
3. Atactic. Substituents are distributed at random along the chain, for example, –DDLDLLLDLDLL–.

Figure 1.2 shows sections of polymer chains of these three types; the substituent R equals phenyl for polystyrene and methyl for polypropylene. The general term for this stereoregularity is *tacticity*, a term derived from the Greek word meaning "to put in order."

Polymers of different tacticity have quite different properties, especially in the solid state. One of the requirements for polymer crystallinity is a high degree of microstructural regularity to enable the chains to pack in an orderly manner. Thus atactic polypropylene is a soft, tacky substance, whereas both isotactic and syndiotactic polypropylenes are highly crystalline.

No polymer is ever 100% crystalline; at best, patches of crystallinity are present in an otherwise amorphous matrix. In some ways, the presence of these domains of crystallinity is equivalent to cross-links, since different chains loop in and out of the same crystal. Although there are similarities in the mechanical behavior of chemically cross-linked and partially crystalline polymers, a significant difference is that the former are irreversibly bonded while the latter are reversible through changes of temperature. Materials in which chemical cross-linking is responsible for the mechanical properties are called thermosetting; those in which this kind of physical cross-linking operates, thermoplastic.

The final type of isomerism we take up in this section involves various possible structures which result from the polymerization of 1,3-dienes. Three important monomers of this type are 1,3-butadiene, 1,3-isoprene, and 1,3-chloroprene, structures [X]-[XII], respectively:

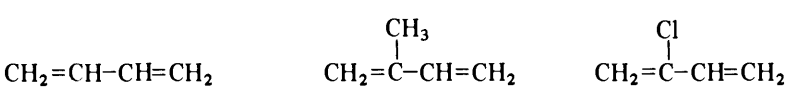

[X] [XI] [XII]

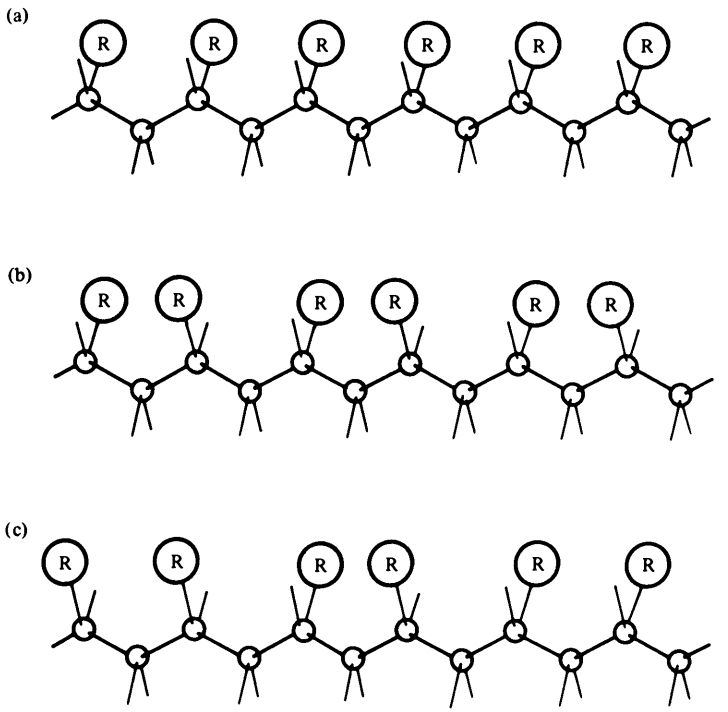

Figure 1.2 Sections of polymer chains of differing tacticity: (a) isotactic (b) syndiotactic (c) atactic.

To illustrate the possible modes of polymerization of these compounds, consider the following reactions of isoprene:

1. 1,2- and 3,4-Polymerizations. As far as the polymer chain backbone is concerned, these compounds could just as well be mono-olefins, since the second double bond is relegated to the status of a substituent group. Because of the reactivity of the latter, however, it might become involved in cross-linking reactions. For isoprene, 1,2- and 3,4-polymerizations yield different products:

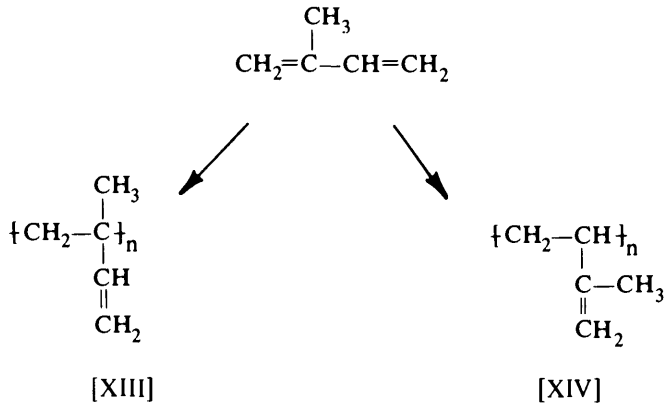

(1.D)

[XIII] [XIV]

These differences do not arise from 1,2- or 3,4-polymerization of butadiene. Structures [XIII] and [XIV] can each exhibit the three different types of tacticity, so a total of six structures can result from this monomer when only one of the olefin groups is involved in the backbone formation.

2. 1,4-Polymerization. This mode of polymerization gives a molecule with double bonds along the backbone of the chain. Again using isoprene as the example,

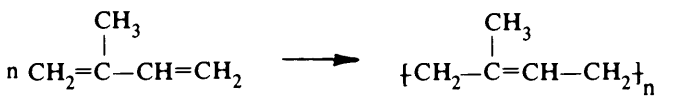

(1.E)

As in all double-bond situations, the adjacent chain sections can be either cis or trans–structures [XV] and [XVI], respectively–with respect to the double bond, producing the following geometrical isomers:

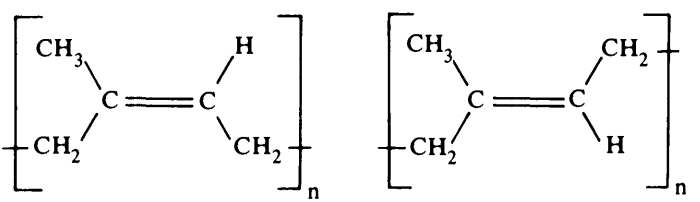

[XV] [XVI]

Figure 1.3 shows several repeat units of cis-1,4-polyisoprene and trans-1,4-polyisoprene. Natural rubber is the cis isomer of 1,4-polyisoprene, and gutta-percha is the trans isomer.

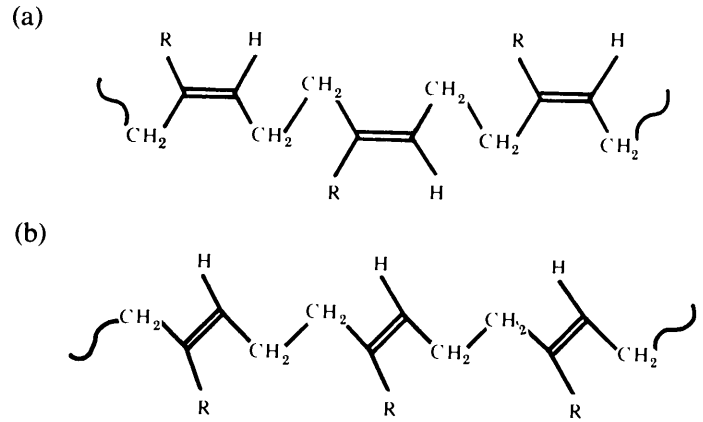

Figure 1.3 1,4-polyisoprene with $R=CH_3$ (a) cis isomer: natural rubber (b) trans isomer: gutta-percha.

3. Polymers of chloroprene (structure [XII]) are called neoprene and copolymers of butadiene and styrene are called SBR, an acronym for styrene-butadiene rubber. Both are used for many of the same applications as natural rubber. Chloroprene displays the same assortment of possible isomers as isoprene; the extra combinations afforded by copolymer composition and structure in SBR offsets the fact that structures [XIII] and [XIV] are identical for butadiene.
4. Although the conditions of the polymerization reaction may be chosen to optimize the formation of one specific isomer, it is typical in these systems to have at least some contribution of all possible isomers in the polymeric product, except in the case of polymers of biological origin, like natural rubber and gutta-percha.

Throughout the past few sections we have ignored the uniqueness of chain ends and focused attention on the repeating portion of the chain. Generally speaking, this will be our attitude throughout this book. An exception is the material of the next section, where we consider the quantitative analysis for end groups as a method for polymer molecular weight determination.

1.7 Molecular Weight by End Group Analysis

The high molecular weight of a polymer is one of the most immediate consequences of the chain structure of these molecules. As indicated in Sec. 1.2, it is also the basis for describing the size of the polymer molecule, either directly or through the degree of polymerization. Most methods for the determination

of the molecular weight of a polymer depend on the properties of polymer solutions. These methods will be taken up in Part III. In this section, however, we shall at least introduce the topic of molecular weight determination by considering those methods based on end group analysis.

The terminal groups of a polymer chain are different in some way from the repeat units that characterize the rest of the molecule. If some technique of analytical chemistry can be applied to determine the number of these end groups in a polymer sample, then the average molecular weight of the polymer is readily evaluated. In essence, the concept is no different than the equivalent procedure applied to low molecular weight compounds. The latter is often included as an experiment in general chemistry laboratory classes. The following steps outline the experimental and computational essence of this procedure:

1. The mass of the sample is determined. Only an analytical balance is required for this.
2. A suitable functional group is assayed in the same sample. In general chemistry and many polymer applications, this is merely the titration of acid groups with a base, or vice versa. Note that only volumetric glassware and a method for end point determination are required to do this.
3. From the volume and concentration of the base, the number of equivalents of the neutralized acid group is readily calculated.
4. The number of grams in a sample divided by the number of equivalents in the same sample gives the gram-equivalent weight of the material.
5. If the number of equivalents per mole is known, the molecular weight is calculated from the equivalent weight by multiplying the latter by the number of equivalents per mole.
6. The method of end group analysis for molecular weight determination is not only simple to understand, but can also be done with ordinary laboratory equipment in many instances.

One limitation of this method that should immediately come to mind is the restriction to relatively low molecular weight polymers. This is a corollary of the fact that chain ends are inconsequential for very long chains. Hence, the sensitivity of the method decreases as the molecular weight of the polymer increases. As a general rule, molecular weights in the neighborhood of 25,000 represent the upper limit for applicability of this method.

Condensation polymers such as polyesters and polyamides are especially well suited to this method of molecular weight determination. For one thing, the molecular weight of these polymers is usually less than for addition polymers. Even more pertinent to the method is the fact that the chain ends in these molecules consist of unreacted functional groups. Using polyamides as an example, we can readily account for the following possibilities:

1. A linear molecule has a carboxyl group at one end and an amino group at the other, such as poly(ϵ-caprolactam):

   $$HOOC-(CH_2)_5\text{-}NHCO-(CH_2)_5\text{-}_nNH_2$$

   In this case there is one functional group of each kind per molecule, and each could titrated as a double check of the method.
2. If a polyamide is prepared in the presence of a large excess of diamine, the average chain will be capped by an amine group at each end:

   $$H_2N-R\text{-}NHCO-R\text{-}_nNH_2$$

   In this case only the amine can be titrated, and two ends are counted per molecule.
3. If a polyamide is prepared in the presence of a large excess of dicarboxylic acid, the average chain will have a carboxyl group at each end:

   $$HOOC-R\text{-}CONH-R\text{-}_nCOOH$$

   Only acid groups are titrated and two ends are counted per molecule.

The foregoing examples point out certain critical aspects of the end group method for molecular weight determination. At least for certain functional groups and down to a certain limit of concentration, end groups can be analyzed. Proceeding from this information to the molecular weight of the polymer requires either knowing or assuming something about the nature of the chain ends in the specific sample under consideration. The alternatives enumerated above emphasize that this must be considered explicitly for each sample. In addition to the variations listed above, the following points should also be considered:

1. Have any amino groups been acylated by reaction with an acid catalyst?
2. Has any decarboxylation occurred as a result of elevated temperatures?
3. Have any ring structures formed from the reaction of two ends of the same molecule?
4. Can branching be ruled out, since it would obviously make the number of chain ends per molecule an unknown quantity?

Comparable but equally specific considerations must be applied to other condensation polymer systems. The following example is an illustration of the application of these ideas to the molecular weight of polyamides.

Example 1.4

Aqueous caprolactam is polymerized alone and in the presence of sebacic acid (S) or hexamethylenediamine (H).† After a 24-hr reaction time, the polymer is isolated and the end groups are analyzed by titrating the carboxyl groups with KOH in benzyl alcohol and the amino groups with *p*-toluenesulfonic acid in trifluoroethanol. The number of milliequivalents of carboxyl group per mole caprolactam converted to polymer, [A*], and the number of milliequivalents of amino groups per mole caprolactam converted to polymer, [B*], are given below for three different runs:

Additive	[A*]	[B*]
None	12.0	11.6
S	39.9	2.4
H	1.87	35.1

Calculate the molecular weights in each case and comment briefly on the results.

Solution

Note the units of the end group concentrations [A*] and [B*]: milliequivalents per mole polymerized monomer. The reciprocal is therefore moles of monomer per milliequivalent of end groups. Accordingly, the molecular weight is given by

$$M = \frac{\text{moles caprolactam}}{\text{mEq specific end group}} \times \frac{113 \text{ g caprolactam}}{\text{moles caprolactam}} \times \frac{1000 \text{ mEq}}{1 \text{ Eq}}$$

$$\times \frac{\text{number of equivalents of specific end groups}}{\text{polymer molecule}}$$

Only the last factor is a little tricky; it is also different with and without additives. With no additive, polycaprolactam can be represented A*BABAB . . . ABAB*, where the A and B are acid and base groups, respectively, and those marked with the asterisk are those analyzed. Thus every molecule has one of each. In this case, then, we use the average of 12.0 and 11.6 as the end group concentration, and unity as the number of ends of each kind to obtain

†H. K. Reimschussel and G. J. Dege, *J. Polym. Sci.* 9:2343 (1971).

$$M = \frac{1}{11.8} \times 113 \times 1000 \times 1 = 9580 \text{ g mol}^{-1}.$$

With either S or H as additives, two different kinds of chain are present: A*BAB ... ABAB* and A*BABAB ... ABABAA* with S or B*BABAB ... ABAB* with H. In these cases the total number of acid and base groups counts the total number of chain ends. There are two equivalents of total chain ends per mole of chains. Therefore, for S, [total ends] = 39.9 + 2.4 = 42.3 and

$$M = \frac{1}{42.3} \times 113 \times 1000 \times 2 = 5340 \text{ g mol}^{-1}$$

and for H, [total ends] = 1.87 + 34.1 = 37.0 and

$$M = \frac{1}{37.0} \times 113 \times 1000 \times 2 = 6110 \text{ g mol}^{-1}$$

Several comments come to mind:

1. As polymers go, none of these is a particularly high molecular weight.
2. No consideration is made of the fact that S and H contribute to M a molecular weight different from M_0.
3. The results of end group analyses must be examined on a system-by-system basis for correct interpretation.
4. The presence of monomers with two functional groups of the same kind limits chain growth and decreases the molecular weight.
5. The molecular weights obtained by this method are averages. This is particularly evident from the situations where additives are present. In these cases, two different kinds of chains result, with those terminated by the same end group being stunted in growth compared to the normal polycaprolactam. Yet it is the total weight of polymer and the total number of ends that are used to evaluate M. This must result in an average molecular weight.

•

In principle, the same concept could be used to determine the molecular weights of materials from any class of polymers, and not just condensation polymers. In practice, the method is less suitable for polymers of the addition type, since these generally have considerably higher molecular weights and less-certain end groups. Modern instrumental techniques, especially spectroscopic techniques, sometimes have sufficient sensitivity to offset the lower concentration of chain ends in addition polymers. The use of radioisotopes in this connection also extends the range of molecular weights which can be determined by this approach. No general principles beyond those already discussed are involved in the more sophisticated methods. As in the cases discussed here, specific consideration must be given to the number of measured chain ends per molecule as well as to the specific analytical chemistry associated with the experimental method employed.

Note that the method of end group analysis is inapplicable to copolymers, since the presence of more than one repeat unit adds extra uncertainty as to the nature of chain ends. The above example included the remark that the molecular weights calculated in the example were average values. In the next section we shall examine this point in greater detail.

1.8 Molecular Weight Averages

The example in the last section argued that polymers of more than one molecular weight must be present when a polymer is prepared in the presence of an additive with two functional groups of the same kind. While this is true, it presents a far too limited explanation for the presence of chains with a distribution of molecular weights in all polymer preparations. We describe this state of affairs by saying that the polymer shows polydispersity with respect to molecular weight or degree of polymerization. Some degree of polydispersity is the normal state for all polymer systems. To see how this comes about, we only need to think of the reactions between monomers that lead to the formation of polymers in the first place. Random encounters between reactive species are responsible for chain growth, so statistical descriptions are appropriate for the resulting product. The situation is reminiscent of the distribution of molecular velocities in a sample of gas. In that case, also, random collisions impart extra energy to some molecules while reducing the energy of others. Only the average energy makes sense in this latter situation and only the average molecular weight makes sense for polymers.

In Chaps. 5 and 6 we shall examine the distribution of molecular weights for condensation and addition polymerizations in some detail. For the present, our only concern is how such a distribution of molecular weights is described. The standard parameters used for this purpose are the mean and standard deviation of the distribution. Although these are well-known quantities, many students are familiar with them only as results provided by a calculator. Since statistical considerations play an important role in several aspects of polymer chemistry, it is appropriate to digress into a brief examination of the statistical way of describing a distribution.

Suppose that a variable of interest, the molecular weight in the present context, displays an assortment of values. Then it is convenient to divide the observed range of molecular weights into 10-20 categories, called classes, and to hypothetically sort the molecules by molecular weight into these different classes. We choose the molecular weight at the center of each class as typifying that class and call that value the class mark. Thus for category 1, the class mark has the value M_1; for category 2, M_2, and so on. After all of the molecules have been sorted into these molecular weight classes, we imagine counting the number that have accumulated in each category. Accordingly, we might find

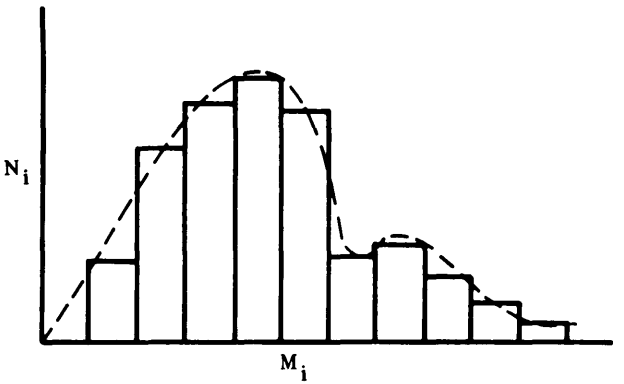

Figure 1.4 Histogram showing the number of molecules N_i having the molecular weight M_i for classes indexed i. The broken line shows how the distribution would be described by a continuous function.

N_1 in class 1, N_2 in class 2, and so forth. In class i there will be N_i molecules of molecular weight M_i. One way of representing the results of this type of inventory procedure is to construct a bar graph called a histogram, like that shown in Fig. 1.4. If we were doing an actual classification instead of a hypothetical one—say, classifying beans instead of molecules—we would lose detail if we used less than about 10 categories, and the effort of classification would be prohibitive if more than about 20 categories were used. As Fig. 1.4 illustrates, however, a number of classes in the range 10–20 does give a reasonable picture of the distribution of M values. Furthermore, as the number of classes increases with each spanning a narrower range, the resulting histogram comes closer and closer to outlining a smooth curve. In the limiting case each class becomes one of the infinitesimally thin slices of calculus. At one extreme, then, the histogram enables us to classify actual data, and at the other it leads to the mathematics of continuous distribution functions. The broken line in Fig. 1.4 shows how a continuous function might look which describes the same system as the histogram approximates. In Chap. 8 we shall see that polymer preparations may be fractionated into molecular weight classes so that a histogram representation of the original distribution is a possibility and not merely a hypothetical exercise.

On the basis of the concepts and notation introduced here, we see that there are several ways of describing a polydisperse system:

1. A continuous distribution function is a mathematical function which gives N as a function of M. This is the most general way of describing the

distribution, since, in principle, all other aspects of the polydispersity can be derived from the continuous distribution function.

2. The histogram is a graphical device which is both attainable in practice and also an approximation to a theoretical distribution function.
3. The mean can be evaluated from the classified data of the histogram; it measures the center of the distribution. The mean (whose symbol is an overbar) is defined as

$$\bar{M}_n = \frac{\Sigma_i N_i M_i}{\Sigma_i N_i} \tag{1.3}$$

This quantity is also called the number (subscript n) average molecular weight.

4. The standard deviation can also be evaluated from the same classified data; it measures the width of the distribution. The standard deviation σ is defined as

$$\sigma = \left(\frac{\Sigma_i N_i (M_i - \bar{M})^2}{\Sigma_i N_i} \right)^{1/2} \tag{1.4}$$

Note that σ^2 has the significance of being the mean value of the square of the deviations of individual M_i values from the mean $\bar{M}$. Accordingly, σ is sometimes called the root mean square (rms) deviation.

In both Eqs. (1.3) and (1.4), the summations are carried out over all classes of data. From a computational point of view, standard deviation may be written in a more convenient form by carrying out the following operations. First both sides of Eq. (1.4) are squared; then the difference $M_i - \bar{M}$ is squared to give

$$\sigma^2 = \frac{\Sigma_i N_i M_i^2}{\Sigma_i N_i} - 2\bar{M} \frac{\Sigma_i N_i M_i}{\Sigma_i N_i} + \bar{M}^2 \tag{1.5}$$

Recalling the definition of the mean, we recognize the first term on the right-hand side of Eq. (1.5) to be the mean value of M^2 and write

$$\sigma^2 = \overline{M^2} - 2\bar{M}^2 + \bar{M}^2 \tag{1.6}$$

It is important to realize that $\overline{M^2} \neq \bar{M}^2$. An alternative to Eq. (1.4) as a definition of standard deviation is, therefore,

$$\sigma = (\overline{M^2} - \bar{M}^2)^{1/2} \tag{1.7}$$

We shall make use of this relationship presently.

Since $\Sigma_i N_i$ represents the total number of molecules N_t in the population we are describing, each of the coefficients in Eqs. (1.3) and (1.4) is the fraction f_i of the total number of molecules in category i:

$$f_i = \frac{N_i}{N_t} \tag{1.8}$$

Introducing this notation means that Eqs. (1.3) and (1.4) may be written as

$$\bar{M} = \Sigma_i f_i M_i \tag{1.9}$$

and

$$\sigma = [\Sigma_i f_i (M_i - \bar{M})^2]^{1/2} \tag{1.10}$$

where the fractions f_i are the weighting factors used in the definition of the average. In the mean and standard deviation, the number fraction is the weighting factor involved.

Finally we define a quantity known as the kth moment of the distribution. In terms of molecular weight,

$$\text{kth moment} = \Sigma_i f_i (M - M_s)^k \tag{1.11}$$

The numerical value of the exponent k determines which moment we are defining, and we speak of these as moments about the value chosen for M_s. Thus the mean is the first moment of the distribution about the origin ($M_s = 0$) and σ^2 is the second moment about the mean ($M_s = \bar{M}$). The statistical definition of moment is analogous to the definition of this quantity in physics. When $M_s = 0$, Eq. (1.11) defines the average value of M^k; this result was already used in writing Eq. (1.6) with k = 2.

Throughout this discussion we have used the numerical fraction of molecules in a class as the weighting factor for that portion of the population. This restriction is not necessary; some other weighting factor could be used equally well. As a matter of fact, one important type of average encountered in polymer chemistry is the case where the mass fraction of the ith component is used as the weighting factor. Defining the mass of material in the ith class as m_i, we write

$$\bar{M}_w = \frac{\Sigma_i m_i M_i}{\Sigma_i m_i} \tag{1.12}$$

This quantity is called the weight average molecular weight, reflecting the chemist's customary carelessness about distinguishing between mass and weight, and is given the symbol $\bar{M}_w$. By contrast, the mean, where number fractions are used, is called the number average molecular weight and is given the symbol $\bar{M}_n$.

The mass of material in a particular molecular weight class is given by the product of the class mark molecular weight and the number of molecules in the class:

$$m_i = N_i M_i \tag{1.13}$$

Substituting this result into Eq. (1.12) gives

$$\bar{M}_w = \frac{\Sigma_i N_i M_i^2}{\Sigma_i N_i M_i} = \frac{\Sigma_i f_i M_i^2}{\Sigma_i f_i M_i} \tag{1.14}$$

which shows that the weight average molecular weight may also be regarded as the ratio of the second moment of the distribution to the first moment, where each of these moments are taken with respect to the origin of the distribution.

The weight average molecular weight of a distribution will always be greater than the number average. This is true because the latter merely counts the contribution of molecules in each class, whereas the former weights their contribution in terms of mass. Thus those molecules with higher molecular weights contribute relatively more to the average when mass fraction rather than number fraction is used as the weighting factor. For all polydisperse systems

$$\frac{\bar{M}_w}{\bar{M}_n} > 1 \tag{1.15}$$

and the amount by which this ratio deviates from unity is a measure of the polydispersity of a sample. In the event that all of the molecules in a sample have the same molecular weight, the summations in Eqs. (1.3) and (1.4) would each consist of a single term and their ratio would equal unity. Such a sample is said to be monodisperse.

In connection with Eq. (1.4), we noted that the standard deviation measures the spread of a distribution; now we see that the ratio $\bar{M}_w/\bar{M}_n$ also measures this polydispersity. The relationship between these two different measures of polydispersity is easily shown. Equation (1.14) may be written as

$$\Sigma_i f_i M_i^2 = \bar{M}_w \Sigma_i f_i M_i = \bar{M}_w \bar{M}_n \tag{1.16}$$

The left-hand side of this expression equals $\overline{M^2}$, so Eq. (1.16) may also be written as

$$\overline{M^2} = \bar{M}_w \bar{M}_n \tag{1.17}$$

Substituting this result into Eq. (1.7) gives

$$\sigma = (\bar{M}_w \bar{M}_n - \bar{M}^2)^{1/2} = \bar{M}_n \left(\frac{\bar{M}_w}{\bar{M}_n} - 1 \right)^{1/2} \tag{1.18}$$

This result shows that the square root of the amount by which the ratio $\bar{M}_w/\bar{M}_n$ exceeds unity equals the standard deviation of the distribution relative to the number average molecular weight. Thus if a distribution is characterized by $\bar{M}_n = 10{,}000$ and $\sigma = 3000$, then $\bar{M}_w/\bar{M}_n = 1.09$. Alternatively, if $\bar{M}_w/\bar{M}_n = 1.50$, then the standard deviation is 71% of the value of $\bar{M}_n$. This shows that reporting the mean and standard deviation of a distribution or the values of M_n and $\bar{M}_w/\bar{M}_n$ gives equivalent information about the distribution. We shall see in a moment that the second alternative is more easily accomplished for samples of polymers. First, however, consider the following example in which we apply some of the equations of this section to some numerical data.

Example 1.5

The first and second columns of Table 1.4 give the number of moles of polymer in six different molecular weight fractions. Calculate $\bar{M}_n$ and $\bar{M}_w$ for this polymer and evaluate σ using both Eqs. (1.7) and (1.18).

Solution

Evaluate the product $n_i M_i$ for each class; this is required for the calculation of both $\bar{M}_n$ and $\bar{M}_w$. Values of this quantity are listed in the third column of Table 1.4. From $\Sigma_i n_i M_i$ and $\Sigma_i n_i$, $\bar{M}_n = 734/0.049 = 15{,}000$. The matter of significant figures will not be strictly adhered to in this example.

The products $m_i M_i$ are mass-weighted contributions and are listed in the fourth column of Table 1.4. From $\Sigma_i m_i$ and $\Sigma_i m_i M_i$, $\bar{M}_w = 113 \times 10^5/734 = 15{,}400$.

The ratio $\bar{M}_w/\bar{M}_n$ is found to be $15{,}400/15{,}000 = 1.026$ for these data. Using Eq. (1.18), we have $\sigma/\bar{M}_n = (1.026 - 1)^{1/2} = 0.162$ or $\sigma = 0.162(15{,}000) = 2430$.

To evaluate σ via Eq. (1.7), differences between M_i and $\bar{M}$ must be considered. The fifth and sixth columns in Table 1.4 list $(M_i - \bar{M}_n)^2$ and $N_i(M_i - \bar{M}_n)^2$ for each class of data. From $\Sigma_i N_i$ and $\Sigma_i N_i (M_i - \bar{M}_n)^2$, $\sigma^2 = 28.1 \times 10^4/0.049 = 5.73 \times 10^6$, and $\sigma = 2390$.

The discrepancy between the two values of σ is not meaningful in terms of significant figures. The standard deviation is 2400.

We shall see that, as polymers go, this is a relatively narrow molecular weight distribution.

•

Table 1.4 Some Classified Molecular Weight Data for a Hypothetical Polymer Used in Example 1.5

N_i (mol)	M_i (g mol^{-1})	m_i (g)	$m_i M_i \times 10^{-5}$ ($g^2 mol^{-1}$)	$(M_i - \bar{M})^2 \times 10^{-6}$ (g^2 mol^{-2})	$N_i (M_i - \bar{M})^2 \times 10^{-4}$ (g^2 mol^{-1})
0.003	10,000	30	3.0	25	7.50
0.008	12,000	96	11.5	9	7.20
0.011	14,000	154	21.6	1	1.10
0.017	16,000	272	43.5	1	1.70
0.009	18,000	162	29.2	9	8.10
0.001	20,000	20	4.0	25	2.50
$\Sigma = 0.049$		$\Sigma = 734$	$\Sigma = 113$	$\Sigma = 70$	$\Sigma = 28.10$

The preceding discussion and example are based on the premise that classified molecular weight data are available. While this is sometimes the case, the average molecular weight of a polydisperse system is usually the information available to characterize the sample. The significant thing about this, however, is the fact that different experimental techniques yield different averages. We shall see in Chap. 8, for example, that osmostic pressure experiments can be interpreted to give the number average molecular weight; in Chap. 10 we shall see that light scattering produces a weight average. Hence these different experimental methods applied to the same sample will provide $\bar{M}_n$ and $\bar{M}_w$, thus yielding some statistical information about the molecular weight distribution.

It is important to realize that this difference in averaging is an intrinsic part of the way different experimental methods "see" a polydisperse system. Accordingly, osmometry effectively counts while light scattering effectively weighs particles of different molecular weight. The overall value of the measured property is the average effect produced by the polydisperse system, with the weighting factors which are appropriate to the specific method. When the measured properties are interpreted in terms of the average polymer responsible for the effect, the difference in averaging procedure shows up in the result. A light-scattering experiment and an osmotic pressure experiment conducted on the same sample will produce two different molecular weights, with light scattering producing the higher value. If we were not aware of this situation, we might very well blame the difference on experimental error instead of recognizing that it is the natural consequence of polydispersity.

Table 1.5 lists the different molecular weight averages most commonly encountered in polymer chemistry. Table 1.5 also includes the definition of these averages for easy reference, some experimental methods that produce them, and cross-references to sections of this volume where the specific techniques are discussed. Note that end group analysis produces a number average molecular weight, since it is a technique based on counting. This is especially evident when we compare end group analysis with the procedure for evaluating $\bar{M}_n$ in Example 1.5. In the latter, $\bar{M}_n$ is given by dividing the total mass of the sample by the total number of moles of polymer it contains. This is exactly what is done in end group analysis.

Table 1.5 also includes two additional types of molecular weight average besides those already discussed. The following remarks describe some features of these two, the z-average molecular weight, and the viscosity average:

1. The z-average molecular weight is defined by the equation

$$\bar{M}_z = \frac{\Sigma_i N_i M_i^3}{\Sigma_i N_i M_i^2} \tag{1.19}$$

Table 1.5 Summary of the Molecular Weight Averages Most Widely Encountered in Polymer Chemistry

Average	Definition	Methods	Section
$\bar{M}_n$	$\frac{\Sigma_i N_i M_i}{\Sigma_i N_i}$	Osmotic pressure and other colligative properties	8.8
		End group analysis	1.7
$\bar{M}_w$	$\frac{\Sigma_i N_i M_i^2}{\Sigma_i N_i M_i}$	Light scattering	10.7
		Sedimentation velocity	9.10
M_z	$\frac{\Sigma_i N_i M_i^3}{\Sigma_i N_i M_i^2}$	Sedimentation equilibrium	9.10
$\bar{M}_v$	$\left(\frac{\Sigma_i N_i M_i^{1+a}}{\Sigma_i N_i M_i}\right)^{1/a}$	Intrinsic viscosity	9.5

From this definition, we see it is the ratio of the third moment of the distribution about the molecular weight origin to the second moment about the origin.

2. The weighting factors used in the determination of the z-average molecular weight are $N_i M_i^2$, which means that higher molecular weight molecules are weighted even more heavily in this average than is the case in the weight average. For the same distribution, the order of the averages is $\bar{M}_z > \bar{M}_w > \bar{M}_n$.
3. The viscosity average is defined by the equation

$$\bar{M}_v = \left(\frac{\Sigma_i N_i M_i^{a+1}}{\Sigma_i N_i M_i}\right)^{1/a} \tag{1.20}$$

where the exponent a is characteristic of the system under investigation and generally lies in the range $0.5 < a < 1.0$. Note that $\bar{M}_v = \bar{M}_w$ when $a = 1$.

4. The viscosity average molecular weight is not an absolute value, but a relative molecular weight based on prior calibration with known molecular weights for the same polymer-solvent-temperature conditions. The parameter a depends on all three of these; it is called the Mark-Houwink exponent, and tables of experimental values are available for different systems.
5. For the viscosity average molecular weight, $\bar{M}_v^a$ may be considered the ratio of the (a + 1)th moment to the first moment of the distribution. Alternatively, $\bar{M}_v^a$ may be viewed as the weight average value of M^a in view of Eq. (1.13).

Note that a statistical study could be done on an electron micrograph like that shown in Fig. 1.1. The dimensions of the blobs could be converted to volumes and then to masses with a knowledge of the density of the deposited polymer. This approach could be organized into a table of classified data from which any of these averages could be calculated.

1.9 The Binomial Distribution and the Random Walk

In this section, we shall examine another application of statistics to polymer chemistry. This time we shall consider the average spatial dimensions of an isolated polymer molecule, especially with regard to its dependence on molecular weight. In this context, we disregard the fact that polymer samples show polydispersity: The distribution of dimensions we are concerned with would be present even if all polymer chains were identical in length. This is because successive chain units are able to rotate along the bonds of the backbone to acquire a jumbled conformation. No two molecules have identical shapes or dimensions, even if the sample is monodisperse. Likewise, the conformation of any particular molecule continuously changes with time owing to thermal fluctuations. Only a statistical description is adequate to characterize this situation.

As a consequence of these various possible conformations, the polymer chains exist as coils with spherical symmetry. Our eventual goal is to describe these three-dimensional structures, although some preliminary considerations must be taken up first. Accordingly, we begin by discussing a statistical exercise called a one-dimensional random walk.

We start this exercise by considering the placement of n successive repeat units in a polymer chain along a straight line, say, the x axis. We assume that the chain is perfectly flexible and that it excludes a negligible volume so that more than one repeat unit can be placed on the same site. We anchor one end of the chain at the origin of the axis and propose to use the toss of a coin to decide on the placement of successive units; that is, if the coin turns up heads (subscript H), we place the next unit one step ahead—an increment of +l in the x direction, where l is the length of the repeat unit. If the coin shows tails (subscript T), the next unit is placed back a step for a change in x value of -l. How far from the origin will the other end of the chain lie after n units are placed on the basis of this random walk? A possible sequence for 10 tosses might be HTTHHTHHTH in a particular exercise; this amounts to 6 steps forward and 4 backward for a net displacement of +2. In this example, the two ends of the chain are separated by only 2 l, even though the fully extended chain would have a length of 10 l. Since the outcome of 10 tosses could be different in another trial of the same exercise, it is clear that we must turn to statistics to describe the average placement of the chain.

For a one-dimensional random walk, the probability of n_H heads after n moves is supplied by application of the bionomial distribution formula:

$$P(n_H, n) = \frac{n!}{n_H!\, n_T!}\; {p_H}^{n_H} {p_T}^{n_T} \tag{1.21}$$

in which the p's are the probabilities of either a head or tail in a single toss and the subscripted n's are the number of heads and tails in the specific exercise. For a fair coin $p_H = p_T = \frac{1}{2}$, but for the time being we shall continue using the more general formula.

The binomial distribution function is one of the most fundamental equations in statistics and finds several applications in this volume. To be sure that we appreciate its significance, we make the following observations about the plausibility of Eq. (1.21):

1. To evaluate the probability that one event *and* another will occur, we multiply the probabilities of the individual events. Thus the probability of tossing two heads is ${p_H}^2$ and that of tossing n_H heads is ${p_H}^{n_H}$.
2. Likewise, the probability of tossing n_T tails is ${p_T}^{n_T}$. The probability of tossing n_H heads and n_T tails is ${p_H}^{n_H}{p_T}^{n_T}$ by the same principle.
3. The probability calculated so far is too low because it describes one specific sequence of heads and tails. From the point of view of net displacement, the sequence does not matter. Hence the above results must be multiplied by the number of different ways this outcome can arise. Instead of tossing one coin n times, we could toss n coins drawn at random from a piggy bank. For the first, we have a choice of n to draw from; for the second, n - 1; for the third, n - 2, and so on. The total possible ways the toss could be carried out is given by the product of these different choices, that is by n!
4. This suggests that $n!{p_H}^{n_H}{p_T}^{n_T}$ gives the desired probability, but now we have gone too far in the opposite direction and overcounted the probability. To appreciate this fact, we recognize that among the n! ways the coins could be tossed, we have included a number of ways that yield the same net outcome achieved through different sequences of tosses. For example, the n! count would include HHHTTT, HTHTHT, and HTTHHT as different, although they each consist of the same number of heads and tails.
5. To correct for this overcounting, we cancel out the number of ways n_H heads can be permuted and the number of ways n_T tails can be permuted. Using the same logic as in item (3), these redundant possibilities are given by $n_H!$ and $n_T!$, respectively. Dividing the result in item (4) by these factorials gives Eq. (1.21).

If we apply Eq. (1.21) to the problem of determining the number of heads occurring in 10 tosses, we find that the probability of, say, 6 heads is given by $(10!/6!4!)\ ½^{10} = 0.205$. That is, heads would occur in 6 of every 10 tosses about 20% of the time. If a large number of 10-mer molecules were being positioned along an axis according to this hypothetical procedure, in about 20% of the cases the end-to-end distance would be 2 l. For an outcome of 8 heads and 2 tails, corresponding to a net forward displacement of 6 steps or an end-to-end distance of 6 l, the probability is $(10!/8!2!)\ ½^{10} = 9.77 \times 10^{-4} \cong 0.1\%$.

It is an easy matter to rewrite Eq. (1.21) in terms of the probability of a displacement x occurring after n tosses. We recognize the following:

1. Each toss is either a head or a tail:

$$n = n_H + n_T \tag{1.22}$$

2. The displacement x after n steps of length l is

$$x = (n_H - n_T)l \tag{1.23}$$

3. Solving Eqs. (1.22) and (1.23) for n_H and n_T gives

$$n_H = ½(n + x/l) \tag{1.24}$$

and

$$n_T = ½(n - x/l) \tag{1.25}$$

4. For a fair coin $p_H = p_T = ½$; there Eq. (1.21) becomes

$$P(n_H, n) = \frac{n!}{[(n + x/l)/2]!\,[(n - x/l)/2]!}\ ½^n \tag{1.26}$$

This result enables us to calculate the probability of any specified outcome for the one-dimensional random walk. We shall continue to develop this one-dimensional relationship somewhat further, since doing so will produce some useful results.

5. For high molecular weight polymers, n is large and the logarithm of large factorials is accurately given by Sterling's approximation,

$$\ln y! \cong y \ln y - y \tag{1.27}$$

for large y.

6. Taking logarithms of both sides in Eq. (1.26) and applying Sterling's approximation gives

$$-\ln P(x, n) = \frac{nl + x}{2l} \ln\left(1 + \frac{x}{nl}\right) + \frac{nl - x}{2l} \ln\left(1 - \frac{x}{nl}\right) \tag{1.28}$$

7. The number of steps is always much larger than the displacement x, since there is a good deal of back-and-forth cancellation. Hence the ratio x/nl is less than unity and the logarithms may be approximated by the leading terms of a series expansion

$$\ln\left(1 + \frac{x}{nl}\right) \cong \frac{x}{nl} - \frac{1}{2}\left(\frac{x}{nl}\right)^2 + \cdots \tag{1.29}$$

in which x can be either positive or negative.

8. Applying Eq. (1.29) to Eq. (1.28) gives

$$\ln P(x, n) \cong -\frac{x^2}{2nl^2} + \cdots \tag{1.30}$$

or

$$P(x, n) = k \exp\left(\frac{-x^2}{2nl^2}\right) \tag{1.31}$$

where the factor k is a constant called a normalization factor.

9. Well-behaved probability functions total unity when they are summed over all possible outcomes. Since Eq. (1.31) is a continuous function—this has been accomplished by getting rid of the factorials—this sum may be written as an integral over all possible values of x:

$$k \int_{-\infty}^{\infty} \exp\left(\frac{-x^2}{2nl^2}\right) dx = 1 \tag{1.32}$$

A probability function which satisfies this criterion is said to be normalized. This will be accomplished when a value of k which satisfies Eq. (1.32) is found.

10. The integral in Eq. (1.32) is known as a gamma function and may be found in tables of integrals. The result of the integration is that

$$k = (2\pi nl^2)^{-1/2} \tag{1.33}$$

Therefore an expression which is equivalent to Eq. (1.21) for the case of large n's is

$$P(x, n) = (2\pi n l^2)^{-1/2} \exp\left(\frac{-x^2}{2nl^2}\right) \tag{1.34}$$

Since we have ended up with a continuous distribution function, it is more appropriate to multiply both sides of Eq. (1.34) by dx and to say that the equation gives the probability of x values between x and x + dx for n steps of length l.

In the next section we shall adapt this probability function to the description of a three-dimensional coil. We conclude this section by noting that Eq. (1.21) may be approximated by two other functions which are used elsewhere in this book. For these general relationships we define ν to be the number of successes—that is, some specified outcome such as tossing a head—out of n tries and define p as the probability of success in a single try. In this amended notation, Eq. (1.21) becomes

$$P(\nu, n) = \frac{n!}{\nu!(n - \nu)!} \, p^{\nu} (1 - p)^{n-\nu} \tag{1.35}$$

In terms of this notation we have the following:

1. The average number of successes is given by

$$\bar{\nu} = np \tag{1.36}$$

and the standard deviation of the distribution of successes is

$$\sigma = [np(1 - p)]^{1/2} \tag{1.37}$$

2. If n is large and p is very small, Eq. (1.35) is approximated by the Poisson distribution

$$P_{Pois} = \frac{e^{-\bar{\nu}} \bar{\nu}^{\nu}}{\nu!} \tag{1.38}$$

3. As an example of the Poisson distribution, consider the case of n = 1000, p = 0.01, and ν = 5. According to the binomial distribution, $P_{bin} = (1000!/995!5!)(0.01)^5(0.99)^{995} = 0.0375$. By Eq. (1.36), $\bar{\nu} = (0.01)(1000) = 10$ and $P_{Pois} = e^{-10} \, 10^5/5! = 0.0378$.

4. If n is large, but without any particular restriction on p, Eq. (1.35) is approximated by the Gaussian or normal distribution

$$P_{norm} = \frac{1}{(2\pi)^{1/2}\sigma} \exp\left[-\frac{1}{2}\left(\frac{\nu - \bar{\nu}}{\sigma}\right)^2\right] \tag{1.39}$$

5. As an example of the normal distribution, consider the case of n = 60, p = 0.20, and ν = 10. According to the binomial distribution, P_{bin} = (60!/ 50!10!)$(0.2)^{10}(0.8)^{50}$ = 0.110. By Eq. (1.36), $\bar{\nu}$ = (0.2)(60) = 12, and by (1.37), $\sigma = [(60)(0.2)(0.8)]^{1/2} = 3.10$, therefore

$$P_{norm} = \frac{1}{3.10(2\pi)^{1/2}} \exp\left[-\frac{1}{2}\left(\frac{10 - 12}{3.10}\right)^2\right] = 0.105$$

6. The proof that these expressions are equivalent to Eq. (1.35) under suitable conditions is found in statistics textbooks. We shall have occasion to use the Poisson approximation to the binomial in discussing crystallization of polymers in Chap. 4, and the distribution of molecular weights of certain polymers in Chap. 6. The normal distribution is the familiar bell-shaped distribution that is known in academic circles as "the curve." We shall use it in discussing diffusion in Chap. 9.

1.10 Size Parameters for Random Coils

Next let us apply random walk statistics to three-dimensional chains. We begin by assuming isolated polymer molecules which consist of perfectly flexible chains.

To isolate polymer chains from one another, we consider a solution which is sufficiently dilute that the domains of the individual polymer molecules are well separated from each other. For the present, we assume the solvent has no influence on the polymer but merely supports the molecule. In fact, this is not generally the case, although it can be achieved by proper choice of solvent or temperature.

The chain is imagined to consist of n units connected to one another by perfectly flexible joints. Figure 1.5a shows the ith and (i + 1)th unit along the backbone of a vinyl polymer according to this model. The three carbon atoms involved in these bonds are numbered for ease of discussing the model. We focus attention at carbon 2, which we picture as lying at the center of a sphere. By hypothesis, the chain is perfectly flexible at C_2 so that the angle θ between the two bonds can have any value between 0° and 360°. Likewise, regardless of the value of θ, there is complete freedom of rotation around bond i connecting C_1 and C_2; that is, the angle ϕ may take on all values between 0° and 360°.

This kind of perfect flexibility means that C_3 may lie anywhere on the surface of the sphere. According to the model, it is not even excluded from C_1. This model of a perfectly flexible chain is not a realistic representation of an actual polymer molecule. The latter is subject to fixed bond angles and experiences some degree of hindrance to rotation around bonds. We shall consider the effect of these constraints, as well as the effect of solvent-polymer interactions, after we explore the properties of the perfectly flexible chain. Even in this revised model, we shall not correct for the volume excluded by the polymer chain itself.

If a chain consists of m bonds of this sort, then there are m + 1 atoms which can act as centers like C_2 in Fig. 1.5. The values of the angles at each successive center are assumed to be independent, so the chain can twist and bend in an enormous number of conformations along its length. This is how the random coil comes about. Figure 1.5b shows a somewhat longer segment of chain. Each carbon atom has the possibility of being anywhere on the surface of the sphere centered at the preceding carbon according to this model.

The one-dimensional random walk of the last section is readily adapted to this problem once we recognize the following connection. As before, we imagine that one end of the chain is anchored at the origin of a three-dimensional coordinate system. Our interest is in knowing, on the average, what will be the distance of the other end of the chain from this origin. A moment's reflection will convince us that the x, y, and z directions are all equally probable as far as the perfectly flexible chain is concerned. Therefore one-third of the repeat units will be associated with each of the three perpendicular directions

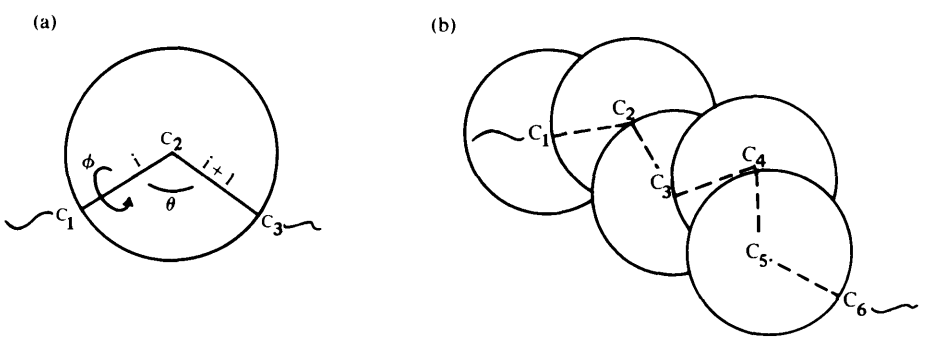

Figure 1.5 Placement of successive polymer segments connected by perfectly flexible joints. In (a), the ith and (i + 1)th bond can be moved through angles ϕ and θ so that carbon 3 can lie anywhere on the surface of a sphere. In (b), the pattern is illustrated for a longer portion of chain.

of the coordinate system. The probability of a displacement x in that direction is given by Eq. (1.34), with n replaced by n/3. Since the x, y, and z directions are equivalent, the same expression holds for P(y, n/3) and P(z, n/3). Thus the probability that the loose end of the chain will be found in a volume element dx dy dz located at a specific set of x, y, z values is the probability that is has *all* of the following:

1. A value of x between x and x + dx.
2. A value of y between y and y + dy.
3. A value of z between z and z + dz.

According to the rules for compounding probabilities, this is given by

$$P(x, y, z, n)\,dx\,dy\,dz = P(x, n/3)\,P(y, n/3)\,P(z, n/3)\,dx\,dy\,dz \tag{1.40}$$

Substituting Eq. (1.34) with n replaced by n/3 for each of the probabilities in (1.40) gives

$$P(x, y, z, n)\,dx\,dy\,dz = \left(2\pi \frac{n}{3} l^2\right)^{-3/2} \exp\left(-\frac{3(x^2 + y^2 + z^2)}{2nl^2}\right) dx\,dy\,dz \tag{1.41}$$

The x, y, and z coordinates of the loose end of the chain can be related to the radial distance r from the origin by

$$x^2 + y^2 + z^2 = r^2 \tag{1.42}$$

In addition, the volume element of interest is not the box dx dy dz shown in Fig. 1.6a but, rather, a spherical shell of radius r and thickness dr as shown in Fig. 1.6b. The result of expressing the volume element in spherical coordinates and integrating over all angles is the replacement

$$dx\,dy\,dz \longrightarrow 4\pi r^2\,dr \tag{1.43}$$

Making these substitutions gives the probability of finding one end of a perfectly flexible chain of n units a distance r from the other end by

$$P(r, n)\,dr = \left(2\pi \frac{n}{3} l^2\right)^{-3/2} 4\pi r^2 \exp\left(\frac{-3r^2}{2nl^2}\right) dr \tag{1.44}$$

Several features of this expression should be noted:

1. The probability is normalized, since Eq. (1.44) was assembled from separately normalized components.

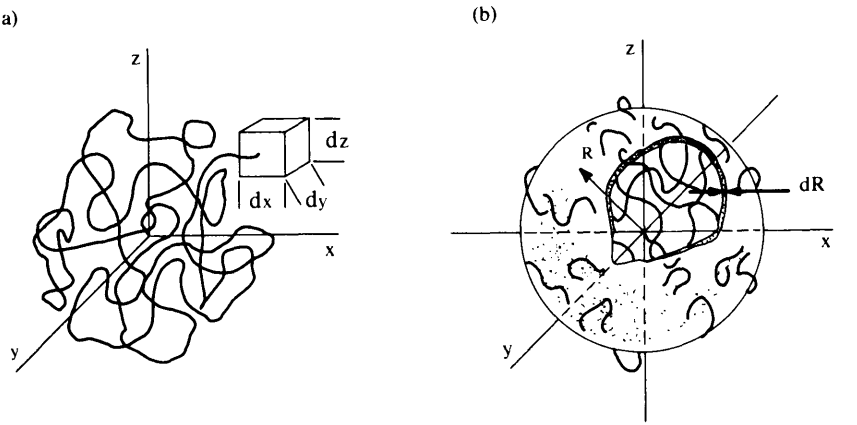

Figure 1.6 A flexible coil attached at the origin at one end and (a) in a volume element dx dy dz at the other end and (b) in a spherical shell of volume $4\pi r^2$ dr. (Reprinted from Ref. 4, p. 116.)

2. The factor containing r^2 increases with increasing r and reflects the fact that there are more locations to place the loose chain end within larger spherical shells, but . . . .
3. The exponential factor decreases with increasing r and reflects the fact that large displacements become decreasingly probable.
4. The overall probability function for the end-to-end distance is the product of these two considerations. Starting at r = 0, the probability increases owing to the r^2 term, passes through a maximum, then decreases as the exponential factor takes over at large r values.
5. This factor is reminiscent of the radial distribution function for electron probability in an atom and the Maxwell distribution of molecular velocities in a gas, both of which pass through a maximum for similar reasons.

With this probability expression, it is an easy matter to calculate the average dimensions of a coil. Because of the back-and-forth character of the x, y, and z components of the random walk, the average end-to-end distance is less meaningful than the average of r^2. The latter squares positive and negative components before averaging and gives a more realistic parameter to characterize the coil. To calculate $\overline{r^2}$, we remember Eq. (1.11) and write

$$\overline{r^2} = \sum_i f_i r_i^2 \tag{1.45}$$

Now we recognize that the weighting factor f_i is precisely what the probability function gives, so we write Eq. (1.45) as

$$\overline{r^2} = \int_0^\infty P(r, n) r^2 \, dr \tag{1.46}$$

where the sum has been replaced by an integral, since we are using a continuous probability function. Substituting Eq. (1.44) for $P(n, r)$ gives

$$\overline{r^2} = 4\pi \left(2\pi \frac{n}{3} l^2\right)^{-3/2} \int_0^\infty r^4 \exp\left(\frac{-3r^2}{2nl^2}\right) dr \tag{1.47}$$

This is also a gamma function and may be solved with the help of a table of integrals. Evaluation of the integral gives the simple result

$$\overline{r^2} = nl^2 \tag{1.48}$$

which is the relationship we have sought.

The coil dimensions are characterized by the root-mean-square (rms) end-to-end distance which Eq. (1.48) shows to increase with the square root of the degree of polymerization. According to Eq. (1.1), the latter is directly proportional to M. Hence two chains of the same polymer compared under the same conditions would have to differ by a factor of 4 in M to show a factor of 2 difference in r_{rms}. We shall return to an examination of the length of the repeat unit l in the next section. Before doing that, however, there is another parameter of considerable importance which is used to characterize polymer coil dimensions, namely, the radius of gyration. It turns out that the radius of gyration r_g is the way chain dimensions enter the theories of viscosity and light scattering, as we shall see in Chaps. 9 and 10, respectively.

For a body that consists of n masses m_i, each separated by a distance r_i from the axis of rotation of the array, the radius of gyration is defined

$$r_g = \left(\frac{\Sigma_i m_i r_i^2}{\Sigma_i m_i}\right)^{1/2} \tag{1.49}$$

We may therefore think of r_g^2 as the weight average value of r^2, by analogy with Eq. (1.12). As a reminder of how the radius of gyration comes to be defined this way, recall that the moment of inertia I of this same body is given by

$$I = \sum_i m_i r_i^2 \tag{1.50}$$

There exists some radial distance from the axis of rotation at which all of the mass could be concentrated to produce the same moment of inertia that the actual distribution of mass possesses. This distance is defined to be the radius of gyration. According to this definition,

$$I = r_g^2 \sum_i m_i = \sum_i m_i r_i^2 \tag{1.51}$$

which leads directly to Eq. (1.49). The relationship between the radius of gyration and the actual dimensions of a body depends on the geometry of that body. Examples of these relationships are derived in many elementary physics textbooks for bodies of simple geometry; Table 10.1 lists several of these results that are pertinent to polymer chemistry. Let us briefly examine what the relationship is for a randomly coiled polymer molecule.

We desire to use the probability function derived above, so we recognize that the mass contribution of the volume element located a distance r from an axis through the center of mass is the product of the mass of a chain unit m_0 times the probability of a chain unit at that location as given by Eq. (1.44). For this purpose, however, it is not the distance from the chain end that matters but, rather, the distance from the center of mass. Therefore we temporarily identify the jth repeat unit as the center of mass and use the index k to count outward toward the chain ends from j. On this basis, Eq. (1.49) may be written as

$$(r_g^2)_j = \frac{\sum_{k=1}^{j} m_0 P(k,r) r^2 + \sum_{k=1}^{n-j} m_0 P(k,r) r^2}{\sum_{i=1}^{n} m_0} \tag{1.52}$$

where the terms in the numerator correspond to the two portions of chain on either side of j, and the denominator equals nm_0. We may cancel the mass of the individual chain units to give

$$(r_g^2)_j = \frac{1}{n}\left(\sum_{k=1}^{j} P(k,r) + \sum_{k=1}^{n-j} P(k,r)\right) r^2 \tag{1.53}$$

Next we recognize that any one of the repeat units can lie at the center of mass of the coil. To incorporate this last consideration, we sum Eq. (1.53) for all values of j and then divided by $\Sigma_j = n$:

$$\overline{r_g^2} = \sum_{j=1}^{n} (r_g^2)_j = \frac{1}{2n^2} \sum_{j=1}^{n} \left(\sum_{k=1}^{j} P(k,r) + \sum_{k=1}^{n-j} P(k,r)\right) r^2 \tag{1.54}$$

This last result includes the factor ½, since all segments are counted twice by the combination of Eqs. (1.53) and (1.54). The double summation also makes the two terms in the brackets equal to two times either one of them. This procedure *averages* over all segments fulfilling the role of center of mass; therefore it is appropriate to identify the quantity evaluated by Eq. (1.59) by the symbol $\overline{r_g^2}$.

Next we may substitute Eq. (1.44) for P(k, r) in Eq. (1.54):

$$\overline{r_g^2} = \frac{1}{n^2} \sum_{j=1}^{n} \sum_{k=1}^{j} \int_0^{\infty} 4\pi r^4 (2\pi kl)^{-3/2} \exp\left(\frac{-3r^2}{2kl^2}\right) dr \tag{1.55}$$

This integral is the same as Eq. (1.47) and its value is given by (1.48). Substituting the latter, with k replacing n, yields

$$\overline{r_g^2} = \frac{1}{n^2} \sum_{j=1}^{n} \sum_{k=1}^{j} kl^2 \tag{1.56}$$

For polymers in which the degree of polymerization is large—a condition already assumed by the use of Eq. (1.48)—the remaining summations may be replaced by integrals

$$\overline{r_g^2} = \int_0^n \left(\int_0^j \frac{l^2}{n^2} \, k \, dk \right) dj = \int_0^n \frac{l^2}{n^2} \, \frac{j^2}{2} \, dj \tag{1.57}$$

or

$$\overline{r_g^2} = \frac{1}{6} nl^2 \tag{1.58}$$

Comparing this last result with Eq. (1.48) shows that

$$\overline{r_g^2} = \frac{1}{6} \overline{r^2} \tag{1.59}$$

As should be expected, both $(\overline{r_g^2})^{1/2}$ and r_{rms} show the same dependence on the degree of polymerization or molecular weight. Since the radius of gyration can be determined experimentally through the measurement of viscosity or light scattering, it is through this quantity that we shall approach the evaluation of l.

1.11 Application to Polymer Chains

In this section we compare actual polymer chains with the perfectly flexible model discussed in the last section. There are four respects in which an actual molecule differs from the idealized model:

1. The angle formed between successive bonds along the chain backbone—θ in Fig. 1.5a—is not free to assume all values, but is fixed at a definite angle depending on the nature of the bond. For the tetrahedral angle associated with carbon-carbon single bonds, $\theta = 109.5°$.
2. The rotation of one carbon-carbon bond around another—say, the $(i + 1)$th around the ith in Fig. 1.5a—is subject to steric hindrance, so that not all values of ϕ are equally probable.
3. Actual polymer repeat units occupy finite volumes and therefore exclude other segments from occupying the same space.
4. To obtain isolated polymer chains, a solvent must be present. The solvent might be selectively excluded or imbibed by the coil, depending on the free energy of interaction, and thereby perturb the coil dimensions.

At first glance it seems problematic whether anything is salvageable from the random walk model with so many areas of difference.

The strategy for rescuing the model based on a highly idealized picture of the chain depends on the following insight. Fixed bond angles and steric hindrance may limit the flexibility of the chain at any specific bond, but these restrictions can be overcome if we consider a somewhat longer segment of the polymer chain; that is, Fig. 1.5a with a full range of values for θ and ϕ is a highly unrealistic model for the backbone of a polymer molecule, even though it is an attractive basis for a theoretical derivation. On the other hand, the six-carbon segment shown in Fig. 1.5b—even if restricted in the allowed possibilities for θ and ϕ—does possess very nearly perfect flexibility. If five restricted bonds are still insufficiently flexible, we may subdivide the actual polymer chain into still longer subsections until they are long enough to qualify as "perfectly flexible." If the subsections so defined have a degree of polymerization ν and an effective length l^*, then the actual polymer chain contains $n/\nu = n^*$ such units. All of the relationships of the last section may now be applied to this chain—which *is* perfectly flexible—consisting of n^* segments of length l^*. Of course, n^* is still directly proportional to n, so we continue to expect the average coil dimensions to increase as $M^{1/2}$; the effective length of an individual step can be regarded as a proportionality constant. Since the radius of gyration can be measured under certain circumstances, the effective step length can be evaluated experimentally through the proportionality between $\overline{r_g^2}$ and n.

With the results of the preceding section thus salvaged, let us look in more detail at the specific areas of discrepancy between the perfectly flexible model

and an actual molecule. At least those deviations which arise from the actual restrictions on θ and ϕ can be dealt with quantitatively.

We begin by considering the fact that θ in Fig. 1.5a is limited to the value 109.5° for the carbon-carbon bonds along the backbone of a vinyl polymer chain. This means that carbon 3 in Fig. 1.5 may not, in fact, lie anywhere on the surface of a sphere, but is limited to positions on the rim of a cone, as shown in Fig. 1.7a. As before, the cone is generated by rotating the (i + 1)th bond between C_2, and C_3 around the ith bond. We shall return to the question of hindrance to this rotation presently. Figure 1.7b shows a longer segment of chain with this restricted bond angle and shows that a high degree of flexibility is still attainable over a somewhat longer portion of chain.

The approach to dealing with this quantitatively is to consider adding together the projections of individual bonds onto the direction of the first and averaging. If the length of the individual bonds is l, then the projection of the second bond onto the direction of the first is $l \cos \theta$, and the projection of the ith onto the direction of the first is $l(\cos \theta)^i$. For large values of n, the average value of r^2 obtained by adding and averaging these projections is

$$\overline{r^2} = nl^2 \frac{1 - \cos \theta}{1 + \cos \theta} = nb^2 \tag{1.60}$$

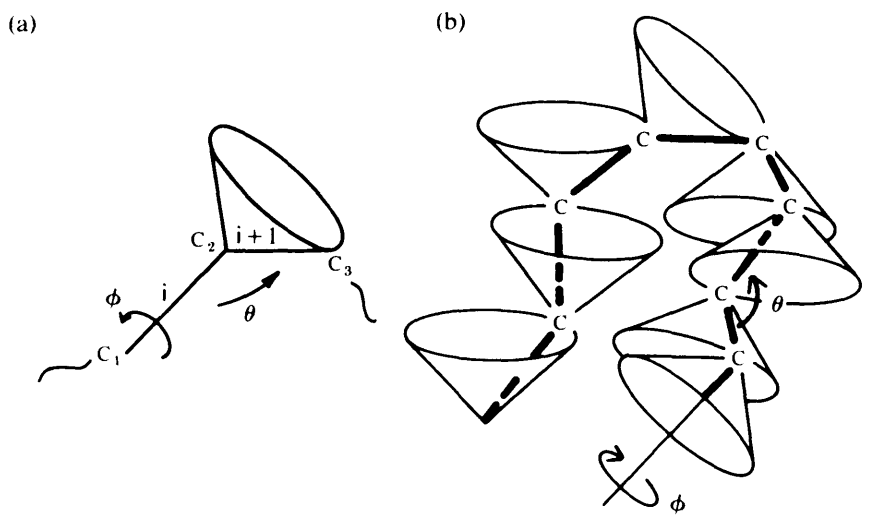

Figure 1.7 Placement of successive polymer segments connected at fixed bond angles. (a) Carbon 3 can lie anywhere on the rim of the cone. (b) This effect is illustrated for a longer portion of chain. [Panel (a) reprinted from Ref. 4, p. 118.]

where b corrects the step length for the effect of fixed bond angles. In the case of tetrahedral bond angles, $\cos 109.5° = -0.333$ so $(1 - \cos\theta)/(1 + \cos\theta) = 2.00$ and $b = \sqrt{2}l$. This result shows that the restriction on bond angles has the effect of increasing the rms end-to-end distance by about 40% over the perfectly flexible case.

The formalism that we have set up to describe chain flexibility readily lends itself to the problem of hindered rotation. Figure 1.8a shows a sawhorse representation of an ethane molecule in which the angle of rotation around the bond is designated by ϕ. Because of electron repulsion between the atoms bonded to

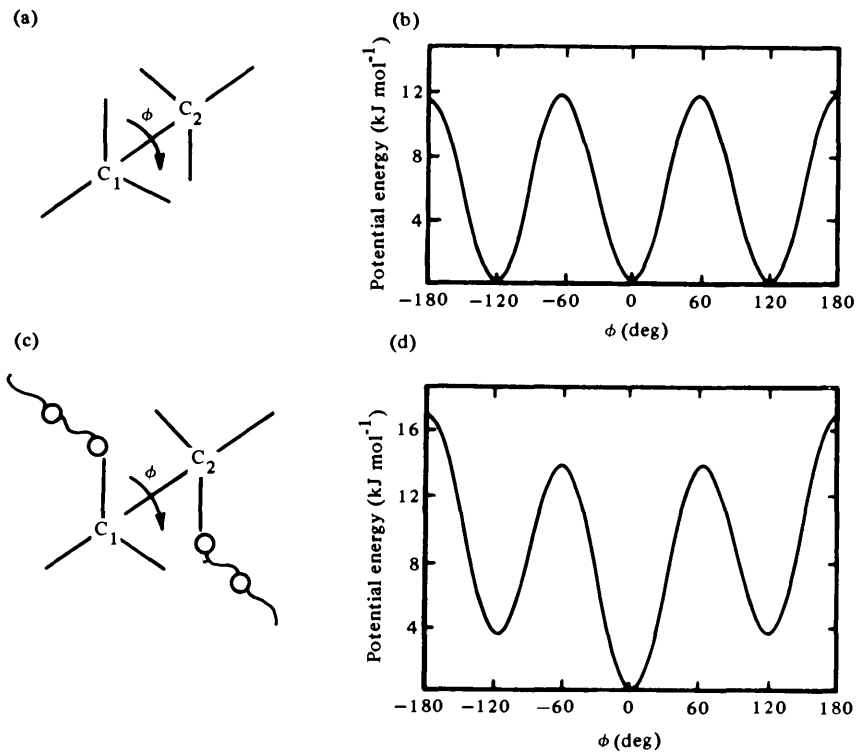

Figure 1.8 Hindered rotation around a carbon-carbon bond. (a) The definition of ϕ (from $\phi = 0$) in terms of the ethane molecule. (b) The potential energy as a function of ϕ. (c) Here ϕ is shown (from $\phi = 0$) for a carbon-carbon bond along a polyethylene backbone. (d) The potential energy for case (c) shown as a function of ϕ. [Panels (b) and (d) reprinted with permission from W. J. Taylor, *J. Chem. Phys.* 16:257 (1948).]

carbons 1 and 2, the potential energy of this molecule varies with the value of ϕ as shown in Fig. 1.8b. If we define $\phi = 0$ to be the conformation shown in Fig. 1.8a, then the potential energy shows the following:

1. A maximum after a rotation through $\pm 60^\circ$ when the hydrogens on adjacent carbon atoms are eclipsed.
2. A minimum after rotation through $\pm 120^\circ$ when the hydrogens are staggered.
3. A maximum after rotation through $\pm 180^\circ$ when they are eclipsed again.
4. Potential energy barriers which are equal in height, on the order of 12 kJ mol^{-1}, for ethane.

For a carbon-carbon bond located along a polymer backbone, the preceding molecular representation must be modified to Fig. 1.8c. The chain segments on either side of the bond of interest are substituents for which the amount of steric hindrance follows a slightly different pattern than for the unsubstituted ethane. Using the same convention for ϕ, we see the following in Fig. 1.8d:

5. The potential energy shows a minimum at $\phi = 0^\circ$, which is defined as the trans conformation.
6. The potential energy shows secondary minima after rotation through $\pm 120^\circ$. These are called gauche conformations, and for polyethylene they are on the order of 4 kJ mol^{-1} higher in energy than the trans conformation.
7. The potential energy barrier associated with the chain segment passing a hydrogen is about 12 kJ mol^{-1} relative to the trans energy, and that of the two chain segments passing each other is about 16 kJ mol^{-1} relative to trans.

A still more intricate pattern of potential energy may be expected if the repeat units of the polymer chain carry other substituents, such as the phenyl groups in polystyrene, but these examples establish the general method for quantitatively describing the effects of steric hindrance on rotation.

Because of the variation in potential energy with the angle of rotation, not all locations on the rim of the cones in Fig. 1.7b are equally favored. The probability of a particular angular position depends on the potential energy at that location, V_ϕ, and an averaging procedure which considers this angular variation must be used to modify Eq. (1.60). The result of this procedure is

$$\overline{r^2} = nl^2 \left(\frac{1 - \cos\theta}{1 + \cos\theta}\right)\left(\frac{1 + \overline{\cos\phi}}{1 - \overline{\cos\phi}}\right) = nb^2 \left(\frac{1 + \overline{\cos\phi}}{1 - \overline{\cos\phi}}\right) \tag{1.61}$$

In this expression, $\overline{\cos\phi}$ is the average value of $\cos\phi$; the weighting factor used to evaluate the average is given by the Boltzmann factor $\exp(-V_\phi/RT)$, where R is the gas constant in the units of V_ϕ and T is in degrees Kelvin. Note that the correction factor introduced by these considerations reduces to unity if

$\overline{\cos \phi} = 0$, the case for free rotation, and increase as $\overline{\cos \phi}$ increases. Qualitatively, then, the effect of hindered rotation is to introduce still further expansion of coil dimensions.

In Chap. 9 we shall apply Eq. (1.44) to describe the probability that a particle has diffused a distance r after n thermal collisions with other molecules. In that context the particle may return to the sites of previous occupancy with no difficulty, but an error is clearly made by the same assumption regarding placement of chain segments. In the random walk derivation, we assumed that no excluded volume effect was operative regarding chain placement. There has been a good deal of research directed toward circumventing this clearly erroneous assumption. We shall not go into any detail in this matter, except for the following assessment of the magnitude of the effect. In computer simulation studies it has been found that the fraction of nonintersecting chains decreases by about 4% per segment added to the chain so that only 1 chain out of about 10^7 could attain a length of 400 units without intersection. The result of this sort of interference is to rule out still more conformations, just as restrictions on θ and ϕ did. Thus we have uncovered still one more factor which tends to increase coil dimensions above the value predicted by Eq. (1.48). Instead of examining the attempts that have been made to deal quantitatively with this source of error, let us look instead at conditions under which it might be offset.

At the beginning of this section we enumerated four ways in which actual polymer molecules deviate from the model for perfectly flexible chains. The three sources of deviation which we have discussed so far all lead to the prediction of larger coil dimensions than would be the case for perfect flexibility. The fourth source of discrepancy, solvent interaction, can have either an expansion or a contraction effect on the coil dimensions. To see how this comes about, we consider enclosing the spherical domain occupied by the polymer molecule by a hypothetical boundary as indicated by the broken line in Fig. 1.9. Only a portion of this domain is actually occupied by chain segments, and the remaining sites are occupied by solvent molecules which we have assumed to be totally indifferent as far as coil dimensions are concerned. The region enclosed by this hypothetical boundary may be viewed as a solution, an we next consider the tendency of solvent molecules to cross in or out of the domain of the polymer molecule.

The thermodynamic criterion for spontaneity is that the change in Gibbs free energy is negative for those processes which occur spontaneously. Thus if the free energy in the domain of the coil is lowered by increasing the number of polymer--solvent contacts, then solvent will be imbibed and the dimensions of the domain will increase as shown in Fig. 1.9. On the other hand, if the free energy is lowered by decreasing the number of polymer–solvent contacts, then solvent is squeezed out and the coil dimensions decrease. It is in this way that polymer–solvent interactions affect the rms values of the end-to-end distance

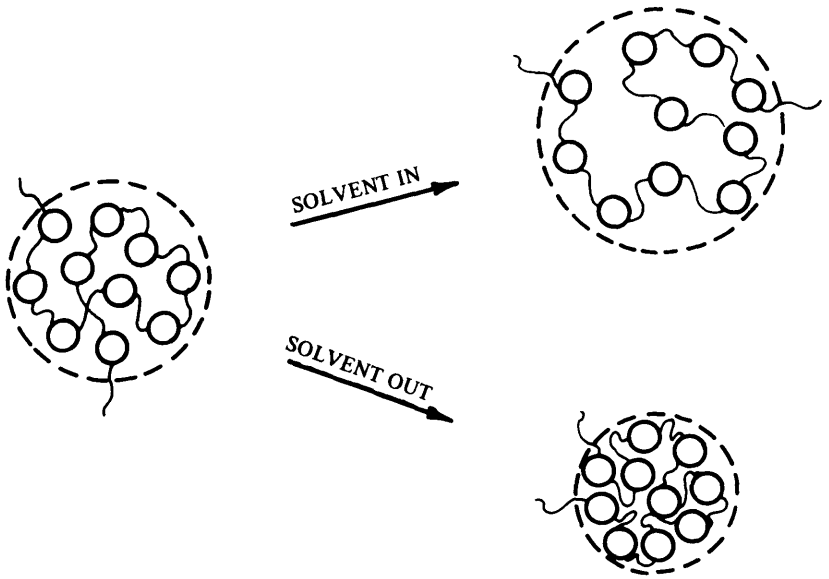

Figure 1.9 The spherical domain of a polymer molecule either expanding by imbibing solvent or contracting by excluding solvent.

and r_g. Quantitative discussion of this point must be deferred until the properties of polymer solutions are considered in Chap. 8. In the meanwhile, however, we can at least introduce some of the vocabulary that is used to describe these situations:

1. A "good solvent" is the technical as well as descriptive term used to identify a solvent which tends to increase coil dimensions. Since this is a consequence of thermodynamically favorable polymer-solvent interactions, good solvents also dissolve polymers more readily in the first place.
2. By contrast, a "poor solvent" is the technical description of a solvent which tends to decrease coil dimensions.
3. The relative goodness of a solvent depends on the temperature as well as the nature of the polymer-solvent system. Solvent goodness can be decreased by changing (generally lowering) the temperature or by adding a poorer solvent, which can result in the precipitation of polymer. Since higher molecular weight polymers are less soluble, controlled regulation of solvent goodness can be employed to fractionate a polydisperse polymer sample.

That state of affairs in which the poorness of the solvent exactly compensates for the excluded volume effect is called a Θ condition or Flory condition, after

P. J. Flory† whose outstanding overall contributions in polymer chemistry won him the Nobel Prize in 1974. Flory's book *Principles of Polymer Chemistry* contains an admirable discussion of these topics.

In summary, we see that the first two sources of deviation can be dealt with quantitatively, while the last two are dispatched by joining them in compensation for one another. (If you can't beat 'em, join 'em!) By convention, the coil dimensions under Θ conditions are given the subscript 0, so we write

$$\overline{r_0^2} = 6\overline{r_{g,0}^2} = nl_0^2 \tag{1.62}$$

where l_0 is the step length under these so-called unperturbed conditions. We shall see in Chap. 8 that Θ conditions can be achieved experimentally, so $\overline{r_{g,0}^2}$ and l_0 are measurable quantities. Table 1.6 lists some values of l_0 calculated from experimental data via Eq. (1.62). Table 1.6 also includes the ratio of these experimental l_0 values to b, the length of a carbon-carbon bond, corrected for fixed bond angles (or whatever distance is appropriate as the length of the repeat unit for non-vinyl polymers). The value of this ratio may be taken as a measure of the factor $(1 + \overline{\cos\phi})/(1 - \overline{\cos\phi})$ in Eq. (1.61). The following example will help clarify the meaning of these quantities.

Example 1.6

A polystyrene sample of molecular weight 10^6 shows an rms end-to-end distance under unperturbed conditions equal to 735 Å. In polystyrene $M_0 = 104$ and the length of the carbon-carbon bond along the backbone is 0.154 nm. Use these data to verify the numbers given for this polymer in Table 1.6.

Solution

For polystyrene of molecular weight 10^6, the degree of polymerization is $10^6/104 = 9620$. Since there are two carbon-carbon bonds associated with each repeat unit, the total number of bonds comprising the random walk is $2(9620) = 1.92 \times 10^4$. According to Eq. (1.48), for a random walk of 1.92×10^4 steps of length 0.154 nm, $\overline{r^2} = (1.92 \times 10^4)(0.154)^2 = 455\ \text{nm}^2$. This is based on the assumption of unrestricted values for θ and ϕ. Limiting θ to the tetrahedral angle leads to the corrected value [Eq. (1.60)], which is double this, or $910\ \text{nm}^2$. Therefore, for fixed bond angles but free rotation around bonds, $r_{rms} = 30.2$ nm = 302 Å. The actual value for this quantity is subject to hindred rotation, so

†Paul J. Flory is another of the "fathers" of polymer chemistry. An interview with Flory appears in the *Journal of Chemical Education*, 54:341 (1977).

Table 1.6 Values of l_0 and b for Some Common Polymers and l_0/b Ratios Which Measure Steric Hindrance via Eq. (1.61)

Polymer	l_0 (nm)	Length of bond, corrected for fixed angles, b (nm)	l_0/b
Polyisobutylene	0.421	$0.154\sqrt{2} = 0.218$	1.93
Polystyrene	0.530	0.218	2.44
Poly(methyl methacrylate)	0.481	0.218	2.20
Poly(acrylic acid)	0.426	0.218	1.96
Poly(dimethyl siloxane)	0.444	0.278	1.60
Natural rubber	0.684	0.402[a]	1.71
Gutta-percha	0.849	0.580[a]	1.46

[a]These values are the total length of the repeat unit, based on appropriate bond lengths and bond angles.
Source: Data from Ref. 3.

the ratio 735/302 = 2.44 equals the correction factor for this effect, $[(1 + \overline{\cos\phi})/(1 - \overline{\cos\phi})]^{1/2}$.

•

The values of the ratio l_0/b are thus seen to be quantitative measures of the hindrance to rotation in these polymers. The following observations are pertinent to the trends in this behavior:

1. Poly(dimethyl siloxane) offers the least steric hindrance of the polymers listed; every other atom along the backbone of the chain is devoid of substituents in this case.
2. Polystyrene with its bulky phenyl substituents shows the largest amount of hindrance of the polymers listed here.
3. In the two polyisoprene isomers, the length of the repeat unit and the steric hindrance factor vary oppositely for the two isomers. The greater end-to-end distance in the trans isomer is the dominant influence on the order of l_0 values.

In a good solvent, the end-to-end distance is greater than the l_0 value owing to the coil expansion resulting from solvent imbibed into the domain of the polymer. The effect is quantitatively expressed in terms of an expansion factor α defined by the relationship

$$\alpha = \frac{l}{l_0} = \frac{r_g}{r_{g,0}} = \frac{r_{rms}}{r_{rms,0}} \tag{1.63}$$

We shall defer a quantitative discussion of this expansion factor until the discussion of solutions in Chaps. 8 and 9.

We end this section with a disclaimer. In spite of the importance of the random coil in polymer chemistry, it must be conceded that this is not the only structure that polymer molecules assume. We have already noted that globular proteins may be cross-linked into tertiary structures best described as ellipsoids of revolution. In crystals, polyethylene folds back and forth along the backbone of the chain. Something on the order of 40 segments exist in the fully extended form in these crystals before the chain folds back on itself and repeats the process. In vinyl polymers the substituents are too bulky to fit into a crystal with only a 0.252-nm repeat distance as provided with the chain in the fully extended zigzag form. In these cases the chains accommodate substituents by twisting subsequent repeat units along the length of the otherwise extended backbone.

The helix is a geometrical structure to which certain polymer molecules are especially well suited. As an example, we consider an isotactic vinyl polymer in which successive repeat units assume alternating trans and gauche conformations. The tacticity is an aspect of the primary structure and the alternating gauche–trans conformations describe a specific situation that we may regard as secondary structure. Our present purpose is to show that this results in a still higher order of structure—tertiary structure—which has helical geometry. Figure 1.10a is an illustration of this conformation for an R-substituted vinyl polymer. This is the observed conformation for such molecules in the crystalline state when R is $-CH_3$, $-C_2H_5$, $-C_3H_7$, $-C_6H_5$, and so on. In Fig. 1.10 the ribbon connects successive R groups, tracing a helix containing three repeat units per turn. To see how such a structure is generated, examine Fig. 1.10a through the following steps (or, better yet, construct a model of the structure):

1. Number successive bonds along the backbone 1, 2, 3, and so on.
2. Bonds 1 and 3 are rotated to trans positions with respect to bond 2. All odd-numbered bonds are in similar situations with respect to the even-numbered bonds.
3. Bonds 1 and 3 are in axial positions in the helix, with bond 2 oriented equatorially.
4. Bonds 2 and 4 are rotated to gauche positions with respect to bond 3. All even-numbered bonds are in similar conformations with respect to the odd-numbered bonds.
5. A consistent direction of twist is maintained; clockwise or counterclockwise rotations are equally probable.

This particular sequence of conformations—trans bonds that advance the helix along the axis, alternating with gauche bonds which provide the twist—takes the chain through a series of relatively low potential energy states and generates a structure with minimum steric hindrance between substituents. If the polymer series is extended to include bulkier substituents, for example,

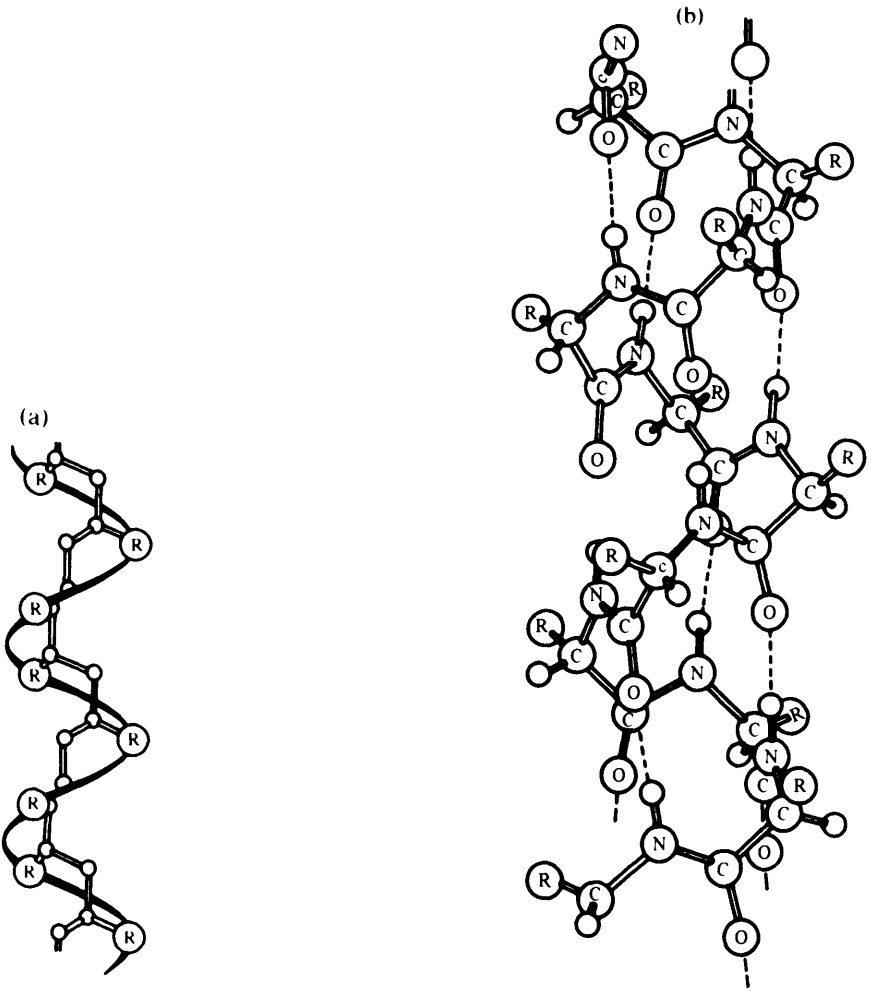

Figure 1.10 Helical conformations in polymer molecules. (a) A vinyl polymer with R substituents has three repeat units per turn. (b) The α helix of the protein molecule is stabilized by hydrogen bonding. [From R. B. Corey and L. Pauling, *Rend. Inst. Lombardo Sci.* 89:10 (1955).]

R = $-CH_2CH(CH_3)_2$, there occurs a modest deviation from a strict 0°-120° alternation which characterizes the trans-gauche sequence. This produces a helical structure with seven repeat units occurring in two turns. Even bulkier substituents, for example, *o*-methyl phenyl, produce still more open helices

with four repeat units per turn as a result of even greater deviation from the rotational positions of lowest potential energy.

In addition to existing as helices in crystals, there is evidence that certain vinyl polymers also show some degree of regular alternation between trans and gauche conformations in solution. In solution, the chain is free from the sort of environmental constraints that operate in a crystal, so the length of the helical sequence in a dissolved isotactic vinyl polymer may be relatively short.

Many polypeptides also assume helical structures in the crystalline state and—in equilibrium with unwound random conformations—in solution. In this case the helix is stabilized by hydrogen bonding between the N–H and O=C groups on successive turns of the helix. Fixed bond angles and bond lengths restrict stable helices to those containing either 3.7 or 5.1 repeat units per turn. The former, commonly called the α helix, is shown in Fig. 1.10b; it possesses about 18 amino acid residues in every five turns. Many globular proteins, for example, myoglobin, contain helical sections in which the helix is interrupted occasionally, the chain bends through a kink, then the helix resumes. Finally, there is the most famous helical structure of all: the DNA double helix. Random coils are not without competition as the structure of polymer molecules!

1.12 Preview of Things to Come

In this chapter we have focused attention on various aspects of individual polymer molecules. In the next three chapters we shall examine some properties of assemblies of polymer molecules. Our interest in these chapters will be mostly directed toward samples of pure polymer; assemblies of high and low molecular weight molecules—polymer solutions—will be discussed in Part III of this book.

We shall divide our discussion of bulk polymers on the basis of the mechanical states of these materials; that is, instead of classification into states based on thermodynamic criteria alone, we favor a system based on the way samples respond to deforming forces. Accordingly, we shall discuss the viscous state in Chap. 2, the elastic and viscoelastic states in Chap. 3, and the glassy and crystalline states in Chap. 4. There are good reasons for choosing these mechanical states as the basis for classification and, incidentally, for presenting this material right at the start of this text. If polymers did not possess the mechanical properties they have, they would, in all likelihood, still be in the category of laboratory curiosities—or disasters. Instead, their sluggish flow, elastic snap, plastic flexibility, and toughness in wear are all marketable properties. Each of these properties is ultimately traceable to the chain structure of polymer molecules. It is not the *amide* in its IUPAC name that makes nylon the important material that it is; it is the *poly* which is primarily responsible!

In Chap. 2, we consider polymers whose molecular weight and/or temperature gives them liquid flow behavior. We shall begin by quantitatively examining what we mean by viscosity and then consider how this property depends on, say, how fast the material is stirred and on the characteristics of the polymer itself. It should not be too surprising that the length of the chain is the most important polymer property in this regard. All we need to do is think of our experience with a plate of spaghetti to get an idea of what happens when we try to induce some motion in a mass of tangled flexible "chains."

Polymers are not alone in displaying elastic properties, but their elasticity is unique in both origin and magnitude. For one thing, the elastic restoring force which acts in polymers increases with increasing temperature, whereas the opposite is true in, say, metals. Again, this is a consequence of the chain structure of the polymer. Stretching a live snake to a "fully extended conformation" may be problematic under the best of conditions, but it will resist all the more if we warm it up besides. We shall see in Chap. 3 that polymer chains behave in pretty much the same way.

Chapter 4 is concerned with the solid forms of polymers. Crystals of any material consist of highly ordered arrays of molecules. In view of the assortment of variations that can occur within polymer chains, it is not surprising that only those polymers with a high degree of chain regularity crystallize. Even crystallizable polymers fall short of complete crystallinity. Those polymers which do not crystallize, whether partly or totally, still solidfy in the mechanical sense at a temperature called the glass transition temperature. Below this temperature the thermal energy available for chain motion is inadequate to allow much relative motion between chains. Low molecular weight materials also form glasses, but the chain structure of polymers makes this behavior one to which polymers are particularly susceptible.

In the next group of chapters—indeed, throughout the book—we shall be talking about a variety of properties of individual polymer molecules and assemblies of these molecules. One concept that should be fairly clear from the discussions of this chapter is that the word *average* should be used as a modifier in almost every statement we make about polymers. This is true in many areas of chemistry: Even an assembly of relatively simple water molecules possesses an assortment of isotopic possibilities; translational, rotational, vibrational, and electronic energy states; and different extents of hydrogen bonding and ionization. Still we speak of *the* water molecule as if it were an invariant species. What we are really talking about is an *average* molecule. Unless we specifically wish to underscore the statistical aspect of a statement, however, the word *average* is generally implied rather than stated. So it will be in this volume. One of the themes of this chapter is the diversity of structures—even down to something as fundamental as molecular weight—that polymers display. Accordingly, the word *average* is even more appropriate as a modifier in polymer

chemistry than in chemistry as a whole. More often than not, however, the actual word is implied rather than stated. Remembering that this is the case is one of the major lessons of this chapter.

Problems

Whenever feasible, the problems in this book are based on data from the original literature. In many instances the values given have been estimated from graphs, transformed from another functional representation, or changed in units. Therefore these quantities do not necessarily reflect the accuracy of the original work, nor is the given number of significant figures always justified. Finally, the data may be used for purposes other than were intended in the original measurement.

1. Cohen and Ramos† describe some phase equilibrium studies of block copolymers of butadiene (B) and isoprene (I). One such polymer is described as having a 2:1 molar ratio of B to I with the following microstructure:

   B – 45% cis-1,4; 45% trans-1,4; 10% vinyl.
   I – over 92% cis-1,4.

   Draw the structure of a portion of this polymer consisting of about 15 segments and having approximately the composition of this polymer.
2. Hydrogenation of polybutadiene converts both cis and trans isomers to the same linear structure and vinyl groups to ethyl branches. A polybutadiene sample of molecular weight 168,000 was found‡ by infrared spectroscopy to contain double bonds consisting of 47.2% cis, 44.9% trans, and 7.9% vinyl. After hydrogenation, what is the average number of backbone carbon atoms between ethyl side chains?
3. Landel§ used a commercial material called Vulcollan 18/40 to study the rubber-to-glass transition of a polyurethane. This material is described as being "prepared from a low molecular weight polyester which is extended and crosslinked . . . by reacting it with naphthalene-1,4-diisocyanate and 1,4-butanediol. The polyester . . . is prepared from adipic acid and a mixture of ethylene and propylene glycols." Draw the structural formula of a portion of the cross-linked polymer which includes the various possible linkages that this description includes. Remember that isocyanates react with active hydrogens; use this fact to account for the cross-linking.

---

†R. E. Cohen and A. R. Ramos, *Macromolecules* 12:131 (1979).
‡W. E. Rochefort, G. G. Smith, H. Rachapudy, V. R. Raju, and W. W. Graessley, *J. Polym. Sci. Polym. Phys.* 17:1197 (1979).
§R. F. Landel, *J. Colloid Sci.* 12:308 (1957).

4. Some polymers are listed below by either IUPAC† (I) names or acceptable trivial (T) names. Draw structural formulas for the repeat units in these polymers and propose an alternative name in the system other than the one given.

   (a) Polymethylene (I).
   (b) Polyformaldehyde (T).
   (c) Poly(phenylene oxide) (T).
   (d) Poly[(2-propyl-1,3-dioxane-4,6-diyl)methylene] (I).
   (e) Poly(1-acetoxyethylene) (I).
   (f) Poly(methyl acrylate) (T).

5. Star polymers are branched molecules with a controlled number of linear arms anchored by one central molecular unit acting as a branch point. Schaefgen and Flory‡ prepared poly(ϵ-caprolactam) four- and eight-pointed stars using cyclohexanone tetrapropionic acid and dicyclohexanone octapropionic acid as branch points. These authors present the following stoichiometric definitions/relations to relate the molecular weight of the polymer to the concentration of unreacted acid groups in the product. Provide the information required for each of the following steps:

   (a) The product has the formula $R\{-CO[-NH(CH_2)_5CO-]_y-OH\}_b$. What is the significance of R, y, and b?
   (b) If Q is the number of equivalents of multifunctional reactant which reacts per mole of monomer and L represents the number of equivalents of unreacted (end) groups per mole monomer, then $\bar{y} = (1 - L)/(Q + L)$. Justify this relationship, assuming all functional groups are equal in reactivity.
   (c) If M_0 is the molecular weight of the repeat unit and M_b is the molecular weight of the original branch molecule divided by b, then the number average molecular weight of the star polymer is $\bar{M}_n = b\{M_0[(1 - L)/(Q + L)] + M_b\}$. Justify this result and evaluate M_0 and M_b for the b = 4 and b = 8 stars.
   (d) Evaluate $\bar{M}_n$ for the following molecules:

	Q	L
b = 4	0.2169	0.0018
b = 8	0.134	0.00093

6. Batzer§ has reported the following data for a fractionated polyester made from sebacic acid and 1,6-hexanediol:

† IUPAC Macromolecular Nomenclature Commission, *Macromolecules* 6:149 (1973).
‡ J. R. Schaefgen and P. J. Flory, *J. Am. Chem. Soc.* 70:2709 (1948).
§ H. Batzer, *Makromol. Chem.* 5:5 (1950).

	Fraction no.								
	1	2	3	4	5	6	7	8	9
Mass (g)	1.15	0.73	0.415	0.35	0.51	0.34	1.78	0.1	0.94
$M \times 10^{-4}$ (g mol^{-1})	1.25	2.05	2.40	3.20	3.90	4.50	6.35	4.1	9.40

Evaluate $\bar{M}_n$, $\bar{M}_w$, and $\bar{M}_z$ from these data.

7. At 25°C, the Mark-Houwink exponent for poly(methyl methacrylate) has the value 0.69 in acetone and 0.83 in chloroform. Calculate (retaining more significant figures than strictly warranted) the value of $\bar{M}_v$ that would be obtained for a sample with the following molecular weight distribution if the sample were studied† by viscometry in each of these solvents:

$N_i \times 10^3$ (mol)	1.2	2.7	4.9	3.1	0.9
$M_i \times 10^{-5}$ (g mol^{-1})	2.0	4.0	6.0	8.0	10.0

8. In addition to r_g and r_{rms}, another way of characterizing coil dimensions is to consider which end-to-end distance has the greatest probability of occurring for specified n and l values. Derive an expression for this most probable value of r, r_m, from Eq. (1.44). Compare the ratio r_{rms}/r_m to the ratio u_{rms}/u_m from the kinetic molecular theory of gases (consult, say, a physical chemistry textbook), where u is molecular velocity. Comment briefly on the significance of the comparison.
9. Random walk statistics also describe the path followed by a diffusing particle. In this case, the number of steps which a particle takes is proportional to the time allowed for diffusion: $n = Kt$, with K the proportionality constant. A totally independent approach to diffusion gives $\overline{r^2} = 2Dt$ as the relationship between the mean-square displacement, time, and the diffusion coefficient of the particle. Use this result to evaluate the constant K. The diffusion coefficients of low molecular weight solutes through low molecular weight solvents, polymers through low molecular weight solvents, and polymers through polymers are on the order of 10^{-9}, 10^{-11}, and 10^{-17} m^2 sec^{-1}, respectively. Calculate the time required for r_{rms} to be 10 nm in each case.
10. For two different esters of cellulose, l_0 values are listed‡ here in two different temperature regions, 30 and 130–140°C:

Ester	T(°C)	l_0 (Å)
Cellulose tributyrate	30	38.6
Cellulose tributyrate	130	14.1
Cellulose tricaprylate	140	17.3

† S. N. Chinai, J. D. Matlock, A. L. Resnick, and R. J. Samuels, *J. Polym. Sci.* 17:391 (1955).
‡ Ref. 3.

Taking the length per repeat unit (i.e., bond angles already considered) as 0.78 nm in each instance, evaluate the factors $(1 + \cos\phi)/(1 - \cos\phi)$ and $\cos\phi$ for each polymer. Ignoring the difference between 130 and 140°C, do you find the difference in steric hindrance between the tributyrate and tricaprylate to be what you expected? Is the effect of temperature on the l_0 value of cellulose tributyrate what you expected? Briefly explain each answer. For each polymer, calculate r_{rms} if $n = 10^4$; also do this for the hypothetical chain with no restrictions to rotation and having the same repeat length.

11. Strauss and Williams† have studied coil dimensions of derivatives of poly(4-vinylpyridine) by light-scattering and viscosity measurements. The derivatives studied were poly(pyridinium) ions quaternized y% with n-dodecyl groups and (1 - y)% with ethyl groups. Experimental coil dimensions extrapolated to Θ conditions and expressed relative to the length of a freely rotating repeat unit are presented here for the molecules in two different environments:

	$r_{rms,0}/n^{1/2}b$	
y	In isopropanol with LiBr	In water with KBr
0	–	2.54
4.8	2.60	2.88
10.3	2.77	2.26
16.3	2.80	1.86
34.1	2.98	1.23

(a) Write three unit structural formulas for poly(4-vinyl pyridine) and for the molecule in which y = 34.1%.

(b) In both solvents the limiting value of $r_{rms,0}/n^{1/2}b$ as $y \to 0$ is similar in magnitude to the value of this quantity for polystyrene as given in Table 1.6. Briefly explain why this might be expected.

(c) The trends in $r_{rms,0}/n^{1/2}b$ with increasing y are different in the two solvents. Propose brief explanations for each of these trends. (Hint: The "micelle" concept is helpful for the water case; look this up in Chap. 6 or surface chemistry texts if unfamiliar.)

12. The special stability of the helix with three repeat units per turn for isotactic vinyl polymers in which the substituent is not too large was discussed in connection with Fig. 1.10a. Rodriguez‡ has suggested a simple paper model which is also helpful in illustrating this structure. The following steps summarize this method; additional details are available in this readily accessible reference.

† U. P. Strauss and B. L. Williams, *J. Phys. Chem.* 65:1390 (1961).

‡ F. Rodriguez, *J. Chem. Educ.* 45:507 (1968).

(a) Construct a triangular prism mandrel by folding construction paper or, even better, transparent plastic sheeting. Axial bonds of the helix lie along the edges—labeled A, B, and C—of this prism.
(b) Equatorial bonds lie on the faces of the prism—labels AB, BC, and CA. The bonds on the faces make an angle of 109.5° with the previous bond in the plane of that face.
(c) To maintain proper bond lengths, the width of each face should be 94.3% (sin 70.5° = 0.943) of the bond length.
(d) Use a felt-tip pen to mark bond 1 along edge A. Bond 2 is then drawn on face AB (measure angle, 109.5°). Bond 3 goes along edge B; bond 4 on face BC, and so on.
(e) Slots are cut into the edges of the mandrel, bisecting the bond angles along the chain. Cards are inserted into the slots onto which chain substituents have been drawn to scale.

Construct such a model for isotactic polypropylene. Estimate the volume of an isobutyl group on the scale of your model and examine whether interference between successive substituents would occur if this were the R group present.

13. The intrinsic viscosity of a solution of particles shaped like ellipsoids of revolution is given by the expression

$$\frac{14}{15} + \frac{(a/b)^2}{15[\ln(2a/b) - 1.5]} + \frac{(a/b)^2}{5[\ln(2a/b) - 0.5]}$$

(Simha equation), where a/b is the length/diameter ratio of these cigar-shaped particles. Doty et al.† measure the intrinsic viscosity of poly(γ-benzyl glutamate) in a chloroform-formamide solution and obtained (approximately) the following results:

Degree of polymerization	98	317	1240	1650
Intrinsic viscosity (dimensionless as in expression above)	13	66	740	1060

Use the Simha equation and these data to criticize or defend the following proposition: These polymer molecules behave like rods whose diameter is 16 Å and whose length is 1.5 Å per repeat unit. The molecule apparently exists in fully extended form in this solvent rather than as random coils.

†P. Doty, A. M. Holtzer, J. H. Bradbury, and E. R. Blout, *J. Am. Chem. Soc.* 76:4493 (1954).

Bibliography

1. Allcock, H. R., and Lampe, F. W., *Contemporary Polymer Chemistry*, Prentice-Hall, Englewood Cliffs, N.J., 1981.
2. Billmeyer, F. W., Jr., *Textbook of Polymer Science*, 2nd ed., Wiley-Interscience, New York, 1971.
3. Flory, P. J., *Principles of Polymer Chemistry*, Cornell University Press, Ithaca, N.Y., 1953.
4. Hiemenz, P. C., *Principles of Colloid and Surface Chemistry*, Marcel Dekker, New York, 1977.
5. Seymour, R. B., and Carraher, C. E., Jr., *Polymer Chemistry, an Introduction*, Marcel Dekker, New York, 1981.

BULK POLYMERS AND THEIR MECHANICAL BEHAVIOR

2

The Viscous State

The fond voyeur
And narcissist alike devoutly peer
Into disorder, the disorder
Being covalent bondings that prefer
Prolonged viscosity and spread loose nets
Photons slip through

The Dance of the Solids, by John Updike

2.1 Introduction

In this chapter we examine the flow behavior of bulk polymers in the liquid state. Such substances are characterized by very high viscosities, a property which is directly traceable to the chain structure of the molecules. All substances are viscous, even low molecular weight gases. The enhancement of this property due to the molecular structure of polymers is one of the most striking features of these materials.

Before we are in a position to discuss the viscosity of polymer melts, we must first give a quantitative definition of what is meant by viscosity and then say something about how this property is measured. This will not be our only exposure to experimental viscosity in this volume—other methods for determining bulk viscosity will be taken up in the next chapter and the viscosity of solutions will be discussed in Chap. 9—so the discussion of viscometry will only be introductory. Throughout we shall be concerned with constant temperature experiments conducted under nonturbulent flow conditions.

There are three major aspects of polymer viscosity discussed in this chapter. First, we shall consider the fact that most bulk polymers display shear-dependent viscosity; that is, this property does not have a single value but varies with the shearing forces responsible for the flow. Second, the molecular weight dependence of polymer viscosity is examined. We may correctly expect a

considerable sensitivity to this parameter, since it is a direct measure of chain length. Third, we shall investigate the effect of chain branching on viscosity.

Our approach in this chapter is to alternate between experimental results and theoretical models to acquire familiarity with both the phenomena and the theories proposed to explain them. We shall consider a model for viscous flow due to Eyring which is based on the migration of vacancies or holes in the liquid. A theory developed by Debye will give a first view of the molecular weight dependence of viscosity; an equation derived by Bueche will extend that view. Finally, a model for the snakelike wiggling of a polymer chain through an array of other molecules, due to deGennes, Doi, and Edwards, will be taken up.

There are a number of important concepts which emerge in our discussion of viscosity. Most of these will come up again in subsequent chapters as we discuss other mechanical states of polymers. The important concepts include free volume, relaxation time, spectrum of relaxation times, entanglement, the friction factor, and reptation. Special attention should be paid to these terms as they are introduced.

2.2 The Coefficient of Viscosity

Before we attempt to discover the molecular origin of the viscosity of a polymer melt, we must first define more quantitatively what we mean by viscosity. As a place to begin, we visualize the fluid as a set of infinitesimally thin layers moving parallel to each other, each with a characteristic velocity. In addition, we stipulate that those fluid layers which are adjacent to nonflowing surfaces have the same velocity as the rigid surfaces. This is another way of stating that there is no slipping at the interface between the stationary and flowing phases and is an experimental fact of fluid behavior at such boundaries. Now suppose we consider a sample of fluid which is maintained at constant temperature, sandwiched between two rigid parallel plates of area A as shown in Fig. 2.1. If a force F is applied to the top plate as shown in Fig. 2.1, that plate and the layer of fluid adjacent to it will accelerate until a steady velocity is reached. As long as the deforming force continues to be applied, this velocity is unchanged. This time-independent behavior is called stationary-state flow and will be our primary concern. During the acceleration that precedes the stationary state, the velocity is a function of time. For our purposes, we shall simply wait until the stationary state is reached and not even question how long it will take. Force per unit area is called stress and is given the symbol σ; we often attach the subscript s to F and σ as a reminder that these operate in a shear mode in this discussion.

In the experiment described in Fig. 2.1, the bottom plate remains in place and the nonslip condition stipulated above requires that the layer of fluid adjacent to the bottom plate also have zero velocity. This situation clearly

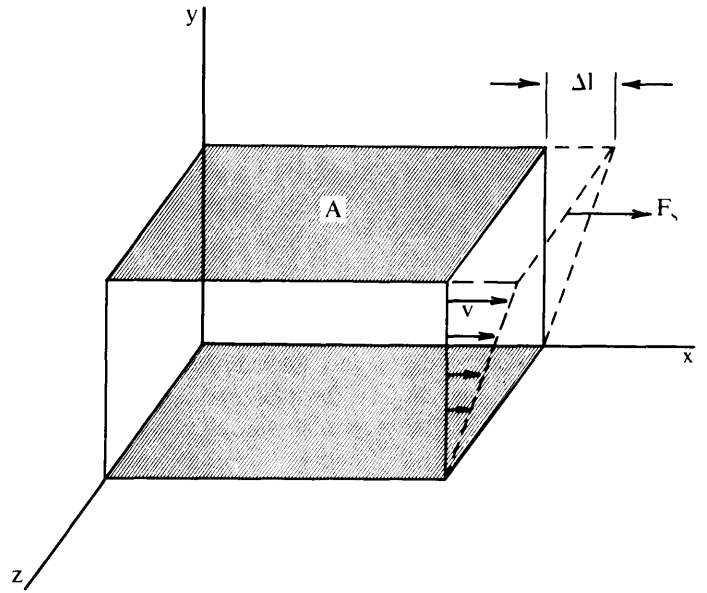

Figure 2.1 The relationship between the applied force per unit area and the velocity used in the definition of viscosity.

requires that the velocity of the fluid vary from layer to layer across the gap between the two rigid plates.

To formulate this mathematically, we write that the top and bottom of these imaginary fluid layers are separated by a distance Δy and differ from each other in velocity by Δv. The ratio $\Delta v/\Delta y$ has units of reciprocal time and is called either the velocity gradient or the rate of shear. The former name is self-explanatory, and the latter may be understood by considering the actual deformation the sample undergoes under the shearing force. During a short time interval Δt, the top layer moves a distance Δl relative to the bottom layer. Accordingly, Δv may be written $\Delta v = \Delta l/\Delta t$ and the velocity gradient may be expressed as $\Delta v/\Delta y = (\Delta l/\Delta t)/\Delta y = (\Delta l/\Delta y)/\Delta t$. The shear displacement Δl divided by the distance over which it vanishes to zero, in this case Δy, is called the shear strain, which we represent by γ. These relationships show that the ratio $\Delta v/\Delta y$ also describes the rate at which the shear strain develops, or, more simply, the rate of shear $\Delta\gamma/\Delta t$, or $\dot{\gamma}$. For the present, we shall represent the velocity gradient by either $\Delta v/\Delta y$ or $\dot{\gamma}$, but the more compact symbol for this quantity is used exclusively in later sections. In summary,

$$\frac{\Delta v}{\Delta y} = \dot{\gamma} = \frac{\Delta l/\Delta y}{\Delta t} \tag{2.1}$$

Now let us invoke our experience with liquids of different viscosities, say, water and molasses, and imagine the magnitude of the shearing force that would be required to induce the same velocity gradient in separate experiments involving these two liquids. Our experience suggests that more force is required for the more viscous fluid. Since the area of the solid plates in this liquid sandwich is also involved, we can summarize this argument by writing a proportionality relation between the shear force per unit area σ_s and the velocity gradient

$$\sigma_s = \eta \frac{\Delta v}{\Delta y} = \eta \dot{\gamma} \tag{2.2}$$

where η is called the coefficient of viscosity of the fluid or, more simply, its viscosity. Equation (2.2) implies that the velocity gradient is exactly the same throughout the liquid. Since this may not be the case over macroscopic distances, our best assurance of generality is to consider the limiting case in which Δy and therefore Δv approach zero. In the limit of these infinitesimal increments Δv and Δy become dv and dy, respectively, so Eq. (2.2) becomes

$$\sigma_s = \eta \frac{dv}{dy} \tag{2.3}$$

Equation (2.3) is called Newton's law of viscosity and those systems which obey it are called Newtonian.

Equation (2.3) describes a straight line of zero intercept if σ_s is plotted versus the velocity gradient. Such a plot is shown in Fig. 2.2. Since the coefficient of viscosity is the slope of this line, this quantity has a single value for Newtonian liquids. Liquids of low molecular weight compounds and their solutions are generally Newtonian, but quite a few different variations from this behavior are also observed. We shall not attempt to catalog all of these variations, but shall only consider the other pattern of behavior shown in Fig. 2.2. This example of non-Newtonian behavior is described as pseudoplastic and is often observed when the material under study is a fluid polymer. Since Eq. (2.3) defines the coefficient of viscosity as the slope of a plot of σ_s versus velocity gradient, it is clear from Fig. 2.2 that pseudoplastic substances are not characterized by a single viscosity. The apparent viscosity at a particular velocity gradient is given by the ratio $\sigma_s/(dv/dy)$. Inspection of Fig. 2.2 reveals that pseudoplastic materials appear less viscous at high rates of shear than at low rates.

The amount of curvature in plots like Fig. 2.2 is a measure of the deviation from Newtonian behavior. We can use the logic of calculus to argue that such curvature becomes less apparent as we examine progressively smaller segments of the line. This statement leads us to two important conclusions:

1. If our objective is to examine non-Newtonian behavior, we must design experiments which permit the relationship between σ_s and dv/dy to be studied over as wide a range as possible. This topic is taken up in the next section.

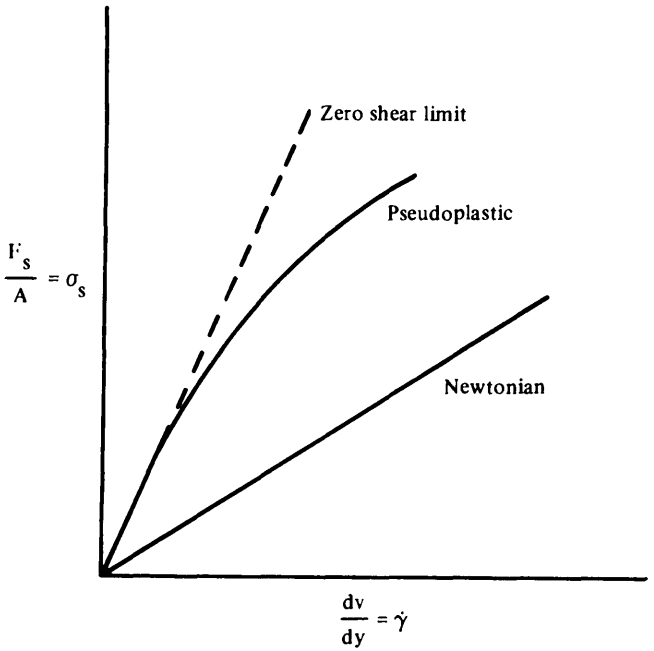

Figure 2.2 Comparison of Newtonian and pseudoplastic behavior.

2. If we wish to avoid the complication of non-Newtonian behavior, we must focus attention on a relatively narrow range of values for dv/dy.

Which range should be considered? The answer is the region near the origin of a plot like Fig. 2.2 for pseudoplastic materials. The slope of the tangent to a pseudoplastic curve at the origin is called the viscosity at zero rate of shear. Note that this is an extrapolation to a limit rather than an observation at zero shear (which corresponds to no flow). We shall use the symbol η_N to indicate the viscosity of a polymer in the limit of zero shear, since the behavior is Newtonian (subscript N) in this region.

To see another interpretation of viscosity, we multiply both sides of Eq. (2.2) by $\Delta v/\Delta y$:

$$\sigma_s \frac{\Delta v}{\Delta y} = \eta \left(\frac{\Delta v}{\Delta y}\right)^2 \tag{2.4}$$

To make sense of this result, we remember that v as introduced in Fig. 2.1 is actually $\Delta x/\Delta t$. Thus the product $F(\Delta v/\Delta y)$ can be written $F(\Delta x/\Delta t)/\Delta y$, and $F(dv/dy)/A$ becomes $F\ \Delta x/A\ \Delta y\ \Delta t$. The product of a force and the distance through which it operates equals an energy ΔE, and the product of A and Δy

equals the volume element ΔV upon which the shearing force described in Fig. 2.1 operates. Therefore $F\,\Delta x/A\,\Delta y\,\Delta t$ is the same as $\Delta E/\Delta V\,\Delta t$. Defining the increment in shear energy dissipated per unit volume by the symbol ΔW, we obtain

$$\frac{\Delta W}{\Delta t} = \eta\left(\frac{\Delta v}{\Delta y}\right)^2 \tag{2.5}$$

As in the parallel case of going from Eq. (2.2) to Eq. (2.3), we take the limit of infinitesimal increments and write

$$\frac{dW}{dt} = \eta\left(\frac{dv}{dy}\right)^2 \tag{2.6}$$

The deforming forces which induce flow in fluids are not recovered when these forces are removed. These forces impart kinetic energy to the fluid, an energy which is dissipated within the fluid. This is the origin of the idea that viscosity represents an internal friction which resists flow. This friction originates from the way molecules of the sample interact during flow.

We conclude this section with a consideration of the units required for η by Eqs. (2.3) and (2.6). To do this, we rewrite these equation in terms of the units of all quantities except η. The units of η must make the expressions dimensionally correct. Force has units of mass times acceleration, or mass length time^{-2}, and area is length^2. Since the velocity gradient has units time^{-1}, the dimensional statement of Eq. (2.3) is

$$\frac{\text{mass length time}^{-2}}{\text{length}^2} = (\eta)\,\text{time}^{-1}$$

Similarly, the rate of energy dissipation in Eq. (2.6) has units energy volume^{-1} time^{-1}, so the dimensions of that equation are

$$\frac{\text{mass length}^2\ \text{time}^{-2}}{\text{length}^3\ \text{time}} = (\eta)\,\text{time}^{-2}$$

In order to satisfy these two defining equations, η must have units mass length^{-1} time^{-1}. In SI units this is kg m^{-1} sec^{-1}. The cgs unit 1 g cm^{-1} sec^{-1} is defined to be 1 poise (1 P). Note that 1 kg m^{-1} s^{-1} = 10 P. At room temperature, water has a viscosity of about 10^{-3} kg m^{-1} sec^{-1}, and other low molecular weight liquids also have viscosities of this magnitude. The viscosity of a polymer depends on the architecture of the polymer molecule and, especially, on the molecular weight of the polymer, as we shall see in Sec. 2.9. To get a feel for the magnitude of polymer viscosities, note that $\eta_N = 3.3 \times 10^4$ kg m^{-1} sec^{-1} at 200°C for a polystyrene sample with $\bar{M}_w = 3.71 \times 10^5$ and that $\eta_N = 7.5 \times 10^5$ kg m^{-1} sec^{-1} at 25°C for poly(dimethyl siloxane) with $\bar{M}_w = 1.34 \times 10^6$.

2.3 Measuring Viscosity: Concentric Cylinder Viscometers

As the numbers cited in the preceding section suggest, the range of viscosities spanned between low and high molecular weight substances is very broad and no single experimental procedure is equally suitable over the entire range. In Chap. 9 we shall discuss the capillary viscometer as a means of measuring the viscosity of dilute polymer solutions. For undiluted fluid polymer samples, our concern in this chapter, this type of viscometer is not particularly useful. For the present we shall focus our attention on a device called the concentric cylinder viscometer. Some of our reasons for interest in this type of viscometer are the following:

1. The basic design is a direct extension of the discussion of the preceding section.
2. The range of applicability is exceptionally wide, approximately 10^{-1}-10^{11} kg m^{-1} sec^{-1}.
3. The design permits different velocity gradients to be considered, so that pseudoplasticity can be investigated if desired.
4. A number of technically important viscosity-measuring devices may be thought of as variants of this basic apparatus.

The illustration that enabled us to define the coefficient of viscosity also suggests a modification which would be experimentally useful. Suppose the two rigid parallel plates of Fig. 2.1 and the intervening layers of fluid were wrapped around the z axis to form two concentric cylinders, with the fluid under consideration in the gap between them. The required velocity gradient is then established by causing one of these cylinders to rotate while the other remains stationary. The velocity is now in the direction described by the angle θ in Fig. 2.3a, and its gradient is in the radial direction r. Thus the velocity gradient in this arrangement may be written dv_θ/dr. As a practical matter, the outer cylinder is part of a cup which holds the fluid, while the inner cylinder is a coaxial bob suspended within the outer cup. Suppose the cup is centered on a turntable which rotates with an angular velocity ω, measured in radians per second. The viscous fluid now transmits a force to the suspended bob which can be measured in terms of the torque on a torsion wire. This arrangement is sketched in Fig. 2.3b. In this representation, the outer cylinder has a radius R and the inner cylinder has a radius fR, where f is some fraction. The closer to unity this fraction is, the narrower will be the gap between the cylinders and the more closely the apparatus will approximate the parallel plate model in terms of which η was defined.

A formal mathematical analysis of the flow in the concentric cylinder viscometer yields the following relationship between the experimental variables and the viscosity:

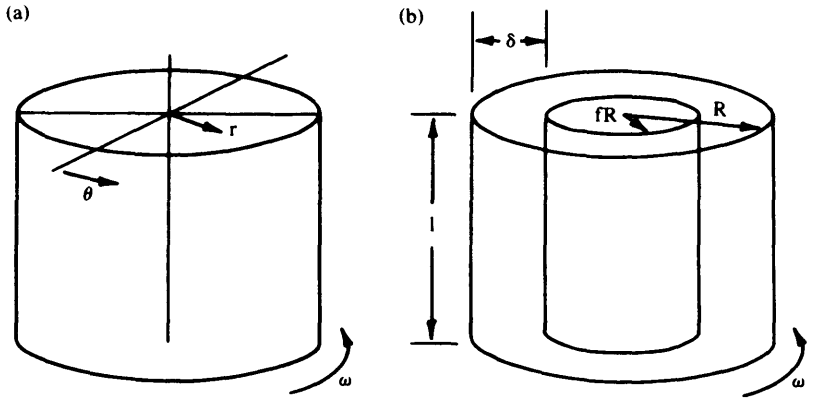

Figure 2.3 Definition of variables for concentric cylinder viscometers; (a) the rotating cylinder and (b) the coaxial cylinders.

$$\text{Torque} = 4\pi\eta l R^2 \omega \frac{f^2}{1 - f^2} \tag{2.7}$$

This equation can be cast into a more recognizable from by assuming that f is very close to unity. In that case we have the following:

1. The radius R also applies to the entire fluid sample. Since torque equals the product of force and R, canceling out one power of R leaves the shearing force acting on the fluid on the left-hand side of Eq. (2.7).
2. The remaining factor R times ω on the right-hand side of Eq. (2.7) can be replaced by the linear velocity v_θ.
3. The factor $1 - f^2$ can be replaced by $2(1 - f)$, since $1 - f^2 = (1 + f)(1 - f)$ and $1 + f \to 2$ as $f \to 1$.
4. The area of contact A between the cylinders and the fluid is $2\pi Rl$; therefore $4\pi lR/R(1 - f^2) = A/(1 - f)R$.
5. The product $(1 - f)R$ is the width of the gap, δ.

Introducing these substitutions in Eq. (2.7) gives

$$\frac{F_s}{A} = \sigma_s = \eta f^2 \frac{v_\theta}{\delta} \tag{2.8}$$

Since v_θ is the difference in velocity between the inner and outer cylinders and δ is the difference in the radial location of the two rigid surfaces, Eq. (2.8) becomes

$$\sigma_s = \eta \frac{dv_\theta}{dr} \tag{2.9}$$

in the limit as $f \to 1$. This is identical to Eq. (2.3) and is the result we anticipated in rolling Fig. 2.1 into a cylinder. Equation (2.7) is more flexible than Eq. (2.8), since its applicability is not limited to vanishingly small gaps.

While conceptually easy to understand, there are several difficulties associated with the concentric cylinder viscometer. Particularly at high rates of shear, it is difficult to maintain constant temperature conditions. Although experimental data can be corrected for some temperature variation, this is an undesirable complication. In the analysis presented above, it appears irrelevant whether the outer cylinder rotates while the force is measured on the inner cylinder or vice versa. It seems that only the direction of the gradient—a matter of sign—would be affected by the reversal. It turns out, however, that there is a greater tendency toward turbulent flow when the inner cylinder rotates. The derivation of Eq. (2.7) is based on the assumption of laminar flow. Instrument design is simplified by using a rotating center spindle so variations of the latter are widely encountered.

A final objection to concentric cylinder viscometers is that the velocity gradient is not uniform throughout the gap. Since a very wide range of shear rates is accessible, it may be quite acceptable to use the average value in the gap to describe a particular experiment. The nonuniformity of the velocity gradient can result in some interesting phenomena for pseudoplastic materials. If the velocity gradient is different in different parts of the gap, then it follows that a pseudoplastic material will show different viscosities in the sheared sample. This manifests itself in a tendency for the sample to flow out of the region of high shear, perhaps climbing the wall where the shear is less. A whole assortment of phenomena of this sort have been studied. Such observations are sometimes called Weissenberg effects.

In the light of the difficulties described above, it is not surprising that in many areas of technology viscosity is measured with rotating devices for which the geometry deviates some from precisely coaxial cylinders. Instruments with modified geometry are simpler to construct and therefore open to such conveniences as interchangeable spindles as well as variable speeds. Although they may lack the precise geometry which permits the absolute determination of viscosity from experimentally measurable parameters, they are sturdy and versatile and permit reproducible observations to be made. These observations may serve as the basis for comparison of relative viscosities of samples measured with the same apparatus, or they may be calibrated with substances of known viscosity so that unknown viscosities may be evaluated. Figure 2.4 is an example of one such commercial apparatus. The instrument shown is the Brookfield digital viscometer, and—with up to eight different speeds and seven different spindles—can measure 56 different average ranges for dv/dr.

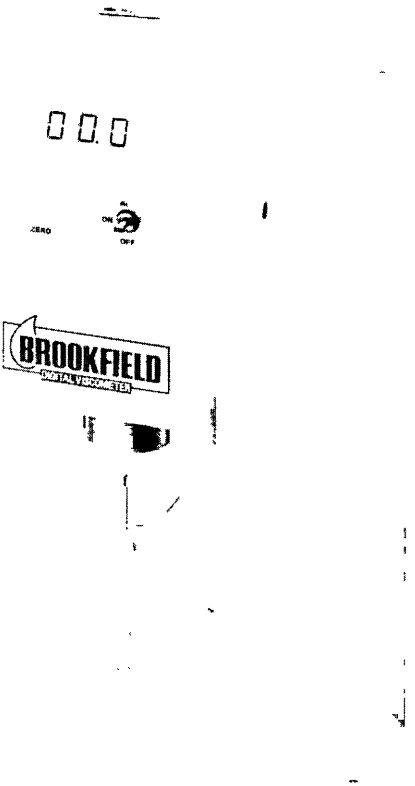

Figure 2.4 A commercial instrument, the Brookfield Digital Viscometer, based on the geometry of the concentric cylinder viscometer. (Photo courtesy of Brookfield Engineering Laboratories, Inc., Stoughton, Mass. 02072.)

2.4 The Power Law for Pseudoplastic Liquids

Figure 2.5 shows some actual experimental data for σ_s versus $\dot{\gamma}$, measured on a sample of polyethylene at 126°C. Note that the data are plotted on log-log coordinates. In spite of the different coordinates, Fig. 2.5 is clearly an example of pseudoplastic behavior as defined in Fig. 2.2. In this and the next several sections, we discuss shear-dependent viscosity. In this section the approach is strictly empirical, and its main application is in correcting viscosities measured

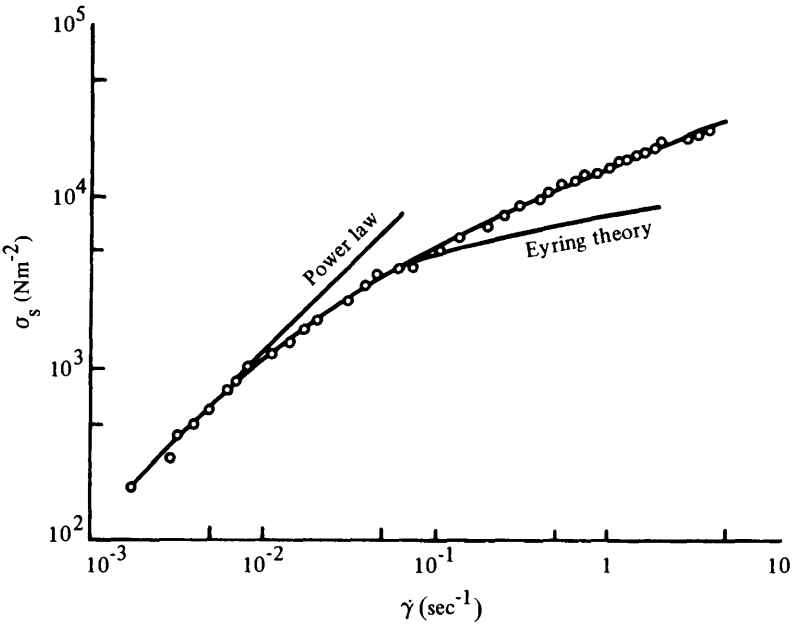

Figure 2.5 Shearing force per unit area versus shear rate. The experimental points are measured for polyethylene, and the labeled lines are drawn according to the relationship indicated. (Data from J. M. McKelvey, *Polymer Processing*, Wiley, New York, 1962.)

at one rate of shear for use under somewhat different shear conditions. In subsequent sections we shall turn to a model for the origin of pseudoplasticity at the molecular level. Although the actual data points in Fig. 2.5 do not describe a straight line, it is apparent that portions of the data over at least an order of magnitude variation in $\dot{\gamma}$ do display linearity. The line labeled "power law" in Fig. 2.5 is an example of such a linear domain. The straight line shown has been drawn with a slope of unity. It can be seen from Fig. 2.5 that other straight lines representing portions of the data at higher rates of shear would be described by lines with slopes less than unity. This is characteristic of pseudoplasticity.

Since any straight line obeys the equation $y = mx + b$, the equation for any tangent drawn in Fig. 2.5 will be

$$\log \sigma_s = m \log \dot{\gamma} + \text{const.} \tag{2.10}$$

where m is the local slope. Taking the antilogs in Eq. (2.10) converts that result to

$$\sigma_s = K\dot{\gamma}^m \tag{2.11}$$

For the straight line in Fig. 2.5 where m = 1.0, this equation expresses direct proportionality between σ_s and $\dot{\gamma}$, the condition of Newtonian behavior. In the non-Newtonian region where $m < 1$, Eq. (2.11) may describe the data over an order of magnitude or so. Next we consider the relationship between the constant K and viscosity. If Eq. (2.11) is solved for K and the resulting expression multiplied and divided by $\dot{\gamma}^{1-m}$, we obtain

$$K = \frac{\sigma_s}{\dot{\gamma}^m} \frac{\dot{\gamma}^{1-m}}{\dot{\gamma}^{1-m}} = \frac{\sigma_s}{\dot{\gamma}} \dot{\gamma}^{1-m} = \eta\dot{\gamma}^{1-m} \tag{2.12}$$

Since K is a constant, two different η-$\dot{\gamma}$ combinations measured in the same regime can be related to each other in the form given by Eq. (2.12) because both factors must equal the same constant; that is,

$$\eta\dot{\gamma}^{1-m} = \eta_r \dot{\gamma}_r^{1-m} \tag{2.13}$$

where one of the η-$\dot{\gamma}$ combinations is distinguished by a subscript, the r signifying a reference or calibration point. Rearranging, this result becomes

$$\eta = \eta_r \left(\frac{\dot{\gamma}}{\dot{\gamma}_r}\right)^{m-1} \tag{2.14}$$

When m = 1.0, as in Fig. 2.5, the exponent becomes zero and the viscosity is independent of $\dot{\gamma}$; when m = 0.7, a factor of 10 change in $\dot{\gamma}$ results in a decrease of viscosity by a factor of 2. This is approximately the case for the data in Fig. 2.5 for $\dot{\gamma}$ values between 10^{-2} and 10^{-1} sec^{-1}. Equation (2.14) and its variations are called power laws. Relationships of this sort are valuable empirical tools for extrapolating either F/A or η over modest ranges of $\dot{\gamma}$. In such an application, the exponent m - 1 and the proportionality constant $\eta_r \dot{\gamma}_r^{1-m}$ are evaluated in a calibration experiment, and Eq. (2.14) is nothing more than a two-parameter empirical equation.

Equation (2.14) has the advantage of simplicity; its drawback is that we learn nothing about either the nature of viscosity or the nature of the sample from the result. In the next few sections we shall propose and develop a molecular model for the flow process. The goals of that development will be not only to describe the data, but also to do so in terms of parameters which have some significance at the molecular level. Before turning to this, it will be helpful if we consider a bit further the form of Eq. (2.14).

The power law developed above uses the ratio of the two different shear rates as the variable in terms of which changes in η are expressed. Suppose that instead of some reference shear rate, values of $\dot{\gamma}$ were expressed relative to some other rate, something characteristic of the flow process itself. In that case Eq. (2.14) or its equivalent would take on a more fundamental significance. In the model we shall examine, the rate of flow is compared to the rate of a chemical reaction. The latter is characterized by a specific rate constant; we shall see that such a constant can also be visualized for the flow process. Accordingly, we anticipate that the molecular theory we develop will replace the variable $\dot{\gamma}/\dot{\gamma}_r$ by a similar variable $\dot{\gamma}/k_R$, where k_R is the rate constant for the flow process.

Figure 2.5 reveals that polymer viscosity approaches Newtonian behavior for sufficiently low rates of shear. From an empirical point of view, this simply means that $m \to 1$ as $\dot{\gamma} \to 0$. From a molecular point of view, in the region of Newtonian behavior the rate of shear is small compared to the rate constant for the flow process. When molecular displacements occur very much faster than the rate of shear ($\dot{\gamma} \ll k_R$), the molecules show maximum efficiency in dissipating the applied forces. When the molecules cannot move fast enough to keep pace with the external forces, they couple with and dissipate those forces to a lesser extent. Thus there is a decrease in viscosity from its upper, Newtonian limit with increasing $\dot{\gamma}/k_R$. The rate constant for the flow process is therefore seen to define a standard against which the rate of shear is to be judged large or small. In the next section we shall consider a molecular model in terms of which this rate constant can be analyzed.

We shall consider a number of different models in this volume. Before proceeding, it might be helpful to remember the status of the model in the methodology of science. Several things come to mind:

1. Models are the handiwork of theoreticians and may be mechanical or electrical analogs, pictorial representations, or purely mathematical constructs.
2. There must be ongoing comparison of experimental results and modelistic predictions. Experiment and theory feed each other.
3. Models necessarily involve approximations: They focus on one facet of behavior to the exclusion of others.
4. Models may succeed in some areas and not in others. This is common and must be remembered in evaluating the success or failure of a model.
5. Models are open to revision. Ideally, the good ones get better and the poor ones are abandoned.
6. There is a tendency among both students and researchers to place more faith in the model than it deserves. Successful models may unify many observations for us and hence be highly valued. The observation always has priority, however.

7. Parameters of interest evaluated via a model may reflect the model as well as the system under consideration.

The statistical model of the random coil discussed in Chap. 1 illustrates many of these items.

2.5 A Model for Flow in Liquids

We begin developing a model for viscous flow for a liquid of small molecules which we can visualize as filling space like beads might fill a beaker. Describing such a beaker as "full" means that it can hold no more beads, and not that it contains no empty space. There are empty spaces in such an assembly due both to the loose, imperfect packing that would ordinarily result from tossing beads into a beaker and to the interstitial spaces between the beads, even in dense packing. The analogous space in a liquid is called the free volume and is responsible for the fact that liquids are compressible. Figure 2.6 represents such an array of spherical particles. We wish to describe the flow of this liquid in terms of steps occurring at the molecular level. We can picture one such elementary step in the flow of the liquid in Fig. 2.6 from left to right by considering the displacement of particle P to hole H. Note that it is equivalent to focus on the hole and consider it being displaced to the left. Since there are fewer holes to account for, the latter process may be easier.

If we were required to pack beads in a beaker, we know from experience that by jostling the container we could achieve some compaction or decrease in free volume. In fact, we can picture the flow of a huge array of beads through a pipe by considering the beaker as a volume element in that pipe. By vibration, the beads are jostled downward; that is, the holes work their way to the top.

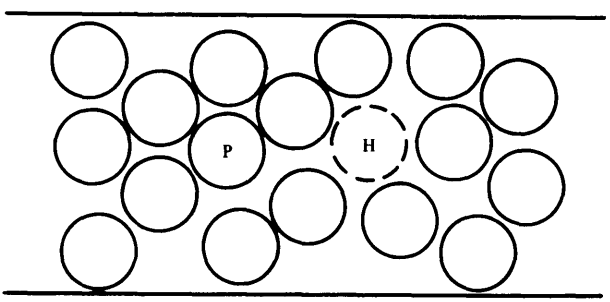

Figure 2.6 Model of a particle P, a hole H, and the bottleneck between them in a liquid of spherical molecules.

Now we imagine the bottom of the beaker being lowered by a small amount such that the lower layers of beads can loosen up a bit. Additional vibration will result in additional compaction as the newly formed holes are worked out. The bottom is then lowered again and the process repeated until the whole array has been moved along an appreciable distance. The entire process can be described in terms of opening holes and moving them through the array. In terms of Fig. 2.6 the exchange of positions between particle P and hole H is the elementary step of this mechanism.

The beads and the holes are necessary to the previous discussion, but by themselves are insufficient to describe the process. The vibration also plays a crucial role. Here, too, our analogy extends to molecular systems, with temperature being the measure of kinetic energy. Because of the free volume present in a liquid, we can imagine each molecule as enclosed by a cage of its neighbors. Because we are concerned with temperatures above absolute zero, these molecules possess thermal energy which is distributed through a variety of different storage modes. When we discuss molecules in the gaseous state where the interactions between neighbors can be neglected, we think of the molecules as moving from place to place, as tumbling in all directions as they move, and as having some parts which oscillate against other parts. We speak of these as translational, rotational, and vibrational modes of energy storage, respectively. An important result of classical physics is the equipartition principle, which says that the energy stored in each of these modes is some multiple of kT, where k is the Boltzmann constant, 1.38×10^{-23} J K^{-1} $molecule^{-1}$, and T is the absolute temperature. Note that this result may be scaled up to apply to a mole of particles simply by multiplying by Avogadro's number N_A. The product of N_A and k is the gas constant R; in SI units R is 8.314 J K^{-1} mol^{-1}. In discussions of thermal energy, kT and RT are often used interchangeably, the understanding being that the former applies "per molecule" while the latter is "per mole."

The equipartition principle is a classic result which implies continuous energy states. Internal vibrations and to a lesser extent molecular rotations can only be understood in terms of quantized energy states. For the present discussion, this complication can be overlooked, since the sort of vibration a molecule experiences in a cage of other molecules is a sufficiently loose one (compared to internal vibrations) to be adequately approximated by the classic result.

Next let us consider the source of resistance to flow. Examination of the path between particle P and hole H in Fig. 2.6 reveals the source of this resistance. The moving particle must pass through the bottleneck formed by neighboring particles along the path between P and H. All of the particles in the assembly are equivalent inasmuch as each vibrates with a certain energy around an equilibrium position separated from neighbors by an average distance. Neither the energy nor the separation are identical for all molecules, but average values for

these quantities are characteristic of the sample. This means that adjacent molecules must be dislodged from their equilibrium positions by the migration of P to H. An expenditure of energy is needed to do this.

Figure 2.7 shows a representation of this situation. The ordinate is an energy axis and the abscissa is called the reaction coordinate and represents the progress of the elementary step. In moving from P to H, the particle simply moves from one equilibrium position to another. In the absence of any external forces, the energy of both the initial and final locations should be the same as shown by the solid line in Fig. 2.7. Between the two minima corresponding to the initial and final positions is the energy barrier arising from the dislodging of the particles neighboring the reaction path from *their* positions of minimum energy.

We conclude this section by noting that the picture we have developed can be extended, with some modification, to polymers relatively easily. From a pictorial point of view, we have compared our system to a beaker of beads. To obtain a representation of polymers we need only to string the beads together. The number of beads on a string gives the degree of polymerization of the polymer. If we string together only a few of the beads and leave most free, the resulting system can be compared to a solution of polymers in a solvent of low

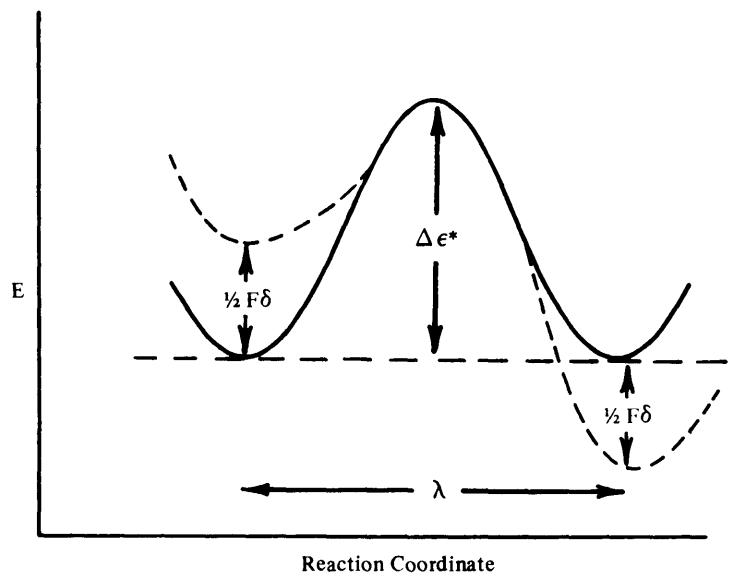

Figure 2.7 Potential energy as a function of location along the reaction coordinate. The solid line describes an undisturbed liquid; the broken line applies to liquids subjected to shearing force.

molecular weight molecules. On the other hand, tying all the beads into strings of more or less uniform length represents a polymer melt. All this can be accomplished in our model without any modification of the basic picture, except that the bead now represents a flow segment rather than an individual molecule. Now, however, the movement of one flow segment necessarily involves adjustment of the location of other segments in the chain in addition to dislodging those in the flow path. This is another consideration which makes it easier to focus attention on the holes, since these are not entrained with other units. We shall see in subsequent sections that a good deal of effort has been directed toward understanding the movement of chains through polymer melts. For our present purposes, however, it is sufficient to continue thinking of the elementary flow step as a flow segment and a hole exchanging positions. Note that the flow segment and the repeat unit of the polymer molecule are not necessarily the same.

2.6 Flow As a Rate Process

In this section we shall examine the analogy between the flow of a liquid and the rate of a chemical reaction. This approach has been developed extensively by Eyring and co-workers and has been applied to a wide variety of deformation processes and systems.

At first glance it may seem strange to compare the rate of fluid flow to the rate of a chemical reaction, but the following analogy may help. The array of particles shown in Fig. 2.6 may be thought of as the "atoms" in a large molecule. Particle P and hole H are clearly different kinds of "atoms." The exchange of positions between P and H is thus comparable to an atomic rearrangement: an isomerization! The rate of such a chemical reaction is generally directly proportional to the concentration of the reacting species C and the proportionality constant is called the specific rate constant:

$$\text{Rate} = k_R C \tag{2.15}$$

This is a phenomenological equation, relating observables; what we seek is the molecular basis for this expression. Eyring's approach focuses attention on the energy barrier along the reaction coordinate as the source of this insight. The molecular situation at the top of the energy barrier is described as an activated complex, so the corresponding theory is called the activated complex theory.

The activated complex theory has been developed extensively for chemical reactions as well as for deformation processes. The full details of the theory are not necessary for us. Instead, it is sufficient to note that k_R can be written as

$$k_R = Ae^{-\Delta\epsilon^*/kT} \tag{2.16}$$

where A gives the frequency with which molecules cross the energy barrier at infinite temperature. The exponential multiplier indicates what fraction of that frequency is achieved at temperature T. As indicated in Fig. 2.7, $\Delta\epsilon^*$ is the height of the energy barrier above the equilibrium energy. It is significant that $\Delta\epsilon^*$ occurs in ratio with kT in Eq. (2.16), since it is thermal energy that allows molecules to pass such barriers. Thus an energy barrier that may be prohibitively high at low temperatures is less of an obstacle at higher temperatures. Note that the exponent must be dimensionless, so that the units of $\Delta\epsilon^*$ and k must be self-consistent; both can be expressed on either a per-molecule or per-mole basis. In the latter case kT becomes RT, as previously noted.

It is generally true and especially clear in the case of the barrier represented by the solid line in Fig. 2.7 that movement in either the forward or the backward direction across the barrier is possible. Hence the *net* rate of the process is written as the difference between the rate forward (subscript f) and the rate backward (subscript b):

$$\text{Net rate} = A\left[(e^{-\Delta\epsilon^*/kT})_f - (e^{-\Delta\epsilon^*/kT})_b\right] C \tag{2.17}$$

where the high-temperature frequency A is taken to be the same in both directions. If we apply Eq. (2.17) to the flow process described by the solid line in Fig. 2.7, we see that the height of the energy barrier is the same in both directions; hence the two exponentials are identical and their difference is zero. There is no net flow, since forward and reverse processes cancel, although at the molecular level fluctuations in density occur. When we examine light scattering in Chap. 10, we shall see that these fluctuations play a role in the discussion of that subject. In the next section we consider how this situation is modified by the application of an external force.

2.7 The Effect of Shearing Forces

In this section we continue our discussion of flow viewed as a rate process, applying our model explicitly to polymer melts. We begin by considering how the energy barrier to flow is modified by the application of an external force. Figure 2.8 will enable us to do this in the case of a shearing force F. Figure 2.8 represents a tangle of polymer molecules. A portion of one chain is shown; its neighbors occupy the shaded region of the diagram. Critical to the development of this picture are the holes labeled H. On the average such vacancies are assumed to be separated by the distance λ, as shown in Fig. 2.8. We are interested in the displacement of the molecule from left to right by suitable segments of the chain exchanging positions with hole H. By appropriate adjustments of position, the effect of this displacement is damped out over the distance λ.

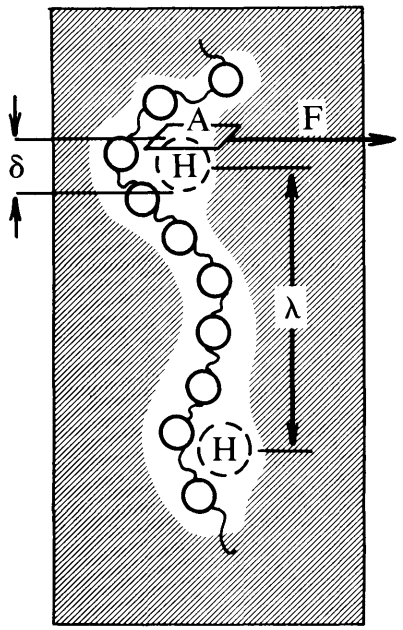

Figure 2.8 Model for the displacement of a polymer chain in relation to a hole H.

The affected portions of the chain define the flow segment according to this picture.

We can imagine that the barrier to this displacement occurs at the midpoint of the forward step $\delta/2$, where δ characterizes the dimensions of the symmetrical holes. Since the product of a force and a distance is energy, we see that the forward motion is facilitated by an amount of energy given by $F\delta/2$. Another way of thinking of this is to imagine that the height of the barrier to the forward motion is lowered by this amount. This is equivalent to starting from an initial state which is higher in energy by $F\delta/2$ than the unstressed fluid. This situation is indicated by the broken line in Fig. 2.7. A corollary of this is that the backward motion is impeded by this extra energy in addition to $\Delta\epsilon^*$. Hence the height of the backward barrier is increased by $F\delta/2$. This is equivalent to initiating the backward migration from a lower-energy state; it is also shown by the broken line in Fig. 2.7.

Under these circumstances the two exponentials in Eq. (2.17) are no longer identical but become

$$\text{Net rate} = A\left[\exp\left(\frac{-(\Delta\epsilon^* - F\delta/2)}{kT}\right) - \exp\left(\frac{-(\Delta\epsilon^* + F\delta/2)}{kT}\right)\right]C = k_R'C \tag{2.18}$$

where the prime on the k_R reminds us that this expression applies when an external force is applied in the direction of the flow. Writing the sum of exponents as the product of two exponentials enables us to rearrange Eq. (2.18) to

$$k'_R = Ae^{-\Delta\epsilon^*/kT}\left(e^{F\delta/2kT} - e^{-F\delta/2kT}\right) = k_R\left(e^{F\delta/2kT} - e^{-F\delta/2kT}\right) \tag{2.19}$$

This expression gives us the rate constant for the net rate of forward flow according to the activated complex theory.

Now let us consider the significance of the factor $\delta k_R/\lambda$. According to Fig. 2.8, δ gives the forward distance a molecule moves in a single flow step and k_R gives the frequency of such steps. The product of the two therefore gives the velocity of forward displacement. Equation (2.1) shows that the rate of shear is given by the velocity at which a shear displacement is propagated divided by the distance over which the displacement develops. In the notation of this model, the latter is λ. Therefore, $\delta k_R/\lambda$ is identical to the rate of shear:

$$\dot{\gamma} = \frac{\delta k_R}{\lambda} \tag{2.20}$$

Combining Eqs. (2.19) and (2.20) gives

$$\dot{\gamma} = \frac{\delta k_R}{\lambda}\left(e^{F\delta/2kT} - e^{-F\delta/2kT}\right) \tag{2.21}$$

The difference in exponentials which occurs in Eq. (2.21) is directly related to the hyperbolic sine function

$$\sinh x = \tfrac{1}{2}\left(e^x - e^{-x}\right) = y \tag{2.22}$$

Accordingly, Eq. (2.21) can be rewritten as

$$\dot{\gamma} = \frac{2\delta k_R}{\lambda}\sinh\left(\frac{F\delta}{2kT}\right) \tag{2.23}$$

Even though they look very different, Eqs. (2.21) and (2.23) are identical.

If we multiply and divide the argument of the sinh by A, we achieve the desired result: a relationship between F/A and $\dot{\gamma}$. Remembering that F/A is the same as σ_s, we write

$$\dot{\gamma} = \frac{2\delta k_R}{\lambda}\sinh\frac{\delta A\sigma_s}{2kT} \tag{2.24}$$

Since the sinh function is less familiar than simple exponentials, an example illustrating Eq. (2.24) may be helpful.

Example 2.1

The σ_s (in N m^{-2}) versus $\dot{\gamma}$ (in sec^{-1}) behavior of poly(dimethyl siloxane) [$\bar{M}_w = 3.2 \times 10^6$] at 25°C has been found to follow the expression

$$\dot{\gamma} = 5.75 \times 10^{-9} \sinh\left(3.60 \times 10^{-3} \frac{F}{A}\right)$$

(a) Find $\dot{\gamma}$ when $\sigma_s = 681$ N m^{-2} and (b) Find σ_s when $\dot{\gamma} = 1.70 \times 10^{-6}$ sec^{-1}.

Solution

(a) Evaluate $\dot{\gamma}$ directly from the expression given, using tables of the sinh function: $3.60 \times 10^{-3}\sigma_s = (3.60 \times 10^{-3})681 = 2.45$; sinh 2.45 = 5.75 from tables of sinh x versus x; or by direct calculation, $5.75 \times 10^{-9}(5.75) = 3.31 \times 10^{-8}$ sec^{-1}. The experimental† value was 3.34×10^{-8} sec^{-1}. (b) Evaluate σ_s from Eq. (2.22), using the inverse sinh: $\dot{\gamma}/5.75 \times 10^{-9} = 1.70 \times 10^{-6}/5.75 \times 10^{-9} = 296$; sin x = 296. We may use tables of sinh x versus x or the identity given in Table 2.1 to find the inverse sinh. The procedure is analogous to finding an antilog: $\sinh^{-1} 296 = x = 6.38$; $6.38 = 3.60 \times 10^{-3}\sigma_s$; $\sigma_s = 1.77 \times 10^3$ N m^{-2}. The experimental‡ value was 1.78×10^3 N m^{-2}.

•

Table 2.1 Some Useful Relationships Involving the Hyperbolic Sine and Inverse Hyperbolic Sine Function

Hyperbolic sine	Inverse hyperbolic sine
Notation $y = \sinh x$	$x = \sinh^{-1} y$
Definition-identity $\sinh x = \frac{1}{2}(e^x - e^{-x})$	$\sinh^{-1} y = \ln(y + \sqrt{y^2 + 1})$
Series expansion $\sinh x = x + \frac{x^3}{3!} + \frac{x^5}{5!} + \cdots$	$\sinh^{-1} y = y - \frac{1}{2}\frac{y}{3} + \frac{1}{2}\frac{3}{4}\frac{y^5}{5} - \cdots$
Limiting values $x \to 0$, $\sinh x \to 0$;	$y \to 0$, $\frac{1}{y}\sinh^{-1} y = 1$;
$x \to \infty$, $\sinh x \cong \frac{1}{2}e^x \to \infty$	$y \to \infty$, $\frac{1}{y}\sinh^{-1} y = 0$
Miscellaneous $\sinh(-x) = -\sinh x$; not periodic	

† D. J. Plazek, W. Dannhauser, and J. D. Ferry, *J. Colloid Sci.* 16:101 (1961).
‡ Ibid.

The example shows that Eq. (2.24) successfully describes the behavior of this polymer under shear over more than two orders of magnitude.

Introduction of the inverse hyperbolic sine function encourages us to take Eq. (2.24) a bit further and derive an expression for η itself. Before continuing, let us remember the following:

1. $\sinh^{-1}$ y is the inverse or arc function, *not* the reciprocal.
2. While less familiar, finding $\sinh^{-1}$ y is no more complicated than finding an antilog.
3. Numerical values of sinh x versus x are tabulated in standard sources (e.g., *The Handbook of Tables for Mathematics*, Chemical Rubber Company) and the tables can be used to evaluate either sinh x or $\sinh^{-1}$ y.
4. The identities for both y = sinh x and x = $\sinh^{-1}$ y in Table 2.1 may be used to calculate these quantities directly, eliminating the need to interpolate.

With this change in notation, Eq. (2.24) becomes

$$\sigma_s = \frac{2kT}{\delta A} \sinh^{-1} \frac{\lambda\dot{\gamma}}{2\delta k_R} = \frac{2kT}{\delta A} \sinh^{-1} \beta\dot{\gamma} \tag{2.25}$$

where we have defined β to replace the cluster of constants:

$$\beta = \frac{\lambda}{2\delta k_R} \tag{2.26}$$

Finally, if we multiply and divide the right-hand side of Eq. (2.25) by $\beta\dot{\gamma}$, we obtain

$$\sigma_s = \frac{2kT\beta}{\delta A} \left(\frac{\sinh^{-1} \beta\dot{\gamma}}{\beta\dot{\gamma}} \right) \dot{\gamma} \tag{2.27}$$

Comparing this result with Eq. (2.2) gives

$$\eta = \frac{2kT\beta}{\delta A} \frac{\sinh^{-1} \beta\dot{\gamma}}{\beta\dot{\gamma}} \tag{2.28}$$

We shall refer to Eq. (2.28) as the Eyring viscosity equation.

In the next section we shall examine the testing and applications of this result; for now we justify the efforts of this section by observing that Eq. (2.28) reduces to two simple cases when the limits presented in Table 2.1 are considered:

$$\eta \to \eta_N = \frac{2kT\beta}{\delta A} \quad \text{as} \quad \beta\dot{\gamma} \to 0 \tag{2.29}$$

and

$$\eta \to 0 \qquad \text{as } \beta\dot{\gamma} \to \infty \tag{2.30}$$

Regardless of the value of β, these limits are obtained at sufficiently small or large values of shear rate; hence we have successfully shown the following:

1. Polymers display Newtonian behavior (η_N = constant) at sufficiently low rates of shear [Eq. (2.29)].
2. Polymers display pseudoplasticity, with apparent viscosity decreasing as $\dot{\gamma}$ increases [Eq. (2.30) and Fig. 2.2].
3. The details of how η varies between these two limits are given by Eq. (2.28).
4. $\beta\dot{\gamma}$, which is proportional to $\dot{\gamma}/k_R$, is a natural variable for describing the dependence of σ_s or η on $\dot{\gamma}$. This result was anticipated in Sec. 2.4.

2.8 Testing the Eyring Equation

While the Eyring equation gives a relationship between σ_s and $\dot{\gamma}$ which allows for both Newtonian and pseudoplastic behavior, the result does not appear too promising. To begin with, the inverse hyperbolic sine function is discouraging and, worse yet, the relationship involves four adjustable parameters: k_R, δ, λ, and A. Having this many parameters imparts a flexibility to the theory which enhances the chance of fitting it to experimental data. On the other hand, we might be hard pressed to find suitable values for these parameters to evaluate η via Eq. (2.25). Furthermore, the possibility of extracting useful molecular information from an equation which contains so many parameters seems slim. To assess this situation more thoroughly, let us reexamine the parameters in Eq. (2.25) and the grouping in which they occur.

Probably the easiest place to begin is with a consideration of the product δA. As defined by Fig. 2.8, δ is the average diameter of a hole and A is its average cross section.

Accordingly, the product δA is about the same as V_h, the volume of the hole. For liquids of low molecular weight, V_h is on the order of 0.5% the volume of the liquid at room temperature, increasing to 2-3% at the boiling point, and larger yet at still higher temperatures. This identification makes δA easier to visualize, but it still leaves us with four parameters: k_R, δ, λ, and V_h.

Next we recognize that δ and λ always appear as a ratio in our theory. If we argue that the hole and the polymer chain have comparable cross-sectional areas, we can multiply both the numerator and denominator of the λ/δ ratio by this cross section and convert it into the ratio V_s/V_h, where V_s is the volume of the flow segment of length λ. While we know neither of these volumes directly, there are indications that V_s/V_h may be on the order of 10-20 for many linear

polymers. Since only the ratio concerns us, we may think of λ/δ or the equivalent V_s/V_h as a single parameter which describes how much larger than the hole the flow segment is. This leaves us with three parameters: k_R, V_h, and V_s/V_h.

Of the adjustable parameters in the Eyring viscosity equation, k_R is the most important. In Sec. 2.4 we discussed the desirability of having some sort of natural rate compared to which rates of shear could be described as large or small. This natural standard is provided by k_R. The parameter k_R entered our theory as the factor which described the frequency with which molecules passed from one equilibrium position to another in a flowing liquid. At this point we will find it more convenient to talk in terms of the period of this vibration rather than its frequency. We shall use τ to symbolize this period and define it as the reciprocal of k_R. In addition, we shall refer to this characteristic period as the relaxation time for the polymer. As its name implies, τ measures the time over which the system relieves the applied stress by the relative slippage of the molecules past one another. In summary,

$$\text{Relaxation time} = \tau = \frac{1}{k_R} \propto \beta \tag{2.31}$$

From now on, we shall use the product $\tau\dot{\gamma}$ instead of $\dot{\gamma}/k_R$ as the natural variable to describe η. Small values of $\tau\dot{\gamma}$ mean that the molecule responds rapidly compared with the duration of the shearing force. Regardless of the value of τ, this condition is met at sufficiently low rates of shear. In terms of Eq. (2.29), polymers are expected to show Newtonian behavior as long as the rate of shear is low enough to allow the molecules to respond; when the velocity gradient is too large, the molecules are unable to keep up, and non-Newtonian behavior results. Thus it is not surprising that low molecular weight liquids are generally Newtonian: They can respond to shear much faster than the more entangled polymer molecules.

Of the various parameters introduced in the Eyring theory, only τ—or β, which is directly proportional to it—will be further considered. We shall see that the concept of relaxation time plays a central role in discussing all the deformation properties of bulk polymers and thus warrants further examination, even though we have introduced this quantity through a specific model.

The concept of free volume is taken up again in Chap. 4.

In the following example we illustrate how values for β and τ can be extracted from experimental data.

Example 2.2

Test the ability of Eq. (2.28) to represent the data of Fig. 2.5, and evaluate β. Estimate τ, recalling that $\beta = \frac{1}{2}(V_s/V_h)\tau \cong 10\tau$.

Table 2.2 Calculated Values for the Evaluation of Eyring Parameters for the Data and the Theoretical Curve of Fig. 2.5

Part I: Evaluation of parameters

$\dot{\gamma}$ (sec^{-1})	F/A ($N\ m^{-2}$)	η ($kg\ m^{-1}\ sec^{-1}$)	η/η_N
0.002	245	123,000	1.00
0.004	491	123,000	1.00
0.008	981	123,000	1.00
0.02	1,960	98,000	0.80
0.04	2,940	73,600	0.60
0.08	4,420	55,200	0.45
0.2	7,650	38,300	0.31
0.4	9,520	23,800	0.19
0.8	14,200	17,800	0.14

Part II: Calculation of theoretical curve

$\dot{\gamma}$ (sec^{-1})	$\beta\dot{\gamma}$ (β = 75 sec)	$\sinh^{-1}(\beta\dot{\gamma})$	$(1/\beta\dot{\gamma})$ $\sinh^{-1}(\beta\dot{\gamma})$	η ($kg\ m^{-1}\ sec^{-1}$)	F/A ($N\ m^{-2}$)
0.002	0.150	0.149	0.993	122,000	245
0.004	0.300	0.296	0.987	121,000	481
0.008	0.600	0.569	0.946	116,000	932
0.02	1.50	1.195	0.797	97,700	1,950
0.04	3.00	1.818	0.606	74,300	2,970
0.08	6.00	2.492	0.415	50,900	4,070
0.2	15.00	3.402	0.227	27,800	5,570
0.4	30.0	4.095	0.137	16,800	6,720
0.8	60.0	4.788	0.080	9,800	7,850

Solution

Apply Eq. (2.27) to some of the data points to evaluate the apparent viscosity at different $\dot{\gamma}$'s. The first section of Table 2.2 shows the results of such calculations. Note that the calculated η's are constant at low $\dot{\gamma}$ values, indicating Newtonian behavior. Table 2.2 also expresses all η values relative to the Newtonian limiting value η_N. Comparison of Eqs. (2.28) and (2.29) shows that η/η_N values decrease from the Newtonian limit by the fraction $\sinh^{-1}(\beta\dot{\gamma})/\beta\dot{\gamma}$.

Next, by trial and error, we try to find a value for y such that $\sinh^{-1} y$ matches one of the η/η_N fractions in Table 2.2, say $\eta/\eta_N = 0.80$. This is easily done using either tables of sinh functions or the equation given in Table 2.1. The following results show that it is possible to place y within a range and then narrow that range without much difficulty. Remember, it is the *inverse* sinh values we are examining:

	Approximation				
	1		2		3
Trial y	1	2	1.40	1.60	1.50
$\sinh^{-1} y$	0.88	1.44	1.14	1.25	1.20
$(1/y)\sinh^{-1} y$	0.88	0.72	0.81	0.78	0.80

Note that the ratio η/η_N equals 0.80 at $\dot{\gamma} = 0.02$ sec^{-1}, so we identify y = 1.50 with $\beta\dot{\gamma}$ when $\dot{\gamma} = 0.02$ sec^{-1}. Therefore $\beta = 1.50/0.02 = 75$ sec and $\tau \cong 7.5$ sec.

Once a value for β has been obtained, we can calculate the value of $(1/\beta\dot{\gamma})\sinh^{-1}(\beta\dot{\gamma})$ for a range of $\beta\dot{\gamma}$ values. These fractions are tabulated in the second part of Table 2.2. We multiply η_N by these fractions to obtain η values and multiply these by $\dot{\gamma}$ to obtain σ_s. Calculated values of $\dot{\gamma}$ and σ_s are also tabulated and the latter are plotted in Fig. 2.5.

•

Examination of Table 2.2 and Fig. 2.5 enables us to judge the success of the Eyring equation. In the region of first deviations from Newtonian behavior the agreement between theory and experiment is excellent. Since the parameters are fitted with these data, no great significance should be attached to the fact that the agreement occurs here rather than elsewhere. Perhaps an equally good fit could be obtained with other parameters for a different range of experimental values. For the parameters used, theory and experiment agree to within 0.5% over an order of magnitude variation of $\dot{\gamma}$ and within 10% for one and a half orders of magnitude. On the log-log scale of Fig. 2.5 the agreement is excellent up to a $\dot{\gamma}$ value of about 1.0 sec^{-1}, at which point theoretical viscosities are less than experimental. One useful application of the Eyring equation is to extrapolate shearing forces, viscosities, and so on, over modest ranges from the conditions where they are measured.

This guarded assessment does not mean that the effort involved in deriving the Eyring equation was wasted—far from it. Several points might be noted:

1. Additional trial and error manipulation of the data might yield agreement over a somewhat wider range of conditions with slightly modified parameters.
2. The system considered in this example was chosen for convenience, not as either a best or worst case example. Eyring and co-workers have published numerous examples in which the theory (slightly modified) fits experimental data quite well.
3. The phenomenon under consideration *is* complicated and the theory developed in the last section is fairly simple—involved, but not really difficult.
4. We have successfully discovered that the transition from Newtonian to pseudoplastic behavior is governed by the product $\tau\dot{\gamma}$, or the relative values of the shear rate and the rate of molecular response.

5. We have found an alternative to the power law, Eq. (2.14), which describes experimental data as well as the latter. In the Eyring approach, however, the curve-fitting parameters have a fundamental significance in terms of a model for the flow process at the molecular level.

Next let us briefly consider how the Eyring equation might be modified to improve its agreement with experiment. As noted in item (4) above, the relaxation time plays a very important role in the theoretical development and the practical application of the Eyring model. A little reflection readily convinces us that it is also the greatest weakness of the theory. Specifically, it seems highly improbable that the slithering of a polymer chain through a tangle of similar chains would be characterized by a single relaxation time. For some of the flow segments, the barrier to displacement may be the consequence of weak London forces which attract all molecules to each other. For other segments the barrier may be much higher owing to a virtual knotting of chains together through entanglements. The response time of a heavily entangled chain is expected to be significantly longer than that for a segment which moves the same way as a nontangled small molecule. This leads us to the idea that a whole spectrum of relaxation times rather than a single value might be a more suitable way to describe the flow process.

Suppose we divide the flow segments into classes according to relaxation times and index the various states by the subscript i. Thus the relaxation time and the component of shear stress borne by the segments in class i are τ_i and F_i, respectively. The applied shear force is related to the F_i's through

$$F = \sum_i f_i F_i \tag{2.32}$$

where f_i represents the fraction of the surface occupied by segments in the ith category. We might question why the summation of effects is conducted over F rather than by assigning to different classes different values of shear rate. The explanation is that all types of segments must experience the same rate of shear; otherwise different classes of segments would move at different rates and the flow process would segregate the different regions. Instead, all experience the same shear rate, with different amounts of stress.

Equations (2.27) and (2.32) may now be combined to give

$$\sigma_s = \left(\frac{2kT}{V_h} \sum_i f_i \beta_i \frac{\sinh^{-1}(\beta_i \dot{\gamma})}{\beta_i \dot{\gamma}} \right) \dot{\gamma} \tag{2.33}$$

In writing this result, we have assumed that the same value of V_h characterizes all classes and have indicated the variation in τ by attaching the subscript i to values of β. The summation is carried out over the entire spectrum of relaxation

times. According to this modification, the viscosity of the system is given by the bracketed terms in Eq. (2.33) rather than by Eq. (2.28).

One of our previous complaints was that we had more parameters than we knew what to do with; Eq. (2.33) makes this problem even worse. It turns out, however, that using only two or three terms of Eq. (2.33) results in a usable equation with improved curve-fitting ability. Techniques have been developed for extracting acceptable parameters from experimental data in these cases (see Problem 4). Figure 2.9, for example, shows data collected from a sample of natural rubber, analyzed according to a two-term version of Eq. (2.33). The line in Fig. 2.9 is drawn according to the equation

$$\sigma_s = (1.50 \times 10^4)(6.01 \times 10^{-5}) \frac{\sinh^{-1}(6.01 \times 10^{-5}\,\dot{\gamma})}{6.01 \times 10^{-5}\,\dot{\gamma}}$$

$$+ (1.80 \times 10^4)(6.80 \times 10^{-3}) \frac{\sinh^{-1}(6.80 \times 10^{-3}\,\dot{\gamma})}{6.80 \times 10^{-3}\,\dot{\gamma}}$$

Note that the second term involves a β value which is about 100 times larger than the β value of the first term. Since the proportionality between β and τ is expected to be about the same for both classes of flow elements, this ratio also

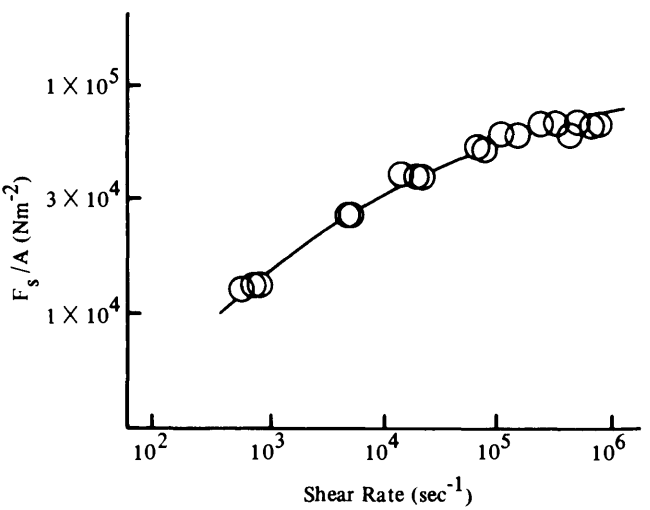

Figure 2.9 F_s/A versus shear rate for natural rubber. The line is drawn according to a two-term version of the Eyring theory. (Redrawn from Ref. 5.)

describes the relative values for the two relaxation times. Furthermore, the weighting factors for the two terms, $2kTf/V_h$, are about the same magnitude, suggesting equal surface concentration of two types of flow segments according to this analysis. This two-term, four-parameter expression accounts for the observed pseudoplasticity over three orders of magnitude of shear rate. The complication of additional terms not only results in a better fit of experimental results, but also makes sense at the molecular level. Especially when subjected to a wide range of impulse times for experimental force, an array of polymer molecules will respond with more than one characteristic relaxation time.

One of the striking omissions from our discussion has been an explicit consideration of polymer molecular weight on the viscous behavior of the sample. This omission will be corrected in the next section.

2.9 The Molecular Weight Dependence of Viscosity: Experimental Aspects

A basic theme throughout this book is that the long-chain character of polymers is what makes them different from their low molecular weight counterparts. Although this notion was implied in several aspects of the discussion of the shear dependence of viscosity, it never emerged explicitly as a variable to be investitated. It makes sense to us intuitively that longer chains should experience higher resistance to flow. Our next task is to examine this expectation quantitatively, first from an empirical viewpoint and then in terms of a model for molecular motion.

Figure 2.10 shows a plot of viscosity versus degree of polymerization for several polymers. Several things should be observed about this graph:

1. Figure 2.10 is drawn on log-log coordinates; more than two orders of magnitude in degree of polymerization are covered.
2. The viscosity values have been displaced vertically from each other by arbitrary amounts for display purposes.
3. The family of curves consist of two straight-line portions, with a change of slope occurring at a degree of polymerization in the range 10^2-10^3.
4. Numerous additional systems could be added to this display; the behavior is quite general.

One of the most striking features of Fig. 2.10 is the change of slope. Let us begin our discussion of this feature by examining the slopes of the linear portions of these lines on either side of the break. Representing the equation of a straight line by $y = ax + b$, we can write an empirical equation for the phenomena shown in Fig. 2.10 as

$$\log \eta = a \log n + b \tag{2.34}$$

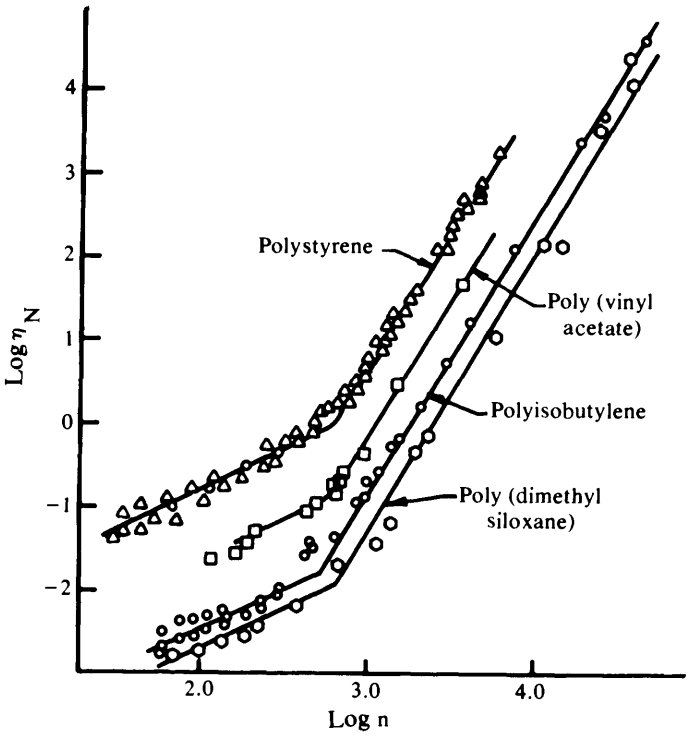

Figure 2.10 Log viscosity versus log molecular weight for several polymers. The lines are displaced vertically for display purposes. [From T. G. Fox and V. R. Allen, *J. Chem. Phys.* 41:344 (1964) with permission.]

where n is the degree of polymerization and a and b are the slope and intercept, respectively, of the linear regions. It is convenient to think of b as a logarithmic quantity also and write b = log B, so Eq. (2.34) becomes

$$\log \eta = a \log n + \log B \tag{2.35}$$

Taking the antilog of both sides yields

$$\eta = Bn^a = B'M^a \tag{2.36}$$

where the second equation follows from the direct proportion between n and the molecular weight M.

The two straight-line portions of the individual graphs are seen to be remarkably parallel, with slopes close to unity below the break and about 3.4 at higher

molecular weights. Since the slope gives the power to which the viscosity depends on molecular weight, we see that the dependence is one of direct proportion for low molecular weights—not too striking a result. For high molecular weights, on the other hand, viscosity shows a spectacular 3.4-power dependence on M. To appreciate the magnitude of this effect, we note that two samples of the same polymer differing by a factor of 2 in molecular weight will differ by a factor of more than 10 in viscosity if they fall on the high side of the break in Fig. 2.10. This extreme sensitivity of polymer viscosity to molecular weight is one of the things that makes a discussion of viscosity so important in polymer chemisty.

The empirical results contained in Fig. 2.10 present us with three challenges:

1. To account for a first-power dependence of viscosity on molecular weight for lower molecular weights.
2. To account for a 3.4-power dependence at higher molecular weights.
3. To account for the transition between the two.

It should be noted that a log-log plot condenses the data considerably and that the transition between a first-power and a 3.4-power dependence occurs over a modest range rather than at a precise cutoff. Nevertheless, the transition is read from the intersection of two lines and is identified as occurring at a degree of polymerization or molecular weight designated n_c or M_c, respectively.

In the next few sections we shall examine some of the theoretical effort which has been directed toward an understanding of these exponents. The principal difference in the theoretical approach to the two regimes of Fig. 2.10 involves the absence or presence of chain entanglements. In discussing the Eyring theory, we saw that different relaxation times might be associated with the relatively loose associations arising from London forces, while the knotting together of chains would result in more sluggish motion. A little reflection will convince us that polymers are not essentially different from any other class of compounds with respect to the first of these interaction modes: All molecules attract one another. The knotting mechanism, by comparison, is unique to long-chain structures, implying an ability of molecules to become entangled. Thus we expect that some sort of critical chain length must be exceeded before the mechanism of entanglement becomes effective. Although precise incorporation of this notion into a theoretical treatment of the phenomena is still incomplete, there is no doubt that this is the source of the breaks in the curves in Fig. 2.10. The subscript c which we have used to designate the degree of polymerization and molecular weight at the break point indicates a critical molecular weight above which entanglement effects make significant contributions to the observed viscosity.

Throughout this section we have spoken of molecular weight as if a single value characterized all samples. This contrasts sharply with the position taken in

Sec. 1.8, where polydispersity in ordinary samples was emphasized. Polydispersity clearly complicates things, especially in the neighborhood of n_c, where a significant number of molecules are too short to show entanglement effects while an equally significant fraction are entangled. We simply note that any study conducted with the intention of a molecular interpretation should be conducted on a sample with as sharp a distribution as possible.

The effect of polydispersity on the fitting of data by Eq. (2.36) may be treated as follows. We assume that, in the absence of entanglements, the observed viscosity of a polydisperse system is simply the average of viscosity contributions of each of the molecular weight fractions present, each weighted by the mass of that particular fraction in a unit volume of sample. The justification for using this weight average instead of some other rests on the theory to be presented in the next section [Eq. (2.56)]. Thus we write

$$\eta_i = K \rho_i M_i \tag{2.37}$$

where η_i, ρ_i, and M_i are, respectively, the viscosity, density, and molecular weight of the ith category of molecules; K is a constant. The experimental density and experimental viscosity are also related through the same relationship, except that some average of the molecular weight—we call it the viscosity average $\bar{M}_v$—is involved:

$$\eta_{ex} = K \rho_{ex} \bar{M}_v \tag{2.38}$$

We further note that $\rho_{ex} = \Sigma_i \rho_i$ and below the threshold for entanglements $\eta_{ex} = \Sigma_i \eta_i$. Substituting these into a combination of Eqs. (2.37) and (2.38) gives

$$\bar{M}_v = \frac{\Sigma_i \rho_i M_i}{\Sigma_i \rho_i} = \frac{\Sigma_i m_i M_i}{\Sigma_i m_i} \tag{2.39}$$

Equation (2.39) is the weight average molecular weight as defined in Sec. 1.8. It is important to note that this result, $\bar{M}_v = \bar{M}_w$, applies only in the case of nonentangled chains where η is directly proportional to M. A more general definition of $\bar{M}_v$ for the case where $\eta \propto M^a$ is

$$\bar{M}_v = \left(\frac{\Sigma_i m_i M_i^a}{\Sigma_i m_i} \right)^{1/a} = \left(\frac{\Sigma_i N_i M_i^{1+a}}{\Sigma_i N_i M_i} \right)^{1/a} \tag{2.40}$$

but this latter result does not apply in the event of chain entanglements (i.e., $a > 1$), since the simple additivity of viscosity contributions breaks down in

that case. As we shall see in Chap. 9, however, values of less than unity are often encountered in the study of the viscosity of polymer solutions. Entanglement is not a problem in dilute systems, so Eq. (2.40) is widely used in connection with solution viscosities.

2.10 A Theory for Viscosity in the Absence of Entanglements

Figure 2.11a shows a velocity gradient in a flowing liquid. Our interest is in the effect of this gradient on a (nonentangled) polymer molecule, regardless of where in the shear apparatus the molecule is located. We wish to set up a coordinate system centered on the molecule of interest. Suppose the center of mass of a polymer molecule is located in the layer labeled v_p in Fig. 2.11a. This is to be our reference point, and we wish to examine the polymer's motion relative to this point. Accordingly, we subtract v_p from each of the velocity vectors of Fig. 2.11a and shift the origin of our coordinate system to the center of mass. Figure 2.11b shows the result of this shift. This transformation enables us to see that the velocity gradient will cause the polymer molecule to rotate in a

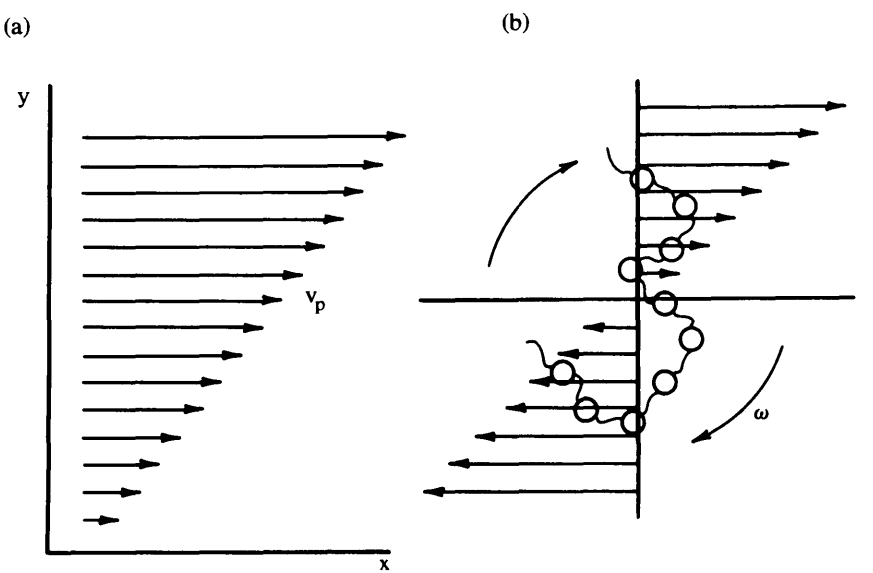

Figure 2.11 (a) The velocity gradient in a flowing liquid. (b) Velocities relative to the center of mass of a polymer molecule.

clockwise direction as shown in Fig. 2.11. Since the velocity gradients in Fig. 2.11 are the result of an applied shearing force, it is apparent that the induced rotation uses energy that was intended to produce translational motion. This is effectively a dissipation of that energy; hence Eq. (2.6) will permit us to evaluate η if the rate of energy dissipation can be related to the rate of shear.

To convert this strategy into an actual result, we must examine the mechanics of two-dimensional rotation. When the shear force is first applied, the molecule experiences an acceleration. Within a short time, however, the shear force and the force of viscous resistance to the particle movement equalize and no further net acceleration occurs. This means that the particle rotates with a constant average angular velocity. This final situation is called a stationary-state condition and is the subject of our attention. Our first problem, then, is to evaluate this average angular velocity. Even though the particle is in a stationary state, its velocity is not absolutely constant, but only constant on the average. To see that this is the case, we return to an inspection of Fig. 2.11b. Those polymer segments along the y axis bear the full brunt of the velocity gradient as an inducement to rotation. It can be shown (e.g., see Schultz's *Polymer Materials Science*) by an analysis of the torque balance under stationary-state conditions that for segments along the y axis (subscript y), $\omega_y = dv/dy$. At the same time those segments which lie along the x axis (subscript x), experience no difference in velocity relative to the center of mass of the molecule: $\omega_x = 0$. The angular velocity of a segment depends on its location relative to the center of mass in the molecule. Because of the symmetry of the rotation, the average angular velocity of a segment is the mean of these two extremes:

$$\omega = \frac{\omega_x + \omega_y}{2} = \frac{1}{2}\frac{dv}{dy} \tag{2.41}$$

Next, suppose we consider the tangential velocity v of segment i in a polymer molecule. The segment is located a distance r from the center of mass of the molecule and possesses an average angular velocity ω. The situation is sketched in Fig. 2.12a. Since $v = r\omega$, it follows that the x and y components of the velocity are given by

$$v_{x,i} = r\omega \sin \theta \tag{2.42}$$

and

$$v_{y,i} = r\omega \cos \theta \tag{2.43}$$

as shown in Fig. 2.12b.

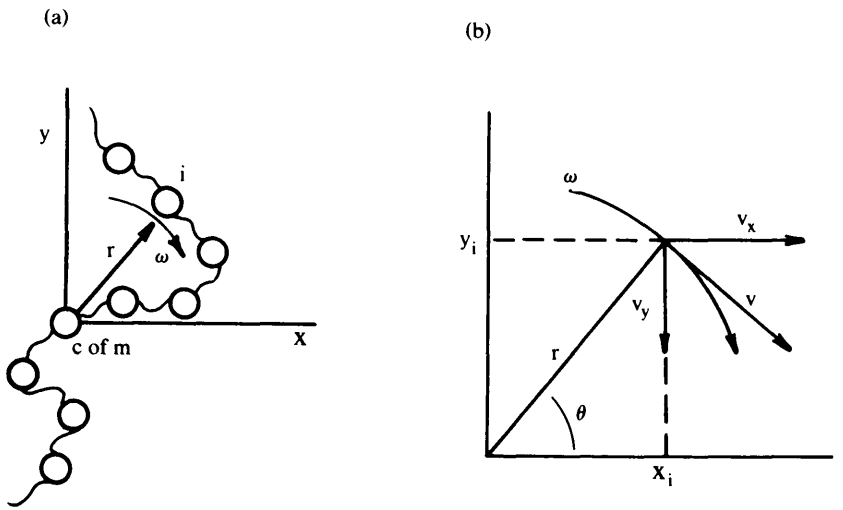

Figure 2.12 (a) Description of segment i in a polymer molecule relative to the center of mass. (b) Velocity components of segment i.

Now we must consider how the frictional force experienced by this segment is related to the tangential velocity whose components are given by these expressions.

In Chap. 9 we shall discuss in considerable detail a parameter called the molecular friction factor f. For velocities that are not too great, the friction factor expresses the proportionality between the frictional force a particle experiences and its velocity:

$$F_{vis} = fv \tag{2.44}$$

This is precisely the kind of thing we are looking for. Before proceeding, let us summarize some important properties of the friction factor:

1. It has the units required by Eq. (2.44), namely, kg sec^{-1} in the SI system.
2. For spherical particles of radius R moving through a medium of viscosity η, Stokes showed that the friction factor is given by

$$f = 6\pi\eta R \tag{2.45}$$

3. For particles of any shape at an absolute temperature T, Einstein showed that f is related to the experimental diffusion coefficient D by the expression

$$f = \frac{kT}{D} \tag{2.46}$$

where k is the Boltzmann constant.

4. The illustrious names associated with these expressions for f show that it is a factor of considerable importance and not merely a concept conjured up for the present discussion.

Strictly speaking, the friction factor as described above applies to a freely moving particle. We shall apply the same defining expression, Eq. (2.44), to the friction factor *per segment*, but shall use the symbol ζ to signify the latter. Note that neither Eq. (2.45) nor Eq. (2.46) can be exactly applied to ζ, since the segments do not move independently. Applying the concept of the segmental friction factor to the ith segment gives

$$F_{vis,i} = \zeta v_i \tag{2.47}$$

Next Eq. (2.47) can be substituted into Eqs. (2.42) and (2.43) to give the x and y components of the viscous force on segment i:

$$F_{x,i} = \zeta r\omega \sin\theta \tag{2.48}$$

and

$$F_{y,i} = \zeta r\omega \cos\theta \tag{2.49}$$

In connection with Eq. (2.6), we used the fact that the product of a viscous force and a velocity gives a rate of energy dissipation, so $F_{x,i}\, v_{x,i} + F_{y,i}\, v_{y,i}$ equals the rate of energy dissipation by segment i. Thus the energy loss per second for the ith segment $(\Delta W/\Delta t)_i$ is

$$\left(\frac{\Delta W}{\Delta t}\right)_i = \zeta r^2 \omega^2 (\sin^2\theta + \cos^2\theta) \tag{2.50}$$

Substituting Eq. (2.41) and recalling that $\sin^2\theta + \cos^2\theta = 1$, Eq. (2.50) becomes

$$\left(\frac{\Delta W}{\Delta t}\right)_i = \frac{1}{4}\zeta r_i^2 \left(\frac{dv}{dy}\right)^2 \tag{2.51}$$

For a polymer molecule consisting of n segments, this result must be summed over all the segments in the molecule to give the energy dissipated per second per polymer molecule $(\Delta W/\Delta t)_p$:

$$\left(\frac{\Delta W}{\Delta t}\right)_p = \sum_{i=1}^{n} \left(\frac{\Delta W}{\Delta t}\right)_i = \frac{1}{4} \zeta \sum_{i=1}^{n} r_i^2 \left(\frac{dv}{dy}\right)^2 \tag{2.52}$$

The summation in Eq. (2.52) corresponds to n times the square of a two-dimensional radius of gyration $r_{g,2D}$ since there is no rotation in the z direction. Our next step, therefore, is to eliminate the summation in Eq. (2.52) and replace it with an expression for $r_{g,2D}$ and then $r_{g,3D}$.

The three-dimensional radius of gyration of a random coil was discussed in Sec. 1.10 and found to equal one-sixth the mean-square end-to-end distance of the polymer [Eq. (1.59)]. What we need now is a connection between two- and three-dimensional radii of gyration. Since the molecule has spherical symmetry $r_{g,3D}^2 = r_{g,x}^2 + r_{g,y}^2 + r_{g,z}^2 = 3r_{g,x}^2$. If only two of these contributions are present, we obtain $(2/3)r_{g,3D}^2 = r_{g,2D}^2$. We use this result and Eq. (1.59) to rewrite Eq. (2.52) in terms of the mean-square end-to-end distance $\overline{r^2}$ in the polymer coil:

$$\left(\frac{\Delta W}{\Delta t}\right)_p = \left(\frac{1}{4}\right)\left(\frac{2}{3}\right)\left(\frac{1}{6}\right) \zeta n \overline{r^2} \left(\frac{dv}{dy}\right)^2 \tag{2.53}$$

This expression gives the rate of energy dissipation per molecule while we seek an expression for the rate per unit volume. In the absence of molecular coupling through entanglement, we can multiply Eq. (2.53) with the number of molecules per unit volume to achieve the desired result. The latter is given by $\rho N_A/M$, where ρ is the density, N_A is Avogadro's number, and M is the molecular weight of the polymer. Equation (2.6) shows that the coefficient of viscosity equals the proportionality factor between the rate of energy dissipation per unit volume and the square of the velocity gradient; therefore we have shown that

$$\eta = \frac{n\zeta \overline{r^2}}{36} \frac{\rho N_A}{M} \tag{2.54}$$

Next we consider a substitution for the mean-square end-to-end distance $\overline{r^2}$. At first glance this seems easy, since Eq. (1.62) gives $\overline{r^2} = nl_0^2$. There are two problems associated with the use of this substitution:

1. The derivation of Eq. (1.62) explicitly requires that n be large, while the notion of nonentanglement which underlies (2.54) precludes large values of n. Since we have not confronted the question of how large is large in either of these derivations, we proceed with this substitution, hoping for a compatibility of n values.
2. The subscript 0 on l implies Θ conditions, a state of affairs characterized in Chap. 1 by the compensation of chain-excluded volume and solvent effects on coil dimensions. In the present context we are applying this result to bulk polymer with no solvent present. We shall see in Chap. 9, however, that coil dimensions in bulk polymers and in solutions under Θ conditions are the same.

With this substitution, Eq. (2.54) becomes

$$\eta = \frac{n^2 \zeta l_0^2}{36} \frac{\rho N_A}{M} \tag{2.55}$$

Using the molecular weight of the repeat unit M_0 as the proportionality factor between n and M, we write

$$\eta = \frac{\zeta l_0^2 \rho N_A}{36 M_0^2} M = \frac{\zeta l_0^2 \rho N_A}{36 M_0} n \tag{2.56}$$

This result was published by Debye in 1946. Since we shall also encounter a light-scattering equation associated with his name, we shall refer to Eq. (2.56) and its variations as the Debye viscosity equation.

It is the presence of ρ in the proportionality factor between η and M in the Debye viscosity equation that justifies the use of this quantity as a weighting factor in the definition of the viscosity average molecular weight [e.g., Eq. (2.37)]. Of the various parameters which appear in Eq. (2.56), only ζ is unfamiliar. While many polymers differ relatively little in l_0, ρ, or even M_0, it turns out that variation in ζ span a wide range. Defining a quantity such as ζ is easy, but if we attempt to assign a numerical value to it, we find ourselves at a loss. Accordingly, the following example gives us an idea of the magnitude of ζ on the basis of some experimental viscosity data.

Example 2.3

At 217°C (490 K) a polyisobutylene sample of $\bar{M}_w$ = 25,000 has a viscosity of about 3 P. Estimate the segmental friction factor for polyisobutylene at this temperature, taking $l_0 = 5.9 \times 10^{-10}$ m and estimating ρ = 1.0 g cm^{-3}.

Solution

First verify that Eq. (2.56) is applicable; this is the case, since $M < M_c$:

$$\text{Number of molecules per unit volume} = \frac{\rho N_A}{\bar{M}_n}$$

$$= \frac{(1 \text{ g cm}^{-3})(6.02 \times 10^{23} \text{ mol}^{-1})}{(2.5 \times 10^4 \text{ g mol}^{-1})} \cong 2.4 \times 10^{19} \text{ cm}^{-3}$$

and the mean-square end-to-end distance

$$\overline{r^2} = \frac{M}{M_0} l_0^2 = \frac{25{,}000}{56} (5.9 \times 10^{-10} \text{ m})^2 = (450)(5.9 \times 10^{-10})^2$$

$$= 1.6 \times 10^{-16} \text{ m}^2$$

Substituting into Eq. (2.56) and solving for ζ yields

$$\zeta = \frac{36\eta}{(M/M_0) l_0^2 (\rho N_A/M)(M/M_0)}$$

$$= \frac{36(0.3 \text{ kg m}^{-1} \text{ sec}^{-1})}{(1.6 \times 10^{-16} \text{ m}^2)(2.4 \times 10^{-25} \text{ m}^{-3})(450)} = 6.3 \times 10^{-12} \text{ kg sec}^{-1}$$

For the same polymer this parameter has values of 4.47×10^{-8} and 5.01×10^{-11} kg sec^{-1} at 298 and 398 K, respectively. Since density is far less sensitive to temperature, these results show that the primary temperature dependence of viscosity is described by the temperature dependence of ζ.

•

2.11 The Segmental Friction Factor

The segmental friction factor introduced in the derivation of the Debye viscosity equation is an important quantity. It will continue to play a role in the discussion of entanglement effects in the theory of viscoelasticity in the next chapter, and again in Chap. 9 in connection with solution viscosity. Now that we have an idea of the magnitude of this parameter, let us examine the range of values it takes on.

To the extent that the segmental friction factor ζ is independent of M, then Eq. (2.56) predicts a first-power dependence of viscosity on the molecular weight of the polymer in agreement with experiment. A more detailed analysis of ζ shows that segmental motion is easier in the neighborhood of a chain end because the wagging chain end tends to open up the structure of the melt and

thus facilitate flow. The number of chain ends per unit volume increases as the molecular weight decreases, suggesting that ζ decreases with decreasing molecular weight. Conversely, the condition that ζ is independent of molecular weight is best realized toward higher molecular weights, where the effect of chain ends on the free volume is less. Since Eq. (2.56) does not apply in the presence of entanglements, we expect the assumption that ζ is independent of M to work best in the vicinity of M_c. At $M \ll M_c$, ζ is sensitive to M, decreasing as M decreases. For example, in studies of poly(vinyl acetate) at 40°C, ζ drops to two-thirds its value at $M = 8 \times 10^5$ for a sample with $M = 2 \times 10^5$.

A much simpler experimental situation for examining ζ arises from a study of the diffusion of small molecules through polymer samples. The small probe molecule is chosen to be similar in size to the repeat unit of the polymer. In diffusing through the polymer, the probe molecule must push its way past individual polymer segments, and presumably experiences comparable resistance to displacement. By suitable analytical techniques—for example, monitoring the progress of an isotopically labeled probe—the diffusion coefficient of the small foreign molecule can be measured. Since this molecule does move freely, its friction factor can be evaluated from the experimental diffusion coefficient via Eq. (2.46). The friction factor so obtained is then identified with the segmental friction factor. Although sensitive to the size and shape of the probe, quite acceptable agreement may be achieved between these "apparent" friction factors and those actually determined from mechanical measurements. For example, *n*-butane, isobutane, and *n*-pentane show "ζ" values of 3.47×10^{-8}, 7.76×10^{-8}, and 3.80×10^{-8} kg sec^{-1} in diffusion experiments into polyisobutelene at 25°C, while the latter has a ζ value of 4.47×10^{-8} kg sec^{-1} when measured directly.

Equation (2.56) not only enables us to understand the basis for the first-power dependence of η on M, but also presents us with a new and important theoretical parameter, the segmental friction factor. We shall see in the next chapter that it is a quantity which can also be extracted from measurements of the viscoelasticity of polymers.

Table 2.3 lists an assortment of polymers in order of decreasing ζ values. The numbers listed were obtained from viscoelastic measurements. Extensive calculations show that viscoelastic and viscosity experiments agree on the magnitude of ζ values for a given sample, although there is a consistent tendency for the values determined from viscosity to be somewhat higher than those determined from viscoelastic measurements. We shall not pursue the cause of this discrepancy, but merely note that it is not sufficient to significantly modify the order of ranking presented in Table 2.3.

The polymers compared in Table 2.3 were not all studied at the same temperature; instead, each was measured at a temperature 100°C above its respective glass transition temperature T_g. We shall discuss the latter in considerable detail

Table 2.3 Segmental Friction Factors Ranked in Order of Decreasing Values for Polymers Compared 100°C Above Their Respective Glass Transition Temperatures

Polymer	T_g (K)	$l_0 \times 10^{10}$ (m)	ζ (kg sec^{-1})
Methyl methacrylate	379	6.9	1.58×10^{-7}
Methoxyethyl methacrylate	293	7.0	9.12×10^{-8}
2-Ethyl butyl methacrylate	284	6.5	5.37×10^{-8}
Ethylene glycol monomethacrylate	366	7.0	4.27×10^{-8}
Ethyl methacrylate	335	5.9	3.98×10^{-8}
Butyl rubber	205	5.9	3.47×10^{-8}
Propoxyethyl methacrylate	253	7.0	2.51×10^{-8}
Polyisobutylene	205	5.9	2.14×10^{-8}
n-Butyl methacrylate	300	6.4	1.70×10^{-8}
n-Hexyl methacrylate	268	7.5	6.61×10^{-9}
n-Octyl methacrylate	253	7.0	4.27×10^{-9}
1-Hexene	218	7.0	3.31×10^{-9}
Urethane rubber	238	~12	9.55×10^{-10}
1,4-Butadiene	172	6.0	6.92×10^{-10}
Methyl acrylate	276	6.8	5.75×10^{-10}
Vinyl acetate	305	6.9	4.79×10^{-10}
cis-Isoprene	200	6.8	3.24×10^{-10}
Styrene	373	7.4	1.12×10^{-10}
1,2-Butadiene	261	7.6	9.77×10^{-11}
Vinyl chloride	347	6.0	3.47×10^{-11}
Dimethyl siloxane	150	6.2	3.16×10^{-11}

Source: Values from Ref. 3.

in Chap. 4. For now it is sufficient to note that this temperature is characteristic of the polymer, just as the critical temperature is a useful reference point in a discussion of liquids and gases. Thus comparing polymers a fixed temperature difference from their individual T_g value is analogous to the comparison of gases at comparable differences from their respective critical temperatures. The law of corresponding states informs us that gases behave similarly when thus compared; a similar principle is being used here.

Inspection of the results presented in Table 2.3 reveals several interesting facts:

1. The samples surveyed span a range of more than three orders of magnitude in ζ values.
2. No significant variation in l_0 value is responsible for this ranking, and no overall pattern in T_g is detectable.

3. All the entries above the broken line in Table 2.3 are disubstituted, and those below, with the exception of poly(dimethyl siloxane), are monosubstituted. Those in the former category consistently have larger values of ζ than the latter.
4. Within a homologous series such as the *n*-butyl-, *n*-hexyl-, and *n*-octyl-substituted methacrylates there is a trend for those polymers with the bulkier substituents to show smaller values of ζ. Note that there is also a correlation between substituent size and T_g within this series.
5. Some data on copolymers of ethylene and propylene (not shown) is also consistent inasmuch as the values of ζ decrease as the ethylene (unsubstituted) content increases.

It will be recalled from the definition of the friction factor, Eq. (2.47), that this parameter gives the force required to impart a unit velocity to a polymer chain segment. This force increases with increasing number of substituents, apparently because the latter interfere with free rotation along the chain backbone and thus impede chain motion. Another effect that arises from the presence of substituents and increases with their bulkiness is a decrease in the efficiency of chain packing in the sample or an increase in free volume. As noted in item (4) above, increasing free volume by bulky substituents decreases ζ. It is gratifying that experiment agrees with our intuitive expectations in this matter, that chain mobility is enhanced by open structure in the liquid and maximum flexibility for the chain.

2.12 Dealing with Entanglements: The Bueche Theory

In our discussion of Fig. 2.10 we saw that the presence of entanglements leads to a change in the molecular weight dependence of viscosity. Note that the onset of entanglements results in a change of slope for the plot of η versus M, not a discontinuity in the plot. With entanglements, η becomes considerably more sensitive to chain length, but it does not jump to infinity. We point this out, since in some ways an entanglement is like a crosslink inasmuch as the fates of two or more chains become interdependent. If entanglement coupling were identical to chemical crosslinking, the entire sample would become essentially one giant molecule and the resulting network would be a nonflowing gel. This is not the case and implies that the chains, though entangled, are still able to move, somehow slipping and sliding past one another.

We begin by assuming that entanglements occur at uniform intervals along the polymer chain, with M_e and n_e representing the molecular weight and degree of polymerization, respectively, between entanglement points. Thus each molecule in the liquid has M/M_e entanglements, or M/M_e molecules somehow attached to it. Our goal is to examine how this encumbrance will increase the force necessary

to move some reference molecule through the sample. We might expect M_c to be at least two times M_e if we picture the first entanglement occurring above M_c as dividing the chain into two portions of average length M_e. This is a very primitive picture and more detailed theories have been developed on the relationship between M_c and M_e.

As with previously developed models, the applied shearing force causes a certain molecule—we shall call it the original molecule (subscript 0)—to move with a velocity v_0. Through entanglements, some fraction s of that velocity is transmitted to another group of molecules entangled with the original. These are called primary couplings and are indicated by the subscript 1. Therefore the velocity of the chains involved through primary coupling with the original chain is

$$v_1 = sv_0 \tag{2.57}$$

In a similar fashion, a fraction of the velocity of the molecules with first-order coupling is transmitted to other molecules entangled with the latter. This is called second-order coupling (subscript 2). Still higher orders of effect radiate from the original molecule in the manner suggested by Fig. 2.13. Because of the

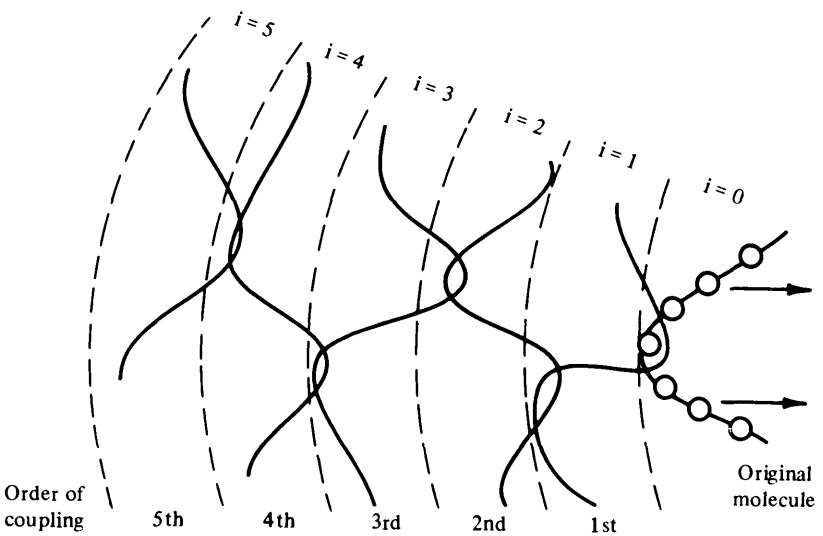

Figure 2.13 Model of several orders of coupling through entanglements according to Bueche theory.

slippage that occurs at each higher-order coupling, successively smaller fractions of the original velocity are transmitted to the higher couplings. For example, the velocity of the molecules entrained through second-order coupling is

$$v_2 = sv_1 = s^2 v_0 \tag{2.58}$$

and for order i the velocity is

$$v_i = s^i v_0 \tag{2.59}$$

Since the slippage factor is a fraction, Eq. (2.59) states in mathematical terms something we realize must be the case, namely, that the effects of entanglements on the neighbors of the original molecule must diminish as we move away from that molecule to prevent the coupling from producing an infinite viscosity.

By analogy with Eq. (2.47), we write the force of viscous resistance experienced by a molecule in an array of uniform molecules of degree of polymerization n as

$$F_{vis} = n\zeta v_0 + C_1 n\zeta s v_0 + C_2 n\zeta s^2 v_0 + \cdots = n\zeta v_0 (1 + C_1 s + C_2 s^2 \cdots) \tag{2.60}$$

where ζ is the segmental friction factor and the C_i values are constants which count the number of effective couplings of order i. The velocity of the original molecule will disappear from our equations just as it did in the Debye theory; hence our next consideration must be the constants C_i.

If this approach is to have any success, the weighting factors C_i must also decrease with increasing i to avoid a catastrophic increase in viscosity due to the proposed web of entanglements. We shall not detail the entire derivation of these C_i values as developed by Bueche but shall only note the following points:

1. Since each molecule has M/M_e entanglements, and each could entrain a different molecule, an upper limit for the number of couplings of order i is given by $(M/M_e)^i$.
2. This last factor overcounts the number of couplings, since the random placement of chain segments makes it improbable that each entanglement will involve a new molecule. Thus an entanglement may be redundant; the chain might already be coupled to the original molecule.
3. Redundancy of another type may arise if a molecule is coupled to the tangle of moving molecules more than once and in couplings of different order. Not only is one coupling sufficient to induce movement, but also the coupling of higher order will have precedence; that is, if a chain is coupled to the original molecule with both a second-order and a fifth-order coupling, it will move with the second-order fraction of v_0. This mode of

attenuation increases with i, since the likelihood of prior involvement increases with i.

Bueche was able to incorporate these ideas into a quantitative theory, the mathematical details of which need not concern us. The result is complex, but simplifies when applied to polymers of very large molecular weight. In this limit the Bueche theory predicts

$$\eta \cong \frac{(\rho N_A)^2}{1728} \frac{l_0^5 \zeta}{M_e^2} \left(\sum_i s^i (2i-1)^{3/2} \right) n^{3.5} \tag{2.61}$$

in which the complicated summation is a numerical constant for a specific value of the slippage factor s.

Equation (2.61) predicts a 3.5-power dependence of viscosity on molecular weight, amazingly close to the observed 3.4-power dependence. In this respect the model is a success. Unfortunately, there are other mechanical properties of highly entangled molecules in which the agreement between the Bueche theory and experiment are less satisfactory. Since we have not established the basis for these other criteria, we shall not go into specific details. It is informative to recognize that Eq. (2.61) contains many of the same factors as Eq. (2.56), the Debye expression for viscosity, which we symbolize η_D. If we factor the Bueche expression so as to separate the Debye terms, we obtain

$$\eta = \eta_D \frac{\rho N_A l_0^3 M_0 S}{48 M_e^2} n^{2.5} = \eta_D \frac{\rho N_A l_0^3 S}{48 M_0} \left(\frac{M}{M_e} \right)^2 n^{1/2} \tag{2.62}$$

where we have used the symbol S to signify the summation involving the slippage factors. In the second form of Eq. (2.62), two of the additional 2.5 powers of n associated with entanglements are expressed in terms of M/M_e. Since the latter gives the number of entanglements per molecule, Eq. (2.62) shows that the effect of entanglements on viscosity increases with the square of the number of entanglements per chain. It must be remembered that Eqs. (2.61) and (2.62) are derived on the premise of entanglements. Note that Eq. (2.62) does not reduce to the Debye limit for $M < M_c$.

Our discussion of Fig. 2.10 and the Debye theory show that polymer chains below a certain critical length move independently and produce a viscosity which depends on the first power of the molecular weight. Longer chains result in entanglements and a greatly increased sensitivity of viscosity to molecular weight. Figure 2.13 on which the Bueche theory is based proposes a model for the effects of entanglement, but we almost feel that it goes overboard. On one side of M_c, chains move independently; on the other, they are meshed in a web which would show infinite viscosity if it were not for the attenuation of the

coupling that Bueche carefully introduced. The problem is that independent chain mobility vanishes at the onset of entanglement according to this model. Since the latter is totally responsible for viscosity below M_c, we might find a model for entanglements more plausible if it continued to allow for the independent movement, however encumbered, of a polymer molecule for $M > M_c$. The concept of reptation introduced in the next section provides just such a model.

2.13 The Reptation Model

Figure 2.14a shows a portion of a polymer chain in which the molecule displays entanglement coupling to two other molecules. The molecule of interest is pictured as passing through a tube or sleeve, which, in turn, weaves between the obstacles presented by entangled neighbors. In terms of this picture, two types of motion can immediately be distinguished: conformational changes occurring within the confines of the tube and escape from the tube by a slalomlike motion through the sleeve. The latter is called reptation. The tube is an artifact which makes it easier to describe and distinguish between these two modes of motion.

The tube is a construct which we might continue to sketch around an emerging chain as it diffuses out of the original sleeve. Instead, it is convenient to start with the tube initially in place and consider how long it takes for the molecule to escape. The initial entanglements which determine the contours of the tube comprise a set of constraints from which the molecule is relaxing, even if only to diffuse into another similar set. Accordingly, we identify this reptation time as a relaxation time τ for the molecule.

In order to draw some conclusions about viscosity from the reptation model, it is again necessary to anticipate some results from Chap. 9 on diffusion. The

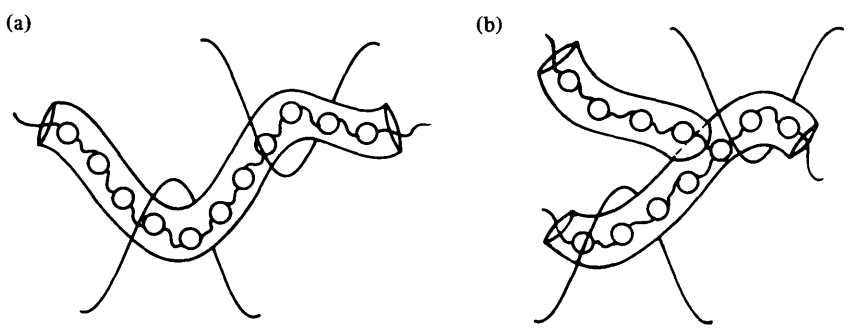

Figure 2.14 Reptation model for entanglements for (a) a linear molecule and (b) a branched molecule.

result we need relates the distance x diffused by a particle, the migration time t, and the diffusion coefficient D:

$$\overline{x^2} = 2Dt \tag{2.63}$$

If we were able to directly observe the meanderings of an individual molecule for a time t as implied by Eq. (2.63), we would find no agreement as to the displacement from one observation to another. Only the average displacement has any significance, and Eq. (2.63) states that it is specifically the squares of the displacements in a large number of experiments that are to be averaged. The situation is reminiscent of the velocities of molecules in a gas sample. Individual molecules may vary widely in velocity, yet the average of the square of individual velocities is a unique property of the gas at the temperature under consideration. Equation (2.63) was derived by Einstein and was applied to the displacements of microscopic colloidal particles by J. Perrin as the basis for an early determination of Avogadro's number. Before we apply Eq. (2.63) to reptation, there are several additional aspects of this relationship that are worth noting:

1. Since the diffusion coefficient is constant for a given material, Eq. (2.63) shows that the time required for a displacement increases with the square of the distance traveled. This can be understood by thinking that the displacement criterion would be met by finding the diffused particle anywhere on the surface of a sphere of radius x after time t if it started at the origin. The surface area of a sphere is proportional to the square of its radius.
2. An alternative way to look at this result is to ignore the averaging procedure required by Eq. (2.63) and regroup the factors $D = (1/2)(x/t)x$. Since x/t is the diffusion velocity, this version shows that the latter decreases as the displacement increases. This apparently strange result arises from the fact that we are dealing with *net* displacement and a diffusing particle follows a very irregular path. Accordingly, longer and longer times are required for larger net displacements.
3. A final interpretation of the regrouped expression given in item (2) is that 2D equals the diffusion velocity for a particle undergoing unit displacement, x = 1 m in the SI system.

With these ideas in mind, let us consider how long it would take for a polymer chain to escape from the tube shown in Fig. 2.14 by reptation.

Without implying anything about the shape of the tube, it is clear that it has the same length as the polymer chain itself, that is, nl_0. This is the displacement of interest in calculating the escape time from the tube. Therefore Eq. (2.63) becomes

$$(nl_0)^2 = 2D_{tube}\tau \tag{2.64}$$

where t has been replaced by τ in recognition of the fact that this characteristic time is in fact the relaxation time. The diffusion coefficient within the tube has been designated on the assumption that sliding along its own contour is an easier mode of motion for a polymer than net translational movement would be. Next we use Eq. (2.46) to replace D_{tube} with the friction factor for the chain in the tube:

$$(nl_0)^2 = 2\frac{kT}{f_{tube}}\tau \tag{2.65}$$

Since the tube friction factor measures the force needed to impart a unit velocity to the chain along the tube direction, we can think of applying this force, one segment at a time, to the diffusing chain. Since the friction factor per segment is ζ, Eq. (2.65) becomes

$$(nl_0)^2 = \frac{2kT}{n\zeta}\tau \tag{2.66}$$

This simple derivation gives us the desired result, a relationship between the relaxation time and the degree of polymerization:

$$\tau = \frac{l_0^2\zeta}{2kT}n^3 = \tau_0 n^3 \tag{2.67}$$

where the segmental relaxation time τ_0 is seen to be $\zeta l_0^2/2kT$ by letting $n = 1$.

The following example will give us a feel for the magnitude of the quantities involved, as well as for the reptition process itself.

Example 2.4

Assuming that Eq. (2.67) applies to small molecules in the limit as $n \to 1$, calculate τ_0, using $D \cong 3 \times 10^{-9}$ m^2 sec^{-1} for a typical low molecular weight molecule. Use this value of τ_0 to estimate τ for a polymer with $n = 10^4$. Based on Eq. (2.63), evaluate D_{tube} and D_p, the net diffusion coefficient for bulk polymer, from these results.

Solution

Assume that kT/ζ can be replaced by D when Eq (2.67) is applied to small molecules. Use a representative value from Table 2.3, say, 6×10^{-10} m, as a value for l_0 and the D value given to estimate τ_0:

$$\tau_0 = \frac{l_0^2}{2D} = \frac{(6 \times 10^{-10}\ \text{m})^2}{2(3 \times 10^{-9}\ \text{m}^2\ \text{sec}^{-1})} = 6 \times 10^{-11}\ \text{sec}$$

The corresponding quantity for a polymer is larger by n^3 according to Eq. (2.67). For $n = 10^4$,

$$\tau = \tau_0 n^3 = (6 \times 10^{-11}\ \text{sec})(10^4)^3 = 60\ \text{sec}$$

Diffusion coefficients are obtained by dividing the square of the length of distance covered by twice this time [Eq. (2.64)]. The length of the reptation tube is nl_0; therefore

$$D_{\text{tube}} = \frac{(nl_0)^2}{2\tau} = \frac{[10^4(6 \times 10^{-10}\ \text{m})]^2}{2(60\ \text{sec})} = 3 \times 10^{-13}\ \text{m}^2\ \text{sec}^{-1}$$

The net displacement of the molecule is very much less than the length of the tube because of the jumbled configuration of the chain. In time τ the net displacement is on the order of the root mean square of the end-to-end distance [Eq. (1.62)]; that is, in Eq. (2.63), $\overline{x^2} = \overline{r_0^2} = nl_0^2$, so for net diffusion

$$D_{\text{net}} = \frac{nl_0^2}{2\tau} = \frac{10^4(6 \times 10^{-10}\ \text{m})^2}{2(60\ \text{sec})} = 3 \times 10^{-17}\ \text{m}^2\ \text{sec}^{-1}$$

Note that the diffusion coefficient for a polymer through an environment of low molecular weight molecules is typically on the order of magnitude of 10^{-11} m^2 sec^{-1}. If the first subscript indicates the diffusing species, and the second the surrounding molecules, and P stands for polymer and S for small molecules, we see that the order of diffusion coefficients is $D_{S,S} > D_{P,S} > D_{P,\text{tube}} > D_{P,P}$, a sequence which makes sense in terms of relative frictional resistance.

•

Before continuing with an application of the reptation model to the viscosity of polymer melts, it is interesting to note that the third-power dependence of relaxation time on degree of polymerization [Eq. (2.67)] has been verified in experiments in which polymer chains are trapped in a network. In one study, for example, styrene-butadiene (S-B) copolymers consisting of blocks of S and of B were mixed with homopolymers of B, the latter with variable molecular weights. The temperature is then lowered such that the S blocks experience phase separation, effectively crosslinking the copolymer network and trapping the chains of pure B. The relaxation behavior of B was then monitored and found to depend on the 3.1 power of n_B—quite acceptable agreement with the predictions of Eq. (2.67). Note the assortment of polymer concepts and phenomena involved in this experiment:

1. Homopolymers versus copolymers.
2. Copolymer microstructure (block structure).

3. Controlled chain length (either by preparation or fractionation).
4. Effective crosslinking by phase separation (could also be accomplished chemically or by crystallization).
5. Direct determination of relaxation time through viscoelastic studies (all mechanical properties involve this important parameter).
6. Tailoring polymeric systems to suit an experimental model.

The behavior of molecules trapped in a network satisfies us that we are on the right track; we continue by applying this relaxation time to viscous behavior.

In connection with a discussion of the Eyring theory, we remarked that Newtonian viscosity is proportional to the relaxation time [Eqs. (2.29) and (2.31)]. What is needed, therefore, is an examination of the nature of the proportionality between the two. At least the molecular weight dependence of that proportionality must be examined to reach a conclusion as to the prediction of the reptation model of the molecular weight dependence of viscosity.

Apart from some numerical coefficients, the details of which we shall forgo, the required proportionality factor involves kT and the concentration of entanglement points. Multiplying Eq. (2.67) by these factors, we obtain

$$\eta \propto kT\left(\frac{M}{M_e}\right)\left(\frac{\rho N_A}{M}\right)\left(\frac{l_0^2\zeta}{2kT}\right) n^3 \tag{2.68}$$

where M/M_e gives the number of entanglements per chain and $\rho N_A/M$ gives the number of chains per unit volume. Since these additional involvements of molecular weight cancel, the relaxation time alone determines the power dependence of viscosity on molecular weight according to the reptation model.

The reptation model, developed largely by de Gennes, Doi, and Edwards, is thus seen to predict a very strong dependence of viscosity on molecular weight, although not quite the 3.4-power dependence observed experimentally. Although not quite as successful in this regard as the Bueche theory, the reptation model is vastly simpler and is consistent with experiments in other areas. Finally, reptation provides us with an excellent model for the discussion of the role of chain branching on viscosity. This is the topic of the next section.

2.14 The Effects of Branching

In the foregoing discussions of theoretical models and experimental results, we have focused on linear polymers. We have seen the effect of chain substituents on viscosity. All other things being equal, bulky substituents tend to decrease ζ and thereby lower η. The effect is primarily due to the opening up of the liquid because of the steric interference with efficient packing arising from the substituents. With side chains of truly polymeric character, the picture is quite different.

Figure 2.14b suggests how the reptation picture for linear chains must be modified by the presence of side chains. While we can visualize the unbranched molecule sliding along its reptation tube relatively easily, the polymeric side chain interferes considerably. Since the side chain is enclosed in its own tube, sliding the main chain along entails withdrawing the side chain from its sleeve and inserting it into a new, equivalent one located a step farther along the contour of the main tube. How long does it take to move this branch chain from one sleeve to another?

If the side chain were an independent molecule, its escape time from its sleeve would be given by Eq. (2.67), with n replaced by the degree of polymerization n_s of the side chain. This is not the case, however, since the loose end of the side chain must retrace its steps out of the sleeve before the other end, the branch point along the backbone, can move. Our interest is in the probability of such a withdrawal path occurring among all the possible modifications of conformation the side chain can undergo. It is clear that the probability of such a path being followed will decrease with increasing n_s, and detailed theoretical analysis of the problem suggests that the probability P depends on the length of the side chain as follows:

$$P = Ae^{-an_s} \tag{2.69}$$

where A and a are constants.

Aside from the side chains, the movement of the backbone along the main reptation tube is still given by Eq. (2.67). With the side chains taken into account, the diffusion velocity must be decreased by multiplying by the probability of the side-chain relocation. Since the diffusion velocity is inversely proportional to τ, Eq. (2.67) must be divided by Eq. (2.69) to give the relaxation time for a chain of degree of polymerization n carrying side chains of degree of polymerization n_s:

$$\tau = A\tau_0 n^3 e^{an_s} \tag{2.70}$$

Comparing Eqs. (2.68) and (2.70) suggests that the effect of branching on η might be an exponential increase with the length of the side chain, provided that the entanglement mechanism is operative for both the branched and unbranched samples being compared:

$$\eta_{br} = \eta_{unbr} e^{an_s} \tag{2.71}$$

or

$$\ln \frac{\eta_{br}}{\eta_{unbr}} = an_s + \text{const.} \tag{2.72}$$

We must be careful in assessing the experimental results on the viscosity of branched polymers. If we compare two polymers of identical molecular weight, one branched and the other unbranched, it is possible that the branched one would show lower viscosity. Two considerations enter the picture here. First, since the side chains contribute to the molecular weight, the backbone chain

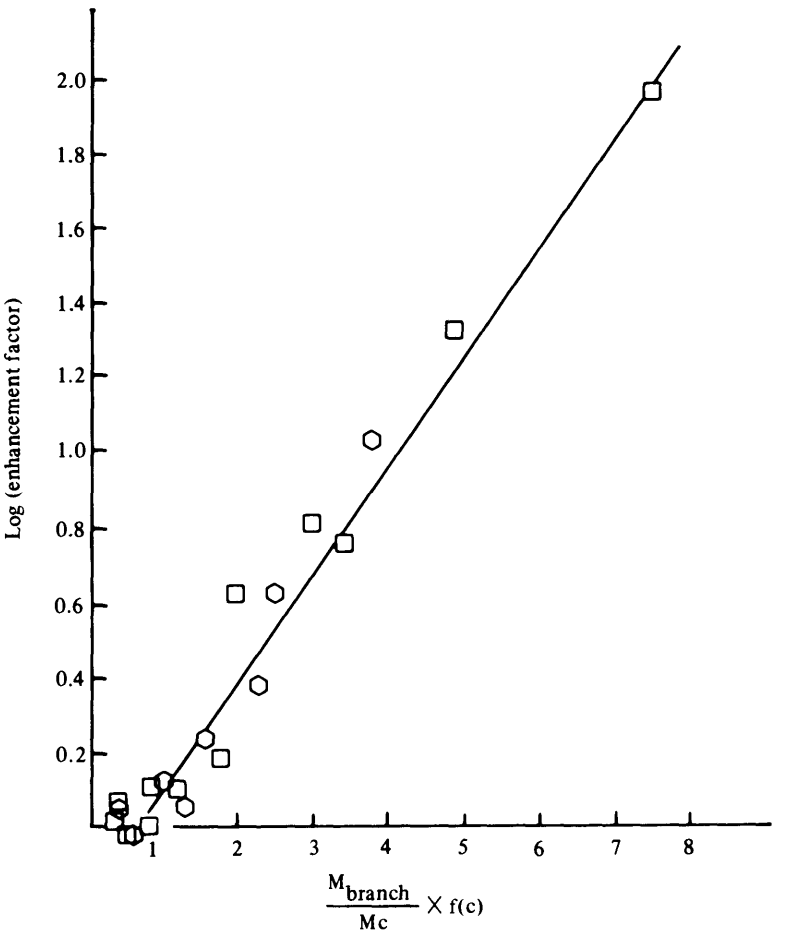

Figure 2.15 Log of viscosity enhancement factor versus parameter measuring branch length for polyisoprene. [Data from W. W. Graessley, T. Masuda, J. E. I. Roovers, and N. Hadjichristidis, *Macromolecules* 9:127 (1976).]

is shorter for the branched polymer. Second, the branched molecule is more compact and may actually be below the entanglement threshold in terms of chain length if not molecular weight. It would then be totally inappropriate to compare its behavior with a linear polymer having entanglements.

Figure 2.15 is a plot of experimental results which is consistent with the relationship given by Eq. (2.72). The systems investigated as the basis for Fig. 2.15 were branched polyisoprene samples. The polymers are called star molecules, consisting of four or six arms of equal length. Some were measured in bulk, and others in solution. The viscosity enhancement factor plotted in Fig. 2.15 is different than a simple ratio of experimental viscosities, but measures essentially the same thing. Likewise, the abscissa values have been multiplied by a function of the concentration of the polymer to reduce data from different experimental conditions to a single line. Since this axis is proportional to n_s, however, the data in Fig. 2.15 are consistent with the predictions of Eq. (2.72). The same research obtained similar results for three-arm polybutadiene stars. Note that the molecular weights of the branches in Fig. 2.15 are listed as multiples of M_c, indicating that the molecules are above the entanglement threshold in all cases.

The molecules used in the study described in Fig. 2.15 were model compounds characterized by a high degree of uniformity. When branching is encountered, it is generally in a far less uniform way. As a matter of fact, traces of impurities or random chain transfer during polymer preparation may result in a small amount of unsuspected branching in samples of ostensibly linear molecules. Such adventitious branched molecules can have an effect on viscosity which far exceeds their numerical abundance. It is quite possible that anomalous experimental results may be due to such effects.

Problems

1. The following are approximate σ_s (in dyne cm^{-2}) versus $\dot{\gamma}$ data† for three different samples of polyisoprene in tetradecane solutions of approximately the same concentration:

†W. W. Graessley, T. Masuda, J. E. L. Rovers, and H. Hadjichristidis, *Macromolecules* 9:127 (1976).

sample:	P-4	S-6	H-3
$\bar{M}_w$ (g mol^{-1})	1.61×10^6	1.95×10^6	1.45×10^6
Description	Linear	Four-armed star	Six-armed star
C (g cm^{-3})	0.0742	0.0773	0.0778
$\dot{\gamma}$ (sec^{-1})	$\sigma_s \times 10^{-3}$	$\sigma_s \times 10^{-3}$	$\sigma_s \times 10^{-2}$
0.6	0.7	–	–
0.8	0.9	–	–
1	1	0.3	–
2	2	0.6	–
4	4	1	0.15
8	5	2	0.3
10	6	3	0.4
20	7	4	0.8
60	–	7	2
100	–	8	4

From plots of these data, estimate the Newtonian viscosity of each of the solutions and the approximate rate of shear at which non-Newtonian behavior sets in. Are these two quantities better correlated with the molecular weight of the polymer or the molecular weight of the "arms"?

2. Wagner and Dillon† have described a low-shear viscometer in which the inside diameter of the outer, stationary cylinder is 30 mm and the outside diameter of the inner, rotating cylinder is 28 mm; the rotor is driven by an electromagnet. The device operates at 135°C and was found to be free of wobble and turbulence for shear rates between 3 and 8 sec^{-1}. The conversion of Eq. (2.7) to Eq. (2.9) shows that $F/A = (\eta)(dv/dr)$ (instrument constant) for these instruments Evaluate the instrument constant for this viscometer.
3. A fluid of viscosity η is confined within the gap between two concentric cylinders as shown in Fig. 2.3b. Consider a cylindrical shell of radius r, length l, and thickness dr located within that gap.
   (a) What is the torque acting on the shell if torque is the product of force and the distance from the axis and $F/A = \eta r\, d\omega/dr$?
   (b) Under stationary-state conditions, the torques at r and at r + dr must be equal, otherwise the shell would accelerate. This means that the torque must be independent of r. Show that this implies the following variation of ω with r: $\omega = -B/2r^2 + C$, where B and C are constants.
   (c) Evaluate the constant B by noting that $\omega = \omega_{ex}$, the experimental velocity, at r = R and $\omega = 0$ at r = fR.
   (d) Combine the results of (a), (b), and (c) to obtain Eq. (2.7).

†H. L. Wagner and J. G. Dillon, *Polym. Prepr.* 22:260 (1981).

4. The two-term version of equaton (2.33) contains four parameters. It may be written as

$$\frac{F}{A} = \left(\alpha_1\beta_1 \frac{\sinh^{-1}(\beta_1\dot{\gamma})}{\beta_1\dot{\gamma}} + \alpha_2\beta_2 \frac{\sinh^{-1}(\beta_2\dot{\gamma})}{\beta_2\dot{\gamma}}\right)\dot{\gamma} = \eta\dot{\gamma}$$

It is sometimes observed that β_1 is sufficiently small that $\sinh^{-1}(\beta_1\dot{\gamma})/\beta_1\dot{\gamma} = 1$ for all $\dot{\gamma}$ values, in other words, an exclusively Newtonian contribution. In such a case $\eta = \eta_N + \alpha_2\beta_2 \sinh^{-1}(\beta_2\dot{\gamma})/\beta_2\dot{\gamma}$. Consider both limiting values of $(1/\beta\dot{\gamma}) \sinh^{-1}(\beta\dot{\gamma})$ from Table 2.1 to suggest a procedure whereby η_N, α_2, and β_2 could be evaluated from experimental data describing F/A versus $\dot{\gamma}$, assuming that this model applies and that data are available over a sufficiently wide range of $\dot{\gamma}$ values.

5. The bulk viscosity of polystyrene ($\bar{M}_w$ = 371,000) at 200°C was measured by Graessley and Segal† at different rates of shear. At low rates of shear η_N = 330,000 P and drops off with $\dot{\gamma}$ approximately as follows:

$\dot{\gamma}$ (sec^{-1})	0.03	0.1	0.3	1	3
η/η_N	0.89	0.76	0.56	0.35	0.22

Does a β value of 1, 10, or 100 sec work best in Eq. (2.28) to describe the variation of η with $\dot{\gamma}$ for this sample? Note that no single-term version of the Eyring theory gives a totally acceptable fit.

6. A slightly different but useful way of defining the viscosity average molecular weight is the following:

$$\overline{M_v^a} = \frac{\Sigma_i f_i M_i M_i^a}{\Sigma_i f_i M_i}$$

where $f_i M_i$ is the weighting factor used to average M_i^a. A satisfactory way of treating many polymer distributions is to define

$$f_i = \frac{1}{\bar{M}_n} e^{-M_i/\bar{M}_n}$$

Then

$$\overline{M_v^a} = \frac{\int_0^\infty f_i M_i^{a+1}\, dM_i}{\int_0^\infty f_i M_i\, dM_i}$$

Combine the last two expressions and integrate to express $\bar{M}_v$ in terms of $\bar{M}_n$ and a. The integrals are standard forms and are listed in integral tables as gamma functions.

†W. W. Graessley and L. Segal, *A.I.Ch.E. J.* 16:261 (1970).

7. Pearson et al.† determined the viscosity average molecular weight of polyisoprene samples working with solutions of the polymer in toluene. For this system, the a value in Eq. (2.40) is known to be 0.74. Use the results of the last problem and tables of gamma functions (e.g., *CRC Handbook of Tables for Mathematics*) to convert the following viscosity average molecular weights to number average molecular weights: 13,300, 31,300, 80,000, 205,000, 220,000, 270,000, 490,000, 560,000, and 1,150,000. If $(M_c)_n$ for polyisoprene is 10^4, estimate the number of entanglements per chain each of these samples would display in the bulk.
8. At 200°C the Newtonian viscosities of polystyrene samples of different molecular weights were studied by Spencer and Dillon‡ and the following results were reported:

$\bar{M}_w \times 10^{-3}$ (g mol^{-1})	η_N (P)
86	3.50×10^3
162	4.00×10^4
196	6.25×10^4
360	4.81×10^5
490	1.89×10^6
508	1.00×10^6
510	1.64×10^6
560	3.33×10^6
710	6.58×10^6

Use these data to determine the exponent of M in the relationship between η_N and M.
9. The Newtonian viscosities of polystyrene samples were measured at 183°C and the following results were reported by Graessley and Segal§:

$\bar{M}_w$ (g mol^{-1})	117,000	179,000	217,000	242,000
η_N (P)	25,700	109,000	190,000	295,000

What power dependence on M does η display according to these results? Comment on the significance of the 3.4-power law according to these data and the results of the last problem.
10. A semiempirical way of extending the Debye equation to molecular weights above M_c is given by multiplying the right-hand side of Eq. (2.56) by $(M/M_c)^{2.4}$. For a poly(dimethyl siloxane) sample of $\bar{M}_w = 1.34 \times 10^6$,

† D. S. Pearson, A. Mera, and W. E. Rochefort, *Polym. Prepr.* 22:102 (1981).
‡ R. S. Spencer and R. E. Dillon, *J. Colloid Sci.* 4:241 (1949).
§ W. W. Graessley and L. Segal, *A.I.Ch.E. J.* 16:261 (1970).

Plazek et al.† measured η_N to be 7.50×10^6 P at 25°C when $\rho = 0.974$ g cm^{-3}. Using 24,500 as the value for M_c and taking the value of l_0 from Table 2.3, estimate the value of ζ which is consistent with these data. How does this value compare with the ζ value listed in Table 2.3?

11. Once the value of the constant and the a value in Eq. (2.36) have been evaluated for a particular system, viscosity measurements constitute a relatively easy method for determining the molecular weight of a polymer. Criticize or defend the following proposition: Since viscosity is so highly dependent on molecular weight for $M > M_c$, a 10% error in η will result in a 34% error in M above M_c, but only a 10% error in M below M_c.
12. A polystyrene sample of relatively narrow molecular weight distribution ($\bar{M}_w/\bar{M}_n = 1.07$) has a molecular weight of 275,000. Its viscosity was found‡ to be 10^7 kg m^{-1} sec^{-1}. Evaluate the S factor in Eq. (2.62) which is compatible with the result, taking $M_e = 16{,}000$ and using $\zeta = 10^{-8}$ kg sec^{-1} and $\rho = 1.0$ g cm^{-3} at 160°C, the temperature of the experiment. Evaluate the first 10 terms of the summation in Eq. (2.61) for s = 0.4 and 0.5 and compare with the experimental S value.
13. A sphere of density ρ_2 and radius R falling through a medium of density ρ_1 and viscosity η experiences three kinds of forces: gravitational, buoyant, and frictional. The latter is given by Eqs. (2.44) and (2.45). During most of the fall (excluding the very beginning and the very end of the path), these forces balance. Use this condition to derive an equation showing how this stationary-state velocity of fall is related to R, ρ_1, ρ_2, and η. This is the basis for the so-called falling-ball viscometer.
14. Plazek et al.† measured the viscosities of a poly(dimethyl siloxane) sample of $\bar{M}_w = 4.1 \times 10^5$ over a range of temperatures using the falling-ball method. Stainless steel ($\rho_2 = 7.81$ g cm^{-3}) balls of two different diameters, 0.1590 and 0.0966 cm, were used at 25°C, where $\rho_1 = 0.974$ g cm^{-3} and $\eta = 8.64 \times 10^4$ P. Use the result derived in the last problem to calculate the ratio of the stationary-state settling velocities for the two different balls. How long would it take the smaller ball to fall a distance of 15 cm under these conditions?
15. At concentrations roughly five times higher than those described in Problem 1, the same polymer samples show§ the following Newtonian viscosities:

	P-4	S-6	H-3
C (g cm^{-3})	0.331	0.326	0.329
η_N (P)	1.35×10^6	3.8×10^7	4.7×10^5

†D. J. Plazek, W. Dannhauser, and J. D. Ferry, *J. Colloid Sci.* 16:101 (1961).
‡S. Onogi, T. Masuda, and K. Kitagawa, *Macromolecules* 3:109 (1970).
§W. W. Graessley, T. Masuda, J. E. L. Roovers, and N. Hadjichristidis, *Macromolecules* 9:127 (1976).

Criticize or defend the following proposition: In dilute solutions, branching affects viscosity only inasmuch as the branched molecule has a more compact shape. At higher concentrations, the effect of branching is closer to a bulk effect.

Bibliography

1. Bueche, F., *Physical Properties of Polymers*, Interscience, New York, 1962.
2. deGennes, P. G., *Scaling Concepts in Polymer Physics*, Cornell University Press, Ithaca, N.Y., 1979.
3. Ferry, J. D., *Viscoelastic Properties of Polymers*, Wiley, New York, 1980.
4. Krausz, A. S., and Eyring, H., *Deformation Kinetics*, Wiley, New York, 1975.
5. Ree, T., and Eyring, H., in *Rheology*, Vol. 2 (F. R. Eirich, Ed.), Academic, New York, 1958.
6. Schultz, J., *Polymer Materials Science*, Prentice-Hall, Englewood Cliffs, N.J., 1974.

3

The Elastic and Viscoelastic States

Our time has seen
The synthesis of polyisoprene
And many cross-linked helixes unknown
To *Robert Hooke*; but each primoridal bean
Knew cellulose by heart . . .

The Dance of the Solids, by John Updike

3.1 Introduction

In this chapter we examine the elastic behavior of polymers. We shall see that this behavior is quite different from the elasticity displayed by metals and substances composed of small molecules. This is a direct consequence of the chain structure of the polymer molecules. In many polymers elasticity does not occur alone, but coupled with viscous phenomena. The combination of these effects is called viscoelasticity. We shall examine this behavior as well.

The elastic and viscoelastic properties of materials are less familiar in chemistry than many other physical properties; hence it is necessary to spend a fair amount of time describing the experiments and the observed response of the polymer. There are a large number of possible modes of deformation that *might* be considered: We shall consider only elongation and shear. For each of these we consider the stress associated with a unit strain and the strain associated with a unit stress; the former is called the modulus, the latter the compliance. Experiments can be time independent (equilibrium), time dependent (transient), or periodic (dynamic). Just to define and describe these basic combinations takes us into a fair amount of detail and affords some possibilities for confusion. Pay close attention to the definitions of terms and symbols.

We shall rely heavily on models again in this chapter; this time they are of two different types. We shall consider elasticity in terms of a molecular model in which the chains are described by random flight statistics. The phenomena of

viscoelastic behavior are also discussed in terms of models, but here they are mechanical equivalents to the whole sample and do not involve molecular parameters. Finally, the Rouse theory for viscoelasticity involves a model that describes the vibrations of molecules in mechanical terms. Like the composite behavior it describes, the beads and springs of the Rouse theory comprise a combination model.

Temperature is an important variable in the discussion of viscoelasticity. For reasons of pedagogy, most consideration of this variable is deferred to the next chapter. This does not mean that temperature is unimportant to the present discussion, only that the agenda is full enough without it.

3.2 Elastic Deformation

The various elastic and viscoelastic phenomena we discuss in this chapter will be developed in stages. We begin with the simplest: the case of a sample that displays a purely elastic response when deformed by simple elongation. On the basis of Hooke's law, we expect that the force of deformation—the stress—and the distortion that results—the strain—will be directly proportional, at least for small deformations. In addition, the energy spent to produce the deformation is recoverable: The material snaps back when the force is released. We are interested in the molecular origin of this property for polymeric materials but, before we can get to that, we need to define the variables more quantitatively.

A quantitative formulation of Hooke's law is facilitated by considering the rectangular sample shown in Fig. 3.1a. If a force F is applied to the face of area A, the original length of the block L_0 will be increased by ΔL. Now consider the following variations:

1. Imagine subdividing the block into two portions perpendicular to the direction of the force, as shown in Fig. 3.1b. Each slice experiences the same force as before, and the same net deformation results. A deformation $\frac{1}{2}\ \Delta L$ is associated with a slice of length $L_0/2$. The same argument could be applied for any number of slices; hence it is the quantity $\Delta L/L_0$ which is proportional to the force.
2. Imagine subdividing the face of the block into two portions of area A/2. A force only half as large would be required for each face to produce the same net distortion. The same argument could be applied for any degree of subdivision; hence it is the quantity F/A which is proportional to $\Delta L/L_0$.
3. Force per unit area along the axis of the deformation is called the uniaxial tension or stress. We shall use the symbol σ as a shorthand replacement for F/A and attach the subscript t to signify tension. The elongation, expressed as a fraction of the original length $\Delta L/L_0$ is called the strain. We shall use γ_t as the symbol for the resulting strain (subscript t for tension). Both σ

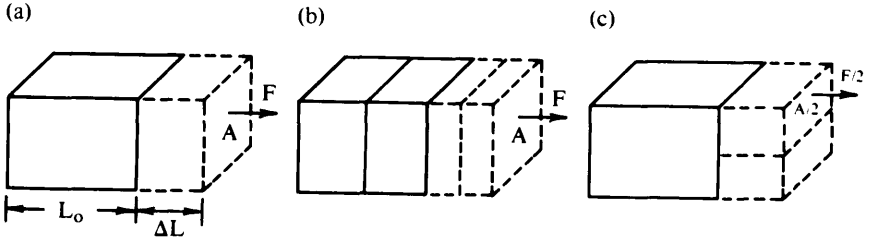

Figure 3.1 (a) The force F applied to area A extends the length of the block from L_0 by an amount ΔL. Parts (b) and (c) illustrate the argument that $F/A \propto \Delta L/L$.

and γ were encountered in the last chapter under conditions of shear. We shall take up shear deformation presently.

With these considerations in mind, we write

$$\sigma_t = E\gamma_t = E\left(\frac{\Delta L}{L_0}\right)_t \tag{3.1}$$

where the proportionality constant E is called the tensile modulus or Young's modulus. Remember, it will be different for different substances and for a given substance at different temperatures. For the present we assume that E is independent of time, but we shall remove this constraint eventually. Since γ is dimensionless, E has the same units as F/A, namely, force length^{-2}, or Nm^{-2} in the SI system. Note that Eq. (3.1) also applies to the case of compression.

There is another aspect of tensile deformation to be considered. The application of a distorting force not only stretches a sample, but it also causes the sample to contract at right angles to the stretch. If w and h represent the width and height of area A in Fig. 3.1, both contract by the same fraction, a fraction which is related in the following way to the strain:

$$\frac{\Delta w}{w} = \frac{\Delta h}{h} = \mu\frac{\Delta L}{L_0} \tag{3.2}$$

where the constant μ is called Poisson's ratio. Poisson's ratio is also a property of the material; it may be written as

$$\mu = \tfrac{1}{2}\left(1 - \frac{1}{V}\frac{dV}{d\gamma}\right) \tag{3.3}$$

where V is the volume of the sample. Thus if the volume does not change on elongation, the fractional contraction in each of the perpendicular directions is half the fractional increase in length. It takes two parameters to describe the response of a sample to tensile force, for example, E and μ. Other constants can be defined, but two are needed for the general case, regardless of how they are defined.

Although we are not specifically interested in time-dependent behavior in this section, it will be helpful to examine the temporal development of the elongation experiment described above. When the force is first applied, the sample begins to stretch, starting from $\Delta L = 0$. Eventually an elongation consistent with the applied force is reached. It is this point in the history of our experiment that we are describing. The time development of the strain is not our concern for the present. Except for the difference between tensile and shear forces, the situation described in Fig. 3.1 resembles Fig. 2.1, the defining figure for viscosity. The sample behaves differently, however. In the case of viscosity, the deformation is more accurately called flow: It is not recovered when the force is removed. For purely elastic behavior, the sample does not flow, and the deformation is fully recoverable. For substances composed of small molecules, nearly perfect Newtonian behavior is associated with the liquid state. Likewise, the solid state is associated with elastic behavior, although the origin of the elasticity is quite different in substances composed of small molecules than for polymers. Many polymers show the superpositioned effects of elastic deformation and viscous flow and in this sense are intermediate between simple liquids and solids. We shall avoid words like *solid* and *liquid* altogether, since the superficial appearance of a sample can be misleading. A specimen can look solid, for example, yet achieve flow deformation over a long period of time. Alternatively, it may appear to flow, but eventually reach an equilibrium deformation. Observation over a long period of time is required for accurate characterization. For the present, we shall assume that our tensile experiment has had all the time it needs to reach its equilibrium deformation. We shall postpone time-dependent viscoelastic behavior until we have dealt with elasticity alone.

Throughout this chapter we shall take a very liberal attitude toward time. When time-dependent properties are examined, we shall examine a time range in seconds spanning 18 powers of 10. On this scale, if the shortest time were 1 sec, the longest would be 3×10^{10} years! Obviously the shortest time must be very much less than 1 sec, but measuring extremely short times is as much of a challenge as measuring extremely long times. The way out of this predicament is to conduct measurements over a range of temperatures. A variation of 100°C in temperature may have the same effect on the viscoelastic properties of a substance as does a time span of 10^{10} sec. Since the former is readily achieved, it is clearly the method of choice. Results determined at different temperatures are subsequently reduced to a common temperature. The extraordinary time scales cited above are the result. The procedure for this reduction

to a common temperature is taken up in the next chapter. In this chapter we shall mostly describe isothermal data—in the reduced form if not experimental—and discuss very long and very short times with equal ease. To maintain contact with reality in the face of this strategy, the time-temperature equivalency should be borne in mind. Although not our primary concern in this chapter, we shall have more than one occasion to point out this equivalency.

Next let us consider the differences in molecular architecture between polymers which exclusively display viscous flow and those which display a purely elastic response. To attribute the entire effect to molecular structure we assume the polymers are compared at the same temperature. Crosslinking between different chains is the structural feature responsible for elastic response in polymer samples. If the crosslinking is totally effective, we can regard the entire sample as one giant molecule, since the entire volume is permeated by a continuous network of chains. This result was anticipated in the discussion of the Bueche theory for chain entanglements in the last chapter, when we observed that viscosity would be infinite with entanglements if there were no slippage between chains.

The details of chemical crosslinking need not concern us, but some examples will illustrate materials with the potential to display elasticity:

1. Natural rubber, cis-1,4-polyisoprene, cross-linked with sulfur. This reaction was discovered by Goodyear in 1839, making it both historically and commercially the most important process of this type. This reaction in particular and crosslinking in general are also called vulcanization.
2. Vinyl polymers cross-linked with divinyl monomers, for example, polystyrene polymerized in the presence of divinyl benzene.
3. Condensation polymers prepared with some monomer of functionality greater than 2, for example, a polyester formed with some glycerol or tricarboxylic acid.
4. Polyethylene cross-linked by irradiation with high-energy electrons.
5. Polysilicones cross-linked by reaction with benzoyl peroxide.

The concentration of crosslink junctions in the network is also important: if too low, flow will be possible; if too high, the maximum attainable elongation will be decreased. From the point of view of theoretical analysis, the length of chain between crosslink points must be long enough to be described by random flight statistics.

Stretching a polymer sample tends to orient chain segments and thereby facilitate crystallization. The incorporation of different polymer chains into small patches of crystallinity is equivalent to additional crosslinking and changes the modulus accordingly. Likewise, the presence of finely subdivided solid particles, such as carbon black in rubber, reinforces the polymer in a way that imitates the effect of crystallites. Spontaneous crystal formation and reinforcement

by fillers are both important in technology, but since they complicate the picture of the polymer network, we shall not consider them further at this time.

Merely having a cross-linked polymer does not guarantee good elastic properties. For the latter, the polymer chains should also have relatively unhindered rotation along the chain backbone so that distortions occur rapidly in response to the applied force. Thus a high local mobility is desirable, while the overall mobility of the chains must be blocked so that they will snap back when the force is removed. High chain mobility also works in favor of promoting crystallinity, and the latter is undesirable if high elasticity is sought. So optimization in the context of mechanical properties consists in finding a polymer with good chain mobility, but not so good as to produce crystallization. From a practical point of view, the glass transition temperature should be well below the temperature at which the elasticity is desired. The glass transition temperatures of a number of polymers are listed in Table 2.3. Inspection of Table 2.3 shows that a number of hydrocarbon polymers–such as 1,4-butadiene, cis-isoprene, butyl rubber, and polyisobutylene–have low values of T_g and thus the potential for a wide working range. We shall have more to say about the glass transition temperature and related phenomena in the next chapter.

The tightrope situation that arises from balancing high mobility, low crystallinity, and optimum crosslinking is often dealt with by using copolymers rather than homopolymers. With chain composition as an additional variable, molecules can be tailored better for specific application situations.

Polymers with the mechanical and chemical properties we have discussed in this section are called elastomers. In the next couple of sections we shall examine the thermodynamic basis for elasticity and then apply these ideas to cross-linked polymer networks.

3.3 Thermodynamics and Elasticity

It is not particularly difficult to introduce thermodynamic concepts into a discussion of elasticity. We shall not explore all of the implications of this development, but shall proceed only to the point of establishing the connection between elasticity and entropy. Then we shall go from phenomenological thermodynamics to statistical thermodynamics in pursuit of a molecular model to describe the elastic response of cross-linked networks.

We begin by remembering the mechanical definition of work and apply that definition to the stretching process of Fig. 3.1. Using the notation of Fig. 3.1, we can write the increment of elastic work we associated with an increment in elongation dL as

$$dw_e = F\,dL \tag{3.4}$$

It is necessary to establish some conventions concerning signs before proceeding further. When the applied force is a tensile force and the distortion is one of stretching, F, dL, and dw_e are all defined to be positive quantities. Thus dw_e is positive when elastic work is done on the system. The work done by the sample when the elastomer snaps back to its original size is a negative quantity.

The classical formulation of the first law of thermodynamics defines the change dU in the internal energy of a system as the sum of heat dq absorbed by the system plus the work dw done on the system:

$$dU = dq + dw \tag{3.5}$$

The element of work is generally written $-p\,dV$, where p is the external pressure, but with the possibility of an elastic contribution, it is $-p\,dV + F\,dL$. With this substitution Eq. (3.5) becomes

$$dU = dq - p\,dV + F\,dL \tag{3.6}$$

A consistent sign convention has been applied to the pressure-volume work term: A positive dV corresponds to an expanded system, and work is done by the system to push back the surrounding atmosphere.

The phenomenological definition for the change in entropy associated with the isothermal, reversible absorption of an element of heat dq is

$$dS = \frac{dq}{T} \tag{3.7}$$

This relationship can be used to replace dq by T dS in Eq. (3.6), since the infinitesimal increments implied by the differentials mean that the system is only slightly disturbed from equilibrium and the process is therefore reversible:

$$dU = T\,dS - p\,dV + F\,dL \tag{3.8}$$

Remember that in this relationship, as in all thermodynamic equations, temperature must be expressed in degrees Kelvin.

A quantity of great importance in chemical thermodynamics is the Gibbs free energy G. The latter is defined in terms of enthalpy H as

$$G = H - TS \tag{3.9}$$

where

$$H = U + pV \tag{3.10}$$

Combining the last two results and taking the derivative gives

$$dG = dU + p\,dV + V\,dp - T\,dS - S\,dT \tag{3.11}$$

Comparing Eq. (3.11) with Eq. (3.8) enables us to replace several of these terms by F dL,

$$dG = V\,dp - S\,dT + F\,dL \tag{3.12}$$

thus establishing the desired connection between the stretching experiment and thermodynamics.

Since G is a state variable and forms exact differentials, an alternative expression for dG is

$$dG = \left(\frac{\partial G}{\partial p}\right)_{T,L} dp + \left(\frac{\partial G}{\partial T}\right)_{p,L} dT + \left(\frac{\partial G}{\partial L}\right)_{p,T} dL \tag{3.13}$$

Comparing Eqs. (3.12) and (3.13) enables us to write

$$F = \left(\frac{\partial G}{\partial L}\right)_{p,T} \tag{3.14}$$

Note this is the same derivation that yields the important results $V = (\partial G/\partial p)_T$ and $S = -(\partial G/\partial T)_p$ when no elastic work is considered. It would be inappropriate for a book like this to digress into thermodynamics any further than this. The two relationships cited above are derived in almost every thermodynamics text; the student is advised to consult a suitable reference and review this material if the treatment above is too abbreviated.

Now we return to the definition of F provided by Eq. (3.14) and differentiate Eq. (3.9) with respect to L, keeping p and T constant:

$$\left(\frac{\partial G}{\partial L}\right)_{p,T} = \left(\frac{\partial H}{\partial L}\right)_{p,T} - T\left(\frac{\partial S}{\partial L}\right)_{p,T} \tag{3.15}$$

The left-hand side of this equation gives F according to Eq. (3.14); therefore

$$F = \left(\frac{\partial H}{\partial L}\right)_{p,T} - T\left(\frac{\partial S}{\partial L}\right)_{p,T} \tag{3.16}$$

This expression is sometimes called the equation of state for an elastomer in analogy to

$$p = \left(\frac{\partial U}{\partial V}\right)_T - T\left(\frac{\partial S}{\partial V}\right)_T \tag{3.17}$$

the thermodynamic equation of state. Note the parallel roles played by length and volume in these two expressions.

Equation (3.16) shows that the force required to stretch a sample can be broken into two contributions: one that measures how the enthalpy of the sample changes with elongation and one which measures the same effect on entropy. The pressure of a system also reflects two parallel contributions, except that the coefficients are associated with volume changes. It will help to pursue the analogy with a gas a bit further. The internal energy of an ideal gas is independent of volume: The molecules are noninteracting so it makes no difference how far apart they are. Therefore, for an ideal gas $(\partial U/\partial V)_T = 0$ and the thermodynamic equation of state becomes

$$p = -T\left(\frac{\partial S}{\partial V}\right)_T \tag{3.18}$$

By analogy, an ideal elastomer is defined as one for which $(\partial H/\partial L)_{p,T} = 0$; in this case Eq. (3.16) becomes

$$F = -T\left(\frac{\partial S}{\partial L}\right)_{p,T} \tag{3.19}$$

Although defined by analogy to an ideal gas, the justification for setting $(\partial H/\partial L)_{p,T} = 0$ cannot be the same for an elastomer as for such a gas. All molecules attact one another, and this attraction is not negligible in condensed phases such as our sample. What the ideality condition requires in an elastomer is that there be no change in the enthalpy of the sample as a result of the stretching process. As long as deformations are not too large, the polymer chain responds to deforming forces by a combination of rotations along the chain backbone that straighten out some of the kinks in the chain and increase the overall end-to-end distance. One way of thinking of this is to imagine that some bond near the middle of a randomly jumbled coil experiences a rotation of 180°, all other angles remaining fixed. Since the nature of the random flight process tends to bring the ends of the chain together, this rotation would have the opposite effect and increase the end-to-end distance. A chain of degree of polymerization n can achieve exactly the same effect by rotations of 180°/n at each repeat unit. If the chain is long enough, this amounts to a slight disturbance of each bond from its equilibrium position. The foregoing implies a cooperative effect along the backbone, while it is actually the average of a

variety of rotations that produces the net effect. Nevertheless, considerable modification of the end-to-end distance in a chain can be accomplished with the expenditure of relatively little energy. To get an idea of the numerical magnitude of this energy, let us consider the following example.

Example 3.1

A cross-linked polymer has a density of 0.94 g cm^{-3} at 25°C and a molecular weight between crosslinks of 28,000. The conformation of one bond in the middle of the molecule changes from trans to gauche, and the molecule opens up by 120°. In *n*-butane, the trans to gauche transformation requires about 3.3 kJ mol^{-1}. Estimate a value for ΔH of stretching based on this model, and use the law of cosines to estimate the magnitude of the "opening up" that results.

Solution

We need to know the number of chains per unit volume and must calculate the result on this basis:

$$\frac{0.94\ \text{g}}{\text{cm}^3} \times \frac{\text{moles polymer}}{28{,}000\ \text{g}} = 3.4 \times 10^{-5}\ \text{moles polymer cm}^{-3}$$

$$\Delta H_{t\to g} = \frac{3300\ \text{J}}{\text{moles monomer}} \times \frac{1\ \text{repeat unit}}{\text{polymer chain}} \times \frac{3.4 \times 10^{-5}\ \text{mol}}{\text{cm}^3}$$

$$= 0.12\ \text{J cm}^{-3}$$

In the present discussion it is the relative magnitudes of ΔH and ΔS which are significant. Several considerations lead us to conclude that this value of ΔH represents an upper limit for this quantity:

1. The same 120° opening can be achieved by a gauche → gauche transition with no difference in energy.
2. Only those bonds in the direction of stretch are elongated; in perpendicular directions they contract. The latter outnumber the former by two to one.
3. Not only does this calculation overcount the number of chains involved, but it makes no attempt to consider any compensation from the perpendicular direction.

We can use the law of cosines to estimate the effect on the end-to-end distance as follows. Picture two vectors of equal length b extending from the center of the chain to each of the ends. In the trans conformation of the center bond the

angle between these vectors is 180° (see Fig. 1.8c), and the end-to-end distance is 2b. In the gauche position at the center bond the angle between these vectors is 60°, and the law of cosines gives

$$r^2 = 2b^2 - 2b^2 \cos 60° = b^2 \quad \text{or} \quad r = b$$

as the end-to-end distance. In terms of this oversimplified model, a single trans → gauche rearrangment changes the end-to-end separation by a factor of 2. We shall estimate ΔS for this process in Example 3.2.

•

For large deformations or for networks with strong interactions—say, hydrogen bonds instead of London forces—the condition for an ideal elastomer may not be satisfied. There is certainly a heat effect associated with crystallization, so $(\partial H/\partial L)_{p,T}$ would not apply if stretching induced crystal formation. The compounds and conditions we described in the last section correspond to the kind of system for which ideality is a reasonable approximation.

Since entropy plays the determining role in the elasticity of an ideal elastomer, let us review a couple of ideas about this important thermodynamic variable:

1. Equation (3.7) gives a simple procedure for evaluating the entropy change accompanying a change of state. At the normal boiling point of a liquid, for example, the heat is absorbed reversibly and equals the heat of vaporization ΔH_v. Since T is constant, the entropy of vaporization is $\Delta H_v/T$. For benzene, for example, $\Delta S_v = (30.8 \text{ k J mol}^{-1})/353 = 87 \text{ J K}^{-1} \text{ mol}^{-1}$.
2. While this is an easy calculation to make, Eq. (3.7) does little to clarify exactly what ΔS means. Phenomenological proofs that ΔS as defined by Eq. (3.7) is a state variable often leave us with little more than a lament for the inefficiency of spontaneous processes.
3. Most chemistry students acquire a much better "feel" for entropy by considering it a measure of the amount of disorder in a system. For example, the fact that ΔS_v is positive immediately makes sense, since the vapor phase is more disordered than the liquid.
4. A quantitative way of dealing with the degree of disorder in a system is to define something called the thermodynamic probability Ω which counts the number of ways in which a particular state can come about. Thus situations we characterize as relatively disordered can come about in more ways than a relatively ordered state, just as an unordered deck of cards compared to a deck arranged by suits.

Chemists learn to use the thermodynamic probability almost instinctively in a qualitative manner; it is quantitatively related to entropy through an equation due to Boltzmann:

$$S = k \ln \Omega \tag{3.20}$$

where k is Boltzmann's constant. As usual, k is replaced by R for calculations on a per mole basis. The difference in entropy between two states of different thermodynamic probability is

$$\Delta S = S_2 - S_1 = k \ln \left(\frac{\Omega_2}{\Omega_1} \right) \tag{3.21}$$

and this is positive when $\Omega_2 > \Omega_1$ and negative when $\Omega_2 < \Omega_1$.

For the evaporation process we mentioned above, the thermodynamic probability of the gas phase is given by the number of places a molecule can occupy in the vapor. This, in turn, is proportional to the volume of the gas (subscript g): $\Omega_g \propto V_g$. In the last chapter we discussed the free volume in a liquid. The total free volume in a liquid is a measure of places for molecules to occupy in the liquid. The thermodynamic probability of a liquid (subscript l) is thus $V_l \propto V_{l,\,free}$. Based on these ideas, the entropy of the evaporation process can be written as

$$\Delta S_v = k \ln \left(\frac{V_g}{V_{l,\,free}} \right) \tag{3.22}$$

for one molecule, or

$$\Delta S_v = k \ln \left(\frac{V_g}{V_{l,\,free}} \right)^N = Nk \ln \left(\frac{V_g}{V_{l,\,free}} \right) \tag{3.23}$$

for N molecules. If N equals Avogadro's number, Eq. (3.23) becomes

$$\Delta S_v = R \ln \left(\frac{V_g}{V_{l,\,free}} \right) \tag{3.24}$$

Neither the volume occupied by a mole of gas at the boiling point nor the free volume of a liquid vary too widely from substance to substance. Taking the former to be about 30,000 ml and the latter to be about 3 ml gives

$$\Delta S_v = R \ln \left(\frac{30{,}000}{3} \right) = (8.314) \ln 10^4 = 77 \text{ J K}^{-1} \text{ mol}^{-1} \tag{3.25}$$

A great many liquids have entropies of vaporization at the normal boiling point in the vicinity of this value (see benzene above), a generalization known as Trouton's rule. Our interest is clearly not in evaporation, but in the elongation of elastomers. In the next section we shall apply Eq. (3.21) to the stretching process for a statistical–and therefore molecular–picture of elasticity.

3.4 Entropy Elasticity

By combining random flight statistics from Chap. 1 with the statistical definition of entropy from the last section, we shall be able to develop a molecular model for the stress–strain relationship in a cross-linked network. It turns out to be more convenient to work with the ratio of stretched to unstretched lengths L/L_0 than with γ itself. Note the relationship between these variables:

$$L = L_0 + \Delta L \tag{3.26}$$

or

$$\alpha - 1 = \gamma_t \tag{3.27}$$

where the elongation α is defined to be L/L_0 while $\gamma_t = \Delta L/L_0$.

The next step in the development of a model is to postulate a perfect network. By definition, a perfect network has no free chain ends. An actual network will contain dangling ends, but it is easier to begin with the perfect case and subsequently correct it to a more realistic picture. We define ν as the number of subchains contained in this perfect network, a subchain being the portion of chain between the crosslink points. The molecular weight and degree of polymerization of the chain between crosslinks are defined to be M_c and n_c, respectively. Note that these same symbols were used in the last chapter with different definitions.

Finally, we assume that the network undergoes an affine deformation. This means that each volume element within the sample deforms in exact proportion to the overall specimen. Since a volume element can be inscribed around a subchain of the network, affine deformation requires that the coordinates describing the ends of subchains also be changed in proportion to changes in the macroscopic dimensions of the sample. Such a situation is represented in Fig. 3.2. In Fig. 3.2 the solid lines represent the volume element and the broken lines suggest the overall sample. Figure 3.2a indicates an unstretched sample; Fig. 3.2b, the same sample after elongation in the z direction ($\alpha = z/z_0$). Assuming that no volume change accompanies the deformation, the x and y dimensions of the volume element as well as the macroscopic specimen are decreased by $1/\alpha^{1/2}$ compared to the original dimensions (subscript 0):

$$\text{Volume} = x_0 y_0 z_0 = \left(\frac{1}{\alpha^{1/2}} x_0\right)\left(\frac{1}{\alpha^{1/2}} y_0\right)(\alpha z_0) \tag{3.28}$$

Next let us apply random walk statistics to the subchain before and after stretching.

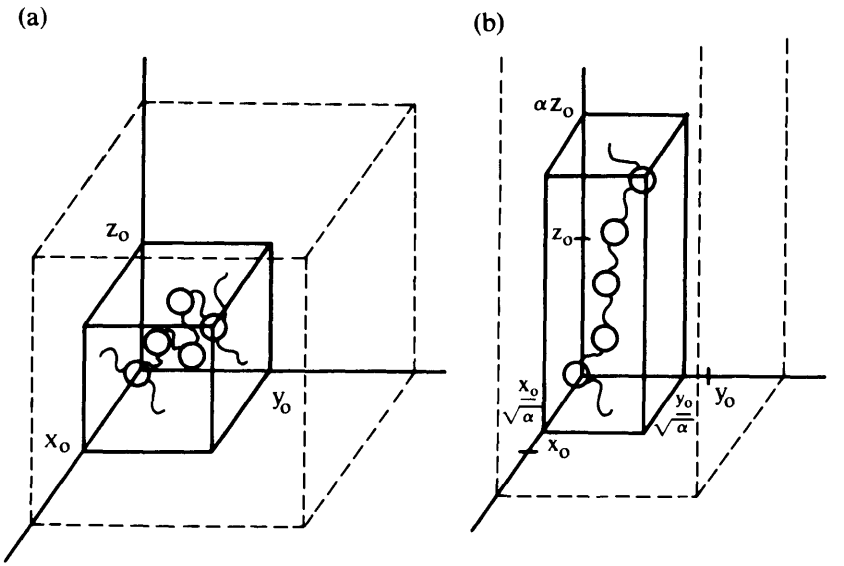

Figure 3.2 The affine deformation of a polymer subchain. (a) The original coordinates of the end of the subchain are x_0, y_0, and z_0. (b) The same coordinates as in (a) are $x_0/\sqrt{\alpha}$, $y_0/\sqrt{\alpha}$, and αz_0.

Equation (1.41) gives the probability of finding one end of a chain with degree of polymerization n in a volume element dx dy dz located at x, y, and z if the other end of the chain is located at the origin. We can use this relationship to describe the unstretched chain shown in Fig. 3.2a; all that is required is to replace n by n_c, the degree of polymerization of the subchain. Therefore for the unstretched chain (subscript u) we write

$$P_u \, dx \, dy \, dz = \left(\frac{2}{3} \pi n_c l_0^2\right)^{-3/2} \exp\left(\frac{-3(x^2 + y^2 + z^2)}{2n_c l_0^2}\right) dx \, dy \, dz \qquad (3.29)$$

After stretching, the z coordinate is increased by α, while x and y are decreased by $\alpha^{-1/2}$, as described by Eq (3.28) and shown in Fig. 3.2b. For this situation (subscript s) the probability becomes

$$P_s \, dx \, dy \, dz = \left(\frac{2}{3} \pi n_c l_0^2\right)^{-3/2} \exp\left(\frac{-3(x^2/\alpha + y^2/\alpha + \alpha^2 z^2)}{2n_c l_0^2}\right) dx \, dy \, dz \qquad (3.30)$$

A moment's reflection will convince us that these probabilities can be used as thermodynamic probabilities in Eq. (3.21) to calculate the entropy change on stretching:

$$S_s - S_u = \Delta S = k(\ln P_s - \ln P_u) \tag{3.31}$$

The only limitations imposed by using these expressions are that the subchains are long enough to be described by random flight statistics and that the elongation is not so large that the average end-to-end distance in the subchain ceases to be large compared to $n_c l_0$. This last requirement is imposed by the approximation introduced in the derivation of Eq. (1.31). Combining the last three results and rearranging gives

$$\Delta S_i = \frac{-3k\left[(1/\alpha - 1)x^2 + (1/\alpha - 1)y^2 + (\alpha^2 - 1)z^2\right]}{2n_c l_0^2} \tag{3.32}$$

for the entropy change of a typical subchain, say, the ith one.

In the volume elements describing individual subchains, the x, y, and z dimensions will be different, so Eq. (3.32) must be averaged over all possible values to obtain the average entropy change per subchain. This process is also easily accomplished by using a result from Chap. 1. Equation (1.62) gives the mean-square end-to-end distance of a subchain as $n_c l_0^2$, and this quantity can also be written as $\overline{x^2} + \overline{y^2} + \overline{z^2}$; therefore

$$\overline{x^2} + \overline{y^2} + \overline{z^2} = n_c l_0^2 \tag{3.33}$$

Because of the random nature of the distribution of repeat units, each contribution to the left-hand side of this expression is equal and

$$\overline{x^2} = \overline{y^2} = \overline{z^2} = \frac{1}{3} n_c l_0^2 \tag{3.34}$$

Using this value for the average value of x^2, y^2, and z^2 in Eq. (3.32) and rearranging gives

$$\overline{\Delta S} = -\frac{3k}{2}\left[\frac{2}{3}\left(\frac{1}{\alpha} - 1\right) + \frac{1}{3}(\alpha^2 - 1)\right] \tag{3.35}$$

or

$$\overline{\Delta S} = -\frac{k}{2}\left(\alpha^2 + \frac{2}{\alpha} - 3\right) \tag{3.36}$$

This expression gives the average entropy change per chain; to get the average for the sample, we multiply by the number ν of subchains in the sample. The total entropy change is

$$\Delta S = -\frac{k\nu}{2}\left(\alpha^2 + \frac{2}{\alpha} - 3\right) \tag{3.37}$$

The quantity in parentheses is always positive for $\alpha > 1$, the case of elongation, making $\Delta S < 0$ for stretching. Therefore ΔS is positive for the opposite process, showing that entropy alone is sufficient to explain the elastomer's snap. To get an idea of the magnitude of this entropy effect, consider the following example.

Example 3.2

Calculate ΔS for a 100% elongation of a polymer sample at 25°C using Eq. (3.37) and compare ΔS with the value of ΔH calculated for the same process in Example 3.1.

Solution

From Example 3.1, $\nu = 3.4 \times 10^{-5}$ mol (expressed per cubic centimeter of sample), and for a 100% elongation $\alpha = 2$. Substitution into Eq. (3.37) gives

$$\Delta S = -\frac{1}{2}\left(\frac{8.314\ \text{J}}{\text{K mol}}\right)\left(\frac{3.4 \times 10^{-5}\ \text{mol}}{\text{cm}^3}\right)\left(2^2 + \frac{2}{2} - 3\right)$$

$$= -2.8 \times 10^{-4}\ \text{J K}^{-1}\ \text{cm}^{-3}$$

To compare with ΔH at 25°C, ΔS must be multiplied by the temperature:

$$T\Delta S = 298(-2.8 \times 10^{-4}) = -0.084\ \text{J cm}^{-3}$$

Comparison of this result with Example 3.1 shows that $T\Delta S$ and ΔH are of the same order of magnitude. Example 3.1 stressed that the value of ΔH estimated there was an upper limit. Experimental results show that the assumption of ideality—while a slight oversimplification—generally introduces an error of less than 10%. Comparison of the two examples shows how much more difficult it is to deal with ΔH than with ΔS in these systems.

•

Recalling that this is an ideal elastomer, we apply Eq. (3.19) to Eq. (3.37) to obtain

$$F = -T\left(\frac{\partial S}{\partial L}\right)_T = -\frac{T}{L_0}\left(\frac{\partial \Delta S}{\partial \alpha}\right) = \frac{kT\nu}{L_0}\left(\alpha - \frac{1}{\alpha^2}\right) \tag{3.38}$$

Dividing both sides of the equation by the cross-sectional area of the sample gives

$$\sigma_t = \frac{F}{A} = kT \frac{\nu}{V} \left(\alpha - \frac{1}{\alpha^2} \right) \tag{3.39}$$

where the product of the cross section and L_0 has been set equal to the volume V of the sample. Note that σ_t changes sign at $\alpha = 1$, as physically required.

Although it is in this form that we compare theoretical predictions with experiment in the next section, it is instructive to express Eq. (3.39) in terms of L/L_0 and then differentiate the result with respect to L:

$$d\sigma_t = kT \frac{\nu}{V} \left(\frac{1}{L_0} + 2L_0^2 L^{-3} \right) dL \tag{3.40}$$

Next we multiply and divide the right-hand side by L to get

$$d\sigma_t = \left[kT \frac{\nu}{V} \left(\alpha + \frac{2}{\alpha^2} \right) \right] \frac{dL}{L} \tag{3.41}$$

Comparing this result with Eq. (3.1) shows that the quantity in brackets equals Young's modulus for an ideal elastomer in a perfect network. Since the number of subchains per unit volume, ν/V, is also equal to $\rho N_A/M_c$, where M_c is the molecular weight of the subchain, the modulus may be written as

$$E = \frac{RT\rho}{M_c} \left(\alpha + \frac{2}{\alpha^2} \right) \tag{3.42}$$

There are several things to notice about this result:

1. The modulus increases with temperature. This behavior is verified by experiment. By contrast, the modulus of metals decreases with increasing T. The difference arises from the fact that entropy is the origin of elasticity in polymers but not in metals.
2. The modulus increases as M_c decreases. This effect on M_c is brought about by increased crosslinking and is consistent with intuitive expectations in this regard.
3. The modulus is not independent of α. For $\alpha \gg 1$, the first term in parentheses predominates and the modulus is directly proportional to α. For $\alpha \ll 1$, the first term is insignificant and E varies as α^{-2}.
4. An interesting limit for small deformation (i.e., $\alpha \cong 1$) is

$$E_{\alpha \cong 1} = \frac{3RT\rho}{M_c} \tag{3.43}$$

showing the condition for Young's modulus to be constant and its value when that condition is met.

5. Carrying out a parallel differentiation on Eq. (3.38) and examining the case of $\alpha \cong 1$ yields

$$dF = \frac{3kT\nu}{L_0^2}\, dL \tag{3.44}$$

Applied to a single chain, $\nu = 1$ and L_0^2 is replaced by Eq. (1.62) to give

$$dF = \frac{3kT}{nl_0^2}\, dL = k_H\, dL \tag{3.45}$$

This equation shows that at small deformations individual chains obey Hooke's law with the force constant $k_H = 3kT/nl_0^2$. This result may be derived directly from random flight statistics without considering a network.

A typical cross-linked polymer at room temperature has $\rho \cong 1$ g cm^{-3} and $M_c \cong 10^4$. According to Eq. (3.43), Young's modulus for such a polymer is $3(8.314 \text{ J K}^{-1} \text{ mol}^{-1})(300 \text{ K})(10^3 \text{ kg m}^{-3})/10 \text{ kg mol}^{-1} = 7.5 \times 10^5 \text{ N m}^{-2}$ which is on the order of the observed magnitude of this quantity for polymers. By contrast, for metals E is on the order of 10^{11} N m^{-2}.

3.5 Experimental Behavior of Elastomers

We have already observed that the entropy theory of elasticity predicts a modulus of the right magnitude and possessing the proper temperature coefficient. Now let us examine the suitability of Eq. (3.39) to describe experimental results in detail.

Figure 3.3 shows a plot of σ_t versus α at 20°C for a sample of natural rubber cross-linked with sulfur. The points are experimental and the solid line is drawn according to Eq. (3.39). The agreement is seen to be very good for α values between 0.4 and 1.3. For greater elongations the theoretical force is initially too large, although at $\alpha \gtrsim 5$ the theoretical line falls below the experimental. Remember, the sample is already increased in length by 30% at $\alpha = 1.3$; however, since elongations approaching 1000% are possible for actual elastomers, the range of success is modest. There is no doubt that the dependence of the modulus on α is correctly given by Eq. (3.42) for small elongations and compressions.

Over the range of fit, matching the dependence of σ_t on α produces only a numerical coefficient and does not constitute a test of the predicted dependence of the modulus on either T or M_c. We have already confirmed that Young's modulus actually does increase with temperature for elastomers. Next let us

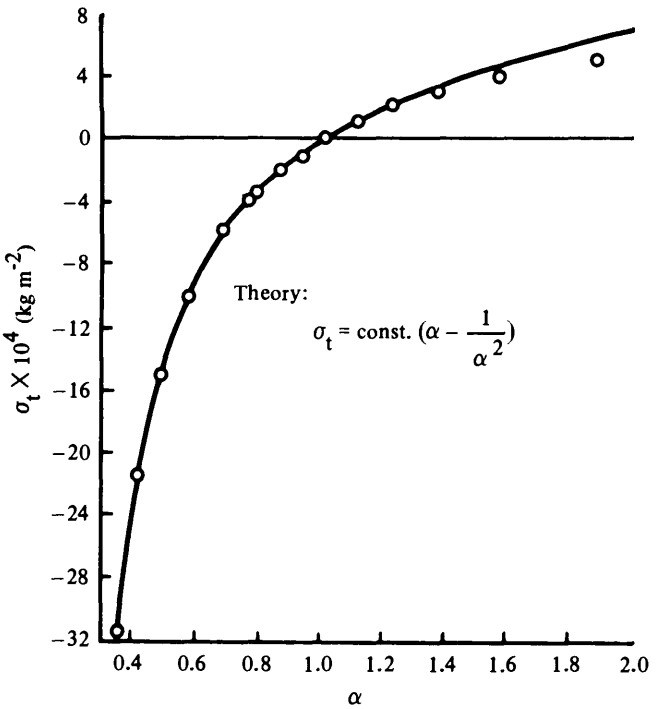

Figure 3.3 Comparison of experiment (points) and theory [Eq. (3.39)] for the entropy elasticity of a sample of cross-linked natural rubber. [From L. R. G. Treloar, *Trans. Faraday Soc.* 40:59 (1944).]

consider experiments which test the predicted effect of M_c on this quantity. The best way to proceed is by considering at the same time the fact that real elastomers do not form perfect networks. By definition, the perfect network has no loose ends. An actual network is cross-linked at random, and a certain fraction of subchains are only dangling appendages to the network. The number of subchains in this category should be subtracted from the total number of subchains, since they do not contribute to the elasticity of the network. Loose ends relax from deformation over a period of time—like the branch chains discussed in connection with viscosity—and do not oppose the deformation with a restoring force. Our problem, then, is to subtract the number of ineffective subchains from the total number ν, since the latter overcounts.

Suppose the un-cross-linked polymer chain has a molecular weight M which, upon crosslinking, is divided into subchains of molecular weight M_c. This means that each subchain is a fraction M_c/M of the original chain. Since the crosslink

points occur at random along the original chain, two of the subchains will be in terminal positions; that is, they will be held to the network by only one crosslink and thus not contribute to elasticity. Therefore $2M_c/M$ is the fraction of subchains which are ineffective and should be subtracted from the total number to give an improved representation of elasticity. With this modification, Eq. (3.39) becomes

$$\sigma_t = \frac{RT\rho}{M_c}\left(1 - \frac{2M_c}{M}\right)\left(\alpha - \frac{1}{\alpha^2}\right) \tag{3.46}$$

Note that as $M \to \infty$, the absolute number of chain ends per unit volume decreases, as does the chain-end correction.

Figure 3.4 is a display of data which confirms the predictions of Eq. (3.46). For T and α constant—the case in these experiments—Eq. (3.46) predicts that a plot of σ_t versus $1/M$ should yield a straight line with an intercept proportional to $1/M_c$. The elastomers on which the experiments were conducted were copolymers of isobutylene containing a small amount of isoprene. The polymers

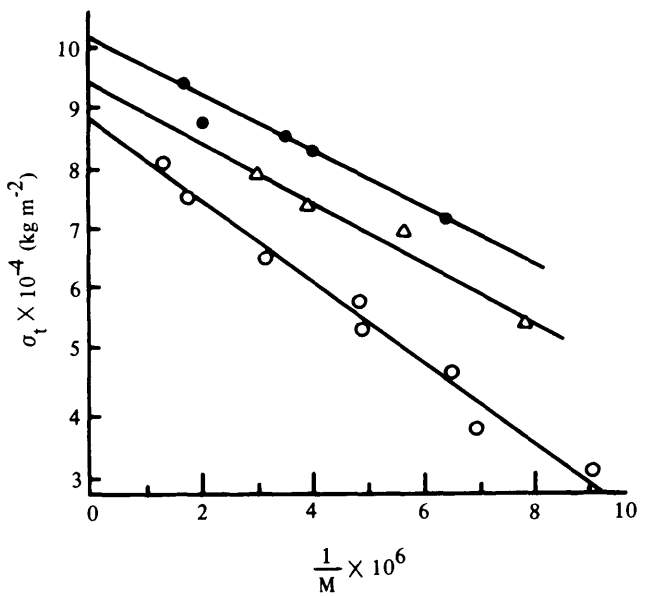

Figure 3.4 σ_t versus M^{-1} for polyisobutylene samples with three different degrees of crosslinking (T and α constant). [Reprinted with permission from P. J. Flory, *Ind. Eng. Chem.* 38:417 (1946). Copyright 1946, American Chemical Society.]

were fractionated into samples of different molecular weight prior to crosslinking. The crosslink sites, the isoprene units, are distributed at random through the polymer; after vulcanization, samples are available with the same values of M_c but different values of M. Elasticity measurements on the latter are plotted in Fig. 3.4. Figure 3.4 shows that copolymers with three different degrees of crosslinking agree with theoretical predictions very well. The sample represented by the open circles in Fig. 3.4 yields a value of M_c = 37,000 when analyzed according to Eq. (3.46). Independent measurement of this quantity through solubility studies gives a value of 35,000. In view of the complexity of the phenomena involved, this must be regarded as excellent agreement.

The entropy theory for elasticity is thus seen to correctly describe the dependence of the modulus on T, ν, and α, at least for small elongations. For distortion of the sample to many times its original length, crystallization due to chain alignment may cause the breakdown of the theory. At intermediate elongations, however, the model should still apply, provided that we have not limited its validity by mathematical approximations. In writing Eq. (3.32) we observed that large deformations might invalidate the assumption that the end-to-end distance in the subchain is small compared to $n_c l_0$. Without going into full mathematical details, let us examine how this constraint can be lifted.

The first step is to write an expression for the energy stored in a network U as a result of the elongation α. This may be written as

$$U = \int_{x_0}^{x_0/\sqrt{\alpha}} F_x \, dx + \int_{y_0}^{y_0/\sqrt{\alpha}} F_y \, dy + \int_{z_0}^{\alpha z_0} F_z \, dz \tag{3.47}$$

where the F's are the x, y, and z components of the distorting force and x_0, y_0, and z_0 are the initial dimensions of the sample. Assuming that the applied force is in the z direction, as in Fig. 3.1, we note that the contraction in the x and y directions is much less than the elongation in z. The x and y components of the force are therefore assumed to obey Hooke's law; that is, $F_x = k_H x$, with k_H given by Eq. (3.45). A similar expression describes F_y, but F_z is described differently because of the greater elongation it experiences. For the latter the the force component may be shown to be

$$F_z = \frac{kT}{l_0}\left[3\frac{r_z}{n_c l_0} + \frac{9}{5}\left(\frac{r_z}{n_c l_0}\right)^3 + \frac{297}{175}\left(\frac{r_z}{n_c l_0}\right)^5 + \cdots\right] \tag{3.48}$$

in which r_z is the z component of the average end-to-end distance in the subchain. Note that Eq. (3.48) gives a force which is identical to the x and y components if $r_z \ll n_c l_0$. Equation (3.48) gives the first three terms in the series expansion of the inverse Langevin function of $r_z/n_c l_0$; this describes

the chain-end separation without assuming stringent limitations on $r/n_c l_0$. Equations (3.48) and (3.45) with $n = n_c$ can be substituted into Eq. (3.47) and the result integrated and then multiplied by ν to give the elastic energy stored per unit volume of elastomer. The derivative of this last quantity with respect to α equals σ_t. When the indicated operations are carried out, the following result is obtained:

$$\sigma_t = \frac{\nu kT}{V}\left\{1 - \frac{1}{\alpha^2} + \frac{1}{3}\sqrt{n_c}\left[3\frac{\alpha}{\sqrt{n_c}} + \frac{9}{5}\left(\frac{\alpha}{\sqrt{n_c}}\right)^3 + \frac{297}{175}\frac{5}{3}\left(\frac{\alpha}{\sqrt{n_c}}\right)^5 + \cdots\right]\right\} \tag{3.49}$$

For the case of $\alpha \ll n_c^{1/2}$, terms higher than first order in this expression are negligible and the result becomes identical to Eq. (3.39). However, the derivation of Eq. (3.49) does not limit its applicability to these small values of α. Figure 3.5 shows that experimental results are still not exactly described by Eq. (3.49), although the general shape of the theoretical and experimental lines is similar.

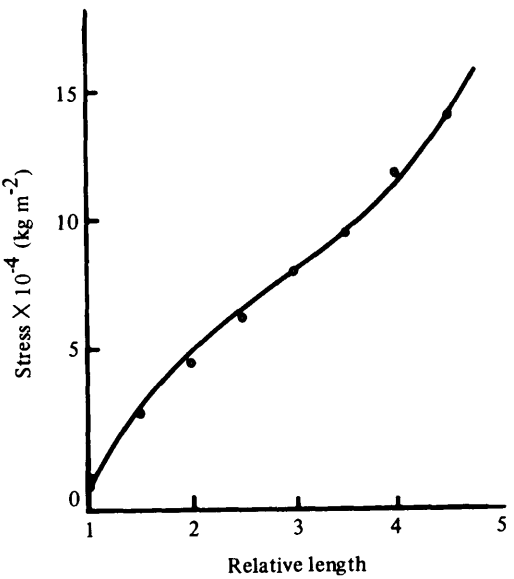

Figure 3.5 Comparison of experiment (points) and theory [Eq. (3.49)] for the entropy elasticity of the same sample shown in Fig. 3.3. [Reprinted with permission from H. M. James and E. Guth, *J. Chem. Phys.* 11:455 (1943).]

In connection with Eq. (3.45) we noted that the deformation of individual chains can be studied directly from random flight statistics. Using equivalent expressions for the x, y, *and* z components of force and following the procedure outlined above gives a more rigorous derivation of Eq. (3.39) than that presented in the last section.

Even better agreement between theory and experiment has been obtained in other theories by abandoning the notion of affine deformation and recognizing that shorter subchains experience a greater strain than do longer subchains for a given stress. We shall not pursue this development any further, however, and shall turn next to a consideration of other types of deformation.

3.6 The Shear Modulus and the Compliances

Until now we have restricted ourselves to consideration of simple tensile deformation of the elastomer sample. This deformation is easy to visualize and leads to a manageable mathematical description. This is by no means the only deformation of interest, however. We shall consider only one additional mode of deformation, namely, shear deformation. Figure 3.6 represents an elastomer sample subject to shearing forces. Deformation in the shear mode is the basis

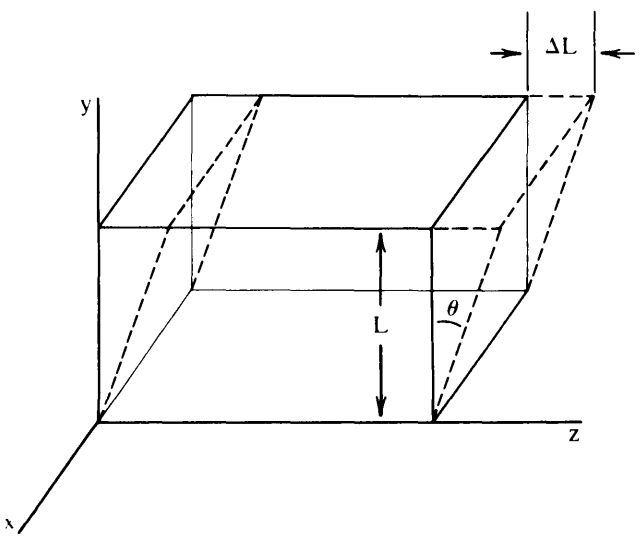

Figure 3.6 Definition of variables to define the shear deformation of an elastic body.

for the definition of viscosity. An examination of elasticity according to the same mode of deformation will make it easy to combine the two for a description of viscoelasticity. We shall begin, however, by describing the purely elastic response to a body under conditions of shear.

By analogy with Eq. (3.1), we seek a description for the relationship between stress and strain. The former is the shearing force per unit area, which we symbolize as σ_s, as in Chap. 2. For shear strain we use the symbol γ_s; it is the rate of change of γ_s that is involved in the definition of viscosity in Eq. (2.2). As in the analysis of tensile deformation, we write the strain $\Delta L/L$, but this time ΔL is in the direction of the force, while L is at right angles to it. These quantities are shown in Fig. 3.6. It is convenient to describe the sample deformation in terms of the angle θ, also shown in Fig. 3.6. For distortion which is independent of time—we continue to consider only the equilibrium behavior—stress and strain are proportional with proportionality constant G:

$$\sigma_s = G\gamma_s = G\frac{\Delta L}{L} = G\tan\theta \cong G\theta \tag{3.50}$$

where the last relationship is based on the fact that $\tan\theta \cong \theta$ for small θ. The factor G is called the shear modulus or the modulus of rigidity. In SI units, G also has units $N\,m^{-2}$.

The shear modulus for an ideal elastomer in a perfect network is not difficult to derive:

1. Equation (3.47) is used with each of the force components given by (3.44). The limits of integration are different for affine deformation under shear at constant volume. In terms of the coordinates shown in Fig. 3.6, there is no change in x, z increases by α, and y decreases by $1/\alpha$.
2. Integration, multiplication by ν, and differentiation with respect to γ yields $\sigma_s = (kT\nu/V)\gamma_s = (RT\rho/M_c)\gamma_s$ and, by comparison with Eq. (3.50), makes the shear modulus

$$G = \frac{RT\rho}{M_c} \tag{3.51}$$

3. This result is the shear equivalent to Eq. (3.42) for tensile deformation. Note the modulus is a constant independent of strain for shear, while this is only true for $\alpha \cong 1$ in the case of tension as shown by Eq. (3.43).

A general relationship between Young's modulus and the shear modulus is

$$G = \frac{E}{2(1+\mu)} \tag{3.52}$$

where μ is Poisson's ratio defined by Eq. (3.3). For constant volume deformations $\mu = \frac{1}{2}$ and $G = E/3$. This same result is obtained when Eq. (3.51) is

compared with Young's modulus under conditions where the latter is a constant, namely, Eq. (3.43).

As long as the moduli are constants, it makes no difference in either a tensile or shear experiment which variable, stress or strain, is independent and which is dependent; that is, we could apply a constant force and measure the strain or induce a constant strain and measure the force responsible. The modulus is the ratio of the stress to the strain. If the ratio were calculated as the ratio of the strain to the stress, the reciprocal of the modulus would result. The latter is called the compliance and is given the symbols D and J for tensile and shear conditions, respectively. When they are independent of time, the moduli and compliances for a particular deformation are simply reciprocals.

The situation is not so simple when these various parameters are time dependent. In the latter case, the moduli, designated by E(t) and G(t), are evaluated by examining the (time dependent) value of σ needed to maintain a constant strain γ_0. By constrast, the time-dependent compliances D(t) and J(t) are determined by measuring the time-dependent strain associated with a constant stress σ_0. Thus whether the deformation mode is tension or shear, the modulus is a measure of the stress required to produce a unit strain. Likewise, the compliance is a measure of the strain associated with a unit stress. As required by these definitions, the units of compliance are the reciprocals of the units of the moduli $m^2\ N^{-1}$ in the SI system.

These distinctions are summarized in Table 3.1 for handy reference. The nomenclature and notation are somewhat confusing, and the situation gets even worse when other sources are consulted. Not all authors use the same notation, so Table 3.1 is useful as a concordance.

As is often the case, models will assist us in understanding the time-dependent moduli and compliances. This time we turn to a purely mechanical model to characterize viscoelastic systems. In their simplest form, the models will consist of two units, a spring and a dashpot. The latter is a cup and bob arrangement where the piston moves through a viscous medium. These units embody the features of elastic and viscous response. We shall characterize the former by a Hookean modulus and the latter by a Newtonian viscosity. Although there are exceptions to these statements, the way the spring and dashpot units are arranged determines whether a modulus or compliance is most readily calculated from a model. For example, if the spring and dashpot are connected in series, we have the following:

1. The net deformation is the sum of the deformations of the individual units.
2. Dividing the stress by the net deformation gives the modulus.
3. A spring and dashpot in series is called a Maxwell model.

Alternatively, if the spring and dashpot are connected in parallel, the following holds:

Table 3.1 Summary of the Names and Notation for Moduli[a] and Compliances[b] Under Equilibrium, Transient, and Dynamic Conditions

Experimental condition	Tension	Shear	Comment
Equilibrium	1. $E = \sigma_t/\gamma_t$	$G = \sigma_s/\gamma_s$	Time independent; E = Young's modulus
	2. $D = 1/E = \gamma_t/\sigma_t$	$J = 1/G = \gamma_s/\sigma_s$	
Transient	1. $E(t) = \sigma_t(t)/\gamma_0$	$G(t) = \sigma_s(t)/\gamma_0$	Time dependent; Subscript 0, held constant in experiment
	2. $D(t) = \gamma_t(t)/\sigma_0$	$J(t) = \gamma_s(t)/\sigma_0$	
Dynamic	1. $E(\omega) = \sigma_t(\omega)/\gamma_0$	$G(\omega) = \sigma_s(\omega)/\gamma_0$	Frequency dependent; Subscript 0, maximum amplitude; all have storage (single prime) and loss (double prime) components
	2. $D(\omega) = \gamma_t(\omega)/\sigma_0$	$J(\omega) = \gamma_s(\omega)/\sigma_0$	

[a] Modulus: Stress per unit strain
[b] Compliance: Strain per unit stress

4. The deformations are the same for each unit and it is the stresses that are added.
5. Dividing the deformation by the stress gives the compliance.
6. A spring and dashpot in parallel is called a Voigt model.

Each of these models will be examined in subsequent sections as devices for describing specific transient experiments.

3.7 The Maxwell Model: Stress Relaxation

Our objectives in this section are twofold: to describe and analyze a mechanical model for a viscoelastic material, and to describe and interpret an experimental procedure used to study polymer samples. We shall begin with the model and then proceed to relate the two. Pay attention to the difference between the model and the actual observed behavior.

Suppose we consider a spring and dashpot connected in series as shown in Fig. 3.7a; such an arrangement is called a Maxwell element. The spring displays a Hookean elastic response and is characterized by a modulus G^*. The dashpot displays Newtonian behavior with a viscosity η^*. These parameters (superscript *) characterize the model; whether they have any relationship to the

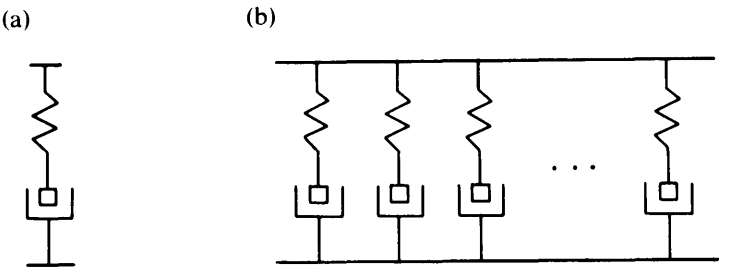

Figure 3.7 Maxwell models consisting of a spring and dashpot in series: (a) single unit and (b) set of units arranged in parallel.

properties of molecules remains to be seen. As a word of caution, it might be observed that other authors frequently use complex numbers for the mathematics of viscoelasticity and use the asterisk to label these complex numbers. We shall avoid the use of complex numbers; for us the asterisk simply labels the modulus or viscosity of a spring or dashpot.

Returning to the Maxwell element, suppose we rapidly deform the system to some state of strain γ_{tot} and secure it in such a way that it retains the initial deformation. Because the material possesses the capability to flow, some internal relaxation will occur such that less force will be required with the passage of time to sustain the deformation. Our goal with the Maxwell model is to calculate how the stress varies with time, or, expressing the stress relative to the constant strain, to describe the time-dependent modulus. Such an experiment can readily be performed on a polymer sample, the results yielding a time-dependent stress relaxation modulus. In principle, the experiment could be conducted in either a tensile or shear mode measuring E(t) or G(t), respectively. We shall discuss the Maxwell model in terms of shear.

In the Maxwell model, the two units are connected in series, so that each bears the full stress individually and the deformations of the elastic and viscous components are additive:

$$\gamma_{tot} = \gamma_{el} + \gamma_{vis} \tag{3.53}$$

In a shear experiment the first of these is given by Eq. (3.50). For the viscous component we do not have an expression for γ, only for the way γ varies with time. Hence it is not possible to develop this relationship any further as an explicit equation, but only as a differential equation. Differentiating Eq. (3.53) with respect to time, we obtain

$$\frac{d\gamma_{tot}}{dt} = \dot{\gamma}_{tot} = \dot{\gamma}_{el} + \dot{\gamma}_{vis} \tag{3.54}$$

and, differentiating (3.50) with G constant, we obtain

$$\dot{\gamma}_{el} = \frac{1}{G^*} \frac{d\sigma}{dt} \tag{3.55}$$

Substituting Eqs. (3.55) and (2.2) into Eq. (3.54) gives .

$$\dot{\gamma}_{tot} = \frac{1}{G^*} \frac{d\sigma}{dt} + \frac{1}{\eta^*} \sigma \tag{3.56}$$

Since the total strain in the experiment is held constant, $d\gamma_{tot}/dt = 0$ and Eq. (3.56) becomes

$$\frac{1}{G^*} \frac{d\sigma}{dt} + \frac{1}{\eta^*} \sigma = 0 \tag{3.57}$$

This is the fundamental differential equation for a shear stress relaxation experiment. The solution to this differential equation is an equation which gives σ as a function of time in accord with experiment.

Example 3.3

Show that the equation $\sigma = \sigma_0 \exp(-G^*t/\eta^*)$ is a solution to Eq. (3.57) where σ_0 is the value of σ at $t = 0$.

Solution

Demonstrating that a function solves a differential equation is easier than finding the solution. All that is required is to perform the indicated differentiation and verify the equality. Remember that σ_0, G^*, and η^* are constants:

$$\frac{d\sigma}{dt} = \sigma_0 e^{-G^*t/\eta^*} \left(- \frac{G^*}{\eta^*} \right)$$

Substitution of the proposed solution and its derivative into Eq. (3.57) gives

$$\frac{1}{G^*} \sigma_0 e^{-G^*t/\eta^*} \left(- \frac{G^*}{\eta^*} \right) + \frac{1}{\eta^*} \sigma_0 e^{-G^*t/\eta^*} = 0$$

as required. Note that G^*/η^* must have units time^{-1}. This is readily verified from the units of the individual quantities as follows: (kg m^{-1} sec^{-2})/(kg m^{-1} sec^{-1}) = sec^{-1}

•

The example verifies that the solution to this differential equation is

$$\sigma = \sigma_0 e^{-G^* t/\eta^*} = \sigma_0 e^{-t/\tau} \tag{3.58}$$

where η^*/G^* has the units of time and is identified as the experimental relaxation time and given the symbol τ.

Equation (3.58) can be written in terms of the shear modulus by dividing both sides of the equation by the constant strain:

$$G(t) = G_0 e^{-t/\tau} \tag{3.59}$$

where G_0 is the value of the time-dependent modulus at $t = 0$. Figure 3.8a shows a plot of this result in linear coordinates, and Fig. 3.8b does the same in log-log coordinates. Note that a semilog plot would be a straight line whose slope would measure τ. Similar results would be obtained for E(t) in the case of tensile deformation. Several things about the relaxation time readily come to mind:

1. It is the time required for σ to drop to 1/e or 37% of its initial value.
2. As a ratio of η^*/G^*, τ is large when η^* is large and G^* is small and decreases with increasing modulus and decreasing viscosity.
3. The Newtonian viscosity is given by the product of the relaxation time and the Hookean modulus. This result was anticipated in the discussion of Eqs. (2.29) and (2.31).

In the last chapter we saw that the molecular relaxation time is the "yardstick" against which times are measured. The experimental relaxation time plays a similar role. This is easily seen by an examination of Fig. 3.8b. For

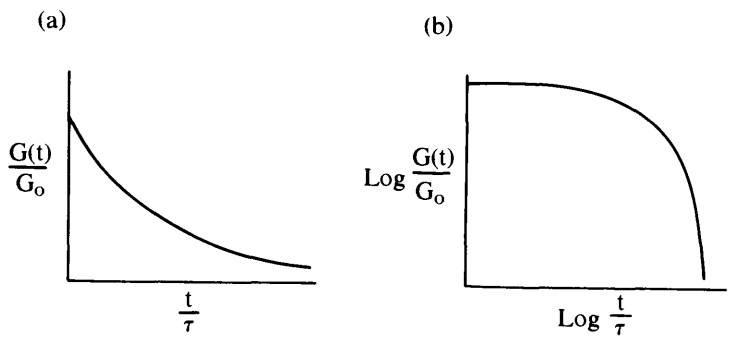

Figure 3.8 Time-dependent shear modulus [as $G(t)/G_0$] versus time (as t/τ): (a) linear coordinates and (b) log-log coordinates.

times very short compared to τ, the ratio $G(t)/G_0$ is essentially constant; that is, the elasticity totally predominates and the modulus is constant. For times which are long compared to τ, the modulus drops to zero, indicating totally viscous behavior. It is only for time scales within roughly one order of magnitude of τ that the combined viscoelastic behavior is observed. Two aspects of this will be developed in subsequent sections:

1. If the applied force varies sinusoidally with time, the period of the oscillation defines the time scale. Quite different mechanical responses are expected at different frequencies. This type of experiment will be described in Secs. 3.10 and 3.11.
2. Viscosity is considerably more sensitive to temperature than elasticity. By varying the temperature, the relaxation time of the polymer will be changed. Hence different mechanical response might be expected on a fixed laboratory time scale for samples examined at different temperatures.
3. Equivalent mechanical behavior can be achieved by either time (or frequency) or temperature manipulation. As noted in Sec. 3.2, results measured at different temperatures can be reduced to a common temperature to describe response over a wide range of times. We shall consider data reduced to a common temperature in this chapter and discuss the reduction process in Chap. 4.

Until now we have been describing the behavior of the Maxwell model in a relaxation experiment. How do these predictions compare with the observed behavior of polymers under the same experimental conditions? Figure 3.9 shows a plot of experimental results for two different un-cross-linked polymers of high molecular weight. One of the samples is polyisobutylene of $M = 1.56 \times 10^6$, the temperature to which the data has been reduced is 25°C, and the time scale is in hours. The second polymer is polystyrene of $M = 2.0 \times 10^5$, the reduced temperature is 135°C and the units of time are seconds. The fact that the reduced temperatures are different should not concern us, nor is it significant that the moduli reported are Young's moduli while Eq. (3.59) was derived for shear. The issue is whether the model predicts the shape of the experimental curves. Since Fig. 3.9 is a double logarithmic plot, it should resemble Fig. 3.8b if the model applies. Our first reaction is that the agreement is not very good. Since these are the first examples of actual time-dependent data we have examined, it will be worthwhile to look at them in some detail. Moving from short to long times in Fig. 3.9, four regions of behavior can be distinguished:

1. At very short times the modulus is on the order of 10^{-10} N m^{-2}, comparable to ordinary window glass at room temperature. In fact, the mechanical behavior displayed in this region is called the glassy state, regardless of the chemical composition of the specimen. Inorganic and polymeric glasses

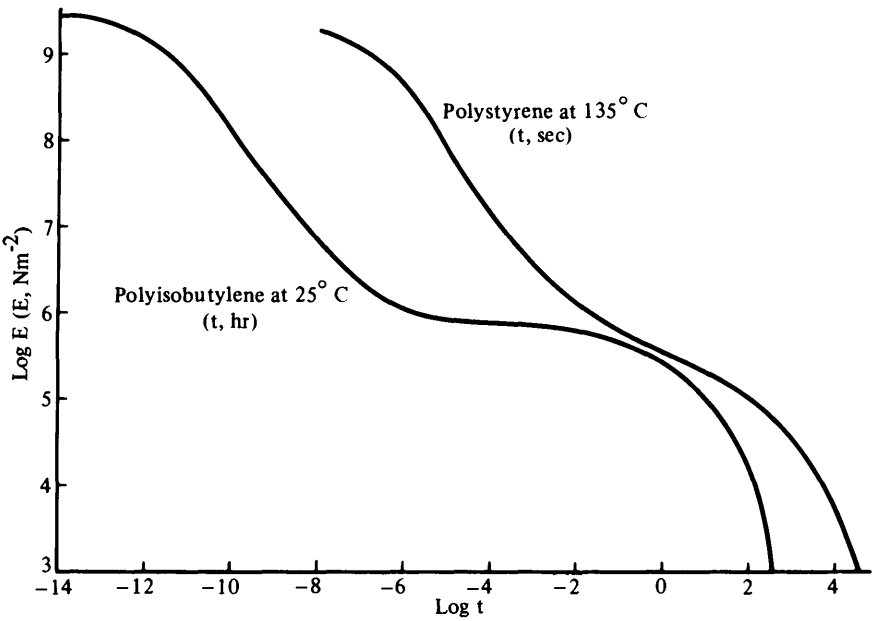

Figure 3.9 Log-log plots of modulus versus time for polyisobutylene at 25°C and polystyrene at 135°C. Note the different units of time for the two substances. (From data of A. V. Tobolsky and E. Catsiff and of H. Fujita and K. Ninomiya. From Ref. 4.)

are very similar in many properties and are often described as being hard, stiff, and brittle. These are the properties displayed by the polymers in Fig. 3.9 for very short periods of observation.

2. At somewhat longer times the modulus undergoes a gradual transition to a value lower by 3 or 4 orders of magnitude than its glassy value. Observed on this time scale, the material has a leathery consistency.
3. At still longer times a more or less pronounced plateau is encountered. The value of the plateau modulus is on the order of 10^6 N m^{-2}, comparable to the effect predicted for cross-linked elastomers in Sec. 3.4. This region is called the rubbery plateau and the sample appears elastic when observed in this time frame.
4. Eventually the modulus begins to drop off rapidly. This is an indication of the onset of flow rather than elastic resistance to deforming forces. The material would display viscous flow for very long periods of observation. Here again we can cite an analogy between inorganic glass and polymers.

The windows in some medieval cathedrals show greater thickness at the bottom than at the top, owing to the slow flow of the glass under the influence of gravity.

One of the things we immediately become aware of in examining a horizontal sweep across Fig 3.9 is that a similar range of behaviors would be encountered for an observation of some standardized duration, if temperature were the independent variable. As a matter of fact, the temperature at which the modulus drops from the glassy to rubbery values is the glass transition temperature. In an isothermal situation this same transition in behavior is characterized by the time required for certain relaxations. From Fig. 3.9 we can immediately conclude that polystyrene has a higher glass transition temperature than polyisobutylene. Table 2.3 lists the T_g values for these as 373 and 205 K, respectively. Next let us examine the meaning of these results.

3.8 Understanding the Modulus: Molecules and Models

The four regions of behavior shown by the polymers in Fig. 3.9 are fairly typical of high molecular weight un-cross-linked polymers. Let us examine the four regions of behavior, this time in terms of what is happening at the molecular level:

1. In the glassy state net movements of the chain backbone are impossible. We may consider this now from two points of view: The time required for movement of the chain is long, and the glassy state is observed when the time of observation is too short for such movements to occur. Alternatively, at low temperatures backbone motion is literally frozen out. The principal difference between a crystalline solid and a glassy solid is in the order (or lack thereof) of the molecular arrangement, not in the magnitude of the modulus. Both glassy and crystalline states are discussed in the next chapter.
2. At the transition between glassy and rubbery behavior, a distinct relaxation occurs. From one viewpoint, the molecules have enough time to jostle into more relaxed conformations; from another, they have enough thermal energy to do so.
3. In the rubbery plateau, a new impediment to movement must be overcome: entanglements along the polymer chain. In discussing the effects of entanglements in Chap. 2, we compared them to crosslinks. Is it any surprise, then, that rubbery behavior similar to that shown by cross-linked elastomers characterizes this region?
4. Chemical crosslinks and entanglements differ, however. The former is permanent, the latter transient. Given sufficient time, even the effects of entanglements can be overcome and stationary-state flow is achieved. An

increase of temperature facilitates the process and produces a similar effect. When the time-dependent modulus of chemically cross-linked polymers is investigated, similar results to Fig. 3.9 are obtained, except that the fourth region is not observed and the modulus of an elastomer is observed at equilibrium.

Now that we have reviewed the phenomena observed in a stress relaxation experiment and the molecular processes occurring therein, let us return to a discussion of the Maxwell model. When we first compared the predictions of the model with experimental observations in the last section, the verdict was rather pessimistic. The foregoing review of the molecular processes which occur reveals the source of the trouble: Two (at least) distinctly different relaxation processes are taking place. At the glass transition, localized displacements of chain segments become feasible. At termination of the rubbery zone, displacements which overcome the more long-range effects of entanglements are possible. Since these different modes of motion meet entirely different types of opposition, the relaxation times may be very different. We allowed for the possibility of more than one relaxation time in discussing the Eyring theory in the last chapter. This possibility is even more plausible in the present context, where significantly different relaxations are visualized.

To quantitatively examine the effect of having two relaxations, suppose we assemble two Maxwell elements in parallel. One of these is characterized by G_1^*, η_1^*, and τ_1; the other by G_2^*, η_2^*, and τ_2. For the sake of discussion we assume the two relaxation times to differ by many orders of magnitude, say, $\tau_1 = 10^{-8}$ sec and $\tau_2 = 10^3$ sec. The values of G* are also different, say, $G_1^* = 10^{10}$ N m^{-2} and $G_2^* = 10^6$ N m^{-2}. Table 3.2 shows the result of calculating G(t) according to Eq. (3.59) for each of these elements separately over a wide range of times. Table 3.2 also lists the sum of the two contributions. Because of the logarithmic time scale, the contribution of the individual Maxwell element is its respective G* value for $t < \tau$. For $t > \tau$, the contribution to G rapidly approaches zero. Provided that the two relaxation times are sufficiently different, the total modulus for the system consisting of two Maxwell elements shows two distinct steps occurring in the vicinity of the individual τ's. Table 3.2 also shows the logarithms of this composite modulus for ease of comparison with Fig. 3.9. From this comparison, it is clear that the two-element mechanical model with widely spaced relaxation times is capable of approximating the behavior of actual polymers in terms of the general features observed. An improvement over Eq. (3.59), therefore, is

$$G(t) = G_{1,0}^* e^{-t/\tau_1} + G_{2,0}^* e^{-t/\tau_2} \tag{3.60}$$

Even with this modification, we note that the model predicts a drop off in modulus which is steeper than observed in the individual steps. This gradual

Table 3.2 Calculated Values of G(t) at Various Times Based on a Model Consisting of Two Maxwell Elements in Parallel ($\tau_1 = 10^{-8}$ sec, $G_1^* = 10^{10}$ N m^{-2}, and $\tau_2 = 10^3$ sec, $G_2^* = 10^6$ N m^{-2})

Log t (sec)	$10^{10}\, e^{-t/10^{-8}}$ (N m^{-2})	$10^6\, e^{t/10^3}$ (N m^{-2})	$\sum_{1+2} G\, e^{-t/\tau}$ (N m^{-2})	$\log \sum_{(1,2)}$ (N m^{-2})
-14.0	1×10^{10}	1×10^6	1×10^{10}	10.00
-12.0	1×10^{10}	1×10^6	1×10^{10}	10.00
-10.0	9.9×10^9	1×10^6	9.9×10^9	10.00
-8.0	3.68×10^9	1×10^6	3.68×10^9	9.57
-7.5	4.23×10^8	1×10^6	4.24×10^8	8.63
-7.0	4.54×10^5	1×10^6	1.45×10^6	6.16
-6.5	1.85×10^{-4}	1×10^6	1×10^6	6.00
-6.0	3.7×10^{-34}	1×10^6	1×10^6	6.00
-4.0	~ 0	1×10^6	1×10^6	6.00
-2.0	~ 0	1×10^6	1×10^6	6.00
0.0	~ 0	9.99×10^5	9.99×10^5	6.00
+2.0	~ 0	9.05×10^5	9.05×10^5	5.96
+3.0	~ 0	3.68×10^5	3.68×10^5	5.57
+3.5	~ 0	4.23×10^4	4.23×10^4	4.63
+4.0	~ 0	4.54×10^1	4.54×10^1	1.66

decline can be viewed as a whole series of steps of the general type described above, except now closely spaced in G* and τ values. Such a set of steps will not be resolved as in Table 3.2, but slightly different elements will contribute to the modulus simultaneously.

The Maxwell model for a set of n elements is shown in Fig. 3.7b. Recall that each element is characterized by its own parameters, for the ith: G_i^*, η_i^*, and τ_i. For a set of n Maxwell elements, Eq. (3.59) becomes

$$G(t) = \sum_{i=1}^{n} G_i(t) = \sum_{i=1}^{n} G_{i,0}^* e^{-t/\tau_i} \tag{3.61}$$

Finally, if a very large number of relaxation times is present, the summation in Eq. (3.61) can be replaced by an integral:

$$G(t) = \int_0^\infty G(\tau) e^{-t/\tau} d\tau \tag{3.62}$$

where $G(\tau)$ is a continuous distribution function which gives the contribution of relaxation times between τ and $\tau + d\tau$. If $G(\tau)$ were known, the modulus could be predicted exactly. Since a logarithmic time scale is almost always used in this type of work, it is more common to multiply and divide the right-hand side of Eq. (3.62) by τ and regroup the terms:

$$G(t) = \int_0^\infty \tau G(\tau) e^{-t/\tau} \frac{d\tau}{\tau} = \int_0^\infty H(\tau) e^{-t/\tau} d \ln \tau \tag{3.63}$$

The factor $\tau G(\tau)$ is called the relaxation spectrum and is given the symbol $H(\tau)$.

In principle, the relaxation spectrum $H(\tau)$ describes the distribution of relaxation times which characterizes a sample. If such a distribution function can be determined from one type of deformation experiment, it can be used to evaluate the modulus or compliance in experiments involving other modes of deformation. In this sense it embodies the key features of the viscoelastic response of a spectrum. Methods for finding a function $H(\tau)$ which is compatible with experimental results are discussed in Ferry's *Viscoelastic Properties of Polymers*. In Sec. 3.12 we shall see how a molecular model for viscoelasticity can be used as a source of information concerning the relaxation spectrum.

3.9 The Voigt Model: Creep

In this section we consider a different experimental situation: the case of creep. In a creep experiment σ is maintained at a constant value and the time dependence of the strain is measured. Thus it is the exact inverse of the relaxation

experiment. As was the case with relaxation, it is convenient to proceed in terms of a model. Although a new model is not required—creep can be discussed in terms of the Maxwell model—it is convenient to approach the subject in terms of a different model. The components of the model are the same as those in the Maxwell model: the spring and the dashpot. This time, however, they are arranged in parallel rather than in series. This simple mechanical model is called a Voigt element and is sketched in Fig. 3.10a.

We shall follow the same approach as the last section, starting with an examination of the predicted behavior of a Voigt model in a creep experiment. We should not be surprised to discover that the model oversimplifies the behavior of actual polymeric materials. We shall continue to use a shear experiment as the basis for discussion, although a creep experiment could be carried out in either a tension or shear mode. Again we begin by assuming that the Hookean spring in the model is characterized by a modulus G*, and the Newtonian dashpot by a viscosity η^*.

Since the strain is the same in both elements in the Voigt model, the applied stress (subscript 0) must equal the sum of the opposing forces arising from the elastic and viscous response of the model:

$$\sigma_0 = \sigma_{el} + \sigma_{vis} \tag{3.64}$$

Substituting Eqs. (2.2) and (3.50) into this relationship yields

$$\sigma_0 = G^*\gamma + \eta^* \frac{d\gamma}{dt} \tag{3.65}$$

In the following example we examine the solution to this differential equation.

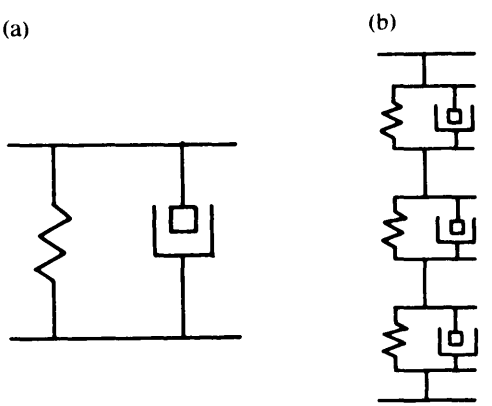

Figure 3.10 Voigt models consisting of a spring and dashpot in parallel: (a) simple Voigt unit and (b) set of units arranged in series.

Example 3.4

Verify that $\gamma(t) = (1/G^*)\sigma_0 + Be^{-G^*t/\eta^*}$ is a solution to Eq. (3.65) and evaluate the constant B for the boundary condition that $\gamma = 0$ at $t = 0$.

Solution

We verify the solution by carrying out the indicated differentiation and substituting back into the differential equation:

$$\frac{d\gamma}{dt} = -\frac{G^*B}{\eta^*} e^{-G^*t/\eta^*} \quad \text{for } \sigma_0, G^*, \text{ and } \eta^* \text{ constant}$$

If we substitute back into Eq. (3.65),

$$\sigma_0 = G^*\left(\frac{1}{B}\sigma_0 + Be^{-G^*t/\eta^*}\right) + \eta^*\left(-\frac{G^*B}{\eta^*} e^{-G^*t/\eta^*}\right)$$

If $\gamma = 0$ at $t = 0$, the solution becomes $0 = (1/G^*)\sigma_0 + B$ or $B = -\sigma_0/G^*$. Therefore we write $\gamma(t) = (\sigma_0/G^*)(1 - e^{-t/\tau})$ using the result of $\tau = \eta^*/G^*$. Dividing through by σ_0 converts $\gamma(t)$ to compliance as defined in Table 3.1.

•

The example shows that the shear compliance of the Voigt material is given by

$$J(t) = \frac{\gamma(t)}{\sigma_0} = \frac{1}{G^*}(1 - e^{-t/\tau}) = J(\infty)(1 - e^{-t/\tau}) \tag{3.66}$$

Figure 3.11a is a plot of this solution, showing how the strain develops exponentially with time. The maximum value of the compliance is attained as $t \to \infty$, hence the upper limits of compliance is designated $J(\infty)$. Since the deformation

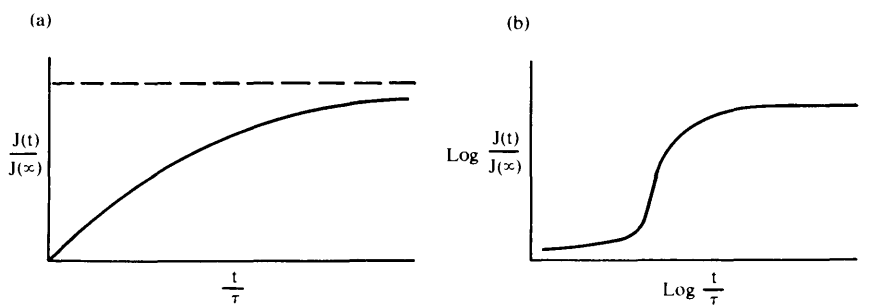

Figure 3.11 Time-dependent shear compliance [as $J(t)/J(\infty)$] versus time (as t/τ): (a) linear coordinates and (b) log–log coordinates.

only gradually approaches this limit, the ratio η^*/G^* is called the retardation time in this kind of experiment. The retardation time of the Voigt element continues to define the time scale of the experiment. A log-log representation of Eq. (3.66) exaggerates the shape of the solution and results in a rather sharp step in compliance at $t = \tau$. This is shown in Fig. 3.11b.

It is interesting to note that the Voigt model is useless to describe a relaxation experiment. In the latter a constant strain was introduced instantaneously. Only an infinite force could deform the viscous component of the Voigt model instantaneously. By constrast, the Maxwell model can be used to describe a creep experiment. Equation (3.56) is the fundamental differential equation of the Maxwell model. Applied to a creep experiment, $d\sigma/dt = 0$ and the equation becomes

$$\frac{d\gamma}{dt} = \frac{1}{\eta^*} \sigma_0 \tag{3.67}$$

Integrating Eq. (3.67) and using $\gamma = \gamma_0$ at $t = 0$ to evaluate the integration constant gives

$$\gamma(t) = \gamma_0 + \frac{\sigma_0}{\eta^*} t \tag{3.68}$$

or

$$J(t) = J(0) + \frac{1}{\eta^*} t \tag{3.69}$$

The Maxwell model thus predicts a compliance which increases indefinitely with time. On rectangular coordinates this would be a straight line of slope $1/\eta^*$, and on log-log coordinates a straight line of unit slope, since the exponent of t is 1 in Eq. (3.69).

As we did in the case of relaxation, we now compare the behavior predicted by the Voigt model—and, for that matter, the Maxwell model—with the behavior of actual polymer samples in a creep experiment. Figure 3.12 shows plots of such experiments for two polymers. The graph is on log-log coordinates and should therefore be compared with Fig. 3.11b. The polymers are polystyrene of molecular weight 6.0×10^5 at a reduced temperature of 100°C and cis-polyisoprene of molecular weight 6.2×10^5 at a reduced temperature of −30°C.

Since the compliance is essentially the inverse of the modulus, it is not surprising that the same four regions of mechanical behavior show up again here. The data for polystyrene is more fully developed, so we shall examine it:

1. At very short times the compliance is low and essentially constant. This is the glassy state where chain motion requires longer times to be observed.

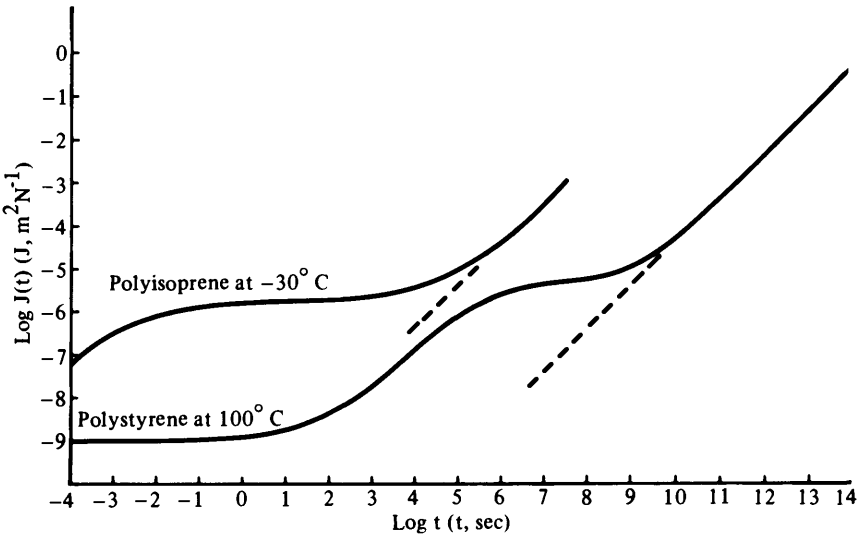

Figure 3.12 Log-log plots of compliance versus time for polystyrene at 100°C and cis-polyisoprene at -30°C. (Data of D. J. Plazek and V. M. O'Rourke and of N. Nemoto, M. Moriwaki, H. Odani, and M. Kurata from Ref. 4.)

The same mechanical behavior would be observed at longer times at lower temperatures.

2. At longer times an increase in compliance marks the relaxation of the glassy state to the rubbery state. Again, an increase of temperature through T_g would produce the same effect.
3. The plateau compliance is characteristic of rubbery behavior where chain entanglements play the role of effective crosslinks.
4. The upswing in compliance from the rubbery plateau marks the onset of viscous flow. In this final stage the slope of the lines (the broken lines in Fig. 3.12) is unity, which means that the compliance increases linearly with time.

As was the case with the modulus, the transitions from one horizontal region of compliance to another is more gradual than that predicted by the model and shown in Fig. 3.11b.

The procedure we followed in adapting the relaxation model to experimental findings immediately suggests how to handle the discrepancies between the model and experiment in the case of creep:

1. The more gradual approach to equilibrium than the model predicts can be taken into account by imagining that the rise consists of a series of n smaller (and unresolved) steps. This is equivalent to expanding the model so that it consists of n Voigt elements as shown in Fig. 3.10b. Each of these Voigt elements is characterized by its own value for G^*, η^*, and τ.
2. With this modification of the model, Eq. (3.66) becomes

$$J(t) = \sum_{i=1}^{n} J_i(t) = \sum_{i=1}^{n} J_i(\infty)\,(1 - e^{-t/\tau_i}) \tag{3.70}$$

or

$$J(t) = \int_0^{\infty} J(\tau)\,(1 - e^{-t/\tau})\,d\tau \tag{3.71}$$

if a continuous distribution of retardation times is considered [compare Eq. (3.62)].
3. In addition to the set of Voigt elements, a Maxwell element could also be included in the model. The effect is to include a contribution given by Eq. (3.69) to the calculated compliance. This long time flow contribution to the compliance is exactly what we observe for non-cross-linked polymers in Fig. 3.12.
4. Therefore, in the most general case, we write for an actual polymer

$$J(t) = J(0) + \frac{t}{\eta^*} + \int_0^{\infty} J(\tau)\,(1 - e^{-t/\tau})\,d\tau \tag{3.72}$$

An advantage of having the relaxation spectrum defined by Eq. (3.63) is that it can be adapted to expressions like this to calculate mechanical behavior other than that initially measured.

The Maxwell and Voigt models of the last two sections have been investigated in all sorts of combinations. For our purposes, it is sufficient that they provide us with a way of thinking about relaxation and creep experiments. Probably one of the reasons that the various combinations of springs and dashpots have been so popular as a way of representing viscoelastic phenomena is the fact that simple and direct comparison is possible between mechanical and electrical networks, as shown in Table 3.3. In this parallel, the compliance of a spring is equivalent to the capacitance of a condenser and the viscosity of a dashpot is equivalent to the resistance of a resistor. The analogy is complete

Table 3.3 Comparison of Mechanical and Electrical Models Consisting of Different Arrangements of Springs and Dashpots or Their Equivalents, Capacitance and Resistance, Respectively

	Mechanical	Electrical
	F/A	Electromotive force
	$\bar{\gamma}$	Charge
	$\dot{\gamma}$	Current
	J	Capacitance
	η	Resistance
Maxwell element	Series	Parallel
Voigt element	Parallel	Series

because electrical work done on a network is stored in capacitors and dissipated by resistors. Likewise, mechanical energy is stored and dissipated by the elastic and viscous units of a mechanical model system. The only word of caution about the use of this analogy is that the rules for combination are reversed—that is, series becomes parallel and vice versa—between the electrical and mechancial networks to produce the close correspondence between the storage and dissipative units. Electrical circuits can thus be designed and analyzed which embody the appropriate features of a model mechanical system. The usefulness of this analogy will be even more evident—although we shall not pursue it—in the next section, in which we take up periodic stress-strain relationships, the mechanical analog of alternating current.

3.10 Dynamic Viscoelasticity

The relaxation and creep experiments that were described in the preceding sections are known as transient experiments. They begin, run their course, and end. A different experimental approach, called a dynamic experiment, involves stresses and strains that vary periodically. Our concern will be with sinusoidal oscillations of frequency ν in cycles per second (Hz) or ω in radians per second. Remember that there are 2π radians in a full cycle, so $\omega = 2\pi\nu$. The reciprocal of ω gives the period of the oscillation and defines the time scale of the experiment. In connection with the relaxation and creep experiments, we observed that the maximum viscoelastic effect was observed when the time scale of the experiment is close to τ. At a fixed temperature and for a specific sample, τ or the spectrum of τ values is fixed. If it does not correspond to the time scale of a transient experiment, we will lose a considerable amount of information about the viscoelastic response of the system. In a dynamic experiment it may

be possible to vary the frequency in such a way that the period and the range of τ values overlap optimally. This sort of dynamic mechanical test yields the maximum amount of information about a viscoelastic substance.

Suppose an oscillating strain of frequency ω is induced in a sample:

$$\gamma = \gamma_0 \sin(\omega t) \tag{3.73}$$

where γ_0 is the maximum amplitude of the strain. If the sample showed only elasticity and obeyed Hooke's law, the stress and strain would be exactly in phase:

$$\sigma = G\gamma = G\gamma_0 \sin(\omega t) = \sigma_0 \sin(\omega t) \tag{3.74}$$

where σ_0 is the maximum amplitude of the stress. The rate of change of the strain is given by

$$\frac{d\gamma}{dt} = \omega\gamma_0 \cos(\omega t) \tag{3.75}$$

If the sample behaves as a Newtonian liquid, the stress is

$$\sigma = \eta\dot{\gamma} = \eta\omega\gamma_0 \cos(\omega t) \tag{3.76}$$

Comparing this result with Eq. (3.74) shows that elastic and viscous forces—occurring separately—are 90° out of phase. In the more general case of the two occurring together, these two components are out of phase by some angle δ.

Next suppose we consider the effect of a periodically oscillating stress on a Voigt element of modulus G* and viscosity η^*. Remember from the last section that for a Voigt element the applied stress equals the sum of the elastic and viscous responses of the model. Therefore, for a stress which varies periodically, Eq. (3.64) becomes

$$\sigma = \sigma_0 \cos(\omega t) = G^*\gamma + \eta^* \frac{d\gamma}{dt} \tag{3.77}$$

In this case, σ_0 is the maximum amplitude of the stress. The solution to this differential equation will give a functional description of the strain in this dynamic experiment. In the following example, we examine the general solution to this differential equation.

Example 3.5

Evaluate the constants B and C in the expression $\gamma = B\cos(\omega t) + C\sin(\omega t)$ so that this equation is a solution to Eq. (3.77).

Solution

Evaluate $d\gamma/dt$ and substitute this and γ into Eq. (3.77):

$$\frac{d\gamma}{dt} = -\omega B\sin(\omega t) + \omega C\cos(\omega t)$$

Therefore $\sigma_0\cos(\omega t) = G^*[B\cos(\omega t) + C\sin(\omega t)] + \eta^*[-\omega B\sin(\omega t) + \omega C\cos(\omega t)]$. For an acceptable solution, coefficients of trigonometric functions must be the same on both sides of the equation. Therefore we can write $\sigma_0 = G^*B + \eta^*\omega C$ and $0 = -\eta^*\omega B + G^*C$. The second of these can be written $C = \eta^*\omega B/G^* = \tau\omega B$. Solving these two simultaneous equations for B and C yields

$$B = \frac{\sigma_0}{G^*(1+\omega^2\tau^2)} \quad \text{and} \quad C = \frac{\sigma_0\tau\omega}{G^*(1+\omega^2\tau^2)}$$

With these values for the constants in the general equation, the latter satisfies the original differential equation.

•

The example shows that we have found an acceptable solution for $\gamma(t)$ for the case of a periodic applied stress. Dividing through by σ_0 gives the appropriate compliance:

$$J(t) = [G^*(1+\omega^2\tau^2)]^{-1}\cos(\omega t) + \omega\tau[G^*(1+\omega^2\tau^2)]^{-1}\sin(\omega t) \qquad (3.78)$$

The frequency-dependent coefficients in this equation are given separate names and symbols to facilitate discussion. Remember it is these coefficients that determine the behavior of the system; the trigonometric functions merely describe the oscillations. The following can be said of the coefficient of the cosine term:

1. It is called the storage compliance and is given the symbol $J'(\omega)$.
2. It is directly related to the energy stored in the sample per cycle of oscillation.
3. It is defined by the expression

$$J'(\omega) = [G^*(1+\omega^2\tau^2)]^{-1} \qquad (3.79)$$

The following can be said of coefficient of the sine term:

4. It is called the loss compliance and is given the symbol $J''(\omega)$.
5. It is directly related to the nonrecoverable or dissipated energy per cycle.
6. It is defined by the expression

$$J''(\omega) = \omega\tau[G^*(1 + \omega^2\tau^2)]^{-1} \tag{3.80}$$

Identical relationships apply to the compliance in a dynamic tensile experiment. Equations (3.79) and (3.80) are plotted in Fig. 3.13.

It is not difficult to understand the behavior of $J'(\omega)$ and $J''(\omega)$ sketched in Fig. 3.13. At low frequencies the motion is slow and the energy loss due to viscous resistance is negligible. The displacement is due essentially to the spring, so the compliance is constant. In Eq. (3.79), $J'(\omega) \to 1/G^*$ as $\omega \to 0$. As the frequency increases, motion is faster and the applied stress becomes more evenly divided between the spring and the dashpot. The elastic portion of the

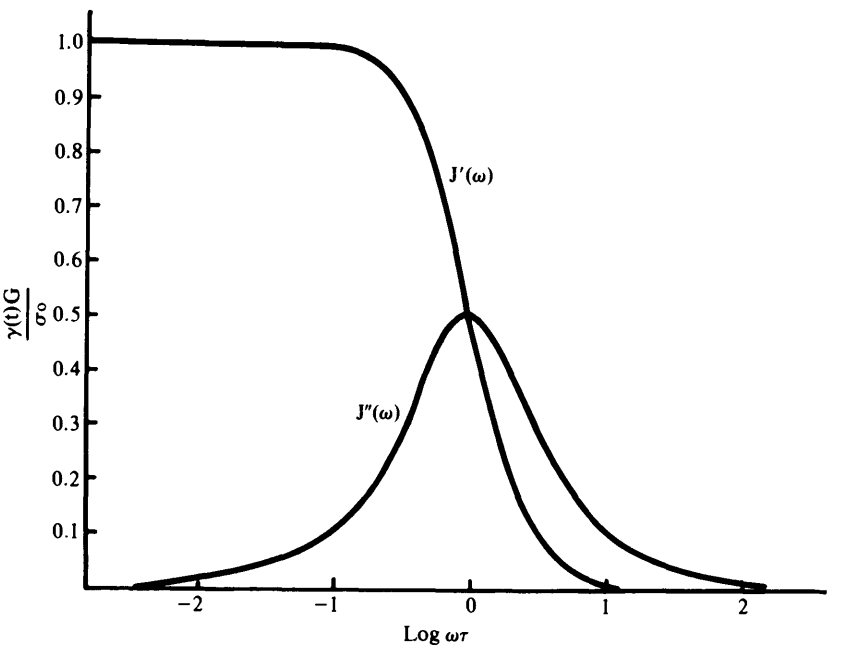

Figure 3.13 Storage compliance $J'(\omega)$ and loss compliance $J''(\omega)$ as functions of $\omega\tau$ as given by Eqs. (3.79) and (3.80).

compliance is therefore less, while the viscous part increases. At very large frequencies the resistance of the dashpot becomes large and effectively suppresses the motion of the spring completely. Also, because the viscosity is so high, the displacement of the dashpot is insignificant. Energy dissipation involves both force and displacement. At high frequencies the former is large but the latter small in the dashpot, so the loss compliance also decreases with increasing $\omega\tau$. In Eq. (3.80) $J''(\omega) \rightarrow (G^*\omega\tau)^{-1} \rightarrow 0$ as $\omega\tau \rightarrow \infty$.

A dynamic modulus can also be evaluated by following a procedure similar to that used for the dynamic compliance above. The modulus is most easily approached by considering a Maxwell element in which case the differential equation analog to Eq. (3.77) is

$$\omega\gamma_0 \cos(\omega t) = \frac{1}{G^*}\frac{d\sigma}{dt} + \frac{1}{\eta^*}\sigma \tag{3.81}$$

Equations (3.77) and (3.81) both have the same general form $dy/dt + Py = Q$, so the general solution—given in Example 3.5—is the same for both, although the values of the constants are different. When the constants are evaluated, the storage and loss components of the modulus are found to be

$$G'(\omega) = \omega^2\tau^2 G^*(1 + \omega^2\tau^2)^{-1} \tag{3.82}$$

and

$$G''(\omega) = \omega\tau G^*(1 + \omega^2\tau^2)^{-1} \tag{3.83}$$

respectively.

The dynamic viscosity is related to the loss component of the shear modulus through the result $\eta_{dyn} = G''/\omega$ As $\omega \rightarrow 0$, the dynamic viscosity approaches the zero shear viscosity of an ordinary liquid, η_N.

We commented above that the elastic and viscous effects are out of phase with each other by some angle δ in a viscoelastic material. Since both vary periodically with the same frequency, stress and strain oscillate with t, as shown in Fig. 3.14a. The phase angle δ measures the lag between the two waves. Another representation of this situation is shown in Fig. 3.14b, where stress and strain are represented by arrows of different lengths separated by an angle δ. Projections of either one onto the other can be expressed in terms of the sine and cosine of the phase angle. The bold arrows in Fig. 3.14b are the components of γ parallel and perpendicular to σ. Thus we can say that $\gamma \cos\delta$ is the strain component in phase with the stress and $\gamma \sin\delta$ is the component out of phase with the stress. We have previously observed that the elastic response is in phase with the stress and the viscous response is out of phase. Hence the ratio of

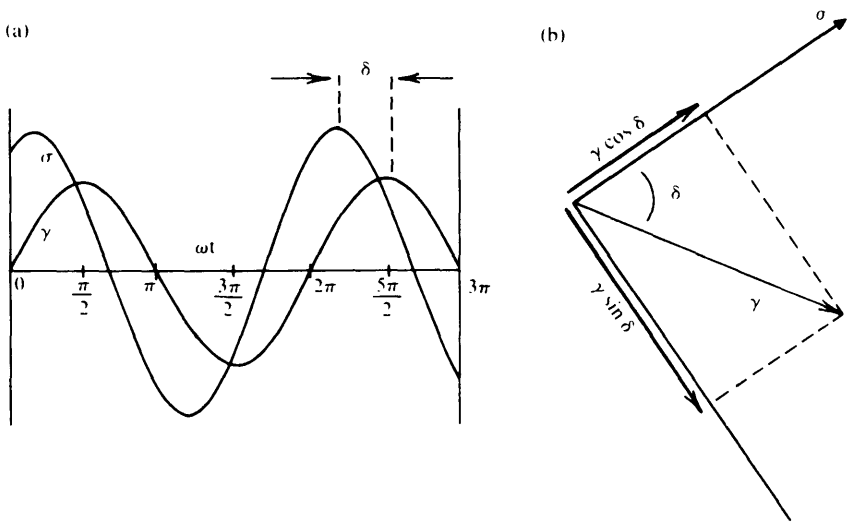

Figure 3.14 General representations of stress and strain out of phase by amount δ: (a) represented by oscillating functions and (b) represented by vectors.

the two measures the relative contributions of these effects. These two contributions are also measured by $J'(\omega)$ and $J''(\omega)$; therefore

$$\frac{\gamma \sin \delta}{\gamma \cos \delta} = \tan \delta = \frac{J''(\omega)}{J'(\omega)} \tag{3.84}$$

where the single parameter $\tan \delta$ is called the loss tangent. The loss tangent is also proportional to the energy loss per cycle, so both $J''(\omega)$ and $\tan \delta$ measure viscous dissipation of mechanical energy in a sample. Often the quantity $\pi \tan \delta$ is reported; it is called the logarithmic decrement.

3.11 The Dynamic Components: Measurement and Interpretation

The wide range of variables involved makes experimental viscoelasticity somewhat difficult to describe. In a particular study the range might be narrowed because of the specific character of the material under investigation. In more general terms, however, such wide ranges of variation are involved that no single experimental design is suitable for all purposes. Figure 3.12, for example, spans 9 orders of magnitude variation in J(t) and 18 orders in t (no wonder log-log

coordinates are standard in this type of work!). In addition, samples can vary from viscous liquids to brittle solids, and there may be restrictions on the size or shape of available samples.

Both stress relaxation and creep experiments have their place in the study of viscoelasticity, but measurement and interpretation of the dynamic mechanical behavior of a polymer gives the most information on the most convenient time scale. We shall describe the experimental aspects of dynamic viscoelasticity only in broad conceptual terms. The actual implementation of these concepts embraces many different kinds of apparatus and experimental routines. In a conceptually simple apparatus for measuring the dynamic components, the sample is sandwiched between two surfaces, one of which is driven with a known periodic displacement. The force at the other side of the gap is measured by a strain gauge. The stress and strain at the two surfaces are proportional to the voltage outputs of electromechanical transducers monitoring each plate. These can be calibrated so that the maximum force F_0 and maximum displacement x_0 are read directly. The signals could be fed into a dual-beam oscilloscope so that the sinusoidal variation of both the stress and strain appear on the screen. The phase angle δ can be measured from this trace, as shown in Fig. 3.14a. Alternatively, the ratio of the two signals can be used to measure the loss tangent directly as indicated by Eq. (3.84). If A is the area of contact between the sample and the plates and h is the separation of the surfaces,

$$J''(t) = \frac{x_0/h}{F_0/A} \sin \delta$$

and

$$J'(t) = \frac{x_0/h}{F_0/A} \cos \delta$$

These equations reveal that sample dimensions must also be known with precision, and, of course, the specimens must be free from defects.

In another type of measurement, the parallel between mechanical and electrical networks can be exploited by using variable capacitors and resistors to balance the impedance of the transducer circuit. These electrical measurements readily lend themselves to computer interfacing for data acquisition and analysis.

A variety of commercial instruments are available for the determination of the viscoelastic behavior of samples. Figure 3.15 shows one such apparatus, the Rheovibron Viscoelastometer. This instrument also takes advantage of the complementarity that exists between time and temperature: It operates at four frequencies over a 175°C temperature range. With accessories, both the frequency range and the temperature range can be broadened still further.

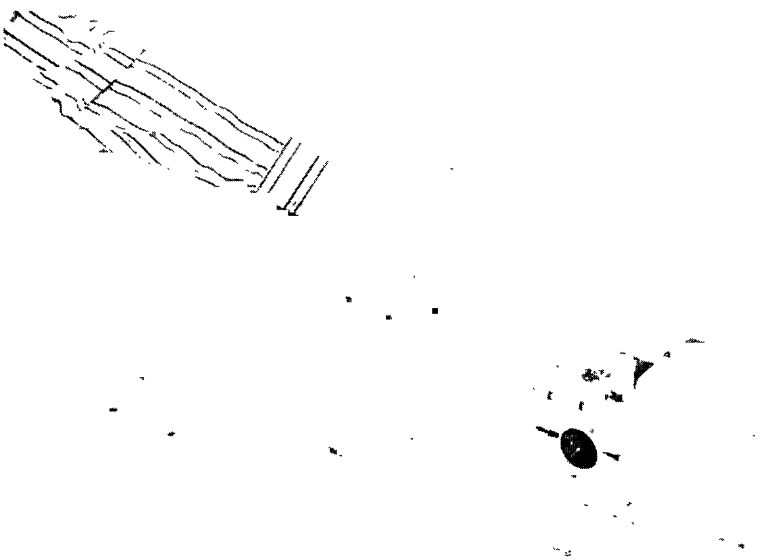

Figure 3.15 The Rheovibron Viscoelastometer, a commercially available instrument for the determination of the dynamic moduli and compliances. [Photo courtesy of Imass, Inc., Accord (Hingham), Mass. 02018.]

Figure 3.16a shows the storage and loss components of the compliance of crystalline polytetrafluoroethylene at 22.6°C. While not identical to the theoretical curve based on a single Voigt element, the general features are readily recognizable. Note that the range of frequencies over which the feature in Fig. 3.16a develops is much narrower than suggested by the scale in Fig. 3.13. This is because the sample under investigation is crystalline. For amorphous polymers, the observed loss peaks are actually broader than predicted by a

Figure 3.16 Some experimental dynamic components. (a) Storage and loss compliance of crystalline polytetrafluoroethylene measured at different frequencies. [Data from E. R. Fitzgerald, *J. Chem. Phys.* 27:1180 (1957).] (b) Storage modulus and loss tangent of poly(methyl acrylate) and poly(methyl methacrylate) measured at different temperatures. (Reprinted with permission from J. Heijboer in D. J. Meier (Ed.), *Molecular Basis of Transitions and Relaxations*, Gordon and Breach, New York, 1978.)

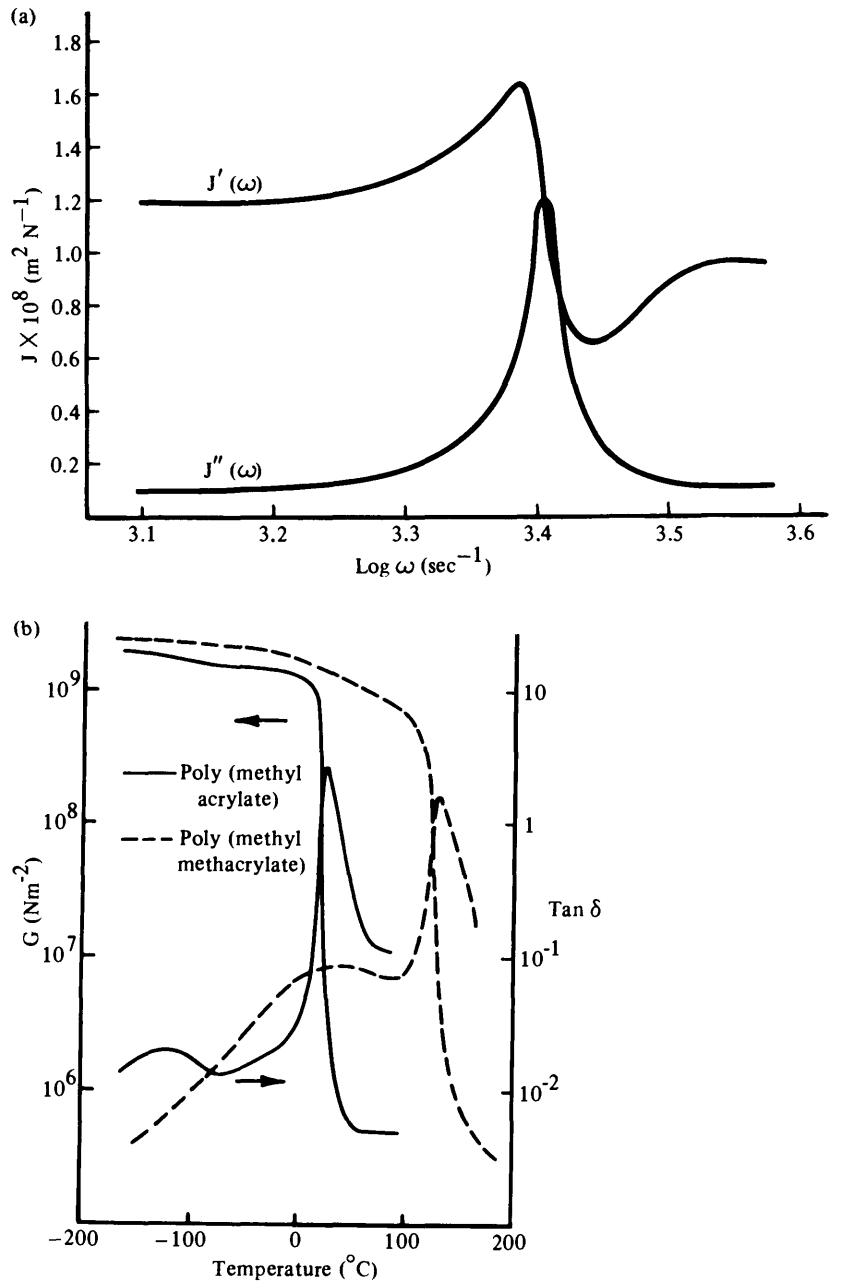
(a)
1.8
1.6
1.4
1.2
1.0
0.8
0.6
0.4
0.2
J X 10^8 (m^2 N^-1)
J' (ω)
J'' (ω)
3.1
3.2
3.3
3.4
3.5
3.6
Log ω (sec^-1)
(b)
10^9
10^8
10^7
10^6
G (Nm^-2)
Poly (methyl acrylate)
Poly (methyl methacrylate)
10
1
10^-1
10^-2
Tan δ
-200
-100
0
100
200
Temperature (°C)

Figure 3.16

single element model. By now, the remedy to this latter situation is becoming commonplace: We simply replace the single element in the model by a set of n elements, each having parameters of G_i^*, η_i^*, and τ_i. For this general system, Eqs. (3.79) and (3.80) become

$$J'(\omega) = \sum_{i=1}^{n} [G_i^*(1 + \omega^2\tau_i^2)]^{-1} \tag{3.85}$$

and

$$J''(\omega) = \sum_{i=1}^{n} \omega\tau_i [G_i^*(1 + \omega^2\tau_i^2)]^{-1} \tag{3.86}$$

for storage and loss, respectively.

The abscissa in Fig. 3.16a is the experimental frequency on a log scale, while log ($\omega\tau$) is plotted in Fig. 3.13. The maximum of the loss compliance occurs at $\omega\tau = 1$ (log 1 = 0) so $\omega = 1/\tau$ at the location of this feature. For the system in Fig. 3.16a, therefore, $\tau = 4 \times 10^{-4}$ sec.

Figure 3.16b is an equivalent diagram in which a different set of variables are employed:

1. The storage modulus rather than compliance is plotted. This is a trivial difference, but note that the modulus is measured at a single frequency, 1 Hz.
2. The loss tangent rather than the loss modulus is plotted, also at 1 Hz.
3. Temperature rather than frequency is the independent variable. We have previously noted the equivalency of these variables. Figure 3.16 may be taken as experimental evidence for that.
4. Temperature variation is not only easy to implement experimentally, but is also more familiar to chemists than the frequency of mechanical oscillations.
5. With T as the independent variable, the transition between glassy and rubbery behavior can be read directly at T_g. Note that T_g is about 100° lower for poly(methyl acrylate) than for poly(methyl methacrylate).
6. An additional interesting feature that emerges from Fig. 3.16b is the smaller loss tangent peak which occurs below T_g. Since backbone motion is essentially frozen out below T_g, this low-temperature peak must measure some energy-dissipating mode of motion that does not involve the main polymer chain. The fact that this feature is so much more prominent in poly(methyl methacrylate) than in poly(methyl acrylate) suggests that the motion involves the methyl group.

The parallel between the loss compliance spectrum—or those of the loss tangent or logarithmic decrement, which are equivalent—and an electromagnetic absorption spectrum should not be overlooked. Several areas of similarity and/or difference can be identified:

1. The electromagnetic spectrum measures the absorption of radiation energy as a function of the frequency of the radiation. The loss spectrum measures the absorption of mechanical energy as a function of the frequency of the stress–strain oscillation.
2. In the electromagnetic spectrum, the energy absorbed makes up the difference between two allowed energy states in the absorber. In the loss spectrum the frequency absorbed closely matches the frequency of dissipative modes of molecular motion in the sample.
3. The electromagnetic spectrum is a quantum effect and the width of a spectral feature is traceable to the Heisenberg uncertainty principle. The mechanical spectrum is a classical resonance effect and the width of a feature indicates a range of closely related τ values for the model elements.
4. The electromagnetic spectrum can be used to "fingerprint" molecules or functional groups. For example, hydroxyl and carbonyl groups absorb different frequencies of infrared radiation. A well-resolved mechanical spectrum can distinguish between the relaxations occurring in, say, crystalline and amorphous regions of the same sample.
5. The amount of a particular component in a sample can be monitored by examining the height of a spectral absorption peak: The reduction of an aldehyde to an alcohol would show up as a decrease in line intensity for the carbonyl and an increase for the hydroxyl peaks in the spectrum. Changes in the relative importance of different relaxation modes in a polymer can also be followed by the corresponding changes in a mechanical spectrum.
6. Theoretical analysis of certain features in the electromagnetic spectrum yields basic molecular parameters such as bond lengths and bond stiffness. We shall see presently that the mechanical spectra can be related to molecular parameters and not just modelistic characteristics as we have used until now.

The following example illustrates an application of the mechanical spectra.

Example 3.6

A diblock copolymer, 71% polyisoprene (I) by weight and 29% polybutadiene (B), was blended in different proportions into a 71%–29% mixture of the individual homopolymers. The loss tangent was measured as a function of temperature for various proportions of copolymer. Two peaks are observed:

Table 3.4 Temperature Coordinate and Relative Height (in Parenthesis) for the Two Loss Tangent Maxima Observed in Mixtures of Isoprene–Butadiene Block Copolymers with Homopolymers of These Two Repeat Units in the Same Proportion[a]

	Temperature (°C) and relative height (arbitrary units)	
Weight percent copolymer	Peak 1	Peak 2
Pure homopolymers	Polyisoprene: -49	Polybutadiene: -82
0	-50 (2.5)	-84 (0.9)
20	-52 (2.6)	-84 (0.8)
40	-54 (2.5)	-85 (0.7)
60	-57 (2.8)	-86 (0.5)
80	-57 (2.6)	-86 (0.5)
100	-58 (2.6)	None

[a]Results interpreted in Example 3.6.
Source: Data from R. R. Cohen and A. R. Ramos, *Macromolecules* 12:131 (1979).

Their temperature coordinate and relative height are listed in Table 3.4. Briefly describe any trends or features of the data and propose an interpretation.

Solution

The system combines having three components and having constant composition, since the copolymer has the same composition as the homopolymer mixture. Listed below are some observations and possible interpretations:

1. The position of the loss tangent maximum is quite different for pure B and pure I, indicating distinctly different T_g values for the two.
2. The homopolymer mixture shows only a minor modification of the two T_g values. This suggests that the two homopolymers are concentrated in separate phases of almost pure polymer.
3. The butadiene peak is absent in the pure copolymer sample. Since this must be a single phase, this phase containing both B and I has a T_g of -58°C.
4. Increasing the copolymer content of the system lowers the T_g of both peaks, but the effect is far more pronounced for the peak associated with I. The latter is essentially constant in height, while the B peak diminishes in height with increasing copolymer. This suggests that the copolymer dissolves preferentially in the polyisoprene.

•

3.12 A Molecular Theory for Viscoelasticity: The Rouse Model

We have relied heavily on the use of models in discussing the viscoelastic behavior of polymers in the transient and dynamic experiments of the last few sections. The models were mechanical, however, and while they provide a way for understanding the phenomena involved, they do not explicitly relate these phenomena to molecular characteristics. To establish this connection is the objective of this section.

The molecular theory begins by subdividing the polymer molecules into subchains with the following properties:

1. The degree of polymerization of the subchain is n_s. If the degree of polymerization of the molecule as a whole is n, then there are n/n_s subchains per molecule. We symbolize the number of subchains per molecule as N_s. Other properties of the subchain—which, incidentally, should not be confused with the chains between crosslink points in elastomers—will also have the subscript s as they emerge.
2. The length of the subchain is sufficient to justify the use of random flight statistics in its description.
3. The mass of the subchain is pictured as concentrated in a bead, connected to adjacent beads by Hookean springs which, individually, obey Eq. (3.45).
4. The displacement of beads representing subchains is resisted by viscous forces which follow Eq. (2.47).
5. Whether the beads representing subchains are imbedded in an array of small molecules or one of other polymer chains changes the friction factor in Eq. (2.47), but otherwise makes no difference in the model. This excludes chain entanglement effects and limits applicability to $M < M_c$, the threshold molecular weight for entanglements.
6. The subchain of this model is an artifact about which we have no information. After developing expressions for the behavior of the subchains, we must describe the latter in terms of the actual polymer chains.

We refer to this model as the bead-spring model and to its theoretical development as the Rouse theory, although Rouse, Bueche, and Zimm have all been associated with its development.

We begin the mathematical analysis of the model, by considering the forces acting on one of the beads. If the sample is subject to stress in only one direction, it is sufficient to set up a one-dimensional problem and examine the components of force, velocity, and displacement in the direction of the stress. We assume this to be the z direction. The subchains and their associated beads and springs are indexed from 1 to N_s; we focus attention on the ith. The absolute coordinates of the beads do not concern us, only their displacements.

Accordingly, we designate z_i as the displacement of the ith bead in the direction of the stress. Since its immediate neighbors also experience some displacement, the springs connecting the ith bead to these neighbors are stretched by the amounts $z_{i+1} - z_i$ and $z_i - z_{i-1}$, respectively. As indicated above, these springs obey Hooke's law with $k_H = 3kT/n_s l_0^2$. The net elastic force on the ith bead is given by the difference between the forces exerted on it by the two connecting springs:

$$F_{el,i} = \frac{3kT}{n_s l_0^2}(z_{i+1} - z_i) - \frac{3kT}{n_s l_0^2}(z_i - z_{i-1}) = \frac{3kT}{n_s l_0^2}(z_{i+1} + z_{i-1} - 2z_i) \tag{3.87}$$

Note that the quantity $n_s l_0^2$ is the mean-square end-to-end distance in the subchain according to Eq. (1.62). We shall designate it $(\overline{r^2})_s$.

The phenomena under discussion are viscoelastic; we have only considered the elastic forces. Next we must incorporate viscous forces. As indicated above, we use Eq. (2.47) to express the proportionality between the viscous resistance to displacement and the velocity of the bead, dz_i/dt:

$$F_{vis,i} = \zeta_s \frac{dz_i}{dt} = n_s \zeta \frac{dz_i}{dt} \tag{3.88}$$

where ζ_s is the friction factor of the subchain. It equals $n_s\zeta$, where ζ is the segmental friction factor discussed in Sec. 2.11. Under stationary-state conditions (and assuming viscous forces to be much larger than inertial forces) the forces given by Eqs. (3.87) and (3.88) equal:

$$\zeta_s \frac{dz_i}{dt} = \frac{3kT}{(\overline{r^2})_s}(z_{i+1} + z_{i-1} - 2z_i) \tag{3.89}$$

for each of the N beads in the polymer, except the two end ones, which experience only one elastic force.

What makes this set of differential equations tricky to solve is the fact that the z values for the two beads adjacent to the ith bead must be taken into account.

The bead and spring model is clearly based on mechanical elements just as the Maxwell and Voigt models were. There is a difference, however. The latter merely describe a mechanical system which behaves the same as a polymer sample, while the former relates these elements to actual polymer chains. As a mechanical system, the differential equations represented by Eq. (3.89) have been thoroughly investigated. The results are somewhat complicated, so we shall not go into the method of solution, except for the following observations:

1. An important part of solving any differential equation is the specification of the boundary conditions. In the present case these can correspond to tension or shear and can be solved to give either a modulus or a compliance.
2. If the viscous contribution were absent, the solution to this problem would be characterized by a resonance frequency close to which the application of small driving forces results in displacements of large amplitude.
3. Including viscosity has the effect of damping the system of vibrators, broadening the range of resonating frequencies, and decreasing the amplitude of the resulting displacement.
4. The solutions describe the vibrational modes of the system. As waves, the solutions are characterized by integers p which essentially count the number of nodes along the chain in a particular mode of vibration. The upper limit of p corresponds to the number of subchains in the molecule N_s.

The shear relaxation modulus of the bead-spring system is given by an expression very much like Eq. (3.61), namely,

$$G(t) = \sum_{p=1}^{N_s} G_p \, e^{-t/\tau_p} \tag{3.90}$$

except that G_p and τ_p are the modulus and relaxation time, respectively, for the wave characterized by the integer p. The value of τ_p in the Rouse theory is given by

$$\tau_p = \left[\frac{24kT}{\langle r^2 \rangle_s \zeta_s} \sin^2 \left(\frac{p\pi}{2(N_s + 1)} \right) \right]^{-1} \tag{3.91}$$

Next we shall examine G_p and τ_p individually.

We return to Eq. (3.45) to describe the elasticity of a subchain. According to that equation, the force can be written

$$F = \frac{3kT}{\sqrt{n_s}\, l_0} \left(\frac{\Delta z}{\sqrt{n_s}\, l_0} \right) = \frac{3kT}{\sqrt{n_s}\, l_0} \gamma$$

where γ is the strain. Dividing both sides of this expression by the cross-sectional area of the subchain converts F to σ and $\sqrt{n_s}\, l_0$ to V_s, the volume of the subchain. This last quantity is given by the reciprocal of the number of subchains per unit volume, which, in turn, is the product of the number of polymer chains per unit volume and the number of subchains per molecule. Putting these results together gives $V_s = (N_s \, \rho N_A / M)^{-1}$. As a result of these considerations, we write the following expression for the tensile modulus:

$$E = \frac{F/A}{\gamma} = \frac{3kT}{V_s} = 3kT \frac{\rho N_A}{M} N_s \tag{3.92}$$

A value one-third this large applies to the shear modulus. We can eliminate N_s from this last result by observing that the limit of Eq. (3.90) as $t \to 0$ is $\sum_{p=1}^{N_s} G_p$, which becomes $N_s G_p$ if all values of G_p are assumed to be equal. Expressing Eq. (3.92) in terms of shear and equating it to $N_s G_p$ gives

$$\frac{RT\rho}{M} = G_p \tag{3.93}$$

Although the notation is different, this result is identical to Eq. (3.51).

Next we turn our attention to τ_p. Equation (3.91) is messy enough for us to accept a certain degree of approximation if some simplification results. For small x, $\sin x \cong x$; therefore

$$\left[\sin^2\left(\frac{p\pi}{2(N_s+1)}\right)\right]^{-1} \cong \frac{4(N_s+1)^2}{\pi^2 p^2}$$

Substituting this approximation into Eq. (3.91) gives

$$\tau_p = \frac{(\overline{r^2})_s \zeta_s}{24kT} \frac{4(N_s+1)^2}{\pi^2 p^2} \cong \frac{(\overline{r^2})_s \zeta_s}{6kT\pi^2 p^2} N_s^2 \tag{3.94}$$

where the second version assumes $N_s \gg 1$.

How are G_p and τ_p related to experimental quantities? We have repeatedly used the ratio of η to G as a definition of τ in this chapter. The experimental viscosity is related to the products of the individual G_p and τ_p values as follows:

$$\eta = \sum_{p=1}^{N_s} \tau_p G_p \tag{3.95}$$

Substituting Eqs. (3.93) and (3.94) into Eq. (3.95) gives

$$\eta = \frac{RT\rho}{M} \frac{(\overline{r^2})_s \zeta_s N_s^2}{6kT\pi^2} \sum_{p=1}^{N_s} \frac{1}{p^2} \tag{3.96}$$

The summation in this equation is known to be equal to $\pi^2/6$ for large values of N_s; therefore we write

$$\eta = \frac{RT\rho}{M} \frac{(\overline{r^2})_s \zeta_s N_s^2}{6kT\pi^2} \frac{\pi^2}{6} = \frac{\rho N_A}{M} \frac{(\overline{r^2})_s \zeta_s N_s^2}{36} \tag{3.97}$$

The remaining step is to eliminate those terms which refer to the subchain by expressing them in terms of the polymer molecule as a whole. Specifically, we recall that $(\overline{r^2})_s = n_s l_0^2$, $\zeta_s = n_s \zeta$, and $N_s = n/n_s$. Substituting into Eq. (3.97), we obtain

$$\eta = \frac{\rho N_A l_0^2 \zeta}{36 M_0} \, n \tag{3.98}$$

which is identical to the Debye viscosity equation, Eq. (2.56). Making this last group of substitutions in Eq. (3.94) gives

$$\tau_p = \frac{n^2 l_0^2 \zeta}{6kT\pi^2 p^2} \tag{3.99}$$

Although the Rouse theory is the source of numerous additional relationships, Eq. (3.98) is a highpoint for us, because it demonstrates that the viscosity we are dealing with in the Rouse theory for viscoelasticity is the same quantity that we would obtain in a flow experiment. Several aspects of this statement deserve amplification:

1. Through the dashpot a viscous contribution was present in both the Maxwell and Voigt models and is essential to the entire picture of viscoelasticity. These have been the viscosities of mechanical units which produce equivalent behavior to that shown by polymers. While they help us understand and describe observed behavior, they do not give us the actual viscosity of the material itself.
2. The viscosity given by Eq. (3.98) not only follows from a different model than the Debye viscosity equation, but it also describes a totally different experimental situation. Viscoelastic studies are done on solid samples for which flow is not measurable. A viscous deformation is present, however, and this result shows that it is equivalent to what would be measured directly, if such a measurement were possible.
3. Although we still need to explain the use of this theory, Eq. (3.98) shows that segmental friction factors are accessible through viscoelastic studies. This fact was anticipated in the list of ζ values given in Table 2.3.

If we combine Eqs. (3.98) and (3.94), we can eliminate N_s from the latter to obtain an expression for the relaxation time of mode p which is free of any reference to the subchain:

$$\tau_p = \frac{6M\eta}{\pi^2 \rho RT} \frac{1}{p^2} \tag{3.100}$$

Setting p = 1 in this expression enables us to identify the cluster of constants

$$\tau_1 = \frac{6M\eta}{\pi^2 \rho RT} \tag{3.101}$$

Now the relaxation times for all higher modes of vibration can be expressed relative to τ_1:

$$\tau_p = \tau_1 p^{-2} \tag{3.102}$$

This result shows that the highest modes of response have the shortest relaxation times and influence the initial response of the sample. Conversely, the longest relaxation time is τ_1, which we can identify with the terminal behavior of the sample. For example, in Fig. 3.9 the final collapse of the modulus at long times occurs at τ_1. An example will show how we can use this idea.

Example 3.7

Inspection of Fig. 3.9 suggests that for polyisobutylene at 25°C, τ_1 is about $10^{2.5}$ hr. Use Eq. (3.101) to estimate the viscosity of this polymer, remembering that $M = 1.56 \times 10^6$. As a check on the value obtained, use the Debye viscosity equation, as modified here, to evaluate M_c, the threshold for entanglements, if it is known that $\zeta = 4.47 \times 10^{-8}$ kg sec^{-1} at this temperature. Both the Debye theory and the Rouse theory assume the absence of entanglements. As a semi-empirical correction, multiply ζ by $(M/M_c)^{2.4}$ to account for entanglements. Since the Debye equation predicts a first-power dependence of η on M, inclusion of this factor brings the total dependence of η on M to the 3.4 power as observed.

Solution

Assume a density of 1.0 g cm^{-3} = 10^3 kg m^{-3}, since no density is given. This assumption will affect the viscosity but will cancel out of the estimation of M_c.

$$\tau_1 = 10^{2.5} \text{ hr} = 1.14 \times 10^6 \text{ sec}$$

$$\eta = \frac{\pi^2 \rho RT \tau_1}{6M}$$

$$= \frac{\pi^2 (10^3 \text{ kg m}^{-3})(8.314 \text{ J K}^{-1} \text{ mol}^{-1})(298 \text{ K})(1.14 \times 10^6 \text{ sec})}{6(1.56 \times 10^3 \text{ kg mol}^{-1})}$$

$$= 2.98 \times 10^9 \text{ kg m}^{-1} \text{ sec}^{-1}$$

Table 2.3 shows that $l_0 = 5.9 \times 10^{-10}$ m and $n = (1.56 \times 10^6)/56 = 2.79 \times 10^4$; therefore

$$\zeta_{app} = \frac{36 M_0 \eta}{\rho N_A l_0^2 n}$$

$$= \frac{36\,(0.056 \text{ kg mol}^{-1})(2.98 \times 10^9 \text{ kg m}^{-1} \text{ sec}^{-1})}{(10^3 \text{ kg m}^{-3})(6.02 \times 10^{23})(5.9 \times 10^{-10} \text{ m})^2\,(2.79 \times 10^4)}$$

$$= 1.09 \times 10^{-3} \text{ kg sec}^{-1}$$

$$\zeta_{app} = \zeta \left(\frac{M}{M_c}\right)^{2.4} \quad \text{hence} \quad \left(\frac{M}{M_c}\right)^{2.4} = \frac{1.09 \times 10^{-3}}{4.47 \times 10^{-8}} = 2.31 \times 10^4$$

$$\frac{M}{M_c} = 65.8 \quad \text{and} \quad M_c = \frac{M}{65.8} = \frac{1.56 \times 10^6}{65.8} = 23{,}700$$

and $n_c = 23{,}700/56 = 423$, which appears quite reasonable compared to the value observed in Fig. 2.10.

•

It should be observed that Eq. (3.102) may be viewed as a distribution function for relaxation times. In fact, if N_s is large enough, integer increments in p may be approximated as continuous p values. This makes τ_p continuous also. The significance of this is that Eq.(3.90) can be written as an integral in analogy with (3.62) if p is continuous:

$$G(t) = \int_0^\infty G_p\, e^{-t/\tau p}\, dp \tag{3.103}$$

Comparison of Eqs. (3.63) and (3.103) reveals

$$H(\tau)\, d \ln \tau = G(\tau)\, d\tau = G_p\, dp \tag{3.104}$$

Taking the log of Eq. (3.102) and differentiating (remember that τ_1 is constant) gives

$$\frac{dp}{d \ln \tau} = -\frac{1}{2}\, p \tag{3.105}$$

Using Eq. (3.93) for G_p, substituting this and Eq. (3.105) into Eq. (3.104) gives $H(\tau)\, d \ln \tau = -(\tfrac{1}{2})\, p\, (RT\rho/M)\, d \ln \tau$. Eliminating p via Eq. (3.100) yields

$$H(\tau) = -\left(\frac{3}{2}\,\frac{RT\rho\eta}{\pi^2 M}\right)^{1/2} \tau^{-1/2} \tag{3.106}$$

Table 3.5 Rouse Theory Expressions for the Modulus (entries labeled 1) and Compliances (entries labeled 2) for Tension and Shear Under Different Conditions[a]

Experimental condition	Tension	Shear
Transient	1. $E(t) = \Sigma_p E_p e^{-t/\tau_p}$	1. $G(t) = \Sigma_p G_p e^{-t/\tau_p}$
	2. $D(t) = \Sigma_p D_p (1 - e^{-t/\tau_p})$	2. $J(t) = \Sigma_p J_p (1 - e^{-t/\tau_p})$
Dynamic components	1. $E'(\omega) = \Sigma_p E_p \omega^2 \tau_p^2 (1 + \omega^2 \tau_p^2)^{-1}$ $E''(\omega) = \Sigma_p E_p \omega \tau_p (1 + \omega^2 \tau_p^2)^{-1}$	1. $G'(\omega) = \Sigma_p G_p \omega^2 \tau_p^2 (1 + \omega^2 \tau_p^2)^{-1}$ $G''(\omega) = \Sigma_p G_p \omega \tau_p (1 + \omega^2 \tau_p^2)^{-1}$
	2. $D'(\omega) = \Sigma_p D_p (1 + \omega^2 \tau_p^2)^{-1}$ $D''(\omega) = \Sigma_p D_p \omega \tau_p (1 + \omega^2 \tau_p^2)^{-1}$	2. $J'(\omega) = \Sigma_p J_p (1 + \omega^2 \tau_p^2)^{-1}$ $J''(\omega) = \Sigma_p J_p \omega \tau_p (1 + \omega^2 \tau_p^2)^{-1}$

[a] For the dynamic components the storage component is designated by a single prime, and the loss component by a double prime.

for the distribution of relaxation times. A theoretical result like this can be used in conjunction with Eq. (3.63) to derive an expression for the shear modulus or the moduli and, with minor differences, the compliances for other modes of deformation.

We observed above that the Rouse expression for the shear modulus is the same function as that written for a set of Maxwell elements, except that the summations are over all modes of vibration and the parameters are characteristic of the polymers and not springs and dashpots. Table 3.5 shows that this parallel extends throughout the moduli and compliances that we have discussed in this chapter. In Table 3.5 we observe the following:

1. G(t) has the same form as Eq. (3.61) for a set of Maxwell elements.
2. J(t) has the same form as Eq. (3.70) for a set of Voigt elements.
3. $J'(\omega)$ and $J''(\omega)$ have the same form as Eqs. (3.79) and (3.80) for a dynamic Voigt system.
4. $G'(\omega)$ and $G''(\omega)$ have the same form as Eqs. (3.82) and (3.83) for a dynamic Maxwell system.

The purpose of these comparisons is simply to point out how complete the parallel is between the Rouse molecular model and the mechanical models we discussed earlier. While the summations in the stress relaxation and creep expressions were included to give better agreement with experiment, the summations in the Rouse theory arise naturally from a consideration of different modes of vibration. It should be noted that all of these modes are overtones of the same fundamental and do not arise from considering different relaxation processes. As we have noted before, different types of encumbrance have different effects on the displacement of the molecules. The mechanical models correct for this in a way the simple Rouse model does not. Allowing for more than one value of ζ, along the lines of Example 3.7, is one of the ways the Rouse theory has been modified to generate two sets of τ_p values. The results of this development are comparable to summing multiple effects in the mechanical models. In all cases the more elaborate expressions describe experimental results better.

Problems

1. A constant force is applied to an ideal elastomer, assumed to be a perfect network. At an initial temperature T_i the length of the sample is l_i. The temperature is raised to T_f and the final length is l_f. Which is larger: l_i or l_f (remember F is a constant and $T_f > T_i$)? Suppose a wheel were constructed with spokes of this same elastomer. From the viewpoint of an observer, the spokes are heated near the 3 o'clock position—say, by exposure to sunlight—while other spokes are shaded. Assuming the torque produced can overcome any friction at the axle, would the observer see the wheel turn clockwise or counterclockwise? How would this experiment contrast, in magnitude and direction, with an experiment using metal spokes?

2. An important application of Eq. (3.39) is the evaluation of M_c. Flory et al.† measured the tensile force required for 100% elongation of synthetic rubber with variable crosslinking at 25°C. The molecular weight of the un-cross-linked polymer was 225,000, its density was 0.92 g cm^{-3}, and the average molecular weight of a repeat unit was 68. Use Eq. (3.39) to estimate M_c for each of the following samples and compare the calculated value with that obtained from the known fraction of repeat units cross-linked:

Fraction cross-linked	0.005	0.010	0.015	0.020	0.025
F/A (lb-force $in.^{-2}$)	61.4	83.2	121.8	148.0	160.0

How important is the end group correction introduced in Eq. (3.46) for this system?

3. The purpose of this problem is to consider numerically the effect of including more than two Maxwell elements in the model for a relaxation experiment. Prepare a table analogous to Table 3.2 for a set of four Maxwell elements having the following properties:

Element number	1	2	3	4
G^* (N m^{-2})	10^9	10^8	10^7	10^6
τ (sec)	10^{-8}	10^{-7}	10^{-6}	10^{-5}

Evaluate G(t) for integral powers of 10 between 10^{-10} and 10^{-3} sec. Use the same table entries to evalute G(t) for a two-element Maxwell model consisting of elements 1 and 4 above. On the same graph plot both sets of results as log G(t) versus log t. Comment on the similarities and differences between the two curves.

4. Stress relaxation studies were conducted on samples of nylon yarn at a constant strain of 2% and the following results were obtained‡:

At 25°C

log t (sec)	0.6	1.0	1.3	1.6	2.0	2.3	2.7	3.0	3.3	3.8
E x 10^{-10} (dyne cm^{-2})	4.00	3.85	3.73	3.60	3.47	3.37	3.25	3.17	3.08	2.98

At 45°C

log t (sec)	0.6	1.0	1.5	1.75	2.15	2.65	3.15	3.40
E x 10^{-10} (dyne cm^{-2})	3.35	3.22	3.08	3.00	2.92	2.83	2.79	2.75

†P. J. Flory, N. Rabjohn, and M. C. Shaffer, *J. Polym. Sci.* 4:225 (1949).

‡T. Murayama, J. H. Dumbleton, and M. L. Williams, *J. Macromol. Sci. Phys.* B-1:1 (1967).

Plot E versus log t for both of these sets of data on the same graph. Now suppose that the units of the 45°C experiment are minutes instead of seconds (this is *not* the case, but we can pretend that it is). On the basis of this imaginary condition, each of the times at 45°C should be multiplied by the factor 60 sec/min to make the comparison with the 25°C data. Apply this "correction" to the 45°C data and plot on the original graph. Be sure to select a scale of the original graph so that "corrected" data can be accommodated; also, label various portions clearly. Briefly comment on the results of this manipulation.

5. Figure 3.12 shows that, at long times, the creep compliance is directly proportional to time for the polymers shown. For polystyrene (M = 600,000) at 100°C, the following values describe the linear portion of the data†:

log J(t) ($m^2\ N^{-1}$)	-1.84	-1.44	-1.05	-0.64	-0.24	+0.16
log t (sec)	12.6	13.0	13.4	13.8	14.2	14.6

Use Eq. (3.69) to evaluate the viscosity of the polymer at this temperature. For polystyrene $M_c \cong 30{,}000$. Use the viscosity value calculated above and the entanglement correction procedure introduced in Example 3.7 to estimate ζ for polystyrene. Take $\rho = 1.04\ g\ cm^{-3}$ and $l_0 = 7.4 \times 10^{-10}$ m for this calculation.

6. Equation (3.77) is the starting point for the derivation of the compliance in a dynamic experiment. This derivation is based on a Voigt model. Working from a Maxwell model with additive strains yields the analogous expressions for the modulus. Starting with Eqs. (3.73) and (3.54), derive Eq. (3.81); then use the function given for γ in Example 3.5—this time written for σ to verify that the storage and loss components of the dynamic modulus have the values given by Eqs. (3.82) and (3.83).
7. In a dynamic experiment $\gamma(t) = \gamma_0 \sin(\omega t)$. The power loss per cycle of oscillation is given by $\int_{\omega t=0}^{\omega t=2\pi} \sigma\, d\gamma$.
   (a) Evaluate the power loss per cycle if the material is a Hookean solid: $\sigma = G\gamma$.
   (b) Evaluate the power loss per cycle if the material is a Newtonian liquid: $\sigma = \eta(d\gamma/dt)$.
   (c) Briefly comment on the significance of these results.
8. Blends of poly(oxytetramethylene glycol) (PTMG) (M = 1000) with poly(tetramethylene terephthalate) (PTMT) were studied‡ for dynamic viscoelastic properties as a function of temperature. For the following percentages by weight PTMG, the temperature coordinate of the loss peak (T_g) and the median plateau modulus vary as follows:

† Data of D. J. Plazek and V. M. O'Rourke, quoted from Ref. 4.

‡ R. W. Seymour, J. R. Overton, and L. S. Corley, *Macromolecules* 8:331 (1975).

Weight percent PTMG	20	25	35	50
T_{max} (°C)	19	10	-3	-35
Modulus (N m^{-2})	13	10	8	4

Criticize or defend the following propositions:

(a) The two polymers combined contribute different degrees of hardness to the blend in proportion to their relative abundance. PTMG is the "hard" component, and PTMT the "soft."

(b) Since a single loss peak is observed, phase separation into hard and soft components does not occur.

(c) Crystallization of PTMT increases the modulus. The crystals function as physical crosslinks in the sample.

9. For the tire cord-rubber composite system, the experimental loss tangent $(\tan \delta)_{ex}$ may be regarded as the sum of two contributions: the loss tangent associated with the individual constituents, assuming perfect adhesion between them, and the loss tangent associated with poor adhesion between the tire and the cord. The first of these contributions, $(\tan \delta)_{perfect}$, is calculated from the properties of the rubber and the cord measured separately. Using the following data‡ to evaluate the adhesion contribution to the loss tangent:

	Nylon-6,6 cord		Poly(ethylene terephthalate) cord	
Adhesive?	Yes	No	Yes	No
$(\tan \delta)_{ex} \times 10^{-3}$:	86.3	108.7	74.4	84.2
$(\tan \delta)_{perfect} \times 10^{-3}$:	68.1	58.5	36.2	27.2

Briefly explain each of the following points: Does it make sense that the loss tangent is larger when a condition of poor adhesion exists between the cord and the rubber? Is the adhesive effective? Is it equally effective for both of the cord materials?

10. The following data were obtained on the same system described in Example 3.6.§ This time the copolymer (C) concentration is fixed at 25% by weight and the proportions of polybutadiene (B) and polyisoprene (I) are varied:

† T. Murayama and E. J. Lawton, *J. Appl. Polym. Sci.* 17:669 (1973).

‡ R. E. Cohen and A. R. Ramos, *Macromolecules* 12:131 (1979).

Weight percent			Temperature (°C) and, in parentheses, relative height (arbitrary units)	
B	I	C	Peak 1	Peak 2
75	0	25	-78 (2.1)	-54 (1.3)
50	25	25	-76 (2.2)	-50 (1.8)
25	50	25	-85 (0.9)	-54 (2.7)
0	75	25		-51 (3.0)

Criticize or defend the following proposition: These data display the same trends described in the example and suggest the same interpretation.

11. Chains of polybutadiene were trapped in the network formed by cooling a butadiene–styrene copolymer until phase separation occurred for the styrene, effectively crosslinking the copolymer. At 25°C the loss modulus shows a maximum which is associated with the free chains. This maximum occurs† at the following frequencies for the indicated molecular weights of polybutadiene:

ω (Hz)	1.3×10^4	63	3.2	0.79	2.5×10^{-2}
$M_w \times 10^{-3}$ (g mol^{-1})	10	57	120	249	634

Evaluate the relaxation time associated with each of these molecular weights and verify that the molecular weight dependence of τ corresponds to the value given in Sec. 2.13.

Bibliography

1. Aklones, J. J., Mac Knight, W. J., and Shen, M., *Introduction to Polymer Viscoelasticity*, Wiley-Interscience, New York, 1972.
2. Alfrey, T., Jr., *Mechanical Behavior of High Polymers*, Interscience, New York, 1948.
3. Bueche, F., *Physical Properties of Polymers*, Interscience, New York, 1962.
4. Ferry, J. D., *Viscoelastic Properties of Polymers*, Wiley, New York, 1980.
5. Flory, P. J., *Principles of Polymer Chemistry*, Cornell University Press, Ithaca, N.Y., 1953.
6. Meares, P., *Polymers: Structure and Bulk Properties*, D. Van Nostrand, London, 1965.

†G. Kraus and K. W. Rollmann, *J. Polym. Sci. Phys.* 15:385 (1977).

4

The Glassy and Crystalline States

The average *polymer*
Enjoys a glassy state, but cools, forgets
To slump, and clouds in closely patterned minuets.

The Dance of the Solids, by John Updike

4.1 Introduction

In this chapter we examine some aspects of the solid states of polymers. There are two different forms in which a polymer can display the mechanical properties we associate with solids: as a crystal or as a glass. Not all polymers are able to crystallize; a high degree of microstructural regularity within the polymer chains is essential for crystallization to occur. Even in those polymers which do crystallize, the degree of crystallinity is less than 100%. Therefore in all cases there is at least some polymer, perhaps all, which is noncrystalline even though the temperature is well below the freezing point. If the temperature is lowered far enough, the glassy state is ultimately formed from the noncrystalline polymer. In the last chapter we saw that glasses are characterized by high values of the moduli and low values of the compliances.

In discussing the low-temperature (and this is only low compared to the region where the material is rubbery or viscous) behavior of polymers, two transitions are possible: the crystal–liquid transition and the glass–liquid transition. In the temperature range between these two transitions we may be dealing with a mixture of orderly crystals and chaotic amorphous polymer. It is possible to classify the literature on the subject as partly ordered and partly chaotic as well. When some unifying principle or perspective is operating, an orderly discussion is possible. When a catalog of diverse behaviors arising from diverse procedures is presented, the subject matter seems chaotic. From the viewpoint of the student trying to get oriented to the subject, the ordered approach is

definitely preferred. From the point of view of fidelity to the actual range of observable behaviors, some chaos is closer to the true picture.

To provide a rational framework in terms of which the student can become familiar with these concepts, we shall organize our discussion of the crystal-liquid transition in terms of thermodynamic, kinetic, and structural perspectives. Likewise, we shall discuss the glass-liquid transition in terms of thermodynamic and mechanistic principles. Every now and then, however, to impart a little flavor of the real world, we shall make reference to such complications as the prior history of the sample, which can also play a role in the solid behavior of a polymer.

A variety of experimental techniques have been employed to research the material of this chapter, many of which we shall not even mention. For example, pressure as well as temperature has been used as an experimental variable to study volume effects. Dielectric constants, indices of refraction, and nuclear magnetic resonsance (NMR) spectra are used, as well as mechanical relaxations, to monitor the onset of the glassy state. X-ray, electron, and neutron diffraction are used to elucidate structure along with electron microscopy. It would take us too far afield to trace all these different techniques and the results obtained from each, so we restrict ourselves to discussing only a few types of experimental data. Our failure to mention all sources of data does not imply that these other techniques have not been employed to good advantage in the study of the topics contained herein.

The material of this chapter and, for that matter, of the two preceding chapters has wide applicability in the area of technology and manufacture. To do justice to this facet of the subject would require a book in itself, so we must settle for a few paragraphs concerned with industrial applications.

4.2 The Glass and Melting Transitions

In the last chapter time was the primary independent variable under consideration. We saw that at short times of observation, polymeric solids take on high values of the modulus, roughly three or four orders of magnitude higher than those shown in the rubbery state of these materials. The transition between the two values of the modulus occurs over a range of times. We also saw that temperature changes produce changes in mechanical properties which parallel those resulting from shifts of time scale. This change in mechanical behavior is called the glass transition, and, when monitored by temperature variation, it occurs as the glass transition temperature. We shall return to an examination of the equivalency of time and temperature with respect to effects on mechanical properties later in this chapter. To begin, however, it is desirable to consider some other properties of matter that change at T_g. Although quite a variety of observations are available to choose from, we shall consider the volume changes which occur in cooling a polymer.

Figure 4.1 illustrates schematically the range of possibilities for variation in specific volume with temperature. Remember that specific volume is the reciprocal of the density; it, rather than density, is chosen to describe these changes in anticipation of the molecular interpretations which follow in Sec. 4.9. Line ABDG in Fig. 4.1 shows how the specific volume changes upon freezing a low molecular weight compound. A few substances—water is the best known example—occupy a larger volume per unit mass in the solid state than in the liquid, and for these the transition at the melting point T_m would be a jump rather than a drop in volume. That is not the main point, however; instead, what is significant is that the transition occurs at a single temperature, the melting point T_m. The slopes of AB and DG measure the coefficients of thermal expansion of liquid and solid, respectively. The temperature variation of the latter is not our interest either; the point is that it is different for solids and liquids. Note that the coefficient of thermal expansion shows a discontinuity at the melting point.

An entirely different pattern of behavior is shown along line ABHI. In this case there is no discontinuity at T_m. The line AB which characterizes the liquid changes slope at T_g to become HI. Actually, the change in slope occurs over a range of temperatures (about 5°), as suggested by Fig. 4.1, but extrapolation of the two linear portions permits T_g to be defined by this method. Region HI characterizes the glassy state, and the threshold for its appearance is the glass

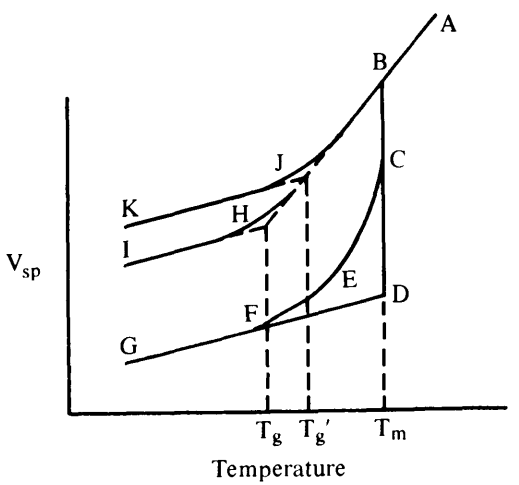

Figure 4.1 Schematic illustration of possible changes in the specific volume of a polymer with temperature. See text for a description of the various lettered phenomena.

transition temperature. The glassy state is also called the vitreous state, and its formation, vitrification. In the region BH, supercooled liquid exists.

In principle, each of the two lines we have discussed could describe the behavior of either high or low molecular weight compounds. This is not to say, however, that each is equally probable for the two classes of compounds. For low molecular weight compounds, special effort must be made to suppress crystallization and achieve glass formation. With polymers, on the other hand, the glassy state is always obtained whether a particular polymer is crystallizable or not. The mere fact that molecular structure allows the possibility of crystal formation does not mean that the latter occurs rapidly or completely: There is often a significant amount of amorphous polymer present, even in a partially crystalline sample. The line ABCEFG in Fig. 4.1 describes the situation of a partly crystalline, partly amorphous polymer. At T_m crystallization begins and the characteristic discontinuity occurs in specific volume (V_{sp}). The sharpness of T_m is not as pronounced for polymers as for low molecular weight compounds, as evidenced by the trailing off in the transition temperature between C and E. In the region EF the volume reflects the supercooling of the amorphous portion of the polymer. The change in slope between segments EF and FG occurs at T_g just as it would in the absence of crystallization. If partial crystallization occurs, the amount of amorphous material is decreased and the change in slope at T_g may be harder to detect in this case.

The line ABJK in Fig. 4.1 is a displaced variation of ABHI in which AB is liquid, BJ is supercooled liquid, and JK is glass. The experimental variable which causes region JK to be offset from HI is the cooling rate, ABJK being the course of the more quickly cooled polymer. Since T_g is identified from the change in slope, it is apparent that T_g is also displaced, appearing at higher temperatures for faster rates of cooling.

The low-temperature (remember that this is a relative term: $T_m = 317°C$ for polyacrylonitrile) behavior of linear polymers may conveniently be divided into three regimes:

1. Above T_m the material is liquid and its viscosity depends on the molecular weight of the polymer and the time scale of the observation, but it would be considered high by all standards.
2. Between T_m and T_g, depending on the regularity of the polymer and on the experimental conditions, this domain may be anything from almost 100% crystalline to 100% amorphous. The amorphous fraction, whatever its abundance, behaves like a supercooled liquid in this region. The presence of a certain degree of crystallinity mimics the effect of crosslinking with respect to the mechanical behavior of a sample.
3. Below T_g the material is hard and rigid with a coefficient of thermal expansion equal to roughly half that of the liquid. With respect to mechanical properties, the glass is closer in behavior to a crystalline solid than to a

liquid. In terms of molecular order, however, the glass more closely resembles the liquid. In this temperature region the noncrystalline fraction acquires the same glassy properties it would have if the crystallization had been suppressed completely. In general terms, there is no difference between linear and cross-linked polymers below T_g.

4. The location of T_g depends on the rate of cooling. The location of T_m is not subject to this variability, but the degree of crystallinity depends on the conditions of the experiment, as well as on the nature of the polymer. For example, if the rate of cooling exceeds the rate of crystallization, there may be no observable change at T_m, even for a crystallizable polymer.

The foregoing description of behaviors introduces us to the phenomena with which we shall be dealing in this chapter. As noted above, both high and low molecular weight compounds are capable of displaying these effects, but the chain structure of the polymer molecules is responsible for the reversed probability of the various possibilities. It is the specific identity of the polymer that anchors these transitions in some particular region of the temperature scale. The regularity of the microstructure of the polymer molecule, along with experimental conditions, determines the extent of crystallization. The glassy state is thus seen as a lowest common denominator shared by all polymers, since 100% crystallinity is virtually impossible. This promotes T_g to the position of importance assumed by T_m for low molecular weight compounds. The fact that the mechanical properties undergo such profound change at T_g also contributes to the significance of this parameter.

Some of the distinctions that we shall have to examine in more detail before proceeding much further are the considerations of order versus disorder, solid versus liquid, and thermodynamics versus kinetics. These dualities are taken up in the next section. With those distinctions as background, we shall examine both the glassy and crystalline states from both the experimental and modelistic viewpoint.

We conclude this section with a few remarks about the measurement of polymer density. This is about as unglamorous an experiment as one can imagine. As a property of matter, we take density very much for granted. The fact that it is conceptually simple, readily available for many materials, and relatively monotonous in its variations all contribute to this attitude. The types of phenomena represented schematically in Fig. 4.1 require careful experimentation on well-defined samples to yield reproducible results. The device that is used to follow volume changes upon cooling is called a dilatometer. The sample is placed in a bulb which is then filled with an inert liquid, generally mercury. The bulb is connected to a capillary so that changes in volume register as variations in the height of the mercury column, just as in a thermometer. For a constant temperature experiments, say, monitoring crystallization at T_m, the volume changes in the capillary correspond identically to changes occurring in

the sample. When temperature variation is involved, the expansion of the mercury due to the temperature change is superimposed on the expansion of the specimen and must be taken into account. To obtain meaningful results it is necessary to standardize the rate at which temperature changes are made and, of course, to have an accurately measured and uniform temperature in the bath surrounding the dilatometer. The sample must be immiscible with the displacement fluid and degassed to prevent entrapment of air. A gas bubble can really raise havoc in this kind of experiment.

4.3 The Thermodynamics of Crystallization: Round I

In dealing with experimental thermodynamics, one of the criteria that a true equilibrium has been established is to approach the state of interest from opposite directions. Accordingly, we are in the habit of thinking of the equilibrium melting point of a crystal or the equilibrium freezing point of the corresponding liquid as occurring at the same temperature. In dealing with polymer crystals, unfortunately, we are not so lucky as to observe this simple behavior. The transition liquid → crystal is so overshadowed by kinetic factors that some workers even question the value of any thermodynamic discussion of the transition in this direction. Furthermore, because of the kinetic complications occurring during the formation of the crystal, the transition crystal → liquid also becomes more involved.

If polymers had infinite molecular weights and formed infinitely large crystals, the thermodynamics of the transition would be simpler, although the kinetics might very well be worse. Assuming, temporarily, that any kinetic complications can be overlooked, we will define the temperature of equilibrium (subscript e) between crystal and liquid for a polymer meeting the infinity criteria stated above as T_e^∞. Subsequently, we will use the superscript ∞ to indicate either infinite crystal dimension, infinite molecular weight, or both; it will be clear from the context which is meant. In such a case the melting point of the crystal would be T_e^∞ and the freezing point of the liquid would also be T_e^∞. The facts that actual molecular weights are less than infinite and that crystals have finite dimensions both tend to lower the equilibrium transition temperature below T_e^∞. The fact that kinetic complications also interfere means, in addition, that the temperature of crystallization T_c does not equal the temperature of melting T_m and that neither equals T_e^∞.

Figure 4.2 illustrates some of these points for poly(1,4-cis-isoprene). The temperature at which the crystals are formed is shown along the abscissa, and the temperature at which they melt, along the ordinate. Note the following observations:

1. The lower the crystallization temperature, the lower the melting point. These facts are connected through consideration of crystal dimensions.

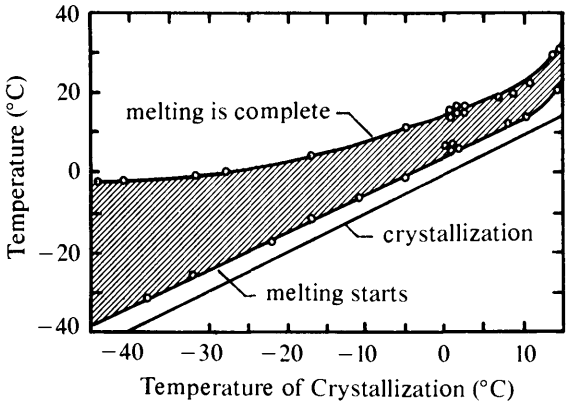

Figure 4.2 Melting temperature of crystals versus temperature of crystallization for poly(1,4-cis-isoprene). Note the temperature range over which melting occurs. [Reprinted with permission from L. A. Wood and N. Bekkedahl, *J. Appl. Phys.* 17:362 (1946).]

2. Melting occurs over a range of temperatures, as in Fig. 4.1. The range narrows as the crystallization temperature increases. This is probably due to a wider range of crystal dimensions and less perfect crystals under the lower temperatures of formation.
3. There is a suggestion of convergence of these lines in the upper right-hand portion of Fig. 4.2. For this polymer T_m^∞ is estimated to be 28°C—not an unreasonable point of convergence for the lines in Fig. 4.2.

We shall take up the kinetics of crystallization in detail in Secs. 4.5 and 4.6. For the present, our only interest is in examining what role kinetic factors play in complicating the crystal-liquid transition. In brief, the story goes like this. Polymers have a great propensity to supercool. If and when they do crystallize, it is an experimental fact that smaller crystal dimensions are obtained the lower the temperature at which the crystallization is carried out. The following considerations supply some additional details:

1. At and near T_m—which is a low temperature for the liquid state of a polymer, whatever its absolute value may be—the viscosity of a polymer melt will be quite high, which is a direct consequence of the encumbered movement of the polymer chains past one another.
2. Polymer crystals form by the chain folding back and forth on itself, with crystal growth occurring by the deposition of successive layers of these folded chains at the crystal edge. The resulting crystal, therefore, takes on a platelike structure, the thickness of which corresponds to the distance between folds.

3. This intricate mode of crystallization requires more time to accomplish than, say, the entry of small ions into growing salt crystals. This, coupled with low chain mobility due to viscous effects, makes the rate of crystallization slow and accounts in part for the fact that with rapid cooling—called quenching—the temperature drops below T_e^∞ without crystallization.
4. The thickness of the crystal plates or lamellae can be measured by x-ray diffraction studies and other methods. It is a well-established fact that thinner lamellae are formed at lower temperatures of crystallization.
5. The thickness depends on the supercooling, which, in turn, is the result of kinetic considerations. Accordingly, crystal thickness is related to T_c, but neither have much to do with T_e^∞.
6. The melting point T_m of the resulting crystal is less than it would be if the crystal had infinite dimensions (T_m^∞). This latter temperature approaches T_e^∞ as $M \to \infty$.

In summary, T_m gives a truer approximation to a valid equilibrium parameter, although it will be less than T_m^∞ owing to the finite dimensions of the crystal and the finite molecular weight of the polymer. We shall deal with these considerations in the next section. For now we assume that a value for T_e^∞ has been obtained and consider the simple thermodynamics of a phase transition.

We begin our application of thermodynamics to polymer phase transitions by considering the fusion (subscript f) process: crystal → liquid.

Figure 4.3a shows schematically how the Gibbs free energy of liquid (subscript l) and crystalline (subscript c) samples of the same material vary with temperature. For constant temperature–constant pressure processes the criterion for spontaneity is a negative value for ΔG, where the Δ signifies the difference final minus initial for the property under consideration. Applying this criterion to Fig. 4.3, we conclude immediately that above T_m^∞, $\Delta G_f = G_l - G_c$ is negative and the process is spontaneous, whereas below T_m^∞, $\Delta G_f > 0$ and it is the reverse process which is spontaneous. At T_m^∞ both phases have the same value of G; at this temperature $\Delta G = 0$ and a condition of equilibrium exists between the phases.

For a particular phase, an increment in Gibbs free energy dG can be expressed in terms of increments of pressure and temperature dp and dT; that is,

$$dG = V\,dp - S\,dT \tag{4.1}$$

where V and S are the volume and entropy of the phase, respectively. Since this is thermodynamics, T is always expressed in degrees Kelvin in these equations. Since G is a state variable and forms exact differentials, Eq. (4.1) can be interpreted to mean

$$\left(\frac{\partial G}{\partial T}\right)_p = -S \tag{4.2}$$

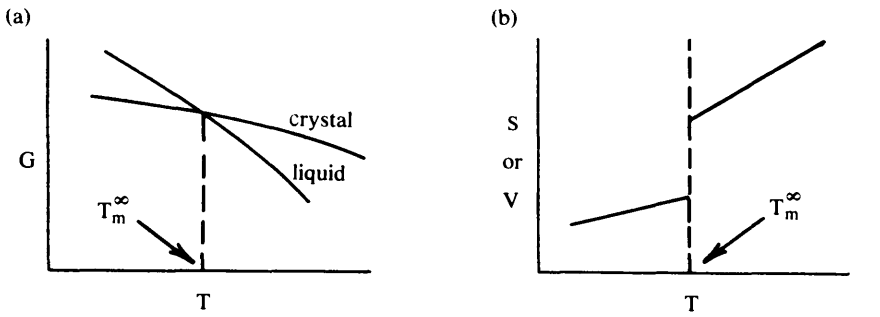

Figure 4.3 Behavior of thermodynamic variables at T_m^∞ for an idealized phase transition: (a) Gibbs free energy and (b) entropy and volume.

and

$$\left(\frac{\partial G}{\partial p}\right)_T = V \tag{4.3}$$

Figure 4.3b is a schematic representation of the behavior of S and V in the vicinity of T_m^∞. Although both the crystal and liquid phases have the same value of G at T_m^∞, this is not the case for S and V (or for the enthalpy H). Since these latter variables can be written as first derivatives of G and show discontinuities at the transition point, the fusion process is called a first-order transition. Vaporization and other familiar phase transitions are also first-order transitions. The behavior of V at T_g in Fig. 4.1 shows that the glass transition is not a first-order transition. One of the objectives of this chapter is to gain a better understanding of what else it might be. We shall return to this in Sec. 4.8.

At T_m^∞, $\Delta G_f = 0$, but ΔS_f, ΔV_f, and ΔH_f have nonzero values. For any constant-temperature process such as fusion,

$$\Delta G = \Delta H - T\,\Delta S \tag{4.4}$$

therefore at equilibrium

$$T_m^\infty = \frac{\Delta H_f}{\Delta S_f} \tag{4.5}$$

This fundamental relationship points out that the temperature at which crystal and liquid are in equilibrium is determined by the balancing of entropy and enthalpy effects. Remember, it is the difference between the crystal and

the liquid that is pertinent; sometimes these differences are not what we might first expect.

Table 4.1 lists values of T_m as well as ΔH_f and ΔS_f per mole of repeat units for several polymers. A variety of experiments and methods of analysis have been used to evaluate these data, and because of an assortment of experimental and theoretical approximations, the values should be regarded as approximate. We assume $T_m \cong T_m^\infty$. In general, both ΔH_f and ΔS_f may be broken into contributions H_0 and S_0 which are independent of molecular weight and increments $\Delta H_{f,1}$ and $\Delta S_{f,1}$ for each repeat unit in the chain. Therefore $\Delta H_f = H_0 + n\,\Delta H_{f,1}$, where n is the degree of polymerization. In the limit of $n \to \infty$, $\Delta H_f \cong n\,\Delta H_{f,1}$ and $\Delta S_f = n\,\Delta S_{f,1}$, so $T_m^\infty = \Delta H_{f,1}/\Delta S_{f,1}$. The values of $\Delta H_{f,1}$ and $\Delta S_{f,1}$ in Table 4.1 are expressed per mole of repeat units on this basis. Since no simple trends exist within these data, the entries in Table 4.1 appear in numbered sets, and some observations concerning these sets are listed here:

1. Polyethylene. The crystal structure of this polymer is essentially the same as those of linear alkanes containing 20–40 carbon atoms, and the values of T_m and $\Delta H_{f,1}$ are what would be expected on the basis of an extrapolation from data on the alkanes. Since there are no chain substituents or intermolecular forces other than London forces in polyethylene, we shall compare other polymers to it as a reference substance.
2. Poly(1,4-cis-isoprene). Although $\Delta H_{f,1}$ is slightly higher than that of polyethylene, it is still completely reasonable for a hydrocarbon. The

Table 4.1 Values of T_m, $\Delta H_{f,1}$, and $\Delta S_{f,1}$ for Several Polymers[a]

Polymer	T_m (°C)	Per mole repeat units	
		$\Delta H_{f,1}$ (J mol^{-1})	$\Delta S_{f,1}$ (J K^{-1} mol^{-1})
1. Polyethylene	137.5	4,020	9.8
2. Poly(1,4-cis-isoprene)	28	4,390	14.5
3. Poly(ethylene oxide)	66	8,280	22.4
4. Poly(decamethylene sebacate)	80	50,200	142.3
Poly(decamethylene azelate)	69	41,840	121.3
5. Poly(decamethylene sebacamide)	216	34,700	71.1
Poly(decamethylene azelamide)	214	36,800	75.3

[a]This notation indicates the contribution to the value for the fusion process (subscript f) per mole of repeat units (subscript 1). Entries are discussed by number in the text.
Source: Data from Ref. 5.

lower T_m is the result of a value of $\Delta S_{f,1}$, which is 50% higher than that of polyethylene. The low melting point of this polymer makes natural rubber a useful elastomer at ordinary temperatures.

3. Poly(ethylene oxide). Although $\Delta H_{f,1}$ is more than double that of polyethylene, the effect is offset by an even greater increase for $\Delta S_{f,1}$. The latter may be due to increased chain flexibility in the liquid caused by the regular insertion of ether oxygens along the chain backbone.
4. Polyesters. The next two polyesters have $\Delta H_{f,1}$ values an order of magnitude higher than polyethylene. Our first thought might be to attribute this to a strong interaction between the polar ester groups. The repeat units of these compounds are considerably larger than in the reference compound, so the $\Delta H_{f,1}$ values should be compared on a per gram basis. When this is done, $\Delta H_{f,1}$ is actually less than for polyethylene. This suggests that the larger value for $\Delta H_{f,1}$ is the result of a greater number of methylene groups contributing London attraction for the polyesters, with the dipole-dipole interaction of the ester groups about the same in both liquid and crystal and therefore contributing little to ΔH_f. When compared on the basis of the number of bonds along the backbone, $\Delta S_{f,1}$ is not exceptional either. Accordingly, T_m is less than polyethylene for these esters.
5. Polyamides. The next two compounds are the amide counterparts of the esters listed under item (4). Although the values of $\Delta H_{f,1}$ are less for the amides than for the esters, the values of T_m are considerably higher. This is a consequence of the very much lower values of $\Delta S_{f,1}$ for the amides. These, in turn, are attributed to the low entropies of the amide in the liquid state owing to the effects of hydrogen bonding and chain stiffness arising from the contribution of the resonance form

These items show that it may be easier to rationalize an observation or trend than to predict it a priori. This state of affairs is not unique to polymers, however. The following example gives another illustration of this type of reasoning.

Example 4.1

The melting points of a series of poly(α-olefin) crystals were studied. All of the polymers were isotactic and had chain substituents of different bulkinesses. Table 4.2 lists some results. Use Eq. (4.5) as the basis for interpreting the trends in these data.

Solution

The bulkiness of the substituent groups increases moving down Table 4.2. Also moving down the table, the melting points decrease, pass through a minimum, and then increase again. As is often the case with reversals of trends such as this, there are two different effects working in opposition in these data:

1. As the bulkiness of the substituents increases, the chains are prevented from coming into intimate contact in the crystal. The intermolecular forces which hold these crystals together are all London forces, and these become weaker as the crystals loosen up owing to substituent bulkiness. Accordingly, the value for the heat of fusion decreases moving down Table 4.2.
2. As the bulkiness of the chain substituents increases, the energy barriers to rotation along the chain backbone increase. As seen in Chap. 1, this decreases chain flexibility in the liquid state. It is flexibility which permits the molecules to experience a large number of conformations and therefore have high entropies. If the flexibility is reduced, the entropy change on melting is less than it would otherwise be. Accordingly, the entropy of fusion decreases moving down the table.

Table 4.2 Values of T_m for Poly(α-olefin) Crystals in Which the Polymer has the Indicated Substituent (Results are Discussed in Example 4.1)

Substituent	T_m(°C)
$-CH_3$	165
$-CH_2CH_3$	125
$-CH_2CH_2CH_3$	75
$-CH_2CH_2CH_2CH_3$	-55
$-CH_2\underset{\displaystyle CH_3}{\underset{\vert}{CH}}-CH_2-CH_3$	196
$-CH_2-\underset{\displaystyle CH_3}{\overset{\displaystyle CH_3}{\overset{\vert}{\underset{\vert}{C}}}}-CH_2-CH_3$	350

Source: Data quoted from F. W. Billmeyer, *Textbook of Polymer Science*, 2nd ed., Wiley-Interscience, New York, 1971.

3. Since $T_m = \Delta H_f/\Delta S_f$, the observed behavior of this series of polymers may be understood as a competition between these effects. For the smaller substituents, the effect on ΔH_f dominates and T_m decreases with bulk. For larger substituents, the effect of ΔS_f dominates and T_m increases with bulk.

The polymers compared all have similar crystal structures but are different from polyethylene, which excludes the possibility for also including the latter in this series. Also note that the isotactic structure of these molecules permits crystallinity in the first place. With less regular microstructure, crystallization would not occur at all.

•

In the discussion of Table 4.1, we acknowledged that there might be some uncertainty in the values of the quantities tabulated, but we sidestepped the origin of the uncertainty. In the next section we shall consider one of these areas: the effect of crystal dimensions of the value of T_m.

4.4 The Thermodynamics of Melting: Round II

Whenever a phase is characterized by at least one linear dimension which is small, the properties of the surface begin to make significant contributions to the observed behavior. We shall examine the structure of polymer crystals in more detail in Sec. 4.7, but for now the following summary of generalizations about these crystals will be helpful:

1. Polymers crystallize in the form of thin plates or lamellae. The thickness of each of these lamellae is on the order of 10 nm.
2. The dimensions of the crystal plates perpendicular to the small dimensions depend on the conditions of the crystallization, but are many times larger than the thickness for a well-developed crystal.
3. The chain direction within the crystal is along the short dimension of the crystal, indicating that the molecule folds back and forth, fire hose fashion, with successive layers of folded molecules accounting for the lateral growth of the platelets.
4. A crystal does not consist of a single molecule, nor does a molecule reside exclusively in a single crystal.
5. The loop formed by the chain as it emerges from the crystal, turns around, and reenters the crystal may be regarded as amorphous polymer, but is insufficient to account for the total amorphous content of most crystalline polymers.
6. Polymer chain ends disrupt the orderly fold pattern of the crystal and tend to be excluded from the crystal and relegated to the amorphous portion of the sample.

7. Variations of all the above points—all the way to the complete failure of a crystallizable polymer to actually crystallize—are possible, depending on experimental conditions.

Since the polymer crystal habit is characterized by plates whose thickness is small, surface phenomena are important. During the early development of the crystal, the lateral dimensions are also small and the effect is even more pronounced. The key to understanding this fact lies in the realization that all phase boundaries possess surface tension and that this surface tension measures the Gibbs free energy stored per unit area of the phase boundary. To get a preliminary feel for the importance of this, suppose we consider a spherical phase of radius r, density ρ, and surface tension γ. The total surface free energy associated with a particle such as this is given by the product of γ and the area of the sphere, or $\gamma(4\pi r^2)$. The total mass of material in the sphere is given by the product of the density and the volume of the sphere, or $\rho(4\pi r^3/3)$. The ratio of the former to the latter gives the Gibbs free energy arising from surface considerations, expressed per unit mass; that is, the surface Gibbs free energy per unit mass is $3\gamma/\rho r$. Since γ is small compared to most other chemical and physical contributions to free energy, surface effects are not generally considered when, say, the ΔG° of formation is quoted for a substance. The above argument shows that this becomes progressively harder to justify as the particle size of the material decreases. The emergence of a new phase implies starting from an r value of zero in the argument above, and the surface contribution to the energy becomes important indeed. Since two phases with their separating surface must already exist for γ to have any meaning, we are spared the embarrassment of the surface free energy becoming infinite at $r = 0$. Nevertheless, it is apparent from the foregoing that the effect of the surface free energy contribution is to increase G. Inspection of Fig. 4.3a shows that an increase in the G value for the crystalline phase arising from its small particle size has the effect of shifting T_m to lower temperatures. The smaller the particle size, the bigger the effect. This is the origin of all superheating, supercooling, and supersaturation phenomena: An equilibrium transition is sometimes overshot because of the difficulty associated with the initiation of a new phase. Likewise, all nucleation practices—cloud seeding, bubble chambers, and the use of boiling chips—are based on providing a site on which the emerging phase can grow.

To develop a more quantitative relationship between particle size and T_m, suppose we consider the melting behavior of the cylindrical crystal sketched in Fig. 4.4. Of particular interest in this model is the role played by surface effects. The illustration is used to define a model and should not be taken too literally, especially with respect to the following points:

1. The geometry of the cylinder is a matter of convenience. Except for numerical coefficients, the results we shall obtain will apply to plates of any cross-sectional shape.

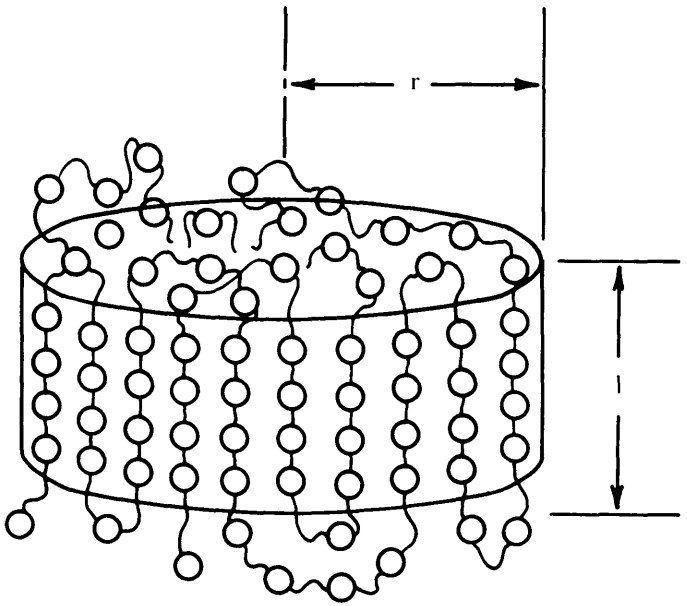

Figure 4.4 Idealized representation of a polymer crystal as a cylinder of radius r and thickness l. Note the folded nature of polymer chains in crystal.

2. The thickness of the plate, while small, is greater than the few repeat units shown.
3. The specific nature of the reentry loops is not the point of this illustration. The sketch shows both hairpin turns and longer loops. Problem 7 at the end of the chapter examines the actual nature of the reentry loop.

To develop this model into a quantitative relationship between T_m and the thickness of the crystal, we begin by realizing that for the transition crystal → liquid, ΔG is the sum of two contributions. One of these is ΔG^{∞}, which applies to the case of a crystal of infinite (superscript ∞) size; the other ΔG^s arises specifically from surface (superscript s) effects which reflect the finite size of the crystal:

$$\Delta G_f = \Delta G^{\infty} + \Delta G^s \tag{4.6}$$

Now each of these can be developed independently.

As in the qualitative discussion above, let γ be the Gibbs free energy per unit area of the interface between the crystal and the surrounding liquid. This is undoubtedly different for the edges of the plate than for its faces, but we

shall not worry about this distinction. The area of each of the circular faces of the cylinder is πr^2, and the area of the edge is $2\pi rl$, where r is the radius of the face and l is the length of the side as shown Fig. 4.4. Since surface is destroyed by the melting process, the contribution of these considerations to ΔG_f is

$$\Delta G^s = -[2(\pi r^2) + 2\pi rl]\gamma = -2\pi r^2\gamma\left(1 + \frac{l}{r}\right) \tag{4.7}$$

For the bulk effect we elect to proceed on the basis of a unit volume (superscript V) and immediately write

$$\Delta G^\infty = (\pi r^2 l)\Delta G_V^\infty \tag{4.8}$$

and

$$\Delta G_V^\infty = \Delta H_V^\infty - T^\infty \Delta S_V^\infty \tag{4.9}$$

In this last result we have retained the superscript ∞ on the T as a reminder that this refers to the infinitely extensive bulk phase; it describes the transition in the absence of surface complications.

When this infinitely extensive phase is in equilibrium with the melt, $\Delta G_V^\infty \to 0$ and $T^\infty \to T_m^\infty$. Accordingly, we can solve Eq. (4.9) for $\Delta S_V^\infty = \Delta H_V^\infty / T_m^\infty$ and substitute this back into Eq. (4.9):

$$\Delta G_V^\infty = \Delta H_V^\infty\left(1 - \frac{T^\infty}{T_m^\infty}\right) \tag{4.10}$$

This gives the values of ΔG_V at any temperature in terms of the two parameters ΔH_V^∞ and T_m^∞. Combining Eqs. (4.6)-(4.8) and (4.10) enables us to write

$$\Delta G_f = (\pi r^2 l)\Delta H_V^\infty\left(1 - \frac{T^\infty}{T_m^\infty}\right) - 2\pi r^2\gamma\left(1 + \frac{l}{r}\right) \tag{4.11}$$

We can now drop the superscript ∞ on the T in the numerator, recognizing that it is merely the temperature at which we are evaluating ΔG for the process $c \to l$ for a crystal characterized by r and l and a polymer characterized by ΔH_V^∞, T_m^∞, and γ. When the value of this ΔG is zero, we have the actual melting point of the crystal of finite dimension T_m. That is,

$$(\pi r^2 l)\Delta H_V^\infty\left(\frac{T_m^\infty - T_m}{T_m^\infty}\right) = 2\pi r^2\gamma\left(1 + \frac{l}{r}\right) \tag{4.12}$$

or

$$\Delta T = T_m^\infty - T_m = 2l^{-1} \frac{\gamma}{\Delta H_V^\infty} (1 + r^{-1}) T_m^\infty \tag{4.13}$$

Note that this equation is dimensionally correct, since γ has units of energy area^{-1} and ΔH_V^∞ has units energy volume^{-1}. Therefore the units of $l\Delta H_V^\infty$ and γ cancel, as do the units of l and r, leaving only temperature units on both sides of the equation. All of the quantities on the right-hand side of the equation are positive (ΔH_V^∞ is the heat of fusion), which means that $T_m^\infty > T_m$, as anticipated. The difference ΔT derived in Eq. (4.13) is called the undercooling, since it represents the melting point lowering due to particle size. Several limiting cases of this equation are of note:

1. If $\gamma = 0$, $\Delta T = 0$, regardless of particle size. This is not expected, however, since chains emerging from a crystal face either make a highly constrained about-face and reenter the crystal or meander off into the liquid from a highly constrained attachment to the solid. In either case, a free-energy contribution is inescapable.
2. As $r \to 0$, $\Delta T \to \infty$, showing that the lateral dimensions of the plate are critical for very small crystals. This makes the crystal nucleation event especially crucial.
3. As $r \to \infty$, which describes well-developed crystals, Eq. (4.13) becomes

$$\Delta T = 2T_m^\infty \frac{\gamma}{\Delta H_V^\infty} l^{-1} \tag{4.14}$$

which shows that an undercooling is still important because of the platelike crystal habit of polymers with limited crystal dimensions along the chain direction.

Equation 4.14 shows that a direct proportionality relationship should exist between crystal thickness l and the ratio $T_m^\infty/\Delta T$; a plot of l versus $T_m^\infty/\Delta T$ should result in a straight line of zero intercept with a slope proportional to $\gamma/\Delta H_V^\infty$. Figure 4.5 shows such a plot for polyethylene in which T_m^∞ was taken to be 137.5°C and the l values were determined by x-ray diffraction. While there is considerable and systematic divergence from the predicted form at large undercoolings, the data show a linear relationship for the higher-temperature region. In the following example we analyze the linear portion of Fig. 4.5 in terms of Eq. (4.14).

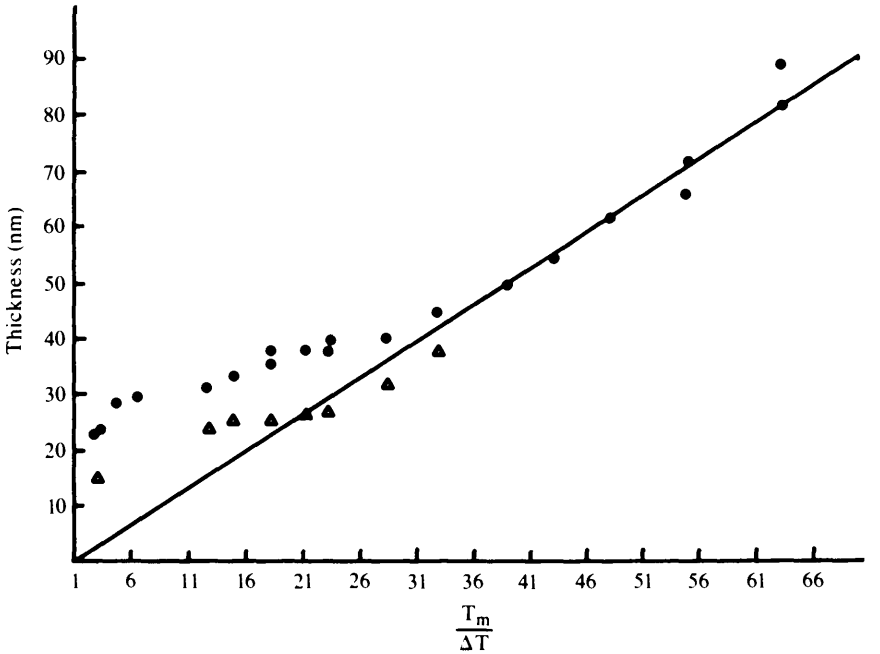

Figure 4.5 Crystal thickness versus $T_m/\Delta T$ for polyethylene. (Reprinted with permission from Ref. 5, copyright 1964, McGraw-Hill.)

Example 4.2

Use Eq. (4.14), the results in Fig. 4.5, and the data in Table 4.1 to estimate a value for γ for polyethylene. Figure 4.10 shows the unit cell of polyethylene; Fig. 4.10b shows the equivalent of two chains emerging from an area 0.740 by 0.493 nm^2. On the basis of the calculated value of γ and the characteristics of the unit cell, estimate the free energy of the fold surface per mole of repeat units.

Solution

Equation (4.14) predicts a straight line of zero intercept and slope $2\gamma/\Delta H_V^\infty$ when l is plotted versus $T_m/\Delta T$. The solid line in Fig. 4.5 has a slope of 650Å/51 = 12.75 Å. Therefore $2\gamma/\Delta H_V^\infty = 12.75 \times 10^{-10}$ m. The value of $\Delta H_{f,1}$ given in Table 4.1 is used for ΔH_V^∞ after the following change of units:

$$\Delta H_V^\infty = \frac{4020\ \text{J}}{\text{mole}} \times \frac{1\ \text{mole}}{28\ \text{g}} \times \frac{1\ \text{g}}{\text{cm}^3} \times \frac{10^6\ \text{cm}^3}{1\ \text{m}^3} = 1.44 \times 10^8\ \text{J m}^{-3}$$

Therefore $\gamma = \frac{1}{2}(12.75 \times 10^{-10}\ \text{m})(1.44 \times 10^8\ \text{J m}^{-3}) = 0.091\ \text{J m}^{-2}$. From the data on the unit cell

$$\frac{0.091\ \text{J}}{\text{m}^2} \times \left(\frac{0.740 \times 0.493\ \text{nm}^2}{\text{unit cell}} \times \frac{1\ \text{m}^2}{10^{18}\ \text{nm}^2}\right) \times \frac{1\ \text{unit cell}}{2\ \text{molecules}}$$

$$\times \frac{6.02 \times 10^{23}\ \text{molecules}}{\text{mol}} = 9990\ \text{J mol}^{-1}$$

Although it applies to a totally different kind of interface, the value of γ calculated in the example is on the same order of magnitude as the γ value for the surface between air and liquids of low molecular weight.

Before concluding this section, there is one additional thermodynamic factor to be mentioned which also has the effect of lowering T_m. Since we shall not describe the thermodynamics of polymer solutions until Chap. 8, a quantitative treatment is inappropriate at this point. However, some relationships familiar from the behavior of low molecular weight compounds may be borrowed for qualitative discussion. The specific effect we consider is that of chain ends. The position we take is that they are "foreign species" from the viewpoint of crystallization.

In this context the repeat units in a polymer may be divided into two classes: those at the ends of the chain (subscript e) and the others which we view as being in the middle (subscript m) of the chain. The mole fraction of each category in a sample is x_e and x_m, respectively. Since all segments are of one type or the other,

$$x_m = 1 - x_e \tag{4.15}$$

the proportion of chain ends increases with decreasing molecular weight; hence x_e decreases with increasing M.

The attitude we adopt in this discussion is that only those chain segments in the middle of the chain possess sufficient regularity to crystallize. Hence we picture crystallization occurring from a mixture in which the concentration of crystallizable units is x_m and the concentration of solute or diluent is x_e. The effect of solute on the freezing (melting) point of a solvent is a well-known result: T_m is lowered. Standard thermodynamic analysis yields the relationship

$$\ln x_m = -\frac{\Delta H_f}{R}\left(\frac{1}{T_m} - \frac{1}{T_m^\infty}\right) \tag{4.16}$$

where R is the gas constant, ΔH_f is the heat of fusion, T_m^∞ is the melting point for a polymer of infinite molecular weight, and T_m is the melting point of the polymer under consideration. This result assumes that the solution is ideal, an assumption we shall not pursue in view of the purely analogous nature of this argument. Combining Eqs. (4.15) and (4.16), expanding the logarithms, and rearranging yields

$$\Delta T = T_m^\infty - T_m = \frac{R x_e T_m T_m^\infty}{\Delta H_f} \tag{4.17}$$

which shows that a freezing point depression is to be expected from an increased concentration of chain ends. At least qualitatively, the effect of other types of defects is expected to also lower T_m. Remember that in the present discussion T_m^∞ is the melting point for a polymer of infinite molecular weight without regard to the crystal size, while Eq. (4.14) is the melting point for a crystal of infinite dimension without regard to molecular weight. The two effects are therefore complementary and are both operative if both particle dimension and molecular weight are small enough to lower the freezing point appreciably.

Throughout this section we have focused attention on the thermodynamic considerations which help explain the lowering and broadening of polymer melting points. The same thermodynamic arguments can be applied to the raising and sharpening of this transition temperature through annealing. When a crystal is maintained at a temperature between the crystallization temperature and the equilibrium melting point, an increase in T_m is observed. This may be understood in terms of the melting of smaller, less-perfect crystals and the redeposition of the polymer into larger, more stable crystals. This is analogous to the procedure of digesting a precipitate prior to filtration. There is more to the story than this, however. The digestion analogy suggests that those crystals which are enlarged simply add more folded chains around their perimeter. In fact, x-ray diffraction studies reveal progressive thickening of lamellae as T_m increases. This means large-scale molecular reorganization within the crystal. Such rearrangements apparently require the molecule to snake along the chain axis, with segments being reeled in and out across the crystal surface. The process of annealing, therefore, not only involves crystal thickening, but also provides the opportunity to work out kinks and defects.

Direct electron-microscopic examination of single crystals subjected to annealing shows a tendency of the platelets to develop holes like Swiss cheese or to develop an irregular perimeter like an amoeba. Each of these transformations has the effect of decreasing the face area of the crystal while increasing the edge area. These modifications occur as a result of the system seeking a lower overall free energy and demonstrate that the assumption made in the derivation of Eq. (4.14) concerning the equality of the face and edge values of γ was an oversimplification.

The last two sections have examined various aspects of the transition at T_m from the thermodynamic viewpoint. In the next section we turn to a kinetic approach to the same transition.

4.5 The Kinetics of Crystallization: The Avrami Equation

The fundamental equilibrium relationships we have discussed in the last sections are undoubtedly satisfied to the extent possible in polymer crystallization, but this possibility is limited by kinetic considerations. To make sense of the latter, both the mechanisms for crystallization and experimental rates of crystallization need to be examined.

The rate of emergence of a new phase must be considered in terms of two other rates: the rate of nucleation and the rate of growth of the nucleated particle. The nucleus is the structural entity which constitutes the growth center and may appear as the result of random fluctuations within the liquid or from the presence of foreign bodies. While seeding by deliberately introduced particles is an important practical matter, it is not our primary concern. Instead we imagine the ongoing conformational changes that occur in liquid polymers. We recognize that among the myriad of shapes possible small regions with the order which is prerequisite for crystal growth will spontaneously and randomly form and redissolve. We may regard these flickering domains as potential embryos for crystal growth.

The rate law describing embryo growth can be written as the product of two factors:

1. A Boltzmann factor in which the energy of crystallization appears in a negative exponent. According to Eq. (4.11), this energy increases–hence the exponential decreases–with increasing r.
2. A preexponential factor in which the frequency of chain addition increases with the surface area of the embryo. This, in turn, increases with increasing r.
3. As the product of two factors which vary oppositely with increasing r, the rate of embryo growth passes through a maximum at some critical (subscript c) dimension.

From a kinetic point of view, therefore, an embryo of radius r_c is an essential intermediate and the value of ΔG_c is analogous to an energy barrier to be overcome along the path to crystallization. As the temperature is lowered, molecular motion slows, delaying the thermal disruption of these embryos. Crystal growth from a large number of nuclei randomly dispersed throughout the melt becomes possible. The migration of polymer molecules to sites of growth is also slowed by the lowering of temperature. While the foregoing considerations are general

for all nucleation phenomena, the high molecular weight of polymers aggravates the problem of crystal nucleation to the point that supercooling a liquid all the way to T_g without appreciable crystallization is commonplace.

In spite of these obstacles, crystallization does occur and the rate at which it develops can be measured. The following derivation will illustrate how the rates of nucleation and growth combine to give the net rate of crystallization. The theory we shall develop assumes a specific picture of the crystallization process. The assumptions of the model and some comments on their applicability follow:

1. The crystals are assumed to be circular disks. This geometry is consistent with previous thermodynamic derivations. It has the advantage of easy mathematical description.
2. The disks are assumed to lie in the same plane. While this picture is implausible for bulk crystallization, it makes sense for crystals grown in ultrathin films, adjacent to surfaces, and in stretched samples. A similar mathematical formalism can be developed for spherical growth and the disk can be regarded as a cross section of this.
3. Nucleation is assumed to begin simultaneously from centers positioned at random throughout the liquid. This is more descriptive of heterogeneous nucleation by foreign bodies introduced at a given moment than of random nucleation. We shall dispense with the requirement of simultaneity below.
4. Growth in the radial direction is assumed to occur at a constant velocity. There is ample experimental justification for this in the case of three-dimensional spherical growth.

Figure 4.6a represents the top view of an array of these disks after the crystals have been allowed to grow for a time t after nucleation. The two disks on the left are widely enough separated to still have room for further growth; the three on the right have impinged upon one another and can grow no more. We shall see in Sec. 4.7 that this latter situation can be observed microscopically.

Suppose we define the rate of radial growth of the crystalline disks as $\dot{r}$. Then disks originating from all nuclei within a distance $\dot{r}t$ of an arbitrary point, say, point x in Fig. 4.6a, will reach that point in an elapsed time t. If the average concentration of nuclei in the plane is N (per unit area), then the average number of fronts $\bar{F}$ which converge on x in this time interval is

$$\bar{F} = \pi(\dot{r}t)^2 N \tag{4.18}$$

If real growth fronts were to impinge on a point like this, their growth would terminate at x. Suppose we imagine point x to be charmed in some way such that any number of growth fronts can pass through it without interference.

If we were to monitor the number of (noninterfering) fronts which cross x in a series of observations, we would expect a distribution of values because of

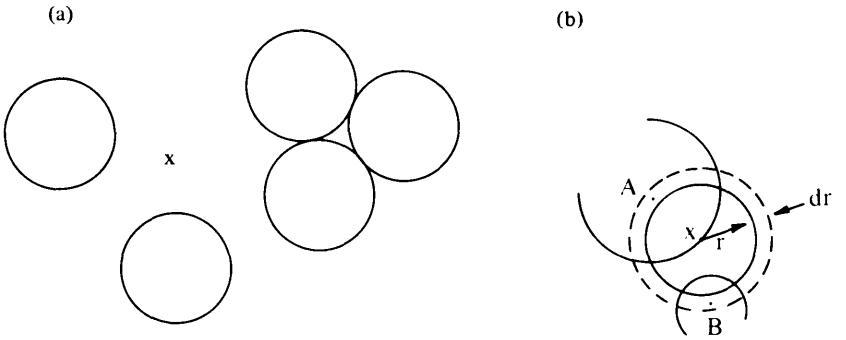

Figure 4.6 The growth of disk-shaped crystals. (a) All crystals have been nucleated simultaneously. All crystals have the same radius rt after an elapsed time t. (b) Nucleation is sporadic. Crystal A has had enough time to reach point x, while B has not, although both originate in the same ring a distance r from x.

the random placement of the nuclei. Furthermore, the distribution of F values is expected to pass through a maximum. Fronts arising from nuclei very close to x can easily cross x in the allotted time, but the area of melt under consideration in this case is small, so the number of fronts is small. As the area around the charmed point x is enlarged, a larger number of nuclei will be encompassed, so the number of fronts crossing x will increase. This increase is offset by the fact that fronts originating from more distant nuclei will require more time to reach x. Therefore the number of fronts which cross x (remember that these are free from interference by hypothesis) will increase, pass through a maximum, and decrease as we allow them to originate from all parts of the sample. This distribution of values for F is our next interest. If a distribution of values is possible, then it can always be characterized by an average value, $\bar{F}$ in this case.

We propose to describe the distribution of the number of fronts crossing x by the Poisson distribution function, discussed in Sec. 1.9. This probability distribution function describes the probability P(F) of a specific number of fronts F in terms of that number and the average number $\bar{F}$ as follows [Eq. (1.38)]:

$$P(F) = \frac{e^{-\bar{F}}\,\bar{F}^{F}}{F!} \tag{4.19}$$

Next we apply this distribution to the case where F = 0, that is, to the case where no fronts have crossed point x. There are several aspects to note about this situation:

1. Since $\bar{F}^0 = 1$ and $0! = 1$, Eq. (4.19) becomes

$$P(0) = e^{-\bar{F}} \tag{4.20}$$

for $F = 0$.

2. The condition of no fronts crossing x is automatically a condition of noninterference, so the special magic postulated for point x poses no problem.
3. Since point x is nonspecific, Eq. (4.20) describes the fraction of observations in which no fronts cross any arbitrary point or the fraction of the area in any one experiment which is crossed by no fronts.
4. This last interpretation makes P(0) the same as the fraction of a sample in the amorphous state. It is conventional to focus on the fraction crystallized θ; therefore the fraction amorphous is $1 - \theta$ and

$$1 - \theta = P(0) = e^{-\bar{F}} \tag{4.21}$$

5. Inverting and taking the logarithm of both sides of Eq. (4.21), we obtain

$$\ln \frac{1}{1 - \theta} = \bar{F} \tag{4.22}$$

Equations (4.18) and (4.22) both describe the same situation and can be equated to each other to give

$$\ln \left(\frac{1}{1 - \theta} \right) = \pi \dot{r}^2 N t^2 \tag{4.23}$$

or

$$\theta = 1 - \exp(-\pi \dot{r}^2 N t^2) \tag{4.24}$$

Remember the units involved here: For $\dot{r}$ they are length time^{-1}; for N, length^{-2}; and for t, time. Therefore the exponent is dimensionless, as required. The form of Eq. (4.24) is such that at small times the exponential equals unity and $\theta = 0$; at long times the exponential approaches zero and $\theta = 1$. In between, an S-shaped curve is predicted for the development of crystallinity with time. Experimentally, curves of this shape are indeed observed. We shall see presently, however, that this shape is also consistent with other mechanisms besides the one considered until now.

In terms of spontaneous crystallization, the assumption that N nuclei commence to grow simultaneously at $t = 0$ is the most unrealistic. We can modify the model to allow for sporadic, spontaneous nucleation by the following

argument. We draw a set of concentric rings in the plane of the disks around point x as shown in Fig. 4.6b. If the radii are r and r + dr for the rings, then the area enclosed between them is $2\pi r\ dr$. We postulate that spontaneous random nucleation occurs with a frequency $\dot{N}$, having units area^{-1} time^{-1}. The rate of formation of nuclei within the ring is therefore $\dot{N}2\pi r\ dr$.

We continue to assume that the crystals so nucleated display a constant rate of radial growth $\dot{r}$. This means that it takes a crystal originating in a ring of radius r around point x a time given by $r/\dot{r}$ to cross x. The crystal labeled A in Fig. 4.6b has had just enough growth time to reach x. On the other hand, a crystal nucleated in this ring after $t - r/\dot{r}$ will not have had time to grow to x. The crystal labeled B in Fig. 4.6b is an example of the latter. It is only nucleation events that occur up to $t - r/\dot{r}$ which have time to grow from the ring of radius r and cross point x by their growth front. The increment in this number of fronts for the ring of radial thickness dr is

$$dF = (\dot{N}2\pi r\ dr)\left(t - \frac{r}{\dot{r}}\right) \tag{4.25}$$

The average number of fronts crossing point x at a time of observation t is the sum of contributions from all rings which are within reach of x in time t. The most distant ring included by this criterion is a distance $\dot{r}t$ from x. The average number of fronts, therefore, is given by integrating Eq. (4.25) for all rings between r = 0 and $r = \dot{r}t$:

$$\bar{F} = 2\pi\dot{N}\int_0^{\dot{r}t} r\left(t - \frac{r}{\dot{r}}\right) dr \tag{4.26}$$

As far as this integration is concerned, $\dot{r}$ and t are constants, so Eq. (4.26) is readily evaluated to give

$$\bar{F} = \frac{1}{3}\pi\dot{N}\dot{r}^2t^3 \tag{4.27}$$

As before, this quantity in relation to the degree of crystallinity is given by Eq. (4.22), so equating the latter to Eq. (4.27) gives

$$\ln\left(\frac{1}{1-\theta}\right) = \frac{\pi}{3}\dot{N}\dot{r}^2t^3 \tag{4.28}$$

or

$$\theta = 1 - \exp\left(-\frac{\pi}{3}\dot{N}\dot{r}^2t^3\right) \tag{4.29}$$

Equations (4.24) and (4.29) are equivalent, except that the former assumes instantaneous nucleation at N sites per unit area while the latter assumes a nucleation rate of $\dot{N}$ per unit area *per unit time*. It is the presence of this latter rate which requires the power of t to be increased from 2 to 3 in this case.

In deriving these results we have focused attention on growth fronts originating elsewhere and crossing point x. We would count the same number if the growth originated at x and we evaluated the number of nucleation sites swept over by the growing front. This change of perspective is immediately applicable to a three-dimensional situation as follows. Suppose we let N represent the number of sites per unit volume (note that this is a different definition than given above) and assume that a spherical growth front emanates from each. Then the average number of fronts which cross nucleation sites in time t is

$$\bar{F} = \frac{4}{3}\pi(\dot{r}t)^3 N \tag{4.30}$$

by analogy with Eq. (4.18). Following the same argument as produced Eq. (4.24), we obtain

$$\theta = 1 - \exp\left(-\frac{4}{3}\pi\dot{r}^3 N t^3\right) \tag{4.31}$$

for the three-dimensional case of simultaneous nucleation (concentration N). Following the argument that produced (4.29), we obtain

$$\theta = 1 - \exp\left(-\frac{\pi}{3}\dot{r}^3\dot{N}t^4\right) \tag{4.32}$$

for the three-dimensional case of sporadic nucleation (rate $\dot{N}$).

Equations (4.24), (4.29), (4.31), and (4.32) all describe different mechanisms for crystallization, yet all have basically the same form:

$$\theta = 1 - \exp(-Kt^m) \tag{4.33}$$

where K is a cluster—different in detail for each case—of numerical and growth constants and m is the power dependence of time. Equation (4.33) is known as the Avrami equation, after one of the researchers who has made contributions in this area. Likewise, the exponent m in Eq. (4.33) is called the Avrami exponent. The latter takes on the values 2, 3, or 4 for the four mechanisms considered above. To acquire some numerical familiarity with the Avrami function, consider the following example.

Example 4.3

Three different crystallization systems show m values of 2, 3, and 4. Calculate the value required for K in each of these systems so that all will show $\theta = 0.5$ after 10^3 sec. Use these m and K values to compare the development of crystallinity with time for these three systems.

Solution

Solve Eq. (4.33) for K and evaluate at $t = 10^3$ sec for each of the m values: $K = [-\ln(1 - \theta)]/t^m$. For m = 2, $K = (\ln 0.5)/(10^3)^2 = 6.93 \times 10^{-7}$ sec^{-2}; for m = 3, $K = 6.93 \times 10^{-10}$ sec^{-3}; for m = 4, $K = 6.93 \times 10^{-13}$ sec^{-4}. Note that the units of K depend on the value of m. Solve Eq. (4.33) for t and evaluate at different θ's for the m and K values involved:

	t in seconds		
θ	m = 2 ($K = 6.93 \times 10^{-7}$)	m = 3 ($K = 6.93 \times 10^{-10}$)	m = 4 ($K = 6.93 \times 10^{-13}$)
0.1	3.89×10^2	5.33×10^2	6.24×10^2
0.2	5.67×10^2	6.85×10^2	7.53×10^2
0.3	7.18×10^2	8.02×10^2	8.47×10^2
0.4	8.59×10^2	9.03×10^2	9.27×10^2
0.5	1×10^3	1×10^3	1×10^3
0.6	1.15×10^3	1.10×10^3	1.07×10^3
0.7	1.32×10^3	1.20×10^3	1.15×10^3
0.8	1.52×10^3	1.32×10^3	1.23×10^3
0.9	1.82×10^3	1.49×10^3	1.35×10^3

These three systems describe a set of crystallization curves that cross at $\theta = 0.5$ and $t = 10^3$ sec. For the case where m = 2, the time span over which the change occurs is widest (1430 sec from $\theta = 0.1$–0.9) and the maximum slope is flattest (7.8×10^{-4} sec^{-1} between $\theta = 0.4$ and 0.6). For m = 4, the range is narrowest (726 sec) and the maximum slope is steepest (1.4×10^{-3} sec).

•

Although two of the mechanisms presented above yield the same power dependence on t, it appears possible to eliminate certain mechanisms by experimentally testing the development of θ with time. A strategy for this is suggested by Eq. (4.28). Taking the logarithm of both sides of that equation gives

$$\ln\left[\ln\left(\frac{1}{1-\theta}\right)\right] = 3 \ln t + \text{const.} \tag{4.34}$$

or for the generalized Avrami equation

$$\ln\left[\ln\left(\frac{1}{1-\theta}\right)\right] = m \ln t + \text{const.} \tag{4.35}$$

Thus the slope of a plot of $\ln[\ln(1-\theta)^{-1}]$ versus ln t will have a slope equal to the Avrami exponent.

Before turning to an examination of this prediction, a few more complications must be mentioned. Until now we have considered the case of disk or spherical growth from simultaneous or sporadic nucleation. Are these the only possibilities? As might be anticipated, the answer is no. Other geometries for growth have been examined; we shall include only the case of the cylinder, which is limited in radius but not in length (i.e., one-dimensional growth) to produce fibrillar structures. Another modification which has been investigated concerns the rate-determining step of the crystallization process. Equation (4.18) and those following from it imply that a contact between the growing disk and the surrounding melt for time t is sufficient for crystallization. Another possibility is that allowance must be made for the diffusion of the molecules to (or from) the growth site. A way of dealing with this assumes that amorphous molecules must diffuse out of the crystal domain to allow space for the crystallizing molecules. For a crystal of radius r, the time required for molecules to diffuse out of this domain is, according to Eq. (2.63), $r = (2Dt)^{1/2}$. In Eq. (4.18) this radius is written $r = \dot{r}t$. Thus, if the growth rate is diffusion controlled, these two expressions for r can be equated and solved for $\dot{r}$:

$$\dot{r} = \left(\frac{2D}{t}\right)^{1/2} \tag{4.36}$$

If this result is substituted into the previous expressions containing $\dot{r}$, the effect is to replace $\dot{r}$ with $(2D)^{1/2}$ and to multiply those t's which accompany $\dot{r}$ by $t^{-1/2}$.

This rather complex array of possibilities is summarized in Table 4.3. Table 4.3 lists the predicted values for the Avrami exponent for the following cases:

1. Growth geometry: fibrillar rod, disk, and sphere.
2. Nucleation mode: simultaneous and sporadic.
3. Rate determination: contact and diffusion.

Those exponents which we have discussed explicitly are identified by equation number in Table 4.3. Other tabulated results are readily rationalized from these. For example, according to Eq. (4.24) for disk (two-dimensional) growth on contact from simultaneous nucleations, the Avrami exponent is 2. If the dimensionality of the growth is increased to spherical (three dimensional), the exponent becomes 3. If, on top of this, the mechanism is controlled by diffusion, the

Table 4.3 Summary of Exponents in the Avrami Equation for Different Crystallization Mechanisms

Avrami exponent	Crystal geometry	Nucleation mode	Rate determination	Equation[a]
0.5	Rod	Simultaneous	Diffusion	
1	Rod	Simultaneous	Contact	
1	Disk	Simultaneous	Diffusion	
1.5	Sphere	Simultaneous	Diffusion	
1.5	Rod	Sporadic	Diffusion	
2	Disk	Simultaneous	Contact	(4.24)
2	Disk	Sporadic	Diffusion	
2	Rod	Sporadic	Contact	
2.5	Sphere	Sporadic	Diffusion	
3	Sphere	Simultaneous	Contact	(4.31)
3	Disk	Sporadic	Contact	(4.29)
4	Sphere	Sporadic	Contact	(4.32)

[a] Equation numbers refer to those relationships discussed explicitly in text.

exponent becomes 1.5. If the nucleation is sporadic in addition, the exponent is increased to 2.5.

While there are several instances of redundancy among the Avrami exponents arising from different pictures of the crystallization process, there is also enough variety to make the experimental value of this exponent a valuable way of characterizing the crystallization process. In the next section we shall examine the experimental side of crystallization kinetics.

4.6 The Kinetics of Crystallization: Experimental Aspects

In order to carry out an experimental study of the kinetics of crystallization, it is first necessary to be able to measure the fraction θ of polymer crystallized. While this is necessary, it is not sufficient; we must also be able to follow changes in the fraction of crystallinity with time. So far in this chapter we have said nothing about the experimental aspects of determining θ. We shall now briefly rectify this situation by citing some of the methods for determining θ. It must be remembered that not all of these techniques will be suitable for kinetic studies.

Since the fractions of crystalline (subscript c) and amorphous (subscript a) polymer account for the entire sample, it follows that we may measure whichever of the two is easiest to determine and obtain the other by difference. Generally, it is some property P_c of the crystalline phase that we are able to

monitor. If this property can be measured for a sample which is 100% crystalline (superscript °) we can compare the value of P_c measured on an actual sample (no superscript) to evaluate θ:

$$\theta = \frac{P_c}{P_c^\circ} \tag{4.37}$$

This relationship is sketched in Fig. 4.7a, which emphasizes that P_c must vary linearly with θ and that P_c° must be available, at least by extrapolation. The heat of fusion is an example of a property of the crystalline phase that can be used this way. It could be difficult to show that the value of ΔH_f is constant per unit mass at all percentages of crystallinity and to obtain a value for ΔH_f° for a crystal free from defects. Therefore, while conceptually simple, the actual utilization of Eq. (4.37) in precise work may not be easy.

Figure 4.7b shows a variation of this in which a property of the sample (no subscript) is found to vary linearly with θ, having a value P_a when $\theta = 0$ and a value P_c when $\theta = 1$. The slope of this line is simply $P_c - P_a$, since the difference of θ values is unity for this difference in P. The equation for the line in Fig. 4.7b is

$$P = P_a + \theta(P_c - P_a) \tag{4.38}$$

which can be solved for θ as a function of P, P_a, and P_c:

$$\theta = \frac{P - P_a}{P_c - P_a} \tag{4.39}$$

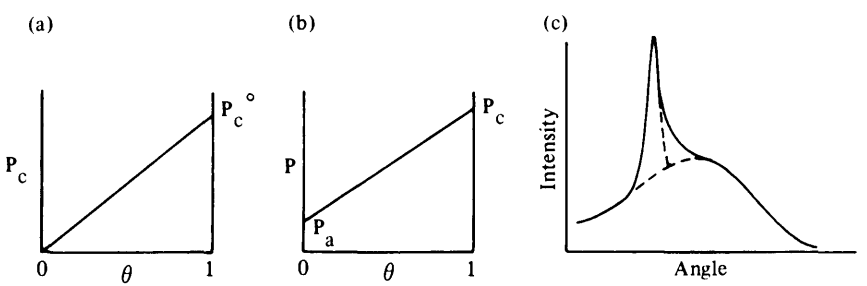

Figure 4.7 Various representations of the properties of a mixture of crystalline and amorphous polymer. (a) The monitored property is characteristic of the crystal and varies linearly with θ. (b) The monitored property is characteristic of the mixture and varies linearly with θ between P_a and P_c. (c) X-ray intensity is measured with the sharp and broad peaks being P_c and P_a, respectively.

If the amorphous component contributes nothing to the measured property (as with heat of fusion), then Eq. (4.39) reduces to Eq. (4.37). Specific volume is an example of a property which has been extensively used in this way to evaluate θ.

Figure 4.7c illustrates how x-ray diffraction techniques can be applied to the problem of evaluating θ. If the intensity of scattered x-rays is monitored as a function of the angle of diffraction, a result like that shown in Fig. 4.7c is obtained. The sharp peak is associated with the crystalline diffraction, and the broad peak, with the amorphous contribution. If the area A under each of the peaks is measured, then

$$\theta = \frac{A_c}{A_c + A_a} \tag{4.40}$$

An obvious difficulty here is deciding the location of the broken line portions of the peaks in the region of overlap. Some features of the infrared absorption spectrum may also be analyzed by the same procedure to yield values for θ.

As noted above, not all techniques which provide information regarding crystallinity are useful to follow the rate of crystallization. In addition to sufficient sensitivity to monitor small changes, the method must be rapid and suitable for isothermal regulation, quite possibly over a range of different temperatures. Specific volume measurements are especially convenient for this purpose. We shall continue our discussion using specific volume as the experimental method.

Although the extent of crystallinity is the variable under consideration, time is the experimental variable. Accordingly, what is done is to identify the specific volume of a sample at t = 0 (subscript 0) with V_a, the volume at t = ∞ (subscript ∞) with V_c, and the volume at any intermediate time (subscript t) with the composite volume. On this basis, Eq. (4.39) becomes

$$\theta = \frac{V_t - V_0}{V_\infty - V_0} \tag{4.41}$$

and the fraction amorphous becomes

$$1 - \theta = \frac{V_\infty - V_t}{V_\infty - V_0} \tag{4.42}$$

Figure 4.8a shows how this quantity varies with time for polyethylene crystallized at a series of different temperatures. Several aspects of these curves are typical of all polymer crystallizations and deserve comment:

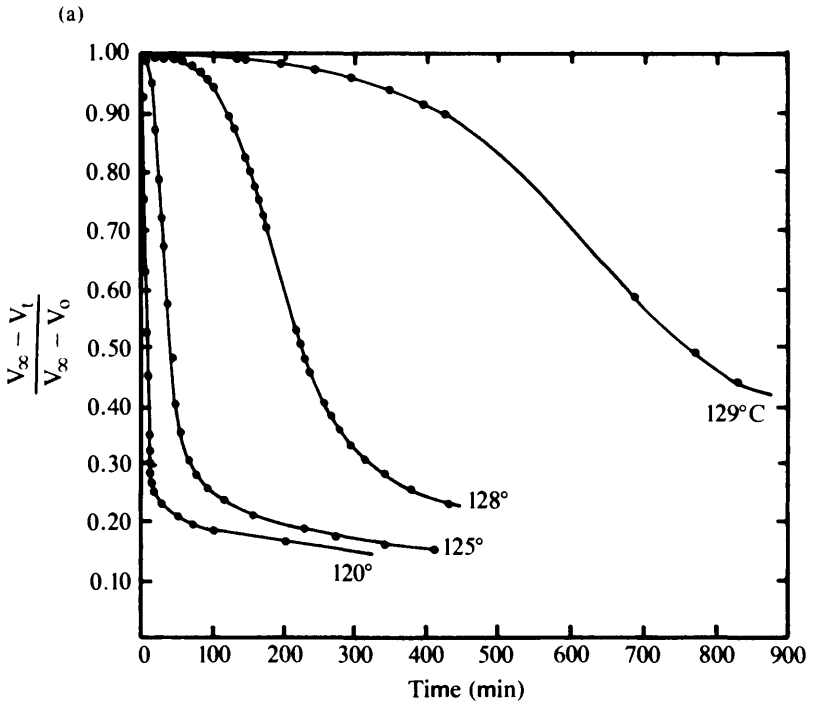

Figure 4.8 Fraction of amorphous polyethylene as a function of time for crystallizations conducted at indicated temperatures: (a) linear time scale and (b) logarithmic scale. Arrows in (b) indicate shifting curves measured at 126 and 130 to 128°C as described in Example 4.4. [Reprinted with permission from R. H. Doremus, B. W. Roberts, and D. Turnbull (Eds.) *Growth and Perfection of Crystals*, Wiley, New York, 1958.]

1. The decrease in amorphous content follows an S-shaped curve. The corresponding curve for the growth of crystallinity would show a complementary but increasing plot. This aspect of the Avrami equation was noted in connection with the discussion of Eq. (4.24).
2. The greater the undercooling, the more rapidly the polymer crystallizes. This is due to the increased probability of nucleation the more supercooled the liquid becomes. Although the data in Fig. 4.8 are not extensive enough to show it, this trend does not continue without limit. As the crystallization temperature is lowered still further, the rate passes through a maximum and then drops off as T_g is approached. This eventual decrease in rate is due to decreasing chain mobility which offsets the nucleation effect.

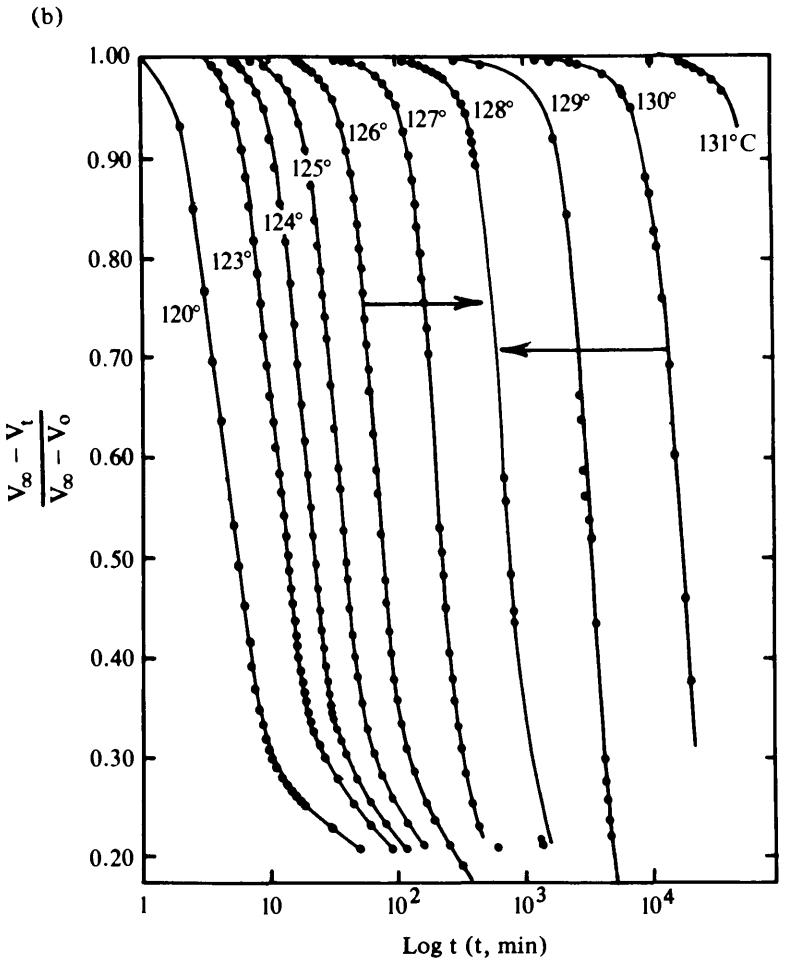

Figure 4.8 *(continued)*

3. Replotting the data on a lorgarithmic time scale as shown in Fig. 4.8b has an interesting effect. Figure 4.8b shows that this modification produces a far more uniform set of S curves. As a matter of fact, if the various curves are shifted along the horizontal axis, they may be superimposed over a wide portion of the transformation. The arrows in Fig. 4.8b show this displacement of the data at 126 and 130°C to correspond to the data at 128°C. This superpositioning is examined in the example below.

Example 4.4

From the lengths of the arrows drawn in Fig. 4.8b, estimate the change in time scale which will produce the same effect on the rate of crystallization as changing the temperature from 130 to 128°C. Do the same for a temperature change from 126 to 128°C.

Solution

At the values of $1 - \theta$ listed below, determine the difference between $(\log t)_{128}$ and $(\log t)_{130}$ and that between $(\log t)_{128}$ and $(\log t)_{126}$.

$1 - \theta$	0.9	0.8	0.7	0.6	0.5	0.4	0.3
$(\log t)_{128} - (\log t)_{126}$	1.00	1.00	1.03	1.00	0.97	0.98	0.97
$(\log t)_{128} - (\log t)_{130}$	-1.30	-1.33	-1.33	-1.35	-1.35	-1.35	

The fact that these differences are as constant as they are for each of the shifts illustrates the validity of the superpositioning procedure. Now consider the average value of these differences:

	Average for 126 → 128°C	Average for 130 → 128°C
$\Delta \log t$	0.99	-1.34
antilog	10	0.046 = 1/22

The significance of these numbers is seen as follows. The average values of $\Delta \log t$ are to be added to the log t values at 126 or 130°C to superimpose the latter curves on the one measured at 128°C. Since these values are added to log t values, the effect is equivalent to multiplying the individual t values at 126 and 130°C by the appropriate antilogs to change the time scale in the individual runs to a common time scale. Using the case of $\theta = 0.5$ as an illustration, we see the following times are required to reach this level of crystallinity:

T (°C)	t observed (min)	t shifted (min)
126	80	80 × 10 = 800
128	800	800 × 1 = 800
130	17,500	17,500 × 0.046 = 800

•

The preceding example of superpositioning is an illustration of the principle of time-temperature equivalency. We referred to this in the last chapter in connection with the mechanical behavior of polymer samples and shall take up the

latter quantitatively in Sec. 4.10. Although time-temperature equivalency with respect to mechanical properties is a different phenomenon, precisely the same formalism as illustrated above applies. In the above sample note that the absolute magnitude of the two separate shifts could be combined so that a change of temperature from 126 to 130°C would involve a difference in log t of about 2.33, the antilog of which is about 214. This shows that a 4°C increase in temperature is equivalent to an expansion in the time scale of the experiment by a factor of 214.

Next let us examine an experimental test of the Avrami equation and the assortment of predictions from its various forms as summarized in Table 4.3. Figure 4.9 is a plot of $\ln[\ln(1-\theta)^{-1}]$ versus ln t for poly(ethylene terephthalate) at three different temperatures. According to Eq. (4.35), this type of

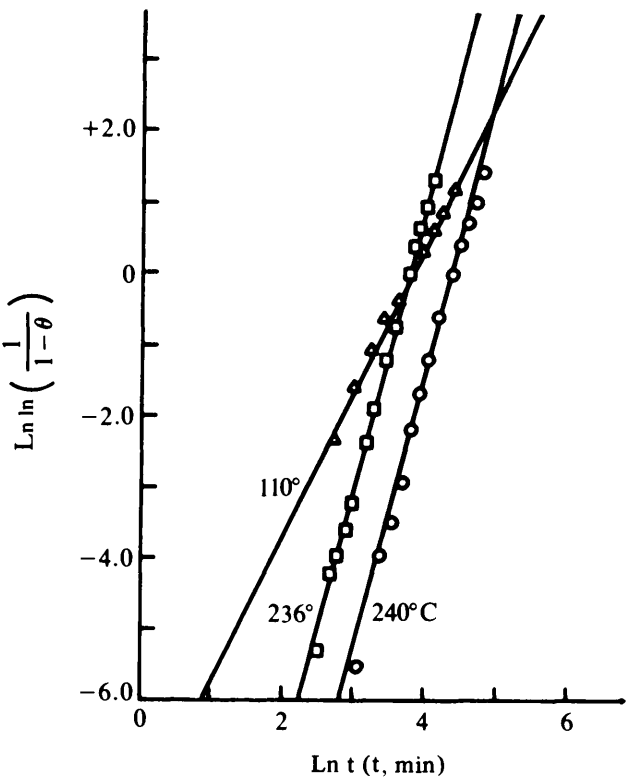

Figure 4.9 Log-log plot of $\ln(1-\theta)^{-1}$ versus time for poly(ethylene terephthalate) at three different temperatures. [Reprinted from L. B. Morgan, *Philos. Trans. R. Soc. London* 247A:13 (1954).]

representation should yield a straight line, the slope of which corresponds to the Avrami exponent. The data in Fig. 4.9 show that linearity is indeed obtained and that the slope equals 2 when the crystallization is carried out at 110°C and changes to 4 at higher temperatures. The melting point of poly(ethylene terephthalate) is 267°C, so when the undercooling is about 25°C, three-dimensional growth with sporadic nucleation is indicated. With an undercooling of 150°C, the mechanism of crystallization is clearly different, although it is not possible to identify the specific combination of factors responsible for the exponent 2. The values of K in Eq. (4.33) are best obtained analytically, once the exponent has been determined graphically. The two K values for the case where m = 4 in Fig. 4.9 are 2.94×10^{-7} min^{-4} at 236°C and 3.13×10^{-8} min^{-4} at 240°C. The mechanism is the same in these two cases, but the rate is more than nine times faster when the temperature is lowered by 4°C. Note that it is not possible to resolve K, which is a cluster of other nucleation and growth parameters, into its constituent factors, even when the value of the exponent identifies the mechanism unambiguously. At both 110 and 120°C, m = 2 and the values of K are 7.93×10^{-4} and 7.45×10^{-3} min^{-2}, respectively. In this region the rate is about 10 times slower when the temperature is lowered by 10°C. Thus both the value of m and the effect on K of changing temperature are different for these two regimes of behavior.

The testing of the Avrami equation reveals several additional considerations of note:

1. The multiple use of logarithms in the analysis presented by Fig. 4.9 obliterates much of the deviation between theory and experiment. More stringent tests can be performed by other numerical methods.
2. Deviations from the Avrami equation are frequently encountered in the long time limit of the data. This is generally attributed to secondary nucleation occurring at irregularities on the surface of crystals formed earlier.
3. Exponents other than integral multiples of one-half are observed. As a matter of fact, a method for determining the Avrami exponent which is based on graphical differentiation rather than logarithmic analysis yields instantaneous m values at particular values of θ rather than a single value averaged over the entire transition. When this method is used, it is found that m increases initially, eventually leveling off.
4. These unpredicted Avrami exponents may be indications that multiple mechanisms are operative and/or that $\dot{r}$ and/or $\dot{N}$ is itself a function of θ.

Experimental results are in general conformity with the Avrami equation, but the interpretation of various observations is still complicated in many instances. One intriguing observation is that the induction period for nucleation is inversely proportional to the length of time the liquid is held in the liquid state after previous melting. This dependence on prior history may be qualitatively understood

by assuming that the last traces of order from the first crystals persist for quite a while and affect the rate of nucleation. It is difficult to handle these complications quantitatively, however. Having looked at some aspects of both the thermodynamics and the kinetics of the crystallization process, it is time to take a look at the crystals themselves. We shall do this in the next section.

4.7 Levels of Structure: Crystal Morphology

In this section we shall examine the various levels of structure displayed by polymers. The term *morphology* is used to describe such features and may be applied to both molecular and macroscopic levels of organization. A general principle that underlies morphological inquiry is the idea of using as a "yardstick" some probe which matches within an order of magnitude or so the linear dimensions of the feature being explored. Accordingly, x-ray diffraction is the preferred technique for investigating the spacing of individual atoms or chains within a crystal, since the wavelength is on the order of 100 pm for this radiation. Both transmission and scanning electron microscopy are valuable techniques for examining individual polymer crystals. The thickness and lateral dimensions of the individual crystals as well as surface topography can be studied by these instruments. Three-dimensional aggregates of single-crystal lamellae have characteristic structures of their own. Since they are ordered on a larger scale of linear dimension, optical microscopy can be used as a probe of structure in those cases.

Although x-ray diffraction yields the most detailed information about crystal morphology at the molecular level, we shall restrict ourselves to a few limited remarks about observations derived by this method. The interpretation of x-ray diffraction patterns is a topic best left to experts, but we note that the characterization of the unit cell is one of the pieces of information which this type of measurement yields. Of the many polymers which have been investigated, none crystallizes so completely or has been studied as thoroughly as polyethylene. Figure 4.10 shows the arrangement of molecules in the polyethylene crystal and outlines the unit cell. By transposing the unit cell through three dimensions, the overall crystal structure is generated. X-ray studies show the dimensions of the unit cell for polyethylene as a = 736 pm, b = 492 pm, and c = 253.4 pm. In regard to this unit cell, we observe the following:

1. The c axis corresponds to both the short axis of the crystal and the axis along the molecular chain. The observed repeat distance in the c direction is what would be expected between successive substituents on a fully extended hydrocarbon chain with normal bond lengths and angles (see Sec. 1.2).
2. The distances between all hydrogen atoms is approximately the same in this structure, so there is no problem with overcrowding.

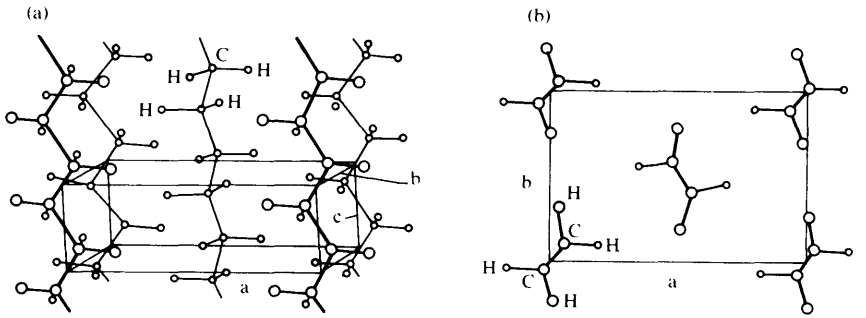

Figure 4.10 Crystal structure of polyethylene: (a) unit cell shown in relation to chains and (b) view of unit cell perpendicular to the chain axis. [Reprinted from C. W. Bunn, *Fibers from Synthetic Polymers*, R. Hill (Ed.), Elsevier, Amsterdam, 1953.]

3. While not overcrowded, the polyethylene structure uses space with admirable efficiency, the atoms filling the available space with 73% efficiency. For contrast, recall that close-packed spheres fill space with 74% efficiency, so polyethylene does about as well as is possible in its utilization of space.

One of the things that can be done with a knowledge of the unit cell dimensions is to calculate the crystal density. This is examined in the following example.

Example 4.5

Use the unit cell dimensions cited above to determine the crystal density of polyethylene. Examine Fig. 4.10 to decide the number of repeat units per unit cell.

Solution

Figure 4.10 shows that the equivalent of two ethylene units are present in each unit cell. Accordingly, the mass per unit cell is

$$\frac{2 \text{ repeat units}}{\text{unit cell}} \times \frac{1 \text{ mol repeat units}}{6.02 \times 10^{23} \text{ repeat units}} \times \frac{28.0 \text{ g}}{1 \text{ mol repeat units}}$$

$$= 9.30 \times 10^{-23} \text{ g (unit cell)}^{-1}$$

Since all angles in the cell are 90°, the volume of the unit cell is

$$\frac{736 \text{ pm} \times 492 \text{ pm} \times 253 \text{ pm}}{\text{unit cell}} \times \left(\frac{1 \text{ cm}}{10^{10} \text{ pm}}\right)^3$$

$$= 9.16 \times 10^{-23} \text{ cm}^3 \text{ (unit cell)}^{-1}$$

The density of the crystal is obtained from the ratio of these two quantities:

$$\rho = \frac{9.30 \times 10^{-23}}{9.16 \times 10^{-23}} = 1.015 \text{ g cm}^{-3}$$

A result such as this could be used in Eq. (4.39) as part of the information needed to determine θ.

•

Next, we consider the electron microscope as a tool for investigating crystallization in polymers. The electron microscope uses the de Broglie waves associated with accelerated electrons to produce an image just as visible light produces an image in an optical microscope. Electromagnets function as lenses for the electron beam and the image is formed on a phosphorescent screen or a photographic plate. Otherwise the electron microscope is completely analogous to the light microscope. The de Broglie wavelength of an electron under typical operating conditions in an electron microscope is on the order of a few picometers. In all types of microscopy it is the resolving power rather than the magnification per se which is the limiting factor. Light is diffracted from the edges of illuminated bodies and this diffraction blurs their boundaries. The resolving power measures the minimum separation between objects that will produce discernably different images in a microscope. As with many optical phenomena, this separation is on the order of the wavelength of the illuminating radiation. Therefore, the resolving power of an electron microscope is potentially smaller by some five orders of magnitude than that achieved by optical microscopes. Two adjunct procedures of electron microscopy find applicability in the study of polymer crystals: shadow casting and dark-field operation.

Shadow casting is used to improve the contrast between a sample and its background and between various details of the sample surface. Because polymer crystals are so thin and mostly consist of atoms of low atomic number (the number of electrons in an atom determines the extent of interaction with the electron beam), some sort of contrast enhancement is important. In the shadowing method the sample is placed in an evacuated chamber and a heavy metal is allowed to evaporate in the same chamber. The position of the metal source is such that the metal vapor strikes the sample at an oblique angle and condenses on the cool surface. The thin metal film thus formed literally casts shadows which enhance the image of the sample. If the angle of incidence of the heavy metal beam is known, the thickness of a crystal or the height of surface protubrances can be determined from the length of the shadow by simple trigonometry.

In dark-field electron microscopy it is not the transmitted beam which is used to construct an image but, rather, a beam diffracted from one facet of the object under investigation. One method for doing this is to shift the aperture of the microscope so that most of the beam is blocked and only those electrons

scattered into the chosen portion of the diffraction pattern contribute to the image. This decreases the intensity of the illumination used to produce the dark-field image and therefore requires longer exposure times, with the attendant modification or even degradation of the polymer. Nevertheless, dark-field operation distinguishes between portions of the sample with different orientations and therefore produces a more three-dimensional representation of the sample.

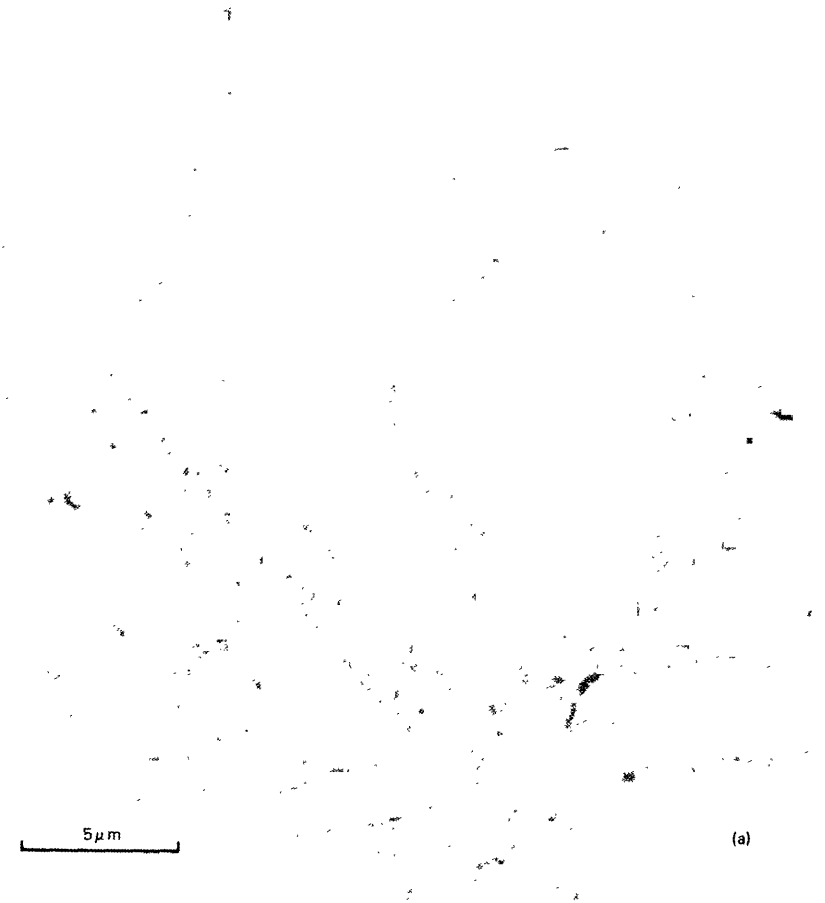

Figure 4.11 Electron micrographs of polyethylene crystals. (a) Dark-field illumination shows crystals to have a hollow pyramid structure. (Reprinted with permission from P. H. Geil, *Polymer Single Crystals*, Interscience, New York, 1963.) (b) Transmission micrograph in which contrast is enhanced by shadow casting [Reprinted with permission from D. H. Reneker and P. H. Geil, *J. Appl. Phys.* 31:1916 (1960).]

Figures 4.11a and b, respectively, are examples of dark-field and direct transmission electron micrographs of polyethylene crystals. The ability of dark-field imaging to distinguish between features of the object which differ in orientation is apparent in Fig. 4.11a. The effect of shadowing is evident in Fig. 4.11b, where those edges of the crystal which cast the shadows display sharper contrast.

The electron micrographs of Fig. 4.11 are more than mere examples of electron microscopy technique. They are the first occasion we have had to actually look at single crystals of polymers. Although there is a great deal to be learned from studies of single crystals by electron microscopy, we shall limit ourselves to just a few observations:

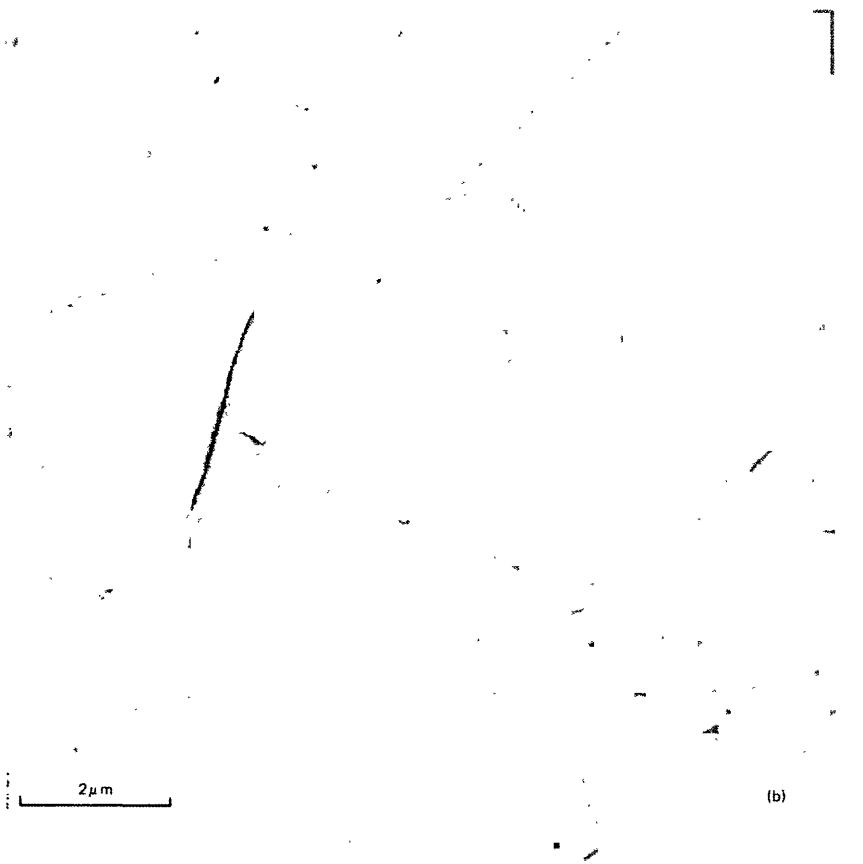

Figure 4.11 *(continued)*

1. Single crystals such as those shown in Fig. 4.11 are not observed in crystallization from the bulk. Crystallization from dilute solutions is required to produce single crystals with this kind of macroscopic perfection. Polymers are not intrinsically different from low molecular weight compounds in this regard.
2. Crystallization conditions such as temperature, solvent, and concentration can influence crystal form. One such modification is the truncation of the points at either end of the long diagonal of the diamond-shaped crystals seen in Fig. 4.11b. Twinning and dendritic growth are other examples of such changes of habit.
3. The polyethylene crystals shown in Fig. 4.11 exist as hollow pyramids made up of planar sections. Since the solvent must be evaporated away prior to electron microscopic observation, the pyramids become buckled, torn, and/or pleated during the course of sample preparation. While the pyramidal morphology is clearly evident in Fig. 4.11a, there is also evidence of collapse and pleating. Likewise, the ridges on the apparently planar crystals in Fig. 4.11b are pleats of excess material that bunches up when the pyramids collapse.
4. Both hollow pyramids and corrugated pyramids are thoroughly documented and fairly well understood. Such structures are consistent with the notion that successive layers of folded chains do not fold at the same place, but offset this fold stepwise to generate the pyramid face. The polymer chains are perpendicular to the planar faces of the pyramid and are therefore tilted at an angle relative to the base of the pyramid.

The foregoing is by no means a comprehensive list of the remarkable structures formed by the crystallization of polymers from solution. The primary objective of this brief summary is the verification that single crystals can be formed and characterized, not only by x-ray diffraction, but by direct electron-microscopic observation. These single crystals are mostly formed from dilute solution, however, and our concern throughout previous parts of this chapter has been the crystallization of polymer from the melt. What is the relationship between these idealized single crystals and the morphological forms which result from crystallization of bulk polymer? We begin to answer this question by considering the microscopic examination of material resulting from the crystallization of polymer melt.

Suppose a bulk-crystallized polymer sample is observed in an optical microscope with the sample placed between Polaroid filters oriented at right angles to each other. In the absence of any sample, the light would be attenuated owing to the 90° angle between the vectors describing the light transmitted by the two filters. With a crystalline sample of polymer in place, however, a display like

Figure 4.12 Spherulites of poly(1-propylene oxide) observed through crossed Polaroid filters by optical microscopy. See text for significance of Maltese cross and banding in these images. [From J. H. MaGill, *Treatise on Materials Science and Technology*, Vol. 10A, J. M. Schultz (Ed.), Academic, New York, 1977, with permission.]

that shown in Fig. 4.12 is generally observed. The field of view becomes at least partially filled with domains called spherulites and which are described by the following general features:

1. They possess spherical symmetry around a center of nucleation. This symmetry projects a perfectly circular cross section if the development of the spherulite is not stopped by contact with another expanding spherulite.

2. A system of mutually impinging spherulites develop into an array of irregular polyhedra, the dimensions of which can be as large as a centimeter or so.
3. The individual spherulite shows up by the characteristic Maltese cross optical pattern under crossed Polaroids, although the Maltese cross is truncated in the event of impinging spherulites.
4. Superimposed on the Maltese cross may be such additional optical features as the banding seen in Fig. 4.12.
5. Spherulites have been observed in organic and inorganic systems of synthetic, biological, and geological origin, including moon rocks, and are therefore not unique to polymers.
6. A larger number of smaller spherulites are produced at larger undercoolings, a situation suggesting nucleation control. Various details of the Maltese cross pattern, such as the presence or absence of banding, may also depend on the temperature of crystallization.

On the basis of a variety of experimental observations, including an analysis of the ubiquitous Maltese cross, a number of aspects of the structure of spherulites have been elucidated. The spherulites are aggregates of lamellar crystals radiating from a nucleation site. The latter can be either a spontaneously formed single crystal or a foreign body. The spherical symmetry is presumably not present at the outset, but develops with time. Apparently, fibrous or lathlike crystals begin branching and fanning out as in dendritic growth. As the lamellae spread out radially and three dimensionally from the nucleus, branching of the crystallites continues to generate the spherical morphology. Figure 4.13 represents schematically the leading edge of some of these fibrils, one of which has just split.

The molecular alignment within these radiating fibers has been determined to be perpendicular to the radius of the individual spherulite. The individual lamellae are similar in organization to the planar faces of pyramidal single crystals; that is, they consist of ribbons on the order of 10-100 nm in thickness, built up from successive layers of folded chains. Growth is accomplished by the addition of successive layers of chains to the ends of the radiating laths. This feature is also indicated schematically in Fig. 4.13. The chain structure of polymer molecules suggests that a given molecule might become involved in more than one lamella and thus link radiating crystallites from the same or adjacent spherulites, as seen in Fig. 4.13. These interlamellar links are not possible in spherulites of low molecular weight compounds, which show poorer mechanical strength as a consequence.

The molecular chain folding is the origin of the Maltese cross which identifies the spherulite under crossed Polaroids. The Maltese cross is known to arise from a spherical array of birefringent particles through the following considerations:

1. The ordered polymer chains are consistently oriented perpendicularly to the radius of the spherulite.

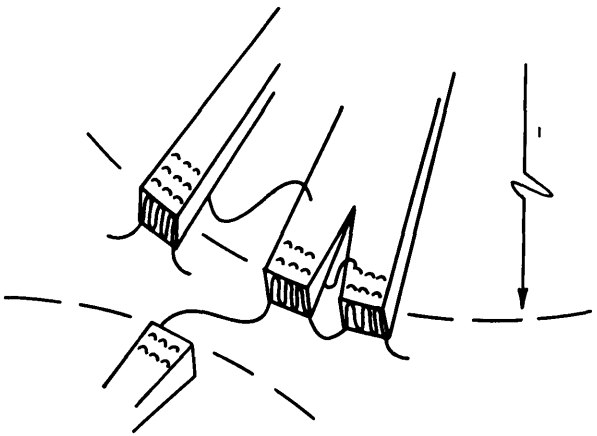

Figure 4.13 Schematic illustration of the leading edge of a lathlike crystal within a spherulite.

2. The index of refraction of most polymers is greater parallel to the chain than normal to the molecular axis. Substances showing this anisotropy of refractive index are said to be birefringent.
3. Items (1) and (2) mean that the refractive index in the tangential direction of the spherulite is generally greater than that along the radius.
4. This birefringence coupled with spherical geometry produces light extinction along the axis of each of the Polaroid filters, hence the 90° angle of the Maltese cross.
5. If the Polaroid filters are held fixed and the sample rotated between them, the Maltese cross remains fixed because of the symmetry of the spherulite.
6. Twisting of the lamellar ribbons along the radial direction is responsible for the banding superimposed on the Maltese cross in Fig. 4.12. From the spacing of the bands, the period of the twist can be calculated and is found to depend on crystallization conditions.

Spherulite morphology in a bulk-crystallized polymer is thus seen to involve ordering at several different levels of organization: individual molecules folded into crystallites which, in turn, are oriented into spherical aggregates. The overall kinetics of such crystallization are consistent with the model of spherical growth from either simultaneous or sporadic nucleations, as discussed in Sec. 4.5. Microscopic observations of growing spherulite fronts even show that the rate of radial growth is constant in isothermal experiments, as postulated in our discussion of crystallization kinetics. The complicated morphology of the spherulite makes it clear that the mechanistic details for bulk crystallization are

oversimplified if growth is visualized as a uniform deposition of polymer molecules on a spherical surface.

We conclude this brief presentation on the types of crystal morphology by briefly describing crystallization under applied stress. We noted this possibility in discussing deviations from the simple model for rubber elasticity under large deformations. Also, stress-induced crystallinity is important in film and fiber technology. When dilute solutions of polymers are stirred rapidly, unusual structures develop which are described as having a shish kebab morphology. These consist of chunks of folded chain crystals strung out along a fibrous central column. In both the "shish" and the "kebab" portions of the structure, the polymer chains are parallel to the overall axis of the structure. Polymers may have a number of obstacles to overcome to crystallize, but once these are surmounted, there seems to be no end to the surprising structures they can produce!

The objective of this chapter is to discuss both the crystalline and the glassy states of polymers. As noted above, only those polymers with the prerequisite order of molecular microstructure can crystallize, but all undergo the glass transition of whatever material remains amorphous at T_g. Thus we conclude this section on structure by observing that the glassy state lacks long-range order, although small domains of short-range order may be larger and last longer for glasses than for liquids because of the lower level of disruptive thermal energy below T_g. Within the glassy state there may be interspersed crystalline patches, but we shall take the position that the glassy state has essentially the same level of order—or lack of order—as the liquid state. With the morphology of the glassy state thus dismissed, we next turn to the question of how the glassy state does differ from the liquid state.

4.8 Thermodynamics and the Glass Transition

The kinetic nature of the glass transition should be clear from the last chapter, where we first identified this transition by a change in the mechanical properties of a sample in very rapid deformations. In that chapter we concluded that molecular motion could simply not keep up with these high-frequency deformations. The complementarity between time and temperature enters the picture in this way. At lower temperatures the motion of molecules becomes more sluggish and equivalent effects on mechanical properties are produced by cooling as by frequency variations. We shall return to an examination of this time-temperature equivalency in Sec. 4.10. First, however, it will be profitable to consider the possibility of a thermodynamic description of the transition which occurs at T_g.

In Secs. 4.3 and 4.4 we discussed the thermodynamics of the crystal → liquid transition. This and other familiar phase equilibria are examples of what are called first-order transitions. There are other less familiar but also well-known

transitions in nature that are not first-order thermodynamic processes. The disappearance of ferromagnetism at a temperature called the Curie point is an example of such a transition. Rather than a discontinuity in S, V, and H, as shown by first-order transitions, these variables merely change slope with increasing temperature. Since this is the sort of behavior which occurs at T_g, it is important to examine this second type of transition in some detail as well. It must be acknowledged from the outset that the applicability of these ideas to T_g is filled with controversy. Time is not a thermodynamic variable, yet we have already seen that the location of T_g depends on the rate at which the temperature variation is carried out. The full picture cannot be developed all at once, however, so for the present we shall ignore this aspect of the behavior and pursue the thermodynamics. We shall have more to say about the time-dependent aspects in later sections.

There is no discontinuity in volume, among other variables, at the Curie point, but there is a change in temperature coefficient of V, as evidenced by a change in slope. To understand why this is called a second-order transition, we begin by recalling the definitions of some basic physical properties of matter:

1. The coefficient of thermal expansion α:

$$\alpha = \frac{1}{V}\left(\frac{\partial V}{\partial T}\right)_p \tag{4.43}$$

2. The isothermal compressibility β:

$$\beta = -\frac{1}{V}\left(\frac{\partial V}{\partial p}\right)_T \tag{4.44}$$

Since V experiences a change of slope at the second-order transition, that is, $(\partial V/\partial T)_p$ and $(\partial V/\partial p)_T$ have different values on each side of the transition, it is α and β that show the discontinuities at the second-order transition rather than V itself. The term *second order* comes about since the quantities showing the discontinuity, α and β among others, may be written as second derivatives of G. That is, we apply Eq. (4.3) to Eqs. (4.43) and (4.44) to obtain

$$\alpha = \frac{1}{V}\left(\frac{\partial V}{\partial T}\right)_p = \frac{1}{V}\frac{\partial}{\partial T}\left[\left(\frac{\partial G}{\partial p}\right)_T\right]_p \tag{4.45}$$

and

$$\beta = -\frac{1}{V}\left(\frac{\partial V}{\partial p}\right)_T = -\frac{1}{V}\left(\frac{\partial^2 G}{\partial p^2}\right)_T \tag{4.46}$$

Figures 4.14a and b are the analogs of Figs. 4.3a and b; they schematically describe second- and first-order transitions, respectively. It is the discontinuity in these second-order properties that characterizes a second-order transition.

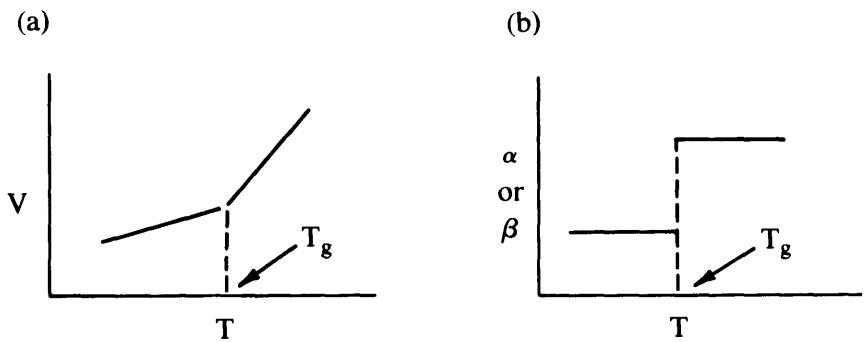

Figure 4.14 Behavior of thermodynamic variables at T_g for a second-order phase transition: (a) volume and (b) coefficient of thermal expansion α and isothermal compressibility β.

Another well-known thermodynamic result, the Clapeyron equation, applies to first-order transitions (subscript 1):

$$\frac{dp}{dT_1} = \frac{\Delta S_1}{\Delta V_1} \tag{4.47}$$

This expression describes the variation of the pressure-temperature coordinates of a first-order transition in terms of the changes in S and V which occur there. The Clapeyron equation cannot be applied to a second-order transition (subscript 2), because ΔS_2 and ΔV_2 are zero and their ratio is undefined for the second-order case. However, we may apply L'Hopital's rule to both the numerator and denominator of the right-hand side of Eq. (4.47) to establish the limiting value of dp/dT_2. In this procedure we may differentiate either with respect to p,

$$\frac{dp}{dT_2} = \frac{(\partial \Delta S_2/\partial p)_T}{(\partial \Delta V_2/\partial p)_T} = \frac{\Delta \alpha}{\Delta \beta} \tag{4.48}$$

or T,

$$\frac{dp}{dT_2} = \frac{(\partial \Delta S_2/\partial T)_p}{(\partial \Delta V_2/\partial T)_p} = \frac{\Delta C_p}{T_2} \frac{1}{V \Delta \alpha} \tag{4.49}$$

to generate some additional expressions. The derivatives of entropy involved in obtaining these equations will be found in any textbook treatment of the

second law. All of the Δ's in these equations refer to the difference in the value of the variable from one side (prime) of T_2 to the other (double prime):

$$\Delta\alpha = \alpha' - \alpha'' \tag{4.50}$$

$$\Delta\beta = \beta' - \beta'' \tag{4.51}$$

and

$$\Delta C_p = C_p' - C_p'' \tag{4.52}$$

The following example illustrates how results like these can be applied.

Example 4.6

On the assumption that the glass transition is a second-order thermodynamic transition, estimate the pressure dependence dT_g/dp of T_g using the following data for poly(vinyl chloride): $T_g = 347$ K, $V_{sp} = 0.75$ cm^3 g^{-1}, $\Delta\alpha = 3.1 \times 10^{-4}$ K^{-1} and $\Delta C_p = 0.068$ cal K^{-1} g^{-1}.†

Solution

Invert Eq. (4.49) and substitute. The ratio of gas constants is convenient for unit conversion:

$$\frac{dT_g}{dp} = \frac{T_g V \Delta\alpha}{\Delta C_p} = \frac{(347 \text{ K})(0.75 \text{ cm}^3 \text{ g}^{-1})(3.1 \times 10^{-4} \text{ K}^{-1})}{(0.068 \text{ cal g}^{-1} \text{ K}^{-1})}$$

$$\times \frac{1.99 \text{ cal}}{82 \text{ atm cm}^3} = 0.029 \text{ K atm}^{-1}$$

This quantity has been measured directly to be 0.016 K atm^{-1}. Note that a pressure change of 60 atm is needed to change T_g by 1 K.

•

Since Eqs. (4.48) and (4.49) both describe the same limit, they must be equal at the second-order transition point:

$$T_2 = \frac{\Delta C_p \, \Delta\beta}{V(\Delta\alpha)^2} \tag{4.53}$$

† J. M. O'Reilly, *J. Polym. Sci.* 57:429 (1962).

For a second-order transition Eq. (4.53) is the analog of Eq. (4.5), which is useful for first-order transitions. Equation (4.53) and the first- and second-order terminology are due to Ehrenfest.

Thermodynamics is an abundant source of relationships and does not let us down with respect to true second-order transitions. The reader will notice that the innocent-looking word *true* crept into the last sentence describing this second-order transition. The implication here is that the glass transition is not "truly" a second-order transition. A moment's reflection reveals that the source of this reservation is the doubt about equilibrium for the glass transition. Implicit throughout all of the thermodynamics in this chapter has been the notion that the phases on either side of a transition, whether first or second order, are in thermodynamic equilibrium. This enters the mathematical formalism right from the start: Eq. (4.1) assumes that the Gibbs free energy of a phase is described by only two variables, in that case p and T. While the glass transition is certainly affected by p and T, it is also dependent on the time of observation, as shown in Fig. 4.1. Because of this time dependence, the glass transition involves more than a simple second-order transition. Several generalizations do seem safe at this point, however:

1. The experimental value of T_g appears at progressively lower temperatures the more slowly the experiment is conducted.
2. Sufficient time must be allowed for thermodynamic equilibrium to be reached in other simpler reactions and transitions.
3. Changes in the conformation of polymer chain backbone occur much more slowly in the vicinity of T_g than most of the molecular processes that serve as examples of simpler equilibria.
4. If a T_g value corresponding to a true second-order transition exists, it is a value lower than those based on short-term observations. The latter should then be regarded as approximations to the true value.

4.9 Free Volume

The foregoing thermodynamic view of the glass transition assumes that equilibrium criteria are satisfied as a sample is cooled through T_g. In this section we shall set aside the issue of thermodynamic equilibrium and simply consider why the mechanical properties of polymers should undergo a dramatic change over a relatively narrow range of temperatures, an observation which was, in the last chapter, our introduction to T_g. In discussing Fig. 4.14, we saw that volume also shows a change in behavior at T_g—a change more typical of second-order than first-order transitions. Since volume is more readily visualized than the mechanical properties, we shall concentrate on the former in the following discussion. The emphasis is not merely a matter of convenience, however, since most attempts to understand T_g involve some concept of free volume.

There are two ways in which the volume occupied by a sample can influence the Gibbs free energy of the system. One of these involves the average distance of separation between the molecules and therefore influences G through the energetics of molecular interactions. The second volume effect on G arises from the contribution of free-volume considerations. In Chap. 2 we described the molecular texture of the liquid state in terms of a model which allowed for vacancies or holes. The number and size of the holes influence G through entropy considerations. Each of these volume effects varies differently with changing temperature and each behaves differently on opposite sides of T_g. We shall call free volume that volume which makes the second type of contribution to G.

On the basis of these ideas, the observed volume of a sample can be written as the sum of the volume occupied by the molecules (subscript 0) and the free volume (subscript f). Acknowledging that each of these is a function of temperature, we write

$$V(T) = V_0(T) + V_f(T) \tag{4.54}$$

The variation in the occupied volume with temperature arises from changes in the amplitude of molecular vibrations with changing T, a variation which affects the excluded volume of the molecules. The free volume, on the other hand, may be viewed as the "elbow room" that molecules require to undergo rotation and translational motion. These modes of motion also increase with increasing temperature, so the associated volume is also expected to increase with T. With decreasing temperature a point may be visualized at which V_f has decreased to a critical value below which the translational and rotational modes of motion are essentially crowded out. In the last chapter we attributed the dramatic difference in moduli between the glassy state and the rubbery state at T_g to an effective freezing out of translational modes of motion of chain backbone segments. According to this picture, then, we identify T_g as the temperature at which V_f reaches this critical size. It will simplify our discussion to assume that below T_g the quantity V_f is constant with further decreases in T. This assumption imposes no constraints on the behavior of V_0 below T_g. On the basis of these ideas, we can write the following expressions for the volume of the sample:

1. Below T_g

$$V(T < T_g) = V_0(T = 0) + V_f(T = 0) + \left(\frac{dV_0}{dT}\right)_g T \tag{4.55}$$

2. At T_g

$$V(T_g) = V_0(T = 0) + V_f(T = 0) + \left(\frac{dV_0}{dT}\right)_g T_g \tag{4.56}$$

3. Above T_g

$$V(T > T_g) = V(T_g) + \left(\frac{d(V_0 + V_f)}{dT}\right)_l (T - T_g) \tag{4.57}$$

The subscripts g and l on the coefficient of volume variation with T indicate that these are determined for the glass and liquid states, respectively. These relationships are indicated geometrically in Fig. 4.15. The broken line in Fig. 4.15 shows the temperature variation of V_0, and the solid line, the actual volume. Presumably V_0 does not undergo any significant change in its temperature variation at T_g, but continues at least some distance beyond T_g with the slope $(dV_0/dT)_g$. At any temperature the difference between the two lines gives the free volume at that temperature. Figure 4.15 illustrates by shading how the free volume funnels down with decreasing temperature to a value too small to allow those types of molecular motion with greater space requirements. Each of the differences used to describe the second-order phase transition as given by Eq. (4.53) can be qualitatively traced to the sort of change implied by Fig. 4.15. Around T_g, for example, the coefficient of expansion of the liquid and glassy states are,

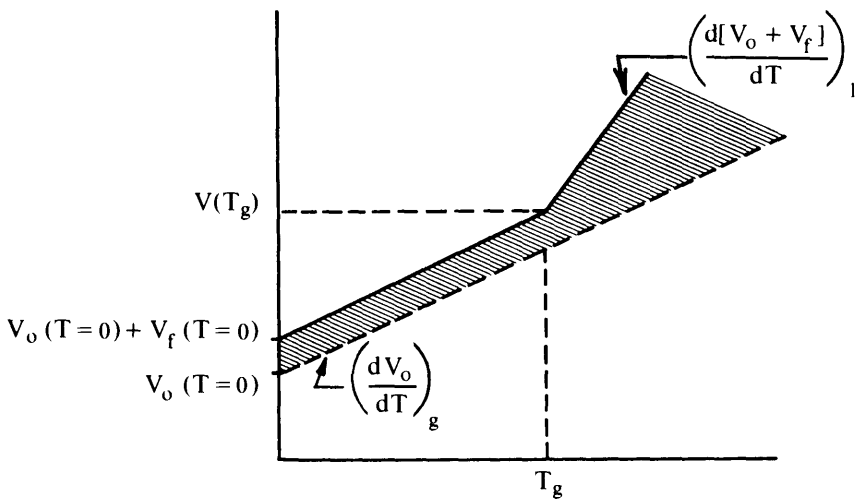

Figure 4.15 Geometrical representation of the temperature variation of the actual volume (solid line) and the "occupied" volume (broken line). The shaded difference indicates the free volume which decreases to a critical value at T_g.

respectively,

$$\alpha_l = \frac{1}{V_g}\left(\frac{d(V_0 + V_f)}{dT}\right)_l \quad \text{and} \quad \alpha_g = \frac{1}{V_g}\left(\frac{dV_0}{dT}\right)_g$$

therefore $\Delta\alpha$ is a measure of the opening up of V_f at T_g. The additional volume above T_g also accounts for the change in compressibility $\Delta\beta$, and the emergence of the associated modes of energy storage accounts for ΔC_p.

In discussing Fig. 4.1 we noted that the apparent location of T_g is dependent on the time allowed for the specific volume measurements. Volume contractions occur for a long time below T_g: The lower the temperature, the longer it takes to reach an equilibrium volume. It is the equilibrium volume which should be used in the representation summarized by Fig. 4.15. In actual practice, what is often done is to allow a convenient and standardized time between changing the temperature and reading the volume. Instead of directly tackling the rate of collapse of free volume, we shall approach this subject empirically, using a property which we have previously described in terms of free volume, namely, viscosity.

The following expression, known as the Dolittle equation, has been found to accurately describe the viscosity of low molecular weight compounds:

$$\eta = A \exp\left(\frac{B(V - V_f)}{V_f}\right) \tag{4.58}$$

where A and B are empirical constants. Dolittle showed that this expression described the viscosity of low molecular weight compounds better than the Arrhenius equation ($\eta = A' e^{-E^*/RT}$), which is generally used for this purpose. Although they relate η to different variables, both the Dolittle and Arrhenius equations have the same functional form. Just as the activation energy E^* measures the height of the energy barrier relative to thermal energy, so $V - V_f$ or V_0 is measured relative to V_f. If both V_0 and V_f are expressed per molecule, the exponent in the Dolittle equation measures the volume of a molecule (V_0 per molecule) relative to the volume of a hole (V_f per hole). When the molecule is large compared to the vacancy it must move into, the viscosity is high; when the molecule is small compared to the hole, the viscosity is low. This is the physical significance of the Dolittle equation, although we should remember that it is basically empirical in origin.

If we define f to be the fraction of volume contributed by the free volume V_f/V, then Eq. (4.58) can be written as

$$\eta = A \exp\left[B\left(\frac{1}{f} - 1\right)\right] \tag{4.59}$$

Now the constant A can be eliminated from Eq. (4.59) by examining the ratio of two values of η with two different values of f (subscripts 1 and 2), remembering that B is a constant. In this case, we write

$$\frac{\eta_1}{\eta_2} = \exp\left\{B\left[\left(\frac{1}{f_1} - 1\right) - \left(\frac{1}{f_2} - 1\right)\right]\right\} = \exp\left[B\left(\frac{1}{f_1} - \frac{1}{f_2}\right)\right] \tag{4.60}$$

or

$$\ln\left(\frac{\eta_1}{\eta_2}\right) = B\left(\frac{1}{f_1} - \frac{1}{f_2}\right) \tag{4.61}$$

which is analogous to the form into which the Arrhenius equation would be cast to evalute E^*.

Next we assume that the state designated by the subscript 2 in Eq. (4.61) corresponds to T_g; we designate the fraction free volume at T_g by f_g. Likewise, state 1 is assumed to be above T_g, where f can be written

$$f = f_g + \alpha_f(T - T_g) \tag{4.62}$$

on the basis of Fig. 4.15. In this expression α_f is the coefficient of expansion of the free volume only. Substitution of f and f_g into Eq. (4.61) gives

$$\ln\left(\frac{\eta(T > T_g)}{\eta(T_g)}\right) = B\left(\frac{1}{f_g + \alpha_f(T - T_g)} - \frac{1}{f_g}\right) = \frac{-(B/f_g)(T - T_g)}{f_g/\alpha_f + (T - T_g)} \tag{4.63}$$

Things appear to have taken a strange turn: We started out discussing the free volume and have ended up with an equation which contains no volume at all! More specifically, we set out to examine the rate at which the free volume collapses at T_g. A final development of Eq. (4.63) will produce the desired result.

In Chap. 9 we shall examine the flow of a solution through a capillary tube. The rate of volume delivery in that case is given by Poiseuille's law [Eq. (9.29)], which states that the time required for a constant volume of liquid to drain out of the capillary is proportional to η/ρ. Accordingly, the viscosity is proportional to the product ρt, and when the delivery times for two liquids are compared in the same capillary,

$$\frac{\eta_1}{\eta_2} = \frac{\rho_1 t_1}{\rho_2 t_2} \tag{4.64}$$

This equation is the basis for viscosity determination by measuring flow times through a capillary. It can also be used to describe a single liquid at two different temperatures, as required for Eq. (4.63). Combining Eqs. (4.63) and (4.64) yields

$$\ln\left(\frac{t(T>T_g)}{t(T_g)}\right) = \frac{-(B/f_g)(T-T_g)}{f_g/\alpha_f + (T-T_g)} - \ln\left(\frac{\rho(T>T_g)}{\rho(T_g)}\right) \tag{4.65}$$

which is approximated by

$$\ln\left(\frac{t(T>T_g)}{t(T_g)}\right) \cong \frac{-(B/f_g)(T-T_g)}{f_g/\alpha_f + (T-T_g)} \tag{4.66}$$

since the variation of ρ with temperature is much less than the variation of η. To simplify the notation, we attach the subscript g to both T and t at the glass transition and use no subscript on either when the temperature exceeds T_g:

$$\ln t - \ln t_g = \frac{-C_1'(T-T_g)}{C_2 + (T-T_g)} \tag{4.67}$$

where the constants C_1' and C_2 replace other clusters of constants. This is an important equation and we shall return to it in the next section. For the present time it is sufficient to note the following:

1. The left-hand side of the equation relates the times required for a specific displacement to occur at T_g and at a distance $T - T_g$ above T_g.
2. The right-hand side of the equation expresses this difference as a function of the temperature difference from T_g.
3. Since $T > T_g$, the negative sign assures that $\ln t_g > \ln t$; that is, the process takes longer at T_g.
4. As $T \to T_g$, the difference between the two times diminishes, dropping to zero when $T = T_g$.

These results make sense physically; what we must remember is that they follow from an analysis of the vanishing free volume.

Several additional observations are in order concerning the use of the Dolittle equation:

1. Although Eq. (4.58) describes the variation of viscosity over a wide range of conditions quite well, it tends to break down toward lower temperatures, precisely where we wish to apply it.
2. Although it is easy to discuss free volume, it is necessary to come up with a numerical value for this quantity in order to test these concepts. There is

some controversy as to which of several different methods of computation gives the best value for V_f and therefore V_0.

3. Although Eq. (4.67) is derived specifically for conditions of $T > T_g$, we shall apply it both above and below T_g in the next section.
4. It is possible to derive an expression equivalent to Eq. (4.67) starting from entropy rather than free volume concepts. We have emphasized the latter approach, since it is easier to visualize and hence to use for qualitative predictions about T_g.
5. Completely aside from the theories which attempt to explain it, the empirical usefulness of Eq. (4.67) is beyond doubt. We shall examine this in detail in the next section.

The collapse of the free volume below a critical size for molecular motion is the perspective on the glass transition that we have taken in this section. This concept is useful to understand the effects of polymer structure on T_g. Table 4.4 lists T_g values for many of the same polymers that were presented in Table 2.3, this time ranked in order of decreasing T_g values. Also listed are values of the clusters of constants shown in Eq. (4.66). Except for polystyrene and poly(dimethyl siloxane), which fall out of place, the broken line divides the hydrocarbons from molecules containing more polar groups of atoms. The following

Table 4.4 Some Polymers Ranked in Order of Decreasing T_g Values, Along with Numerical Values for Quantities Appearing in the Dolittle Equation

Polymer	T_g (K)	B/f_g	f_g/α (K)	f_g
Molecules containing polar groups				
Methyl methacrylate	388	76.9	76.5	0.013
Styrene	373	31.3	50.8	0.032
Ethyl methacrylate	335	40.0	67.6	0.025
n-Butyl methacrylate	300	38.5	100	0.026
Methyl acrylate	276	41.7	45.3	0.024
n-Hexyl methacrylate	268	40.0	132	0.025
n-Octyl methacrylate	253	37.0	108	0.027
Urethane rubber	238	35.7	32.9	0.028
Hydrocarbons				
1-Hexene	218	50.0	20.6	0.020
Butyl rubber	205	38.5	108	0.026
Polyisobutylene	205	38.5	104	0.026
1,4-Butadiene	172	25.6	60.9	0.039
Dimethyl siloxane	150	14.1	68.9	0.071

Source: Data from J. D. Ferry, *Viscoelastic Properties of Polymers*, John Wiley and Sons, New York, 1980.

list of generalizations is based in part on Table 4.4 and on various additional observations:

1. Hydrocarbons without bulky side groups are held together by London forces, the weakest of intermolecular attractions. This means that the free volume tends to be large for these compounds, so a relatively large amount of cooling is necessary before the free volume collapses. Thus T_g is low for these compounds.
2. The effect of a bulky substituent like a phenyl group on the hydrocarbon chain apparently decreases chain flexibility sufficiently to allow more intimate alignment between molecules, less free volume, and therefore a high value for T_g.
3. In the methacrylate homologous series, the effect of side-chain bulkiness is just the opposite. In this case, however, the pendant groups are flexible and offer less of an obstacle to free rotation than the phenyl group in polystyrene. As chain bulk increases, molecules are wedged apart by these substituents, free volume increases, and T_g decreases.
4. The presence of two substituents rather than one (compare methyl methacrylate with methyl acrylate) increases chain stiffness, decreases V_f, and increases T_g.
5. An extra amount of free volume is associated with chain ends, which are capable of wagging in a way that is not possible in the middle of a chain. Accordingly, as molecular weight decreases, V_f increases, which, in turn, decreases T_g. The following expression has been found to describe this molecular weight dependence:

$$T_g = T_g^{\infty} - \frac{K}{M} \tag{4.68}$$

   where T_g^{∞} is the glass transition temperature of a polymer of infinite molecular weight and K is a constant.
6. The effect of branching is to increase the number of chain ends and, therefore, free volume, which decreases T_g. Conversely, crosslinking ties together separate molecules, decreases the number of loose ends, and raises T_g.
7. Copolymers show different effects on T_g, depending on the microstructure of the molecule. Block copolymers show two values of T_g, each being the value appropriate to the respective homopolymer. Random copolymers show T_g values which are intermediate between the values of the homopolymers. It has been found that the following averaging procedure describes this intermediate T_g value:

$$\frac{1}{T_g} = w_1 \left(\frac{1}{T_g}\right)_1 + w_2 \left(\frac{1}{T_g}\right)_2 \tag{4.69}$$

   where the w's are weight fractions of components 1 and 2.

8. The presence of low molecular weight molecules between polymer chains has the effect of pushing the chains apart, effectively increasing V_f. The resulting decrease in T_g can significantly widen the range of usefulness of a polymer, so the importance of such diluents—called plasticizers in view of this effect—in technology is very great.

4.10 Time-Temperature Equivalency

In this section we resume our examination of the equivalency of time and temperature in the determination of the mechanical properties of polymers. In the last chapter we had several occasions to mention this equivalency, but never developed it in detail. In examining this, we shall not only acquire some practical knowledge for the collection and representation of experimental data, but also shall gain additional insight into the free-volume aspect of the glass transition.

In describing the various mechanical properties of polymers in the last chapter, we took the attitude that we could make measurements on any time scale we chose, however long or short, and that such measurements were made in isothermal experiments. Most of the experimental results presented in Chap. 3 are representations of this sort. In that chapter we remarked several times that these figures were actually the result of reductions of data collected at different temperatures. Now let us discuss this technique; our perspective, however, will be from the opposite direction: taking an isothermal plot apart.

Because so many orders of magnitude of time are spanned in comprehensive studies of mechanical behavior, plots of experimental results like that shown in, say, Fig. 3.9, require a long horizontal axis. As a graphical expediency, such a figure could be cut in half at the midpoint. The second half of the data points could then be shifted to the left and plotted beneath the larger, short-duration moduli. Since a logarithmic time scale is used in Fig. 3.9, this compressed graph is simply described by noting that for the second segment of the divided curve the log t values should all be increased by log a, the amount by which the displaced section has been shifted. An even greater telescoping of the data is accomplished by dividing the original full curve into three or more segments and then shifting successive sections onto a single, shortened coordinate system. Figure 4.16 shows schematically the results of such a procedure when the parent curve is divided into three sections. Figure 4.16a shows the following decomposition of the full curve:

1. The segment between t_2 and t_3 is shifted to the left by an amount log a so that log t_2 is displaced to overlap log t_1.
2. The segment between t_3 and t_4 is shifted to the left by an amount log a' so that log t_3 is displaced to log t_1 also.

Figure 4.16b shows the following for the "stacked" segments:

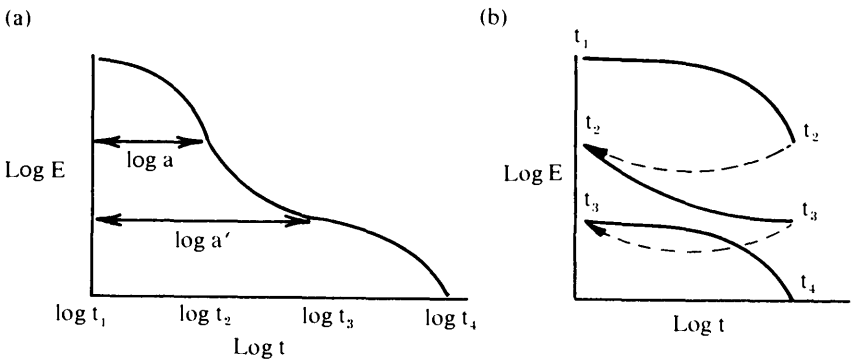

Figure 4.16 Schematic illustration showing how an experimental plot of modulus against log t (a) can be telescoped (b) by shifting successvie segments by an amount designated as log a.

3. t_1, t_2, and t_3 all overlap on the left edge of the log t scale, and t_2, t_3, and t_4 all overlap on the right.
4. In this case a narrower range of log t values is needed to represent the data and this can be narrowed still further by dividing the original curve into an even larger number of segments.

It is apparent that the curve in Fig. 4.16a could be reconstructed from the version in Fig. 4.16b with a knowledge of the displacements, log a and log a′.

The foregoing points are all fairly obvious to science and engineering students who have drawn and studied numerous graphs. The point of this discussion is not merely the telescoping of data by graphical manipulation; instead, it is an empirical fact that measurements of moduli or compliances over a modest range of times or frequencies at a variety of different temperatures produce a set of curves resembling Fig. 4.16b. If the full curve of Fig. 4.16a can be reconstructed from the pieces in Fig. 4.16b, then it must be possible to shift segments measured at different temperatures to produce a full curve by making the individual segments connect with one another. In such a procedure we have the following:

1. Measurements at one of the temperatures will be left unchanged. Data from other temperatures are shifted to bring them into line with the unmoved data.
2. The amount by which the individual isothermal results are shifted, log a_T for an experiment at temperature T, will be different for each T.
3. Shifts can be to either the right or the left; that is, log a_T can be either negative or positive.
4. The final composite curve is called the master curve at the temperature of the unmoved isotherm.

The isothermal curves of mechanical properties in Chap. 3 are actually master curves constructed on the basis of the principles described here. Note that the manipulations are formally similar to the superpositioning of isotherms for crystallization in Fig. 4.8b, except that the objective here is to connect rather than superimpose the segments. Figure 4.17 shows a set of stress relaxation moduli measured on polystyrene of molecular weight 1.83×10^5. These moduli were measured over a relatively narrow range of readily accessible times and over the range of temperatures shown in Fig. 4.17. We shall leave as an assignment the construction of a master curve from these data (Problem 10).

The procedure described above is an application of the time-temperature correspondence principle. By shifting a set of plots of modulus (or compliance) versus time (or frequency) at any temperature (subscript 1) along the log t axis, we obtain the value of that mechanical property at another time and temperature (subscript 2). Using the shear modulus as an example, the time-temperature correspondence principle states

$$G(t_1, T_1) = G(t_2, T_2) \tag{4.70}$$

at the point of overlap. We drop the subscript on time in the master curve; therefore Eq. (4.70) becomes

$$G\left(\frac{t}{a_{T_1}}, T_1\right) = G\left(\frac{t}{a_{T_2}}, T_2\right) \tag{4.71}$$

Note that subtracting an amount log a_T from the coordinate values along the abscissa is equivalent to dividing each of the t's by the appropriate a_T value. This means that times are represented by the reduced variable t/a_T in which t is expressed as a multiple or fraction of a_T which is called the shift factor. The temperature at which the master curve is constructed is an arbitrary choice, although the glass transition temperature is widely used. When some value other than T_g is used as a reference temperature, we shall designate it by the symbol T_0.

We shall presently examine the physical significance of the shift factors, since they quantitatively embody the time-temperature equivalence principle. For the present, however, we shall regard these as purely empirical parameters. The following list enumerates some pertinent properties of a_T:

1. At T_0, $a_T = 1$; no shift of time scale is required.
2. For $T > T_0$, $a_T < 1$, which corresponds to $\log a_T < 0$. These values are used when the curves are shifted to the right. The effect on the mechanical properties is equivalent to expanding the time scale, since we express time as t/a_T.
3. For $T < T_0$, $a_T > 1$, which corresponds to $\log a_T > 0$. These values are used

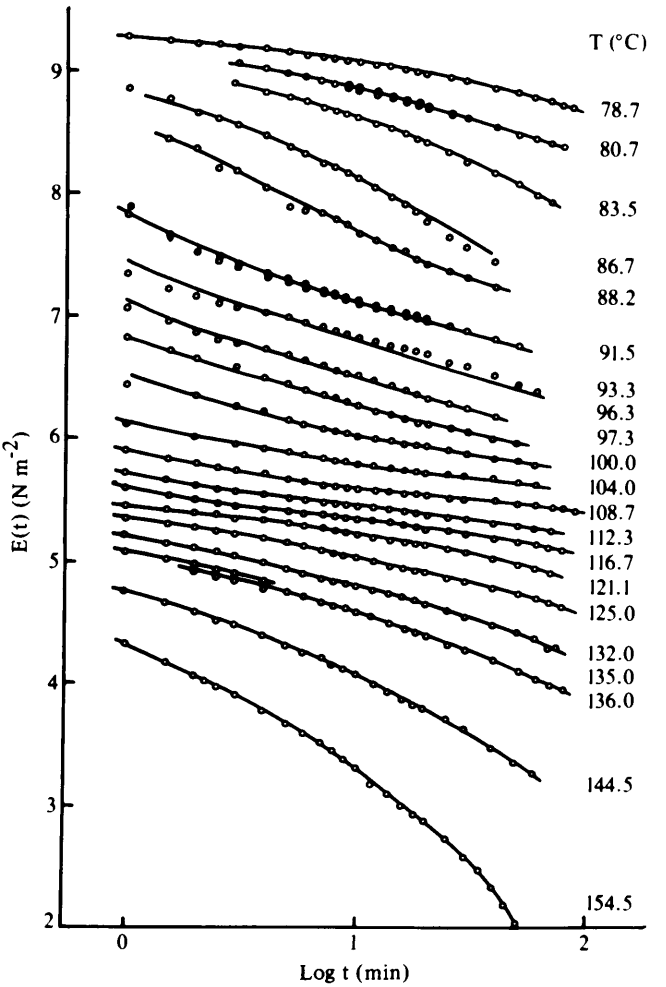

Figure 4.17 Experimental stress relaxation moduli of polystyrene measured over about two orders of magnitude in time at the temperatures indicated. [Reprinted with permission from H. Fujita and K. Ninomiya, *J. Polym. Sci.* 24:233 (1957).]

when curves are shifted to the left. The effect on the mechanical properties is equivalent to compressing the time scale.

All amorphous polymers show remarkably similar results when values of log a_T are plotted versus $T - T_0$. Manipulation of these data shows that the empirically determined shift factors can be fitted by the expression

$$\log a_T = \frac{-C_1(T - T_0)}{C_2 + (T - T_0)} \tag{4.72}$$

where C_1 and C_2 are constants. This equation is known as the WLF equation, for Williams, Landel, and Ferry, the researchers who discovered it. Note that when $T_0 = T_g$, the right-hand side of Eq. (4.72) is identical to Eq. (4.67). It is no wonder that this is the case; Eq. (4.67) is an expression for the difference in ln t values for a fixed amount of deformation at two different temperatures. This is precisely what log a_T does also. The only difference between Eqs. (4.67) and (4.72) is the use of natural logarithms in the former and logarithms to the base 10 in the latter. Accordingly, the constants in the numerator of the two equations are related as follows: $C_1 = C_1'/2.303$; C_2 is the same in both. Since it is easier to study mechanical properties and carry out time-temperature superpositioning than to study volume contraction, the constants listed in Table 4.4 were obtained from the former.

Rearrangement of Eq. (4.72) suggests a method for evaluating the constants C_1 and C_2 from experimental results. We write

$$\frac{T - T_g}{\log a_T} = -\frac{C_2}{C_1} - \frac{1}{C_1}(T - T_g) \tag{4.73}$$

which is an equation of the type $y = mx + b$ if we identify y as $(T - T_g)/(\log a_T)$ and x as $T - T_g$. Then the slope m equals $-1/C_1$, and the intercept b equals $-C_2/C_1$. Thus if the empirical shift factors for different temperatures are analyzed according to Eq. (4.73), the slope and intercept can be used to evaluate C_1 and C_2:

$$C_1 = -\frac{1}{\text{slope}} \tag{4.74}$$

and

$$C_2 = -\frac{\text{intercept}}{\text{slope}} \tag{4.75}$$

The parameters f_g and α_f can be evaluated from C_1 and C_2 by virtue of the definition of the latter:

$$f_g = \frac{B}{2.303C_1} \tag{4.76}$$

and

$$\alpha_f = \frac{B}{2.303C_1C_2} \tag{4.77}$$

The factor B in Eq. (4.58) is close to unity; hence the reciprocals of the

values B/f_g in Table 4.4 give the fraction of free volume in the various polymers at the glass transition temperature. According to this interpretation of the shift factors, the free volume of many polymers is remarkably constant and close to 2.5%. Despite the coherent picture presented here, there is controversy about the validity of this uniform value for V_f. It has been argued that the fraction of free volume at T_g should be up to five times larger than the WLF value.

We conclude this section with an example illustrating the application of the WLF equation using the data in Fig. 4.17.

Example 4.7

Use values of the constants for polystyrene from Table 4.4 to calculate the shift factors needed to connect those segments in Fig. 4.17 measured at 96.3 and 108.7°C, with the isotherm measured at $T_g = 100.0$°C. Are the values reasonable?

Solution

For polystyrene, $B/f_g = 31.3$ and $f_g/\alpha = 50.8$ from Table 4.4. Using Eq. (4.66), we obtain the following. At $t = 96.3$°C, or $T - T_g = -3.7$°C,

$$\ln a_T = \frac{-31.3(-3.7)}{50.8 - 3.7} = 2.46, \quad \log a_T = 1.07, \quad a_T = 11.8$$

At $T = 108.7$°C, or $T - T_g = 8.7$°C,

$$\ln a_T = \frac{-31.3(8.7)}{50.8 + 8.7} = -4.58, \quad \log a_T = -1.99, \quad a_T = 0.0103$$

At 96.3°C, $\log E \cong 6.5$ when $\log t = 1$. Subtracting the calculated value of $\log a_T$ from this gives a reduced value for $\log t \cong 0$. This is the time at which $\log E \cong 6.5$ at 100°C. Stated differently, $E \cong 10^{6.5}$ N m^{-2} after 10 min at 97.3°C and after 1 min at 100°C. Therefore $t/a_T = 10/11.8$ min = 0.85 min $\cong$ 1 min, showing this to be a reasonable value.

At 108.7°C, $\log E \cong 5.9$ when $\log t = 0$. Subtracting the calculated value of $\log a_T$ from this gives a reduced value for $\log t \cong 2$. On the other hand, the time at which $\log E \cong 5.9$ at 100°C is about 20 min, or $\log t \cong 1.3$. This value is less satisfactory. In terms of reduced variables, $E \cong 10^{5.9}$ N m^{-2} after 1 min at 108.7°C and after 1/0.0103 min $\cong$ 100 min at 100°C. This last value should be closer to 20 min.

•

The limited success of the previous example should not be a cause for alarm, since the constants listed in Table 4.4 are "best" values and will not necessarily

work equally well for all observations. The calculated values are certainly of the right magnitude, and we must bear in mind the difficulties involved in estimating values from a logarithmic scale. In addition, Eq. (4.66) was used in this example. This is an approximation based on the assumption that ρ does not change appreciably over the range of temperatures under examination. In precise work, the moduli being matched up should be corrected to the reference temperature by multiplying individual values by the ratio $T_0\rho_0/T\rho$ (subscript 0, reference state; no subscript, result being shifted) before attempting the superpositioning. This ratio is clearly very close to unity in the example.

4.11 Polymer Processing Technology

We conclude this chapter and wrap up the last three chapters with a few remarks about the application of the ideas contained herein to polymer technology. Chapters 2-4 have been concerned with various aspects of the mechanical states of polymers. The opinion was expressed in Chap. 1 that if polymers did not possess the mechanical properties they have, this whole class of compounds might be relegated to the category of laboratory curiosities. On the basis of any number of criteria—the number of scientists employed, the number of industries involved, the number of publications released, the number of patents issued—polymer science proves to be very viable indeed.

The history of individual polymers as well as the history of the discipline itself is one of symbiosis between pure science and applied technology. Haward (Ref. 3) makes this point clear in his discussion of polystyrene. When the latter emerged on the scene in the late 1930s to early 1940s, it was taken up by academic researchers but largely rejected by those in industry. It was a perfect polymer for fundamental, academic-type research. It could be prepared reproducibly and, because of its solubility, fractionated by molecular weight and characterized by solution properties. By contrast, its high T_g value made it brittle under many potential use conditions, and hence initially unattractive for applications. Eventually what Haward describes as an "irresistible combination of four favorable properties" led to industrial research into polystyrene applications. The "favorable four" were low cost, good appearance, rigidity, and processability. Through the use of plasticizers, the development of dispersions of rubber in polystyrene (called high-impact polystyrene), and the development of copolymers, the initial objections to brittleness were overcome. In 1981 the styrene industry produced about 2.2×10^6 metric tons of monomer for use in homo- and copolymers.

From the point of view of technology, it is convenient to classify polymers as thermosetting and thermoplastic. The former "set" by chemical crosslinks introduced during fabrication and hence do not change appreciably in their deformability with changes in temperature. Thermoplastics, on the other hand, soften and/or melt on heating and can therefore be altered in shape by heating

or frozen in shape by cooling. The choice between these two classes is governed by the permanence or elasticity desired in the ultimate application of the material. We saw in Chap. 3 that the presence of crystalline regions and, to a lesser extent, entanglements can give thermoplastic materials similar mechanical properties to elastomers, at least under some conditions.

For pedagogical reasons we have attempted to concentrate on essentially pure polymers in these chapters. From the point of view of technology this creates a fairly narrow view of those systems where polymers find application. Dispersed particles are introduced into polymers as fillers in many applications. These are essentially two-phase systems and include such examples as colloidal carbon dispersed in rubber, pigments dispersed in coatings, and rubber dispersed in high-impact polystyrene. By contrast, plasticizers may be considered to form true, homogeneous solutions with polymers. The plasticizer is often present in relatively small amounts, so, from the point of view of the polymer as solute, these systems are often highly concentrated solutions. Both homogeneous and heterogeneous mixtures are probably more widely used in polymer technology than are pure bulk polymers. It is unfortunate that both the level and length of this book make it impossible to devote more space to these topics. In Chaps. 8-10 we shall return to the topic of polymer solutions, although the emphasis will be placed on systems which are dilute with respect to polymer.

One area of technology that has been the source and motivation for much polymer research, particularly with respect to mechanical properties, is the fiber industry. While many of the basic principles of the last three chapters find application in fiber technology, it must also be acknowledged at the outset that there is a great deal of empirical know-how in addition to fundamental science involved in the production of commercial fibers. The most widely used fiber-forming processes are called melt and wet (or solution) spinning. In both, the polymer is extruded from the small holes of a device called a spinneret to produce a crude fiber. In melt spinning molten polymer is used, while in wet spinning a solution is the source of the polymer. In melt spinning the polymer solidifies by air cooling after extrusion from the spinneret; in wet spinning the polymer solution is emitted into a nonsolvent which causes the precipitation of the polymer. In both cases the polymeric fibers are stretched before being wound onto a spool. Melt spinning is used with thermally stable polymers such as polyolefins, while wet spinning is useful for thermally unstable or sensitive polymers such as poly(acrylonitrile). High temperatures are required for melt spinning, and the cost of the required energy is a disadvantage of this method. The need for solvent recovery is the disadvantage of wet spinning.

When we speak of the solidification of the extruded polymer, we use the term in the broadest sense: It includes crystallization, vitrification, or both. The extent of the drawing of the fibers and the rate and temperature of the drawing affect the mechanical properties of the fiber produced. This conclusion should be evident from a variety of ideas presented in the last three chapters:

1. At the molecular level, stretching extends polymer coils and facilitates crystallization.
2. The nucleation, growth, and morphology of crystals are influenced by both temperature and stress.
3. The presence of spherulites or smaller crystallites is comparable to crosslinking and affects not only the moduli and compliances, but also the ultimate properties such as yield strength and ultimate elongation.
4. Both thermodynamic and kinetic aspects of mixed systems (e.g., the precipitation step in wet spinning) involve the properties of the other components (solvent and nonsolvent in wet spinning) as well as the polymer.

Two other processing techniques, namely, injection molding and calendering, should also be mentioned. In the first of these a heat-softened polymer is injected into a cavity or die, where it is allowed to cool and set. From the point of view of process efficiency, it is desirable to cool the product as rapidly as possible so that the mold can be refilled. From the point of view of the product, the rate of cooling determines the degree of crystallization. This influences the density, which, in turn, affects the linear dimensions of the finished product. In some instances, meeting tolerances specified for a product may be at cross-purposes with efficient equipment utilization. Calendering is the process of rolling a polymeric sample to produce films which can be used as such or layered on a substrate as a coating. As usual, time and temperature are important variables in this process. In addition, either uniaxial or biaxial stretching can be introduced to influence the extent of chain ordering and the attendant consequences of the latter.

4.12 Preview of Things to Come

In the last three chapters we have examined the mechanical properties of bulk polymers. Although the structure of individual molecules has not been our primary concern, we have sought to understand the influence of molecular properties on the mechanical behavior of polymeric materials. We have seen, for example, how the viscosity of a liquid polymer depends on the substituents along the chain backbone, how the elasticity depends on crosslinking, and how the crystallinity depends on the stereoregularity of the polymer. In the preceding chapters we took the existence of these polymers for granted and focused attention on their bulk behavior. In the next three chapters these priorities are reversed: Our main concern is some of the reactions which produce polymers and the structures of the products formed.

In the next group of chapters we shall discuss condensation or step-growth polymers and polymerizations in Chap. 5, addition or chain-growth polymers and polymerizations in Chap. 6, and copolymers and stereoregular polymers in Chap. 7. It should not be inferred from this that these are the only classes of polymers and polymerization reactions. Topics such as ring-opening polymeri-

zation, anionic polymerization, cationic polymerization, and diene polymerization could all be added to the list above and expanded into full chapters. As it is, the first three are relegated to sections within other chapters; the last is neglected entirely. The emphasis given to various topics was decided on the basis of the concepts that their inclusion would illustrate. It does not mean that the topics we have shortchanged are unimportant.

The mechanism of the reactions we shall discuss provides the basis for their classification. Thus the step-growth mechanism applies when chains form one link at a time, while the chain-growth mechanism applies when an avalanche of links form in succession. Even though the mechanisms are quite different in this regard, there are certain common features to their analysis. For example, regardless of the mechanism under consideration, the size of the molecule doing the reacting can be neglected. In both mechanisms, assembling a giant molecule from low molecular weight repeat units is a random process: Statistics play an important role in describing both.

In contrast with the last three chapters, descriptive reaction chemistry plays a large part in the next three chapters. The "steps" in step-growth polymerization are esterification, amidation, and other such reactions; the "chains" in the chain-growth mechanism involve free radicals, ions, and coordinated species as active centers. Reactive functional groups are required for step growth, and reactive double bonds for the chain mechanism. It is not just the chemistry of the monomers that distinguishes between the different polymerizations. Catalysts are also required for virtually all polymerizations, and these determine the nature of the reaction intermediate and thus dictate the mechanism as well as influence the rate of the reaction. Depending on the nature of the catalyst used, polystyrene can be polymerized via free-radical, anion, cation, or coordination species as intermediates. As expected, there are differences in the rates of these various possible reactions. In addition, the products also differ in molecular weight, molecular weight distribution, and, perhaps, tacticity. Generally these latter properties are as important or more important than the rate itself.

Specifically chemical considerations are especially evident in Chap. 7, where copolymers and stereoregular polymers are discussed. Since two monomers are required for the formation of a copolymers, the differences in their reactivity affects both the composition of the product and the distribution of components in it. Likewise, the catalysts that produce stereoregularity are highly specific, highly reactive, and poorly understood chemical reagents.

Problems

1. Illers and Hendus† measured the melting points of polyethylene crystals whose thickness was varied by controlling the conditions of crystallization

† K. H. Illers and H. Hendus, *Makromol. Chem.* 113:1 (1968).

and which was measured by x-ray diffraction. The following results were obtained:

T_m (°C)	139.4	137.5	136.0	134.9	131.9	127.9	117.0
l (Å)	1750	758	481	392	258	177	100

Prepare a plot of T_m versus l^{-1}, and from the intercept and slope respectively, evaluate T_m^∞ and γ from these data. Compare the values obtained with quantities given in Table 4.1 and Example 4.2 (use the latter as a source for ΔH_V^∞).

2. From the data in Fig. 4.8b, estimate the shift factors required to displace the data at $\theta = 0.5$ (consider only this point) so that all runs superimpose on the experiment conducted at 128°C at $\theta = 0.5$. Either a ruler or proportional dividers can be used to measure displacements. Criticize or defend the following proposition: Whether a buffered aqueous solution of H_2O_2 and I^-, containing small amounts of $S_2O_3^{2-}$ and starch, appears blue or colorless depends on both the time and the temperature. This standard general chemistry experiment could be used to demonstrate the equivalency of time and temperature. The pertinent reactions for the "iodine clock" are

$$H_2O_2 + 2I^- + 2H^+ \xrightarrow{\text{slow}} I_2 + 2H_2O$$

$$I_2 + 2S_2O_3^{2-} \xrightarrow{\text{fast}} 2I^- + S_4O_6^{2-}$$

$$I_2 + \text{starch} \xrightarrow{\text{fast}} \text{blue complex}$$

3. The crystallization of poly(ethylene terephthalate) at different temperatures after prior fusion at 294°C has been observed† to follow the Avrami equation with the following parameters applying at the indicated temperatures:

T (°C)	m	K (min)
110	2	3.49×10^{-4}
180	3	1.35
240	4	5.05×10^{-8}

Calculate the time required for θ to reach values 0.1, 0.2, . . . , 0.9 for each of these situations. Graph θ versus t using the results calculated at 110 and 240°C, plotting both in the same figure. Because of the much larger K at 180°C, the crystallization occurs much faster at this temperature than at

†F. D. Hartley, F. W. Lord, and L. B. Morgan, *Philos. Trans. R. Soc. London* 247A:23 (1954).

either 110 or 240°C. Multiply each of the times calculated at 180°C by the arbitrary constant 60 and plot the data thus shifted on the same coordinates as the other curves. What generalization appears concerning the relative slopes at $\theta = 0.5$?

4. Poly(ethylene terephthalate) was crystallized at 110°C and the densities were measured† after the indicated time of crystallization:

t (min)	ρ (g cm^{-3})	t (min)	ρ (g cm^{-3})
0	1.3395	35	1.3578
5	1.3400	40	1.3608
10	1.3428	45	1.3625
15	1.3438	50	1.3655
20	1.3443	60	1.3675
25	1.3489	70	1.3685
30	1.3548	80	1.3693

Using density as the property measured to determine crystallinity, evaluate θ as a function of time for these data. By an appropriate graphical analysis, determine the Avrami exponent (in doing this, ignore values of $\theta < 0.15$, since errors get out of hand in this region). Calculate (rather than graphically evaluate) the value of K consistent with your analysis.

5. The crystallization rate of isotactic polypropylene (M_w = 181,000, T_m = 172°C) was studied under various patterns of temperature change. Solids were melted at T_f, held at T_f for 1 hr, and then crystallized at T_c. The following Avrami exponents were observed.‡

	Avrami exponent		
T_f (°C)	T_c = 150°C	T_c = 155°C	T_c = 160°C
190	–	3.1	3.5
210	2.9	3.3	4.1
220	3.1	3.8	–
230	3.1	4.0	–

On the basis of these observations, criticize or defend the following propositions:

(a) When both T_f and T_c are low, the Avrami exponents are consistent with three-dimensional growth on contact with sporadic nucleation.

† A. Keller, G. R. Lester, and L. B. Morgan, *Philos. Trans. R. Soc. London* 247A:1 (1954).
‡ P. Parrini and G. Corrieri, *Makromol. Chem.* 62:83 (1963).

(b) The change in m can be interpreted as arising from a change in either the growth geometry or nucleation situation. That is, the change in m for [T_f and T_c low] → [T_f and T_c high] could arise from either the change spherical → disk geometry or the change sporadic → simultaneous nucleation.

(c) The changes in m are consistent with the idea that under some conditions nuclei from the original solid survive the period in the melt and nucleate the recrystallization.

6. The polymers listed below are all known to form unit cells in which all of the angles are 90°. Use this fact plus the data† given to complete the following table:

Polymer	M_0	Unit cell dimensions (Å) a	b	c	Number of repeat units per cell	Density (g cm^{-3})
Polystyrene	104.1	—— =	——	6.63	18	1.126
Polyisobutene	56.1	6.94	11.96	——	16	0.937
Poly(vinyl chloride	62.5	10.11	5.27	5.12	4	——
Nylon 8	——	4.9	4.9	~22	2	1.038
Poly(methyl methacrylate)	100.1	21.08	12.17	10.55	——	1.23

7. Chemical evidence for chain folding in polyethylene crystals is obtained by etching polymer crystals with fuming nitric acid, which cleaves the chain at the fold surface. The resulting chain fragments are separated chromatographically and their molecular weights determined by osmometry. The folded chain is pictured as crossing through the crystal, emerging and folding back, then reentering and recrossing the crystal, and so on. According to this picture, the shortest chain showing up in the chromatograms should equal the crystal thickness in length. The second shortest chain exceeds twice this value by some amount which measures the length of the loop made by the chain outside the crystal. Molecular weights for the two shortest chains observed in an experiment‡ of this sort were 1260 and 2530. Since the cleaved chains end in nitro and carboxyl groups, 60 should be subtracted from each of these molecular weights to give the polyethylene chain weight. Calculate the degree of polymerization of each molecule and the chain length (use the length of the unit cell along the chain axis, 2.53 Å, as the distance per repeat unit). Compare the latter with the crystal thickness determined by x-ray diffraction, 105 Å. What does the ratio of chain lengths for the first and second peaks suggest about the tightness of folding?

† Data from Ref. 2.

‡ T. Williams, D. J. Blundell, A. Keller, and I. M. Ward, *J. Polym. Sci.* A-2,6:1613 (1968).

8. Hirai and Eyring† assembled the following data from diverse sources (scarcely any two pieces of data were measured in the same laboratory, much less on the same sample):

	V_{sp} ($cm^3\ g^{-1}$)	ΔC_p ($erg\ K^{-1}\ g^{-1}$)	$\Delta\alpha$ (K^{-1})	$\Delta\beta$ ($cm^2\ dyne^{-1}$)
Rubber	1.1	5×10^6	4.0×10^{-4}	1×10^{-11}
Polystyrene	1.0	7.7×10^6	1.75×10^{-4}	3×10^{-12}
Polyisobutylene	1.1	4.0×10^6	4.5×10^{-4}	3×10^{-11}

Use these data to evaluate T_g, assuming that the latter is a true second-order transition. Compare your results with the values in Table 4.4 and comment on the agreement or lack thereof.

9. The time-temperature superpositioning principle was applied ‡ to the maximum in dielectric loss factors measured on poly(vinyl acetate). Data collected at different temperatures were shifted to match at $T_g = 28°C$. The shift factors for the frequency (in hertz) at the maximum were found to obey the WLF equation in the following form: $\log \omega + 6.9 = [19.6(T - 28)]/[42 + (T - 28)]$. Estimate the fractional free volume at T_g and α for the free volume from these data. Recalling from Chap. 3 that the loss factor for the mechanical properties occurs at $\omega\tau = 1$, estimate the relaxation time for poly(vinyl acetate) at 40 and 28.5°C.
10. Construct a master curve at 135°C from the data in Fig. 4.17 and determine the values of $\log a_T$ at each temperature. A relatively easy way to do this (especially without digital data) is to trace or photocopy Fig. 4.17 onto a transparent film. Place this transparency over a piece of paper and transfer the segment corresponding to T_0 to this paper. This is the beginning of the master curve. Slide the overlay to the right (or left) to connect segments measured at temperatures directly above (or below) T_0 with the segment at T_0. Now transfer (slipping a piece of carbon paper under the transparency is convenient) these segments to the paper on which the master curve is to be built up. On each segment (including T_0) place a mark at a convenient vertical reference, say, $\log t = 0$. Continue extending the master curve by this procedure, being careful to maintain a constant base line with perpendicular verticals. A ruler can be used to measure the displacement of the $\log t = 0$ mark at each temperature from $\log t = 0$ at T_0. These distances can then be converted to $\log a_T$ values by calibration of the horizontal displacements with the original figure.
11. Suppose you wanted to estimate the viscosity of a polystyrene sample at 125°C using the Debye viscosity equation, but the only available value

† N. Hirai and H. Eyring, *J. Polym. Sci.* 37:51 (1959).

‡ S. Matsuoka, G. E. Johnson, H. E. Bair, and E. W. Angerson, *Polym. Prepr.* 22:280 (1981).

of ζ is at T_g + 100°C = 200°C (see Table 2.3). Comparing Eq. (4.71) with the Rouse theory [Eq. (3.90)] suggests that a_T and τ_p play comparable roles in each and that these two are proportional to each other: $a_T = Kn^2\zeta l_0^2/6\pi^2 p^2 kT$ [Eq. (3.99)], with K the proportionality constant. According to this idea, the temperature dependence of ζ can be estimated from a knowledge of the shift factors: $a_{T_1}/a_{T_2} = (\zeta_{T_1}/T_1)/(\zeta_{T_2}/T_2)$. This neglects any temperature dependence of l_0. Use the constants for polystyrene from Table 4.4 to calculate log a_T at 125 and 200°C. From these values and ζ_{200}, estimate ζ_{125}. Use the Debye viscosity equation to estimate η_{125} for polystyrene, for which n = 100 (i.e., no entanglements). If the actual viscosity were 2.54×10^4 kg m^{-1} sec^{-1}, how much of an error would this imply for ζ_{125}? (Use ρ = 1 g cm^{-3} and $l_0 = 7.4 \times 10^{-10}$ m throughout.)

12. Williams and Ferry† measured the dynamic compliance of poly(methyl acrylate) at a number of temperatures. Curves measured at various temperatures were shifted to construct a master curve at 25°C, and the following shift factors were obtained:

T (°C)	log a_T	T (°C)	log a_T
25.00	0	54.90	-3.88
29.75	-0.98	59.95	-4.26
34.85	-1.80	64.70	-4.58
39.70	-2.42	69.50	-4.88
44.90	-3.00	80.35	-5.42
49.95	-3.47	89.15	-5.72

Test whether these data obey the WLF equation; if so, evaluate the constands C_1 and C_2. Note that $T_0 \neq T_g = 3$°C in these data.

Bibliography

1. Aklonis, J. J., MacKnight, W. J., and Shen, M., *Introduction to Polymer Viscoelasticity*, Wiley-Interscience, New York, 1972.
2. Geil, P. H., *Polymer Single Crystals*, Interscience, New York, 1963.
3. Haward, R. N. (Ed.), *The Physics of Glassy Polymers*, Wiley, New York, 1973.
4. MaGill, J. H., *Treatise on Material Science and Technology*, Vol. 10, J. M. Schultz (Ed.), Academic, New York, 1977.
5. Mandelkern, L., *Crystallization of Polymers*, McGraw-Hill, New York, 1964.

† M. L. Williams and J. D. Ferry, *J. Colloid Sci.* 9:474 (1954).

SOME IMPORTANT CLASSES OF POLYMERS AND POLYMERIZATION REACTIONS

5

Condensation or Step-Growth Polymerization

I'd get the urge to go splurging on hose, nylons, a dozen of those!
Now, rich or poor, we're enduring instead woolens which itch!
Rayons that spread!
I'll be happy When The Nylons Bloom Again!

When The Nylons Bloom Again, words by
George Marion, Jr. music by Thomas "Fats" Waller

5.1 Introduction

In Sec. 1.4 we discussed the classification of polymers into the categories of addition or condensation. At that time we noted that these classifications could be based on the following:

1. The stoichiometry of the polymerization reaction (small molecule eliminated?).
2. The composition of the backbone of the polymer (atoms other than carbon present?).
3. The mechanism of the polymerization (stepwise or chain reaction?).

It is the third of these criteria that offers the most powerful insight into the nature of the polymerization process for this important class of materials. We shall frequently use the terms *step-growth* and *condensation polymers* as synonyms, although by the end of the chapter it will be apparent that step-growth polymerization encompasses a wider range of reactions and products than either criteria (1) or (2) above would indicate.

The chapter is organized in a spiral fashion. First, we examine how the degree of polymerization and its distribution vary with the progress of the polymerization reaction, with the latter defined both in terms of stoichiometry and time. In the first round, we consider these topics for simple reaction

mixtures, those in which the proportions of reactants agree exactly with the stoichiometry of the reactions. After this we consider two important classes of condensation or step-growth polymers: polyesters and polyamides. In the second round of the spiral we consider nonstoichiometric proportions of reactants and monomers which introduce branching and crosslinking into the products. We then discuss some formaldehyde-based polymers which serve as examples of cross-linked systems. We conclude the chapter with a description of some more-or-less exotic step-growth polymers and a digression into a third class of polymers: those based on ring-opening reactions.

5.2 Condensation Polymers: One Step at a Time

As the name implies, step-growth polymers are formed through a series of steps and high molecular weight materials result from a large number of steps. Although our interest is in high molecular weight, long-chain molecules, a crucial premise of this chapter is that these molecules can be effectively discussed in terms of the individual steps which lead to the formation of the polymer. Thus polyesters and polyamides (among many others) are substances which result from the occurrence of many steps in which ester or amide linkages between reactants are formed. Central to our discussion is the idea that these steps may be treated in essentially the same way, whether they occur between small molecules or polymeric species. We shall return to a discussion of the implications and justification of this assumption throughout this chapter.

To see why the assumption of equal reactivity is so important to step-growth polymers, recall from Table 1.2 the kind of chemical reactions which produce typical condensation polymers:

1. Polyesters. Successive reactions between diols and dicarboxylic acids:

$$n\text{HO–R–OH} + n\text{HOOC–R'–COOH} \rightarrow \left\{\text{O–R–O–}\overset{\overset{\text{O}}{\|}}{\text{C}}\text{–R'–}\overset{\overset{\text{O}}{\|}}{\text{C}}\right\}_n + 2n\text{H}_2\text{O} \tag{5.A}$$

2. Polyamides. Successive reactions between diamines and dicarboxylic acids:

$$n\text{H}_2\text{N–R–NH}_2 + n\text{HOOC–R'–COOH} \rightarrow \left\{\overset{\overset{\text{H}}{|}}{\text{N}}\text{–R–}\overset{\overset{\text{H}}{|}}{\text{N}}\text{–}\overset{\overset{\text{O}}{\|}}{\text{C}}\text{–R'–}\overset{\overset{\text{O}}{\|}}{\text{C}}\right\}_n + 2n\text{H}_2\text{O} \tag{5.B}$$

3. General. Successive reactions between difunctional monomer A–A and difunctional monomer B–B:

$$n\text{A–A} + n\text{B–B} \rightarrow \{\text{A–A–B–B}\}_n + \cdots \tag{5.C}$$

Since the two reacting functional groups can be located in the same reactant molecule, we add the following:

4. Poly(amino acids).

$$n\mathrm{H_2N{-}\underset{\displaystyle R}{\underset{|}{C}}{-}COOH} \rightarrow \left(\mathrm{N{-}\underset{\displaystyle R}{\underset{|}{C}}{-}C}\right)_n + n\mathrm{H_2O} \qquad (5.D)$$

5. General.

$$n\mathrm{A{-}B} \rightarrow \left(\mathrm{A{-}B}\right)_n + \cdots \qquad (5.E)$$

Of course, in reactions (5.A) and (5.B) the hydrocarbon sequences R and R′ can be the same or different, contain any number of carbon atoms, be linear or cyclic, and so on. Likewise, the general reactions (5.C) and (5.E) certainly involve hydrocarbon sequences between the reactive groups A and B. The notation involved in these latter reactions is particularly convenient, however, and we shall use it extensively in this chapter. It will become clear as we proceed that the stoichiometric proportions of reactive groups—A and B in the above notation—play an important role in determining the characteristics of the polymeric product. Accordingly, we shall confine our discussions for the present to reactions of the type given by (5.E), since equimolar proportions of A and B are assured by the structure of this monomer.

Table 5.1 presents a hypothetical picture of how reaction (5.E) might appear if we examined the distribution of product molecules in detail. Row 1 of Table 5.1 shows the initial pool of monomers, 10 molecules in this example. Row 2 shows a possible composition after a certain amount of reaction has occurred. We shall see in Sec. 5.4 that the particular condensations which

Table 5.1 Hypothetical Step-Growth Polymerization of 10 AB Molecules[a]

Line	Molecular species present
1	AB AB AB AB AB AB AB AB AB AB
2	AbaB AbaB AbaB AbaB AB AB
3	AbababaB AbaB AbabaB AB
4	AbababaB AbabababaB AB
5	AbababaB AbabababababaB
6	AbabababababababababaB

[a]A and B represent two different functional groups and ab is the product of their reaction with each other. Consult the text for a discussion of the line-by-line development of the reaction.

account for the difference between lines 1 and 2 are not highly probable. Our objective here is not to assess the probability of certain reactions—as a matter of fact, we would be at a loss to try this—but, rather, to consider some possibilities. Stoichiometrically, we can still account for the initial set of 10 A groups and 10 B groups; we indicate those that have reacted with each other as ab groups. The same conservation of atom groupings would be obtained if line 2 showed one trimer, two dimers, and three monomers instead of the four dimers and two monomers indicated. Other combinations could also be assembled. These possibilities indicate one of the questions that we shall answer in this chapter: How do the molecules distribute themselves among the different possible species as the reaction proceeds?

Line 3 of Table 5.1 shows the mixture after two more reaction steps have occurred. Again the components we have elected to show are an arbitrary possibility. Stoichiometric considerations rule out certain combinations and/or proportions of products, although these are less stringent for a more realistic picture involving a larger starting number of monomer molecules. For the monomer system we have chosen, the concentration of A and B groups in the initial monomer sample are equal to each other and equal to the concentration of monomer. In this case the assay of either A groups or B groups in the mixture may be used to monitor the progress of the reaction. Choosing the number of A groups for this purpose, we see that this quantity drops from 10 to 6 to 4, respectively, as we proceed through lines 1, 2, and 3 of Table 5.1. What we wish to point out here is the fact that the 10 initial monomers are now present in four molecules, so the number average degree of polymerization is only 2.5, even though only 40% of the initial reactive groups remain. Another question is thus raised: In general, how does the average molecular weight vary with the extent of the reaction?

The reaction mixture in line 4 of Table 5.1 is characterized by an average degree of polymerization of $10/3 = 3.3$, with only 30% of the functional groups remaining. This means that 70% of the possible reactions have already occurred, even though we are still dealing with a very low average degree of polymerization. Note that the average degree of polymerization would be the same if the 70% reaction of functional groups led to the mixture AbababababababaB and two AB's. This is because the initial 10 monomers are present in three molecules in both instances and is a consequence of the fact that we are using number averages to talk about these possibilities. The weight averages would be different in the two cases. This poses still another question: How does the molecular weight *distribution* vary with the extent of reaction?

By line 5, the reaction has reached 80% completion and the number average value of the degree of polymerization $\bar{n}_n$ is 5. Although we have considered this slowly evolving polymer in terms of the extent of reaction, another question starts to be worrisome: How long is this going to take?

Line 6 represents the end of the reaction as far as linear polymer is concerned. Of the 10 initial A groups, 1 is still unreacted, but this situation raises the possibility that the decamer shown in line 6—or for that matter, some other n-mer, including monomer—might form a ring compound, thereby eliminating functional groups without advancing the polymerization. Thus the question, What about rings?

It is an easy matter to generalize the procedure we have been following and express the number average degree of polymerization in terms of the extent of reaction, regardless of the initial sample size. We have been dividing the initial number of monomers present by the total number of molecules present after any extent of reaction. Each molecular species—whether monomer or polymer of any n—contains just one A group. The total number of monomer molecules is therefore equal to the initial (superscript 0) number of A groups ν_A^0; the total number of molecules at any extent of reaction (no superscript) is equal to the number of A groups ν_A present at that point. The number average degree of polymerization is therefore given by

$$\bar{n}_n = \frac{\nu_A^0}{\nu_A} \tag{5.1}$$

It is convenient to define the fraction of reacted functional groups in a reaction mixture by a parameter p, called the extent of reaction. Thus p is the fraction of A groups which have reacted at any stage of the process, and 1 - p is the fraction unreacted:

$$1 - p = \frac{\nu_A}{\nu_A^0} \tag{5.2}$$

or

$$p = 1 - \frac{\nu_A}{\nu_A^0} \tag{5.3}$$

Comparing Eqs. (5.1) and (5.2) enables us to write

$$\bar{n}_n = \frac{1}{1 - p} \tag{5.4}$$

This expression is consistent with the analysis of each of the lines in Table 5.1 as presented above and provides a general answer to one of the questions posed there. It is often a relatively easy matter to monitor the concentration of functional groups in a reaction mixture as we saw in discussing end group analysis as a method for molecular weight determination in Sec. 1.7. Equation (5.4) is

a quantitative summary of the end group method for determining n. Example 1.4 showed that the details of interpreting end group data depends on consideration of the specific polymer mixture. Accordingly, we reiterate that Eq. (5.4) assumes equal numbers of A and B groups, with none of either lost in nonpolymer reactions.

From line 6 in Table 5.1, we see that $\bar{n}_n = 10$ when $p = 0.9$. The fact that this is also the maximum value for n is an artifact of the example. In a larger sample of monomers higher average degrees of polymerization are attainable. Equation (5.4) enables us to calculate that $\bar{n}_n$ becomes 20, 100, and 200, respectively, for extents of reaction of 0.950, 0.990, and 0.995. These considerations point out why condensation polymers are often of relatively modest molecular weight: Achieving the extents of reaction required for very high molecular weights may be difficult to accomplish.

Each of the questions raised in the last few paragraphs will be answered during the course of this chapter, some for systems considerably more involved than the one considered here. Before proceeding further, we should question one premise which underlies the entire discussion of Table 5.1: How does the chemical reactivity of A and B groups depend on the degree of polymerization of the reaction mixture? In Table 5.1 successive entries were generated by simply linking together at random those species present in the preceding line. We have thus assumed that, as far as reactivity is concerned, an A reacts as an A and a B as a B, regardless of the size of the molecule to which the group is attached. If this is valid, it results in a tremendous simplification; otherwise we shall have to characterize reactivity as a function of molecular weight, degree of polymerization, extent of reaction, and so on.

One of the most sensitive tests of the dependence of chemical reactivity on the size of the reacting molecules is the comparison of the rates of reaction for compounds which are members of a homologous series with different chain lengths. Studies by Flory and others on the rates of esterification and saponification of esters were the first investigations conducted to clarify the dependence of reactivity on molecular size. The rate constants for these reactions are observed to converge quite rapidly to a constant value which is independent of molecular size, after an initial dependence on molecular size for small molecules. The effect is reminiscent of the discussion on the uniqueness of end groups in connection with Example 1.1. In the esterification of carboxylic acids, for example, the rate constants are different for acetic, propionic, and butyric acids, but constant for carboxylic acids with 4–18 carbon atoms. This observation on nonpolymeric compounds has been generalized to apply to polymerization reactions as well. The latter are subject to several complications which are not involved in the study of simple model compounds, but when these complications are properly considered, the independence of reactivity on molecular size has been repeatedly verified.

The foregoing conclusion does not mean that the rate of the reaction proceeds through Table 5.1 at a constant value. The rate of reaction depends on the concentrations of reactive groups, as well as on the reactivities of the latter. Accordingly, the rate of the reaction decreases as the extent of reaction progresses. When the rate law for the reaction is extracted from proper kinetic experiments, specific reactions are found to be characterized by fixed rate constants over a range of $\bar{n}_n$ values.

Among the complications that can interfere with this conclusion is the possibility that the polymer becomes insoluble beyond a critical molecular weight or that the low molecular weight by-product molecules accumulate as the viscosity of the mixture increases and thereby shift some equilibrium to favor reactants. Note that we do not express reservations about the effect of increasing viscosity on the mobility of the polymer molecules themselves. Apparently it is not the migration of the center of mass of the molecule as a whole that determines the reactivity but, rather, the mobility of the chain ends which carry the reactive groups.

Figure 5.1 suggests that reactive end groups may be brought into contact by rotation around perhaps only a few bonds, an effect which is independent of chain length. In Chap. 2 we discussed the motion of chain segments in terms of entrapment within cages of neighboring groups. This same effect will promote the reaction of A and B once they find themselves in the same cage, indicated by the broken line in Fig. 5.1. It may take some time for the two reactive groups to diffuse together, but it will also take a while for them to diffuse apart; this provides the opportunity to react. The rate at which independent A and B groups convert to ab linkages is thus seen to depend on the relative rates of three processes: the rate at which the groups diffuse together, the rate at which they diffuse apart, and the rate at which the trapped A and B species react to form ab.

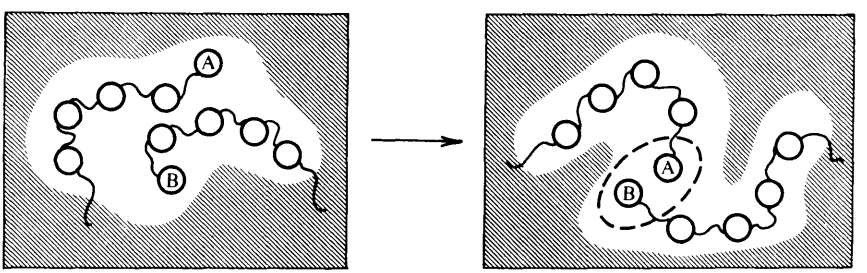

Figure 5.1 The reaction of A and B groups at the ends of two different chains. Note that rotations around only a few bonds will bring A and B into the same cage of neighboring groups, indicated by the broken line enclosure.

These considerations can be expressed quantitatively by writing the overall process in terms of the following mechanism

$$-A + -B \underset{k_o}{\overset{k_i}{\rightleftharpoons}} (-A + B-) \qquad (5.F)$$

$$(-A + B-) \xrightarrow{k_r} -ab-$$

where the parentheses represent the state in which the two reactive groups are trapped together in the same cage, as seen in Fig. 5.1, and the k's are rate constants which typify the individual steps: k_i and k_o measure the rates of group diffusion in and out of the cage, respectively, and k_r measures the rate of reaction.

Since this is the first occasion we have had to examine the rates at which chemical reactions occur, a few remarks about mechanistic steps and rate laws seem appropriate. The reader who feels the need for additional information on this topic should consult the discussions which will be found in any physical chemistry text.

As a brief review we recall the following:

1. The rate of a process is expressed by the derivative of a concentration (square brackets) with respect to time, d[ ]/dt. If the concentration of a reaction product is used, this quantity is positive; if a reactant is used, it is negative and a minus sign must be included. Also, each derivative d[ ]/dt should be divided by the coefficient of that component in the chemical equation which describes the reaction so that a single rate is described, whichever component in the reaction is used to monitor it.
2. A rate law describes the rate of a reaction as the product of a constant k, called the rate constant, and various concentrations, each raised to specific powers. The power of an individual concentration term in a rate law is called the order with respect to that component, and the sum of the exponents of all concentration terms gives the overall order of the reaction. Thus in the rate law Rate = $k[X]^1[Y]^2$, the reaction is first order in X, second order in Y, and third order overall.
3. A rate law is determined experimentally and the rate constant evaluated empirically. There is no necessary connection between the stoichiometry of a reaction and the form of the rate law.
4. A mechanism is a series of simple reaction steps which, when added together, account for the overall reaction. The rate law for the individual steps of the mechanism may be written by inspection of the mechanistic steps. The coefficients of the reactants in the chemical equation describing the step become the exponents of these concentrations in the rate law for

that step. The term *molecularity* is sometimes used instead of *order* to distinguish between the rates of mechanistic steps and experimental rate laws.

5. Frequently it is possible to write more than one mechanism which is compatible with an observed rate law. Thus ability to account for an experimental rate law is a necessary but not sufficient criterion for the correctness of the mechanism.

These ideas are readily applied to the mechanism described by reaction (5.F). To begin with, the rate at which ab links are formed is first order with respect to the concentration of entrapped pairs. In this sense the latter behaves as a reaction intermediate or transition state according to this mechanism. Therefore

$$\text{Rate of ab formation} = k_r[(-A + B-)] \tag{5.5}$$

These entrapped pairs, in turn, form at a rate given by the rate at which the two groups diffuse together minus the rate at which they either diffuse apart or are lost by reaction:

$$\frac{d[(-A + B-)]}{dt} = k_i[A][B] - k_o[(-A + B-)] - k_r[(-A + B-)] \tag{5.6}$$

The concentration of entrapped pairs is assumed to exist at some stationary-state (subscript s) level in which the rates of formation and loss are equal. In this stationary state $d[(-A + B-)]/dt = 0$ and Eq. (5.6) becomes

$$[(-A + B-)]_s = \frac{k_i}{k_o + k_r}[A][B] \tag{5.7}$$

where the subscript reminds us that this is the stationary-state value. Substituting Eq. (5.7) into Eq. (5.5) gives

$$\text{Rate of ab formation} = \frac{k_i k_r}{k_o + k_r}[A][B] \tag{5.8}$$

We shall have considerably more to say about this type of kinetic analysis when we discuss chain-growth polymerizations in Chap. 6.

According to the mechanism provided by reactions (5.F) and the analysis given by Eq. (5.8), the rate of polymerization is dependent upon the following:

1. The concentrations of both A and B, hence the reaction slows down as the conversion to polymer progresses, and . . . .
2. The three constants associated with the rates of the individual steps in reactions (5.F).

3. If the rate of chemical reaction is very slow compared to the rate of group diffusion ($k_r \ll k_i, k_o$), then Eq. (5.8) reduces to

$$\text{Rate of ab formation} = \frac{k_i}{k_o} k_r [A][B] \tag{5.9}$$

4. The two constants k_i and k_o describe exactly the same kind of diffusional processes and differ only in direction. Hence they have the same dependence on molecular size, whatever that might be, and that dependence therefore cancels out.
5. The reaction step in mechanism (5.F) is entirely comparable to the same reaction in low molecular weight systems. Such reactions involve considerably larger activation energies than physical processes like diffusion and, hence, do proceed slowly.
6. If $k_r \gg k_i, k_o$, then Eq. (5.8) reduces to

$$\text{Rate of ab formation} = k_i [A][B] \tag{5.10}$$

Note that the rate law in this case depends only on k_i and any size dependence for this constant would not cancel out.

Both Eqs. (5.9) and (5.10) predict rate laws which are first order with respect to the concentration of each of the reactive groups; the proportionality constant has a different significance in the two cases, however. The observed rate laws which suggest a reactivity that is independent of molecular size and the a priori expectation cited in item (5) regarding the magnitudes of different kinds of k values lend credibility to the version presented as Eq. (5.9).

Our objective in the preceding argument has been to justify the attitude that each ab linkage forms according to the same rate law, regardless of the extent of the reaction. While our attention is focused on the rate laws, we might as well consider the question, raised above, about the actual rates of these reactions. This is the topic of the next section.

5.3 Kinetics of Step-Growth Polymerization

In this section we turn to a consideration of the experimental side of condensation kinetics. The kind of ab links which have been most extensively studied are ester and amide groups, although numerous additional systems could also be cited. In many of these the carbonyl group is present and is believed to play an important role in stabilizing the actual chemical transition state involved in the reactions. The situation can be represented by the following schematic reaction:

$$R-\overset{\overset{O}{\|}}{C}-X + Y^- \longrightarrow \left[R-\overset{\overset{O}{|}}{\underset{\underset{X}{|}}{C}}-Y\right]^- \longrightarrow R-\overset{\overset{O}{\|}}{C}-Y + X^- \qquad (5.G)$$

in which the intermediate is stabilized by coordination with protons, metal ions, or other Lewis acids. The point of this is to emphasize that the kinds of reactions we are considering are often conducted in the presence of an acid catalyst, frequently something like a sulfonic acid or a metal oxide. The purpose of a catalyst is to modify the rates of a reaction, so we must be attentive to the situation with respect to catalysts. For the present we assume a constant concentration of catalyst and attach a subscript c to the rate constant to remind us of the assumption. Accordingly, we write

$$-\frac{d[A]}{dt} = k_c[A][B] \qquad (5.11)$$

which is consistent with both Eqs. (5.9) and (5.10). We expect the constant k_c to be dependent on the concentration of the catalyst in some way which means that Eq. (5.11) may be called a pseudo-second-order rate law. We shall presently consider these reactions in the absence of external catalysts. For now it is easier to proceed with the catalyzed case.

Equation (5.11) is the differential form of the rate law which describes the rate at which A groups are used up. To test a proposed rate law and to evaluate the rate constant it is preferable to work with the integrated form of the rate law. The integration of Eq. (5.11) yields different results, depending on whether the concentrations of A and B are the same or different:

1. We define [A] and [B] as the instantaneous concentrations of these groups at any time t during the reaction, and $[A]_0$ and $[B]_0$ as the concentrations of these groups at t = 0.
2. If $[A]_0 = [B]_0$, the integration of Eq. (5.11) yields

$$\frac{1}{[A]} - \frac{1}{[A]_0} = k_c t \qquad (5.12)$$

3. If $[A]_0 \neq [B]_0$, the integration yields

$$\frac{1}{[A]_0 - [B]_0} \ln\left(\frac{[A][B]_0}{[A]_0[B]}\right) = k_c t \qquad (5.13)$$

Both of these results are readily obtained; we examine the less obvious relationship in item (3) in the following example.

Example 5.1

By differentiation, verify that Eq. (5.13) is a solution to Eq. (5.11) for the conditions given.

Solution

Neither $[A]_0$ nor $[B]_0$ are functions of t, although both [A] and [B] are. We write the latter two as $[A] = [A]_0 - x$ and $[B] = [B]_0 - x$. Substitute these results into Eq. (5.13) and differentiate:

$$d\left[\ln\left(\frac{[A]_0 - x}{[B]_0 - x}\right)\right] + d\left[\ln\left(\frac{[B]_0}{[A]_0}\right)\right] = ([A]_0 - [B]_0)\,k_c\,dt$$

$$\left(\frac{[B]_0 - x}{[A]_0 - x}\right)\left(\frac{([B]_0 - x)(-1) - ([A]_0 - x)(-1)}{([B]_0 - x)^2}\right) dx = \frac{([A]_0 - [B]_0)\,dx}{([A]_0 - x)([B]_0 - x)}$$

$$= ([A]_0 - [B]_0)\,k_c\,dt$$

$$\frac{dx}{dt} = k_c([A]_0 - x)([B]_0 - x) = k_c[A][B]$$

Since $d[A]/dt = -dx/dt$ by the definition of x, this proves Eq. (5.13) to be a solution to Eq. (5.11). Equation (5.13) is undefined in the event $[A]_0 = [B]_0$, but in this case the expression is inapplicable anyhow. Since A and B react in a 1:1 proportion, their concentrations are identical at all stages of reaction if they are equal initially. In this case, Eq. (5.11) would reduce to a simple second-order rate law which integrates to Eq. (5.12).

•

We shall proceed on the assumption that $[A]_0$ and $[B]_0$ are equal. As noted above, the case of both reactive groups on the same molecule is a way of achieving this condition. Accordingly, we rearrange Eq. (5.12) to give the instantaneous concentration of unreacted A groups as a function of time:

$$[A] = \frac{[A]_0}{1 + k_c[A]_0 t} \tag{5.14}$$

At this point it is convenient to recall the extent of reaction parameter defined by Eq. (5.3). If we combine Eqs. (5.2) and (5.14), we obtain

$$1 - p = \frac{1}{1 + k_c[A]_0 t} \tag{5.15}$$

or

$$\frac{1}{1-p} = 1 + k_c [A]_0 t \tag{5.16}$$

Alternatively, we can incorporate Eq. (5.4) into the present discussion and write

$$\bar{n}_n = 1 + k_c [A]_0 t \tag{5.17}$$

These last expressions provide two very useful views of the progress of a condensation polymerization reaction with time. Equation (5.14) describes how the concentration of A groups asymptotically approaches zero at long times; Eq. (5.17) describes how the degree of polymerization increases linearly with time.

Equation (5.16) predicts a straight line when $1/(1 - p)$ is plotted against t. Figure 5.2 shows such a plot for adipic acid reacted with 1,10-decamethylene glycol and diethylene glycol. In both cases the esterifications were catalyzed by *p*-toluene sulfonic acid. Interpreting the slopes of these lines in terms of Eq. (5.16) and in the light of actual initial concentrations gives values of k_c equal to 0.013 and 0.097 kg eq^{-1} min^{-1}, respectively, for diethylene glycol at 109°C and decamethylene glycol at 161°C. Note that the units for these constants imply group concentrations expressed as equivalents per kilogram; mass rather than volume units are often used for concentration, since large volume changes may occur during polymerization.

Although the results presented in Fig. 5.2 appear to verify the predictions of Eq. (5.16), this verification is not free from controversy. This controversy arises because various workers in this field employ different criteria in evaluating the success of the relationships we have presented in fitting experimental polymerization data. One school of thought maintains that an adequate kinetic description of a process must apply to the data over a large part of the time of the experiment.

A second point of view maintains that a rate law correctly describes a process when it applies over a wide portion of the concentration change which occurs during a reaction. Each of these criteria seeks to maximize the region of fit, but the former emphasizes maximizing the range of t while the latter maximizes the range of p. Both standards tolerate deviations from their respective ideals at the beginning and/or the end of the experiment. Deviations at the beginning of a process are rationalized in terms of experimental uncertainties at the point of mixing or modelistic difficulties upon attainment of stationary-state conditions.

The existence of these two different standards for success would be of academic interest only if the analysis we have discussed applied to experimental

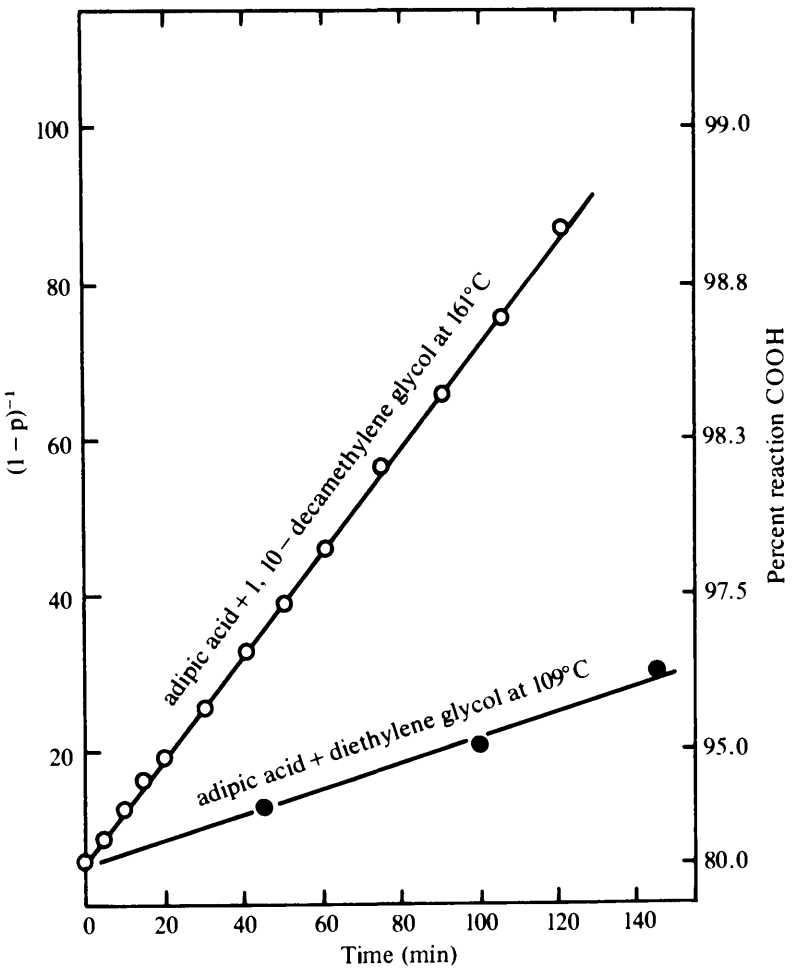

Figure 5.2 Plots of $(1 - p)^{-1}$ (left-hand ordinate) and p (right-hand ordinate) versus time for the catalyzed esterifications shown. [From Ref. 1, used with permission. Data cited from S. D. Hamann, D. H. Solomon, and J. D. Swift, *J. Macromol. Sci. Chem.* A2:153 (1968); P. J. Flory, *J. Am. Chem. Soc.* 61: 3334 (1939).]

results over most of the time range *and* over most extents of reaction as well. Unfortunately, this is not the case in all of the systems which have been investigated. Reference 5, for example, shows one particular set of data—adipic acid and diethylene glycol at 166°C, the same reactants at a different temperature as

the system in Fig. 5.2—analyzed according to two different rate laws. This system obeys one rate law between p = 0.50 and 0.85 that represents 15% of the duration of the experiment, and another rate law between p = 0.80 and 0.93 which spans 45% of the reaction time. These would be rated differently by the two different standards above. This sort of dilemma is not unique to the present problem, but arises in many situations where one variable undergoes a large percentage of its total change while the other variable undergoes only a small percent of its change. In the present context a way out of the dilemma is to accept the attitude that only the latter stages of the reaction are significant, since it is only beyond, say, p = 0.80 that it makes sense to consider the process as one of polymerization. According to this viewpoint, it is only at large extents of reaction that polymeric products are formed and, hence, the kinetics of *polymerization* should be based on a description of this part of the process. This viewpoint intentionally focuses attention on a relatively modest but definite range of p values. Since the reaction is necessarily slow as the number of unreacted functional groups decreases, this position tends to maximize the time over which the rate law fits the data.

Examination of the right-hand ordinate of Fig. 5.2 shows that the data presented there represent only about the last 20% of the range of p values. The zero of the time scale has thus been shifted to pick up the analysis of the reaction at this point.

We commented above that deviations at the beginning or the end of kinetics experiments can be rationalized, although the different schools of thought would disagree as to what constitutes "beginning" and "end." Now that we have settled upon the polymer range, let us consider specifically why deviations occur from a simple second-order kinetic analysis in the case of catalyzed polymerizations. At the beginning of the experiment, say, up to p = 0.5, the concentrations of A and B groups change dramatically, even though the number average degree of polymerization has only changed from monomer to dimer. By ordinary polymeric standards, we are still dealing with a low molecular weight system which might be regarded as the solvent medium for the formation of polymer. During this transformation, however, 50% of the very polar A groups and 50% of the very polar B groups have been converted to the less polar ab groups. Thus a significant change in the polarity of the polymerization medium occurs during, say, the first half of the change in p, even though an insignificant amount of true polymer has formed. In view of the role of ionic intermediates as suggested by reaction (5.G), the polarity of the reaction medium might very well influence the rate law during this stage of the reaction.

At the other end of the reaction, deviations from idealized rate laws are attributed to secondary reactions such as degradations of acids, alcohols, and amines through decarboxylation, dehydration, and deamination, respectively. The step-growth polymers which have been most widely studied are simple

condensation products such as polyesters and polyamides. Although we shall take up these classes of polymers specifically in Secs. 5.5 and 5.6, respectively, it is appropriate to mention here that these are typically equilibrium reactions as represented by the following equations:

$$-R_1-\overset{\overset{O}{\|}}{C}-OH + HO-R_2- \rightleftarrows -R_1-\overset{\overset{O}{\|}}{C}-O-R_2- + H_2O \tag{5.H}$$

and

$$-R_1-\overset{\overset{O}{\|}}{C}-OH + H_2N-R_2- \rightleftarrows -R_1-\overset{\overset{O\ H}{\|\ |}}{C}-N-R_2- + H_2O \tag{5.I}$$

In order to achieve large p's and high molecular weights, it is essential that these equilibria be shifted to the right by removing the by-product molecule, water in these reactions. This may be accomplished by heating, a partial vacuum, or purging with an inert gas, or some combination of the three. These treatments also open up the possibility of reactant loss due to volatility, which may accumulate to a significant source of error for reactions which are carried out to large values of p.

Until now we have been discussing the kinetics of catalyzed reactions. Losses due to volatility and side reactions also raise questions as to the validity of assuming a constant concentration of catalyst. Of course, one way of avoiding this issue is to omit an outside catalyst; reactions involving carboxylic acids can be catalyzed by these compounds themselves. Experiments conducted under these conditions are informative in their own right and not merely as means of eliminating errors in the catalyzed case. As noted in connection with the discussion of reaction (5.G), the intermediate is stabilized by coordination with a proton from the catalyst. In the case of autoprotolysis by the carboxylic acid reactant, the rate-determining step is probably the slow reaction of intermediate [I]:

$$\left[\begin{array}{c} H \\ O \\ | \\ R_1-C-OH \\ | \\ HO-R_2 \end{array}\right]^{\oplus} {}^{\ominus}OOC-R_1$$

[I]

Since this intermediate involves an additional equivalent of acid functional groups, the rate law for the disappearance of A groups becomes

$$-\frac{d[A]}{dt} = k_u [A]^2 [B] \tag{5.18}$$

on the assumption that A represents carboxyl groups. In this case k_u is the rate constant for the uncatalyzed reaction. This differential rate law is the equivalent of Eq. (5.11) for the catalyzed reaction. Equation (5.18) is readily integrated for the case where $[A]_0 = [B]_0$, in which case it becomes

$$-[A]^{-3}\, d[A] = k_u\, dt \tag{5.19}$$

This integrates to

$$\frac{1}{[A]^2} - \frac{1}{[A]_0^2} = 2k_u t \tag{5.20}$$

where $[A]_0$ is the concentration of A at $t = 0$. Thus for the uncatalyzed case we have the following:

1. The rate law is third order.
2. Since $A/A_0 = 1 - p$, Eq. (5.20) may be written as

$$\frac{1}{(1-p)^2} = 1 + 2k_u [A]_0^2 t \tag{5.21}$$

   which shows that a plot of $(1 - p)^{-2}$ increases linearly with t.
3. Since $A_0/A = \bar{n}_n$, Eq. (5.21) becomes

$$(\bar{n}_n)^2 = 1 + 2k_u [A]_0^2 t \tag{5.22}$$

   which shows that $\bar{n}_n$ increases more gradually with t than in the catalyzed case, all other things being equal.

Figure 5.3 shows the data for the uncatalyzed polymerization of adipic acid and 1,10-decamethylene glycol at 161°C plotted according to Eq. (5.21). The various provisos of the catalyzed case apply here also, so it continues to be appropriate to consider only the final stages of the conversion to polymer. From these results, k_u is about 4.3×10^{-3} kg^2 eq^{-2} min^{-1} at 161°C.

We conclude this section with a numerical example which serves to review and compare some of the important relationships we have considered.

Example 5.2

Assuming that $k_c = 10^{-1}$ kg eq^{-1} min^{-1}, $k_u = 10^{-3}$ kg^2 eq^{-2} min^{-1}, and $[A]_0 = 10$ eq kg^{-1}, calculate the times required for p to reach values 0.2, 0.4,

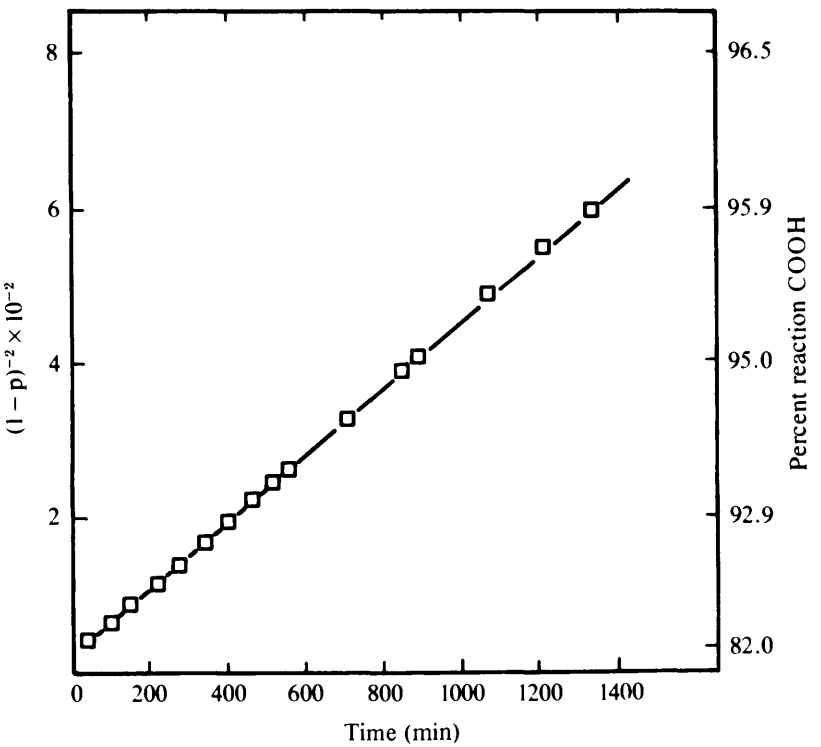

Figure 5.3 Plot of $(1 - p)^{-2}$ (left-hand ordinate) and p (right-hand ordinate) versus time for an uncatalyzed esterification. [From S. D. Hamann, D. H. Solomon, and J. D. Swift, *J. Macromol. Sci. Chem.* A2:153 (1968).]

0.6, and so on, for both catalyzed and uncatalyzed polymerizations, assuming that Eqs. (5.14) and (5.20), respectively, apply to the entire reaction. Compare the results obtained in terms of both the degree of polymerization and the fraction of unreacted A groups as a function of time.

Solution

Since we are asked to evaluate t, $\bar{n}_n$, and $[A]/[A]_0$ for specific values of p, it is convenient to summarize the following relationships:

1. Eq. (5.4): $\bar{n}_n = 1/(1 - p)$.
2. Eq. (5.2): $[A]/[A]_0 = 1 - p$.
3. Eq. (5.17): $t = (\bar{n}_n - 1)/k_c[A]_0 = \bar{n}_n - 1$ if catalyzed, since $10^{-1}(10) = 1$.

4. Eq. (5.22): $t = (\bar{n}_n^2 - 1)/2k_u[A]_0^2 = (\bar{n}_n^2 - 1)(5)$ if uncatalyzed, since $2(10^{-3})(10)^2 = 0.2$.

Using these relationships the following table is developed:

			Time (min)	
p	$[A]/[A]_0$	$\bar{n}_n$	Catalyzed	Uncatalyzed
0.2	0.8	1.25	0.25	2.8
0.4	0.6	1.67	0.67	8.9
0.6	0.4	2.50	1.5	26
0.8	0.2	5.00	4.0	120
0.9	0.1	10.0	9.0	500
0.95	0.05	20.0	19	2.0×10^3
0.99	0.01	100	99	5.0×10^4
0.992	0.008	120	119	7.2×10^4
0.998	0.002	500	499	1.3×10^6

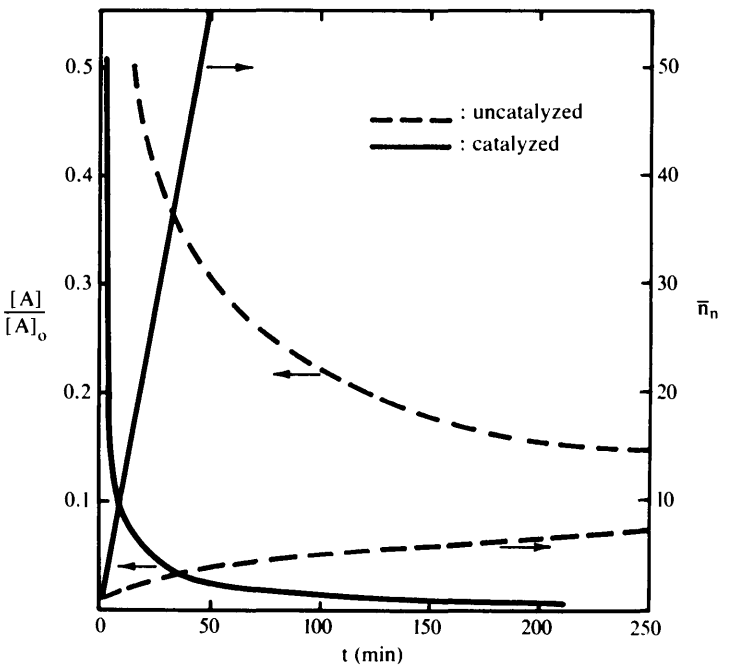

Figure 5.4 Comparison of catalyzed (solid lines) and uncatalyzed (broken lines) polymerizations using results calculated in Example 5.2. Here 1 - p (left-hand ordinate) and $\bar{n}_n$ (right-hand ordinate) are plotted versus time.

A graphical comparison of the trends appearing here is presented in Fig. 5.4. The importance of the catalyst is readily apparent in this hypothetical but not atypical system: To reach $\bar{n}_n = 5$ requires 4 min in the catalyzed case and 120 min without any catalyst, assuming that the same rate law describes the entire reaction in each case.

•

The question posed in Sec. 5.2—how long will it take to reach a certain extent of reaction or degree of polymerization?—is now answered. As is often the case, the answer begins, "It all depends . . . ."

5.4 Distributions of Molecular Sizes

In this section we turn our attention to two other questions raised in Sec. 5.2, namely, how do the molecules distribute themselves among the different possible species and how does this distribution vary with the extent of reaction? Since a range of species is present at each stage of the polymerization, it is apparent that a statistical answer is required for these questions. This time, our answer begins, "On the average . . . ."

We shall continue basing our discussion on the step-growth polymerization of the hypothetical monomer AB. In Sec. 5.7 we shall take a second look at this problem for the case of unequal concentrations of A and B groups. For now, however, we assure this equality by considering a monomer which contains one group of each type. In a previous discussion of the polymer formed from this monomer, we noted that remnants of the original functional groups are still recognizable, although modified, along the backbone of the polymer chain. This state of affairs is emphasized by the notation Ababab . . . abaB in which the a's and b's of the ab linkages are groups of atoms carried over from the initial A and B reactive groups. In this type of polymer molecule, then, there are n - 1 a's and 1 A if the degree of polymerization of the polymer is n. The a's differ from the A's precisely in that the former have undergone reaction while the latter have not. At any point during the polymerization reaction the fraction of the initial number of A groups which have reacted to become a's is given by p, and the fraction which remains as A's is given by 1 - p. In these expressions p is the same extent of reaction defined by Eq. (5.3).

With these ideas in mind, we now turn to the question of evaluating the fraction of n-mers in a mixture as a function of p. The fraction of molecules of a particular type in a population is just another way of describing the probability of such a molecule. Hence our restated objective is to find the probability of an n-mer in terms of p. We symbolize this quantity P(n, p). Since the n-mer consists of n - 1 a's and 1 A, its probability is the same as the probability of finding n - 1 a's and 1 A in the same molecule. Recalling from Chap. 1 how such probabilities are compounded, we write

$$P(n, p) = p_a^{n-1} p_A^{1} \tag{5.23}$$

where p_a and p_A are the probabilities of individual a and A groups, respectively. These probabilities, in turn, are given by their fractional abundance at any point in the reaction; that is, $p_a = p$ and $p_A = 1 - p$. Substituting these results into Eq. (5.23) gives

$$P(n, p) = p^{n-1}(1 - p) \tag{5.24}$$

The probability of an n-mer is converted to the number of n-mer molecules in the reaction mixture N_n by multiplying P(n, p) and the total number of molecules N (no subscript) in the mixture after the reaction has occurred to the extent p:

$$N_n = Np^{n-1}(1 - p) \tag{5.25}$$

Note that N_n/N gives the mole fraction of n-mers in a mixture at an extent of reaction p. As we have seen before, $N = (1 - p) A_0$, since each molecule in the mixture contains one unreacted A group. Incorporating this result into Eq. (5.25) yields

$$N_n = p^{n-1}(1 - p)^2 N_0 \tag{5.26}$$

where N_0 is the total number of monomers present initially; $N_0 = A_0$ for AB monomers. This result may be used to evaluate the number of molecules of whatever degree of polymerization we elect to consider in terms of p and N_0. As such, it provides the answer to one of the questions posed earlier.

Figure 5.5 is a plot of the ratio N_n/N versus n for several values of p. Several features are apparent from Fig. 5.5 concerning the number distribution of molecules among the various species present:

1. On a number basis, the fraction of molecules decreases with increasing n, regardless of the value of p. The distributions in Table 5.1 are unrealistic in this regard.
2. As p increases, the proportion of molecules with smaller n values decreases and the proportion with larger n values increases.
3. The combination of effects described in item (2) tends to flatten the curves as p increases, but not to the extent that the effect of item (1) disappears.

The number average degree of polymerization for these mixtures is easily obtained by recalling the definition of the average from Sec. 1.8. It is given by the sum of all possible n values, with each multiplied by its appropriate weighting factor, provided by Eq. (5.24):

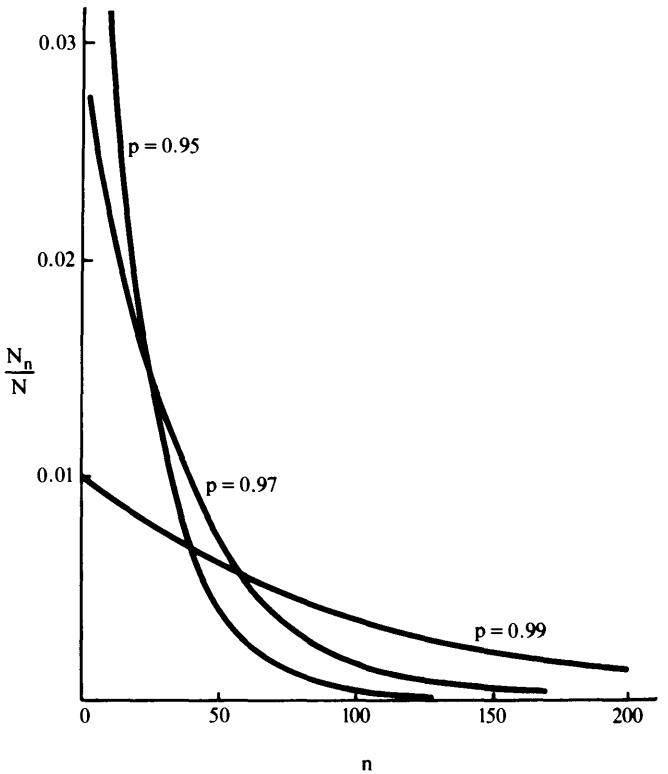

Figure 5.5 Number fraction n-mers as a function of n for several values of p.

$$\bar{n}_n = \sum_{n=1}^{N_0} nP(n, p) = \sum_{n=1}^{\infty} np^{n-1}(1 - p) \tag{5.27}$$

Note that the upper limit of the second summation has been shifted from N_0 to ∞ for mathematical reasons. The change is of little practical significance, since Eq. (5.24) drops off for very large values of n. To simplify the summation in Eq. (5.27) consider the following steps:

1. Write out a few terms of the summation so that it appears less abstract:

$$\bar{n}_n = 1p^0(1 - p) + 2p^1(1 - p) + 3p^2(1 - p) + \cdots$$

2. Factor the quantity 1 − p from each term:

$$= (1 - p)(1p^0 + 2p^1 + 3p^2 + \cdots)$$

3. The remaining series of terms is given by $(1 + p + p^2 + \cdots)^2$, as is easily verified by squaring the latter:

   $= (1 - p)(1 + p + p^2 + p^3 + \cdots)^2$

4. The series $1 + p + p^2 + \cdots$ is given by $1/(1 - p)$, as may be verified by long division:

   $= (1 - p)(1 - p)^{-2}$

Simplification of the summation in Eq. (5.27) thus yields

$$\bar{n}_n = \frac{1}{1 - p} \tag{5.28}$$

Of course, this is the same result that was obtained more simply in Eq. (5.4). The earlier result, however, was based on purely stoichiometric considerations and not on the detailed distribution as is the present result.

Next we turn our attention to the distribution of the molecules by weight among the various species. A corollary of this is the determination of the weight average molecular weight and the ratio $\bar{M}_w/\bar{M}_n$.

We begin by recognizing that the weight fraction w_n of n-mers in the polymer mixture at any value of p equals the ratio of the mass of n-mer in the mixture divided by the mass of the total mixture. The former is given by the product nN_nM_0, where M_0 is the molecular weight of the repeat unit; the latter is given by N_0M_0. Therefore we write

$$w_n = \frac{nN_n}{N_0} \tag{5.29}$$

into which Eq. (5.26) may be substituted to give

$$w_n = np^{n-1}(1 - p)^2 \tag{5.30}$$

The weight fraction of n-mers is plotted as a function of n in Fig. 5.6 for several large value of p. Inspection of Fig. 5.6 and comparison with Fig. 5.5 reveals the following:

1. At any p, very small and very large values of n contribute a lower weight fraction to the mixture than do intermediate values of n. This arises because of the product nN_n in Eq. (5.29): N_n is large for monomers, in which case n is low, and N_n decreases as n increases. At intermediate values of n, w_n goes through a maximum.

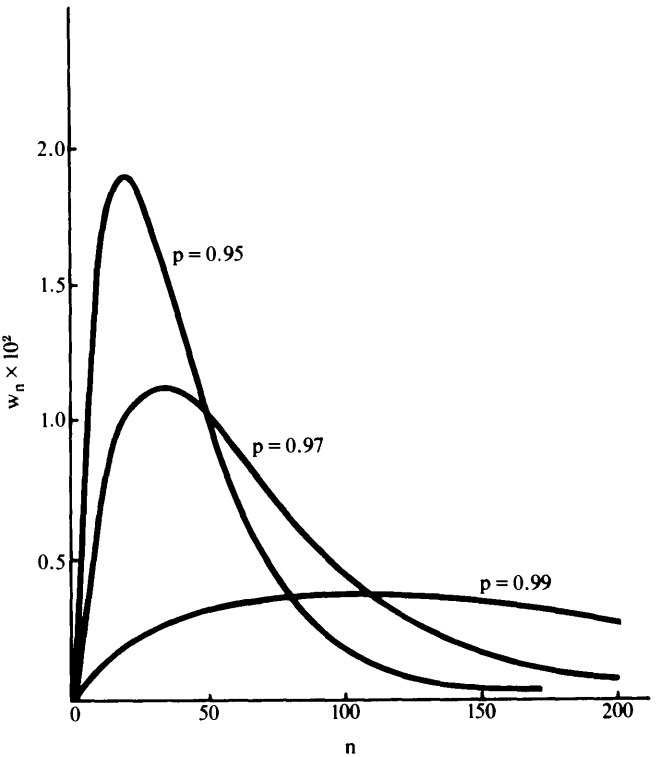

Figure 5.6 Weight fraction of n-mers as a function of n for several values of p.

2. As p increases, the maximum in the curves shifts to larger n values and the tail of the curve extends to higher values of n.
3. The effect in item (2) is not merely a matter of shifting curves toward higher n values as p increases, but reflects a distinct broadening of the distribution of n values as p increases.

The weight average degree of polymerization is obtained by averaging the contributions of various n values using weight fractions as weighting factors in the averaging procedure:

$$\bar{n}_w = \frac{\sum_{n=1}^{N_0} nw_n}{\sum_{n=1}^{N_0} w_n} = \frac{\sum_{n=1}^{\infty} n^2 p^{n-1}(1-p)^2}{\sum_{n=1}^{\infty} np^{n-1}(1-p)^2} \tag{5.31}$$

where the upper limit on n has been extended to infinity as before. Again we examine the simplification of the summations through the following steps:

1. Since each term in the numerator and the denominator contains the factor $(1 - p)^2$, this common factor cancels out:

$$\bar{n}_w = \frac{\sum_{n=1}^{\infty} n^2 p^{n-1}}{\sum_{n=1}^{\infty} np^{n-1}}$$

2. Write out a few terms of the remaining series:

$$= \frac{1 + 4p + 9p^2 + 16p^3 + \cdots}{1 + 2p + 3p^2 + 4p^3 + \cdots}$$

3. This ratio can be reduced by long division:

$$= 1 + 2p + 2p^2 + 2p^3 + \cdots = (2 + 2p + 2p^2 + \cdots) - 1$$

$$= 2(1 + p + p^2 + \cdots) - 1$$

4. As noted above, $1 + p + p^2 + \cdots = 1/(1 - p)$; hence

$$= \frac{2}{1 - p} - 1$$

Performing these manipulations on Eq. (5.31) shows that

$$\bar{n}_w = \frac{1 + p}{1 - p} \tag{5.32}$$

which is the desired result.

We saw in Chap. 1 that the ratio $\bar{M}_w/\bar{M}_n$ is widely used in polymer chemistry as a measure of the width of a molecular weight distribution. If the effect of chain ends is disregarded, this ratio is the same as the corresponding ratio of n values:

$$\frac{\bar{M}_w}{\bar{M}_n} = \frac{\bar{n}_w}{\bar{n}_n} = 1 + p \tag{5.33}$$

where the ratio of Eq. (5.32) to Eq. (5.4) has been used. Table 5.2 lists values of $\bar{n}_w$, $\bar{n}_n$, and $\bar{n}_w/\bar{n}_n$ for a range of high p values. Note that $\bar{n}_w/\bar{n}_n \to 2$ as $p \to 1$. In light of Eq. (1.18), the standard deviation of the molecular distribution is equal to $\bar{M}_n$ for the polymer sample produced by this polymerization. In a manner of speaking, the molecular weight distribution is as wide as the average is high! The broadening of the distribution with increasing p is dramatically

Table 5.2 Values of $\bar{n}_n$, $\bar{n}_w$, and $\bar{M}_w/\bar{M}_n$ for Various Large Values of p

p	$\bar{n}_n$	$\bar{n}_w$	$\bar{n}_w/\bar{n}_n$
0.90	10.0	19.0	1.90
0.92	12.5	24.0	1.92
0.94	16.7	32.3	1.94
0.96	25.0	49.0	1.96
0.98	50.0	99.0	1.98
0.990	100	199	1.990
0.992	125	249	1.992
0.994	167	332	1.994
0.996	250	499	1.996
0.998	500	999	1.998

shown by comparing the values in Table 5.2 with the situation at a low p value, say, p = 0.5. At p = 0.5, $\bar{n}_n = 2$, $\bar{n}_w = 3$, and $\bar{n}_w/\bar{n}_n = 1.5$.

Since Eqs. (5.15) and (5.21), respectively, give p as a function of time for the catalyzed and uncatalyzed polymerizations, the distributions discussed in the last few paragraphs can also be expressed with time as the independent variable instead of p.

The results we have obtained on the basis of the hypothetical monomer AB are also applicable to polymerizations between monomers of the AA and BB type, as long as the condition [A] = [B] is maintained. We shall extend the arguments of this section to conditions in which [A] $\neq$ [B] in Sec. 5.7 and to monomers of the type A$\perp$A in Sec. 5.8. In the meanwhile we interrupt this line of reasoning by considering a few actual condensation polymers as examples of step-growth systems. The actual systems we discuss will serve both to verify and reveal the limitations of the concepts we have been discussing. In addition, they point out some of the topics which still need clarification. We anticipate some of the latter points by noting the following:

1. When [A] $\neq$ [B], both ends of the growing chain tend to be terminated by the group which is present in excess. Subsequent reaction of such a molecule involves reaction with the limiting group. The effect is a decrease in the maximum attainable degree of polymerization.
2. When a monofunctional reactant is present—one containing a single A or B group—the effect is also clearly a decrease in the average degree of polymerization. It is precisely because this type of reactant can only react once that it is sometimes introduced into polymer formulations, thereby eliminating the possibility of long-term combination of chain ends.

3. When monomers of the type $A\perp^{A}A$ or even greater functionality are involved, the effect of their incorporation into the growing polymer chain is to introduce a branch point into the polymer.
4. In some cases of multifunctional monomers the possibility exists for branches on branches, which ultimately result in cross-linked products and effectively infinite molecular weights well before p reaches unity.

Polyesters and polyamides are two of the most studied step-growth polymers, as well as being substances of great commercial importance. We shall consider polyesters in the next section, and polyamides in Sec. 5.6.

5.5 Polyesters

The preceding discussions of the kinetics and molecular weight distributions in the step-growth polymerization of AB monomers are clearly exemplified by the esterification reactions of such monomers as glycolic acid or ω-hydroxydecanoic acid. Therefore one method for polyester synthesis is the following:

1. Esterification of a hydroxycarboxylic acid.

Several other chemical reactions are also widely used for the synthesis of these polymers. This list enumerates some of the possibilities and Table 5.3 illustrates these reactions by schematic chemical equations:

2. Esterification of a diacid and a diol.
3. Ester interchange with alcohol.
4. Ester interchange with ester.
5. Esterification of acid chlorides.
6. Lactone polymerization.

We have not attempted to indicate the conditions of temperature, catalyst, solvent, and so on, for these various reactions. For this type of information, references that deal specifically with synthetic polymer chemistry should be consulted. In the next few paragraphs we shall comment on the various routes to polyester formation in the order summarized above and followed in Table 5.3.

The studies summarized in Figs. 5.2 and 5.3 are examples of reaction 2 in Table 5.3. While bifunctional reactants are the sort we have emphasized until now, both monofunctional compounds and monomers with functionality greater than 2 are present in some polymerization processes, either intentionally or adventitiously. The effect of the monofunctional reactant is clearly to limit chain growth. As noted above, a functionality greater than 2 results in branching. A type of polyester that includes mono-, di-, and trifunctional monomers is the so-called alkyd resin. A typical example is based on the polymerization of phthalic acid (or anhydride), glycerol, and an unsaturated monocarboxylic acid. The following suggests the structure of a portion of such a polyester:

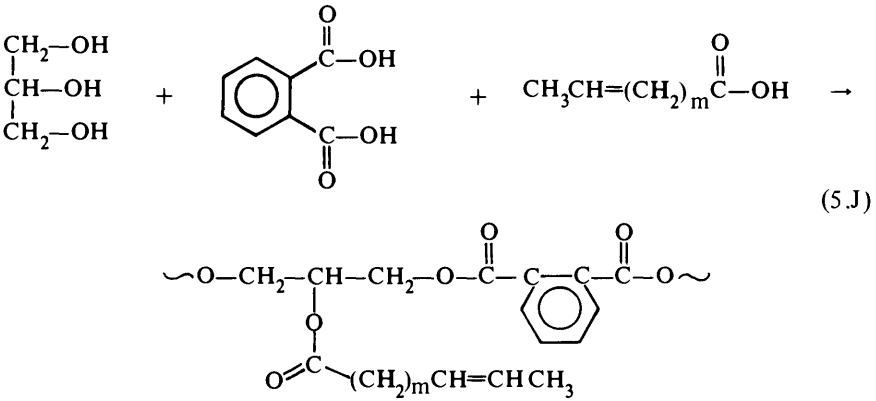

(5.J)

The presence of the unsaturated substituent along this polyester backbone gives this polymer crosslinking possibilities through a secondary reaction of the double bond. These polymers are used in paints, varnishes, and lacquers, where the ultimate cross-linked product results from the oxidation of the double bond as the coating cures. A cross-linked polyester could also result from reaction (5.J) without the unsaturated carboxylic acid, but the latter would produce a gel in which the entire reaction mass solidified and is not as well suited to coatings applications as the polymer that crosslinks upon "drying."

Many of the reactions listed at the beginning of this section are acid catalyzed, although a number of basic catalysts are also employed. Esterifications are equilibrium reactions, and the reactions are often carried out at elevated temperatures for favorable rate and equilibrium constants and to shift the equilibrium in favor of the polymer by volatilization of the by-product molecules. An undesired feature of higher polymerization temperatures is the increased probability of side reactions such as the dehydration of the diol or the pyrolysis of the ester. Basic catalysts produce less of the undesirable side reactions.

Ester interchange reactions are valuable, since, say, methyl esters of dicarboxylic acids are often more soluble and easier to purify than the diacid itself. The methanol by-product is easily removed by evaporation. Poly(ethylene terephthalate) is an example of a polymer prepared by double application of reaction 4 in Table 5.3. The first stage of the reaction is conducted at temperatures below 200°C and involves the interchange of dimethyl terephthalate with ethylene glycol

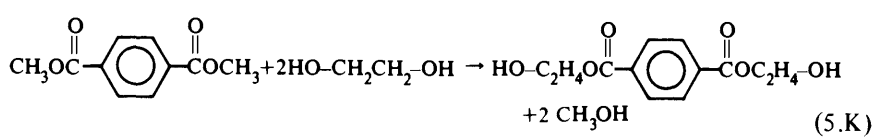

(5.K)

Table 5.3 Some Schematic Reactions for the Formation of Polyesters

1. Esterification of a hydroxycarboxylic acid:

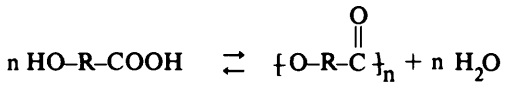

2. Esterification of diacid and diol:

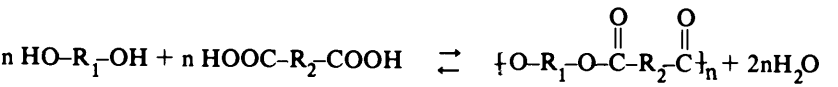

3. Ester interchange with alcohol:

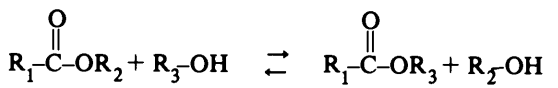

4. Ester interchange with ester:

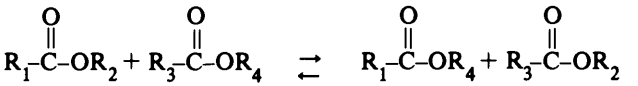

5. Esterification of acid chlorides (Schotten-Baumann reaction):

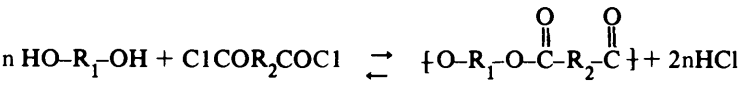

6. Lactone polymerization:

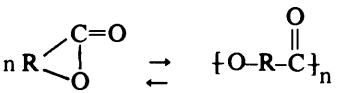

The rate of this reaction is increased by using excess ethylene glycol, and removal of the methanol is assured by the elevated temperature. Polymer is produced in the second stage after the temperature is raised above the melting point of the polymer, about 260°C.

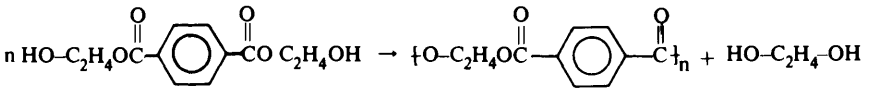

(5.L)

The ethylene glycol liberated by reaction (5.L) is removed by lowering the pressure or purging with an inert gas. Because the ethylene glycol produced by reaction (5.L) is removed, proper stoichiometry is assured by proceeding via the intermediate, bis(2-hydroxyethyl) terephthalate; otherwise the excess glycol used initially would have a deleterious effect on the degree of polymerization. Poly(ethylene terephthalate) is more familiar by some of its trade names: Mylar as a film and Dacron, Kodel, or Terylene as fibers; it is also known by the acronym PET.

Ester interchange reactions like that shown in reaction 4 in Table 5.3 can be carried out on polyesters themselves to produce a scrambling between the two polymers. Studies of this sort between high and low molecular weight prepolymers result in a single polymer with the same molecular weight distribution as would have been obtained from a similarly constituted diol-diacid mixture by direct polymerization. This is true when the time-catalyst conditions allow the randomization to reach equilibrium. If the two prepolymers are polyesters formed from different monomers, the product of the ester interchange reaction will be a copolymer of some sort. If the reaction conditions (time-catalyst) favor esterification, the two chains will merely link together and a block copolymer results. If the conditions favor the ester interchange reaction, then a scrambled copolymer molecule results. These possibilities underscore the idea that the derivations of the preceding sections are based on complete equilibrium among all molecular species present during the condensation reaction.

Example 5.3

It has been hypothesized that cross-linked polymers would have better mechanical properties if interchain bridges were located at the ends rather than the center of chains. To test this, low molecular weight polyesters were synthesized†

†A. Szayna, *Ind. Eng. Chem. Prod. Res. Dev.* 2:105 (1963).

from a diol and two different diacids: one saturated, the other unsaturated. The synthetic procedure was such that the unsaturated acid units were located at either the center (centrene) or the ends (endene) of the chains. Some pertinent aspects of the overall experiment are listed here:

		Endene	Centrene
Step 1:	8 hr at about 150–200°C		
	Maleic anhydride (mol)	0	2.0
	Succinic anhydride (mol)	2.0	0
	Diethylene glycol (mol)	3.0	3.0
Step 2:	About ½ hr at about 120–130°C		
	Maleic anhydride (mol)	2.0	0
	Succinic anhydride (mol)	0	2.0
	Catalyst	0	0
Step 3:	30% styrene + catalyst		
	16 hr at 55°C + 1 hr at 110°C		
	Elastic modulus	21,550	16,500

On the basis of these facts, do the following:

1. Comment on the likelihood that the comonomers are segregated as the names of these polymers suggest.
2. Sketch the structure of the average endene and centrene molecules, as well as the structure of one of the cross-linked products.
3. Comment on the results in terms of the initial hypothesis.

Solution

1. Since the reaction conditions are mild in step 2 (only 6% as much time allowed as in step 1 at a lower temperature) and no catalyst is present, it seems unlikely that any significant amount of ester scrambling occurs. Isomerization of maleate to fumarate is also known to be insignificant under these conditions.
2. The idealized structures of these molecules are

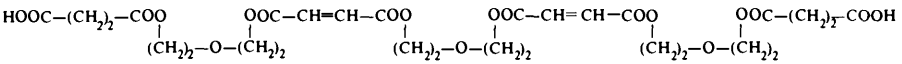

Centrene

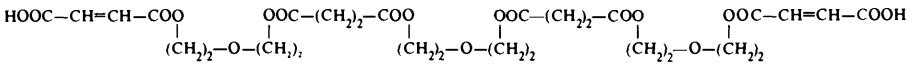

Endene

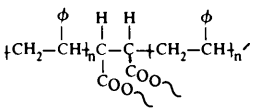

Cross-linked
Centrene

3. A cross-linked product with unsaturation at the chain ends does, indeed, have a higher modulus. This could be of commercial importance and indicates that industrial products might be formed by a nonequilibrium process precisely for this sort of reason.

•

Acid chlorides are generally more reactive than the parent acids, so polyester formation via reaction 5 in Table 5.3 can be carried out in solution and at lower temperatures, in contrast with the bulk reactions of the melt as described above. Again, the by-product molecules must be eliminated either by distillation or precipitation. The method of interfacial condensation, described in the next section, can be applied to this type of reaction.

The formation of polyesters from the polymerization of lactones (reaction 6 in Table 5.3) is a ring-opening reaction that may follow either a step-growth or chain mechanism, depending on conditions. For now our only concern is to note that the equilibrium representing this reaction in Table 5.3 describes polymerization by the forward reaction and ring formation by the back reaction. Rings clearly compete with polymers for monomer in all polymerizations. Throughout the chapter we have assumed that all competing side reactions including ring formation could be neglected. We shall examine the factors which influence the ring-polymer equilibrium in Sec. 5.10.

5.6 Polyamides

The discussion of polyamides parallels that of polyesters in many ways. To begin with, polyamides may be formed from an AB monomer, in this case amino acids:

1. Amidation of amino acids.

Additional synthetic routes which closely resemble the polyesters are also available. Several more of these are listed below and are illustrated by schematic reactions in Table 5.4:

2. Amidation of a diacid and a diamine.
3. Interchange reactions.
4. Amidation of acid chlorides.
5. Lactam polymerization.

We only need to recall the trade name of synthetic polyamides, nylon, to recognize the importance of these polymers and the reactions employed to prepare them. Remember from Sec. 1.5 the nylon system for naming these

Table 5.4 Some Schematic Reactions for the Formation of Polyamides

1. Amidation of amino acids:

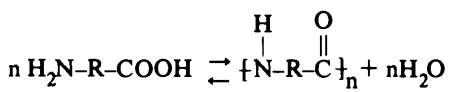

2. Amidation of diacid and diamine:

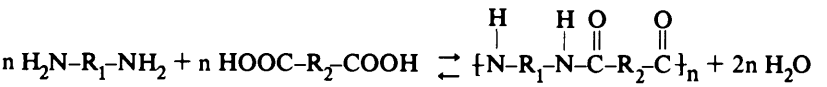

3. Interchange reactions:

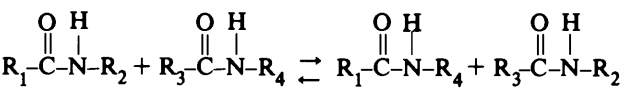

4. Amidation of acid chlorides:

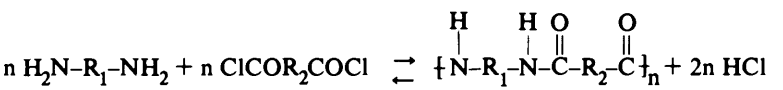

5. Lactam polymerization:

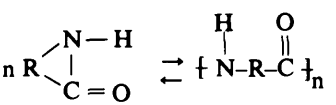

compounds: the first number after the name gives the number of carbon atoms in the diamine, and the second, the number of carbons in the diacid.

The diacid-diamine amidation described in reaction 2 in Table 5.4 has been widely studied in the melt, in solution, and in the solid state. When equal amounts of two functional groups are present, both the rate laws and the molecular weight distributions are given by the treatment of the preceding sections. The stoichiometric balance between reactive groups is readily obtained by precipitating the 1:1 ammonium salt from ethanol:

$$H_2N{-}R_1{-}NH_2 + HOOC{-}R_2{-}COOH \longrightarrow \begin{matrix} H_3N^{\oplus}{-}R_1{-}{}^{\oplus}NH_3 \\ {}^{\ominus}OOC{-}R_2{-}COO^{\ominus} \end{matrix} \qquad (5.M)$$

This compound is sometimes called a nylon salt. The salt $\rightleftarrows$ polymer equilibrium is more favorable to the production of polymer than in the case of polyesters, so this reaction is often carried out in a sealed tube or autoclave at about 200°C until a fairly high extent of reaction is reached; then the temperature is raised and the water driven off to attain the high molecular weight polymer.

The process represented by reaction 2 in Table 5.4 actually entails a number of additional equilibrium reactions. Some of the equilibria that have been considered include the following:

$$\sim NH_3^+ + {}^-OOC\sim \rightleftarrows \sim CONH_2\sim + H_2O \qquad (5.N)$$

$$\sim COOH + H_2O \rightleftarrows \sim COO^- + H_3O^+ \qquad (5.O)$$

$$\sim NH_2 + H_2O \rightleftarrows \sim NH_3^+ + OH^- \qquad (5.P)$$

$$2H_2O \rightleftarrows H_3O^+ + OH^- \qquad (5.Q)$$

$$\sim COOH + H^+ \rightleftarrows \sim C(OH)_2^+ \qquad (5.R)$$

$$\sim C(OH)_2^+ + H_2N\sim \rightleftarrows \sim CONH\sim + H^+ + H_2O \qquad (5.S)$$

Reaction (5.N) describes the nylon salt $\rightleftarrows$ nylon equilibrium. Reactions (5.O) and (5.P) show proton transfer with water between carboxyl and amine groups. Since proton transfer equilibria are involved, the self-ionization of water, reaction (5.Q), must also be included. Especially in the presence of acidic catalysts, reactions (5.R) and (5.S) are the equilibria of the acid-catalyzed intermediate described in general in reaction (5.G). The main point in including all of these equilibria is to indicate that the precise concentration of A and B

groups in a diacid–diamine reaction mixture is a complicated function of the moisture content and the pH, as well as the initial amounts of reactants introduced. Because of the high affinity for water of the various functional groups present, the complete removal of water is impossible: The equilibrium moisture content of molten nylon-6,6 at 290°C under steam at 1 atm is 0.15%. Likewise, the various ionic possibilities mean that at both high and low pH values the concentration of un-ionized carboxyl or amine groups may be considerably different from the total concentration—without regard to state of ionization—of these groups. As usual, upsetting the stoichiometric balance of the reactive groups has a lowering effect on the degree of polymerization attainable. The abundance of high-quality nylon products is evidence that these complications have been overcome in practice.

Amide interchange reactions of the type represented by reaction 3 in Table 5.4 are known to occur more slowly than direct amidation; nevertheless, reactions between high and low molecular weight polyamides result in a polymer of intermediate molecular weight. The polymer is initially a block copolymer of the two starting materials, but randomization is eventually produced.

As with polyesters, the amidation reaction of acid chlorides may be carried out in solution because of the enhanced reactivity of acid chlorides compared with carboxylic acids. A technique known as interfacial polymerization has been employed for the formation of polyamides and other step-growth polymers, including polyesters, polyurethanes, and polycarbonates. In this method the polymerization is carried out at the interface between two immiscible solutions, one of which contains one of the dissolved reactants, while the second monomer is dissolved in the other. Figure 5.7 shows a polyamide film forming at the interface between an aqueous solution of a diamine layered on a solution of a diacid chloride in an organic solvent. In this form interfacial polymerization is part of the standard repertoire of chemical demonstrations. It is sometimes called the nylon rope trick because of the filament of nylon produced by withdrawing the collapsed film.

The amidation of the reactive groups in interfacial polymerization is governed by the rates at which these groups can diffuse to the interface where the growing polymer is deposited. Accordingly, new reactants add to existing chains rather than interacting to form new chains. This is different than the bulk mechanism we have discussed elsewhere in this chapter, and it is evident that a higher molecular weight polymer results from this difference.

The HCl by-product of the amidation reaction is neutralized by also dissolving an inorganic base in the aqueous layer in interfacial polymerization. The choice of the organic solvent plays a role in determining the properties of the polymer produced, probably because of differences in solvent goodness for the resulting polymer. Since this reaction is carried out at low temperatures, the complications associated with side reactions can be kept to a minimum.

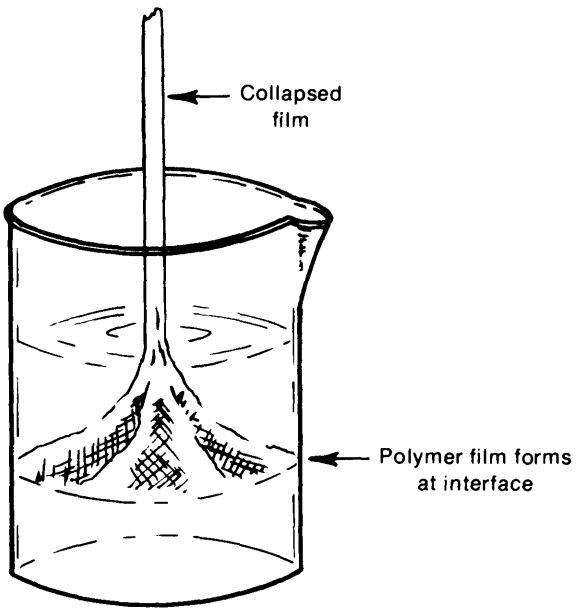

Figure 5.7 Sketch of an interfacial polymerization with the collapsed polymer film being withdrawn from the surface between the immiscible phases. [Redrawn with permission from P. W. Morgan and S. L. Kwolek, *J. Chem. Educ.* 36:182 (1959); copyright by the American Chemical Society.]

Polymer yield may be increased by increasing the area of the interface between the two solutions by stirring.

Lactam polymerization represented by reaction 5 in Table 5.4 is another example of a ring-opening reaction, the reverse of which is a possible competitor with polymer for reactants. We shall discuss this situation in Sec. 5.10.

The various mechanical properties of polyamides may be traced in many instances to the possibility of intermolecular hydrogen bonding between the polymer molecules and to the relatively stiff chains these substances possess. The latter, in turn, may be understood by considering still another equilibrium, this one among resonance structures along the chain backbone:

$$\sim C(=O)-N(H)\sim \rightleftarrows \sim C(-O^{\ominus})=N^{\oplus}(H)\sim \qquad (5.T)$$

The combination of strong intermolecular forces and high chain stiffness accounts for the high melting points of polyamides through application of Eq. (4.5).

The remarks of this and the last section are only a small fraction of what might be said about these important materials. We have commented on some aspects of the polymerization processes and of the polymers themselves that have a direct bearing on the concepts discussed here and elsewhere in this volume. This material provides an excellent example of the symbiosis between theoretical and application-oriented points of view. Each stimulates and reinforces the other with new challenges, although it must be conceded that many industrial processes reach a fairly high degree of empirical refinement before the conceptual basis is quantitatively developed.

5.7 Stoichiometric Imbalance

We now turn to two of the problems we have sidestepped until now. In this section we consider the polymerization of reactants in which a stoichiometric imbalance exists in the numbers of reactive groups A and B. In the next section we shall consider the effect of monomers with a functionality greater than 2.

In prior sections dealing with the quantitative aspects of step-growth polymerization, we focused attention on monomers of the AB type to assure equality of reactive groups. The results obtained above also apply to AA and BB polymerizations, provided that the numbers of reactive groups are equal. There are obvious practical difficulties associated with the requirement of stoichiometric balance. Rigorous purification of monomers is difficult and adds to the cost of the final product. The effective loss of functional groups to side reactions imposes restrictions on the range of experimental conditions at best and is unavoidable at worst. These latter considerations apply even in the case of the AB monomer. We have already stated that the effect of the imbalance of A and B groups is to lower the eventual degree of polymerization of the product. A quantitative assessment of this limitation is what we now seek.

We define the problem by assuming the polymerization involves AA and BB monomers and that the B groups are present in excess. We define ν_A and ν_B to be the numbers of A and B functional groups, respectively. The number of either of these quantities in the initial reaction mixture is indicated by a superscript 0; the numbers at various stages of reaction have no superscript. The stoichiometric imbalance is defined by the ratio r, where

$$r = \frac{\nu_A{}^0}{\nu_B{}^0} \tag{5.34}$$

This ratio cannot exceed unity by definition of the problem.

As with other problems with stoichiometry, it is the less abundant reactant that limits the product. Accordingly, we define the extent of reaction p to be the fraction of A groups that have reacted at any point. Since A and B groups

react in a 1:1 proportion, the number of B groups that have reacted when the extent of reaction has reached p equals $p\nu_A^0$, which, in turn, equals $pr\nu_B^0$. The product pr gives the fraction of B groups that have reacted at any point. With these definitions in mind, the following relationships are readily seen:

1. The number of unreacted functional groups after the reaction reaches extent p is

$$\nu_A = (1 - p)\nu_A^0 \tag{5.35}$$

and

$$\nu_B = (1 - pr)\nu_B^0 = (1 - pr)\frac{\nu_A^0}{r} \tag{5.36}$$

2. The total number of chain ends is the sum of Eqs. (5.35) and (5.36):

$$\nu_{ends} = \left(1 - p + \frac{1 - pr}{r}\right)\nu_A^0 \tag{5.37}$$

3. The total number of chains is half the number of chain ends:

$$N_{chains} = \frac{1}{2}\left(1 + \frac{1}{r} - 2p\right)\nu_A^0 \tag{5.38}$$

4. The total number of repeat units distributed among these chains is the number of monomer molecules present initially:

$$N_{repeat\ units} = \frac{1}{2}\nu_A^0 + \frac{1}{2}\nu_B^0 = \frac{1}{2}\left(1 + \frac{1}{r}\right)\nu_A^0 \tag{5.39}$$

The number average degree of polymerization is given by dividing the number of repeat units by the number of chains, or

$$\bar{n}_n = \frac{1 + 1/r}{1 + 1/r - 2p} = \frac{1 + r}{1 + r - 2pr} \tag{5.40}$$

As a check that we have done this correctly, note that Eq. (5.40) reduces to the previously established Eq. (5.28) when r = 1.00.

One distinction that should be pointed out involves the comparison of Eqs. (5.1) and (5.40). In the former we considered explicitly the AB monomer, while the latter is based on the polymerization of AA and BB monomers. In both instances $\bar{n}_n$ is obtained by dividing the total number of monomer molecules initially present by the total number of chains after the reaction has occurred to extent p. Following the same procedure for different reaction

mixtures results in a different definition of the repeat unit. In the case of the AB monomer, the repeat unit is the ab entity, which differs from AB by the elimination of the by-product molecule. In the case of the AA and BB monomers, the repeat unit in the polymer is the aabb unit, which differs from AA + BB by two by-product molecules. Equation (5.1) counts the number of ab units in the polymer directly. Equation (5.40) counts the number of aa plus bb units. The number of aa plus bb units is twice the number of aabb units. Rather than attempting to formalize this distinction by introducing more complex notation, we simply point out that application of the formulas of this chapter to specific systems must be accompanied by a reflection on the precise meaning of the calculated quantity for the system under consideration. There is nothing particularly unique about this admonition: No equation should be used mindlessly by just plugging in numbers and submitting an answer.

The distinction pointed out in the last paragraph carries over to the evaluation of $\bar{M}_n$ from $\bar{n}_n$. We assume that the chain length of the polymer is great enough to make unnecessary any correction for the uniqueness of chain ends. In such a case the molecular weight of the polymer is obtained from the degree of polymerization by multiplying the latter by the molecular weight of the repeat unit. The following examples illustrate the distinction under consideration:

1. Polymerization of an AB monomer is illustrated by the polyester formed from glycolic acid. The repeat unit in this polymer has the structure $(-O-CH_2-\overset{\overset{O}{\|}}{C}-)$ and $M_0 = 58$. Neglecting end groups, we have $\bar{M}_n = 58\,\bar{n}_n$, with $\bar{n}_n$ given by Eq. (5.1).
2. Polymerization of AA and BB monomers is illustrated by butane-1,4-diol and adipic acid. The aabb repeat unit in the polymer has an M_0 value of 200. If Eq. (5.4) is used to evaluate $\bar{n}_n$, it gives the number of aa plus bb units; therefore $\bar{M}_n = 200(\bar{n}_n)/2$.
3. An equivalent way of looking at the conclusion of item (2) is to recall that Eq. (5.40) gives the (number average) number of monomers of both kinds in the polymer and multiply this quantity by the average molecular weight of the two kinds of units in the structure: (88 + 112)/2 = 100.

Equation (5.40) also applies to the case when some of the excess B groups present are in the form of monofunctional reagents. In this latter situation the definition of r is modified somewhat (and labeled with a prime) to allow for the fact that some of the B groups are in the BB-type monomers (unprimed) and some are in the monofunctional (primed) molecules:

$$r' = \frac{\nu_A}{\nu_B + 2\nu_B'} \tag{5.41}$$

The parameter r′ continues to measure the ratio of the number of A and B groups; the factor 2 enters since the monofunctional reagent has the same effect on the degree of polymerization as a difunctional molecule with two B groups and, hence, is doubly effective compared to the latter. With this modification taken into account, Eq. (5.40) enables us to quantitatively evaluate the effect of stoichiometric imbalance or monofunctional reagents, whether these are intentionally introduced to regulate $\bar{n}_n$ or whether they arise from impurities or side reactions.

The parameter r varies between 0 and 1; as such it has the same range as p. Although the quantitative effect of r and p on n is different, the qualitative effect is similar for each: Higher degrees of polymerization are obtained the closer each of these fractions is to unity. Table 5.5 shows some values of n calculated from Eq. (5.40) for several combinations of (large values of) r and p. Inspection of Table 5.5 reveals the following:

1. For any value of r, n is greater for larger values of p; this conclusion is the same whether the proportions of A and B are balanced or not.
2. The final 0.05 increase in p has a bigger effect on n at r values that are closer to unity than for less-balanced mixtures.
3. For any value of p, n is greater for larger values of r; stoichiometric imbalance lowers the average chain length of the preparation.
4. A 0.05 increase in r produces a much bigger increase in n at p = 1.00 than in mixtures that have reacted to a lesser extent.

An interesting special case of Eq. (5.40) occurs when p = 1.00. In this case Eq. (5.40) becomes

$$\bar{n}_n = \frac{1 + r}{1 - r} \tag{5.42}$$

The following example illustrates some of the concepts developed in this section.

Table 5.5 Some Values of n Calculated by Eq. (5.40) for Several Values of r and p Close to Unity

	p			
r	0.95	0.97	0.99	1.00
0.95	13.5	18.2	28.3	39.0
0.97	15.5	22.3	39.9	65.7
0.99	18.3	28.7	66.8	199
1.00	20.0	33.3	100	∞

Example 5.4

It is desired to prepare a polyester with $\bar{M}_n = 5000$ by reacting 1 mol of butane-1,4-diol with 1 mol of adipic acid.

1. Calculate the value of p at which the reaction should be stopped to obtain this polymer, assuming perfect stoichiometric balance and neglecting end group effects on $\bar{M}_n$.
2. Assuming that 0.5 mol % of the diol is lost to polymerization by dehydration to olefin, what would be the value of $\bar{M}_n$ if the reaction were carried out to the same extent as in (1)?
3. How could the loss in (2) be offset so that the desired polymer is still obtained?
4. Suppose the total number of carboxyl groups in the original mixture is 2 mol, of which 1.0% is present as acetic acid to render the resulting polymer inert to subsequent esterification. What value of p would be required to produce the desired polymer in this case, assuming no other stoichiometric imbalance?

Solution

The various expressions we have developed in this section relating p to the size of the polymer are all based on $\bar{n}_n$. Accordingly, we note that the average reactant molecule in this mixture has a molecular weight of 100 as calculated above. Therefore the desired polymer has a value of $\bar{n}_n = 50$ based on this concept.

1. We use Eq. (5.28) for the case of equal numbers of A and B groups and find that $p = 1 - 1/n = 0.980$. Even though Eq. (5.28) is derived for an AB monomer, it applies to this case with the "average monomer" as the repeat unit.
2. Component AA is the diol in this case and $\nu_A = 0.995$ mol; therefore $r = 0.995/1.00 = 0.995$. We use Eq. (5.40) and solve for $\bar{n}_n$ with $p = 0.980$ and $r = 0.995$:

$$\bar{n}_n = \frac{1.995}{1.995 - 2(0.995)(0.980)} = 44.5$$

and $\bar{M}_n = 44.5(100) = 4450$ g mol^{-1}

3. The effect of the lost hydroxyl groups can be offset by carrying out the polymerization to a higher extent of reaction. We use Eq. (5.40) and solve for p with $\bar{n}_n = 50$ and $r = 0.995$:

$$p = \left(1 - \frac{1}{n}\right)\left(\frac{1 + r}{2r}\right) = \left(1 - \frac{1}{50}\right)\frac{1.995}{1.990} = 0.9825$$

4. The monofunctional reagent B′ is the acetic acid in this case and the number of monofunctional carboxyl groups is $2(0.010) = 0.020 = \nu_{B'}$. The number of B groups in BB monomers is $1.980 = \nu_B$. We use Eq. (5.41) to define r′ for this situation, assuming the number of hydroxyl groups equals 2.00 mol:

$$r' = \frac{2.00}{1.980 + 2(0.020)} = 0.990$$

Equation (5.40) is now solved for p using n = 50 and r′ = 0.990:

$$p = \left(1 - \frac{1}{n}\right)\left(\frac{1 + r'}{2r'}\right) = \left(1 - \frac{1}{50}\right)\frac{1.990}{1.980} = 0.9849$$

It will be remembered from Sec. 5.3 that a progressively longer period of time is required to shift the reaction to larger values of p. In practice, therefore, the effects of side reactions and monofunctional reactants are often not compensated by longer polymerization times, but are accepted in the form of lower molecular weight polymers.

Next let us examine the effect of monomers with functionality greater than 2 on step-growth polymers.

5.8 Branching and Crosslinking

We noted above that the presence of monomer with a functionality greater than 2 results in branched polymer chains. This in turn produces a three-dimensional network of polymer under certain circumstances. The solubility and mechanical behavior of such materials depend critically on whether the extent of polymerization is above or below the threshold for the formation of this network. The threshold is described as the gel point, since the reaction mixture sets up or gels at this point. We have previously introduced the term *thermosetting* to describe these cross-linked polymeric materials. Because their mechanical properties are largely unaffected by temperature variations—in contrast to thermoplastic materials which become more fluid on heating—step-growth polymers that exceed the gel point are widely used as engineering materials.

For simplicity, we assume that the reaction mixture still contains only A and B as reactive groups, but that either one (or both) of these is present (totally or in part) in a molecule that contains more than two of the reactive groups. We use f to represent the number of reactive groups in a molecule when this quantity exceeds 2, and represent a multifunctional molecule A_f or B_f. For example, the monomer $A\overset{A}{\perp}A$ corresponds to f = 3. Several reaction possibilities (all written for f = 3) come to mind in the presence of multifunctional reactants:

1. AA and BB plus either A_f or B_f:

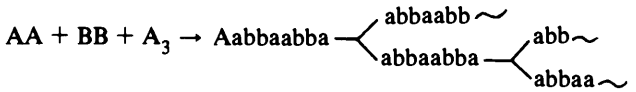

(5.U)

2. AA and B_f or BB and A_f:

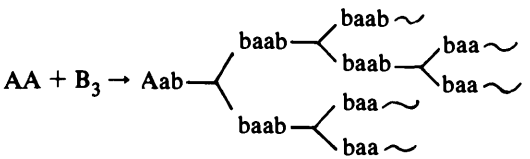

(5.V)

3. AB with either AA and B_f or BB and A_f:

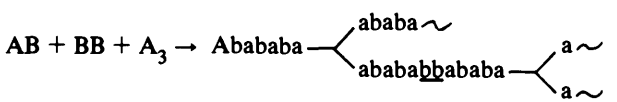

(5.W)

4. A_f and B_f:

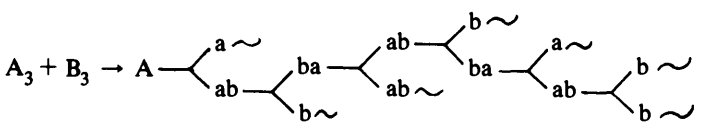

(5.X)

5. Other possibilities include the involvement of still another functional group capable of reaction with A and/or B.

Reaction (5.W) is interesting inasmuch as either the AA or BB monomer must be present to produce crosslinking. Polymerization of AB with only A_f (or B_f) introduces a single branch point, but no more, since all chain ends are misoriented for further incorporation of branch points. Including the AA or BB molecule reverses this. The bb unit which accomplishes this in reaction (5.W) is underscored.

What we seek next is a quantitative relationship between the extent of the polymerization reaction, the composition of the monomer mixture, and the point of gelation. We shall base our discussion on the system described by reaction (5.U); other cases are derived by similar methods. To further specify the system we assume that A groups limit the reaction and that B groups are present in excess. Two parameters are necessary to characterize the reaction mixture:

1. The ratio of the initial number of A to B groups as defined by the factor r. given by Eq. (5.34). The total number of A groups from both AA and A_f are included in this application of r.
2. The fraction of A groups present in multifunctional molecules as defined by the ratio

$$\rho = \frac{\nu_{\text{A from Af}}}{\nu_{\text{A, total}}} \tag{5.43}$$

There are two additional useful parameters which characterize the reaction itself:

3. The extent of reaction p is again based on the group present in limiting amount. For the system under consideration, p is the fraction of A groups that have reacted.
4. The probability that a chain segment is capped at both ends by a branch unit is described by the branching coefficient α. The branching coefficient is central to the discussion of gelation, since whether gelation occurs or not depends on what happens after capping a section of chain with a potential branch point.

The methods we consider have been developed by Stockmayer and Flory and have been applied to quite a variety of polymer systems and phenomena.

Our approach to the problem of gelation proceeds through two stages: First we consider the probability that AA and BB polymerize until all chain segments are capped by an A_f monomer; then we consider the probability that these are connected together to form a network. The actual molecular processes occur at random and not in this sequence, but mathematical analysis is feasible if we consider the process in stages. As long as the same sort of structure results from both the random and the subdivided processes, the analysis is valid.

The arguments we employ are statistical, so we recall that the probability of a functional group reacting is given by the fraction of groups that have reacted at any point, and the probability of a sequence of events is the product of their individual probabilities. We continue to use the concept that functional group reactivity is independent of the size of the molecule to which the group is attached. One additional assumption that enters when multifunctional monomers are considered is that all A groups in A_f are of equal reactivity.

Now let us consider the probability that a section of polymer chain is capped at both ends by potential branch points:

1. The first step is the condensation of a BB monomer with one of the A groups of an A_f molecule:

$$A_f + BB \longrightarrow A_{f-1}\ abB$$

Since all A groups have the same reactivity by hypothesis, the probability of this occurrence is simply p.

2. The terminal B group reacts with an A group from AA rather than A_f:

   $$A_{f-1}\ abB + AA \longrightarrow A_{f-1}\ abbaA$$

   The fraction of unreacted B groups is rp, so this gives the probability of reaction for B. Since ρ is the fraction of A groups on multifunctional monomers, rp must be multiplied by $1 - \rho$ to give the probability of B reacting with an AA monomer. The total probability for the chain shown is the product of the probabilities considered until now:

   $$p[rp(1 - \rho)]$$

3. The terminal A group reacts with another BB:

   $$A_{f-1}\ abbaA + BB \longrightarrow A_{f-1}\ abbaabB$$

   The probability of this step is again p, and the total probability is

   $$p[rp(1 - \rho)p]$$

4. Additional AA and BB molecules condense into the chain to give a sequence of n bbaa units:

   $$A_{f-1}\ abbaabB + AA + BB \longrightarrow \longrightarrow \longrightarrow A_{f-1}\ a(bbaa)_n bB$$

   We have just evaluated the probability of one such unit; the probability for a series of n units is just the product of the individual probabilities:

   $$p[rp(1 - \rho)p]^n$$

5. The terminal B group reacts with an A group from a multifunctional monomer:

   $$A_{f-1}\ a(bbaa)_n bB + A_f \longrightarrow A_{f-1}\ a(bbaa)_n bbaA_{f-1}$$

   The probability of B reacting is rp and the fraction of these reactions with A_f molecules is $rp\rho$. The probability of the entire sequence is

   $$p[rp(1 - \rho)p]^n rp\rho$$

6. In the general expression above, n can have any value from 0 to ∞, so the probability for all possibilities is the sum of the individual probabilities.

Note that a different procedure is used for compounding probabilities here: the sum instead of the product. This time we are interested in *either* n = 0 *or* n = 1 *or* n = 2, and so forth. We have previously required the first A–B reaction *and* the second A–B reaction *and* the third A–B reaction and so on.

Since the branching coefficient gives the probability of a chain segment being capped by potential branch points, the above development describes this situation:

$$\alpha = \sum_{n=0}^{\infty} rp^2\rho\,[rp^2(1-\rho)]^n \tag{5.44}$$

The summation applies only to the quantity in brackets, since it alone involves n. Representing the bracketed quantity by Q, we note that $\Sigma_1^{\infty} Q^n = 1 + Q + Q^2 + \cdots = 1/(1 - Q)$; therefore

$$\alpha = \frac{rp^2\rho}{1 - rp^2(1-\rho)} \tag{5.45}$$

We have now completed the first stage of the problem we set out to consider. We have arrived at the probability that chains are capped at both ends by potential branch points. The second stage of the derivation is concerned with the reaction between these chain ends via the remaining f − 1 reactive A groups. By hypothesis, the mixture contains an excess of B groups, so there are still unreacted BB monomers or other polymer chain segments with terminal B groups which can react with the A_{f-1} groups we have been considering. Table 5.6 shows the connecting of such groups—by BB molecules for simplicity—for several values of f. For each of the situations shown in Table 5.6, converting the boxed A BB A groups into a condensed abba sequence amounts to linking into a linear polymer the capped segments which had been separate until now. Since the capped ends have f − 1 remaining functional groups at this point, a linear condensation product results when any one of these groups reacts. Thus 1/(f − 1) is the probability of this particular eventuality.

Our interest from the outset has been in the possibility of crosslinking which accompanies inclusion of multifunctional monomers in a polymerizing system. Note that this does not occur when the groups enclosed in boxes in Table 5.6 react; however, any reaction *beyond* this for the terminal A groups will result in a cascade of branches being formed. Therefore a critical (subscript c) value for the branching coefficient occurs at

$$\alpha_c = \frac{1}{f-1} \tag{5.46}$$

For an extent of reaction corresponding to $\alpha > \alpha_c$, gelation is predicted to occur.

Table 5.6 Schematic Illustration Showing the Formation of a Linear Polymer by the Reaction of One of the f − 1 Reactive Groups at the End of a Portion of Polymer

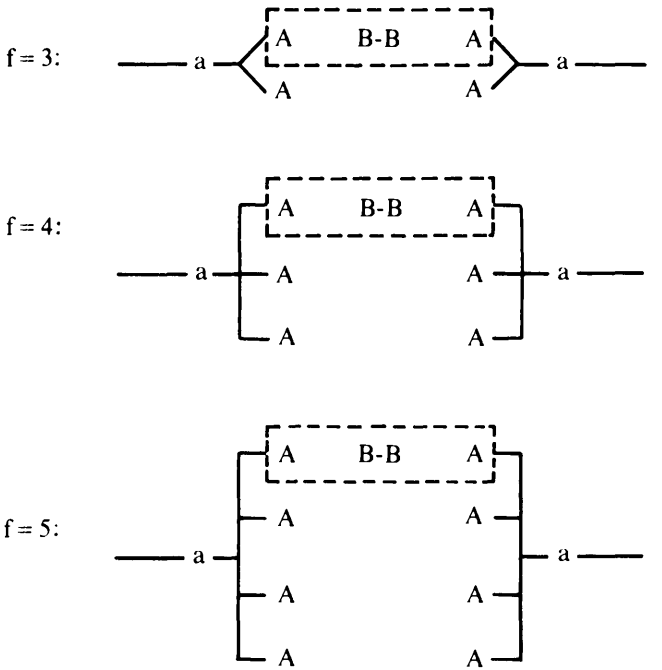

Combining Eqs. (5.45) and (5.46) and rearranging gives the critical extent of reaction for gelation p_c as a function of the properties of the monomer mixture r, ρ, and f:

$$p_c = \frac{1}{[r + r\rho(f - 2)]^{1/2}} \tag{5.47}$$

This equation describes the extent of reaction at which the system is predicted to gel.

Equation (5.47) is of considerable practical utility in view of the commercial importance of three-dimensional polymer networks. Some reactions of the sort we have considered are carried out on a very large scale: Imagine the consequences of having a polymer preparation solidify in a large and expensive reaction vessel because the polymerization reaction went a little too far! Considering this kind of application, we might actually be relieved to know that Eq. (5.47) errs in the direction of underestimating the extent of reaction at

gelation. This comes about because some reactions of the multifunctional branch points result in intramolecular loops which are wasted as far as network formation is concerned. This possibility is readily apparent in Table 5.6.

As an example of the quantitative testing of Eq. (5.47), consider the polymerization of diethylene glycol (BB) with adipic acid (AA) in the presence of 1,2,3-propane tricarboxylic acid (A_3). The critical value of the branching coefficient is 0.50 for this system by Eq. (5.46). For an experiment in which r = 0.800 and ρ = 0.375, p_c = 0.953 by Eq. (5.47). The critical extent of reaction, determined by titration, in the polymerizing mixture at the point where bubbles fail to rise through it was found experimentally to be 0.9907. Calculating back from Eq. (5.45), the experimental value of p_c is consistent with the value $\alpha_c = 0.578$.

Examination of several special cases of Eq. (5.47) gives us a better appreciation of the several factors which operate in that relationship:

1. If $\nu_A^0 = \nu_B^0$ and r = 1,

$$p_c = \frac{1}{[1 + \rho(f - 2)]^{1/2}} \tag{5.48}$$

2. Using the case of f = 3 and ρ = 0.3 as an example, p_c = 0.877 when r = 1 in contrast to, say, 0.886 when r = 0.98. This illustrates that failure to maintain stoichiometric balance continues to have a limiting effect on polymerization in this case also.
3. If $\nu_A^0 < \nu_B^0$ (r < 1) and all A groups are present as A_f (ρ = 1),

$$p_c = \frac{1}{[r + r(f - 2)]^{1/2}} \tag{5.49}$$

4. Using the case of f = 3 and r = 0.98 as an example, p_c = 0.714 when ρ = 1 in contrast to, say, 0.886 when ρ = 0.3. The higher the proportion of groups present as branch points, the lower the threshold for gelation.

It is apparent that numerous other special systems or effects could be considered to either broaden the range or improve the applicability of the derivation presented. Our interest, however, is in illustrating concepts rather than exhaustively exploring all possible cases, so we shall not pursue the matter of gelation further. Instead, we conclude this section with a brief examination of the molecular weight averages in the system generated from AA, BB, and A_f. For simplicity, we restrict our attention to the case of $\nu_A^0 = \nu_B^0$. As an approach to the number average degree of polymerization, it is useful to define the average functionality $\bar{f}$ of a monomer as

$$\bar{f} = \frac{\Sigma_i N_i f_i}{\Sigma_i N_i} \tag{5.50}$$

where N_i and f_i are the number of molecules and the functionality of the ith component in the reaction mixture, respectively. The summations are over all monomers. If N is the total number of molecules present in the reaction mixture at an extent of reaction p and N_0 is the number of molecules present initially, then $2(N_0 - N)$ is the number of functional groups that have reacted and $\bar{f}N_0$ is the total number of groups initially present. Two conclusions follow immediately from these concepts:

$$\bar{n}_n = \frac{N_0}{N} \tag{5.51}$$

and

$$p = \frac{2(N_0 - N)}{\bar{f}N_0} \tag{5.52}$$

Elimination of N from these expressions gives

$$\bar{n}_n = \frac{2}{2 - p\bar{f}} \tag{5.53}$$

This result is known as the Carothers equation. It is apparent that this expression reduces to Eq. (5.4) for the case of $\bar{f} = 2$. Furthermore, when $\bar{f}$ exceeds 2, as in the $AA/BB/A_f$ mixture under consideration, then $\bar{n}_n$ is increased over the value obtained at the same p for $\bar{f} = 2$. A numerical example will help clarify these relationships:

Example 5.5

An AA, BB, and A_3 polymerization mixture is prepared in which $\nu_A^0 = \nu_B^0 = 3.00$, with 10% of the A groups contributed by A_3. Use Eq. (5.53) to calculate $\bar{n}_n$ for p = 0.970 and p for $\bar{n}_n = 200$. In each case compare the results with what would be obtained if no multifunctional A were present.

Solution

Determine the average functionality of the mixture. The total number of functional groups is 6.00 mol, but the total number of molecules initially present must be determined. Using $3N_{A_3} + 2N_{AA} = 3.00$ and $3N_{A_3}/3 = 0.100$, we obtain that $N_{AA} = 1.350$ and $N_{A_3} = 0.100$. Since $N_B = 1.500$, the total number of moles initially present is $N_0 = 1.350 + 0.100 + 1.500 = 2.950$:

$$\bar{f} = \frac{0.100(3) + 1.350(2) + 1.500(2)}{2.950} = \frac{6.000}{2.950} = 2.034$$

Solve Eq. (5.53) with p = 0.970 and $\bar{f} = 2.034$:

$$\bar{n}_n = \frac{2}{2 - 0.97(2.034)} = 73.8$$

For comparison, solve Eq. (5.4) with p = 0.970:

$$\bar{n}_n = \frac{1}{1 - 0.970} = 33.3$$

Solve Eq. (5.53) with n = 200 and $\bar{f} = 2.034$:

$$p = \frac{(1 - 1/\bar{n}_n)(2)}{\bar{f}} = \frac{0.995(2)}{2.034} = 0.978$$

Solve Eq. (5.4) with n = 200:

$$p = \left(1 - \frac{1}{\bar{n}_n}\right) = \left(1 - \frac{1}{200}\right) = 0.995$$

For a fixed extent of reaction, the presence of multifunctional monomers in an equimolar mixture of reactive groups increases the degree of polymerization. Conversely, for the same mixture a lesser extent of reaction is needed to reach a specified $\bar{n}_n$ with multifunctional reactants than without them. Remember that this entire approach is developed for the case of stoichiometric balance. If the numbers of functional groups are unequal, this effect works in opposition to the multifunctional groups.

•

The Carothers approach, being an end group method, is limited to the number average degree of polymerization and gives no information concerning the breadth of the distribution. A statistical approach to the degree of polymerization yields expressions for both $\bar{n}_n$ and $\bar{n}_w$. Reference 2 contains a derivation of these quantities for the self-polymerization of A_f monomers. Although this specific system appears very different from the one we have considered, the essential aspects of the two different averaging procedures are applicable to the system we have considered as well. The results obtained for the A_f case are

$$\bar{n}_n = \frac{1}{1 - \alpha f/2} \tag{5.54}$$

and

$$\bar{n}_w = \frac{1 + \alpha}{1 - \alpha(f - 1)} \tag{5.55}$$

from which it follows that

$$\frac{\bar{n}_w}{\bar{n}_n} = \frac{(1 + \alpha)(1 - \alpha f/2)}{1 - \alpha(f - 1)} \tag{5.56}$$

The value of α to be used in these expressions is given by Eq. (5.45) for the specific mixture under consideration. At the point of gelation $\alpha_c = 1/(f - 1)$ according to Eq. (5.46). Equation (5.55) shows that $\bar{n}_w$ becomes infinite at this point while $\bar{n}_n$ remains finite. This merely means that there are still many molecules present at the gel point in addition to the network molecule of essentially infinite molecular weight. The ratio $\bar{n}_w/\bar{n}_n$ indicates an immense expansion of the degree of heterogeneity as $\alpha \to \alpha_c$. Expressions are also available to describe the distribution of molecules in that fraction of material that is not incorporated into the network beyond the point of gelation.

5.9 Some Cross-linked Step-Growth Polymers

In this section we examine some examples of cross-linked step-growth polymers. The systems we shall describe are thermosetting polymers of considerable industrial importance. The chemistry of these polymerization reactions is more complex than the hypothetical AB reactions of our models. We choose to describe these commercial polymers rather than model systems which might conform better to the theoretical developments of the last section both because of the importance of these materials and because the theoretical concepts provide a framework for understanding more complex systems, even if they are not quantitatively successful.

The materials we shall discuss are all polymers of formaldehyde which may be viewed as methylene glycol in the presence of water:

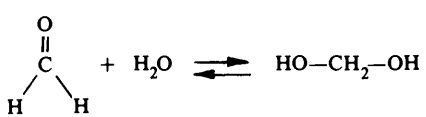

(5.Y)

This particular representation makes it easy to visualize formaldehyde as a step-growth monomer of functionality 2. Our principal interest is in the reactions of formaldehyde with the active hydrogens in phenol, urea, and melamine, compounds [II]–[IV], respectively:

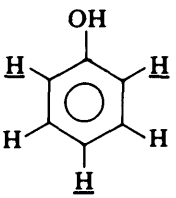

[II]

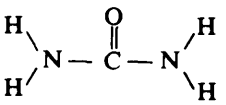

[III]

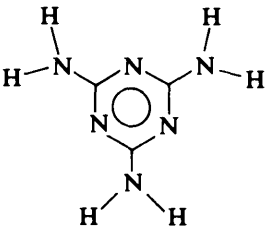

[IV]

The hydrogen atoms shown in these monomers (only those underlined in phenol) are the active hydrogens, so these compounds have nominal functionalities of 3, 4, and 6, respectively. Note that a monosubstituted phenol would have a functionality of 2 and would be incapable of crosslinking.

At first glance it appears that these systems do conform fully to the discussion above; this is an oversimplification, however. The ortho and para hydrogens in phenol are not equal in reactivity, for example. In addition, the technology associated with these polymers involves changing the reaction conditions as the polymerization progresses to shift the proportions of several possible reactions. Accordingly, the product formed depends on the nature of the catalyst used, the proportions of the monomers, and the temperature. Sometimes other additives or fillers are added as well.

Industrial phenol-formaldehyde polymerization is a complex process, but the following reactions suggest the successive stages and the possible linkages involved:

1. Formation of methylol derivatives of phenol:

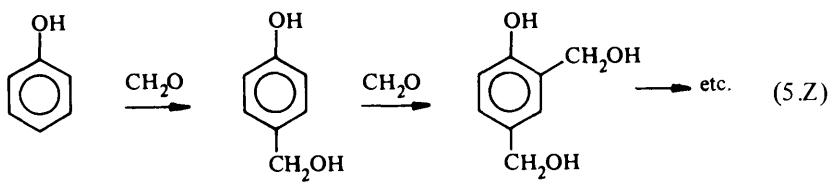

(5.Z)

these species may be regarded as the true monomers for the production of polymer. The reactions shown are catalyzed by either acid or base.

2. Formation of low molecular weight polymer with chains capped by phenol repeat units:

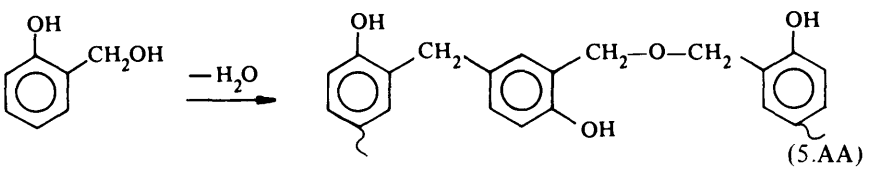

(5.AA)

Stopping the polymer at this point requires the ratio of formaldehyde to phenol to be less than unity. Both methylene and ether bridges are known to be present. The reaction is either acid or base catalyzed, and branching is uncommon at this stage. The products are variously known as A stage resins, novolacs, or resole prepolymers.

3. Formation of final cross-linked polymer:

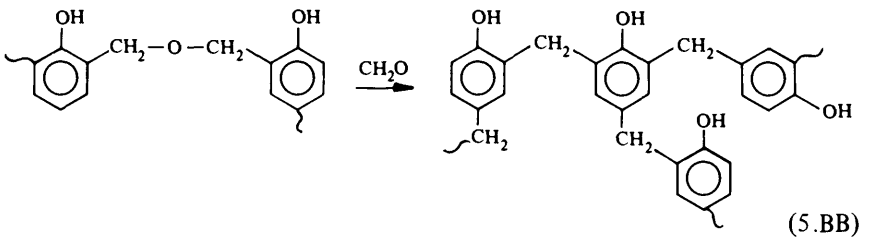

(5.BB)

This reaction is carried out under base-catalyzed conditions and with a formaldehyde/phenol ratio greater than unity. The resulting product is called a C state resin or resite.

Not all of the hydrogens in phenol are equally reactive. Under acid conditions the quinoid structure

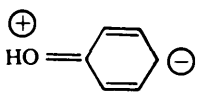

is stabilized as a reaction intermediate favoring the para additions of the protonated formaldehyde molecule. There are also indications that the reaction of one position alters the reactivity of others, so the reactivity depends on the extent of the reaction as well. Hence the assumption that we made in the last section concerning the equal reactivity of all A groups is not justified here. Nevertheless, the previously developed theory can be used to back-calculate from experimental results the effective parameters of the reaction mixtures. Table 5.7 lists some data for three different phenol-formadehyde resins formulated with various ratios of reactants. Weight and number average degrees of polymerization were measured experimentally on these products, and Eqs. (5.54) and (5.55) were used to evaluate α and f from these data. The variation in α reflects the differences in the polymerization mixture; the fact that f values turn out to be as nearly constant as they are suggests that phenol quite consistently displays this effective functionality. Strictly speaking, nonintegral f values are meaningless in terms of the theory presented in the last section, but differences in reactivity and the diversity of possible linkages are quantified to some extent by the concept of effective functionality defined in this way.

Table 5.7 Calculated Values of α and f for Phenol–formaldehyde Resins Formed from Different Proportions of Reactants and Based on Experimental Values of $\bar{n}_n$ and $\bar{n}_w$

Quantity	Resin I	Resin II	Resin III
Phenol–formaldehyde	1.667	1.227	1.176
$\bar{n}_{n,ex}$	2.12	3.51	4.28
$\bar{n}_{w,ex}$	3.64	8.89	11.68
α_{calc}	0.455	0.611	0.677
f_{calc}	2.32	2.35	2.27

Source: M. F. Drumm and J. R. LeBlanc, *Step-Growth Polymerizations*, D. H. Solomon (Ed.), Marcel Dekker, New York, 1972, p. 196.

In the polymerization scheme presented above, the A stage corresponds roughly to $\alpha < \alpha_c$, and the C stage to $\alpha > \alpha_c$; the products are soluble and fusible in the former, and insoluble and infusible in the latter. Presuming that the C stage is the product ultimately sought, it may be formed directly in one step or in two steps through subsequent reaction of the resole prepolymer. Phenol-formaldehyde resins find applications in the manufacture of molded products, as adhesives in products such as plywood, and as protective coatings. This type of polymer, first investigated by Baekeland in 1872, was one of the first synthetic polymers.

Polymers produced by the reactions of urea and melamine with formaldehyde are collectively known as amino resins. In most respects the preparation and properties of these polymers parallel the story of the phenolic resins. The nominal functionality (as opposed to the effective functionality) increases in the order phenol < urea < melamine. As might be anticipated from the effect of this order on crosslinking potential, the hardness and strength of C stage polymers follows the order melamine > urea > phenol. Other properties such as moisture resistance and color are traceable to chemical properties of the monomers other than explicitly polymeric considerations. The amino resins have less moisture resistance and lighter color than the corresponding phenolics. As with the phenolic resins, these polymers also proceed through the methylol intermediates with subsequent linkage through either methyl or ether bridges. They are also commercially available at various stages of polymerization. At the A stage they are used in the textile industry to impart "permanent press" characteristics to cotton and rayon. At the C stage they are used as molding and laminating resins, particularly in applications where their lack of color is an asset.

5.10 Rings 'n Things

From the beginning of this chapter we have acknowledged that ring formation is a possible reaction in the type of monomer mixtures we have considered. We have consistently ignored this complication. In this section we shall remedy this situation. At the same time we shall also consider the polymerizability of cyclic monomers. The formation of polyesters from lactones and of polyamides from lactams, reactions given in Tables 5.3 and 5.4, respectively, are examples of the latter. At first these two issues appear quite different, but the relative stability of rings versus linear structures is at the heart of each. Accordingly, we shall discuss ring formation as a competition to polymerization and ring opening as a mode of polymerization as two areas where the same general principles find application.

In the matter of ring stability it is the number of atoms in the ring that is of central importance. In the following equations l, m, and m′ represent the number of ring (l) and backbone (m, m′) *atoms* in the species shown. Note that for linear species m and m′ are proportional to the degree of polymerization but are more suitable for present purposes than the latter. The following general reactions are pertinent to the present discussion:

1. Monomers reacting to form a ring:

$$A\text{–}A + B\text{–}B \longrightarrow \overset{\frown}{ab}\underset{\smile}{ab}_{[l]} \tag{5.CC}$$

2. Monomers reacting to form a linear molecule:

$$A\text{–}A + B\text{–}B \longrightarrow A\text{–}ab\text{–}B_{[m]} \tag{5.DD}$$

3. Cyclic molecules opening to a linear form:

$$\overset{\frown}{ab}\underset{\smile}{ab}_{[l]} \longrightarrow A\text{–}ab\text{–}B_{[m]} \tag{5.EE}$$

4. Rings combining with linear molecules to form longer linear species:

$$\overset{\frown}{ab}\underset{\smile}{}_{[l]} + A\text{–}B_{[m]} \longrightarrow A\text{–}ab\text{–}B_{[m']} \tag{5.FF}$$

Although the number of ring atoms is the structural feature upon which we focus attention, we shall use the criteria of thermodynamics and kinetics to assess the feasibility of the reactions listed above.

Reaction (5.EE) is particularly useful for the discussion of thermodynamic considerations because of the way differences in thermodynamic state variables are independent of path. Accordingly, if we know the value of ΔG for reaction (5.EE), we have characterized the following:

1. The spontaneity (or lack thereof) of reaction (5.EE) as written.
2. The spontaneity (or lack thereof) of its reverse: the cyclization of a linear molecule.
3. The difference between the values of ΔG for reactions (5.CC) and (5.DD), making it less important to characterize these latter reactions separately.

Reaction (5.FF) summarizes the way high molecular weight polymers form from ring-opening reactions. The reaction ignores the start of the whole process by not showing the origin of the initial linear species, but—as an end effect—that step represents a small part of the entire polymerization process. The reaction as shown is analogous to the neglect of chain initiation and termination in describing vinyl polymerization as was done in reaction (1.A).

Ring-opening polymerization is a distinct category of polymerization, sharing common features with both step-growth and addition polymerization. For example, step-growth polymer chains continue to grow throughout the entire reaction, as we saw in Sec. 5.3; chains continue to grow throughout the entire duration of the ring-opening reaction also. In step-growth polymerization reaction between groups on any molecular species is possible, as we saw in Sec. 5.2; only monomers react with growing chains in ring-opening polymerizations, as shown by reaction (5.FF). This latter feature also characterizes addition polymerization.

As a distinct class of polymerization, ring opening is entirely deserving of a chapter of its own in a polymer chemistry text. Ample material exists to justify such separate treatment. Unfortunately, no course or textbook is ever long enough to cover everything, and certain topics get shortchanged. Such is the fate of ring-opening polymerizations in this book.

We now turn specifically to the thermodynamics and kinetics of reactions (5.EE) and (5.FF). The criterion for spontaneity in thermodynamics is $\Delta G < 0$ with $\Delta G = \Delta H - T\,\Delta S$ for an isothermal process. Thus it is both the sign and magnitude of ΔH and ΔS and the magnitude of T that determine whether a reaction is thermodynamically favored or not. As usual in thermodynamics, the Δ's are taken as products minus reactants, so the conclusions apply to the reactions as written. If a reaction is reversed, products and reactants are interchanged and the sign of the ΔG is reversed also.

Several qualitative predictions can be made concerning the ring-opening reaction described by (5.EE):

1. The reaction involves breaking a bond, which requires the input of energy; hence we expect that $\Delta H > 0$.
2. Although there is no change in the number of molecules, the linear molecule can take on more conformations than the ring; hence we expect that $\Delta S > 0$.
3. Precise numerical values for either ΔH or ΔS will depend on the degree of strain in the ring structure, among other things.

4. The fact that both ΔH and ΔS are expected to be positive for reaction (5.EE) means that ΔG tends to be negative at higher temperatures and positive at lower temperatures. Thus linear molecules tend to be favored over rings at higher temperatures. We have seen elsewhere in this chapter that step-growth polymerizations are usually conducted at elevated temperatures.
5. The temperature at which ΔG changes sign (i.e., where $\Delta G = 0$) is given by the ratio $\Delta H/\Delta S$ if these quantities are independent of T. The temperature at which rings become favored depends on the specific values of ΔH and ΔS, and, again, this is a matter of ring size.

Even at the qualitative level of the discussion above, it is difficult to make predictions regarding the spontaneity of the ring-opening polymerization reaction (5.FF):

1. Regarding ΔH, one bond is broken and a similar bond is formed in a linear product. The linear molecule is unstrained, but the magnitude of the strain relief upon ring opening depends on the ring size.
2. Regarding ΔS, ring opening tends to increase entropy through the increase of possible conformations; the linkage of two separate molecules decreases the translational entropy. The latter effect is probably larger, but the net balance depends on ring size.

Thus consideration of both reactions (5.EE) and (5.FF) forces us to examine the stability of cyclic structures as a function of ring size.

The rather special status of five- and six-membered rings is already familiar from organic chemistry. Because of the general stability associated with rings of this size, both reactions (5.EE) and (5.FF) are expected to be less favored when the ring compounds have this size, that is, when $l = 5$ or 6. To see the basis for this conclusion, let us consider some of the evidence for stain in cyclic compounds.

One of the classic methods for evaluating ring strain is to compare the heat of combustion per methylene group of cyclic hydrocarbons as a function of ring size. When this is done, $\Delta H_c/CH_2$ is found to decrease progressively and dramatically as the number of ring atoms increases from 3 to 6, increase through a slight maximum for $7 \lesssim l \lesssim 11$, and then slowly drop back to the same minimum observed for $l = 6$. The following example also deals with cyclic alkanes and relates the matter of ring size to the ring $\rightleftarrows$ polymer equilibrium.

Example 5.6

For the reaction

$$\text{Cyclic alkane } (CH_2)_l \text{ (liq)} \rightleftarrows \text{polymer (cryst)}$$

the following values of ΔH° and ΔS° have been estimated at 25°C:

l	ΔH° (kJ mol^{-1})	ΔS° (J K^{-1} mol^{-1})
4	-105.0	-55.2
6	+2.9	+10.5
8	-34.7	+37.2

Evaluate ΔG^0 and K_{eq} at 25°C for each of the polymerization reactions and comment on the results.

Solution

We use the relationships $\Delta G^\circ = \Delta H^\circ - T\,\Delta S^\circ$ and $\Delta G^\circ = -RT \ln K_{eq}$, being careful about units: T = 298 K and R = 8.314 J K^{-1} mol^{-1}. Using the above values of ΔH° and ΔS°, the following are readily calculated:

l	ΔG° (kJ mol^{-1})	$\ln K_{eq}$	K_{eq}
4	-88.5	35.7	3.3×10^{15}
6	-0.19	0.08	1.08
8	-45.8	18.5	1.1×10^{8}

Several observations come to mind:

1. For both l = 4 and l = 8, the polymer is favored over the ring to a far greater degree than for l = 6. In the latter case the difference between ΔH° and $T\,\Delta S^\circ$ is so small that there is probably no justification for retaining as many figures as shown in the calculated results.
2. For l = 4, ΔH° makes a favorable contribution to ΔG°, while the contribution of ΔS° is unfavorable. The effect of the former outweighs the latter.
3. For l = 6 the contribution of ΔH° is unfavorable and that of ΔS° is favorable. The specific values make T = 298 K very close to the equilibrium temperature. This implies that the reaction is shifted to favor polymer at higher temperatures and to favor the cyclic monomer at lower temperatures. Since the difference between ΔH° and $T\,\Delta S^\circ$ is so small, the temperature dependence of ΔH° and ΔS° could alter this conclusion.
4. For l = 8 both ΔH° and ΔS° contribute favorably to ΔG°.

•

Thus both combustion and polymerization data indicate a stabilization of rings in the neighborhood of l = 6.

Generally speaking, the replacement of carbon atoms in the rings by –O– or –NH– causes relatively minor alterations in the picture of ring stability. For

Table 5.8 Values for ΔH and ΔS for the Ring-Opening Polymerization, Reaction (5.FF), for Monomers with the Indicated Values of l

l	ΔH (kJ mol^{-1})	ΔS (J K^{-1} mol^{-1})
5	-5.4	-30.5
6	-4.6	-25.1
7	-12.6	-4.6
8	-23.8	-16.7
9	-40.2	–
13	-6.3	–

Source: G. Odian, *Principles of Polymerization*, 1st ed., McGraw-Hill, New York, 1970. Used with the permission of the McGraw-Hill Book Company.

evidence of this, we turn to the data in Table 5.8, which applies to the ring-opening polymerization reaction (5.FF). Table 5.8 lists values of ΔH and ΔS for the reaction of monomers with several different l values. The values of ΔH follow the same trend as discussed above for the combustion data. ΔS passes through a maximum as ring size increases. If we assume that ΔH and ΔS values in Table 5.8 apply at 400 K, $\Delta G = -12.3$ kJ mol^{-1} for $l = 7$, ϵ-caprolactam, while this quantity is +3.7 kJ mol^{-1} for $l = 5$ (2-pyrrolidone) and +2.9 kJ mol^{-1} for $l = 6$ (2-piperidone). The negative value of ΔG for the polymerization of ϵ-caprolactam results in the formation of the important product nylon-6. The positive values of ΔG for rings with $l = 5$ and $l = 6$ reflects the special stability of rings of this size.

Thermodynamics provides only one of the criteria for polymerizability. A favorable value for ΔG says nothing about the rate of a reaction. It is not particularly difficult to see that a reaction like the reverse of (5.EE) becomes kinetically improbable for large values of m, that is, for the cyclization of a large linear molecule. For the terminal A and B groups of a single chain to react with each other for ring closure, they must first diffuse together. We have seen in Chap. 1 that for long chains the end-to-end distance varies with the square root of the degree of polymerization, or with $m^{1/2}$ in the present context. The volume associated with a length of this magnitude varies with length^3, or $m^{3/2}$. Hence as m increases, the concentration of chain ends varies with $m^{-3/2}$. By contrast, the probability that an A group reacts with a B group from another molecule depends on the number of molecules present, and the number of chains in a reaction mixture varies with m^{-1}. Hence as m increases, reaction between different molecules becomes increasingly favored over ring closure simply by a dilution effect. Use of random walk statistics clearly limits the above

argument to chains which are considerably longer than others we have discussed in this section.

At the smaller end of the size range, kinetic studies show that the ease of formation of lactones, cyclic esters, and cyclic anhydrides is greatest in the neighborhood of five- or six-atom rings, drops to a minimum in the range of 8- to 12-membered rings, and then increases and levels off at a low plateau value for still larger rings. The broad minimum in the rate of formation of rings with $8 \lesssim l \lesssim 12$ is attributed to the crowding between chain hydrogens in the interior of the rings in this size range.

On the basis of both thermodynamic and kinetic evidence—both of which are interpretable in terms of the strain associated with rings of certain sizes or similar structural factors—we see that only rings with five or six atoms have any significant stability. Accordingly, we conclude the following:

1. AA and BB monomers and also AB monomers invariably react to form predominantly linear structures in all but the rather special case where the ring structure in reaction (5.CC) has a value of $l = 5$ or 6. This explains why so many of the monomers in step-growth polymerizations are tetra-, hexa-, and decamethylene compounds.
2. The cyclization of a polymer that has already grown through the dimer or trimer stage is also insignificant.
3. The formation of polymers by the ring-opening reaction (5.FF) requires an initiator to get the reaction started, and perhaps a catalyst to assure a suitable rate, but otherwise is quite feasible for $l \lesssim 4$ and $l \gtrsim 7$.

We conclude this section by citing some examples of ring-opening polymerizations. Table 5.9 lists several examples of ring-opening polymerizations. In addition to the reactions listed, we recall the polymerizations of lactones and lactams exemplified by equations in Table 5.3 and 5.4, respectively.

Ring-opening polymerizations are catalyzed by a wide variety of substances, including the bases OH^- and RO^- and the acids H^+ and BF_3; water is also used as a catalyst. The reactions proceed by the opening of the ring by the catalyst to form an active species,

$$\overset{\frown}{\text{ab}} + \text{C} \longrightarrow \text{Ca–b}^* \qquad \text{(5.GG)}$$

followed by the subsequent attachment of additional monomers to the active site,

$$\text{Cab}^* + \overset{\frown}{\text{ab}} \longrightarrow \text{Cabab}^* \longrightarrow \longrightarrow \text{polymer} \qquad \text{(5.HH)}$$

Table 5.9 Some Typical Ring-Opening Polymerization Reactions

1. Epoxides:

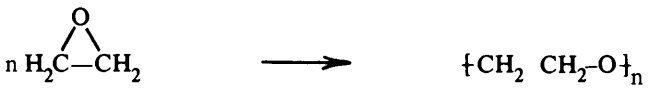

2. Cyclic formals (formaldehyde–cyclic ether dimer):

3. Cyclic sulfides (including S_8):

4. Alkylenimines:

5. Cyclic acetals (trioxane: cyclic trimer of formaldehyde):

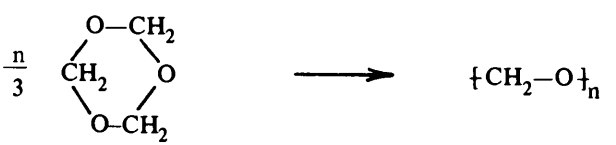

6. Cyclic siloxanes:

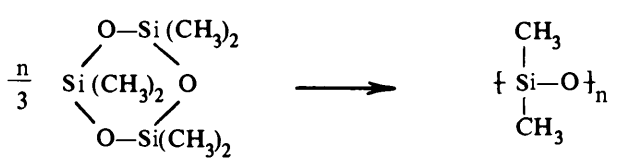

5.11 More Rings

The search for substances which qualify for proposed applications has always been a driving force for the synthesis and characterization of new compounds. This is especially true in polymer chemistry, where it is the potential of polymers as engineering materials that often stimulates research. Polymeric materials frequently fail to be serviceable in engineering applications for one of the following reasons:

1. They lack resistance to solvents or other chemicals.
2. They lack thermal stability at high temperatures.
3. They are not sufficiently rigid.

To some extent each of these objections is met by the presence of either chemical or crystallite crosslinking in the polymer. Another approach which complements the former is to incorporate rings into the backbone of the chemical chain. As an example, contrast the polyesters formed between ethylene glycol and either suberic or terephthalic acid. Structures [V] and [VI], respectively, indicate the repeat units in these polymers:

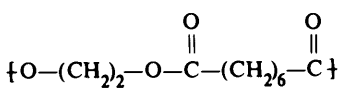

[V]

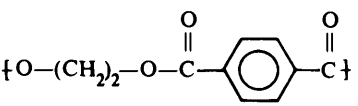

[VI]

In both instances the two carboxyl groups are separated by six carbons, but these occur as six methylene groups in the suberate and as a benzene ring in the terephthalate. The suberate melts at about 62°C and the terephthalate at about 260°C. At least in part, this difference is traceable to the greater chain stiffness of the backbone containing the ring structure, which decreases the ΔS for the melting process and increases the melting point according to Eq. (4.5). This same stiffness enhances the crystallizability and increases the various deformation moduli both through the chain stiffness and the crystallinity. The improved interchain attraction in the stiffer chains decreases the solubility of these materials, and this in itself contributes to their diminished susceptibility to chemical attack. In addition, the backbone rings effectively provide multiple strands along the polymer so that there is a possibility for the polymer to remain intact even if one strand is cleaved.

Once the potential associated with this aspect of molecular architecture is recognized, the principles of the last section coupled with the richness of organic (and inorganic) chemistry suggest numerous synthetic possibilities. We shall not attempt to be comprehensive in discussing this facet of polymer chemistry; instead we cite only a few examples of step-growth polymers which incorporate

successively greater proportions of ring character into the chain backbone. These examples will also remind us that polyesters, polyamides, and formaldehyde polymers are not the only kinds of polymers possible from monomers with two or more functional groups.

Aromatic polyimides are the first example we shall consider of polymers with a rather high degree of backbone ring character. This polymer is exemplified by the condensation product of pyromellitic dianhydride [VII] and *p*-aminoaniline [VIII]:

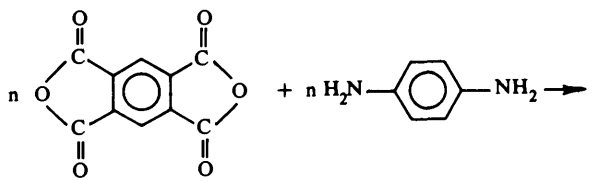

[VII] [VIII]

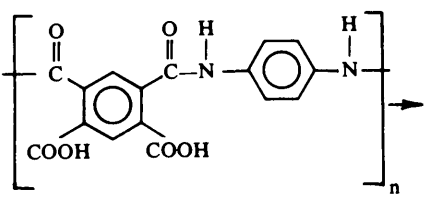

[IX]

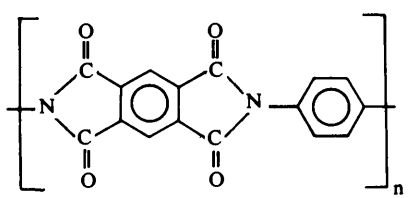

[X] (5.II)

This polymerization is carried out in the two stages indicated above precisely because of the insolubility and infusibility of the final product. The first-stage polyamide, structure [IX], is prepared in polar solvents and at relatively low temperatures, say, 70°C or less. The intermediate is then introduced to the intended application—for example, a coating or lamination—then the second-stage cyclization is carried out at temperatures in the range 150-300°C. Note the formation of five-membered rings in the formation of the polyimide, structure [X], and also that the proportion of acid to amine groups is 2:1 for reaction (5.II).

When the proportion of acid to amine groups is reversed—namely, 1:2—a process rather similar to reaction (5.II) yields a polymer which ultimately contains the five-membered imidazole ring. This reaction is also carried out in the stages listed below and illustrated by reaction (5.JJ):

1. The diphenyl ester of the diacid [XI] is used to prevent side reactions such as decarboxylation.
2. The condensation of the monomers with the elimination of water and the formation of a polyimine [XII] occurs at temperatures around 250°C.
3. This first-stage polymer is then introduced into the application environment, where the final cyclization reaction occurs.
4. The polyimidazole [XIII] is formed by heating to 350-400°C, with the elimination of phenol and ring closure:

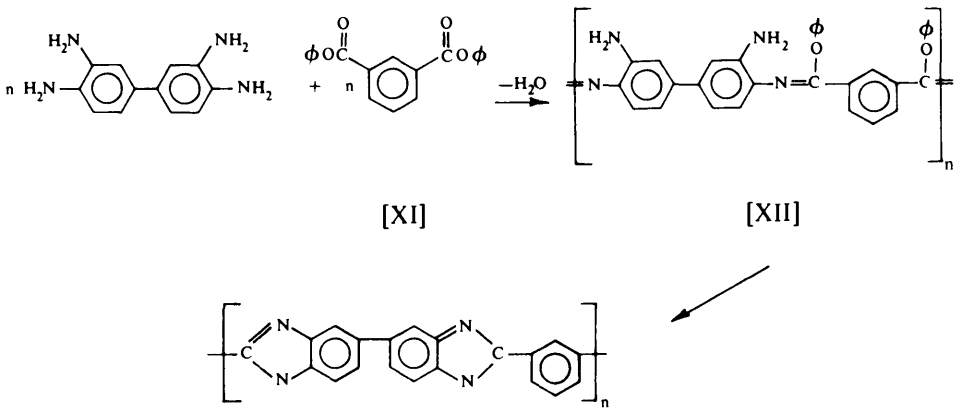

[XI] [XII]

[XIII] (5.JJ)

Another interesting structure with a high degree of ring character along the backbone is the product obtained by the reaction of 1,4-cyclohexanedione [XIV] and pentaerythritol [XV]:

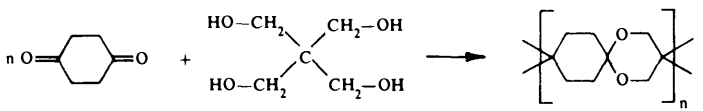

[XIV] [XV] (5.KK)

The backbone here is made up of six-membered rings in which the two rings share a common atom. These are called spiro polymers.

Lastly, we consider a class of compounds called ladder polymers, which are made up of a double-stranded backbone that is linked at regular intervals into rings so that the schematic structure is

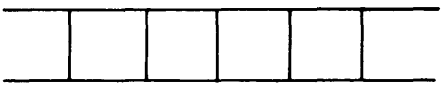

Spiro polymers are also sometimes classified as ladder polymers, and molecules in which the ladder structure is interrupted by periodic single bonds are called semiladders. Consisting entirely of fused ring structures, ladder polymers possess very rigid chains with excellent thermal stability.

Discussion of ladder polymers also enables us to introduce a step-growth polymerization that deviates from the simple condensation reactions which we have described almost exclusively in this chapter. The Diels–Alder reaction is widely used in the synthesis of both ladder and semiladder polymers. In general, the Diels–Alder reaction occurs between a diene [XVI] and a dienophile [XVII] and yields an adduct with a ring structure [XVIII]:

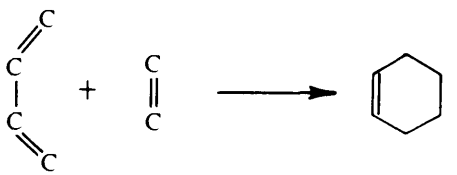

(5.LL)

[XVI] [XVII] [XVIII]

Since the six carbons shown above have 10 additional bonds, the variety of substituents they carry or the structures they can be a part of is quite varied, making the Diels–Alder reaction a powerful synthetic tool in organic chemistry. A moment's reflection will convince us that a molecule like structure [XVI] is monofunctional from the point of view of the Diels–Alder condensation. If the Diels–Alder reaction is to be used for the preparation of polymers, the reactants must be bis-dienes and bis-dienophiles. If the diene, the dienophile, or both are part of a ring system to begin with, a polycyclic product results. One of the first high molecular weight polymers prepared by this synthetic route was the product resulting from the reaction of 2-vinyl butadiene [XIX] and benzoquinone [XX]:

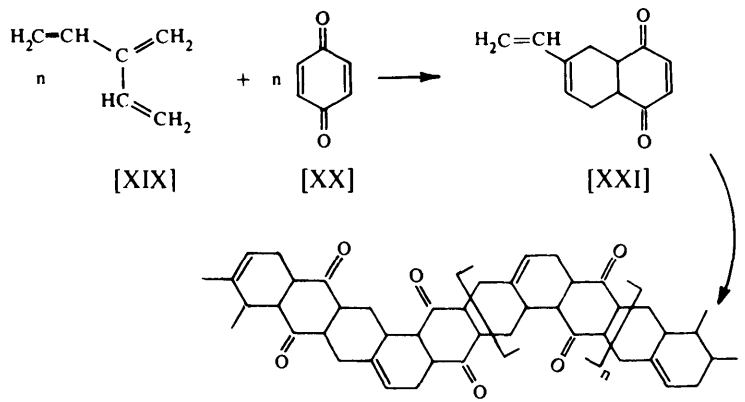

[XIX] [XX] [XXI] (5.MM)

The bifunctionality of the bis-diene and bis-dienophile monomers is apparent from the condensation product, structure [XXI], which still contains a diene and a dienophile in the same molecule. This polymer is crystalline, indicating a high degree of stereoregularity in the condensed rings. It decomposes to a graphitic material before melting.

It is also possible for a single monomer to behave as both diene and dienophile. Heating diacetylene [XXII] produces an infusible material which may be rationalized as follows:

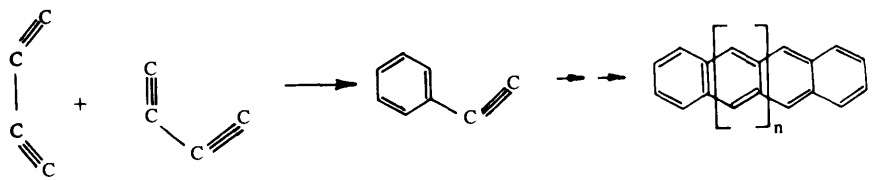

[XXII] (5.NN)

Because of the versatility of the Diels–Alder reaction, an impressive assortment of complex ladder and semiladder polymers have been synthesized; this continues to be a fruitful area of research.

Problems

1. Howard† describes a model system used to test the molecular weight distribution of a condensation polymer: "The polymer sample was an acetic acid-stabilized equilibrium nylon-6,6. Analysis showed it to have the following end group composition (in equivalents per 10^6 g):acetyl = 28.9,

†G. J. Howard, *J. Polym. Sci.* 37:310 (1959).

amine = 35.3 and carboxyl = 96.5. The number average degree of polymerization is, therefore, 110 and the conversion degree (= extent of reaction) = 0.9909." Verify the self-consistency of these numbers.

2. Haward et al.† have reported some research in which a copolymer of styrene and hydroxyethylmethacrylate was cross-linked by hexamethylene diisocyanate. Draw the structural formula for a portion of this cross-linked polymer and indicate what part of the molecule is the result of a condensation reaction and what part results from addition polymerization. These authors indicate that the crosslinking reaction is carried out in sufficiently dilute solutions of copolymer that the crosslinking is primarily intramolecular rather than intermolecular. Explain the distinction between these two terms and why concentration affects the relative amounts of each.
3. The polymerization of β-carboxymethyl caprolactam has been observed to consist of initial isomerization via a second-order kinetic process followed by condensation of the isomer to polymer:

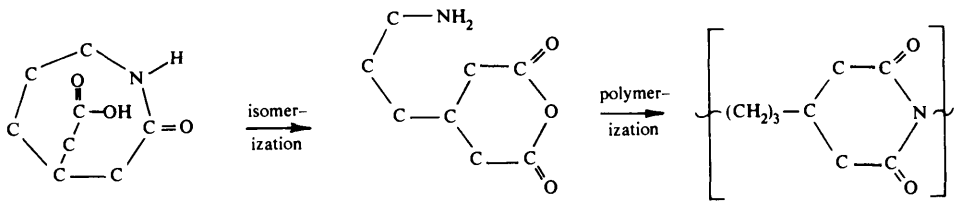

The rate of polymerization is thus first order in ν_{NH_2} and first order in $\nu_{(CO)_2O}$ or second order overall. Since $\nu_{NH_2} = \nu_{(CO)_2O}$, rate = kc^2, if catalyzed; third order is expected under uncatalyzed conditions. The indirect evaluation of c was accomplished by measuring the amount of monomer reacted, and the average degree of polymerization of the mixture was determined by viscosity at different times. The following data‡ were obtained at 270°C (the early part of the experiment gives nonlinear results).

t (min)	c (mole fraction)	t (min)	c (mole fraction)
20	0.042	90	0.015
30	0.039	110	0.013
40	0.028	120	0.012
50	0.024	150	0.0096
60	0.021	180	0.0082
80	0.018		

† R. N. Haward, B. M. Parker, and E. F. T. White, *Adv. Chem.* 91:498 (1969).
‡ H. K. Reimschuessel, *Adv. Chem.* 91:717 (1969).

Graphically test whether these data indicate catalyzed or uncatalyzed conditions and evaluate the rate constant for polymerization at 270°C. Propose a name for the polymer.

4. Examination of Fig. 5.5 shows that N_n/N is greater for n = 40 at p = 0.97 than at either p = 0.95 or p = 0.99. This is generally true: Various n-mers go through a maximum in numerical abundance as p increases. Show that the extent of reaction at which this maximum occurs varies with n as follows: $p_{max} = (n - 1)/(n + 1)$. For a catalyzed AB reaction, extend this expression to give a function for the time required for an n-mer to reach its maximum numerical abundance. If $k_c = 2.47 \times 10^{-4}$ liter mol^{-1} sec^{-1} at 160.5°C for the polymerization of 12-hydroxystearic acid,† calculate the time at which 15-mers show their maximum abundance if the initial concentration of monomer is 3.0 M.
5. In the presence of a pyridine–cuprous chloride catalyst, the following polymerization occurs:

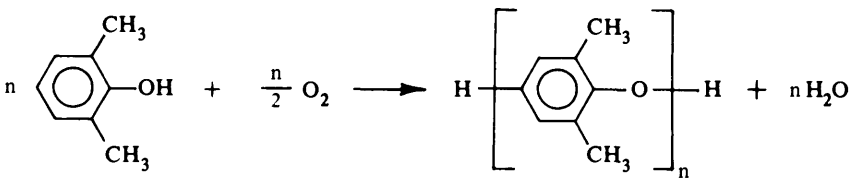

(monomer)

In an investigation to examine the mechanism of this reaction, the dimer (n = 2)

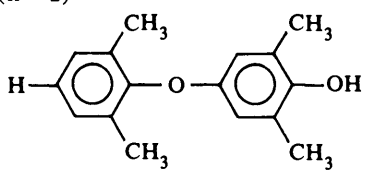

was used as a starting material. The composition of the mixture was studied as the reaction progressed and the accompanying results were obtained‡:

Percent of theoretical O_2 absorbed	Weight percent composition in reaction mixture			
	Monomer	Dimer	Trimer	Tetramer
9	1	69	15	9
12	1.5	68	24	9
20	3	38.5	23	9
35	6	26	21	11
60	11	4	4	1
80	1	0	0	0

†C. E. H. Bawn and M. B. Huglin, *Polymer* 3:257 (1962).

‡G. D. Cooper and A. Katchman, *Adv. Chem.* 91:660 (1969).

Plot a family of curves, each of different n, with composition as the y axis and O_2 absorbed as the x axis. Evaluate w_n by Eq. (5.30) for n = 1, 2, 3, and 4 and $0.1 \leqslant p \leqslant 0.9$ in increments of 0.1. Plot these results (w_n on y axis) on a separate graph drawn to the same scale as the experimental results. Compare your calculated curves with the experimental curves with respect to each of the following points: (1) coordinates used, (2) general shape of curves, and (3) labeling of curves.

6. The polymer described in the last problem is commercially called poly (phenylene oxide), which is not a proper name for a molecule with this structure. Propose a more correct name. Use the results of the last problem to criticize or defend the following proposition: The experimental data for dimer polymerization can be understood if it is assumed that one molecule of water *and* one molecule of monomer may split out in the condensation step. Steps involving incorporation of the monomer itself (with only water split out) also occur.
7. Taylor† carefully fractionated a sample of nylon-6,6 and determined the weight fraction of different n-mers in the resulting mixture. The following results were obtained:

n	$w_n \times 10^{-4}$	n	$w_n \times 10^{-4}$
12	6.5	311	15.2
35	19.6	334	14.1
58	29.4	357	13.0
81	33.0	380	11.5
104	35.4	403	11.0
127	36.5	426	9.1
150	33.0	449	7.2
173	27.6	472	6.5
196	25.2	495	4.9
219	22.9	518	4.3
242	19.4	541	3.9
265	18.5	564	3.3
288	16.8		

Evaluate $\bar{n}_w$ from these data; then use Eq. (5.32) to calculate the corresponding value of p. Calculate the theoretical weight fraction of n-mers using this value of p and a suitable array of n values. Plot your theoretical curve and the above data points on the same graph. Criticize or defend the following proposition: Although the fit of the data points is acceptable with this value of p, it appears that a slightly smaller value of p would give an even better fit.

† G. B. Taylor, *J. Am. Chem. Soc.* 69:638 (1947).

8. Paper chromatograms were developed for 50:50 blends of nylon-6,6 and nylon-6,10 after the mixtures had been heated at 290°C for various periods of time. The following observations† describe the chromatograms after the indicated times of heating:

   0 hr—two spots with R_f values of individual polymers.
   1/4 hr—two distinct spots, but closer together than those of 0 hr.
   1/2 hr—spots are linked together.
   3/4 hr—one long, diffuse spot.
   1½ hr—one compact spot, intermediate R_f value.

   On the basis of these observations, criticize or defend the following proposition: The fact that the separate spots fuse into a single spot of intermediate R_f value proves that block copolymers form between the two species within the blend upon heating.

9. Reimschuessel and Dege‡ polymerized caprolactam in sealed tubes containing about 0.0205 mol H_2O per mole caprolactam. In addition, acetic acid (V), sebacic acid (S), hexamethylene diamine (H), and trimesic acid (T) were introduced as additives into separate runs. The following table lists (all data per mole caprolactam) the amounts of additive present and the analysis for end groups in various runs:

Additives	Moles additive	$-COOH$ (mEq)	$-NH_2$ (mEq)
None	–	5.40	4.99
V	0.0205	19.8	2.3
S	0.0102	21.1	2.3
H	0.0102	1.24	19.7
T	0.0067	22.0	2.5

   Neglecting end group effects, calculate $\bar{M}_n$ for each of these polymers from the end group data. Are the trends in molecular weight qualitatively what would be expected in terms of the role of the additive in the reaction mixture? Explain briefly.

10. In the study described in the last problem, caprolactam was polymerized for 24 hr at 225°C in sealed tubes containing various amounts of water. $\bar{M}_n$ and $\bar{M}_w$ were measured for the resulting mixture by osmometry and light scattering, respectively, and the following results were obtained§:

†C. W. Ayers, *J. Appl. Chem.* 4:444 (1954).
‡H. K. Reimschuessel and G. J. Dege, *J. Polym. Sci.* A-1:2343 (1971).
§Ibid.

Moles H_2O ($\times 10^3$)/mole caprolactam	$\bar{M}_n \times 10^{-3}$	$\bar{M}_w \times 10^{-3}$
49.3	13.4	20.0
34.0	16.4	25.6
25.6	17.9	29.8
20.5	19.4	36.6

Use the molecular weight ratio to calculate the apparent extent of reaction of the caprolactam in these systems. Is the variation in p qualitatively consistent with your expectations of the effect of increased water content in the system? Plot p versus moisture content and estimate by extrapolation the equilibrium moisture content of nylon-6 at 255°C. Does the apparent equilibrium moisture content of this polymer seem consistent with the value given in Sec. 5.6 for nylon-6,6 at 290°C?

11. At 270°C adipic acid decomposes† to the extent of 0.31 mol % after 1.5 hr. Suppose an initially equimolar mixture of adipic acid and diol achieves a value of p = 0.990 after 1.5 hr. Compare the expected and observed values of $\bar{n}_n$ in this experiment. Criticize or defend the following proposition: The difference between the observed and expected values would be even greater than calculated above if, instead of the extent of reaction being measured analytically, the value of p expected (neglecting decomposition) after 1.5 hr were calculated by an appropriate kinetic equation.
12. The Carothers equation can also be used as the basis for an estimate of the extent of reaction at gelation. Consider the value implied for each of the parameters in the Carothers equation at the threshold of gelation and derive a relationship between p_c and $\bar{f}$ on the basis of this consideration. Compare the predictions of the equation you have derived with those of Eq. (5.47) for a mixture containing 2 mol A_3, 7 mol AA, and 10 mol BB. Criticize or defend the following proposition: The Carothers equation gives a higher value for p_c than Eq. (5.47) because the former is based on the fraction of reactive groups that have reacted and hence considers wasted loops that the latter disregards.
13. For monomers of the AB type, reactions (5.CC) and (5.DD) become AB → (ab) and 2AB → AbaB, respectively. If k_r and k_l are the respective rate constants for these reactions, derive an expression which gives the ring to linear ratio in the product as a function of AB concentration and the two rate constants. Criticize or defend the following proposition‡: To obtain a test of Eq. (5.47) without the complications of intramolecular condensations, a series of otherwise identical polymeriztion reactions could be carried out on monomer mixtures at different concentrations. By

†V. V. Korshak and S. V. Vinogradova, *Polyesters*, Pergamon, Oxford, 1965.

‡W. H. Stockmayer and L. L. Weil, in *Advancing Fronts in Chemistry*, S. B. Twiss (Ed.), Reinhold, New York, 1945.

measuring the values of p_c obtained at different concentrations and extrapolating to zero concentration, an uncomplicated test of gelation theory is obtained.

Bibliography

1. Allcock, H. R., and Lampe, F. W., *Contemporary Polymer Chemistry*, Prentice-Hall, Englewood Cliffs, N.J., 1981.
2. Flory, P. J., *Principles of Polymer Chemistry*, Cornell University Press, Ithaca, N.Y., 1953.
3. Frisch, K. C., and Reegen, S. L. (Eds.), *Ring Opening Polymerization*, Marcel Dekker, New York, 1969.
4. Odian, G., *Principles of Polymerization*, 2nd ed., Wiley, New York, 1981.
5. Solomon, D. H. (Ed.), *Step Growth Polymerizations*, Marcel Dekker, New York, 1972.

6

Addition or Chain-Growth Polymerization

I remember snow, Soft as feathers, Sharp as thumb tacks, . . .
And ice, like vinyl, on the streets,
Cold as silver, White as sheets.

I Remember, words and music by Stephen Sondheim

6.1 Introduction

We indicated in Chap. 1 that the category of addition polymers is best characterized by the mechanism of the polymerization reaction rather than by the addition reaction itself. This is known to be a chain mechanism, so in the case of addition polymers we have chain reactions producing chain molecules. One of the things to bear in mind is the double and different use of the word *chain* in this discussion. The word *chain* continues to offer the best description of the large polymer molecules. A chain reaction, on the other hand, describes a whole series of successive events triggered by some initial occurrence. We sometimes encounter this description of highway accidents in which one traffic mishap on a fogbound highway results in a pileup of colliding vehicles that can extend for miles. In nuclear reactors a cascade of fission reactions occurs which is initiated by the capture of the first neutron. In both of these examples some initiating event is required. This is also true in chain-growth polymerization.

In the above examples the size of the chain can be measured by considering the number of automobile collisions that result from the first accident, or the number of fission reactions which follow from the first neutron capture. When we think about the number of monomers that react as a result of a single initiation step, we are led directly to the degree of polymerization of the resulting molecule. In this way the chain mechanism and the properties of the polymer chains are directly related.

Chain reactions do not go on forever. The fog may clear and the improved visibility ends the succession of accidents. Neutron-scavenging control rods may be inserted to shut down a nuclear reactor. The chemical reactions which terminate polymer chain reactions are also an important part of the polymerization mechanism. Killing off the reactive intermediate that keeps the chain going is the essence of these termination reactions. Some unusual polymers can be formed without this termination; these are called living polymers.

The kind of reaction which produces a dead polymer from a growing chain depends on the nature of the reactive intermediate. These intermediates may be free radicals, anions, or cations. We shall devote most of this chapter to a discussion of the free-radical mechanism, since it readily lends itself to a very general treatment. The discussion of ionic intermediates is not as easily generalized.

In this chapter we deal exclusively with homopolymers. The important case of copolymers formed by the chain mechanism is taken up in the next chapter. The case of copolymerization offers an excellent framework for the comparison of chemical reactivities between different monomer molecules. Accordingly, we defer this topic until Chap. 7, although it is also pertinent to the differences in the homopolymerization reactions of different monomers.

6.2 Chain-Growth and Step-Growth Polymerizations: Some Comparisons

Our primary purpose in this section is to point out some of the similarities and differences between step-growth and chain-growth polymerizations. In so doing we shall also have the opportunity to indicate some of the different types of chain-growth polymerization systems.

In Chap. 5 we saw that step-growth polymerizations occur, one step at a time, through a series of relatively simple organic reactions. By treating the reactivity of functional groups as independent of the size of the molecule carrying the group, the entire course of the polymerization is described by the conversion of these groups to their condensation products. Two consequences of this are that both high yield and high molecular weight require extensive reaction to occur. By contrast, chain-growth polymerization occurs by introducing an active growth center into a monomer, followed by the addition of monomers to that center by a chain-type kinetic mechanism. The active center is ultimately killed off by a termination step. The (average) degree of polymerization that characterizes the system depends on the frequency of addition steps relative to the termination steps. Thus high molecular weight polymer is achieved almost immediately. The only thing that is accomplished by allowing the reaction to proceed somewhat further is an increased yield of polymer. The molecular weight of the product is relatively unaffected. This simple picture tends to

break down at high extents of conversion. For this reason we shall focus attention in this chapter on low conversions to polymer, except in those cases where noted otherwise.

Step-growth polymerizations can be schematically represented by one of the individual reaction steps $\sim A + B\sim \longrightarrow \sim ab\sim$ with the realization that the species so connected can be any molecules containing A and B groups. Chain-growth polymerization, by contrast, requires at least three distinctly different kinds of reactions to describe the mechanism. These three types of reactions will be discussed in the following sections in considerable detail. For now our purpose is to introduce some vocabulary rather than develop any of these beyond mere definitions. The principal steps in the chain growth mechanism are the following:

1. Initiation. An active species I* is formed by the decomposition of an initiator molecule I:

$$I \longrightarrow I^* \tag{6.A}$$

2. Propagation. The initiator fragment reacts with a monomer M to begin the conversion to polymer; the center of activity is retained in the adduct. Monomers continue to add in some way until molecules are formed with degree of polymerization n:

$$I^* + M \longrightarrow IM^* \xrightarrow{M} IMM^* \longrightarrow\longrightarrow\longrightarrow IM_n^* \tag{6.B}$$

   If n is large enough, the initiator fragment—an end group—need not be written explicitly.

3. Termination. By some reaction, generally involving two polymers containing active centers, the growth center is deactivated, resulting in dead polymer:

$$M_n^* + M_{n'}^* \longrightarrow \text{dead polymer} \tag{6.C}$$

Elsewhere in this chapter we shall see that other reactions—notably, chain transfer and chain inhibition—also need to be considered to give a more fully developed picture of chain-growth polymerization, but we shall omit these for the time being. Much of the argumentation of this chapter is based on the kinetics of these three mechanistic steps. We shall describe the rates of the three general kinds of reactions by the notation R_i, R_p, and R_t for initiation, propagation, and termination, respectively.

In the last chapter we presented arguments supporting the idea that reactivity is independent of molecular size. Although the chemical reactions are certainly different in this chapter and the last, we shall continue to maintain this position

for addition polymerization also. For step-growth polymerization this assumption simplified the discussion tremendously and at the same time needed careful qualification. We recall that the equal reactivity premise is valid only after an initial size dependence for smaller molecules. The same variability applies to the propagation step of addition polymerizations for short-chain oligomers, although things soon level off and the assumption of equal reactivity holds. We are thus enabled to treat all propagation steps by the single rate constant k_p. Since the total polymer may be the product of hundreds of such steps, no serious error is made in neglecting the variation that occurs in the first few steps.

In Sec. 5.3 we rationalized that, say, the first 50% of a step-growth reaction might be different from the second 50% because the reaction causes dramatic changes in the polarity of the reaction mixture. We shall see that, under certain circumstances, the rate of addition polymerization accelerates as the extent of conversion to polymer increases due to a composition-dependent effect on termination. In spite of these deviations from the assumption of equal reactivity at all extents of reaction, we continue to make this assumption because of the simplification it allows. We then seek to explain the deviations from this ideal or to find experimental conditions—low conversions to polymer—under which the assumptions apply. This kind of thing is common in chemistry: Most discussions of gases begin with the ideal gas law and describe real gases as deviating from the ideal at high pressures and approaching the ideal as pressure approaches zero.

The active centers that characterize addition polymerization are of two types: free radicals and ions. Throughout most of this chapter we shall focus attention on the free-radical species, since these lend themselves most readily to generalization. Ionic polymerizations not only proceed through different kinds of intermediates but, as a consequence, yield quite different polymers. Depending on the charge of the intermediate, ionic polymerizations are classified as anionic or cationic. These two types of polymerization are discussed in Secs. 6.10 and 6.11, respectively.

In the last chapter we saw that two reactive groups in a molecule are the norm for the formation of linear step-growth polymers. A pair of monofunctional reactants might undergo essentially the same reaction, but no polymer is produced because no additional functional groups remain to react. On the other hand, if a molecule contains more than two reactive groups, then branched or cross-linked products result from step-growth polymerizations. By comparison, a wide variety of unsaturated monomers undergo chain-growth polymerization. A single kind of monomer suffices—more than one yields a copolymer—and only one double bond per monomer may result in branching or crosslinking. For example, the 1,3-addition reaction of butadiene results in a chain which has a substituent vinyl group capable of branch formation. Divinyl benzene is an example of a bifunctional monomer which is used as a crosslinking agent in

chain-growth polymerizations. We shall be primarily concerned with various alkenes as the monomers of interest; however, the carbon–oxygen double bond in aldehydes and ketones can also serve as the unsaturation required for addition polymerization. The polymerization of alkenes yields a carbon atom backbone, while the carbonyl group introduces carbon and oxygen atoms into the backbone. The inadequacy of backbone composition as a basis for distinguishing between addition and condensation polymers is now apparent from both sides. We saw in the last chapter that condensation polymers could be formed with exclusively carbon backbones.

It might be noted that most (not all) alkenes are polymerizable by the chain mechanism involving free-radical intermediates, whereas the carbonyl group is generally not polymerized by the free-radical mechanism. Carbonyl groups and some carbon–carbon double bonds are polymerized by ionic mechanisms. Monomers display far more specificity where the ionic mechanism is involved than with the free-radical mechanism. For example, acrylamide will polymerize through an anionic intermediate but not a cationic one, *N*-vinyl pyrrolidones by cationic but not anionic intermediates, and halogenated olefins by neither ionic species. In all of these cases free-radical polymerization is possible.

The initiators which are used in addition polymerizations are sometimes called catalysts, although strictly speaking this is a misnomer. A true catalyst is recoverable at the end of the reaction, chemically unchanged. This is not true of the initiator molecules in addition polymerizations. Monomer and polymer are the initial and final states of the polymerization process, and these govern the thermodynamics of the reaction; the nature and concentration of the intermediates in the process, on the other hand, determine the rate. This makes initiator and catalyst synonyms for the same material: The former term stresses the effect of the reagent on the intermediate, and the latter its effect on the rate. The term *catalyst* is particularly common in the language of ionic polymerizations, but this terminology should not obscure the importance of the initiation step in the overall polymerization mechanism.

In the next three sections we consider initiation, termination, and propagation steps in the free-radical mechanism for addition polymerization. One should bear in mind that two additional steps, inhibition and chain transfer, are being ignored at this point. We shall take up these latter topics in Sec. 6.8.

6.3 Initiation

In this section we discuss the initiation step of free-radical polymerization. This discussion is centered around initiators and their decomposition behavior. The first requirement for an initiator is that it be a source of free radicals. In addition, the radicals must be produced at an acceptable rate at convenient temperatures; have the required solubility behavior; transfer their activity to

monomers efficiently; be amenable to analysis, preparation, purification, and so on. Some of the most widely used initiator systems are listed below, and Table 6.1 illustrates their behavior by typical reactions:

1. Organic peroxides or hydroperoxides.
2. Azo compounds.
3. Redox systems.
4. Thermal or light energy.

Peroxides and hydroperoxides are useful as initiators because of the low dissociation energy of the O–O bond in these compounds. This very property makes the range of possible compounds somewhat limited because of the instability of these reagents. In the case of azo compounds the homolysis is driven by the liberation of the very stable N_2 molecule, despite the relatively high dissociation energy of the C–N bond. The redox systems listed in Table 6.1 have the advantage of water solubility, although redox systems which operate in organic solvents are also available. One advantage of the redox reactions as a source of free radicals is the fact that these reactions often proceed faster and at lower temperatures than the thermal homolysis of the peroxide and azo compounds.

The initiation reactions shown under the heading of electromagnetic radiation in Table 6.1 indicate two possibilities of a large number of examples that might be cited. One mode of photochemical initiation shown involves the direct excitation of the monomer with subseqent bond rupture. The second example cited is the photolytic fragmentation of initiators such as alkyl halides and ketones. Because of the specificity of light absorption, photochemical initiators include a wider variety of compounds than those which decompose thermally. Photosensitizers can also be used to absorb and transfer radiation energy to either monomer or initiator molecules. Finally we note that high-energy radiation such as x rays and γ rays and particulate radiation such as α or β particles also produce free radicals. These latter sources of radiant energy are nonselective and produce a wider array of initiating species. Even though these high-energy radiations produce both ionic and free-radical species, the polymerizations that are so initiated follow the free-radical mechanism almost exclusively, except at very low temperatures, where ionic intermediates become more stable. We shall not deal further with these high-energy sources of initiating radicals, but we shall return to light as a photochemical initiator because of its role in the evaluation of kinetic rate constants.

All of the reactions listed in Table 6.1 produce free radicals, so we are presented with a number of alternatives for initiating a polymerization reaction. Our next concern is in the fate of these radicals or, stated in terms of our interest in polymers, the efficiency with which these radicals initiate polymerization. Since these free radicals are relatively reactive species, there are a variety of

Table 6.1 Some Examples of Initiation Reactions

1. Organic peroxides or hydroperoxides:

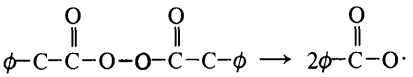

Benzoyl peroxide

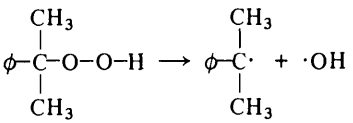

Cumyl hydroperoxide

2. Azo compounds:

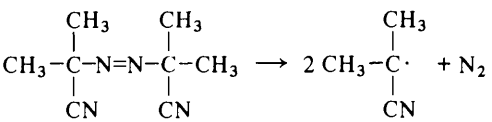

2,2′-Azobisisobutyronitrile (AIBN)

3. Redox systems:

$$H_2O_2 + Fe^{2+} \longrightarrow OH^- + Fe^{3+} + \cdot OH$$

$$S_2O_8^{2-} + Fe^{2+} \longrightarrow SO_4^{2-} + Fe^{3+} + SO_4^{-}\cdot$$

4. Electromagnetic radiation:

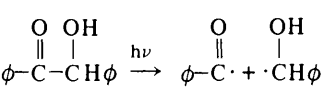

Benzoin

processes they can undergo as alternatives to adding to monomers to commence the formation of polymer.

In discussing mechanism (5.F) in the last chapter we noted that the entrapment of two reactive species in the same solvent cage may be considered a transition state in the reaction of these species. Reactions such as the thermal homolysis of peroxides and azo compounds result in the formation of two radicals already trapped together in a cage that promotes direct recombination, as with the 2-cyanopropyl radicals from 2,2′-azobisisobutyronitrile (AIBN),

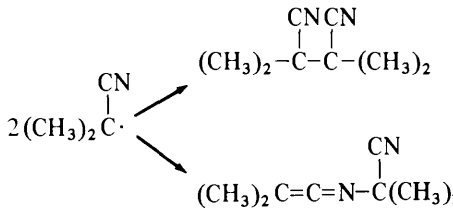

(6.D)

or the recombination of degradation products of the initial radicals, as with acetoxy radicals from acetyl peroxide,

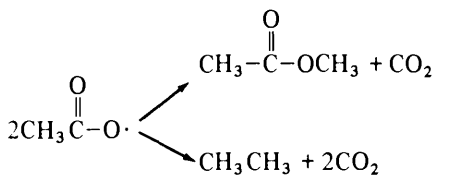

(6.E)

In both of these examples, initiator is consumed, but no polymerization is started.

Once the radicals diffuse out of the solvent cage, reaction with monomer is the most probable reaction in bulk polymerizations, since monomers are the species most likely to be encountered. Reaction with polymer radicals or initiator molecules cannot be ruled out, but these are less important because of the lower concentration of the latter species. In the presence of solvent, reactions between the initiator radical and the solvent may effectively compete with polymer initiation. This depends very much on the specific chemicals involved. For example, carbon tetrachloride is quite reactive toward radicals because of the resonance stabilization of the solvent radical produced [I]:

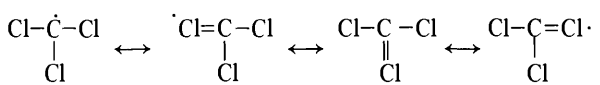

[I]

While this reaction with solvent continues to provide free radicals, these may be less reactive species than the original initiator fragments. We shall have more to say about the transfer of free-radical functionality to solvent in Sec. 6.8.

The significant thing about these and numerous other side reactions that could be described for specific systems is the fact that they lower the efficiency of the initiator in promoting polymerization. To quantify this concept we define the initiator efficiency f to be the following fraction:

$$f = \frac{\text{Radicals incorporated into polymer}}{\text{radicals formed by initiator}} \tag{6.1}$$

The initiator efficiency is not an exclusive property of the initiator alone, but depends on the conditions of the polymerization experiment, including the solvent. In many experimental situations, f lies in the range 0.3–0.8. The efficiency should be regarded as an empirical parameter whose value is determined experimentally. Several methods are used for the evaluation of initiator efficiency, the best being the direct analysis for initiator fragments as end groups compared to the amount of initiator consumed, with proper allowances for stoichiometry. As an end group method, this procedure is difficult in addition polymers, where molecular weights are higher than in condensation polymers. Research with isotopically labeled initiators is particularly useful in this application. Since this quantity is so dependent on the conditions of the experiment, it should be monitored for each system studied.

Scavengers such as diphenylpicrylhydrazyl radicals [II] react with other radicals and thus provide an indirect method for analysis of the number of free radicals in a system:

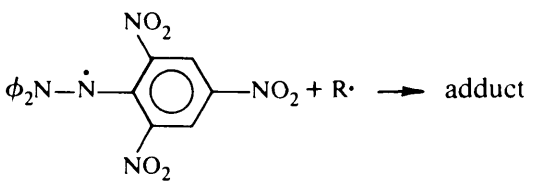

(6.F)

[II]

The diphenylpicrylhydrazyl radical itself is readily followed spectrophotometrically, since it loses an intense purple color on reacting. Unfortunately this reaction is not always quantitative.

We recall some of the ideas of kinetics from the summary given in Sec. 5.2 and recognize that the rates of initiator decomposition can be developed in terms of the reactions listed in the Table 6.1. Using the change in initiator radical concentration $d[I\cdot]/dt$ to monitor the rates, we write the following:

1. For peroxides and azo compounds

$$\frac{d[I\cdot]}{dt} = 2k_d[I] \tag{6.2}$$

where k_d is the rate constant for the homolytic decomposition of the initiator and [I] is the concentration of the initiator. The factor 2 appears because of the stoichiometry in these particular reactions.

2. For redox systems

$$\frac{d[I\cdot]}{dt} = k[Ox][Red] \tag{6.3}$$

where the bracketed terms describe the concentrations of oxidizing and reducing agents and k is the rate constant for the particular reactants.

3. For photochemical initiation

$$\frac{d[I\cdot]}{dt} = 2\phi' I_{abs} \tag{6.4}$$

where I_{abs} is the intensity of the light absorbed and the constant ϕ' is called the quantum yield. The factor 2 is again included for reasons of stoichiometry.

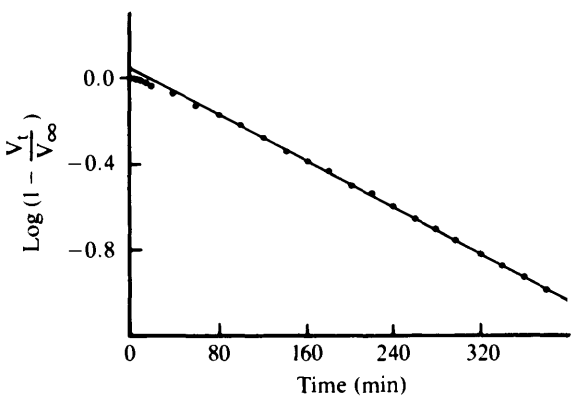

Figure 6.1 Volume of nitrogen evolved from the decomposition of AIBN at 77°C plotted according to the first-order rate law as discussed in Example 6.1. [Reprinted with permission from L. M. Arnett, *J. Am. Chem. Soc.* 74:2027 (1952), copyright 1952 by the American Chemical Society.]

Since $\frac{1}{2}\, d[I\cdot]/dt = -d[I]/dt$ in the case of the azo initiators, Eq. (6.2) can also be written as $-d[I]/dt = k_d[I]$ or, by integration, $\ln([I]/[I]_0) = -k_d t$, where $[I]_0$ is the initiator concentration at $t = 0$. Figure 6.1 shows a test of this relationship for AIBN in xylene at 77°C. Except for a short induction period, the data points fall on a straight line. The evaluation of k_d from these data is presented in the following example.

Example 6.1

The deomposition of AIBN in xylene at 77°C was studied† by measuring the volume of N_2 evolved as a function of time. The volumes obtained at time t and $t = \infty$, are V_t and V_∞, respectively. Show that the manner of plotting used in Fig. 6.1 is consistent with the integrated first-order rate law and evaluate k_d.

Solution

The ratio $[I]/[I]_0$ gives the fraction of initiator remaining at time t. The volume of N_2 evolved is the following:

1. $V_0 = 0$ at $t = 0$ when no decomposition has occurred.
2. V_∞ at $t = \infty$ when complete decomposition has occurred.
3. V_t at time t when some fraction of initiator has decomposed.

Following the logic of Sec. 4.6, the fraction decomposed at t is given by $(V_t - V_0)/(V_\infty - V_0)$ and the fraction remaining at t is $1 - (V_t - V_0)/(V_\infty - V_0) = (V_\infty - V_t)/(V_\infty - V_0)$. Since $V_0 = 0$, this becomes $(V_\infty - V_t)/V_\infty$ or $[I]/[I]_0 = 1 - V_t/V_\infty$. Therefore a plot of $\ln(1 - V_t/V_\infty)$ versus t is predicted to be linear with slope $-k_d$. If logarithms to base 10 are used, the slope equals $-k_d/2.303$.

From Fig. 6.1,

$$\text{Slope} = \frac{-0.4 - (-0.8)}{160 - 320} = -2.5 \times 10^{-3}\ \text{min}^{-1} = \frac{-k_d}{2.303}$$

$$k_d = 5.8 \times 10^{-3}\ \text{min}^{-1}$$

•

Next we assume that a fraction f of these initiator fragments actually reacts with monomer to transfer the radical functionality to monomer:

$$I\cdot + M \xrightarrow{f} IM\cdot \qquad (6.G)$$

† L. M. Arnett, *J. Am. Chem. Soc.* 74:2027 (1952).

As indicated in the last section, we regard the reactivity of the species $IM_n\cdot$ to be the same regardless of the value of n. Accordingly, all subsequent additions to IM· in reaction (6.G) are propagation steps and reaction (6.G) represents the initiation of polymerization. Although it is premature at this point, we disregard end groups and represent the polymeric radicals of whatever size by the symbol M·. Accordingly, we write the following for the initiation of polymer radicals:

1. By peroxides and azo compounds,

$$\frac{d[M\cdot]}{dt} = 2fk_d[I] \tag{6.5}$$

2. By redox systems,

$$\frac{d[M\cdot]}{dt} = fk[Ox][Red] \tag{6.6}$$

3. By photochemical initiation,

$$\frac{d[M\cdot]}{dt} = 2f\phi'\mathbf{I}_{abs} = 2\phi\mathbf{I}_{abs} \tag{6.7}$$

where we have combined the factors f and ϕ' into a composite quantum yield ϕ, since both of the separate factors are measures of efficiency.

Any one of these expressions gives the rate of initiation R_i for the particular catalytic system employed. We shall focus attention on the homolytic decomposition of a single initiator as the mode of initiation throughout most of this chapter, since this reaction typifies the most widely used free-radical initiators. Appropriate expressions for initiation which follows Eq. (6.6) are readily derived.

An important application of photochemical initiation is in the determination of the rate constants which appear in the overall analysis of the chain-growth mechanism. Although we shall take up the details of this method in Sec. 6.6, it is worthwhile to develop Eq. (6.7) somewhat further at this point. It is not possible to give a detailed treatment of light absorption here. Instead, we summarize some pertinent relationships and refer the reader who desires more information to textbooks of physical or analytical chemistry. The following results will be useful:

1. The intensity of light transmitted (subscript t) through a sample $\mathbf{I}_t$ depends on the intensity of the incident (subscript 0) light $\mathbf{I}_0$, the thickness l of the sample, and the concentration [c] of the absorbing species,

$$I_t = I_0 e^{-\alpha[c]l} \tag{6.8}$$

where the proportionality constant α is called the absorption coefficient and is a property of the absorber.

2. The absorbance A as measured by spectrophotometers is defined as

$$A = \log_{10}\left(\frac{I_0}{I_t}\right) \tag{6.9}$$

The variation in absorbance with wavelength reflects the wavelength dependence of α.

3. Since I_{abs} equals the difference $I_0 - I_t$,

$$I_{abs} = I_0(1 - e^{-\alpha[c]l}) \tag{6.10}$$

If the exponent in Eq. (6.10) is small—which means dilute solutions in practice, since most absorption experiments are done where α is large—then the exponential can be expanded, $e^x \cong 1 + x + \cdots$, with only the leading terms retained to give

$$I_{abs} = I_0(\alpha[c]l) \tag{6.11}$$

4. Substituting this result into Eq. (6.7) gives

$$\frac{d[M\cdot]}{dt} = 2\phi I_0 \alpha[c]l \tag{6.12}$$

where [c] is the concentration of monomer or initiator for the two reactions shown in Table 6.1.

Note that Eqs. (6.5) and (6.12) are both first-order rate laws, although the physical significance of the proportionality factors is quite different in the two cases. The rate constants shown in Eqs. (6.5) and (6.6) show a temperature dependence described by the Arrhenius equation:

$$k = Ae^{-E^*/RT} \tag{6.13}$$

where E^* is the activation energy, which is interpreted as the height of the energy barrier to a reaction as discussed in Sec. 2.6. Activation energies are evaluated from experiments in which rate constants are measured at different temperatures. Taking logarithms of both sides of Eq. (6.13) gives $\ln k = \ln A - E^*/RT$. Therefore E^* is obtained from the slope of a plot of $\ln k$ against $1/T$. As usual, T is in degrees Kelvin and R and E^* are in the same energy units.

Table 6.2 Rate Constants (at Temperature Given) and Activation Energies for Some Initiator Decomposition Reactions

Initiator	Solvent	T (°C)	k_d (sec^{-1})	E_d* (kJ mol^{-1})
2,2′-Azobisisobutyronitrile	Benzene	70	3.17×10^{-5}	123.4
	CCl_4	40	2.15×10^{-7}	128.4
	Toluene	100	1.60×10^{-3}	121.3
t-Butyl peroxide	Benzene	100	8.8×10^{-7}	146.9
Benzoyl peroxide	Benzene	70	1.48×10^{-5}	123.8
	Cumene	60	1.45×10^{-6}	120.5
t-Butyl hydroperoxide	Benzene	169	2.0×10^{-5}	170.7

Source: Data from J. C. Masson in Ref. 3.

Since E* is positive according to this picture, the form of the Arrhenius equation assures that k gets larger as T increases. This means that a larger proportion of molecules have sufficient energy to surmount the energy barrier at higher temperatures. This of course assumes that thermal energy is the source of E*, something that is not the case in photoinitiated reactions. The effective first-order rate constants k and $I_0\alpha l$—for thermal initiation and photoinitiation, respectively—do not show the same temperature dependence. The former follows the Arrhenius equation, while the latter cluster of terms in Eq. (6.12) is essentially independent of T.

The activation energies for the decomposition (subscript d) reaction of several different initiators in various solvents are shown in Table 6.2. Also listed are values of k_d for these systems at the temperature shown. The Arrhenius equation can be used in the form $\ln(k_{d,1}/k_{d,2}) = -(E^*/R)(1/T_1 - 1/T_2)$ to evaluate k_d values for these systems at temperatures different from those given in Table 6.2.

6.4 Termination

The formation of initiator radicals is not the only process that determines the concentration of free radicals in a polymerization system. Polymer propagation itself does not change the radical concentration; it merely changes one radical to another. Termination steps also occur, however, and these remove radicals from the system. We shall discuss combination and disproportionation reactions as modes of termination.

Termination by combination results in the simultaneous destruction of two radicals by direct coupling:

$$M_n\cdot + \cdot M_{n'} \longrightarrow M_{n+n'} \tag{6.H}$$

The degree of polymerization values in the two combining radicals can have any value, and the molecular weight of the product molecule will be considerably higher on the average than the radicals so terminated. The polymeric product molecule contains two initiator fragments per molecule by this mode of termination.

Termination by disproportionation comes about when an atom, usually hydrogen, is transferred from one polymer radical to another:

$$M_{n-1}-CH_2-\underset{\underset{X}{|}}{\overset{\overset{H}{|}}{C}}\cdot + \cdot\underset{\underset{X}{|}}{\overset{\overset{H}{|}}{C}}-CH_2-M_{n'-1} \longrightarrow M_{n-1}-CH_2CH_2X + CHX=CH-M_{n'-1} \tag{6.I}$$

This mode of termination produces a negligible effect on the molecular weight of the reacting species, but it does produce a terminal unsaturation in one of the dead polymer molecules. Each polymer molecule contains one initiator fragment when termination occurs by disproportionation.

A kinetic analysis of the two modes of termination is quite straightforward, since each mode of termination involves a bimolecular reaction between two radicals. Accordingly, we write the following:

1. For general termination,

$$R_t = \frac{-d[M\cdot]}{dt} = 2k_t[M\cdot]^2 \tag{6.14}$$

   where R_t and k_t are the rate and rate constant for termination (subscript t) and the factor 2 enters because two radicals are lost for each termination step.

2. The polymer radical concentration in Eq. (6.14) represents the total concentration of all such species, regardless of their degree of polymerization; that is,

$$[M\cdot] = \sum_{\text{all } n} [M_n\cdot] \tag{6.15}$$

3. For combination,

$$R_t = \frac{-d[M\cdot]}{dt} = 2k_{t,c}[M\cdot]^2 \tag{6.16}$$

   where the subscript c specifically indicates termination by combination.

4. For disproportionation,

$$R_t = \frac{-d[M\cdot]}{dt} = 2k_{t,d}[M\cdot]^2 \tag{6.17}$$

where the subscript d specifically indicates termination by disproportionation.

5. In the event that the two modes of termination are not distinguished, Eq. (6.14) represents the sum of Eqs. (6.16) and (6.17), or

$$k_t = k_{t,c} + k_{t,d} \tag{6.18}$$

Combination and disproportionation are competitive processes and do not occur to the same extent for all polymers. For example, at 60°C termination is virtually 100% by combination for polyacrylonitrile and 100% by disproportionation for poly(vinyl acetate). For polystyrene and poly(methyl methacrylate), both reactions contribute to termination, although each in different proportions. Each of the rate constants for termination individually follows the Arrhenius equation, so the relative amounts of termination by the two modes is given by

$$\frac{\text{Termination by combination}}{\text{termination by disproportionation}} = \frac{k_{t,c}}{k_{t,d}} = \frac{A_{t,c}\, e^{-E_{t,c}^*/RT}}{A_{t,d}\, e^{-E_{t,d}^*/RT}}$$

$$= \frac{A_{t,c}}{A_{t,d}} \exp\left(\frac{-(E_{t,c}^* - E_{t,d}^*)}{RT}\right) \tag{6.19}$$

Since the disproportionation reaction requires bond breaking, which is not required for combination, $E_{t,d}^*$ is expected to be greater than $E_{t,c}^*$. This causes the exponential to be large at low temperatures, making combination the preferred mode of termination under these circumstances. Note that at higher temperatures this bias in favor of one mode of termination over another decreases as the difference in activation energies becomes smaller relative to the thermal energy RT. The experimental results on modes of termination cited above make it apparent that this qualitative argument must be applied cautiously. The actual determination of the partitioning between the two modes of termination is best accomplished by analysis of end groups, using the difference in end group distribution noted above.

Table 6.3 lists the activation energies for termination (these are overall values, not identified as to mode) of several different radicals. The rate constants for termination at 60°C are also given. We shall see in Sec. 6.6 how these constants are determined.

Table 6.3 Rate Constants at 60°C and Activation Energies for Some Termination Reactions

Monomer	E_t^* (kJ mol^{-1})	$k_{t,60^\circ} \times 10^{-7}$ (liter mol^{-1} sec^{-1})
Acrylonitrile	15.5	78.2
Methyl acrylate	22.2	0.95
Methyl methacrylate	11.9	2.55
Styrene	8.0	6.0
Vinyl acetate	21.9	2.9
2-Vinyl pyridine	21.0	3.3

Source: Data from R. Korus and K. F. O'Driscoll in Ref. 3.

The assumption that k values are constant over the entire duration of the reaction breaks down for termination reactions in bulk polymerizations. Here, as in Sec. 5.2, we can consider the termination process—whether by combination or disproportionation—to depend on the rates at which polymer molecules can diffuse into (characterized by k_i) or out of (characterized by k_o) the same solvent cage and the rate at which chemical reaction between them (characterized by k_r) occurs in that cage. In Chap. 5 we saw that two limiting cases of Eq. (5.8) could be readily identified:

1. Rate of diffusion > rate of reaction [Eq. (5.9)]:

$$k_t = \frac{k_i}{k_o} k_r \tag{6.20}$$

2. This situation seems highly probable for *step-growth* polymerization because of the high activation energy of many condensation reactions. The constants for the diffusion-dependent steps, which might be functions of molecular size or the extent of the reaction, cancel out.
3. Rate of reaction > rate of diffusion [Eq. (5.10)]:

$$k_t = k_i \tag{6.21}$$

4. This situation is expected to apply to radical termination, especially by combination, because of the high reactivity of the trapped radicals. Only one constant appears which depends on the diffusion of the polymer radicals, so it cannot cancel out and may be the source of a dependence of the rate constant on the extent of reaction or degree of polymerization.

Figure 6.2 shows how the percent conversion of methyl methacrylate to polymer varies with time. These experiments were carried out in benzene at

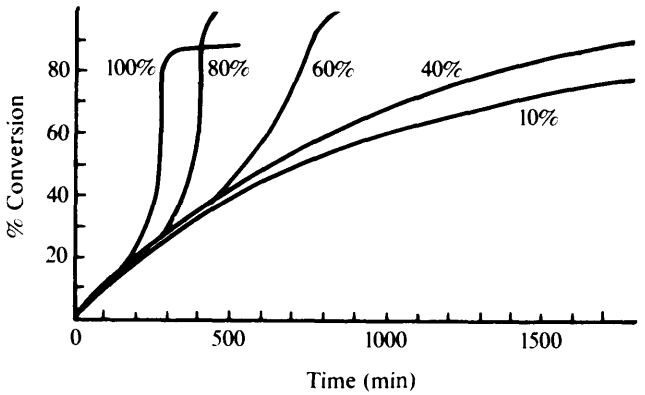

Figure 6.2 Acceleration of the polymerization rate for methyl methacrylate at the concentrations shown in benzene at 50°C. [Reprinted from G. V. Schulz and G. Haborth, *Makromol. Chem.* 1:106 (1948).]

50°C. The different curves correspond to different concentrations of monomer. Up to about 40% monomer, the conversion varies smoothly with time, gradually slowing down at higher conversions owing to the depletion of monomer. At high concentrations, however, the polymerization starts to show an acceleration between 20 and 40% conversion. This behavior, called the Trommsdorff effect, is attributed to a decrease in the rate of termination with increasing conversion. This, in turn, is due to the increase in viscosity which has an adverse effect on k_t through Eq. (6.21). Considerations of this sort are important in bulk polymerizations where high conversion is the objective, but this complication is something we wish to avoid. Hence we shall be mainly concerned with solution polymerization and/or low degrees of conversion where k_t may be justifiably treated as a true constant. We shall see in Sec. 6.8 that the introduction of solvent is accompanied by some complications of its own, but we shall ignore this possibility for now.

Polymer propagation steps do not change the total radical concentration, so we recognize that the two opposing processes, initiation and termination, will eventually reach a point of balance. This condition is called the stationary state and is characterized by a constant concentration of free radicals. Under stationary-state conditions (subscript s) the rate of initiation equals the rate of termination. Using Eq. (6.2) for the rate of initiation (that is, two radicals produced per initiator molecule) and Eq. (6.14) for termination, we write

$$2fk_d[I] = 2k_t[M\cdot]_s^2 \tag{6.22}$$

or

$$[M\cdot]_s = \left(\frac{fk_d}{k_t}\right)^{1/2} [I]^{1/2} \tag{6.23}$$

This important equation shows that the stationary-state free-radical concentration increases with $[I]^{1/2}$ and varies directly with $k_d^{1/2}$ and inversely with $k_t^{1/2}$. The concentration of free radicals determines the rate at which polymer forms and the eventual molecular weight of the polymer, since each radical is a growth site. We shall examine these aspects of Eq. (6.23) in the next section. We conclude this section with a numerical example which concerns the stationary-state radical concentration for a typical system.

Example 6.2

For an initiator concentration which is constant at $[I]_0$, the *non-stationary-state* radical concentration varies with time according to the following expression:

$$\frac{[M\cdot]}{[M\cdot]_s} = \frac{\exp[(16fk_dk_t[I]_0)^{1/2}t] - 1}{\exp[(16fk_dk_c[I]_0)^{1/2}t] + 1}$$

Calculate $[M\cdot]_s$ and the time required for the free-radical concentration to reach 99% of this value using the following as typical values for constants and concentrations: $k_d = 1.0 \times 10^{-4}$ sec^{-1}, $k_t = 3 \times 10^7$ liter mol^{-1} sec^{-1}, $f = \frac{1}{2}$, and $[I]_0 = 10^{-3}$ M. Comment on the assumption $[I] = [I]_0$ that is made in deriving the non-stationary-state equation.

Solution

Use Eq. (6.23) to evaluate $[M\cdot]_s$ for the system under consideration:

$$[M\cdot]_s = \left(\frac{fk_d}{k_t}[I]_0\right)^{1/2} = \left(\frac{(\frac{1}{2})(1.0 \times 10^{-4})(10^{-3})}{3 \times 10^7}\right)^{1/2} = (1.67 \times 10^{-15})^{1/2}$$

$$= 4.08 \times 10^{-8} \text{ mol liter}^{-1}$$

This low level of concentration is typical of free-radical polymerizations. Next we inquire how long it will take the free-radical concentration to reach $0.99[M\cdot]_s$, or 4.04×10^{-8} mol liter^{-1} in this case. Let $a = (16fk_dk_t[I]_0)^{1/2}$ and rearrange the expression given to solve for t when $[M\cdot]/[M\cdot]_s = 0.99$: $0.99(e^{at} + 1) = e^{at} - 1$, or $1 + 0.99 = e^{at}(1 - 0.99)$. Therefore the product $at = \ln(1.99/0.01) = \ln 199 = 5.29$, and $a = [16(\frac{1}{2})(1.0 \times 10^{-4})(3 \times 10^7)(10^{-3})]^{1/2} = 4.90$ sec^{-1}. Hence $t = 5.29/4.90 = 1.08$ sec. This short period is also typical of the time required to reach the stationary state.

The assumption that $[I] = [I]_0$ may be assessed by examining the integrated form of Eq. (6.2) for this system and calculating the ratio $[I]/[I]_0$ after 1.08 sec:

$$\ln\left(\frac{[I]}{[I]_0}\right) = -k_d t = -(1.0 \times 10^{-4})(1.08) = -1.08 \times 10^{-4}$$

$$\frac{[I]}{[I]_0} = 0.99989$$

Over the time required to reach the stationary state, the initiator concentration is essentially unchanged. As a matter of fact, it would take about 100 sec for [I] to reach $0.99[I]_0$ and about 8.5 min to reach $0.95[I]_0$, so the assumption that $[I] = [I]_0$ is entirely justified over the short time involved.

•

6.5 Propagation

The propagation of polymer chains is easy to consider under stationary-state conditions. As the preceding example illustrates, the stationary state is reached very rapidly, so we lose only a brief period at the start of the reaction by restricting ourselves to the stationary state. Of course, the stationary-state approximation breaks down at the end of the reaction also, when the radical concentration drops toward zero. We shall restrict our attention to relatively low conversion to polymer, however, to avoid the complications of the Trommsdorff effect. Therefore deviations from the stationary state at long times need not concern us.

Consideration of reaction (6.B) leads to

$$\frac{-d[M]}{dt} = k_p[M][M\cdot] \tag{6.24}$$

as the expression for the rate at which monomer is converted to polymer. In writing this expression, we assume the following:

1. The radical concentration has the stationary-stage value given by Eq. (6.23).
2. k_p is a constant independent of the size of the growing chain and the extent of conversion to polymer.
3. The rate at which monomer is consumed is equal to the rate of polymer formation R_p:

$$\frac{-d[M]}{dt} = \frac{d[\text{polymer}]}{dt} = R_p \tag{6.25}$$

Combining Eqs. (6.23) and (6.24) yields

$$R_p = k_p[M]\left(\frac{fk_d}{k_t}\right)^{1/2}[I]^{1/2} = k_{app}[M][I]^{1/2} \tag{6.26}$$

in which the second form reminds us that an experimental study of the rate of polymerization yields a single constant (subscript app) which the mechanism reveals to be a composite of three different rate constants. Equation (6.26) shows that the rate of polymerization is first order in monomer and half order in initiator and depends on the rate constants for each of the three types of steps—initiation, propagation, and termination—that make up the chain mechanism. Since the concentrations change with time, it is important to realize that Eq. (6.26) gives an instantaneous rate of polymerization at the concentrations considered. The equation can be applied to the initial concentrations of monomer and initiator in a reaction mixture only to describe the initial rate of polymerization. Unless stated otherwise, we shall assume the initial conditions apply when we use this result.

The initial rate of polymerization is a measurable quantity. The amount of polymer formed after various times in the early stages of the reaction can be determined directly by precipitating the polymer and weighing. Alternatively, some property such as the volume of the system (or the density, the refractive index, or the viscosity) can be measured. Using an analysis like that followed in Sec. 4.6 or Example 6.1, we can relate the values of the property measured at t, $t = 0$, and $t = \infty$ to the fraction of monomer converted to polymer. If the rate of polymerization is measured under known and essentially constant concentrations of monomer and initiator, then the cluster of contants $(fk_p^2k_d/k_t)^{1/2}$ can be evaluated from the experiment. As noted above, f is best investigated by end group analysis. Even with the factor f excluded, experiments on the rate of polymerization still leave us with a single numerical value for a cluster of three constants: one equation with three unknowns. Two other measurable relationships among these unknowns must be found if the individual constants are to be resolved. In anticipation of this development, we list values of k_p and the corresponding activation energies for several common monomers in Table 6.4.

Equation (6.26) is an important result which can be expressed in several alternate forms:

1. The variation in monomer concentration may be taken into account by writing the equation in the integrated form and treating the initiator concentration as constant at $[I]_0$ over the interval considered:

$$\ln\left(\frac{[M]}{[M]_0}\right) = -\left(\frac{fk_p^2k_d}{k_t}[I]_0\right)^{1/2}t \tag{6.27}$$

where $[M] = [M]_0$ at $t = 0$.

Table 6.4 Rate Constants at 60°C and Activation Energies for Some Propagation Reactions

Monomer	E_p^* (kJ mol^{-1})	$k_{p,60°} \times 10^{-3}$ (liter mol^{-1} sec^{-1})
Acrylonitrile	16.2	1.96
Methyl acrylate	29.7	2.09
Methyl methacrylate	26.4	0.515
Styrene	26.0	0.165
Vinyl acetate	18.0	2.30
2-Vinyl pyridine	33.0	0.186

Source: Data from R. Korus and K. F. O'Driscoll in Ref. 3.

2. Instead of using $2fk_d[I]$ for the rate of initiation, we can simply write this latter quantity as R_i, in which case the stationary-state radical concentration is

$$[M\cdot]_s = \left(\frac{R_i}{2k_t}\right)^{1/2} \tag{6.28}$$

and the rate of polymerization becomes

$$R_p = \left(\frac{k_p^2}{2k_t}\right)^{1/2} R_i^{1/2}[M] \tag{6.29}$$

If the rate of initiation is investigated independently, the rate of polymerization measures a cluster of k_p and k_t.

3. Alternatively, Equations (6.6) and (6.7) can be used as expressions for R_i in Eq. (6.29) to describe redox or photoinitiated polymerization.

Figure 6.3 shows some data which constitute a test of Eq. (6.26). In Fig. 6.3a, R_p and [M] are plotted on a log-log scale for a constant level of redox initiator. The slope of this line, which indicates the order of the polymerization with respect to monomer, is unity, showing that the polymerization of methyl methacrylate is first order in monomer. Figure 6.3b is a similar plot of the initial rate of polymerization—which essentially maintains the monomer at constant concentration—versus initiator concentration for several different monomer-initiator combinations. Each of the lines has a slope of ½, indicating a half-order dependence on [I] as predicted by Eq. (6.26).

The apparent rate constant in Eq. (6.26) follows the Arrhenius equation and yields an apparent activation energy:

$$\ln k_{app} = \ln A_{app} - \frac{E_{app}^*}{RT} \tag{6.30}$$

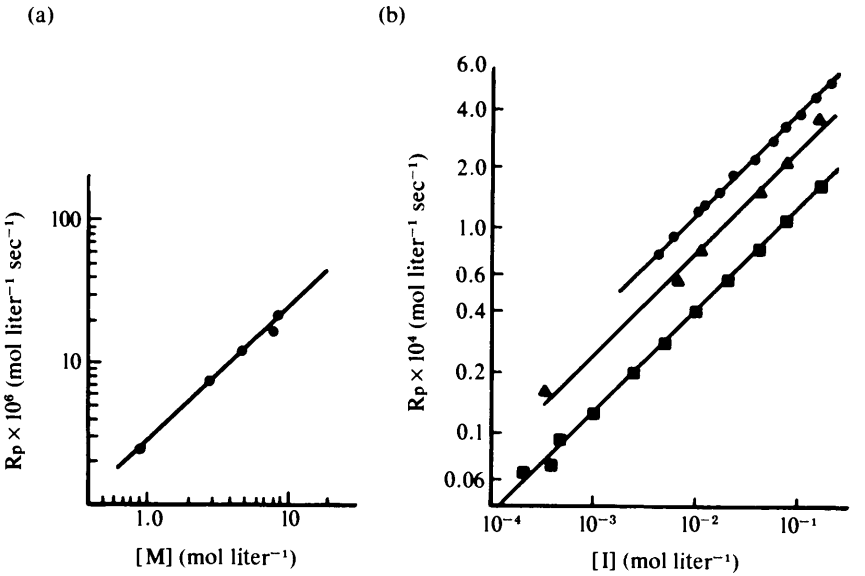

Figure 6.3 Log-log plots of R_p versus concentration which verify the order of the kinetics with respect to the constituent varied. (a) Monomer (methyl methacrylate) concentration varied at constant initiator concentration. [Data from T. Sugimura and Y. Minoura, *J. Polym. Sci.* A-1:2735 (1966).] (b) Initiator concentration varied: AIBN in methy methacrylate (○), benzoyl peroxide in styrene (□), and benzoyl peroxide in methyl methacrylate (△). (From P. J. Flory, *Principles of Polymer Chemistry*, copyright 1953 by Cornell University, used with permission.)

The mechanistic analysis of the rate of polymerization and the fact that the separate constants individually follow the Arrhenius equation means that

$$\ln k_{app} = \ln k_p \left(\frac{k_d}{k_t}\right)^{1/2} = \ln A_p \left(\frac{A_d}{A_t}\right)^{1/2} - \frac{E_p^* + E_d^*/2 - E_t^*/2}{RT} \tag{6.31}$$

This enables us to identify the apparent activation energy in Eq. (6.30) with the difference in E* values for the various steps:

$$E_{app}^* = E_p^* + \frac{E_d^*}{2} - \frac{E_t^*}{2} \tag{6.32}$$

Equation (6.32) allows us to conveniently assess the effect of temperature variation on the rate of polymerization. This effect is considered in the following example.

Example 6.3

Using typical activation energies out of Tables 6.2-6.4, estimate the percent change in the rate of polymerization with a 1°C change in temperature at 50°C for thermally initiated and photinitiated polymerization.

Solution

Write Eq. (6.26) in the form

$$\ln R_p = \ln k_{app} + \ln[M] + \tfrac{1}{2} \ln[I]$$

Taking the derivative, treating [M] and [I] as constants with respect to T while k is a function of T:

$$d \ln R_p = \frac{dR_p}{R_p} = d \ln k_{app}$$

Expand $d \ln k_{app}$ by means of the Arrhenius equation via Eq. (6.31):

$$\frac{dR_p}{R_p} = d \ln A_{app} - d\left(\frac{E_{app}^*}{RT}\right) = \frac{E_{app}^*}{RT^2} dT$$

Substitute Eq. (6.32) for E_{app}^*:

$$\frac{dR_p}{R_p} = \frac{E_p^* + E_d^*/2 - E_t^*/2}{RT^2} dT$$

Finally we recognize that a 1°C temperature variation can be approximated as dT and that $(dR_p/R_p) \times 100$ gives the approximate percent change in the rate of polymerization. Taking average values of E* from the appropriate tables, we obtain $E_d^* = 145$, $E_t^* = 16.8$, and $E_p^* = 24.9$ kJ mol^{-1}. For thermally initiated polymerization

$$\frac{dR_p}{R_p} = \frac{(24.9 + 145/2 - 16.8/2)(10^3)(1)}{(8.314)(323)^2} = 0.103$$

or 10.3% per degree Celsius.

For photoinitiation there is no activation energy for the initiator decomposition; hence

$$\frac{dR_p}{R_p} = \frac{(24.9 - 16.8/2)(10^3)(1)}{(8.314)(323)^2} = 1.90 \times 10^{-2}$$

or 1.90% per degree Celsius.

Note that the initiator decomposition makes the largest contribution to E*; therefore photoinitiated processes display a considerably lower temperature dependence for the rate of polymerization.

•

Suppose we consider the ratio

$$R_p/R_i = \frac{-d[M]/dt}{-d[I]/dt}$$

under conditions where an initiator yields one radical, where f = 1 and where the final polymer contains one initiator fragment per molecule. For this set of conditions the ratio gives the number of monomer molecules polymerized per chain initiated, which is the degree of polymerization. A more general development of this idea is based on a quantity called the kinetic chain length $\bar{\nu}$. The kinetic chain length is defined as the ratio of the number of propagation steps to the rate of initiation, regardless of the mode of termination:

$$\bar{\nu} = \frac{R_p}{R_i} = \frac{R_p}{R_t} \tag{6.33}$$

where the second form of this expression uses the stationary-state condition $R_i = R_t$. The significance of the kinetic chain length is seen in the following statements:

1. For termination by disproportionation

$$\bar{\nu} = \bar{n}_n \tag{6.34}$$

2. For termination by combination

$$\bar{\nu} = \tfrac{1}{2}\bar{n}_n \tag{6.35}$$

3. $\bar{\nu}$ is an average quantity—indicated by the overbar—since not all kinetic chains are identical any more than all molecular chains are.

Using Eqs. (6.26) and (6.17) for R_p and R_t, respectively, we write

$$\bar{\nu} = \frac{k_p[M\cdot][M]}{2k_t[M\cdot]^2} = \frac{k_p[M]}{2k_t[M\cdot]} \tag{6.36}$$

This may be combined with Eq. (6.23) to give the stationary-state value for $\bar{\nu}$:

$$\bar{\nu} = \frac{k_p[M]}{2k_t(fk_d[I]/k_t)^{1/2}} = \frac{k_p[M]}{2(fk_tk_d[I])^{1/2}} \tag{6.37}$$

As with the rate of polymerization, we see from Eq. (6.37) that the kinetic chain length depends on the monomer and initiator concentrations and on the constants for the three different kinds of kinetic processes that constitute the mechanism. When the initial monomer and initiator concentrations are used, Eq. (6.37) describes the initial polymer formed. The initial degree of polymerization is a measurable quantity, so Eq. (6.37) provides a second functional relationship, different from Eq. (6.26), between experimentally available quantities—$\bar{n}_n$, [M], and [I]—and theoretically important parameters—k_p, k_t, and k_d. Note that the mode of termination which establishes the connection between $\bar{\nu}$ and $\bar{n}_n$ and the value of f are both accessible through end group characterization. Thus we have a second equation with three unknowns; one more and the evaluation of the individual kinetic constants from experimental results will be feasible.

There are several additional points about Eq. (6.37) that are worthy of comment. First it must be recalled that we have intentionally ignored any kinetic factors other than initiation, propagation, and termination. We shall see in Sec. 6.8 that another process, chain transfer, has significant effects on the molecular weight of a polymer. The result we have obtained, therefore, is properly designated as the kinetic chain length without transfer. A second observation is that $\bar{\nu}$ depends not only on the nature and concentration of the monomer, but also on the nature and concentration of the catalyst. The latter determines the number of different sites competing for the addition of monomer, so it is not surprising that $\bar{\nu}$ is decreased by increases in either k_d or [I]. Finally, we observe that both k_p and k_t are properties of a particular monomer. The relative molecular weight that a specific monomer tends toward—all other things being equal—is characterized by the ratio $k_p/k_t^{1/2}$ for a monomer. Using the values in Tables 6.3 and 6.4, we see that $k_p/k_t^{1/2}$ equals 0.678 for methyl acrylate and 0.0213 for styrene at 60°C. The kinetic chain length for poly(methyl acrylate) is thus expected to be about 32 times greater than for polystyrene if the two are prepared with the same initiator (k_d) and the same concentrations ([M] and [I]). Extension of this type of comparison to the degree of polymerization requires that the two polymers compared show the same proportion of the modes of termination. Thus for vinyl acetate (subscript V) relative to acrylonitrile (subscript A) at 60°C, with the same provisos as above, $\bar{\nu}_V/\bar{\nu}_A = 6$ while $\bar{n}_{n,V}/\bar{n}_{n,A} = 3$ because of differences in the mode of termination for the two.

The proviso "all other things being equal" in discussing the last point clearly applies to temperature as well, since the kinetic constants are highly sensitive to temperature. To evaluate the effect of temperature variation on the molecular weight of an addition polymer, we follow the same sort of logic as was used in Example 6.3:

1. Take logarithms of Eq. (6.37):

$$\ln \bar{\nu} = \ln k_p (k_t k_d)^{-1/2} + \ln \left(\frac{[M]}{2(f[I])^{1/2}} \right) \tag{6.38}$$

2. Differentiate with respect to T, assuming the temperature dependence of the concentrations is negligible compared to that of the rate constants:

$$\frac{d\bar{\nu}}{\bar{\nu}} = d \ln k_p - \tfrac{1}{2} d \ln (k_t k_d) \tag{6.39}$$

3. By the Arrhenius equation $d \ln k = -d(E^*/RT) = (E^*/RT^2)\, dT$; therefore

$$\frac{d\bar{\nu}}{\bar{\nu}} = \frac{E_p^* - E_t^*/2 - E_d^*/2}{RT^2}\, dT \tag{6.40}$$

It is interesting to compare the application of this result to thermally initiated and photoinitiated polymerizations as we did in Example 6.3. Again using the average values of the constants from Tables 6.2–6.4 and using T = 50°C, we calculate that $\bar{\nu}$ *decreases* about 6.5% per degree Celsius for thermal initiation and *increases* about 2% per degree for photoinitiation. It is clearly the large activation energy of the initiator dissociation which makes the difference in the two cases. This term is omitted in the case of photoinitiation, where the temperature increase produces a bigger effect on propagation than on termination. On the other hand, for thermal initiation an increase in temperature produces a large increase in the number of growth centers, with the attendant reduction of the average kinetic chain length.

Photoinitiation is not as important as thermal initiation in the overall picture of free-radical chain-growth polymerization. The foregoing discussion reveals, however, that the contrast between the two modes of initiation does provide insight into and confirmation of various aspects of addition polymerization. The most important application of photoinitiated polymerization is in providing a third experimental relationship among the kinetic parameters of the chain mechanism. We shall consider this in the next section.

6.6 Radical Lifetime

In the preceding section we observed that both the rate of polymerization and the degree of polymerization under stationary-state conditions can be interpreted to yield some cluster of the constants k_p, k_t, and k_d. The situation is summarized diagramatically in Fig. 6.4. The circles at the two bottom corners

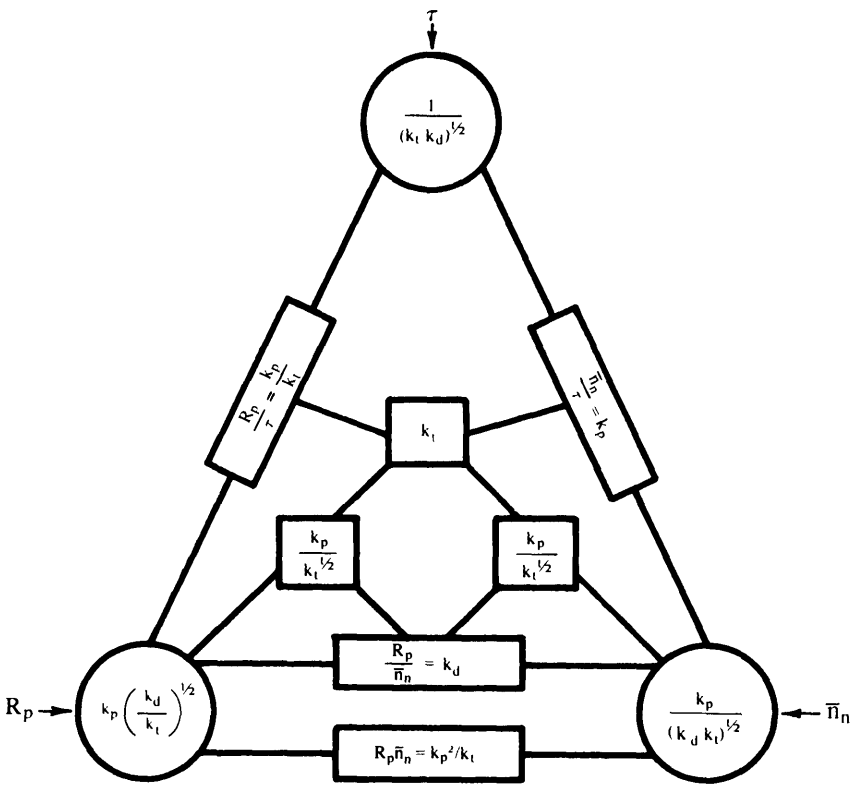

Figure 6.4 Schematic relationship between various experimental quantities (R_p, $\bar{n}_n$, and τ) and the rate constants (k_d, k_p, and k_t) derived therefrom.

of the triangle indicate the particular grouping of constants obtainable from the measurement of R_p or $\bar{n}_n$, as shown. By combining these two sources of data in the manner suggested in the boxes situated along the lines connecting these circles, k_d can be evaluated, as well as the ratio k_p^2/k_t. Using this stationary-state data, however, it is not possible to further resolve the propagation and termination constants. Another relationship is needed to do this. A quantity called the radical lifetime $\bar{\tau}$ supplies the additional relationship and enables us to move off the base of Fig. 6.4.

To arrive at an expression for the radical lifetime, we return to Eq. (6.24), which may be interpreted as follows:

1. d[M]/dt gives the rate at which monomers enter polymer molecules. This, in turn, is given by the product of the number of growth sites, [M·], and

the rate at which monomers add to each growth site. On the basis of Eq. (6.24), the rate at which monomers add to a radical is given by $k_p[M]$.

2. If $k_p[M]$ gives the number of monomers added per unit time, then $1/k_p[M]$ equals the time elapsed per monomer addition.
3. If we multiply the time elapsed per monomer added to a radical by the number of monomers in the average chain, then we obtain the time during which the radical exists. This is the definition of the radical lifetime. The number of monomers in a polymer chain is, of course, the degree of polymerization. Therefore we write

$$\bar{\tau} = \frac{\bar{n}_n}{k_p[M]} \tag{6.41}$$

4. The degree of polymerization in Eq. (6.41) can be replaced with the kinetic chain length, and the resulting expression simplified. To proceed, however, we must choose between the possibilities described by Eqs. (6.34) and (6.35). Assuming termination by disproportionation, we replace $\bar{n}_n$ by $\bar{\nu}$, using Eq. (6.37):

$$\bar{\tau} = \frac{k_p[M]}{2(fk_tk_d[I])^{1/2}} \frac{1}{k_p[M]} = \frac{1}{2(fk_tk_d[I])^{1/2}} \tag{6.42}$$

5. The radical lifetime is an average quantity, indicated by the overbar.

We shall see presently that the lifetime of a radical can be measured. When such an experiment is conducted with a known concentration of initiator, then the cluster of constants $(k_tk_d)^{-1/2}$ can be evaluated. This is indicated at the apex of the triangle in Fig. 6.4.

There are several things about Fig. 6.4 that should be pointed out:

1. In going from the experimental quantities R_p, $\bar{n}_n$, and $\bar{\tau}$ to the associated clusters of constants, it has been assumed that the monomer and initiator concentrations are known and essentially constant. In addition, the efficiency factor f has been left out, the assumption being that still another type of experiment has established its value.
2. By following the lines connecting two sources of circled information, the boxed result in the perimeter of the triangle may be established. Thus k_p is evaluated from τ and $\bar{n}_n$.
3. Here k_p can be combined with one of the various k_p/k_t ratios to permit the evaluation of k_t.

We can use the constants tabulated elsewhere in the chapter to get an idea of a typical radical lifetime. Choosing 10^{-3} M AIBN as the initiator ($k_d = 0.85 \times 10^{-5}$ sec^{-1} at 60°C) and vinyl acetate as the monomer (terminates entirely by

disproportionation, $k_t = 2.9 \times 10^7$ liter mol^{-1} sec^{-1} at 60°C). Taking f = 1 for the purpose of calculation, we find $\tau = \frac{1}{2}[(1.0)(2.9 \times 10^7)(0.85 \times 10^{-5})(10^{-3})]^{-\frac{1}{2}} = 1.01$ sec. This figure contrasts sharply with the times required to obtain high molecular weight molecules in step-growth polymerizations.

Since the radical lifetime provides the final piece of information needed to independently evaluate the three primary kinetic constants—remember, we are still neglecting chain transfer—the next order of business is a consideration of the measurement of $\bar{\tau}$.

A widely used technique for measuring radical lifetime is based on photoinitiated polymerization using a light source which blinks on and off at regular intervals. In practice, a rotating opaque disk with a wedge sliced out of it is interposed between the light and the reaction vessel. Thus the system is in darkness when the solid part of the disk is in the light path and is illuminated when the notch passes. With this device, called a rotating sector, the relative lengths of the light and dark periods can be controlled by the area of the notch, and the frequency of the flickering can be controlled by the velocity of rotation of the disk. For simplicity, we shall consider light and dark periods of equal duration, although this need not be the case.

When results are compared for polymerization experiments carried out at different frequencies of blinking, it is found that the rate depends on that frequency. To see how this comes about, we must examine the variation of radical concentration under non-stationary-state conditions. This consideration dictates the choice of photoinitiated polymerization, since in the latter it is almost possible to turn on or off—with the blink of a light—the source of free radicals. The qualifying *almost* in the previous sentence is actually the focus of our attention, since a short but finite amount of time is required for the radical concentration to reach $[M\cdot]_s$ and a short but finite amount of time is required for it to drop back to zero after the light goes out.

Suppose the radical concentration begins at zero when the light is first turned on at t = 0 (unprimed t represents time in the light; primed t, time in the dark). The radical concentration then increases toward the stationary-state value during the time of illumination. We have already encountered in Example 6.2 the expression which describes the approach of $[M\cdot]$ to $[M\cdot]_s$. The equation is readily derived, but we leave it for Problem 6 at the end of the chapter and simply write the final result:

$$[M\cdot] = [M\cdot]_s \frac{\exp(8R_ik_t)^{\frac{1}{2}}t - 1}{\exp(8R_ik_t)^{\frac{1}{2}}t + 1} \tag{6.43}$$

When $R_i = 2fk_d[I]$, this expression is identical to that given in the example. For photochemical initiation, either Eq. (6.7) or (6.12) can be used for R_i. The result obtained with Eq. (6.12) is particularly informative, since it explicitly

shows the dependence of the radical growth in the system on the incident light intensity I_0. Likewise, the stationary-state free-radical concentration itself depends on the light intensity. Equating Eqs. (6.12) and (6.14), we obtain

$$[M\cdot]_s = \left(\frac{\phi\alpha l[c]}{k_t}\right)^{1/2}\sqrt{I_0} \tag{6.44}$$

where [c] is the concentration of the light-absorbing species. Figure 6.5a shows schematically how the actual radical concentration approaches the stationary-state value.

Next we assume that the light is turned off after the radical concentration has reached $[M\cdot]_s$. Even in the dark the radicals will continue to undergo termination according to Eq. (6.14). Since this occurs without replacement owing to the darkness, the radical concentration decreases with time according to the integrated form of Eq. (6.14):

$$\frac{1}{[M\cdot]} = 2k_t t' + \text{const.} \tag{6.45}$$

The constant of integration in this expression could be evaluated by remembering that $[M\cdot] = [M\cdot]_s$ at $t' = 0$ (prime representing darkness). A qualitative sketch of the decay of the radical concentration is shown in Fig. 6.5b.

If the light source is switched on and off and held for long periods of equal duration in either light or darkness, then the radical concentration in the system will consist of an alternation between the situation described in Figs. 6.5a and b. Because we have specified that the duration of each phase is long, the net behavior is essentially a series of plateaus in which the illumination is either I_0 or zero and the radical concentration is either $[M\cdot]_s$ or zero, with brief transitions in between. This is illustrated in Fig. 6.5c. The concentration of radicals is consistent with I_0, but is present only half of the time; hence the rate of polymerization is only half what it would be for the same illumination operating continuously.

Now suppose we consider another extreme of the same type of experiment. This time we alternate extremely short light and dark periods of equal duration. If we again start with $[M\cdot] = 0$ when the light goes on, we expect the type of behavior shown in Fig. 6.5d, where the radical buildup is interrupted by the extinction of the light before it reaches $[M\cdot]_s$. We could use Eq. (6.43) to evaluate the maximum radical concentration achieved, $[M\cdot]_{max}$, if that were the desired information. The decay of the radical concentration in the dark commences from $[M\cdot]_{max}$ and follows Eq. (6.45). This time the constant integration is evaluated from the fact that $[M\cdot] = [M\cdot]_{max}$ at $t' = 0$. During the dark phase the radical concentration drops to a nonzero value $[M\cdot]_{min}$ before the

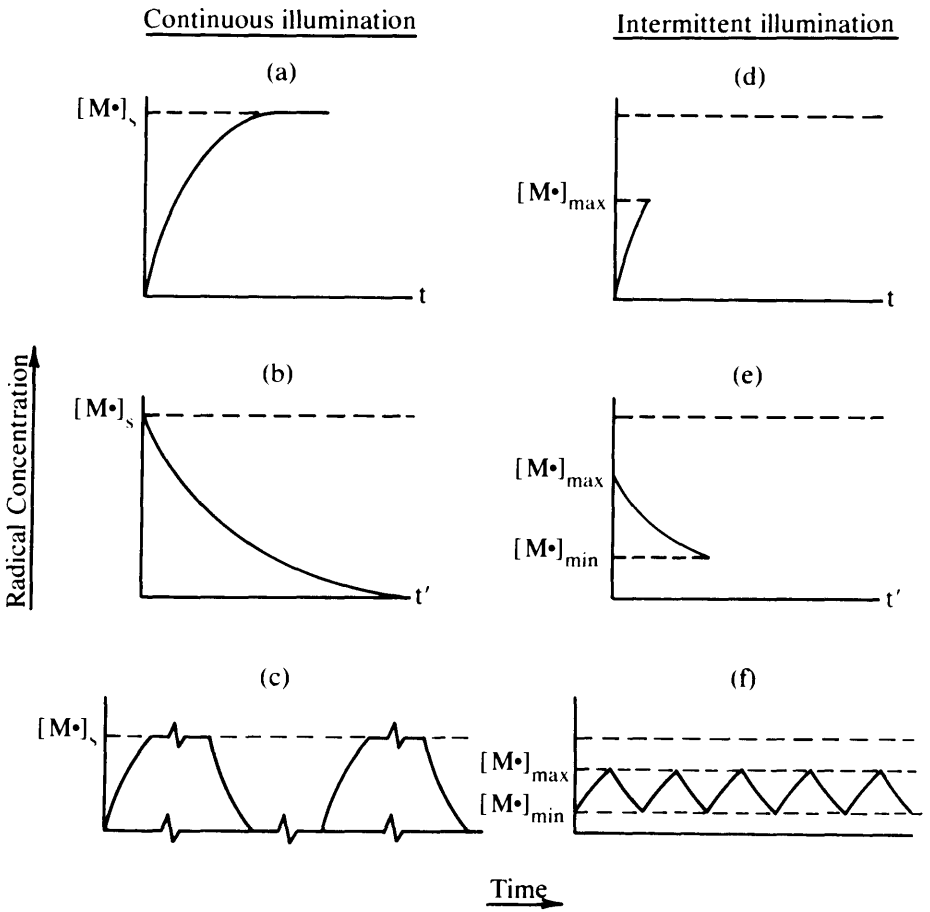

Figure 6.5 Schematic illustrations showing the variation of [M·] with time under conditions of continuous illumination (a–c) and intermittent illumination (d–f). The time in darkness is indicated as t'.

light switches back on again. This is qualitatively sketched in Fig. 6.5e and could be assessed quantitatively via Eq. (6.45). With rapid blinking, the radical concentration alternates between $[M\cdot]_{max}$ and $[M\cdot]_{min}$, as seen in Fig. 6.5f. Although the light is on half the time in this experiment, just as it was in the case of the slower blinking, the concentration of free radicals is always lower, since the time of illumination is never sufficient to reach $[M\cdot]_s$.

As the frequency of blinking increases, the range between $[M\cdot]_{max}$ and $[M\cdot]_{min}$ will narrow, approaching a plateau value below $[M\cdot]_s$ in the limit of

very fast flashing. The radical concentration in this case is consistent with an intensity of illumination $I_0/2$, since the blinking is too fast to cause a perceptible fluctuation in radical concentration, but only half the radiation energy is deposited in the system as would be the case for continuous illumination.

With these ideas as background, we can now consider the formation of polymer in experiments conducted under different conditions of illumination. The rate of polymerization is proportional to the concentration of radicals present in a system. For photoinitiated polymerization this quantity can be changed by varying the frequency of blinking. Thus the rate of polymerization can be measured in a system that is constant with respect to reagents, concentrations, and temperature, but which differs in conditions of illumination. On the basis of the foregoing discussion, we conclude the following for light of intensity I_0:

1. For continuous illumination (i.e., stationary state)

$$(R_p)_{cont} \propto \sqrt{I_0}$$

2. For intermittent illumination with very slow blinking

$$(R_p)_{slow} \propto \tfrac{1}{2} \sqrt{I_0}$$

3. For intermittent illumination with very fast blinking

$$(R_p)_{fast} \propto \sqrt{I_0/2}$$

Thus if we were to compare the rate of polymerization with intermittent illumination relative to that with continuous illumination, but under otherwise identical conditions, we would observe the following limits for equal periods of light and dark:

1. Slow blinking:

$$\frac{(R_p)_{slow}}{(R_p)_{cont}} = \tfrac{1}{2} \tag{6.46}$$

2. Fast blinking:

$$\frac{(R_p)_{fast}}{(R_p)_{cont}} = \frac{1}{\sqrt{2}} \tag{6.47}$$

If the dark period is m times longer than the lit period, then the fraction of time that the sample is illuminated is $1/(1 + m)$($m = 1$ for the case considered above).

For this general case the limits become the following:

3. Slow blinking:

$$\frac{(R_p)_{slow}}{(R_p)_{cont}} = \frac{1}{m+1} \tag{6.48}$$

4. Fast blinking:

$$\frac{(R_p)_{slow}}{(R_p)_{cont}} = \frac{1}{(m+1)^{1/2}} \tag{6.49}$$

Throughout the foregoing discussion, we have used terms like *slow* and *fast blinking* and *long* and *short periods of illumination*. The question that should have been stirring throughout this discussion is, How long a period of time is a lengthy illumination? or How slow is slow? The answer is that times are judged long or short compared to the lifetime of the radical. The radical, after all, is the species that "sees" the light; it is on *its* terms that intervals are described as long or short. Accordingly, we might ask how the rate of polymerization under intermittent illumination might compare with $(R_p)_{cont}$ when the time of illumination is on the order of $\bar{\tau}$.

The rate of polymerization under conditions where the period of illumination is comparable to $\bar{\tau}$ is obtained by integrating Eq. (6.24) in the following form:

$$\int dM = k_p[M]\left\{\int [M\cdot]\, dt + \int [M\cdot]\, dt'\right\} \tag{6.50}$$

The left-hand side of this expression gives the amount of monomer converted to polymer in one light-dark cycle. The first term on the right is integrated over one light period, using Eq. (6.43) for $[M\cdot]$, while the second term is integrated over one dark period, using Eq. (6.45) for $[M\cdot]$. The integration is rather messy, so we forgo the details and simply present the final result. Assuming equal periods for light and dark and expressing the result relative to the stationary-state rate, we integrate Eq. (6.50) to obtain the following result:

$$\frac{(R_p)_{blink}}{(R_p)_{cont}} = \tfrac{1}{2}\left[1 + \frac{\bar{\tau}}{t}\ln\left(\frac{[M\cdot]_{max}/[M\cdot]_{min} + [M\cdot]_{max}/[M\cdot]_s}{1 + [M\cdot]_{max}/[M\cdot]_s}\right)\right] \tag{6.51}$$

In the more general case where the dark period is m times longer than the light period, the factor ½ in Eq. (6.51) is replaced by $1/(1+m)$. This result is used by evaluating $[M\cdot]_{max}$, $[M\cdot]_{min}$, and $[M\cdot]_s$ using Eqs. (6.43), (6.45), and (6.44), respectively, for the conditions of the experiment. Then the ratio $(R_p)_{blink}/(R_p)_{cont}$ is evaluated for different values of the ratio τ/t. The results

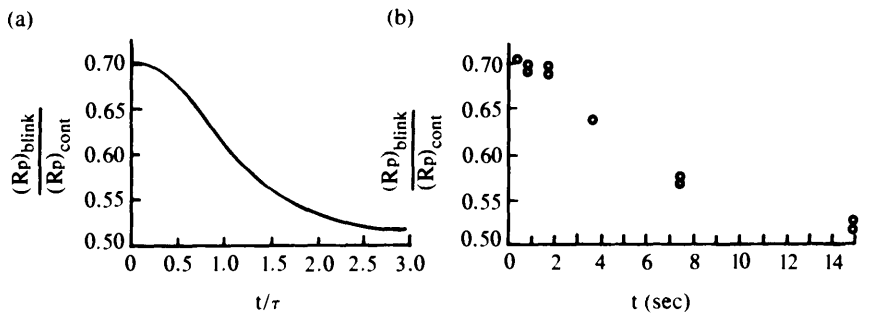

Figure 6.6 Plot of $(R_p)_{blink}/(R_p)_{cont}$ versus time: (a) theoretical curves with time expressed in units of τ and (b) experimental points for methyl acrylate. [Redrawn from Ref. 2.]

are plotted to yield a master curve such as that shown in Fig. 6.6a. Figure 6.6b shows some experimental points measured for the polymerization of methyl acrylate. By plotting the master curve and the data points on the same scale and then sliding the master curve along the ordinate until the points fall on the curve, it is possible to identify the time at which $t/\bar{\tau}$ equals unity. Applying this method to the data in Fig. 6.6 gives a value of $\bar{\tau}$ equal to about 6.5 sec for the system studied.

The superpositioning of experimental and theoretical curves to evaluate a characteristic time is reminiscent of the time-temperature superpositioning described in Sec. 4.10. This parallel is even more apparent if the theoretical curve is drawn on a logarithmic scale, in which case the distance by which the curve has to be shifted measures $\log \bar{\tau}$. Note that the limiting values of the ordinate in Fig. 6.6 correspond to the limits described in Eqs. (6.46) and (6.47). Because this method effectively averages over both the buildup and the decay phases of radical concentration, it affords an experimentally less demanding method for the determination of $\bar{\tau}$ than alternative methods which utilize either the buildup or the decay portions of the non-stationary-state free-radical concentration.

To gain some additional familiarity with the concept of radical lifetime and to see how this quantity can be used to determine the absolute value of a kinetic constant, consider the following example.

Example 6.4

The polymerization of ethylene at 130°C and 1500 atm was studied using different concentrations of the initiator, 1-*t*-butylazo-1-phenoxycyclohexane.

The rate of initiation was measured directly and radical lifetimes were determined using the rotating sector method. The following results were obtained.†

Run	$\bar{\tau}$ (sec)	$R_i \times 10^9$ (mol liter^{-1} sec^{-1})
5	0.73	2.35
6	0.93	1.59
8	0.32	12.75
12	0.50	5.00
13	0.29	14.95

Demonstrate that the variations in the rate of initiation and $\bar{\tau}$ are consistent with free-radical kinetics and evaluate k_t.

Solution

Since the rate of initiation is measured, we can substitute R_i for the terms $(2fk_d[I])^{1/2}$ in Eq. (6.42) to give

$$\bar{\tau} = \frac{1}{(2k_tR_i)^{1/2}} \quad \text{or} \quad k_t = \frac{1}{2\bar{\tau}^2R_i}$$

If the data follow the kinetic scheme presented here, the values of k_t calculated for the different runs should be constant:

Run	$k_t \times 10^{-8}$ (liter mol^{-1} sec^{-1})
5	3.99
6	3.64
8	3.83
12	4.00
13	3.98
Average	3.89

Even though the rates of initiation span almost a 10-fold range, the values of k_t show a standard deviation of only 4%, which is excellent in view of experimental errors. Note that the rotating sector method can be used in high-pressure experiments and other unusual situations, a characteristic it shares with many optical methods in chemistry.

† T. Takahashi and P. Ehrlich, *Polym. Prepr.* 22:203 (1981).

In the next section we shall examine the distribution of molecular weights for polymerization which follows the chain-growth mechanism.

6.7 Distribution of Molecular Weights

Until this point in the chapter we have intentionally avoided making any differentiation among radicals on the basis of the degree of polymerization of the radical. Now we seek a description of the molecular weight distribution of addition polymer molecules. Toward this end it becomes necessary to consider radicals of different n values. We begin by writing a kinetic expression for the concentration of radicals of degree of polymerization n, which we designate $[M_n\cdot]$. This rate law will be the sum of three contributions:

1. An increase which occurs by addition of monomer to the radical $M_{n-1}\cdot$.
2. A decrease which occurs by addition of a monomer to the radical $M_n\cdot$.
3. A decrease which occurs by the termination of $M_n\cdot$ with some other undifferentiated radical $M\cdot$.

The change in $[M_n\cdot]$ under stationary-state conditions equals zero for all values of n; hence we write

$$d[M_n\cdot] = k_p[M][M_{n-1}\cdot] - k_p[M][M_n\cdot] - 2k_t[M_n\cdot][M\cdot] = 0 \tag{6.52}$$

which can be rearranged to

$$\frac{[M_n\cdot]}{[M_{n-1}\cdot]} = \frac{k_p[M]}{k_p[M] + 2k_t[M\cdot]} \tag{6.53}$$

Dividing the numerator and denominator of Eq. (6.53) by $2k_t[M\cdot]$ and recalling the definition of $\bar{\nu}$ provided by Eq. (6.36) enables us to express this result more succinctly as

$$\frac{[M_n\cdot]}{[M_{n-1}\cdot]} = \frac{\bar{\nu}}{1+\bar{\nu}} \tag{6.54}$$

Next let us consider the following sequence of multiplications:

$$\frac{[M_n\cdot]}{[M_{n-1}\cdot]}\frac{[M_{n-1}\cdot]}{[M_{n-2}\cdot]}\frac{[M_{n-2}\cdot]}{[M_{n-3}\cdot]}\cdots\frac{[M_{n-(n-2)}\cdot]}{[M_{n-(n-1)}\cdot]} = \frac{[M_n\cdot]}{[M_1\cdot]} \tag{6.55}$$

This shows that the number of n-mer radicals relative to the number of the smallest radicals is given by multiplying the ratio $[M_n\cdot]/[M_{n-1}\cdot]$ by n - 2 analogous ratios. Since each of the individual ratios is given by $\bar{\nu}/(1+\bar{\nu})$, we can write Eq. (6.55) as

$$\frac{[M_n\cdot]}{[M_1\cdot]} = \frac{[M_n\cdot]}{[M_{n-1}\cdot]} \left(\frac{\bar{\nu}}{1+\bar{\nu}}\right)^{n-2} \tag{6.56}$$

or

$$[M_{n-1}\cdot] = [M_1\cdot] \left(\frac{\bar{\nu}}{1+\bar{\nu}}\right)^{(n-1)-1} \tag{6.57}$$

Since it is more convenient to focus attention on n-mers than (n - 1)-mers, the corresponding expression for the n-mer is written by analogy:

$$[M_n\cdot] = [M_1\cdot] \left(\frac{\bar{\nu}}{1+\bar{\nu}}\right)^{n-1} \tag{6.58}$$

Dividing both sides of Eq. (6.58) by $[M\cdot]$, the total radical concentration, gives the number fraction of n-mer radicals in the total radical population. This ratio is the same as the number of n-mers N_n in the sample containing a total of N (no subscript) polymer molecules:

$$\frac{N_n}{N} = \frac{[M_n\cdot]}{[M\cdot]} = \frac{[M_1\cdot]}{[M\cdot]} \left(\frac{\bar{\nu}}{1+\bar{\nu}}\right)^{n-1} \tag{6.59}$$

The ratio $[M_1\cdot]/[M\cdot]$ in Eq. (6.59) can be eliminated by reexamining Eq. (6.52) explicitly for the M_1 radical:

1. Write Eq. (6.52) for $M_1\cdot$, remembering in this case that the leading term describes initiation:

$$d[M_1\cdot] = R_i - k_p[M][M_1\cdot] - 2k_t[M_1\cdot][M\cdot] = 0 \tag{6.60}$$

2. Rearrange under stationary-state conditions:

$$[M_1\cdot] = \frac{R_i}{k_p[M] + 2k_t[M\cdot]} \tag{6.61}$$

The total radical concentration under stationary-state conditions can be similarly obtained:

3. Write Eq. (6.22) using the same notation for initiation as in (6.60):

$$d[M\cdot] = R_i - 2k_t[M\cdot]^2 = 0 \tag{6.62}$$

4. Rearrange under stationary-state conditions:

$$[M\cdot] = \frac{R_i}{2k_t[M\cdot]} \tag{6.63}$$

5. Take the ratio of Eq. (6.61) to Eq. (6.63):

$$\frac{[M_1\cdot]}{[M\cdot]} = \frac{2k_t[M\cdot]}{k_p[M] + 2k_t[M\cdot]} = \frac{1}{1+\bar{\nu}} \tag{6.64}$$

Combining Eq. (6.64) with Eq. (6.59) gives

$$\frac{N_n}{N} = \frac{1}{1+\bar{\nu}}\left(\frac{\bar{\nu}}{1+\bar{\nu}}\right)^{n-1} = \frac{1}{\bar{\nu}}\left(\frac{\bar{\nu}}{1+\bar{\nu}}\right)^{n} \tag{6.65}$$

This expression gives the number fraction or mole fraction of n-mers in the polymer and is thus equivalent to Eq. (5.25) for step-growth polymerization.

The kinetic chain length $\bar{\nu}$ may also be viewed as merely a cluster of kinetic constants and concentrations which was introduced into Eq. (6.54) to simplify the notation. As an alternative, suppose we define for the purposes of this chapter a fraction p such that

$$p = \frac{\bar{\nu}}{1+\bar{\nu}} = \frac{k_p[M]}{k_p[M] + 2k_t[M\cdot]} \tag{6.66}$$

It follows from this definition that $1/(1 + \bar{\nu}) = 1 - p$, so Eq. (6.65) can be rewritten as

$$\frac{N_n}{N} = (1-p)p^{n-1} \tag{6.67}$$

This change of notation now expresses Eq. (6.65) in exactly the same form as its equivalent in Sec. 5.4. Several similarities and differences should be noted in order to take full advantage of the parallel between this result and the corresponding material for condensation polymers from Chap. 5:

1. In Chap. 5, p was defined as the fraction (or probability) of functional groups that had reacted at a certain point in the polymerization. According to the current definition provided by Eq. (6.66), p is the fraction (or probability) of propagation steps among the combined total of propagation and termination steps. The quantity 1 - p is therefore the fraction (or

probability) of termination steps. An addition polymer of degree of polymerization n has undergone n - 1 propagation steps and one termination step. Therefore it makes sense to describe its probability in the form of Eq. (6.67).

2. It is apparent from Eq. (6.66) that $p \to 1$ as $\bar{\nu} \to \infty$; hence those same conditions which favor the formation of a high molecular weight polymer also indicate p values close to unity.
3. In Chap. 5 all molecules—whether monomer or n-mers of any n—carry functional groups; hence the fraction described by Eq. (5.24) applies to the entire reaction mixture. Equation (6.67), by contrast, applies only to the radical population. Since the radicals eventually end up as polymers, the equation also describes the polymer produced. Unreacted monomer is specifically excluded, however.
4. Only one additional stipulation needs to be made before adapting the results that follow from Eq. (5.24) to addition polymers. The mode of termination must be specified to occur by disproportionation to use the results of Sec. 5.4 in this chapter, since termination by combination obviously changes the particle size distribution. We shall return to the case of termination by combination presently.
5. For termination by disproportionation (subscript d), we note that $p = k_p[M]/(k_p[M] + 2k_{t,d}[M\cdot])$, and by analogy with Eqs. (5.28), (5.32), and (5.33),

$$(\bar{n}_n)_d = \frac{1}{1 - p} \tag{6.68}$$

$$(\bar{n}_w)_d = \frac{1 + p}{1 - p} \tag{6.69}$$

$$\left(\frac{\bar{n}_w}{\bar{n}_n}\right)_d = 1 + p \to 2 \quad \text{as} \quad p \to 1 \tag{6.70}$$

Because of Eq. (6.66), $(\bar{n}_n)_d$ can also be written as $1 + \bar{\nu} \cong \bar{\nu}$ for large $\bar{\nu}$, which is the result already obtained in Eq. (6.34). Figures 5.5 and 5.6 also describe the distribution by number and the distribution by weight of addition polymers, if the provisos enumerated above are applied.

To deal with the case of termination by combination, it is convenient to write some reactions by which an n-mer might be formed. Table 6.5 lists several specific chemical reactions and the corresponding rate expressions as well as the general form for the combination of an (n - m)-mer and an m-mer. On the assumption that all $k_{t,c}$ values are the same, we can write the total rate of change of $[M_n\cdot]$:

Table 6.5 Some Free Radical Combination Reactions Which Yield n-mers and Their Rate Laws

Reaction	Rate law
$M_{n-1}\cdot + M_1\cdot \longrightarrow M_n$	$\frac{d[M_n]}{dt} = k_{t,c}[M_{n-1}\cdot][M_1\cdot]$
$M_{n-2}\cdot + M_2\cdot \longrightarrow M_n$	$\frac{d[M_n]}{dt} = k_{t,c}[M_{n-2}\cdot][M_2\cdot]$
$M_{n-3}\cdot + M_3\cdot \longrightarrow M_n$	$\frac{d[M_n]}{dt} = k_{t,c}[M_{n-3}\cdot][M_3\cdot]$
⋮	⋮
$M_{n-m}\cdot + M_m\cdot \longrightarrow M_n$	$\frac{d[M_n]}{dt} = k_{t,c}[M_{n-m}\cdot][M_m\cdot]$

$$\left(\frac{d[M_n\cdot]}{dt}\right)_{tot} = k_{t,c}\sum_{m=1}^{n-1}[M_{n-m}\cdot][M_m\cdot] \tag{6.71}$$

For the special case of $n - m = m = n/2$, $k_{t,c}$ is only half as large as for the combination of dissimilar radicals, but this effect is offset in Eq. (6.71) by the fact that the sumation counts all combinations twice except that where $n - m = m = n/2$.

The fraction of n-mers formed by combination may be evaluated by dividing $d[M_n\cdot]/dt$ by $\Sigma_n d[M_n\cdot]/dt$. Assuming that termination occurs exclusively by combination, then

$$\sum_n \frac{d[M_n\cdot]}{dt} = k_{t,c}[M\cdot]^2 \tag{6.72}$$

and the number fraction of n-mers formed by combination (subscript c) is

$$\left(\frac{N_n}{N}\right)_c = \frac{d[M_n\cdot]/dt}{\Sigma_n\, d[M_n\cdot]/dt} = \frac{k_{t,c}\sum_{m=1}^{n-1}[M_{n-m}\cdot][M_m\cdot]}{k_{t,c}[M\cdot]^2} \tag{6.73}$$

Equation (6.67) can be used to relate $[M_{n-m}\cdot]$ and $[M_m\cdot]$ to the total radical concentration:

$$[M_{n-m}\cdot] = (1 - p)p^{(n-m)-1}[M\cdot] \tag{6.74}$$

and

$$[M_m \cdot] = (1 - p)p^{m-1}[M \cdot] \tag{6.75}$$

Therefore

$$\left(\frac{N_n}{N}\right)_c = \frac{k_{t,c} \sum_{m=1}^{n-1} (1 - p)p^{n-m-1} [M \cdot](1 - p)p^{m-1}[M \cdot]}{k_{t,c}[M \cdot]^2}$$

$$= \sum_{m=1}^{n-1} (1 - p)^2 p^{n-2} \tag{6.76}$$

The index m drops out of the last summation; we compensate for this by multiplying the final result by n - 1 in recognition of the fact that the summation adds up n - 1 identical terms. Accordingly, the desired result is obtained:

$$\left(\frac{N_n}{N}\right)_c = (n - 1)(1 - p)^2 p^{n-2} \tag{6.77}$$

This expression is plotted in Fig. 6.7 for several large values of p. Although it shows a number distribution of polymers terminated by combination, the distribution looks quite different from Fig. 5.5, which describes the number distribution for termination by disproportionation. In the latter N_n/N decreases monotonically with increasing n. With combination, however, the curves go through a maximum which reflects the fact that the combination of two very small or two very large radicals is a less probable event than a more random combination.

Expressions for the various averages are readily derived from Eq. (6.77) by procedures identical to those used in Sec. 5.4. We only quote the final results for the case where termination occurs exclusively by combination:

$$(\bar{n}_n)_c = \frac{2}{1 - p} \tag{6.78}$$

$$(\bar{n}_w)_c = \frac{2 + p}{1 - p} \tag{6.79}$$

$$\left(\frac{\bar{n}_w}{\bar{n}_n}\right)_c = \frac{2 + p}{2} \tag{6.80}$$

These various expressions differ from their analogs in the case of termination by disproportionation by the appearance of occasional 2's. These terms arise

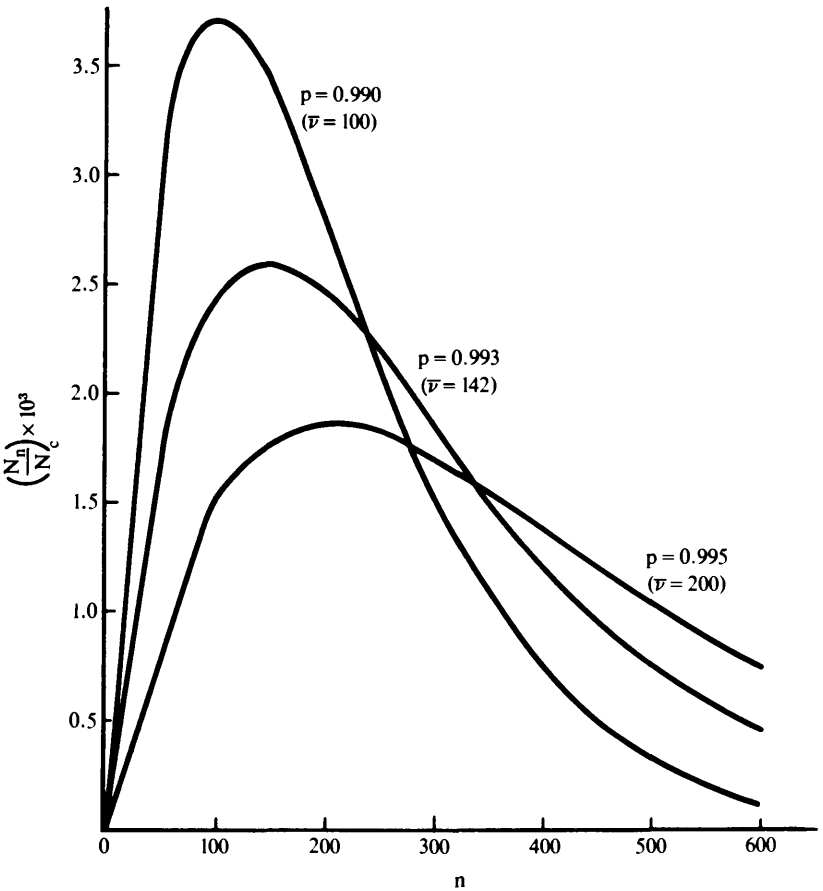

Figure 6.7 Number fraction of n-mers as a function of n for termination by combination. Drawn according to Eq. (6.77) for values of p indicated.

precisely because two chains are combined in this mode of termination. Again using Eq. (6.66), we note that $(\bar{n}_n)_c = 2(1 + \bar{\nu}) \cong 2\bar{\nu}$ for large $\bar{\nu}$, a result which was already given as Eq. (6.35).

One rather different result that arises from the case of termination by combination is seen by examining the limit of Eq. (6.80) for large values of p:

$$\frac{\bar{n}_w}{\bar{n}_n} \longrightarrow \frac{2+1}{2} = 1.5 \quad \text{as} \quad p \longrightarrow 1 \tag{6.81}$$

This contrasts with a limiting ratio of 2 for the case of termination by disproportionation. Since $\bar{M}_n$ and $\bar{M}_w$ can be measured, this difference is potentially a method for determining the mode of termination in a polymer system. In most instances, however, termination occurs by some proportion of both modes. Although general expressions exist for the various averages and their ratio when both modes of termination are operative, molecular weight data are generally not sufficiently precise to allow the proportions of termination modes to be determined in this way.

Throughout this section we have used mostly p and $\bar{\nu}$ to describe the distribution of molecular weights. It should be remembered that these quantities are defined in terms of various concentrations and therefore change as the reactions proceed. Accordingly, the results presented here are most simply applied at the start of the polymerization reaction when the initial concentrations of monomer and initiator can be used to evaluate p or $\bar{\nu}$. The termination constants are known to decrease with the extent of conversion of monomer to polymer, and this effect also complicates the picture at high conversions. Note, also, that chain transfer has been excluded from consideration in this section, as elsewhere in the chapter. We shall consider chain transfer reactions in the next section.

6.8 Chain Transfer

The three-step mechanism for free-radical polymerization represented by reactions (6.A)-(6.C) does not tell the whole story. Another type of free-radical reaction, called chain transfer, may also occur. This is unfortunate in the sense that it complicates the neat picture presented until now. On the other hand, this additional reaction can be turned into an asset in actual polymer practice. One of the consequences of chain transfer reactions is a lowering of the kinetic chain length and hence the molecular weight of the polymer without necessarily affecting the rate of polymerization.

Chain transfer arises when a hydrogen or some other atom, say, X in general, is transferred from some molecule in the system to the polymer radical. This terminates the growth of the original radical but replaces it with a new one: the fragment of the species from which X was extracted. These latter molecules will be designated by attaching the letter X to their symbol in this discussion. Thus if chain transfer involves an initiator molecule, we represent the latter IX in this section. Chain transfer can occur with any molecule in the system. The following reactions specifically describe transfer to initiator, monomer, solvent, and polymer molecules:

1. Transfer to initiator, IX:

$$M_n\cdot + IX \rightarrow M_nX + I\cdot \tag{6.J}$$

2. Transfer to monomer, MX:

$$M_n\cdot + MX \rightarrow M_nX + M\cdot \tag{6.K}$$

3. Transfer to solvent, SX:

$$M_n\cdot + SX \rightarrow M_nX + S\cdot \tag{6.L}$$

4. Transfer to polymer, M_mX:

$$M_n\cdot + M_mX \rightarrow M_nX + M_m\cdot \tag{6.M}$$

5. General, transfer to RX:

$$M_n\cdot + RX \rightarrow M_nX + R\cdot \tag{6.N}$$

It is apparent from these reactions how chain transfer lowers the molecular weight of a chain-growth polymer. The effect of chain transfer on the rate of polymerization depends on the rate at which the new radicals reinitiate polymerization:

$$R\cdot + M \xrightarrow{k_R} RM\cdot \longrightarrow \xrightarrow{k_p} \longrightarrow RM_n\cdot \tag{6.O}$$

If the rate constant k_R is comparable to k_p, the substitution of a polymer radical with a new radical has little or no effect on the rate of polymerization. If $k_R \ll k_p$, the rate of polymerization will be decreased by chain transfer.

The kinetic chain length has a slightly different definition in the presence of chain transfer. Instead of being simply the ratio R_p/R_t, it is redefined to be the rate of propagation relative to the rates of *all* other steps that compete with propagation; specifically, termination and transfer (subscript tr):

$$\bar{\nu}_{tr} = \frac{R_p}{R_t + R_{tr}} \tag{6.82}$$

The transfer reactions follow second-order kinetics, the general rate law being

$$R_{tr} = k_{tr}[M_n\cdot][RX] \tag{6.83}$$

where k_{tr} is the rate constant for chain transfer to a specific compound RX. Since chain transfer can occur with several different molecules in the reaction mixture, Eq. (6.82) becomes

$$\bar{\nu}_{tr} = \frac{k_p[M\cdot][M]}{\left\{2k_t[M\cdot]^2 + k_{t,IX}[M\cdot][IX] + k_{tr,MX}[M\cdot][MX] + k_{tr,SX}[M\cdot][SX] + k_{tr,M_nX}[M\cdot][M_nX]\right\}}$$

$$= \frac{k_p[M]}{2k_t[M\cdot] + \Sigma k_{tr,RX}[RX]} \tag{6.84}$$

where the summation is over all pertinent RX species. It is instructive to examine the reciprocal of this quantity:

$$\frac{1}{\bar{\nu}_{tr}} = \frac{2k_t[M\cdot]}{k_p[M]} + \frac{\Sigma k_{tr,RX}[RX]}{k_p[M]} \tag{6.85}$$

Since the first term on the right-hand side is the reciprocal of the kinetic chain length in the absence of transfer, this becomes

$$\frac{1}{\bar{\nu}_{tr}} = \frac{1}{\bar{\nu}} + \frac{\Sigma k_{tr,RX}[RX]}{k_p[M]} \tag{6.86}$$

This notation is simplified still further by defining the ratio of constants

$$\frac{k_{tr,RX}}{k_p} = C_{RX} \tag{6.87}$$

which is called the chain transfer constant for the monomer in question to molecule RX:

$$\frac{1}{\bar{\nu}_{tr}} = \frac{1}{\bar{\nu}} + \sum_{\text{all RX}} C_{RX}\frac{[RX]}{[M]} \tag{6.88}$$

It is apparent from this expression that the larger the sum of chain transfer terms becomes, the smaller will be $\bar{\nu}_{tr}$.

The magnitude of the individual terms in the summation depends on both the specific chain transfer constants and the concentrations of the reactants under consideration. The former are characteristics of the system and hence quantities over which we have little control; the latter can often be adjusted to study a particular effect. For example, chain transfer constants are generally obtained under conditions of low conversion to polymer where the concentration of polymer is low enough to ignore the transfer to polymer. We shall return below to the case of high conversions where this is not true.

If an experimental system is investigated in which only one molecule is significantly involved in transfer, then the chain transfer constant to that

material is particularly easy to obtain. If we assume that species SX is the only molecule to which transfer occurs, Eq. (6.88) becomes

$$\frac{1}{\bar{\nu}_{tr}} = \frac{1}{\bar{\nu}} + C_{SX}\frac{[SX]}{[M]} \tag{6.89}$$

This suggests that polymerizations should be conducted at different ratios of [SX]/[M] and the molecular weight measured for each. Equation (6.89) shows that a plot of $1/\bar{\nu}_{tr}$ versus [SX]/[M] should be a straight line of slope C_{SX}. Figure 6.8 shows this type of plot for the polymerization of styrene at 100°C in the presence of four different solvents. The fact that all show a common intercept as required by Eq. (6.89) shows that the rate of initiation is unaffected by the nature of the solvent. The following example examines chain transfer constants evaluated in this situation.

Example 6.5

Estimate the chain transfer constants for styrene to isopropylbenzene, ethylbenzene, toluene, and benzene from the data presented in Fig. 6.8. Comment

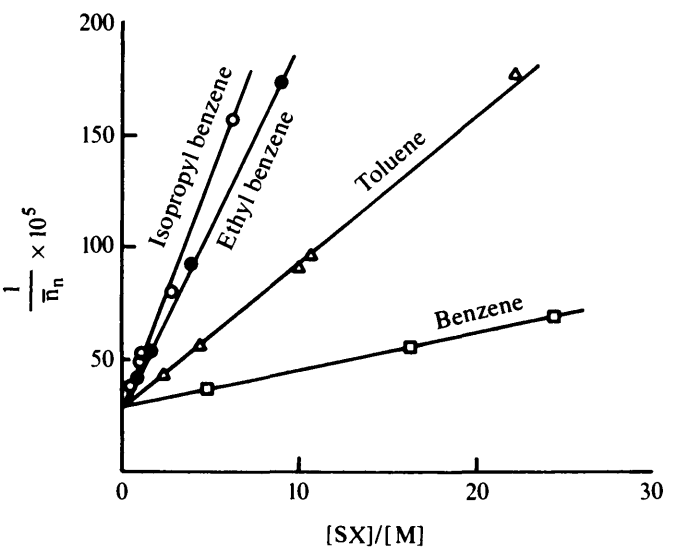

Figure 6.8 Effect of chain transfer to solvent according to Eq. (6.89) for polystyrene at 100°C. Solvents used were ethyl benzene (●), isopropyl benzene (○), toluene (△), and benzene (□). [Data from R. A. Gregg and F. R. Mayo, *Discuss. Faraday Soc.* 2:328 (1947).]

on the relative magnitude of these constants in terms of the structure of the solvent molecules.

Solution

The chain transfer constants are given by Eq. (6.89) as the slopes of the lines in Fig. 6.8. These are estimated to be as follow:

SX	i-C_3H_7	C_2H_5	CH_3	H
$C_{SX} \times 10^4$	2.08	1.38	0.55	0.16

The relative magnitudes of these constants are consistent with the general rule that benzylic hydrogens are more readily abstracted than those attached directly to the ring. The reactivity of the benzylic hydrogens themselves follows the order tertiary > secondary > primary, which is a well-established order in organic chemistry. The benzylic radical resulting from hydrogen abstraction is resonance stabilized. For toluene, as an example,

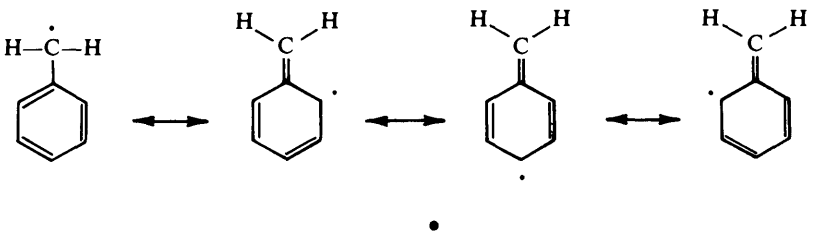

In certain commercial processes it is essential to regulate the molecular weight of the addition polymer either for ease of processing or because low molecular weight products are desirable for particular applications such as lubricants or plasticizers. In such cases the solvent or chain transfer agent is chosen and its concentration selected to produce the desired value of $\bar{\nu}_{tr}$. Certain mercaptans have especially large chain transfer constants for many common monomers and are especially useful for molecular weight regulation. For example, styrene has a chain transfer constant to n-butyl mercaptan equal to 21 at 60°C. This is about 10^7 times larger than the chain transfer constant to benzene at the same temperature.

Chain transfer to initiator or monomer cannot always be ignored. It may be possible, however, to evaluate the transfer constants to these substances by investigating a polymerization without added solvent or in the presence of a solvent for which C_{SX} is known to be negligibly small. In this case the transfer constants C_{IX} and C_{MX} can be determined from experiments in which $\bar{\nu}_{tr}$ (via

$\bar{M}_n$ and $\bar{n}_n$) and R_p are measured. The following steps outline a procedure for accomplishing this:

1. By Eqs. (6.14), (6.24), and (6.33),

$$\frac{1}{\bar{\nu}} = \frac{R_t}{R_p} = \frac{k_t R_p}{k_p [M]^2} \tag{6.90}$$

2. Solving Eq. (6.26) for [IX], we have

$$[IX] = \frac{k_t R_p^2}{f k_d k_p^2 [M]^2} \tag{6.91}$$

3. Substitute Eqs. (6.90) and (6.91) into (6.88) to obtain

$$\frac{1}{\bar{\nu}_{tr}} = \frac{k_t R_p}{k_p [M]^2} + C_{MX} + C_{IX} \frac{k_t R_p^2}{f k_d k_p^2 [M]^3} \tag{6.92}$$

4. Plot $1/\bar{\nu}_{tr}$ versus R_p. If the plot is linear, $C_{IX} = 0$ and the intercept gives the value of C_{MX}. If the plot is nonlinear, the term containing R_p^2 will become insignificant before the term which is first order in R_p as $R_p \to 0$, assuring that the plot becomes linear if examined at sufficiently low R_p values. In this case too the intercept gives C_{MX}.
5. Once the value of C_{MX} has been obtained, Eq. (6.92) can be rearranged to

$$\left(\frac{1}{\bar{\nu}_{tr}} - C_{MX}\right) \frac{1}{R_p} = \frac{k_t}{k_p [M]^2} + C_{IX} \frac{k_t R_p}{f k_d k_p^2 [M]^3} \tag{6.93}$$

   If the left-hand side is plotted against R_p, the slope yields the value of C_{IX}, assuming all other kinetic constants are known.

Fairly extensive tables of chain transfer constants have been assembled on the basis of investigations of this sort. For example, the values of C_{MX} for acrylamide at 60°C is 6×10^{-5}, and that for vinyl chloride at 30°C is 6.3×10^{-4}. Likewise, for methyl methacrylate at 60°C, C_{IX} is 0.02 to benzoyl peroxide and 1.27 to *t*-butyl hydroperoxide.

As noted above, chain transfer to polymer does not interfere with the determination of other transfer constants, since the latter are evaluated at low conversions. In polymer synthesis, however, high conversions are desirable and extensive chain transfer can have a dramatic effect on the properties of the product. This comes about since chain transfer to polymer introduces branching into the product:

$$\sim CH_2-\underset{\displaystyle X}{\overset{\displaystyle Y}{\underset{|}{\overset{|}{C}}}}\sim + M\cdot \rightarrow MX + \sim CH_2-\underset{\cdot}{\overset{Y}{\underset{|}{\overset{|}{C}}}}\sim \xrightarrow{M} \sim CH_2-\underset{(M)_n}{\overset{Y}{\underset{|}{\overset{|}{C}}}}\sim \qquad (6.P)$$

A moment's reflection reveals that the effect on $\bar{\nu}$ of transfer to polymer is different from the effects discussed above inasmuch as the overall degree of polymerization is not decreased by such transfers. Although transfer to polymer is shown in one version of Eq. (6.84), the present discussion suggests that this particular transfer is not pertinent to the effect described. Investigation of chain transfer to polymer is best handled by examining the extent of branching in the product. We shall not pursue the matter of evaluating the transfer constants, but shall consider instead two specific examples of transfer to polymer.

Remember from Sec. 1.3 that graft copolymers have polymeric side chains which differ in the nature of the repeat unit from the backbone. These can be prepared by introducing a prepolymerized sample of the backbone polymer into a reactive mixture—i.e., one containing a source of free radicals—of the side-chain monomer. As an example, consider introducing polybutadiene into a reactive mixture of styrene:

$$\sim CH_2-CH=CH-CH_2\sim + \sim CH_2-\underset{\phi}{\overset{H}{\underset{|}{\overset{|}{C}}}}\cdot \rightarrow \sim CH_2-\underset{\phi}{\underset{|}{CH_2}} + \sim \underset{\cdot}{\overset{H}{\underset{|}{\overset{|}{C}}}}-CH=CH-CH_2\sim$$

$$\text{styrene} \xrightarrow{\rightarrow\rightarrow\rightarrow} \sim \overset{H}{\underset{|}{\overset{|}{C}}}-CH=CH-CH_2\sim \qquad (6.Q)$$

$$\overset{CH_2}{\underset{H-C-\phi}{\underset{|}{\overset{|}{\quad}}}}_n$$

This procedure is used commercially to modify the properties of polybutadiene.

A second example of chain transfer to polymer is provided by the case of polyethylene. In this case the polymer product contains mainly ethyl and butyl side chains. At high conversions such side chains may occur as often as once every 15 backbone repeat units on the average. These short side chains are thought to arise from transfer reactions with methylene hydrogens along the same polymer chain. This process is called backbiting and reminds us of the stability of rings of certain sizes and the freedom of rotation around unsubstituted—beyond hydrogen—bonds:

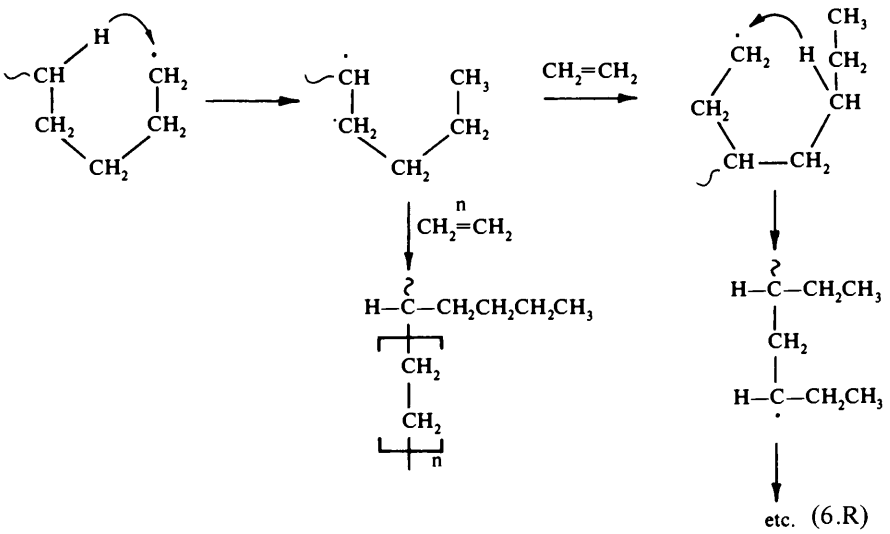

(6.R)

We conclude this section by noting an extreme case of chain transfer, a reaction which produces radicals of such low reactivity that polymerization is effectively suppressed. Reagents that accomplish this are added to commercial monomers to prevent their premature polymerization during storage. These substances are called either retarders or inhibitors, depending on the degree of protection they afford. Such chemicals must be removed from monomers prior to use, and failure to achieve complete purification can considerably affect the polymerization reaction.

Inhibitors and retarders differ in the extent to which they interfere with polymerization, and not in their essential activity. An inhibitor is defined as a substance which blocks polymerization completely until it is either removed or consumed. Thus failure to totally eliminate an inhibitor from purified monomer will result in an induction period in which the inhibitor is first converted to an inert form before polymerization can begin. A retarder is less efficient and merely slows down the polymerization process by competing for radicals.

Benzoquinone [III] is widely used as an inhibitor:

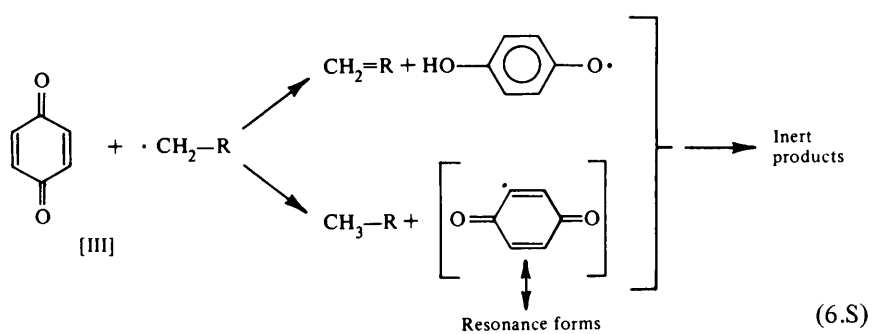

(6.S)

The resulting radical is stabilized by electron delocalization and eventually reacts with either another inhibitor radical by combination (dimerization) or disproportionation or with an initiator or other radical.

Molecular oxygen contains two unpaired electrons and has the distinction of being capable of both initiating and inhibiting polymerization. It functions in the latter capacity by forming the relatively unreactive peroxy radical:

$$\cdot O{-}O\cdot + M\cdot \rightarrow M{-}O{-}O\cdot \qquad (6.T)$$

Inhibitors are characterized by inhibition constants which are defined as the ratio of the rate constant for transfer to inhibitor to the propagation constant for the monomer in analogy with Eq. (6.87) for chain transfer constants. For styrene at 50°C the inhibition constant of *p*-benzoquinone is 518, and that for O_2 is 1.5×10^4. *The Polymer Handbook* (Ref. 3) is an excellent source for these and most other rate constants discussed in this chapter.

6.9 Techniques of Polymerization: Emulsion Polymerization

A number of chain-growth polymers are commercially produced on a high tonnage basis, and the technology of polymerization deserves some comment even though it is not our main emphasis in this volume. Many important monomers polymerize with the evolution of large amounts of heat. This can result in temperature increases, increased kinetic constants, and accelerated reaction rates—in short, to runaway reactions—unless the heat is dissipated. Many important monomers are toxic, carcinogenic, or both and hence must be processed carefully for the safety of workers in the industry and users of the products. These facts, plus the diversity of monomers employed and the assortment of end uses for polymer products, make the choice of a polymerization technique a highly specific matter. In this section we shall discuss some of the possibilities.

Several polymerization techniques are in widespread usage. Our discussion is biased in favor of methods that reveal additional aspects of addition polymerization and not on the relative importance of the methods in industrial practice. We shall discuss four polymerization techniques: bulk, solution, suspension, and emulsion polymerization.

Bulk and solution polymerizations are more or less self-explanatory, since they operate under the conditions we have assumed throughout most of this chapter. A bulk polymerization may be conducted with as few as two components: monomer and initiator. Production polymerization reactions are carried out to high conversions which produces several consequences we have mentioned previously:

1. The rate process for termination is hindered through the Trommsdorff effect.
2. Because of the decrease in R_t, R_p and $\bar{\nu}$ increase as the percent conversion increases.
3. This produces even greater increases in viscosity, with the attendant increase in the difficulty of heat removal and processing.
4. Very strong stirring equipment is needed for mixing because of the high viscosity, and long tubular reactors with low cross-sectional area are needed for heat exchange.
5. Use of chain transfer agents may be indicated to regulate $\bar{\nu}$ and thus avoid some of the difficulties mentioned in items (3) and (4).

Solution polymerization is the name given to the technique of polymer formation in the presence of a solvent. The polymer may not have the same solubility in the solvent as the monomer, so the system may become heterogeneous with the formation of polymer. Although there is an increase in viscosity as polymer concentration in the system increases, the effect is mitigated by the presence of solvent, and autoacceleration through the Trommsdorff mechanism is less troublesome than in bulk polymerizations. This permits easier stirring and better heat exchange than in the bulk. The solvent is ordinarily chosen to show low chain transfer so that high molecular weight polymer is obtained. Solvent recovery must be considered as part of the overall process and this, of course, adds to the cost of this method.

A technique called suspension polymerization is sometimes employed with water-insoluble monomers. In this procedure the monomer is suspended by agitation as small drops in an aqueous medium. The diameters of the drops are in the range of micrometers to millimeters in this technique. Coalescence of the monomer drops is prevented by stirring and by addition of water-soluble polymers like gelatin or by suspending clay particles like kaolin in the mixture. Oil-soluble initiators are used so that each monomer drop behaves as a miniature bulk polymerization system. The advantage of suspension polymerization is the ease of heat removal, and a disadvantage is the need to separate the polymer from the suspending medium and wash it free of additives. Suspension polymerization is also called pearl polymerization because of the appearance of the polymer produced.

The fourth and most interesting of the polymerization techniques we shall consider is called emulsion polymerization. It is important to distinguish between suspension and emulsion polymerization, since there is a superficial resemblance between the two and their terminology has potential for confusion: A suspension of oil drops in water is called an emulsion. Water-insoluble monomers are used in the emulsion process also, and the polymerization is carried out in the presence of water; however, the following significant differences also exist:

1. Water-soluble initiators are used.
2. Polymerization occurs in particles whose dimensions are in the nanometer size range, perhaps 10^3 times smaller than the particles in suspension polymerization.
3. Emulsifying agents which are soaps or detergents play a central role in the emulsion polymerization process.
4. The kinetics of polymerization are considerably different from those we have considered elsewhere in this chapter.

These differences have been extensively researched and their origin is quite well understood. We shall present only an abbreviated discussion of the topic, however.

Before we examine the polymerization process itself, it is essential to understand the behavior of the emulsifier molecules. This class of substances is characterized by molecules which possess a polar or ionic group or head and a hydrocarbon chain or tail. The latter is often in the 10–20 carbon atom size range. Dodecyl sulfate ions, from sodium dodecyl sulfate, are typical ionic emulsifiers. These molecules have the following properties which are pertinent to the present discussion:

1. They are water soluble because of the polar head, if one assumes that the tail is not too long.
2. They lower the free energy of an interface between water and some other phase—for example, with air or hydrocarbon—by concentrating in the surface region. At the surface they may be visualized as having their polar heads in the water and their hydrophobic "water-fearing" tails in the other phase. This is called adsorption; such materials are said to be surface active and are also called surfactants. The role of these materials in washing and laundering applications is a consequence of their adsorption behavior.
3. At low concentrations surfactant molecules adsorbed at the surface are in equilibrium with other molecules in solution. Above a threshold concentration, called the critical micelle concentration (cmc, for short), another equilibrium must be considered. This additional equilibrium is that between individual molecules in solution and clusters of emulsifier molecules known as micelles.
4. When micelles are formed just above the cmc, they are spherical aggregates in which surfactant molecules are clustered, tails together, to form a spherical particle. At higher concentrations the amount of excess surfactant is such that the micelles acquire a rod shape or, eventually, even a layer structure.

Figure 6.9 represents schematically the formation of a micelle by the association of n surfactant molecules. The cutaway view of the spherical micelle shows the hydrocarbon interior of these particles. Incidentally, it is this sort of reversible

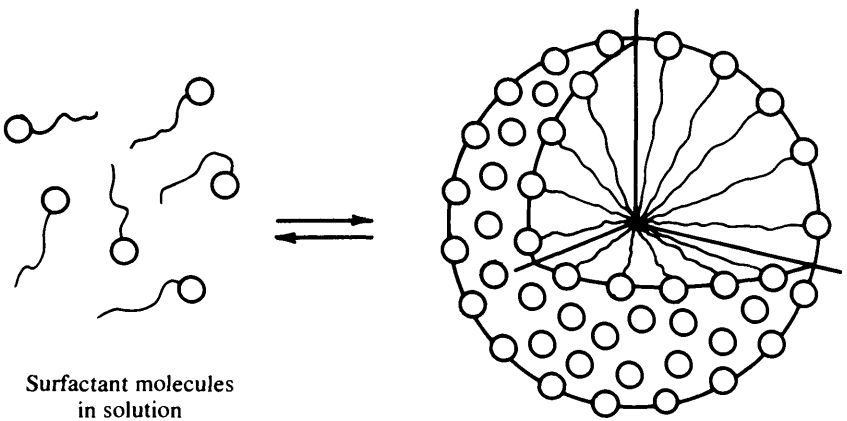

Figure 6.9 Schematic illustration of the micellization process. Cutaway view of spherical micelle shows hydrocarbon interior with polar heads on surface.

association between molecules that was once thought to hold polymers together before covalent structures were accepted.

With this picture in mind, let us consider what happens when monomer is stirred into a surfactant solution—which also contains a water-soluble initiator—above the cmc.

The surfactant is initially distributed through three different locations: dissolved as individual molecules or ions in the aqueous phase, at the surface of the monomer drops, and as micelles. The latter category holds most of the surfactant. Likewise, the monomer is located in three places. Some monomer is present as individual molecules dissolved in the water. Some monomer diffuses into the oily interior of the micelle, where its concentration is much greater than in the aqueous phase. This process is called solubilization. The third site of monomer is in the dispersed droplets themselves. Most of the monomer is located in the latter, since these drops are much larger, although far less abundant, than the micelles. Figure 6.10 is a schematic illustration of this state of affairs during emulsion polymerization.

Polymerization begins in the aqueous phase with the decomposition of the initiator. The free radicals produced initiate polymerization by reacting with the monomers dissolved in the water. The resulting polymer radicals grow very slowly because of the low concentration of monomer, but as they grow they acquire surface active properties and eventually enter micelles. There is a possibility that they become adsorbed at the oil-water interface of the monomer

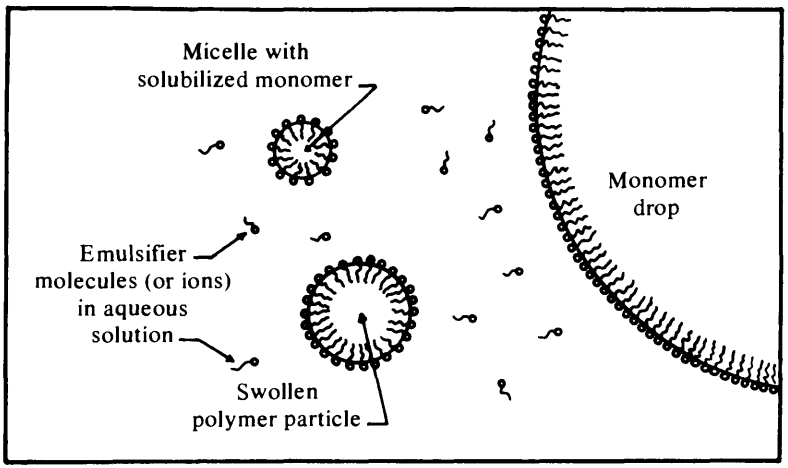

Figure 6.10 Schematic representation of the distribution of surfactant in an emulsion polymerization. Note the relative sizes of suspended particles. [From J. W. Vanderhoff, E. B. Bradford, H. L. Tarkowski, J. B. Shaffer, and R. M. Wiley, *Adv. Chem.* 34:32 (1962).]

drop, but this fate is inconsequential because the micelles are numerically so much more abundant. Once a radical enters a micelle, it polymerizes rapidly, since the concentration of solubilized monomer in the micelle is high. As this overall process continues, there is a general flux of monomer from the droplets to the micelles. The latter expand at the expense of the former. In fact, a micelle that is the locus of polymer growth is rapidly disrupted by the formation of polymer, so that it is no longer appropriate to even consider it a micelle. It is more accurate to consider it a polymer particle swollen by unreacted monomer, with the whole thing covered by adsorbed surfactants. There is a redistribution of surfactant as the polymerization progresses, with more adsorbed on polymer and less on monomer drops. The number of micelles also decreases, since this is the primary reservoir for surfactant.

It takes an initial period—stage one of the process—to get these various processes balanced out; but, after this first stage, polymerization progresses according to a straightforward pattern. We shall continue discussing only the stage which is analogous to a stationary state. The general flux of free radicals is from the aqueous phase into the micelle-swollen polymer particles, of which there are N* per unit volume in a particular experiment. The entry of the first radical into a micelle initiates the formation of a polymer chain; the arrival of a second radical terminates chain growth. A third radical entering a given particle will initiate a second chain, the the fourth radical terminates its growth, and so

on. Within one of these particles, then, there is either zero or one growing chain at any time. Since the entry of radicals into particles is random, there is a 50:50 chance that any one of the N* micelle-swollen polymer particles is the site of polymer growth at any given moment. In other words, the rate of polymerization is proportional to half the concentration of such particles, N*/2. The rate of polymerization in the second stage of emulsion polymerization, R_p^*, also depends on the concentration of monomer in the micelle [M*]; so we can write

$$R_p^* = k_p[M^*]\left[\frac{N^*}{2}\right] \tag{6.94}$$

The kinetic chain length in emulsion polymerization $\bar{\nu}^*$ is also readily derived by considering what happens in a single particle. The rate of propagation within a single particle is given by $k_p[M^*]$, while the rate of termination is identical to the rate at which radicals enter the micelle-swollen polymer particle. This, in turn, is equal to the rate of initiation of radicals divided by N* under second-stage reaction conditions. Therefore the kinetic chain length is

$$\bar{\nu}^* = \bar{n}_n^* = \frac{k_p[M^*]}{R_i/N^*} = \frac{k_p[M^*][N^*]}{2fk_d[I]} \tag{6.95}$$

This also gives $\bar{n}_n^*$, because the small terminating radical has essentially no effect on the degree of polymerization.

It is informative to compare Eqs. (6.94) and (6.95) with Eqs. (6.26) and (6.37), their counterparts for bulk polymerization. In the latter $R_p \propto [M][I]^{1/2}$, while $\bar{\nu} \propto [M][I]^{-1/2}$. Thus, if an initiator concentration were chosen to produce a predetermined value of $\bar{\nu}$, the rate would also be locked in to a particular value. Increasing [I] to increase R_p would have a deleterious effect on the molecular weight of the product. By contrast, in emulsion polymerization, the rate of polymerization is independent of the initiator concentration. Both R_p^* and $\bar{\nu}^*$ depend on the number of micelle-swollen polymer particles in the second stage of the reaction, but this is primarily governed by the nature and concentration of the surfactant, the temperature, and the concentration of electrolytes which affect the cmc. In emulsion polymerization it is possible to achieve both high rates of polymerization and high degrees of polymerization without being caught in the inverse dependence on [I] that characterizes bulk polymerization. The contrast in these behaviors is illustrated quantitatively by the following example:

Example 6.6

In an emulsion polymerization experiment at 60°C the number of micelles per unit volume is 5.0×10^{15} liter^{-1} and the monomer concentration in the micelle

is 5 M. Calculate R_p^* and $\bar{\nu}^*$ for this experiment, assuming the value of k_p from Table 6.4. Compare the calculated quantities for the emulsion polymerization with R_p and $\bar{\nu}$ for the bulk polymerization of styrene, assuming the same temperature, the same concentration of monomer, and the absence of chain transfer. In both cases take the rate of initiation to be 1.0×10^{-9} mol liter^{-1} sec^{-1}. What would be the effect on R_p and $\bar{\nu}$ in each of these cases if R_i were decreased by a factor of 4?

Solution

Assemble the pertinent equations. For emulsion polymerization, we take Eqs. (6.94), $R_p^* = k_p[M^*][N^*/2]$, and (6.95), $\bar{\nu}^* = k_p[M^*][N^*]/R_i = 2R_p^*/R_i$. For bulk polymerization, with the data given, we take Eqs. (6.29), $R_p = k_p(R_i/2k_t)^{1/2}[M]$, and (6.33), $\bar{\nu} = R_p/R_i$. From Tables 6.3 and 6.4, the appropriate constants at 60°C are $k_p = 165$ liter mol^{-1} sec^{-1} and $k_t = 2.9 \times 10^7$ liter mol^{-1} sec^{-1}. Direct substitution leads to the following results:

$$R_p^* = 165(5)\left[\tfrac{1}{2}\left(5 \times 10^{15} \frac{\text{micelles}}{\text{liter}} \times \frac{1 \text{ molecule}}{\text{micelle}} \times \frac{1 \text{ mol}}{6.02 \times 10^{23} \text{ molecules}}\right)\right]$$

$$= 3.41 \times 10^{-6} \text{ mol liter}^{-1} \text{ sec}^{-1}$$

and

$$R_p = 165(5)\left(\frac{1.0 \times 10^{-9}}{2(2.9 \times 10^7)}\right)^{1/2} = 3.41 \times 10^{-6} \text{ mol liter}^{-1} \text{ sec}^{-1}$$

In this example the number of micelles per unit volume is exactly twice the stationary-state free-radical concentration; hence the rates are identical. Although the numbers were chosen in this example to produce this result, neither N* nor M* are unreasonable values in actual emulsion polymerizations.

$$\bar{\nu}^* = \frac{2R_p^*}{R_i} = \frac{2(3.41 \times 10^{-6})}{(1.0 \times 10^{-9})} = 6820$$

$$\bar{\nu} = \frac{R_p}{R_i} = \frac{3.41 \times 10^{-6}}{1.0 \times 10^{-9}} = 3410$$

The difference of a factor of 2 between these values comes about because the conditions were chosen to give the same rates. Since a given micelle-swollen polymer particle is active only half of the time, it must produce chains which are twice as long to polymerize at the same rate as the bulk case. Reducing R_i by 1/4 produces the following effects on the calculated quantities:

R_p*—no effect, since R_i does not appear in Eq. (6.94); therefore $R_p^* = 3.41 \times 10^{-6}$ mol liter^{-1} sec^{-1}.

R_p—rate reduced by ½, since $R_p \propto R_i^{1/2}$ in Eq. (6.29); therefore $R_p = 1.71 \times 10^{-6}$ mol liter^{-1} sec^{-1}.

$\bar{\nu}$*—increased by a factor of 4, since $\bar{\nu}^* \propto R_i^{-1}$ in Eq. (6.95); therefore $\bar{\nu}^* = 27{,}300$.

$\bar{\nu}$—increased by a factor of 2, since $\bar{\nu} \propto R_p/R_i \propto 4 \times 1/2$ in Eq. (6.33); therefore $\bar{\nu} = 6820$.

•

Emulsion polymerization also has the advantages of good heat transfer and low viscosity, which follow from the presence of the aqueous phase. The resulting aqueous dispersion of polymer is called a latex. The polymer can be subsequently separated from the aqueous portion of the latex or the latter can be used directly in eventual applications. For example, in coatings applications—such as paints, paper coatings, floor polishes—soft polymer particles coalesce into a continuous film with the evaporation of water after the latex has been applied to the substrate.

There is a great deal more that could be said about emulsion polymerization or, for that matter, about free-radical polymerization in general. We shall conclude our discussion of the free-radical aspect of chain-growth polymerization at this point, however. This is not the end of chain-growth polymerization, however. There are four additional topics to be considered:

1. Addition polymerization through anionic active species. This is discussed in the next section.
2. Chain-growth polymerization through cationic active species. This is taken up in Sec. 6.11.
3. Chain-growth copolymerization. This topic is considered in Chap. 7.
4. Stereoregular polymerization. This is also taken up in Chap. 7.

Ionic polymerizations, whether anionic or cationic, should not be judged to be unimportant merely because our treatment of them is limited to two sections in this text. Although there are certain parallels between polymerizations which occur via free-radical and ionic intermediates, there are also numerous differences. An important difference lies in the more specific chemistry of the ionic mechanism. While the free-radical mechanism is readily discussed in general terms, this is much more difficult in the ionic case. This is one of the reasons why only relatively short sections have been allotted to anionic and cationic polymerizations. The body of available information regarding these topics is extensive enough to warrant a far more elaborate treatment, but space limitations and the more specific character of the material are the reasons for the curtailed treatment.

Stereoregular polymerizations strongly resemble anionic polymerizations. We discuss these in greater detail in Chap. 7 because of their microstructure rather than the ionic intermediates involved in their formation.

6.10 Anionic Polymerization

Both modes of ionic polymerization are described by the same vocabulary as the corresponding steps in the free-radical mechanism for chain-growth polymerization. However, initiation, propagation, transfer, and termination are quite different than in the free-radical case and, in fact, different in many ways between anionic and cationic mechanisms. Our comments on the ionic mechanisms will touch many of the same points as the free-radical discussion, although in a far more abbreviated form.

The kinds of vinyl monomers which undergo anionic polymerization are those with electron-withdrawing substituents such as the nitrile, carboxyl, and phenyl groups. We represent the catalysts as AB in this discussion; these are substances which break into a cation (A^+) and an anion (B^-) under the conditions of the reaction. In anionic polymerization it is the basic anion which adds across the double bond of the monomer to form the active center for polymerization:

$$CH_2=C(R)(H) + AB \longrightarrow B-CH_2-C^{\ominus}(R)(H)\ A^{\oplus} \qquad (6.U)$$

The electron-withdrawing R group helps stabilize this anion. Chemically, these initiator ions are species like hydroxide, cyanide, amide, alkyl, or aryl ions, the latter two from organometallics such as alkyl or aryl compounds of lithium or aluminum. There is an inverse relationship between the electron-withdrawing tendency of a substituent and the required basicity of the catalyst. Substituents which are strongly electron withdrawing like nitrile can be polymerized with relatively weak bases like hydroxide ion, while phenyl requires a stronger base like the amide ion. Note that the base adds to the more positive carbon atom away from the electron-withdrawing substituent.

The reaction medium plays a very important role in all ionic polymerizations. Likewise, the nature of the ionic partner to the active center—called the counterion or gegenion—has a large effect also. This is true because the nature of the counterion, the polarity of the solvent, and the possibility of specific solvent-ion interactions determines the average distance of separation between the ions in solution. It is not difficult to visualize a whole spectrum of possibilities, from completely separated ions to an ion pair of partially solvated ions to an ion pair of unsolvated ions. The distance between the centers of the ions is different in

each of these situations, and this has a large effect on the ease of monomer addition to the active site.

Once the polymerization has been initiated by the addition of a catalyst to the monomer, propagation occurs by the entry of successive monomers between the ions of the active species:

$$B{-}CH_2{-}\underset{\displaystyle H}{\overset{\displaystyle R}{\overset{|}{\underset{|}{C}}}}{}^{\ominus}A^{\oplus} + (n-1)M \longrightarrow BM_n{}^{\ominus}A^{\oplus} \tag{6.V}$$

It is apparent why the distance of separation between the ions—hence the nature of the medium—is highly influential at this step.

In ionic polymerizations termination by combination does not occur, since all of the polymer ions have the same charge. In addition, there are solvents such as dioxane and tetrahydrofuran in which chain transfer reactions are unimportant for anionic polymers. Therefore it is possible for these reactions to continue without transfer or termination until all monomer has reacted. Evidence for this comes from the fact that the polymerization can be reactivated if a second batch of monomer is added after the initial reaction has gone to completion. In this case the molecular weight of the polymer increases, since no new growth centers are initiated. Because of this absence of termination, such polymers are called living polymers.

While living polymers can be prepared, there are some substances like water, alcohols, and carbon dioxide which are highly effective in terminating chain growth:

$$BM_n{}^{\ominus}A^{\oplus} + H_2O \longrightarrow BM_nH + AOH \tag{6.W}$$

$$BM_n{}^{\ominus}A^{\oplus} + CO_2 \longrightarrow BM_nCOO{}^{\ominus}A^{\oplus} \xrightarrow{HCl} BM_nCOOH + ACl \tag{6.X}$$

In practice, it is very difficult to completely exclude water and CO_2, so chain termination is often induced by these reactions.

An interesting situation is obtained when the catalyst-solvent system is such that the initiator is essentially 100% dissociated before monomer is added and no termination or transfer reactions occur. In this case all chain initiation occurs rapidly when monomer is added, since no time-dependent initiator breakdown is required. If the initial concentration of catalyst is $[AB]_0$, then chain growth starts simultaneously at $[B^-]_0$ centers per unit volume. The rate of polymerization is given by the analog of Eq. (6.24):

$$R_p = \frac{-d[M]}{dt} = k_p[B^-]_0[M] \tag{6.96}$$

which integrates to

$$[M] = [M]_0 e^{-k_p[B^-]_0 t} \tag{6.97}$$

if $[M] = [M]_0$ at $t = 0$. Since no termination occurs, the kinetic chain length at any point during the reaction is given by the amount of monomer reacted at that point, $[M]_0 - [M]$, divided by the number of chain-growth centers:

$$\bar{\nu} = \frac{[M]_0 - [M]}{[B^-]_0} \tag{6.98}$$

Combining Eqs. (6.97) and (6.98) gives

$$\bar{\nu} = \frac{[M]_0}{[B^-]_0}(1 - e^{-k_p[B^-]_0 t}) \tag{6.99}$$

which approaches $[M]_0/[B]_0$ as $t \to \infty$.

The first living polymer studied in detail was polystyrene polymerized with sodium naphthalenide in tetrahydrofuran at low temperatures:

1. The catalyst is prepared by the reaction of sodium metal with naphthalene and results in the formation of a radical ion:

(6.Y

2. These green radical ions react with styrene to produce the red styrene radical anions:

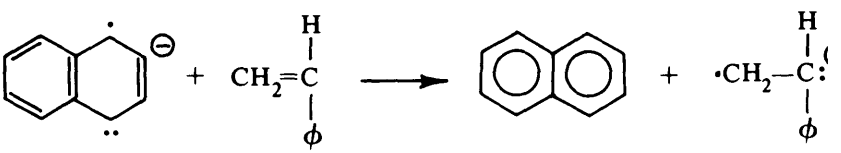

(6.Z

3. The latter undergo radical combination to form the dianion, which subsequently polymerizes:

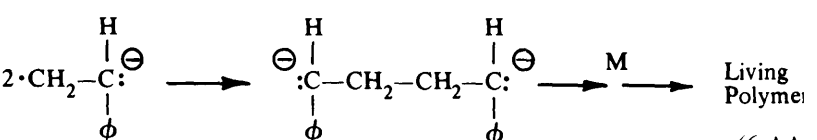

(6.AA

In this case the degree of polymerization is $2\bar{\nu}$ because of the combination step.

The molecular weight distribution for a polymer like that described above is remarkably narrow compared to free-radical polymerization or even to ionic polymerization in which transfer or termination occurs. The sharpness arises from the nearly simultaneous initiation of all chains and the fact that all active centers grow as long as monomer is present. The following steps outline a quantitative treatment of this effect:

1. The first monomer addition to the active center occurs by the reaction

$$B\text{–}M_1^{\ominus}A^{\oplus} + M \longrightarrow B\text{–}M_2^{\ominus}A^{\oplus} \tag{6.BB}$$

for which the rate law is

$$-\frac{d[BM_1^-]}{dt} = k_p[BM_1^-][M] \tag{6.100}$$

2. Substitution of Eq. (6.97) into Eq. (6.100) yields

$$\frac{d[BM_1^-]}{[BM_1^-]} = -k_p[M]_0 \exp(-k_p[B^-]_0 t)\, dt \tag{6.101}$$

Since $[BM_1^-] = [B]_0$ at $t = 0$, Eq. (6.101) can be integrated to

$$[BM_1^-] = [B^-]_0 \exp\left(-\frac{[M]_0}{[B^-]_0}\left(1 - e^{-k_p[B^-]_0 t}\right)\right) \tag{6.102}$$

Consideration of Eq. (6.99) permits Eq. (6.102) to be written as

$$[BM_1^-] = [B^-]_0\, e^{-\bar{\nu}} \tag{6.103}$$

3. The species $BM_2^{\ominus}$ is formed by reaction (6.BB) and lost by

$$BM_2^{\ominus}A^{\oplus} + M \longrightarrow BM_3^{\ominus}A^{\oplus} \tag{6.CC}$$

Therefore the expression for $d[BM_2^-]/dt$ is given by

$$\frac{d[BM_2^-]}{dt} = k_p[BM_1^-][M] - k_p[BM_2^-][M] \tag{6.104}$$

which becomes

$$\frac{d[BM_2^-]}{dt} = k_p[M]_0 e^{-k_p[B^-]_0 t}([B^-]_0 e^{-\bar{\nu}} - [BM_2^-]) \quad (6.105$$

by substitution of Eqs. (6.97) and (6.103). Differentiation of Eq. (6.99 with respect to t shows that $d\bar{\nu} = k_p[M]_0 e^{-k_p[B^-]_0 t}\,dt$. Therefore Eq (6.105) can be written as

$$\frac{d[BM_2^-]}{d\bar{\nu}} + [BM_2^-] = [B^-]_0 e^{-\bar{\nu}} \quad (6.106$$

4. This is a standard differential equation for which the solution is given by

$$[BM_2^-] = [B^-]_0\,\bar{\nu}\,e^{-\bar{\nu}} \quad (6.107$$

We shall examine the solution to this equation in an example below. From the ratio of Eq. (6.106) to Eq. (6.103), note that $[BM_2^-]/[BM_1^-] = \bar{\nu}$

5. The same sequence of steps outlined in items (3) and (4) can be followed to give the concentrations of n-mer anions resulting from n - 1 additions to the original active site:

$$[BM_n^-] = \frac{1}{(n-1)!}\,[B^-]_0\,\bar{\nu}^{n-1}\,e^{-\bar{\nu}} \quad (6.108$$

The expression shows that one extra factor $\bar{\nu}$ enters for each addition and that each successive expression is divided by an extra integer which counts the number of additions to the original growth center.

6. Since the total number of polymer chains is proportional to $[B^-]_0$, the number N_n of n-mers in a population of N polymer molecules is given by

$$\frac{N_n}{N} = \frac{[BM_n^-]}{[B^-]_0} = \frac{1}{(n-1)!}\,\bar{\nu}^{n-1}\,e^{-\bar{\nu}} \quad (6.109$$

Inasmuch as $\bar{\nu}$ is the mean values for n, Eq. (6.109) shows that the distribution for the degree of polymerization follows the Poisson function, Eq (1.38).

The integration of Eq. (6.106) is central to the kinetic proof that living polymers follow Poisson statistics. The solution of this differential equation is illustrated in the following example.

Example 6.7

Show that Eq. (6.107) is a solution to Eq. (6.106). Also consider the extension of the method to $[BM_3^-]$ and $[BM_4^-]$.

Solution

The integrating factor for Eq. (6.106) is $e^{\bar{\nu}}$; therefore multiply the equation through by this factor: $(d[BM_2^-]/d\bar{\nu})\,e^{\bar{\nu}} + [BM_2^-]e^{\bar{\nu}} = [B^-]_0$. Recognize that the left-hand side of the equation is $d([BM_2^-]e^{\bar{\nu}})/d\bar{\nu}$, so the expression becomes

$$d([BM_2^-]e^{\bar{\nu}}) = [B^-]_0 d\bar{\nu}$$

This equation integrates to

$$[BM_2^-]e^{\bar{\nu}} = [B^-]_0\bar{\nu} + \text{const.}$$

where the constant of integration is found to be zero from the fact that at $t = 0$ both $\bar{\nu}$ and $[BM_2^-] = 0$. Rearrangement converts this to $[BM_2^-] = [B^-]_0\bar{\nu}e^{-\bar{\nu}}$ which is Eq. (6.107).

The same set of relationships beginning from Eq. (6.104) can be written for $[BM_3^-]$ and $[BM_4^-]$ and solved by the same procedure. Some key steps are set forth below:

For $[BM_3^-]$	For $[BM_4^-]$
$\dfrac{d[BM_3^-]}{dt} = k_p[M]\left\{[BM_2^-] - [BM_3^-]\right\}$	$\dfrac{d[BM_4^-]}{dt} = k_p[M]\,([BM_3^-] - [BM_4^-])$
$\dfrac{d[BM_3^-]}{d\bar{\nu}} + [BM_3^-] = [B^-]_0\bar{\nu}\,e^{-\bar{\nu}}$	$\dfrac{d[BM_4^-]}{d\bar{\nu}} + [BM_4^-] = [BM_3^-]$
$e^{\bar{\nu}}\left(\dfrac{d[BM_3^-]}{d\bar{\nu}} + [BM_3^-]\right) = [B^-]_0\,\bar{\nu}$	$e^{\bar{\nu}}\left\{\dfrac{d[BM_4^-]}{d\bar{\nu}} + [BM_4^-]\right\} = \dfrac{1}{2}\bar{\nu}^2\,[B^-]_0$
$\int d(e^{\bar{\nu}}\,[BM_3^-]) = [B^-]_0 \int \bar{\nu}\,d\bar{\nu}$	$\int d(e^{\bar{\nu}}[BM_4^-]) = \dfrac{1}{2}[B^-]_0 \int \bar{\nu}^2\,d\bar{\nu}$
$e^{\bar{\nu}}\,[BM_3^-] = [B^-]_0\,\dfrac{1}{2}\bar{\nu}^2$	$e^{\bar{\nu}}[BM_4^-] = \dfrac{1}{3}\,\dfrac{1}{2}\,[B^-]_0\,\bar{\nu}^3$
$[BM_3^-] = \dfrac{1}{2}\bar{\nu}^2\,e^{-\bar{\nu}}\,[B^-]_0$	$[BM_4^-] = \dfrac{1}{3!}\bar{\nu}^3\,[B^-]_0$

These examples show that the power of $\bar{\nu}$ and the factorial are one less than the degree of polymerization for the ion under consideration.

•

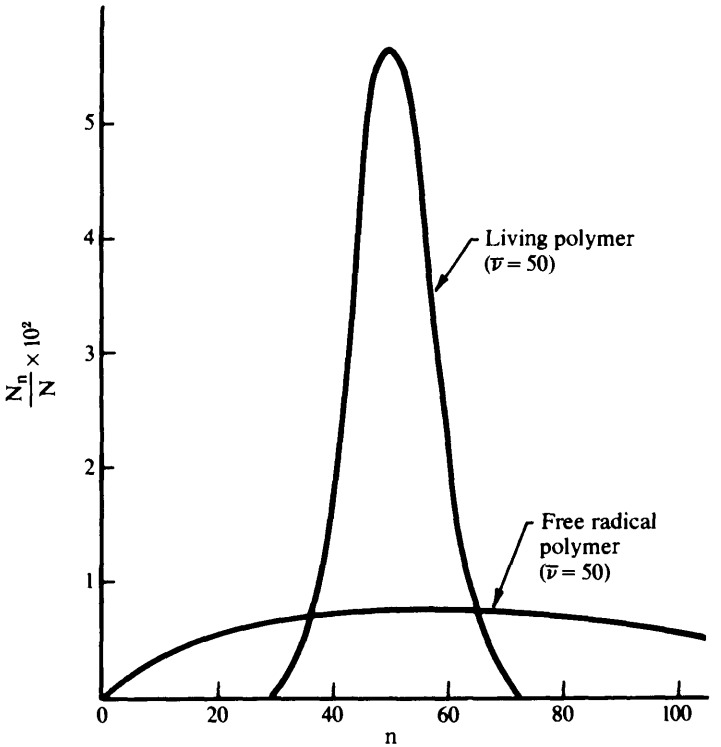

Figure 6.11 Comparison of the number distribution of n-mers for polymers prepared from anionic and free-radical active centers, both with $\bar{\nu} = 50$.

That the Poisson distribution results in a narrower distribution of molecular weights than is obtained with termination is shown by Fig. 6.11. Here N_n/N is plotted as a function of n for $\bar{\nu} = 50$, for living polymers as given by Eq. (6.109), and for conventional free-radical polymerization as given by Eq. (6.77). This same point is made by considering the ratio $\bar{M}_w/\bar{M}_n$ for the case of living polymers. This ratio may be shown to equal

$$\frac{\bar{n}_w}{\bar{n}_n} = 1 + \frac{\bar{\nu}}{(\bar{\nu}+1)^2} \tag{6.110}$$

which is equal to 1.02 for $\bar{\nu} = 50$ and approaches unity as $\bar{\nu} \to \infty$ in contrast to a ratio of 1.5 (for combination) or 2 (for disproportionation) for the free-radical mechanism.

6.11 Cationic Polymerization

Just as anionic polymerizations show certain parallels with the free-radical mechanism, so too can cationic polymerization be discussed in terms of the same broad outline. There are some differences from the anionic systems, however, so the fact that both proceed through ionic intermediates should not be overextended.

The principal differences between cationic and anionic polymerizations center around the following points:

1. A single catalyst is often not sufficient in cationic polymerizations; frequently a cocatalyst is required.
2. Chain transfer is far more important than in the anionic case, so we do not encounter living polymers in cationic systems.
3. Total dissociation of the initiator system is rare, so the simplifications we explored for this condition in the anionic case cannot be used.

We shall consider these points below. The mechanism for cationic polymerization continues to include initiation, propagation, transfer, and termination steps, and the rate of polymerization and the kinetic chain length are the principal quantities of interest.

In cationic polymerization the active species is the ion which is formed by the addition of a proton from the initiator system to a monomer. For vinyl monomers the type of substituents which promote this type of polymerization are those which are electron supplying, like alkyl, 1,1-dialkyl, aryl, and alkoxy. Isobutylene and α-methyl styrene are examples of monomers which have been polymerized via cationic intermediates.

The catalysts for cationic polymerization are either protonic acids or Lewis acids, such as H_2SO_4 and $HClO_4$ or BF_3, $AlCl_3$, and $TiCl_4$:

1. The Lewis acids must be used with a protonic cocatalyst such as water or methanol which generates protons through the following kinds of equilibria:

$$BF_3 + H_2O \rightleftarrows F_3BOH^- + H^+$$

$$AlCl_3 + H_2O \rightleftarrows Cl_3AlOH^- + H^+ \qquad (6.DD)$$

$$TiCl_4 + CH_3OH \rightleftarrows Cl_4TiOCH_3^- + H^+$$

With insufficient catalyst these equilibria lie too far to the left, while excess cocatalyst destroys the catalyst and/or terminates the chain. The optimum proportion of catalyst and cocatalyst varies with the system employed and also with the solvent for a specific system.

2. Protonic acids dissociate to some extent in the nonaqueous reaction mixtures to produce an equilibrium concentration of protons:

$$H_2SO_4 \rightleftarrows H^+ + HSO_4^-$$
$$HClO_4 \rightleftarrows H^+ + ClO_4^- \qquad (6.EE)$$

3. The general formula for the initiator species can be written H^+B^-, where the degree of separation or ion pairing depends on the polarity of the medium and the possibility of specific solvation interactions. If we represent the equilibrium constant for the reactions in (6.DD) and (6.EE) by K, the initiator concentration can be written as

$$[H^+B^-] = K[\text{Lewis acid}][\text{cocatalyst}] \qquad (6.111)$$

or

$$[H^+B^-] = K[\text{protonic acid}] \qquad (6.112)$$

The proton adds to the more negative carbon atom in the olefin to initiate chain growth:

$$CH_2{=}C(R)(H) + H^+B^- \longrightarrow CH_3{-}C^{\oplus}(R)(H)\,B^{\ominus} \qquad (6.FF)$$

The electron-releasing R group helps stabilize this cation. As with anionic polymerization, the separation of the ions and hence the ease of monomer insertion depends on the reaction medium. The propagation reaction may be written as

$$CH_3{-}C^{\oplus}(R)(H)\,B^{\ominus} + (n-1)\,M \longrightarrow M_n{}^{\oplus}B^{\ominus} \qquad (6.GG)$$

Aldehydes can also polymerize in this manner, the corresponding reactions for $O{=}CH_2$ being

$$H^+B^- + O{=}CH_2 \longrightarrow H{-}O{-}C^{\oplus}(H)(H)\,B^{\ominus} \xrightarrow{O=CH_2} \longrightarrow \longrightarrow H\{O{-}CH_2\}_n^{\oplus}B^{\ominus} \qquad (6.HH)$$

Formaldehyde polymerizes even without added catalyst, but it is possible that traces of formic acid act as adventitious catalysts in this system.

One of the side reactions that can complicate cationic polymerization is the possibility of the ionic repeat unit undergoing the well-known carbonium ion rearrangement during the polymerization. The following example illustrates this situation.

Example 6.8

It has been observed† that poly(1,1-dimethyl propane) is the product when 3-methylbutene-1 is polymerized with $AlCl_3$ in ethyl chloride at -130°C. Write structural formulas for the expected repeat units and those observed and propose an explanation.

Solution

The structures expected and found are sketched here:

Expected

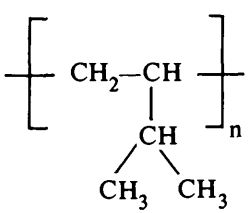

Found

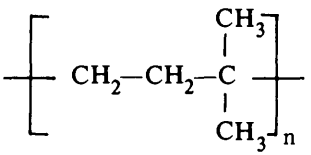

The conversion of the cationic intermediate of the monomer to the cation of the product occurs by a hydride shift between adjacent carbons:

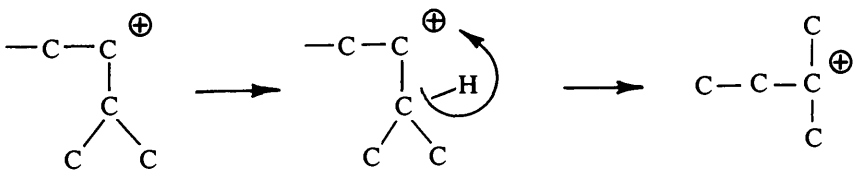

This is a well-known reaction in organic chemistry which is favored by the greater stability of the tertiary cation compared to the secondary ion.

† J. P. Kennedy and R. M. Thomas, *Makromol. Chem.* 53:28 (1962).

The extent of such reactions depends on the monomer structure as well as the temperature and the solvent.

As intimated above, termination occurs in these systems by reactions with water or other proton sources:

$$M_n^{\oplus}B^{\ominus} + H_2O \longrightarrow M_nOH + HB \tag{6.II}$$

Chain transfer reactions to monomer and/or solvent also occur and lower the kinetic chain length without affecting the rate of polymerization:

$$M_n^{\oplus}B^{\ominus} + M \longrightarrow M_n + M^{\oplus}B^{\ominus} \tag{6.JJ}$$

A detailed kinetic analysis depends on the specifics of the initiation and termination-transfer steps. We shall illustrate only one combination; other possibilities are done similarly:

1. For initiation involving a cocatalyst, say, water,

$$R_i = k_i[H^+B^-][M] = k_iK[\text{Lewis acid}][H_2O][M] \tag{6.113}$$

2. For termination by transfer to monomer,

$$R_{tr} = k_{tr}[M_n^+][M] \tag{6.114}$$

3. Under stationary-state conditions, $R_i = R_{tr}$; therefore

$$[M_n^+]_s = \frac{k_iK[\text{Lewis acid}][H_2O]}{k_{tr}} \tag{6.115}$$

4. The rate of polymerization is given by $k_p[M][M_n^+]$; hence

$$R_p = \frac{k_pk_iK[\text{Lewis acid}][H_2O][M]}{k_{tr}} \tag{6.116}$$

5. Even though the catalyst may be only partially converted to H^+B^-, the concentration of these ions may be on the order of 10^5 times greater than the concentration of free radicals in the corresponding stationary state of the radical mechanism. Likewise, k_p for ionic polymerization is on the order of 100 times larger than the sum of the constants for all termination and transfer steps. By contrast, $k_p/k_t^{1/2}$, which is pertinent for the radical mechanism, is typically on the order of 10^{-1}. These comparisons illustrate that ionic polymerizations occur very fast even at low temperatures.

6. Applying the Arrhenius equation to Eq. (6.116) shows that the apparent activation energy for the overall rate of polymerization is given by

$$E_{app}^* = E_i^* + E_p^* - E_{tr}^* \tag{6.117}$$

In some cases E_{tr}^* may be larger than $E_i^* + E_p^*$, which leads to the unusual situation where the rate of the polymerization reaction decreases with increasing temperature. The specifics here depend on the reaction system, including the solvent.

7. The kinetic chain length is given by the ratio R_p/R_{tr} or

$$\bar{\nu} = \frac{k_p}{k_{tr}} = \frac{1}{C_M} \tag{6.118}$$

where C_M is the chain transfer constant to monomer. These constants tend to be about two orders of magnitude larger than their counterparts for the radical mechanism at the temperatures of the respective reactions. There continues to be a significant dependence on the solvent and the nature of the catalyst as far as chain transfer is concerned.

Problems

1. The efficiency of AIBN in initiating polymerization at 60°C was determined by Bevington et al.† by the following strategy. They measured R_p and $\bar{\nu}$ and calculated $R_i = R_p/\bar{\nu}$. The constant k_d was measured directly in the system, and from this quantity and the measured ratio $R_p/\bar{\nu}$ the fraction f could be determined. The following results were obtained for different concentrations of initiator:

[I] (g liter^{-1})	$R_p/\bar{\nu} \times 10^8$ (mol liter^{-1} sec^{-1})
0.0556	0.377
0.250	1.57
0.250	1.72
1.00	6.77
1.50	10.9
2.50	17.1

Using $k_d = 0.0388$ hr^{-1}, evaluate f from these data.

2. AIBN was synthesized using ^{14}C-labeled reagents and the tagged compound was used to initiate polymerization of methyl methacrylate and styrene.

† J. C. Bevington, J. H. Bradbury, and G. M. Burnett, *J. Polym. Sci.* 12:469 (1954).

Samples of initiator and polymers containing initiator fragments were burned to CO_2. The radioactivity of uniform (in sample size and treatment) CO_2 samples was measured in counts per minute (cpm) by a suitable Geiger counter. A general formula for the poly(methyl methacrylate) with its initiator fragments is $(C_5H_8O_2)_n(C_4H_6N)_m$, where n is the degree of polymerization for the polymer and m is either 1 or 2, depending on the mode of termination. The specific activity measured in the CO_2 resulting from combustion of the polymer relative to that produced by the initiator is

$$\frac{\text{Activity of C in polymer}}{\text{activity of C in initiator}} = \frac{4m}{5n + 4m} \cong \frac{4m}{5n}$$

From the ratio of activities and measured values of n, the average number of initiator fragments per polymer can be determined. Carry out a similar argument for the ratio of activities for polystyrene and evaluate the average number of initiator fragments per molecule for each polymer from the following data†:

Methyl methacrylate		Styrene	
$\bar{M}_n$	Counts per minute	$\bar{M}_n$	Counts per minute
444,000	20.6	383,000	25.5
312,000	30.1	117,000	86.5
298,000	29.0	114,000	89.5
147,000	60.5	104,000	96.4
124,000	76.5	101,000	113.5
91,300	103.4		
89,400	104.6		

For both sets of data, the radioactivity from the labeled initiator gives 96,500 cpm when converted to CO_2.

3. In the same research described in Example 6.4, the authors‡ measured the following rates of polymerization:

Run number	$R_p \times 10^4$ (mol liter^{-1} sec^{-1})
5	3.40
6	2.24
8	6.50
12	5.48
13	7.59

They also reported a k_p value of 1.2×10^4 liter mol^{-1} sec^{-1}, but the concentrations of monomer in each run were not given. Use these value of

† J. C. Bevington, H. W. Melville, and R. P. Taylor, *J. Polym. Sci.* 12:449 (1954).

‡ T. Takahashi and P. Ehrlich, *Polym. Prepr.* 22:203 (1981).

R_p and k_p and the values of $\bar{\tau}$ and k_t given in Example 6.4 to evaluate [M] for each run. As a double check, evaluate [M] from these values of R_p (and k_p) and the values of R_i and k_t given in the example.

4. In a series of experiments at 60°C, the rate of polymerization of styrene agitated in water containing persulfate initiator was measured† for different concentrations of sodium dodecyl sulfate emulsifier. The following results were obtained:

[surfactant] $\times 10^3$ (mol liter^{-1})	R_p (% min^{-1})
3.8	~0.08
4.8	~0.08
5.00	~0.08
6.00	0.40
6.25	0.75
6.8	0.77
7.2	0.79
7.8	0.80

Propose an explanation for this variation in R_p. Over the same range of surfactant concentrations, R_p for vinyl acetate is roughly constant at about 1.1% min^{-1}. Criticize or defend the following proposition: Since vinyl acetate is about 70 times more soluble in water than styrene at 30°C, the former undergoes solution polymerization in the aqueous phase while styrene displays true emulsion polymerization under suitable conditions.

5. Arnett‡ initiated the polymerization of methyl methacrylate in benzene at 77°C with AIBN and measured the initial rates of polymerization for the concentrations listed:

[M] (mol liter^{-1})	$[I]_0 \times 10^4$ (mol liter^{-1})	$R_p \times 10^3$ (mol liter^{-1} min^{-1})
9.04	2.35	11.61
8.63	2.06	10.20
7.19	2.55	9.92
6.13	2.28	7.75
4.96	3.13	7.31
4.75	1.92	5.62
4.22	2.30	5.20
4.17	5.81	7.81
3.26	2.45	4.29
2.07	2.11	2.49

† S. Okamura and T. Motoyama, *J. Polym. Sci.* 58:221 (1962).

‡ L. M. Arnett, *J. Am. Chem. Soc.* 74:2027 (1952).

Use these data to evaluate the cluster of constants $(fk_d/k_t)^{1/2} k_p$ at this temperature. Evaluate $k_p/k_t^{1/2}$ using Arnett's finding that $f = 1.0$ and assuming the k_d value determined in Example 6.1 for AIBN at 77°C in xylene also applies in benzene.

6. Since propagation does not change the number of radicals in the system, the rate of change of the radical concentration under non-stationary-state conditions is given by $d[M\cdot]/dt = 2k_d f[I] - 2k_t[M\cdot]^2$. For the short induction period before the stationary-state concentration of radicals is reached, [I] may be regarded as a constant at the initial value $[I]_0$. Making this assumption and using a table of integrals, show by integration that this equation yields Eq. (6.43), the relationship used in Example 6.2, for the nonstationary value of $[M\cdot]$ at time t.
7. The lifetime of polystyrene radicals at 50°C was measured† by the rotating sector method as a function of the extent of conversion to polymer. The following results were obtained:

Percent conversion	$\bar{\tau}$ (sec)
0	2.29
32.7	1.80
36.3	9.1
39.5	13.9
43.8	18.8

Propose an explanation for the variation observed.

8. The equations derived in Sec. 6.7 are based on the assumption that termination occurs exclusively by either disproportionation or combination. This is usually not the case: Some proportion of each is the more common case. If A equals the fraction of termination occurring by disproportionation, we can write $\bar{n}_n = A[1/1 - p] + (1 - A)[2/(1 - p)]$ and $\bar{n}_w/\bar{n}_n = A(1 + p) + (1 - A)[(2 + p)/2]$. From measurements of $\bar{n}_n$ and $\bar{n}_w/\bar{n}_n$ it is possible *in principle* to evaluate A and p. May and Smith‡ have done this for a number of polystyrene samples. A selection of their data for which this approach seems feasible is presented:

$\bar{n}_n$	$\bar{n}_w/\bar{n}_n$
1129	1.60
924	1.67
674	1.73
609	1.74

† M. S. Matheson, E. E. Auer, E. B. Bevilacqua, and J. E. Hart, *J. Am. Chem. Soc.* 73:1700 (1951).

‡ J. A. May, Jr., and W. B. Smith, *J. Phys. Chem.* 72:216 (1968).

Since p is very close to unity, it is adequate to assume this value and evaluate A from $\bar{n}_w/\bar{n}_n$ and then use the value of A so obtained to evaluate a better value of p from $\bar{n}_n$.

9. In the research described in the last problem, the authors† determined the following distribution of molecular weights by a chromatographic procedure:

n	$w_n/w_{tot} \times 10^4$	n	$w_n/w_{tot} \times 10^4$
100	3.25	800	6.88
200	5.50	900	6.10
300	6.80	1200	4.20
400	7.45	1500	2.90
500	7.91	2000	1.20
600	7.82	2500	0.50
700	7.18	3000	0.20

They asserted that the points are described by the expression $w_n/w_{tot} = An(1-p)^2 p^{n-1} + 0.5(1-A)(n)(n-1)(1-p)^3 p^{n-2}$, with A = 0.65 and p = 0.99754. In this expression w_n/w_{tot} is the weight fraction n-mer. Calculate some representative points for this function and plot the theoretical and experimental points on the same graph. On the basis of Eq. (5.30) and the notation of the last problem, extract from the expression given the weight fraction n-mer resulting from termination by combination.

10. Palit and Das‡ measured $\bar{\nu}_{tr}$ at 60°C for different values of the ratio [SX]/[M] and evaluated C_{SX} and $\bar{\nu}$ for vinyl acetate undergoing chain transfer with various solvents. Some of their measured and derived results are tabulated below (the same concentrations of AIBN and monomer were used in each run):

Solvent	$\bar{\nu}$	$\bar{\nu}_{tr}$	[SX]/[M]	$C_{SX} \times 10^4$
t-Butyl alcohol	6580	3709	–	0.46
Methyl isobutyl ketone	6670	510	0.492	–
Diethyl ketone	6670	–	0.583	114.4
Chloroform	–	93	0.772	125.2

Assuming that no other transfer reactions occur, calculate the values missing from the table. Criticize or defend the following proposition: The $\bar{\nu}$ values obtained from the limit [SX]/[M] → 0 show that the AIBN initiates polymerization identically in all solvents.

† J. A. May, Jr., and W. B. Smith, *J. Phys. Chem.* 72:216 (1968).

‡ S. R. Palit and S. K. Das, *Proc. R. Soc. London* 226A:82 (1954).

11. Gregg and Mayo† studied the chain transfer between styrene and carbon tetrachloride at 60 and 100°C. A sample of their data is given below for each of these temperatures:

At 60°C		At 100°C	
$[CCl_4]/[\text{styrene}]$	$\bar{\nu}_{tr}^{-1} \times 10^5$	$[CCl_4]/[\text{styrene}]$	$\bar{\nu}_{tr}^{-1} \times 10^5$
0.00614	16.1	0.00582	36.3
0.0267	35.9	0.0222	68.4
0.0393	49.8	0.0416	109
0.0704	74.8	0.0496	124
0.1000	106	0.0892	217
0.1643	156		
0.2595	242		
0.3045	289		

Evaluate the chain transfer constant (assuming that no other transfer reactions occur) at each temperature. By means of an Arrhenius analysis, estimate $E_{tr}^* - E_p^*$ for this reaction. Are the values of $\bar{\nu}$ in the limit of no transfer in the order expected for thermal polymerization? Explain.

12. Soum and Fontanille‡ prepared a living polymer of 2-vinyl pyridine using benzyl picolyl magnesium as the initiator. The values of $\bar{M}_n$ were measured experimentally for polymers prepared with different concentrations of initiator and different initial concentrations of monomer. The results are given below; calculate the theoretical molecular weights expected if polymerization proceeds completely from 100% predissociated initiator and compare the theoretical and experimental values:

$[I] \times 10^4$ (mol liter^{-1})	$[M]_0 \times 10^2$ (mol liter^{-1})	$\bar{M}_n$ (g mol^{-1})
4.8	8.2	20,000
3.7	8.5	25,000
1.7	7.1	46,000
4.8	7.1	17,000
5.8	7.3	14,000
1.5	15.0	115,000

13. Ionic polymers may exist as undissociated, unsolvated ion pairs; undissociated ion pairs solvated to some extent; solvated ions dissociated to some extent; or some combination of these. The propagation rate constant k_p and the dissociation equilibrium constant K of the lithium salt of anionic

† R. A. Gregg and F. R. Mayo, *J. Am. Chem. Soc.* 70:2373 (1948).

‡ A. Soum and M. Fontanille, in *Anionic Polymerization*, J. E. McGrath (Ed.), ACS Symposium Series, Vol. 166 (1981).

polystyrene were measured in tetrahydrofuran containing various amounts of dioxane. The dielectric constant of the mixed solvents was also determined as a measure of polarity: The lower the dielectric constant, the less polar the medium. The following are some of the results obtained†:

Volume percent dioxane	Dielectric constant	k_p (liter mol^{-1} sec^{-1})	K
0	7.39	65,000	$\sim 2 \times 10^{-7}$
26.0	5.95	257	9×10^{-9}
47.6	4.81	~80	1.8×10^{-10}
69.4	3.75	6.1	Too small
84.8	2.93	~1.5	to measure
100.0	2.20	~0.9	reliably

Criticize or defend the following proposition: The decrease in K with increasing dioxane content is consistent with the diminished solvent properties for ions of substances with low dielectric constant. The decrease in k_p is quantitatively explained by this decrease in free ion concentration, since k_p eventually approaches a limiting value for unsolvated ion pairs.

14. The following table shows the values of ΔH°_{298} for the gas phase reactions $X(g) + H^+(g) \rightarrow HX^+(g)$ where X is an olefin.

X	XH^+	ΔH°_{298} (kJ mol^{-1})
$CH_2{=}CH_2$	$CH_2CH_3^+$	-640
$CH_3CH{=}CH_2$	$CH_3CH_2CH_2^+$	-690
$CH_3CH{=}CH_2$	$CH_3C^+HCH_3$	-757
$CH_3CH_2CH{=}CH_2$	$CH_3CH_2CH_2CH_2^+$	-682
$CH_3CH{=}CHCH_3$	$CH_3CH_2C^+HCH_3$	-782
$(CH_3)_2C{=}CH_2$	$(CH_3)_2CHCH_2^+$	-695

Use these data‡ to quantitatively comment on each of the following points:

(a) The cation is stabilized by electron-supplying alkyl substituents.
(b) The carbonium ion rearrangement of *n*-propyl ions to *i*-propyl ions is energetically favored.
(c) With the supplementary information that $\Delta H^\circ_{f,298}$ of 1-butene and cis-2-butene are +1.6 and -5.8 kJ mol^{-1}, respectively, evaluate the ΔH_{298} for the rearrangement *n*-butyl to sec-butyl ions and compare with the corresponding isomerization for the propyl cations.

†M. van Beylen, D. N. Bhattacharyya, J. Smid, and M. Szwarc, *J. Phys. Chem.* 70:157 (1966).

‡P. H. Plesch (Ed.), *Cationic Polymerization*, Macmillan, New York, 1963.

(d) Of the monomers shown, only isobutene undergoes cationic polymerization to any significant extent. Criticize or defend the following proposition: The above data explain this fact by showing that this is the only monomer of those listed which combines a sufficiently negative ΔH for protonation with the freedom from interfering isomerization reactions.

Bibliography

1. Allcock, H. R., and Lampe, F. W., *Contemporary Polymer Chemistry*, Prentice-Hall, Englewood Cliffs, N.J., 1981.
2. Bagdasan'yan, K. S., *Theory of Free Radical Polymerization*, Israel Program for Scientific Translations, Jerusalem, 1968.
3. Brandup, J., and Immergut, E. H., and McDowell, W. (Eds.), *Polymer Handbook*, 2nd ed., Wiley, New York, 1975.
4. Ham, G. E. (Ed.), *Vinyl Polymerization*, Marcel Dekker, New York, 1967.
5. North, A. M., *The Kinetics of Free Radical Polymerization*, Pergamon, New York, 1966.
6. Odian, G., *Principles of Polymerization*, 2nd ed., Wiley, New York, 1981.
7. Smith, D. A. (Ed.), *Addition Polymers: Formation and Characterization*, Plenum Press, New York, 1968.

7

Polymers with Microstructure
Copolymers and Stereoregular Polymers

In a Rolls or a van
Wrapped in mink or Saran
Any way that you can
Come back to me!

Come Back to Me, words by Alan Jay Lerner, music by Burton Lane

7.1 Introduction

All polymer molecules have unique features of one sort or another at the level of individual repeat units. Occasional head-to-head or tail-to-tail orientations, random branching, and the distinctiveness of chain ends are all examples of such details. In this chapter we shall focus attention on two other situations which introduce variation in structure into polymers at the level of the repeat unit: the presence of two different monomers or the regulation of configuration of successive repeat units. In the former case copolymers are produced, and in the latter polymers with differences in tacticity. Although the products are quite different materials, their microstructure can be discussed in very similar terms. Hence it is convenient to discuss the two topics in the same chapter.

In the discussion of these combined topics, we use statistics extensively because the description of microstructure requires this kind of approach. This is the basis for merging a discussion of copolymers and stereoregular polymers into a single chapter. In other respects these two classes of materials and the processes which produce them are very different and their description leads us into some rather diverse areas.

The formation of copolymers involves the reaction of (at least) two kinds of monomers. This means that each must be capable of undergoing the same propagation reaction, but is is apparent that quite a range of reactivities is compatible with this broad requirement. We shall examine such things as the polarity of monomers, the degree of resonance stabilization they possess and the steric

hindrance they experience in an attempt to understand these differences in reactivity. There are few types of reactions for which chemists are successful in explaining all examples with general concepts such as these. Polymerization reactions are no exception. Even for the specific case of free-radical copolymerization, we shall see that reactivity involves the interplay of all these considerations.

To achieve any sort of pattern in configuration among successive repeat units in a polymer chain, the tendency toward random addition must be overcome. Although temperature effects are pertinent here—remember that high temperature is the great randomizer—real success in regulating the pattern of successive additions involves the use of catalysts which "pin down" both the monomer and the growing chain so that their reaction is biased in favor of one mode of addition or another. We shall discuss the Ziegler-Natta catalysts which accomplish this and shall discover these to be complicated systems for which no single mechanism is entirely satisfactory.

For both copolymers and stereoregular polymers, experimental methods for characterizing the products often involve spectroscopy. We shall see that nuclear magnetic resonance (NMR) spectra are particularly well suited for the study of tacticity. This method is also used for the analysis of copolymers.

In spite of the assortment of things discussed in this chapter, there are also a variety of topics that could be included but which are not owing to space limitations. We do not discuss copolymers formed by the step-growth mechanism, for example, or the use of Ziegler-Natta catalysts to regulate geometrical isomerism in, say, butadiene polymerization. Some other important omissions are noted in passing in the body of the chapter.

7.2 Copolymer Composition

We begin our discussion of copolymers by considering the free-radical polymerization of a mixture of two monomers, M_1 and M_2. This is already a narrow view of the entire field of copolymers, since more than two repeat units can be present in copolymers and, in addition, mechanisms other than free-radical chain growth can be responsible for copolymer formation. The essential features of the problem are introduced by this simpler special case, so we shall restrict our attention to this system.

The polymerization mechanism continues to include initiation, termination, and propagation steps. This time, however, there are four distinctly different propagation reactions:

$$-M_1\cdot + M_1 \xrightarrow{k_{11}} -M_1M_1\cdot \tag{7.A}$$

$$-M_1\cdot + M_2 \xrightarrow{k_{12}} -M_1M_2\cdot \tag{7.B}$$

$$-M_2\cdot + M_1 \xrightarrow{k_{21}} -M_2M_1\cdot \tag{7.C}$$

$$-M_2\cdot + M_2 \xrightarrow{k_{22}} -M_2M_2\cdot \tag{7.D}$$

Each of these reactions is characterized by a propagation constant which is labeled by a two-digit subscript: The first number identifies the terminal repeat unit in the growing radical, and the second identifies the adding monomer. The rate laws governing these four reactions are

$$R_{p,11} = k_{11}[M_1\cdot][M_1] \tag{7.1}$$

$$R_{p,12} = k_{12}[M_1\cdot][M_2] \tag{7.2}$$

$$R_{p,21} = k_{21}[M_2\cdot][M_1] \tag{7.3}$$

$$R_{p,22} = k_{22}[M_2\cdot][M_2] \tag{7.4}$$

In writing Eqs. (7.1)-(7.4) we make the customary assumption that the kinetic constants are independent of the size of the radical and we indicate the concentration of all radicals, whatever their chain length, ending with the M_1 repeat unit by the notation $[M_1\cdot]$. This formalism therefore assumes that only the nature of the radical chain end influences the rate constant for propagation. We refer to this as the terminal control mechanism. If we wished to consider the effect of the next-to-last repeat unit in the radical, each of these reactions and the associated rate laws would be replaced by two alternatives. Thus reaction (7.A) becomes

$$-M_1M_1\cdot + M_1 \xrightarrow{k_{111}} -M_1M_1M_1\cdot \tag{7.E}$$

$$-M_2M_1\cdot + M_1 \xrightarrow{k_{211}} -M_2M_1M_1\cdot \tag{7.F}$$

and Eq. (7.1) becomes

$$R_{p,111} = k_{111}[M_1M_1\cdot][M_1] \tag{7.5}$$

$$R_{p,211} = k_{211}[M_2M_1\cdot][M_1] \tag{7.6}$$

when the effect of the next-to-last, or penultimate, unit is considered. For now we shall restrict ourselves to the simpler case where only the terminal unit determines behavior, although systems in which the penultimate effect is important are well known.

It is the magnitude of the various k values in Eqs. (7.1)-(7.4) that describes the intrinsic kinetic differences between the various modes of addition, and the k's plus the concentrations of the different species determine the rates at which the four kinds of additions occur. It is the proportion of different steps which determines the composition of the copolymer produced.

Monomer M_1 is converted to polymer by reactions (7.A) and (7.C); therefore the rate at which this occurs is the sum of $R_{p,11}$ and $R_{p,21}$:

$$-\frac{d[M_1]}{dt} = k_{11}[M_1\cdot][M_1] + k_{21}[M_2\cdot][M_1] \tag{7.7}$$

Likewise, reactions (7.B) and (7.D) convert M_2 to polymer, and the rate at which this occurs is the sum of $R_{p,12}$ and $R_{p,22}$:

$$-\frac{d[M_2]}{dt} = k_{12}[M_1\cdot][M_2] + k_{22}[M_2\cdot][M_2] \tag{7.8}$$

The ratio of Eqs. (7.7) and (7.8) gives the relative rates of the two monomer additions and, hence, the ratio of the two kinds of repeat units in the copolymer:

$$\frac{d[M_1]}{d[M_2]} = \frac{k_{11}[M_1\cdot][M_1] + k_{21}[M_2\cdot][M_1]}{k_{12}[M_1\cdot][M_2] + k_{22}[M_2\cdot][M_2]} \tag{7.9}$$

We saw in the last chapter that the stationary-state approximation is applicable to free-radical homopolymerizations, and the same is true of copolymerizations. Of course, it takes a brief time for the stationary-state radical concentration to be reached, but this period is insignificant compared to the total duration of a polymerization reaction. If the total concentration of radicals is constant, this means that the rate of crossover between the different types of terminal units is also equal, or that $R_{p,21} = R_{p,12}$:

$$k_{12}[M_1\cdot][M_2] = k_{21}[M_2\cdot][M_1] \tag{7.10}$$

or

$$\frac{[M_1\cdot]}{[M_2\cdot]} = \frac{k_{21}[M_1]}{k_{12}[M_2]} \tag{7.11}$$

Combining Eqs. (7.9) and (7.11) yields the important copolymer composition equation:

$$\frac{d[M_1]}{d[M_2]} = \frac{[M_1]}{[M_2]}\,\frac{(k_{11}/k_{12})[M_1] + [M_2]}{(k_{22}/k_{21})[M_2] + [M_1]} \tag{7.12}$$

Although there are a total of four different rate constants for propagation, Eq. (7.12) shows that the relationship between the relative amounts of the two monomers incorporated into the polymer and the composition of the monomer feedstock involves only two ratios of different pairs of these constants. Accordingly, we simplify the notation by defining

$$r_1 = \frac{k_{11}}{k_{12}} \tag{7.13}$$

and

$$r_2 = \frac{k_{22}}{k_{21}} \tag{7.14}$$

With these substitutions, Eq. (7.12) becomes

$$\frac{d[M_1]}{d[M_2]} = \frac{[M_1]}{[M_2]} \frac{r_1[M_1] + [M_2]}{r_2[M_2] + [M_1]} = \frac{1 + r_1[M_1]/[M_2]}{1 + r_2[M_2]/[M_1]} \tag{7.15}$$

Mayo and collaborators were among the earliest workers to clarify the relationship between copolymer and monomer solution compositions.

The ratio $d[M_1]/d[M_2]$ is the same as the ratio of the numbers of each kind of repeat unit in the polymer formed from the solution containing M_1 and M_2 at concentrations $[M_1]$ and $[M_2]$, respectively. Henceforth we shall designate this ratio as n_1/n_2. Since the composition of the monomer solution changes as the reaction progresses, Eq. (7.15) applies to the feedstock as prepared only during the initial stages of the polymerization. Subsequently, the instantaneous concentrations in the prevailing mixture apply unless monomer is added continuously to replace that which has reacted and maintain the original composition of the feedstock. We shall assume that it is the initial product formed that we describe when we use Eq. (7.15) so as to remove uncertainty as to the monomer concentrations.

As an alternative to the ratios n_1/n_2 and $[M_1]/[M_2]$ in Eq. (7.15), it is convenient to describe the composition of both the polymer and the feedstock in terms of the mole fraction of each monomer. Defining F_i as the mole fraction of the ith component in the polymer and f_i as the mole fraction of component i in the monomer solution, we observe that

$$F_1 = 1 - F_2 = \frac{d[M_1]}{d[M_1] + d[M_2]} \tag{7.16}$$

and

$$f_1 = 1 - f_2 = \frac{[M_1]}{[M_1] + [M_2]} \tag{7.17}$$

Combining Eqs. (7.15) and (7.16) into (7.17) yields

$$F_1 = \frac{r_1 f_1^2 + f_1 f_2}{r_1 f_1^2 + 2 f_1 f_2 + r_2 f_2^2} \tag{7.18}$$

This equation relates the composition of the copolymer formed to the instantaneous composition of the feedstock and to the parameters r_1 and r_2 which characterize the specific system. Figure 7.1 shows a plot of F_1 versus f_1 – the mole fractions of component 1 in the copolymer and monomer mixture, respectively – for several arbitrary values of the parameters r_1 and r_2. Inspection of Fig. 7.1 brings out the following points:

1. If $r_1 = r_2 = 1$, the copolymer and the feed mixture have the same composition at all times. In this case Eq. (7.18) becomes

$$F_1 = \frac{f_1(f_1 + f_2)}{(f_1 + f_2)^2} = f_1$$

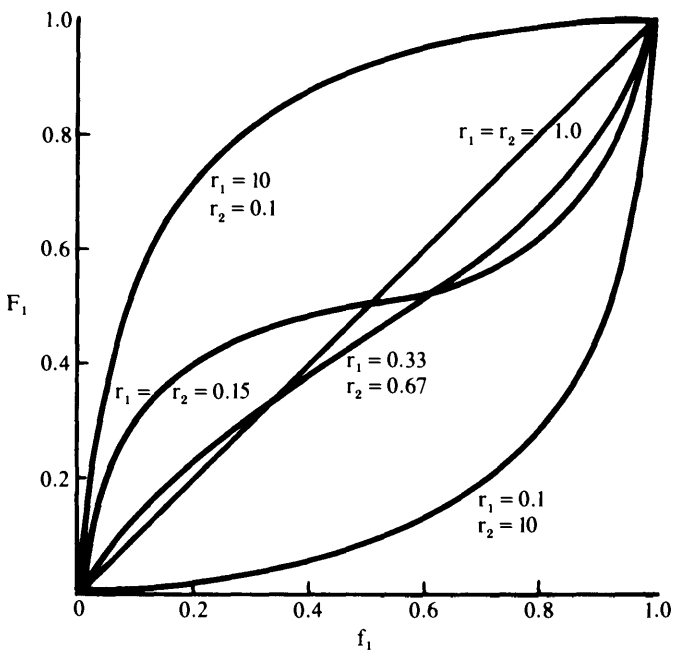

Figure 7.1 Mole fraction of component 1 in copolymers (F_1) and feedstock (f_1) for various values of r_1 and r_2.

2. If $r_1 = r_2$, the copolymer and the feed mixture have the same composition at $f = 0.5$. In this case Eq. (7.18) becomes $F_1 = (r + 1)/2(r + 1) = 0.5$.
3. If $r_1 = r_2$, with both values less than unity, the copolymer is richer in component 1 than the feed mixture for $f_1 < 0.5$, and richer in component 2 than the feed mixture for $f_1 > 0.5$.
4. If $r_1 = r_2$, with both values greater than unity, an S-shaped curve passing through the point (0.5, 0.5) would also result, but in this case reflected across the 45° line compared to item (3).
5. If $r_1 \neq r_2$, with both values less than unity, the copolymer starts out richer in monomer 1 than the feed mixture and then crosses the 45° line, and is richer in component 2 beyond this crossover point. At the crossover point the copolymer and feed mixture have the same composition. The monomer ratio at this point is conveniently solved from Eq. (7.15):

$$\left(\frac{[M_1]}{[M_2]}\right)_{\text{cross}} = \frac{1 - r_2}{1 - r_1} \tag{7.19}$$

   For the case of $r_1 = 0.33$ and $r_2 = 0.67$ shown in Fig. 7.1, $[M_1]/[M_2]$ equals 0.5 and $f_1 = 0.33$. This mathematical analysis shows that a comparable result is possible with both r_1 and r_2 greater than unity, but is not possible for $r_1 > 1$ and $r_2 < 1$.
6. When $r_1 = 1/r_2$, the copolymer composition curve will be either convex or concave when viewed from the F_1 axis, depending on whether r_1 is greater or less than unity. The further removed from unity r_1 is, the farther the composition curve will be displaced from the 45° line. This situation is called ideal copolymerization. The example below explores the origin of this terminology.

There is a parallel between the composition of a copolymer produced from a certain feed and the composition of a vapor in equilibrium with a two-component liquid mixture. The following example illustrates this parallel when the liquid mixture is an ideal solution and the vapor is an ideal gas.

Example 7.1

An ideal gas obeys Dalton's law; that is, the total pressure is the sum of the partial pressures of the components. An ideal solution obeys Raoult's law; that is, the partial pressure of the ith component in a solution is equal to the mole fraction of that component in the solution times the vapor pressure of pure component i. Use these relationships to relate the mole fraction of component 1 in the equilibrium vapor to its mole fraction in a two-component solution and relate the result to the ideal case of the copolymer composition equation.

Solution

We define F_1 to be the mole fraction of component 1 in the vapor phase and f_1 to be its mole fraction in the liquid solution. Here p_1 and p_2 are the vapor pressures of components 1 and 2 in equilibrium with an ideal solution and p_1^0 and p_2^0 are the vapor pressures of the two pure liquids. By Dalton's law, $p_{tot} = p_1 + p_2$ and $F_1 = p_1/p_{tot}$, since these are ideal gases and p is proportional to the number of moles. By Raoult's law, $p_1 = f_1 p_1^0$, $p_2 = f_2 p_2^0$, and $p_{tot} = f_1 p_1^0 + f_2 p_2^0$. Combining the two gives

$$F_1 = \frac{f_1 p_1^0}{f_1 p_1^0 + f_2 p_2^0} = \frac{f_1 (p_1^0/p_2^0)}{f_1 (p_1^0/p_2^0) + f_2}$$

Now examine Eq. (7.18) for the case of $r_1 = 1/r_2$:

$$F_1 = \frac{r_1 f_1^2 + f_1 f_2}{r_1 f_1^2 + 2 f_1 f_2 + (1/r_1) f_2^2} = \frac{r_1 f_1 (r_1 f_1 + f_2)}{(r_1 f_1 + f_2)^2} = \frac{r_1 f_1}{r_1 f_1 + f_2}$$

This is identical to the ideal liquid-vapor equilibrium if r_1 is identified with p_1^0/p_2^0.

The vapor pressure ratio measures the intrinsic tendency of component 1 to enter the vapor phase relative to component 2. Likewise, r_1 measures the tendency of M_1 to add to $M_1\cdot$ relative to M_2 adding to $M_1\cdot$. In this sense there is a certain parallel, but it is based on $M_1\cdot$ as a reference radical and hence appears to be less general than the vapor pressure ratio. Note, however, that $r_1 = 1/r_2$ means $k_{11}/k_{12} = k_{21}/k_{22}$. In this case the ratio of rate constants for monomer 1 relative to monomer 2 is the same regardless of the reference radical examined. This shows the parallelism to be exact.

•

Because of this parallel with liquid-vapor equilibrium, copolymers for which $r_1 = 1/r_2$ are said to be ideal. For those nonideal cases in which the copolymer and feedstock happen to have the same composition, the reaction is called an azeotropic polymerization. Just as in the case of azeotropic distillation, the composition of the reaction mixture does not change as copolymer is formed if the composition corresponds to the azeotrope. The proportion of the two monomers at this point is given by Eq. (7.19).

In this section we have seen that the copolymer composition depends to a large extent on the four propagation constants, although it is sufficient to consider these in terms of the two ratios r_1 and r_2. In the next section we shall examine these ratios in somewhat greater detail.

7.3 Reactivity Ratios

The parameters r_1 and r_2 are the vehicles by which the nature of the reactants enter the copolymer composition equation. We shall call these radical reactivity ratios, although similarly defined ratios also describe copolymerizations that involve ionic intermediates. There are several important things to note about radical reactivity ratios:

1. The single subscript used to label r is the index of the radical.
2. r_1 is the ratio of two propagation constants involving radical 1: The ratio always compares the propagation constant for the same monomer adding to the radical relative to the propagation constant for the addition of the other monomer. Thus if $r_1 > 1$, $M_1\cdot$ adds M_1 in preference to M_2; if $r_1 < 1$, $M_1\cdot$ adds M_2 in preference to M_1.
3. Although r_1 is descriptive of radical $M_1\cdot$, it also depends on the identity of the "other"; the pair of parameters r_1 and r_2 are both required to characterize a particular system and the product $r_1 r_2$ is used to quantify this by a single parameter.
4. The reciprocal of a radical reactivity ratio is sometimes used to quantitatively express the reactivity of monomer M_2 by comparing its rate of addition to radical $M_1\cdot$ relative to the rate of M_1 adding to $M_1\cdot$.
5. As the ratio of two rate constants, the radical reactivity ratio follows the Arrhenius equation with an apparent activation energy equal to the difference in the activation energies for the individual constants. Thus for r_1, $E_{app}^* = E_{p,11}^* - E_{p,12}^*$. Since the activation energies for propagation are not large to begin with, their difference is even smaller. Accordingly, the temperature dependence of r is relatively small.

The reactivity ratios of a copolymerization system are the fundamental parameters in terms of which the system is described. Since the copolymer composition equation relates the compositions of the product and the feedstock, it is clear that values of r can be evaluated from experimental data in which the corresponding compositions are measured. We shall consider this evaluation procedure in Sec. 7.7, where it will be found that this approach is not as free of ambiguity as might be desired. For now we shall simply assume that we know the desired r values for a system; in fact, extensive tabulations of such values exist. An especially convenient source of this information is the *Polymer Handbook* (Ref. 4). Table 7.1 lists some typical r values at 60°C.

Although Table 7.1 is rather arbitrarily assembled, note that it contains no systems for which r_1 and r_2 are *both* greater than unity. Indeed, such systems are very rare. We can understand this by recognizing that, at least in the extreme case of very large r's, these monomers would tend to simultaneously homopolymerize. Because of this preference toward homopolymerization, any copolymer that does form in systems with r_1 and r_2 both greater than unity will

Table 7.1 Values of Reactivity Ratios r_1 and r_2 and the Product $r_1 r_2$ for a Few Copolymers at 60°C

M_1	M_2	r_1	r_2	$r_1 r_2$
Acrylonitrile	Methyl vinyl ketone	0.61	1.78	1.09
	Methyl methacrylate	0.13	1.16	0.15
	α-Methyl styrene	0.04	0.20	0.008
	Vinyl acetate	4.05	0.061	0.25
Methyl methacrylate	Styrene	0.46	0.52	0.24
	Methacrylic acid	1.18	0.63	0.74
	Vinyl acetate	20	0.015	0.30
	Vinylidene chloride	2.53	0.24	0.61
Styrene	Vinyl acetate	55	0.01	0.55
	Vinyl chloride	17	0.02	0.34
	Vinylidene chloride	1.85	0.085	0.16
	2-Vinyl pyridine	0.55	1.14	0.63
Vinyl acetate	1-Butene	2.0	0.34	0.68
	Isobutylene	2.15	0.31	0.67
	Vinyl chloride	0.23	1.68	0.39
	Vinylidene chloride	0.05	6.7	0.34

Source: L. J. Young in Ref. 4.

be a block-type polymer with very long sequences of a single repeat unit. Since such systems are only infrequently encountered, we shall not consider them further.

Table 7.1 also lists the product $r_1 r_2$ for the systems included. These products lie in the range between zero and unity, and it is instructive to consider the character of the copolymer produced toward each of these extremes.

In the extreme case where $r_1 r_2 = 0$ because both r_1 *and* r_2 equal zero, the copolymer adds monomers with perfect alternation. This is apparent from the definition of r, which compares the addition of the same monomer to the other monomer for a particular radical. If both r's are zero, there is no tendency for a radical to add a monomer of the same kind as the growing end, whichever species is the terminal unit. When only one of the r's is zero, say r_1, then alternation occurs whenever the radical ends with an $M_1 \cdot$ unit. There is thus a tendency toward alternation in this case, although it is less pronounced than in the case where both r's are zero. Accordingly, we find increasing tendency toward alternation as $r_1 \to 0$ and $r_2 \to 0$, or, more succinctly, as the product $r_1 r_2 \to 0$.

At the other end of the commonly encountered range we find the product $r_1 r_2 \rightarrow 1$. As noted above, this limit corresponds to ideal copolymerization and means the two monomers have the same relative tendency to add to both radicals. Thus if $r_1 = 10$, monomer 1 is 10 times as likely to add to $M_1 \cdot$ than monomer 2. At the same time $r_2 = 0.1$, which also means that monomer 1 is 10 times as likely to add to $M_2 \cdot$ than monomer 2. In this case the radicals exert the same influence, so the monomers add at random in a proportion governed by the specific values of the r's.

Recognition of these differences in behavior points out an important limitation on the copolymer composition equation. The equation describes the overall composition of the copolymer, but gives no information whatsoever about the distribution of the different kinds of repeat units within the polymer. While the overall composition is an important property of the copolymer, the details of the microstructural arrangement is also a significant feature of the molecule. It is possible that copolymers with the same overall composition have very different properties because of differences in microstructure. Reviewing the three categories presented in Chap. 1, we see the following:

1. Alternating structures [I] are promoted by $r_1 \rightarrow 0$ and $r_2 \rightarrow 0$:

$$M_1M_2M_1M_2M_1M_2M_1M_2M_1M_2M_1M_2M_1M_2M_1M_2M_1M_2M_1M_2$$

[I]

2. Random structures [II] are promoted by $r_1 r_2 \rightarrow 1$:

$$M_1M_2M_2M_2M_1M_1M_2M_1M_1M_2M_1M_2M_1M_2M_1M_2M_2M_1M_1M_2$$

[II]

3. Block structures [III] are promoted by $r_1 r_2 > 1$:

$$M_1M_1M_1M_1M_1M_1M_1M_1M_1M_1M_2M_2M_2M_2M_2M_2M_2M_2M_2M_2$$

[III]

Each of these polymers has a 50:50 proportion of the two components, but the products probably differ in properties. As examples of such differences, we note the following:

4. Alternating copolymers, while relatively rare, are characterized by combining the properties of the two monomers along with structural regularity. We saw in Chap. 4 that a very high degree of regularity—extending all the

way to stereoregularity in the configuration of the repeat units—is required for crystallinity to develop in polymers. Although they fall short of perfect regularity, copolymers with alternating structures are capable of interactions which order separate chains, and this, in turn, can affect their solubility, chemical reactivity, and mechanical properties.

5. Random copolymers tend to average the properties of the constituent monomers in proportion to the relative abundance of the two comonomers.
6. Block copolymers are closer to blends of homopolymers in properties, but without the latter's tendency to undergo phase separation. As a matter of fact, diblock copolymers can be used as surfactants to bind immiscible homopolymer blends together and thus improve their mechanical properties. Block copolymers are generally prepared by sequential addition of monomers to living polymers, rather than by depending on the improbable $r_1 r_2 > 1$ criterion in monomers.

We shall return to the topic of copolymer properties in Sec. 7.8.

Returning to the data of Table 7.1, it is apparent that there is a good deal of variability among the r values displayed by various systems. We have already seen the effect this produces on the overall copolymer composition; we shall return to the matter of microstructure in Sec. 7.6. First, however, let us consider the obvious question. What factors in the molecular structure of two monomers govern the kinetics of the different addition steps? This question is considered in the few next sections; for now we look for a way to systematize the data as the first step toward an answer.

We noted above that the product $r_1 r_2$ can be used to locate a copolymer along an axis between alternating and random structures. It is by means of this product that some values from Table 7.1, supplemented by other results for additional systems, have been organized in Fig. 7.2. Figure 7.2 has been constructed according to the following general principles:

1. Various monomers are listed along the base of a triangle.
2. The triangle is subdivided into an array of diamonds by lines drawn parallel to the two sides of the triangle.
3. The spacing of the lines is such that each monomer along the base serves as a label for a row of diamonds.
4. Each diamond marks the intersection of two such rows and therefore corresponds to two comonomers.
5. The $r_1 r_2$ product for the various systems is the number entered in each diamond.
6. The individual monomers have been arranged in such a way as to achieve to the greatest extent possible values of $r_1 r_2$ that approach zero toward the apex of the triangle and values of $r_1 r_2$ which approach unity toward the base of the triangle.

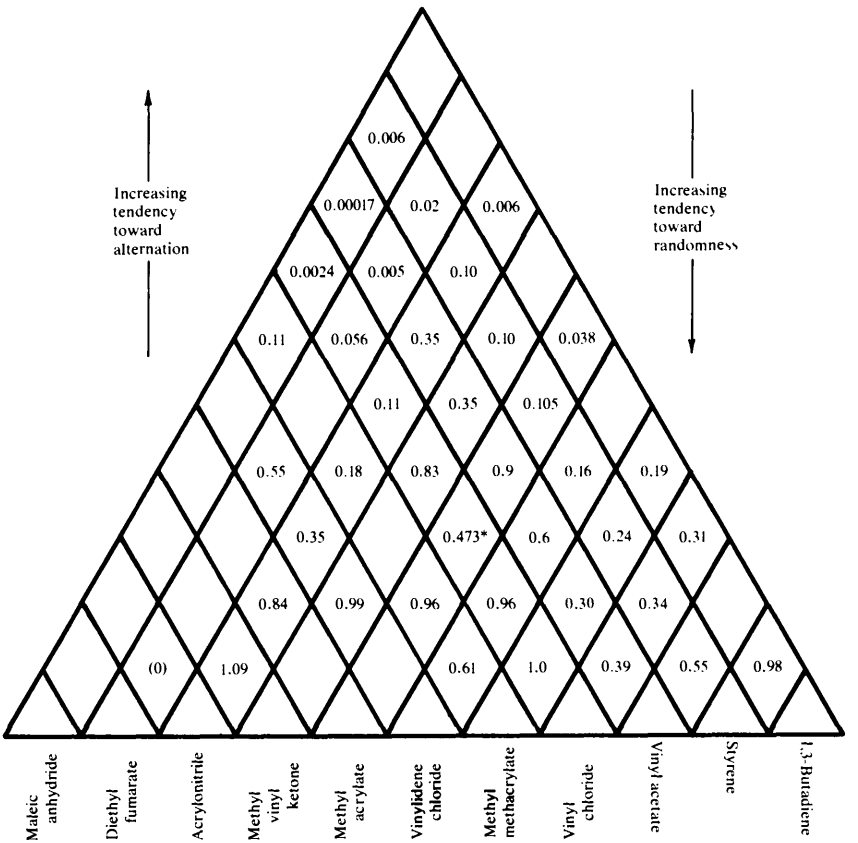

Figure 7.2 The product $r_1 r_2$ for copolymers whose components define the intersection where the numbers appear. See the text for details of placement. The value marked * is determined in Example 7.5. Other values are from Ref. 4.

Before proceeding with a discussion of this display, it is important to acknowledge that the criteria for monomer placement can be met only in part. For one thing, there are combinations for which data are not readily available. Incidentally, not all of the $r_1 r_2$ values in Fig. 7.2 were measured at the same temperature, but, as noted above, temperature effects are expected to be relatively unimportant. Also, there are outright exceptions to the pattern sought: Generalizations about chemical reactions always seem to be plagued by these. In spite of some reversals of ranking, the predominant trend moving upward from the base along any row of diamonds is a decrease in $r_1 r_2$ values.

From the geometry of this triangular display, it follows immediately—if one overlooks the exceptions—that the more widely separated a pair of comonomers are in Fig. 7.2, the greater is their tendency toward alternation. Conversely the closer they are together, the greater their tendency toward randomness We recognize a parallel here to the notion that widely separated elements in the periodic table will produce more polar bonds than those which are closer together and vice versa.

This is a purely empirical and qualitative trend. The next order of business is to seek an explanation for its origin in terms of molecular structure. If we focus attention on the electron-withdrawing or electron-donating attributes of the substituent(s) on the double bond, we find that the substituents of monomers which are located toward the right-hand corner of the triangle in Fig. 7.2 are recognized as electron donors in organic chemistry. Likewise, the substituents in monomers located toward the left-hand corner of the triangle are electron acceptors. The demarcation between the two regions of behavior is indicated in Fig. 7.2 by reversing the direction of the lettering at this point. Pushing this point of view somewhat further, we conclude that the sequence acetoxy < phenyl < vinyl is the order of increase in electron-donating tendency. Chloro < carbonyl < nitrile is the order of increase in electron-withdrawing tendency The positions of diethyl fumarate and vinylidene chloride relative to their mono-substituted analogs indicates that "more is better" with respect to these substituent effects. The location of methyl methacrylate relative to methyl acrylate also indicates additivity, this time with partial compensation of opposing effects

Any discussion based on reactivity ratios is kinetic in origin and therefore reflects the mechanism or, more specifically, the transition state of a reaction The transition state for the addition of a vinyl monomer to a growing radical involves the formation of a partial bond between the two species, with a corresponding reduction of the double-bond character of the vinyl group in the monomer:

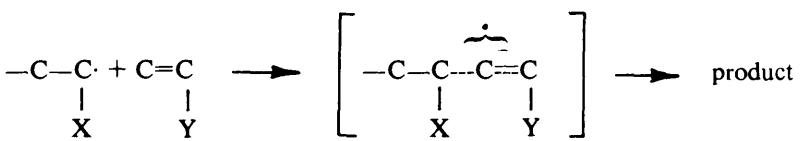

(7.G)

If substituent X is an electron donor and Y an electron acceptor, then the partial bond in the transition state is stabilized by a resonsance form [IV] which attributes a certain polarity to the emerging bond:

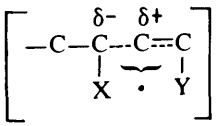

[IV]

The contribution of this polar structure to the bonding lowers the energy of the transition state. This may be viewed as a lower activation energy for the addition step and thus a factor which promotes this particular reaction. The effect is clearly larger the greater the difference in the donor-acceptor properties of X and Y. The transition state for the successive addition of the same monomer (whether X or Y substituted) is structure [V]:

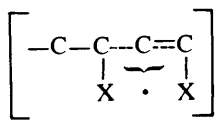

[V]

This involves a more uniform distribution of charge because of the identical substituents and thus lacks the stabilizing effect of the polar resonance form. The activation energy for this mode of addition is greater than that for alternation, at least when X and Y are sufficiently different.

Although we use the term *resonance* in describing the effect of polarity in stabilizing the transition state in alternating copolymers, the emphasis of the foregoing is definitely on polarity rather than resonance per se. It turns out, however, that resonance plays an important role in its own right in free-radical polymerization, even if polarity effects are ignored. In the next section we examine some evidence for this and consider the origin of this behavior.

7.4 Resonance and Reactivity

The tendency toward alternation is not the only pattern in terms of which copolymerization can be discussed. The activities of radicals and monomers may also be examined as a source of insight into copolymer formation. The reactivity of radical 1 copolymerizing with monomer 2 is measured by the rate constant k_{12}. The absolute value of this constant can be determined from copolymerization data (r_1) and studies yielding absolute homopolymerization constants (k_{11}):

$$k_{12} = \frac{k_{11}}{r_1} \tag{7.20}$$

Table 7.2 lists a few cross-propagation constants calculated by Eq. (7.20). Far more extensive tabulations than this have been prepared by correlating copolymerization and homopolymerization data for additional systems. Examination of Table 7.2 shows that the general order of increasing *radical* activity is

styrene < acrylonitrile < methyl acrylate < vinyl acetate

An additional observation is that any one of these species shows the reverse order of reactivity for the corresponding monomers. As *monomers*, the order of reactivity in Table 7.2 is

styrene > acrylonitrile > methyl acrylate > vinyl acetate

These and similar rankings based on more extensive comparisons are summarized in terms of substituents in Table 7.3.

An important pattern to recognize among the substituents listed in Table 7.3 is this: Those which have a double bond conjugated with the double bond in the olefin are the species which are more stable as radicals and more reactive as monomers. The inverse relationship between the stability of monomers and radicals arises precisely because monomers gain (or lose) stability by converting to the radical: The greater the gain (or loss), the greater (or less) the incentive for the monomer to react. It is important to realize that the ability to form conjugated structures is associated with a substituent whether it is in a monomer or a radical. Conjugation allows greater electron delocalization, which, in turn, lowers the energy of the system that possesses this feature.

Comparison of the range of k_{12} along horizontal rows and vertical columns in Table 7.2 suggests that resonance stabilization produces a bigger effect in the radical than in the monomer. After all, the right- and left-hand columns in Table 7.2 (various radicals) differ by factors of 100–1000, while the top and

Table 7.2 Values of the Cross-Propagation Constants k_{12} for Four Monomer-Radical Combinations

	Radical			
Monomer	Styrene	Acrylonitrile	Methyl acrylate	Vinyl acetate
Styrene	145	49,000	14,000	230,000
Acrylonitrile	435	1,960	2,510	46,000
Methyl acrylate	203	1,310	2,090	23,000
Vinyl acetate	2.9	230	230	2,300

Source: Ref. 4.

Table 7.3 List of Some Substituents Ranked in Terms of Their Effects on Monomer and Radical Reactivity

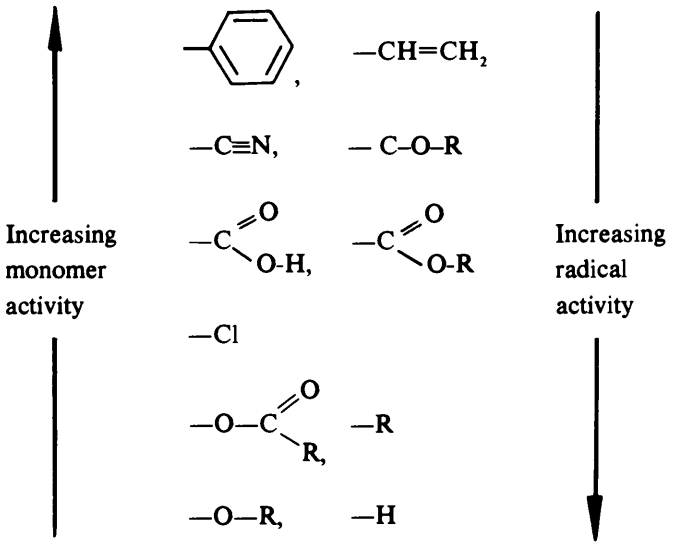

bottom rows (various monomers) differ only by factors of 50–100. In order to examine this effect in more detail, consider the addition reaction of monomer M to a reactant radical R· to form a product radical P·. What distinguishes these species is the presence or absence of resonance stabilization (subscript rs). If the latter is operative, we must also consider which species benefit from its presence. There are four possibilities:

1. Unstabilized monomer converts stabilized radical to unstabilized radical:

$$R_{rs}\cdot + M \rightarrow P\cdot \qquad (7.H)$$

   There is an overall loss of resonance stabilization in this reaction. Since it is a radical which suffers the loss, the effect is larger than in the reaction in which . . . .

2. Stabilized monomer converts stabilized radical to another stabilized radical:

$$R_{rs}\cdot + M_{rs} \rightarrow P_{rs}\cdot \qquad (7.I)$$

   Here too there is an overall loss of resonance stabilization, but it is monomer stabilization which is lost, and this is energetically less costly than reaction (7.H).

3. Unstabilized monomer converts unstabilized radical to another unstabilized radical:

$$R\cdot + M \rightarrow P\cdot \tag{7.J}$$

This reaction suffers none of the reduction in resonance stabilization that is present in reactions (7.H) and (7.I). It is energetically more favored than both of these, but not as much as the reaction in which . . . .

4. Stabilized monomer converts unstabilized radical to stabilized radical:

$$R\cdot + M_{rs} \rightarrow P_{rs}\cdot \tag{7.K}$$

This reaction converts the less effective resonance stabilization of a monomer to a more effective form of radical stabilization. This is the most favorable of the four reaction possibilities.

In summary, we can rank these reactions in terms of their propagation constants as follows:

$$R_{rs}\cdot + M < R_{rs}\cdot + M_{rs} < R\cdot + M < R\cdot + M_{rs}$$

Systems from Table 7.2 which correspond to these situations are the following:

Radical	Styrene	<	styrene	<	vinyl acetate	<	vinyl acetate
	+		+		+		+
Monomer	vinyl acetate		styrene		vinyl acetate		styrene

Note that this inquiry into copolymer propagation rates also increases our understanding of the differences in free-radical homopolymerization rates. It will be recalled that in Sec. 6.1 a discussion of this aspect of homopolymerization was deferred until copolymerization was introduced. The trends under consideration enable us to make some sense out of the rate constants for propagation in free-radical homopolymerization as well. For example, in Table 6.4 we see that k_p values at 60°C for vinyl acetate and styrene are 2300 and 165 liter mol^{-1} sec^{-1}, respectively. The relative magnitude of these constants can be understod in terms of the sequence above.

Resonance stabilization energies are generally assessed from thermodynamic data. If we define ϵ_i to be the resonance stabilization energy of species i, then the heat of formation of that species will be less by an amount ϵ_i than for an otherwise equivalent molecule without resonance. Likewise, the ΔH for a reaction which is influenced by resonance effects is less by an amount $\Delta\epsilon$ (Δ is the usual difference: products minus reactants) than the ΔH for a reaction which is otherwise identical except for resonance effects:

$$\Delta H_{rs} = \Delta H_{no\ rs} - \Delta\epsilon \tag{7.21}$$

Thus if we consider the homopolymerization of ethylene (no resonance possibilities),

$$-CH_2-CH_2\cdot + CH_2=CH_2 \longrightarrow -CH_2CH_2CH_2CH_2\cdot$$
$$\Delta H_{no\ rs} = -88.7\ \text{kJ mol}^{-1} \tag{7.L}$$

as a reference reaction, and compare it with the homopolymerization of styrene (resonance effects present),

$$-CH_2-\underset{\phi}{CH}\cdot + CH_2=\underset{\phi}{CH} \longrightarrow -CH_2-\underset{\phi}{CH}-CH_2-\underset{\phi}{CH}\cdot$$
$$\Delta H_{rs} = -69.9\ \text{kJ mol}^{-1} \tag{7.M}$$

we find a value of $\Delta\epsilon = -19\ \text{kJ mol}^{-1}$, according to Eq. (7.21). Reaction (7.M) is a specific example of the general reaction (7.I), and the negative value of $\Delta\epsilon$ in this example indicates the overall loss of resonance stabilization which is characteristic of (7.I).

Although it is not universally true that the activation energies of reactions parallel their heats of reaction, this is approximately true for the kind of addition reaction we are discussing. Accordingly, we can estimate $E^* = k\,\Delta H$, with k an appropriate proportionality constant. If we consider the difference between two activation energies by combining this idea with Eq. (7.21), the contribution of the nonstabilized reference reaction drops out of Eq. (7.21) and we obtain

$$E_{11}^* - E_{12}^* = k[-\Delta\epsilon_{11} - (-\Delta\epsilon_{12})]$$
$$= -(\epsilon_{P_1\cdot} - \epsilon_{R_1\cdot} - \epsilon_{M_1}) + (\epsilon_{P_2\cdot} - \epsilon_{R_1\cdot} - \epsilon_{M_2}) \tag{7.22}$$

In writing the second version of this, the proportionality constant has been set equal to unity as a simplification. Note that the resonance stabilization energy of the reference radical $R_1\cdot$ also cancels out of this expression.

The temperature dependence of the reactivity ratio r_1 also involves the $E_{11}^* - E_{12}^*$ difference through the Arrhenius equation; hence

$$r_1 \propto \exp\left(\frac{\epsilon_{P_1\cdot} - \epsilon_{M_1}}{RT}\right) \exp\left(\frac{-(\epsilon_{P_2\cdot} - \epsilon_{M_2})}{RT}\right) \tag{7.23}$$

An analogous expression can be written for r_2:

$$r_2 \propto \exp\left(\frac{\epsilon_{P_2\cdot} - \epsilon_{M_2}}{RT}\right) \exp\left(\frac{-(\epsilon_{P_1\cdot} - \epsilon_{M_1})}{RT}\right) \tag{7.24}$$

According to this formalism, the following applies:

1. The reactivity ratios are proportional to the product of two exponential numbers.
2. Each exponential involves the difference between the resonance stabilization energy of the radical and monomer of a particular species.
3. The positive exponent is associated with the same species as identifies the r (i.e., for r_1, $M_1 \rightarrow P_1\cdot$), while the negative exponent is associated with the other species (for r_1, $M_2 \rightarrow P_2\cdot$).

We might be hard pressed to estimate the individual resonance stabilization energies in Eqs. (7.23) and (7.24), but the qualitative application of these ideas is not difficult. Consider once again the styrene-vinyl acetate system:

1. Define styrene to be monomer 1 and vinyl acetate to be monomer 2.
2. The difference in resonance stabilization energy $\epsilon_{P_1\cdot} - \epsilon_{M_1} > 1$, since styrene is resonance stabilized and the effect is larger for the radical than the monomer.
3. The difference $\epsilon_{P_2\cdot} - \epsilon_{M_2} \cong 0$, since neither the radical nor the monomer of vinyl acetate shows appreciable stabilization.
4. Therefore, according to Eqs. (7.23) and (7.24), $r_1 > 1$ while $r_2 < 1$.
5. The experimental values for this system are $r_1 = 55$ and $r_2 = 0.01$.

Although this approach does correctly rank the parameters r_1 and r_2 for the styrene-vinyl acetate system, this conclusion was already reached qualitatively above, using the same concepts and without any mathematical manipulations. One point that the quantitative derivation makes clear is that explanations of copolymer behavior based exclusively on resonance concepts fail to describe the full picture. All that we need to do is examine the product $r_1 r_2$ as given by Eqs. (7.23) and (7.24), and the shortcoming becomes apparent. According to these relationships, the product $r_1 r_2$ always equals unity, yet we saw in the last section that experimental $r_1 r_2$ values generally lie between zero and unity. We also saw that polarity effects could be invoked to rationalize the $r_1 r_2$ product.

The situation may be summarized as follows:

1. If resonance effects *alone* are considered, it is possible to make some sense of the ranking of various propagation constants.
2. In this case only random microstructure is predicted.
3. If polarity effects *alone* are considered, it is possible to make some sense out of the tendency toward alternation.
4. In this case homopolymerization is unexplained.

The way out of this dilemma is easily stated, although not easily acted upon. It is not adequate to consider *any one* of these approaches for the explanation of something as complicated as these reactions. Polarity effects and resonance are *both* operative, and, if these still fall short of explaining all observations, there is another old standby to fall back on: steric effects.

Resonance, polarity, and steric considerations are all believed to play an important role in copolymerization chemistry, just as in other areas of organic chemistry. Things are obviously simplified if only one of these is considered; but it must be remembered that doing this necessarily reveals only one facet of the problem. Nevertheless, there are times, particularly before launching an experimental investigation of a new system, when some guidelines are very useful. The following example illustrates this point.

Example 7.2

It is proposed to polymerize the vinyl group of the hemin molecule with other vinyl comonomers to prepare model compounds to be used in hemoglobin research. Considering hemin and styrene to be species 1 and 2, respectively, use the resonance concept to rank the reactivity ratios r_1 and r_2.

Solution

Hemin is the complex between protoporphyrin and iron in the +3 oxidation state. Iron is in the +2 state in the heme of hemoglobin. The molecule has the following structure:

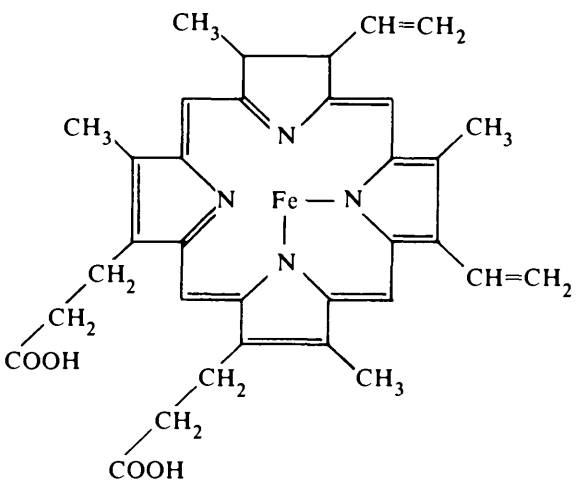

It is apparent from the size of the conjugated system here that numerous resonance possibilities exist in this species in both the radical and the molecular form. Styrene also has resonance structures in both forms. On the principle that these effects are larger for radicals than monomers, we conclude that the difference $\epsilon_P - \epsilon_M > 0$ for both hemin and styrene. On the principle that greater resonance effects result from greater delocalization, we expect the difference to be larger for hemin than for styrene. According to Eq. (7.23), $r_1 \propto e^{\text{larger}}\, e^{-\text{smaller}} > 1$. According to Eq. (7.24), $r_2 \propto e^{\text{smaller}}\, e^{-\text{larger}} < 1$. Experimentally, the values for these parameters turn out to be $r_1 = 65$ and $r_2 = 0.18$.

•

In the next section we shall consider an attempt to combine both resonance and polarity effects.

7.5 The Price-Alfrey Equation

In the last two sections we have considered—separately—the effects of resonance and polarity on copolymerization. While these concepts provide some insights into various observations, it is artificial to consider either one of them operating exclusively. In fact, resonance and polarity features are both active in most molecules. A method for merging their contributions is clearly desirable.

Another troublesome aspect of the reactivity ratios is the fact that they must be determined and reported as a pair. It would clearly simplify things if it were possible to specify one or two general parameters for each monomer which would correctly represent its contribution to all reactivity ratios. Combined with the analogous parameters for its comonomer, the values r_1 and r_2 could then be evaluated. This situation parallels the standard potential of electrochemical cells which we are able to describe as the sum of potential contributions from each of the electrodes that comprise the cell. With x possible electrodes, there are $x(x - 1)/2$ possible electrode combinations. If $x = 50$, there are 1225 possible cells, but these can be described by only 50 electrode potentials. A dramatic data reduction is accomplished by this device. Precisely the same proliferation of combinations exists for monomer combinations. It would simplify things if a method were available for data reduction such as that used in electrochemistry.

An approach to copolymerization has been advanced by Price and Alfrey which attempts to both combine resonance and polarity considerations and accomplish the data reduction strategy of the last paragraph. It should be conceded at the outset that the Price-Alfrey method is only semiquantitative in its success. Its greatest usefulness is probably in providing some orientation to a new system before launching an experimental investigation.

The Price-Alfrey approach begins by defining three parameters—P, Q, and e—for each of the comonomers in a reaction system. We shall see presently that the parameter P is rapidly eliminated from the theory. As a result, the Price-Alfrey system is also called the Q-e scheme for copolymerization.

For the reaction of radical i with monomer j, Price and Alfrey assume that the cross-propagation rate constant can be written as

$$k_{ij} = P_i Q_j e^{-e_i e_j} \tag{7.25}$$

In this equation P and Q are parameters that describe the reactivity of the radical and monomer of the designated species, and the values of e measure the polarity of the two components without distinguishing between monomer and radical.

From Eqs. (7.13) and (7.14), the reactivity ratios can be written

$$r_1 = \frac{Q_1}{Q_2} \exp\left[-e_1(e_1 - e_2)\right] \tag{7.26}$$

and

$$r_2 = \frac{Q_2}{Q_1} \exp\left[-e_2(e_2 - e_1)\right] \tag{7.27}$$

Finally, Eqs. (7.26) and (7.27) can be combined to give

$$r_1 r_2 = \exp\left[(e_1 - e_2)(e_2 - e_1)\right] = \exp\left[-(e_1 - e_2)^2\right] \tag{7.28}$$

That these expressions do combine resonance and polarity effects can be seen as follows:

1. If molecules 1 and 2 differ widely in polarity, then the exponent in Eq. (7.28) will be large and the exponential will be small. We saw in Sec. 7.3 that alternation is favored by large differences in polarity and is described by small values of $r_1 r_2$.
2. If molecules 1 and 2 are identical in polarity, then $e_1 - e_2$ in Eqs. (7.26) and (7.27) is zero and $r_1 = Q_1/Q_2$ and $r_2 = Q_2/Q_1$. Comparing these limits with Eqs. (7.23) and (7.24) leads to the result

$$Q_j = \exp\left(\frac{(\epsilon_{P_j \cdot} - \epsilon_{M_j})}{RT}\right) \tag{7.29}$$

3. This last identification makes the Q's strictly a matter of resonance, whereas the general concept of "reactivity" also includes steric effects. The effects

of polarity are explicitly handled by the e's and are not therefore lumped together with these other concepts.

4. There are no inherent restrictions on Q and e; hence the individual reactivity ratios can take on a wide range of values.

An advantage of the Price-Alfrey system is that each monomer is characterized by its own values for Q and e, which are assumed to be independent of the nature of the comonomer. Thus if Q and e values were available for all monomers, then these could be combined at will to generate the parameters r_1 and r_2 which define copolymer composition and microstructure. This feature makes data reduction and predictions about new systems feasible. The only problem is that Q and e cannot be evaluated independently for a particular monomer any more than the potential of a single electrode can be measured. In electrochemistry we get around the latter problem by assigning to the hydrogen electrode under standard conditions a potential contribution of 0.0000 V. The choice of this electrode and this assignment of potential are arbitrary, but, once accepted, they permit other electrode potentials to be evaluated relative to the standard. A similar procedure is followed for the Q and e values. The reference monomer is chosen to be styrene and the parameters are assigned the following values: $Q_{sty} = 1.0$ and $e_{sty} = -0.8$. In their original work Price and Alfrey assigned styrene an e value of -1.0, but this was revised to the present value, which gives better agreement with experimental reactivity ratios.

This last statement shows that expressing Q and e values relative to the values for styrene is not identical to the procedure for electrode potentials. In the latter, cell potentials are calculated correctly from electrode potentials, regardless of the value assigned to the reference. The Price-Alfrey system is only semiquantitative; values are assigned which give the best average fit to the largest number of monomers. This is accomplished more effectively by assigning styrene an e value of -0.8. In this respect the Q-e values are like bond dissociation energies in which the properties of a variety of different compounds are considered to find the strength of an "average" bond. Both bond energies and Q-e values fall short of expectations when specific effects are present which separate a particular system from the "average."

Table 7.4 lists the Q and e values for an assortment of common monomers. The extremes in the column of e values in Table 7.4 –which are listed in order– quantify the range of donor-acceptor properties which is used as the basis for ranking in Fig. 7.2. The Q values perform a similar ranking with respect to resonance effects. The eight different Q-e combinations in Table 7.4 allow the estimation of r_1 and r_2 values for 28 different copolymers. Of course, in these systems Q and e values were assigned to give the best fit to r values which had already been measured. As an illustration of the predictive values of the Q-e scheme, consider the following example:

Table 7.4 Values of the Price–Alfrey Q and e Values for a Few Common Monomers

Monomer	Q	e
Acrylonitrile	0.60	1.20
Methyl vinyl ketone	1.0	0.7
Methyl acrylate	0.42	0.60
Methyl methacrylate	0.74	0.40
Vinyl chloride	0.044	0.20
Vinyl acetate	0.026	-0.22
Styrene (standard)	1.0	-0.8
Butadiene	2.39	-1.05

Source: L. J. Young in Ref. 4.

Example 7.3

Reactivity ratios for the *N*-vinylphthalimide (molecule 1)-styrene (molecule 2) system were measured, and found† to be $r_1 = 0.075$ and $r_2 = 8.3$. Use these values to estimate values of Q and e for *N*-vinylphthalimide; then estimate the parameters r_1 and r_2 for system in which molecule 2 is vinyl acetate.

Solution

Since styrene is used as the standard in the Price-Alfrey system, $Q_2 = 1.0$ and $e_2 = -0.8$. Use these values and the experimental r_1 and r_2 values for the styrene-*N*-vinylphthalimide system to evaluate Q_1 and e_1: Using Eq. (7.28), we have $r_1 r_2 = e^{-(e_1 - e_2)^2} = 0.075(8.3) = 0.623$, $\ln 0.623 = -[e_1 - (-0.8)]^2$, and $e_1 + 0.8 = \pm 0.688$. The phthalimide substituent is expected to be more electronegative than phenyl, so we choose the negative root; therefore $e_1 = -0.688 - 0.8 = -1.49$. Using Eq. (7.26), we have $r_1 = (Q_1/Q_2)\, e^{-e_1(e_1 - e_2)}$, $0.075 = (Q_1/1)\, e^{-(-1.49)(-0.688)}$, $Q_1 = 0.21$. Next we let vinyl acetate be monomer 2 and obtain the Q and e values for this monomer from Table 7.4: $Q_2 = 0.026$ and $e_2 = -0.22$. Using the Q and e values for *N*-vinylphthalimide calculated above, we find from Eq. (7.26), $r_1 = (Q_1/Q_2)\, e^{-e_1(e_1 - e_2)} = (0.21/0.026)\, e^{-(-1.49)[-1.49-(-0.22)]} = 1.22$, and, from Eq. (7.27), $r_2 = (Q_2/Q_1)\, e^{-e_2(e_2 - e_1)} = (0.026/0.21)\, e^{-(-0.22)[-0.22-(-1.49)]} = 0.16$. The experimental values of the reactivity ratios in this system are $r_1 = 2.4$ and $r_2 = 0.07$. Working backward from *these* data gives $Q_1 = 0.50$ and $e_1 = -1.56$ for *N*-vinylphthalimide.

•

This example also illustrates that "best-fit" values of Q and e are not absolute.

† Data from Ref. 4.

7.6 A Closer Look at Microstructure

In Sec. 7.3 we noted that variations in the $r_1 r_2$ product led to differences in the microstructure of the polymer, even when the overall composition of two compared systems is the same. Structures [I]-[III] are examples of this situation. In this section we shall take a closer look at this variation, using the approach which is best suited for this kind of detail: statistics.

Suppose we define as p_{ij} the probability that a unit of type i is followed in the polymer by a unit of type j, where both i and j can be either 1 or 2. Since an i unit must be followed by either an i or a j, the fraction of ij sequences out of all possible sequences defines p_{ij}:

$$p_{ij} = \frac{\text{number of ij sequences}}{\text{number of ij sequences + number of ii sequences}} \tag{7.30}$$

This equation can also be written in terms of the propagation rates of the different types of addition steps which generate the sequences:

$$p_{ij} = \frac{R_{ij}}{R_{ij} + R_{ii}} = \frac{k_{ij}[M_i\cdot]\,[M_j]}{k_{ij}[M_i\cdot]\,[M_j] + k_{ii}[M_i\cdot]\,[M_i]} \tag{7.31}$$

For the various possible combinations in a copolymer, Eq. (7.31) becomes

$$p_{11} = \frac{k_{11}[M_1\cdot]\,[M_1]}{k_{11}[M_1\cdot]\,[M_1] + k_{12}[M_1\cdot]\,[M_2]} = \frac{r_1[M_1]}{r_1[M_1] + [M_2]} \tag{7.32}$$

$$p_{12} = \frac{[M_2]}{r_1[M_1] + [M_2]} \tag{7.33}$$

$$p_{22} = \frac{k_{22}[M_2\cdot]\,[M_2]}{k_{22}[M_2\cdot]\,[M_2] + k_{21}[M_2\cdot]\,[M_1]} = \frac{r_2[M_2]}{r_2[M_2] + [M_1]} \tag{7.34}$$

$$p_{21} = \frac{[M_1]}{r_2[M_2] + [M_1]} \tag{7.35}$$

Note that $p_{11} + p_{12} = p_{22} + p_{21} = 1$. In writing these expressions we make the assumption that only the terminal unit of the radical influences the addition of the next monomer. This same assumption was made in deriving the copolymer composition equation. We shall have more to say below about this so-called terminal assumption.

Next let us consider the probability of finding a sequence of repeat units in a copolymer which is exactly ν_1 units of M_1 in length. This may be represented as $M_2(M_1)_{\nu_1}M_2$. Working from left to right in this sequence, we note the following:

1. If the addition of monomer M_1 to a radical ending with M_2 occurs L times in a sample, then there will be a total of L sequences, of unspecified length, of M_1 units in the sample.
2. If $\nu_1 - 1$ consecutive M_1 monomers add to radicals capped by M_1 units, the total number of such sequences is expressed in terms of p_{11} to be $Lp_{11}^{\nu_1-1}$.
3. If the sequence contains exactly ν_1 units of type M_1, then the next step must be the addition of an M_2 unit. The probability of such an addition is given by p_{12}, and the number of such sequences is $Lp_{11}^{\nu_1-1}p_{12}$.
4. Note that we use the symbol ν_i to indicate the number of M_i units in a particular sequence. This should be distinguished from n_i, which gives the total number of M_i units in the copolymer without regard to their distribution in various sequences.

Since L equals the total number of M_1 sequences of any length, the fraction of sequences of length ν_1, ϕ_{ν_1}, is given by

$$\phi_{\nu_1} = p_{11}^{\nu_1-1} p_{12} \tag{7.36}$$

The similarity of this derivation to those in Secs. 5.4 and 6.7 should be apparent. Substitution of the probabilities given by Eqs. (7.32) and (7.33) leads to

$$\phi_{\nu_1} = \left(\frac{r_1[M_1]}{r_1[M_1] + [M_2]}\right)^{\nu_1-1} \left(\frac{[M_2]}{r_1[M_1] + [M_2]}\right) \tag{7.37}$$

A similar result can be written for ϕ_{ν_2}. These expressions give the fraction of sequences of specified length in terms of the reactivity ratios of the copolymer system and the composition of the feedstock. Figure 7.3 illustrates by means of a bar graph how ϕ_{ν_1} varies with ν_1 for two polymer systems prepared from equimolar solutions of monomers. The shaded bars in Fig. 7.3 describe the system for which $r_1r_2 = 0.03$, and the unshaded bars describe $r_1r_2 = 0.30$. Table 7.5 shows the effect of variations in the composition of the feedstock for the system $r_1r_2 = 1$. The following observations can be made concerning Fig. 7.3 and Table 7.5:

1. In all situations, the fraction ϕ_{ν_1} decreases with increasing ν_1.
2. Figure 7.3 shows that for $r_1r_2 = 0.03$, about 85% of the M_1 units are sandwiched between two M_2's. We have already concluded that low values of the r_1r_2 product indicate a tendency toward alternation.
3. Figure 7.3 also shows that the proportion of alternating M_1 units decreases and the fraction of longer sequences increases as r_1r_2 increases. The 50 mol % entry in Table 7.5 shows that the distribution of sequence lengths gets flatter and broader for $r_1r_2 = 1$, the random case.

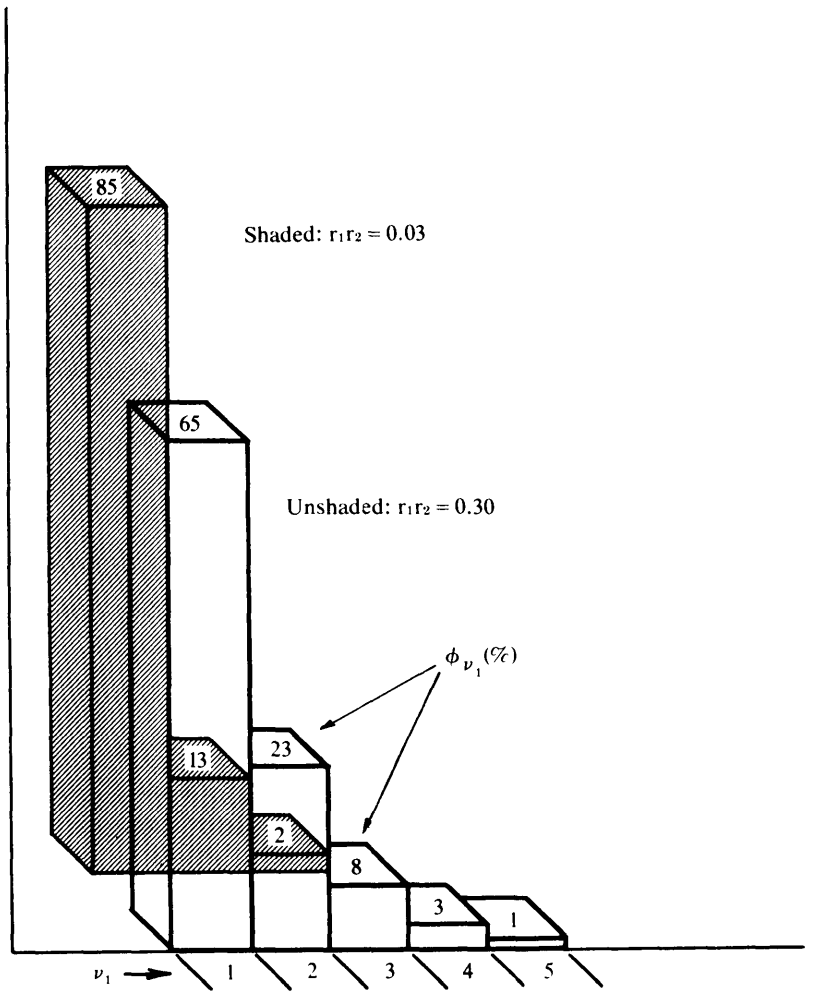

Figure 7.3 Fraction of n_1 sequences of the indicated length for copolymers prepared from equimolar feedstocks with $r_1 r_2 = 0.03$ (shaded) and $r_1 r_2 = 0.30$ (unshaded). [Data from C. Tosi, *Adv. Polym. Sci.* 5:451 (1968).]

4. Table 7.5 also shows that increasing the percentage of M_1 in the monomer solution flattens and broadens the distribution of sequence lengths. Similar results are observed for lower values of $r_1 r_2$, but the broadening is less pronounced when the tendency toward alternation is high.

Table 7.5 Fraction of M_1 Sequences of Length n_1 for Copolymers Prepared from Feedstocks of Different Composition for a System with $r_1 r_2 = 1$

	ν_1											
$f_1 \times 100$	1	2	3	4	5	6	7	8	9	10	11	12
10	90.00	9.00	0.90	0.09								
20	80.00	16.00	3.20	0.64	0.13							
30	70.00	21.00	6.30	1.89	0.57	0.17	0.05					
40	60.00	24.00	9.60	3.84	1.54	0.62	0.25	0.10	0.04			
50	50.00	25.00	12.50	6.25	3.13	1.56	0.78	0.39	0.20	0.10	0.05	
60	40.00	24.00	14.40	8.64	5.18	3.11	1.87	1.12	0.67	0.40	0.24	0.14
70	30.00	21.00	14.70	10.29	7.20	5.04	3.53	2.47	1.73	1.21	0.85	0.59
80	20.00	16.00	12.80	10.24	8.19	6.55	5.24	4.19	3.36	2.68	2.15	1.72
90	10.00	9.00	8.10	7.29	6.56	5.90	5.31	4.78	4.30	3.87	3.59	3.23

Source: C. Tosi, *Adv. Polym. Sci.* 5:451 (1968).

Next we consider the average value of the sequence length for M_1, $\bar{\nu}_1$. Combining Eqs. (1.9) and (7.36) gives

$$\bar{\nu}_1 = \frac{\sum_{\nu_1=1}^{\infty} \nu_1 \phi_{\nu_1}}{\sum_{\nu_1=1}^{\infty} \phi_{\nu_1}} = \frac{\sum_{\nu_1=1}^{\infty} \nu_1 p_{11}^{\nu_1-1} p_{12}}{\sum_{\nu_1=1}^{\infty} p_{11}^{\nu_1-1} p_{12}} \tag{7.38}$$

Simplifying this result involves the same infinite series that we examined in connection with Eq. (5.27); therefore we can write immediately

$$\bar{\nu}_1 = \frac{1}{1 - p_{11}} = \frac{1}{p_{12}} \tag{7.39}$$

By combining Eqs. (7.33) and (7.39), we obtain

$$\bar{\nu}_1 = 1 + r_1 \frac{[M_1]}{[M_2]} \tag{7.40}$$

A value for $\bar{\nu}_2$ is obtained by similar operations:

$$\bar{\nu}_2 = 1 + r_2 \frac{[M_2]}{[M_1]} \tag{7.41}$$

The following example demonstrates the use of some of these relationships pertaining to microstructure.

Example 7.4

The hemoglobin molecule contains four heme units. It is proposed to synthesize a hemin (molecule 1)-styrene (molecule 2) copolymer such that $\bar{\nu}_1 = 4$ in an attempt to test some theory concerning hemoglobin. As noted in Example 7.2, $r_1 = 65$ and $r_2 = 0.18$ for this system. What should be the proportion of monomers to obtain this average hemin sequence length? What is the average styrene sequence length at this composition? Does this system seem like a suitable model if the four hemin clusters are to be treated as isolated from one another in the theory being tested? Also evaluate ϕ_{ν_1} for several values of ν_1 bracketing $\bar{\nu}_1$ to get an idea of the distribution of these values.

Solution

Use Eq. (7.40) to evaluate $[M_1]/[M_2]$ for $r_1 = 65$ and $\bar{\nu}_1 = 4$:

$$\frac{[M_1]}{[M_2]} = \frac{\bar{\nu}_1 - 1}{r_1} = \frac{4 - 1}{65} = 0.046 \quad \text{and} \quad \frac{[M_2]}{[M_1]} = 21.7$$

Use this ratio of concentrations in Eq. (7.41) to evaluate $\bar{\nu}_2$:

$$\bar{\nu}_2 = 1 + r_2 \frac{[M_2]}{[M_1]} = 1 + 0.18(21.7) = 4.9$$

The number of styrene units in an average sequence is a little larger than the length of the average hemin sequence. It is not unreasonable to describe the hemin clusters as isolated, on the average, in this molecule. The product $r_1 r_2 = 11.7$ in this system, which also indicates a tendency toward block formation. Use Eq. (7.37) with $[M_1]/[M_2] = 0.046$ and the r_1 and r_2 values to evaluate ϕ_ν:

$$\phi_\nu = \left(\frac{65(0.046)}{65(0.046)+1}\right)^{\nu-1}\left(\frac{1}{65(0.046)+1}\right)$$

$$= \left(\frac{2.99}{3.99}\right)^{\nu-1}\left(\frac{1}{3.99}\right) = (0.749)^{\nu-1}(0.251)$$

Solving for several values of ν, we obtain the following:

ν	1	2	3	4	5	6
ϕ_ν	0.251	0.188	0.140	0.105	0.079	0.059

The distribution of sequence lengths is very broad.

•

For the systems represented in Fig. 7.3 and the equimolar case in Table 7.5, the average sequence lengths are $\bar{\nu}_1 = 1.173$ for $r_1 r_2 = 0.03$, $\bar{\nu}_1 = 1.548$ for $r_1 r_2 = 0.30$, and $\bar{\nu}_1 = 2.000$ for $r_1 r_2 = 1.0$.

Equations (7.40) and (7.41) suggest a second method, in addition to the copolymer composition equation, for the experimental determination of reactivity ratios. If the average sequence length can be determined for a feedstock of known composition, then r_1 and r_2 can be evaluated. We shall return to this possibility in the next section. In anticipation of applying this idea, let us review the assumptions and limitation to which Eqs. (7.40) and (7.41) are subject:

1. The instantaneous monomer concentration must be used. Except at the azeotrope, this changes as the conversion of monomers to polymer progresses. As in Sec. 7.2, we assume that either the initial conditions apply (little change has taken place) or that monomers are continuously being added (replacement of reacted monomer).

2. The kinetic analysis described by Eqs. (7.32) and (7.33) assumes that no repeat unit in the radical other than the terminal unit influences the addition. The next-to-last unit in the radical as well as those still farther from the growing end are assumed to have no effect.
3. Item (2) requires that each event in the addition process be independent of all others. We have consistently assumed this throughout this chapter, beginning with the copolymer composition equation. Until now we have said nothing about testing this assumption. Consideration of copolymer sequence lengths offers this possibility.

We have suggested above that both the copolymer composition equation and the average sequence length offer possibilities for experimental evaluation of the reactivity ratios. Note that in so doing we are finding parameters which fit experimental results to the predictions of a model. Nothing about this tests the model itself. It could be argued that obtaining the same values for r_1 and r_2 from the fitting of composition and microstructure data would validate the model. It is not likely, however, that both types of data would be available and of sufficient quality to make this unambiguous. We shall examine the experimental side of this in the next section.

Statistical considerations make it possible to test the assumption of independent additions. Let us approach this topic by considering an easier problem: coin tossing. Under conditions where two events are purely random—as in tossing a fair coin—the probability of a specific sequence of outcomes is given by the product of the probabilities of the individual events. The probability of tossing a head followed by a head—indicated HH—is given by

$$p_{HH} = p_H p_H \tag{7.42}$$

If the events are not independent, provision must be made for this, so we define a quantity called the conditional probability. For the probability of a head *given the prior event* of a head, this is written $p_{H/H}$, where the first quantity in the subscript is the event under consideration and that following the slash mark is the prior condition. Thus $p_{T/H}$ is the probability of a tail following a head. If the events are independent, $p_{H/H} = p_H$; if not, then $p_{H/H}$ must be evaluated as a separate quantity. If the coin being tossed were biased, that is, if successive events are not independent, Eq. (7.42) becomes

$$p_{HH} = p_{H/H}\, p_H \tag{7.43}$$

We recall that the fraction of times a particular outcome occurs is used to estimate probabilities. Therefore we could evaluate $p_{H/H}$ by counting the number of times N_H the first toss yielded a head and the number of times N_{HH} two tosses yielded a head followed by a head and write

$$p_{H/H} = \frac{p_{HH}}{p_H} = \frac{N_{HH}}{N_H} \tag{7.44}$$

This procedure is readily extended to three tosses. For a fair coin the probability of three heads is the cube of the probability of tossing a single head:

$$p_{HHH} = p_H p_H p_H \tag{7.45}$$

If the coin is biased, conditional probabilities must be introduced:

$$p_{HHH} = p_{H/HH} p_{H/H} p_H \tag{7.46}$$

Using Eq. (7.44) to eliminate $p_{H/H}$ from the last result gives

$$p_{HHH} = p_{H/HH} \left(\frac{p_{HH}}{p_H} \right) p_H \tag{7.47}$$

or

$$p_{H/HH} = \frac{p_{HHH}}{p_{HH}} = \frac{N_{HHH}}{N_{HH}} \tag{7.48}$$

If we were testing whether a coin were biased or not, we would use ideas like these as the basis for a test. We could count, for example, HHH and HH sequences and divide them according to Eq. (7.48). If $p_{H/HH} \neq p_H$, we would be suspicious!

A similar logic can be applied to copolymers. The story is a bit more complicated to tell, so we only outline the method. If penultimate effects operate, then the probabilities p_{11}, p_{12}, and so on, defined by Eqs. (7.32)–(7.35) should be replaced by conditional probabilities. As a matter of fact, the kind of conditional probabilities needed must be based on the two preceding events. Thus reactions (7.E) and (7.F) are two of the appropriate reactions, and the corresponding probabilities are $p_{1/11}$ and $p_{1/21}$. Rather than work out all of the possibilities in detail, we summarize the penultimate model as follows:

1. A total of eight different reactions are involved, since each reaction like (7.A) is replaced by a pair of reactions like (7.E) and (7.F).
2. There are eight different rate laws and rate constants associated with these reactions. Equation (7.1), for example, is replaced by Eqs. (7.5) and (7.6).
3. The eight rate constants are clustered in four ratios which define new reactivity ratios. Thus r_1 as defined by Eq. (7.13) is replaced by $r_1' = k_{111}/k_{112}$ and $r_1'' = k_{211}/k_{212}$ while r_2 [Eq. (7.14)] is replaced by $r_2' = k_{222}/k_{221}$ and $r_2'' = k_{122}/k_{121}$.

4. The probability p_{11} as given by Eq. (7.32) is replaced by the conditional probability $p_{1/11}$, which is defined as

$$p_{1/11} = \frac{k_{111}[M_1M_1\cdot][M_1]}{k_{111}[M_1M_1\cdot][M_1] + k_{112}[M_1M_1\cdot][M_2]} = \frac{r_1'[M_1]/[M_2]}{1 + r_1'[M_1]/[M_2]} \tag{7.49}$$

There are eight of these conditional probabilities, each associated with the reactions described in item (1).

5. The probability p_{11} can be written as the ratio $N_{M_1M_1}/N_{M_1}$ using Eq. (7.44). This is replaced by $p_{1/11}$, which is given by the ratio $N_{M_1M_1M_1}/N_{M_1M_1}$ according to Eq. (7.48).
6. Equation (7.32) shows that p_{11} is constant for a particular copolymer if the terminal model applies; therefore the ratio $N_{M_1M_1}/N_{M_1}$ also equals this constant. Equation (7.49) shows that $p_{1/11}$ is constant for a particular copolymer if the penultimate model applies; therefore the ratio $N_{M_1M_1M_1}/N_{M_1M_1}$ also equals this constant, but the ratio $N_{M_1M_1}/N_{M_1}$ does not have the same value.

These observations suggest how the terminal mechanism can be proved to apply to a copolymerization reaction if experiments exist which permit the number of sequences of a particular length to be determined. If this is possible, we should count the number of M_1's (this is given by the copolymer composition) and the number of M_1M_1 and $M_1M_1M_1$ sequences. Specified sequences, of any definite composition, of two units are called dyads; those of three units, triads; those of four units, tetrads; those of five units, pentads; and so on. Next we examine the ratio $N_{M_1M_1}/N_{M_1}$ and $N_{M_1M_1M_1}/N_{M_1M_1}$. If these are the same, then the mechanism is shown to have terminal control; if not, it *may* be penultimate control. To prove the penultimate model it would also be necessary to count the number of M_1 tetrads. If the tetrad/triad ratio were the same as the triad/dyad ratio, the penultimate model is proved.

This situation can be generalized. If the ratios do not become constant until the ratio of pentads to tetrads is considered, then the unit before the next to last—called the antepenultimate unit—plays a role in the addition. This situation has been observed for propylene oxide–maleic anhydride copolymers.

The foregoing discussion has been conducted in terms of M_1 sequences. Additional relationships of the sort we have been considering also exist for dyads, triads, and so forth, of different types of specific composition. Thus an ability to investigate microstructure experimentally allows some rather subtle mechanistic effects to be studied. In the next section we shall see how such information is obtained.

7.7 Copolymer Composition and Microstructure: Experimental Aspects

As we have already seen, it is the reactivity ratios of a particular copolymer system that determines both the composition and microstructure of the polymer. Thus it is important to have reliable values for these parameters. At the same time it suggests that experimental studies of composition and microstructure can be used to evaluate the various r's.

Evaluation of reactivity ratios from the copolymer composition equation requires only composition data—that is, analytical chemistry—and has been the method most widely used to evaluate r_1 and r_2. As noted in the last section, this method assumes terminal control and seeks the best fit of the data to that model. It offers no means for testing the model and, as we shall see, is subject to enough uncertainty to make even self-consistency difficult to achieve.

Microstructure studies, by contrast, offer both a means to evaluate the reactivity ratios and also to test the model. The capability to investigate this type of structural detail was virtually nonexistent until the advent of modern instrumentation and even now is limited to sequences of modest length.

In this section we shall use the evaluation of reactivity ratios as the unifying theme; the experimental methods constitute the new material introduced.

The copolymer composition equation relates the r's to either the ratio [Eq. (7.15)] or the mole fraction [Eq. (7.18)] of the monomers in the feedstock and repeat units in the copolymer. To use this equation to evaluate r_1 and r_2, the composition of a copolymer resulting from a feedstock of known composition must be measured. The composition of the feedstock itself must be known also, but we assume this poses no problems. The copolymer specimen must be obtained by proper sampling procedures, and purified of extraneous materials. Remember that monomers, initiators, and possibly solvents are involved in these reactions also, even though we have been focusing attention on the copolymer alone. The proportions of the two kinds of repeat unit in the copolymer is then determined by either chemical or physical methods. Elemental analysis has been the chemical method most widely used, although analysis for functional groups is also employed.

If we represent the percent by weight of an element in monomer i as $(\%)_i$ and the molecular weight of the monomer (repeat unit) by $M_{0,i}$, then the mass of that element in a sample is

$$\text{Element mass} = n_1 M_{0,1}(\%)_1 + n_2 M_{0,2}(\%)_2 \tag{7.50}$$

The total mass of the sample is

$$\text{Sample mass} = n_1 M_{0,1} + n_2 M_{0,2} \tag{7.51}$$

since n_i represents the total number of M_i units in the copolymer. Therefore th percent by weight of the element in the copolymer is

$$\text{Percent} = \frac{n_1 M_{0,1}(\%)_1 + n_2 M_{0,2}(\%)_2}{n_1 M_{0,1} + n_2 M_{0,2}} \times 100 \tag{7.52}$$

Dividing numerator and denomintor by $n_1 + n_2$ and remembering that $F_1 \cdot F_2 = 1$ gives

$$\text{Percent} = \frac{F_1 M_{0,1}(\%)_1 + (1 - F_1) M_{0,2}(\%)_2}{F_1 M_{0,1} + (1 - F_1) M_{0,2}} \times 100 \tag{7.53}$$

which gives F_1 in terms of elemental composition and known parameters

Since the copolymer equation involves both r_1 and r_2 as unknowns, at leas two polymers prepared from different feedstocks must be analyzed. It i preferable to use more than this minimum number of observations and t rearrange the copolymer composition equation into a linear form so tha graphical methods can be employed to evaluate the r's. Several ways to lineariz the equation exist:

1. Rearrange Eq. (7.18) to give

$$\frac{f_1(1 - 2F_1)}{F_1(1 - f_1)} = r_1 \left(\frac{f_1^2 (F_1 - 1)}{F_1 (1 - f_1)^2} \right) + r_2 \tag{7.54}$$

   This is the equation of a straight line, so r_1 and r_2 can be evaluated fron the slope and intercept of an appropriate plot.
2. In terms of ratios rather than fractions, Eq. (7.54) may be written as

$$\frac{[M_1]/[M_2]}{n_1/n_2} \left(\frac{n_1}{n_2} - 1 \right) = r_1 \frac{([M_1]/[M_2])^2}{n_1/n_2} - r_2 \tag{7.55}$$

   This expression is also of the form $y = mx + b$ if $x = ([M_1][M_2]^{-1})^2 (n_1/n_2)$ and $y = [M_1][M_2]^{-1}/(n_1/n_2)(n_1/n_2 - 1)$, so the slope and inter cept yield r_1 and $-r_2$, respectively. This type of analysis is known as Finemann-Ross plot.
3. This last expression can be rearranged in several additional ways which yiel linear plots:

$$\frac{y}{x} = -r_2 \frac{1}{x} + r_1 \tag{7.56}$$

$$x = \frac{1}{r_1} y + \frac{r_2}{r_1} \tag{7.57}$$

$$\frac{x}{y} = \frac{r_1}{r_2}\frac{1}{y} + \frac{1}{r_1} \tag{7.58}$$

Each of these last forms weigh the errors in various data points differently, so some may be more suitable than others, depending on the precision of the data. Ideally all should yield the same values of the reactivity ratios.

The following example illustrates the use of Eq. (7.54) to evaluate r_1 and r_2.

Example 7.5

The data in Table 7.6 list the mole fraction of methyl acrylate in the feedstock and in the copolymer for the methyl acrylate (M_1)-vinyl chloride (M_2) system. Use Eq. (7.54) as the basis for the graphical determination of the reactivity ratios which describe this system.

Solution

We calculate the variables to be used as ordinate and abscissa for the data in Table 7.6 using Eq. (7.54):

Ordinate = $f_1(1 - 2F_1)/F_1(1 - f_1)$	Abscissa = $f_1^2(F_1 - 1)/F_1(1 - f_1)^2$
0.0217	-0.0083
-0.1036	-0.0143
-0.2087	-0.0316
-0.3832	-0.0486
-0.6127	-0.0832
-0.9668	-0.1315
-2.8102	-0.2792
-6.4061	-0.7349

Least-squares analysis of these values gives a slope $r_1 = 8.929$ and an intercept $r_2 = 0.053$. Figure 7.4 shows these data plotted according to Eq. (7.54). The line is drawn with the least-squares slope and intercept. The last point on the left in Fig. 7.4, which this line passes through, corresponds to $F_1 = 0.983$ and $f_1 = 0.867$. Because the functional form plotted involves the small differences $F_1 - 1$ and $1 - f_1$, this point is also subject to the largest error. This illustrates the value of having alternate methods for analyzing the data. The authors of this research carried out several different analyses of this same data; the values they obtained for r_1 and r_2 averaged over the various methods were $r_1 = 9.616 \pm 0.603$ and $r_2 = 0.0853 \pm 0.0239$. The standard deviations of about 6 and 28% in r_1 and r_2 analyzed *from the same data* indicate the hazards of this method for determining r values.

•

Table 7.6 Values of F_1 as a Function of f_1 for the Methyl Acrylate (M_1)-Vinyl Chloride (M_2) System (Data used in Example 7.5)

f_1	F_1	f_1	F_1
0.075	0.441	0.421	0.864
0.154	0.699	0.521	0.900
0.237	0.753	0.744	0.968
0.326	0.828	0.867	0.983

Source: Data from E. L. Chapin, G. Ham, and R. Fordyce, *J. Am. Chem. Soc.* 70:538 (1948).

In spite of the compounding of errors to which it is subject, the foregoing method was the best procedure for measuring reactivity ratios until the analysis of microstructure became feasible. Let us now consider this development.

Most of the experimental information concerning copolymer microstructure has been obtained by physical methods based on modern instrumental methods. Techniques such as ultraviolet (UV), visible, and infrared (IR) spectroscopy, NMR spectroscopy, and mass spectroscopy have all been used to good advantage in this type of research. Advances in instrumentation and computer interfacing combine to make these physical methods particularly suitable to answer the question we pose: With what frequency do particular sequences of repeat units occur in a copolymer.

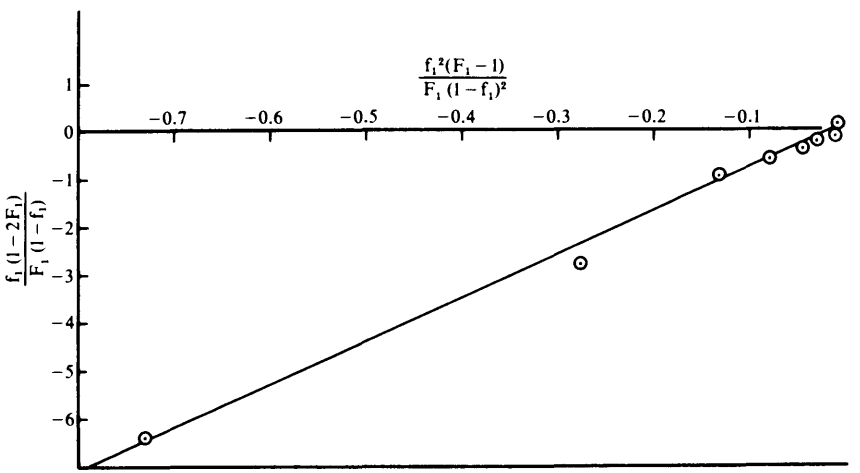

Figure 7.4 Finemann-Ross plot of the data in Table 7.6 and Example 7.5.

The choice of the best method for answering this question is governed by the specific nature of the system under investigation. Few general principles exist beyond the importance of analyzing a representative sample of suitable purity. Our approach is to consider some specific examples. In view of the diversity of physical methods available and the number of copolymer combinations which exist, a few examples barely touch the subject. They will suffice to illustrate the concepts involved, however.

Spectroscopic techniques based on the absorption of UV or visible radiation depend on the excitation of an electron from one quantum state to another. References in physical and/or analytical chemistry should be consulted for additional details, but the present summary is sufficient for our purposes:

1. The excitation energy ΔE measures the spacing between the final (subscript f) and initial (subscript i) quantum states of the electron:

$$\Delta E = E_f - E_i \tag{7.59}$$

   This difference is positive for absorbed energy.
2. The energy absorbed is proportional to the frequency of the radiation, with Planck's constant ($h = 6.63 \times 10^{-34}$ J sec) the factor of proportionality:

$$\Delta E = h\nu = h\frac{c}{\lambda} \tag{7.60}$$

   In the second version of this equation c is the speed of light, and λ the wavelength of the radiation.
3. The more widely separated two states are in energy, the shorter the wavelength of the radiation absorbed. Since vibrational quantum states are more closely spaced than electronic states, the former transitions are induced by IR radiation.
4. Different light-absorbing groups, called chromophores, absorb characteristic wavelengths, opening the possibility of qualitative analysis based on the location of an absorption peak.
5. If there is no band overlap in a spectrum, the absorbance at a characteristic wavelength is proportional to the concentration of chromophores present. This is the basis of quantitative analysis using spectra. With band overlap, things are more complicated but still possible.
6. The proportionality between the concentration of chromophores and the measured absorbance [Eqs. (6.8) and (6.9)] requires calibration. With copolymers this is accomplished by chemical analysis for an element or functional group that characterizes the chromophore, or, better yet, by the use of isotopically labeled monomers.

An elegant example of a system investigated by UV-visible spectroscopy is the copolymer of styrene (molecule 1) and 1-chloro-1,3-butadiene (molecule 2). These molecules quantitatively degrade with the loss of HCl upon heating in base solution. This restores 1,3-unsaturation to the butadiene repeat unit:

$$-(CHCl-CH=CH-CH_2)_n-CH_2-\underset{\phi}{CH}- \xrightarrow{-nHCl} -(CH=CH-CH=CH)_n-CH_2-\underset{\phi}{CH}- \tag{7.N}$$

It is these conjugated double bonds that are the chromophores of interest in this system. What makes this particularly useful is the fact that the absorption maximum for this chromophore is displaced to longer wavelengths the more conjugated bonds there are in a sequence. Qualitatively, this can be understood in terms of a one-dimensional particle-in-a-box model for which the energy level spacing is inversely proportional to the square of the length of the box. In this case the latter increases with the length of the conjugated polyene system. This in turn depends on the number of consecutive butadiene repeat units in the copolymer. For an isolated butadiene molecule dehydrohalogenation produces one pair of conjugated double bonds; two adjacent butadienes, four conjugated double bonds; three adjacent butadienes, six conjugated double bonds; and so on. Sequences of these increasing lengths are expected to absorb at progressively longer wavelengths.

The spectrum shown in Fig. 7.5 shows the appropriate portion of the spectrum for a copolymer prepared from a feedstock for which $f_1 = 0.153$ It turns out that each polyene produces a set of three bands: The dyad is identified with the peaks at $\lambda = 298$, 312, and 327 nm; the triad, with $\lambda = 347$ 367, and 388 nm; and the tetrad with $\lambda = 412$ and 437 nm. Apparently one of the tetrad bands overlaps that of the triad and is not resolved. Likewise only one band (at 473 nm) is observed for the pentad. The identification of these features can be confirmed with model compounds and the location and *relative* intensities of the peaks has been shown to be independent of copolymer composition.

Once these features have been identified, the spectra can be interpreted in terms of the numbers of dyads, triads, tetrads, and pentads (?) of the butadiene units and compared with predicted sequences of various lengths. Further consideration of this system is left for Problems 4-6 at the end of the chapter

Nuclear magnetic resonance (NMR) spectroscopy is another physical technique which is especially useful for microstructure studies. Because of the sensitivity of this technique to an atom's environment in a molecule, NMR is useful for a variety of microstructural investigations: We shall consider the application to copolymers now and to questions of stereoregularity in Sec. 7.11.

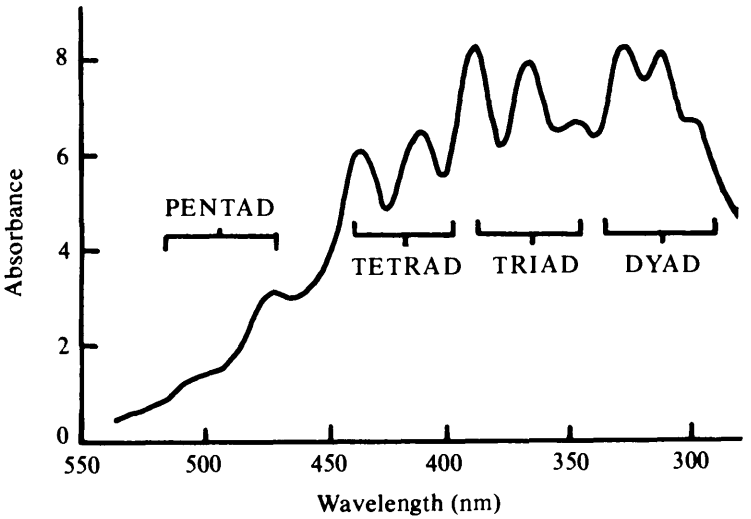

Figure 7.5 Ultraviolet–visible spectrum of dehydrohalogenated copolymers of styrene-1-chloro-1,3-butadiene. [Redrawn with permission from A. Winston and P. Wichacheewa, *Macromolecules* 6:200 (1973), copyright 1973 by the American Chemical Society.]

Nuclear magnetic resonance has become such an importnat technique in organic chemistry that contemporary textbooks in the subject discuss its principles quite thoroughly, as do texts in physical and analytical chemistry. We note only a few pertinent highlights of the method:

1. Certain nuclei—we shall only discuss ^{1}H, but ^{13}C is becoming increasingly important—possess magnetic moments and show two quantum states in a magnetic field.
2. If energy of the proper frequency is supplied, a transition between these quantum states occurs with the absorption of an amount of energy equal to the separation of the states. The frequency of the absorbed radiation lies in the radio-frequency range and depends on the local magnetic field at the atom in question.
3. In practice, NMR spectrometers vary the magnetic field strength and measure the value at which a constant radio frequency is absorbed.
4. The electrons in a molecule also have magnetic moments and set up secondary magnetic fields which partly screen each atom from the applied field. Thus atoms in different chemical environments display resonance at slightly different magnetic fields.

5. The displacement δ of individual resonances from that of a standard are small and are measured in parts per million (ppm) relative to the applied field. These chemical shifts are characteristic of a proton in a specific environment.
6. The interaction between nuclei splits resonances into multiple peaks, the number and relative intensity of which also assist in qualitative identification of the proton responsible for the absorption.
7. Splitting is most commonly caused by the interaction of protons on adjacent carbons with the proton of interest. If there are m equivalent hydrogens on an adjacent carbon, the proton of interest produces m + 1 peaks by this coupling.
8. More distant coupling is revealed in high magnetic fields. Unresolved fine structures in a field of one strength may be resolved at higher fields where more subtle long-range influences can be probed.

The use of NMR spectroscopy to characterize copolymer microstructure takes advantage of this last ability to discern environmental effects which extend over the length of several repeat units. This capability is extremely valuable in analyzing the stereoregularity of a polymer, and we shall have more to say about it in that context in Sec. 7.11.

For the case of copolymers, suppose we consider the various triads of repeat units. There are six possibilities: $M_1M_1M_1$, $M_1M_1M_2$, $M_2M_1M_2$, $M_2M_2M_2$, $M_2M_2M_1$, and $M_1M_2M_1$. These can be divided into two groups of three, depending on the identity of the central unit. Thus the center of a triad can be bracketed by two monomers identical to itself, different from itself, or by one of each. In each of these cases the central repeat unit is in a different environment, and a characteristic proton in that repeat unit will resonate at a different location, depending on the effect of that environment.

As a specific example, consider the ester methoxy group in poly(methyl methacrylate). The hydrogens in this group are magnetically equivalent and hence produce a single resonance at $\delta = 3.74$ ppm. Now suppose we look for this same resonance feature in the copolymer of methyl methacrylate (M_1) and acrylonitrile (M_2). Figure 7.6 shows the 60-MHz spectrum of several of these copolymers in the neighborhood of the methoxy resonance. Three resonance peaks rather than one are observed. Figure 7.6 also lists the methyl methacrylate content of each of these polymers. As the methyl methacrylate content decreases, the peak on the right decreases and that on the left increases. We therefore identify the right-hand peak with the $M_1M_1M_1$ sequence, the left-hand peak to $M_2M_1M_2$, and the peak in the center to $M_1M_1M_2$. The $M_1M_1M_1$ peak occurs at the same location as in the methyl methacrylate homopolymer. The areas under the three peaks give the relative proportions of

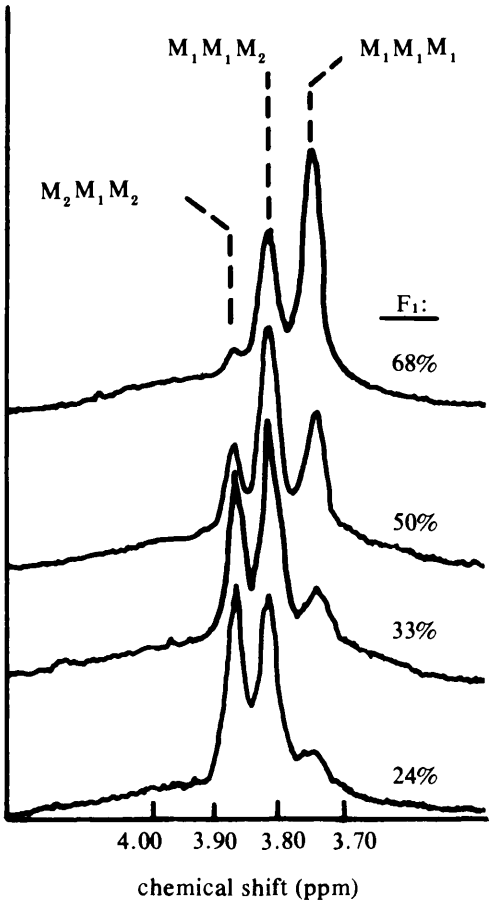

Figure 7.6 Chemical shift (from hexamethyldisiloxane) for acrylonitrile-methyl methacrylate copolymers of the indicated methyl methacylate (M_1) content. Methoxyl resonances are labeled as to the triad source. [From R. Chujo, H. Ubara, and A. Nishioka, *Polym. J.* 3:670 (1972).]

the three sequences. In the following example we consider some results on dyad sequences determined by comparable procedures in vinylidene chloride-isobutylene copolymers.

Example 7.6

The mole fractions of various dyads in the vinylidine chloride (M_1)-isobutylen (M_2) system were determined† by NMR spectroscopy. A selection of the value obtained are listed below, as well as the compositions of the feedstocks fron which the copolymers were prepared:

	Mole fraction of dyads		
f_1	11	12	22
0.584	0.68	0.29	–
0.505	0.61	0.36	–
0.471	0.59	0.38	–
0.130	–	0.67	0.08
0.121	–	0.66	0.10
0.083	–	0.64	0.17

Assuming terminal control, evaluate r_1 from each of the first three sets o data, and r_2 from each of the last three.

Solution

Equations (7.32) and (7.34) provide the method for evaluating the r's from th data given. We recognize that a 12 dyad can come about from 1 adding to 2 as well as from 2 adding to 1; therefore we use half the number of 12 dyad as a measure of the number of additions of monomer 2 to chain end 1 Accordingly, by Eq. (7.30),

$$p_{11} = \frac{N_{11}}{N_{11} + (1/2)N_{12}} = \frac{2N_{11}}{2N_{11} + N_{12}} \quad \text{and} \quad p_{22} = \frac{2N_{22}}{2N_{22} + N_{12}}$$

Since $[M_1]/[M_2] = f_1/(1 - f_1)$, Eq. (7.31) can be written

$$p_{11} = \frac{r_1[f_1/(1 - f_1)]}{1 + r_1[f_1/(1 - f_1)]} \quad \text{and} \quad p_{22} = \frac{r_2[(1 - f_1)/f_1]}{1 + r_2[(1 - f_1)/f_1]}$$

†J. B. Kinsinger, T. Fischer, and C. W. Wilson, *Polym. Lett.* 5:285 (1967).

From $\frac{2N_{11}}{2N_{11} + N_{12}} = \frac{r_1 [f_1/(1 - f_1)]}{1 + r_1 [f_1/(1 - f_1)]}$

From $\frac{2N_{22}}{2N_{22} + N_{12}} = \frac{r_2 [(1 - f_1)/f_1]}{1 + r_2 [(1 - f_1)/f_1]}$

f_1	r_1	f_1	r_2
0.584	3.33	0.130	0.036
0.505	3.32	0.121	0.042
0.471	3.48	0.083	0.048
Average	3.38	Average	0.042

Particularly when r values are close to zero, this method for evaluating small r's is superior to the graphical analysis of composition data (compare Example 7.5 and Fig. 7.4).

•

By making measurements at higher magnetic fields, it is possible to resolve spectral features arising from still longer sequences. As a matter of fact, the authors of the research described in the last example were able to measure the fractions of tetrads of different composition in the same vinylidene chloride-isobutylene copolymer. Based on the longer sequences, they concluded that the penultimate model describes this system better than the terminal model, although the shortcomings of the latter are not evident in the example. Problems 7 and 8 at the end of the chapter also refer to this system.

Before examining NMR applications to problems of stereoregularity, let us conclude the discussion of copolymers by considering some copolymer applications.

7.8 Applications of Copolymers

Any list of copolymer applications would be as extensive as the applications of polymers in general. We shall only consider a few items in which the two-component nature of the copolymer plays an explicit role in determining the properties of the polymer. In addition, we shall examine several additional concerns which come up when applications technology is considered.

The properties of a copolymer can be viewed as hybrids of the properties of the separate homopolymers. Because of this, a good deal of refinement can be introduced into these properties by the use of copolymers. The situation is analogous to the use of pure liquids or binary solutions as solvents. The number of binary combinations, $n(n - 1)/2$ as noted above, greatly exceeds the number of pure liquids, and any one of these combinations can be prepared over a range of compositions. Just as mixed solvents offer a wider range of properties than

pure liquids in, say, developing a chromatogram, so it is with copolymers. Th analogy extends a bit further. Problems of limited miscibility can make certai solution compositions unattainable. Likewise, some copolymer composition are not achievable because of the reactivity ratios for a system.

Even the limitations imposed by reactivity ratios—while real enough—are no as severe as our presentation suggests. The reason for this is that the same pai of comonomers may have very different r values when polymerized via anioni or cationic intermediates rather than free radicals. We have elected to concen trate on the latter, but the former may also be used to synthesize copolymer in some instances. Figure 7.7 illustrates this situation for the styrene (monome 1)-methyl methacrylate system, showing how the copolymer composition F_1 varies with feed composition f_1 for the polymer produced by the three differen mechanisms. This indicates that an equimolar feedstock produces a copolyme which is mostly styrene in the cationic case, mostly methyl methacrylate in th anionic case, and roughly equimolar in the free-radical case. As we saw i Chap. 6, ionic polymerizations tend to be highly selective, so the extra flexibilit this adds to copolymer applications is somewhat limited. Another alternativ is three-component systems; we shall not pursue this possibility.

There are a number of physical properties of copolymers that are directl related to the multicomponent character of these materials and which ar

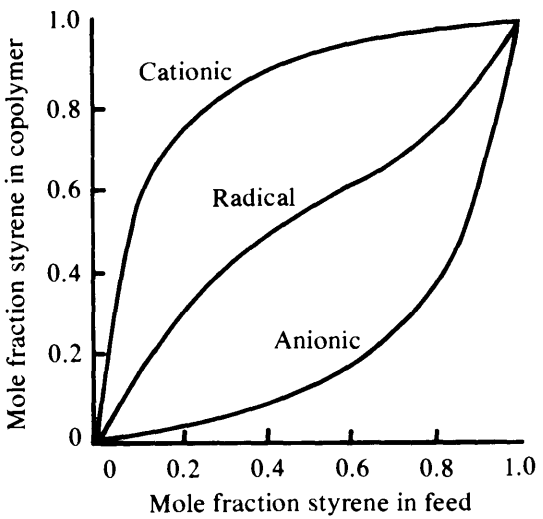

Figure 7.7 F_1 versus f_1 for styrene (M_1)-methyl methacrylate (M_2) copoly mers prepared by the mechanisms indicated. [From D. C. Pepper, *Q. Revie London* 8:88 (1954).]

utilized in various application situations. Solubility is perhaps the most easily visualized of these because of the familiar dictum: Like dissolves like. Thus copolymers may vary in their solubility in certain solvents, depending on their composition. For example, styrene-methyl methacrylate copolymers show increases in solubility in ester solvents as the methyl methacrylate content increases. This consideration is not merely of interest in dissolving polymers, but also affects such things as wet strength, swelling, and plasticizer compatibility.

In Chap. 4 we discussed the crystallizability of polymers and the importance of this property on the mechanical behavior of the bulk sample. Following the logic that leads to Eq. (4.17), the presence of a comonomer lowers T_m for a polymer. Carrying this further, we can compare a copolymer to an alloy in which each component lowers the melting point of the other until a minimum-melting eutectic is produced. Similar trends exist in copolymers.

Copolymers can be used to introduce a mixture of chemical functionalities into a polymer. Acidic and basic substituents can be introduced, for example, through comonomers like acrylic acid and vinyl pyridine. The resulting copolymers show interesting amphoteric behavior, reversing their charge in solution with changes of pH.

Finally, the dielectric properties of a nonpolar polymer are modified by inclusion of even small amounts of a polar comonomer. In coatings applications the presence of polar repeat units in an otherwise nonpolar polymer reduces the tendency for static buildup during manufacture, printing, and ultimate use. On the other hand, in dielectric applications this increases the power loss and must be kept to a minimum, even to the exclusion of polar initiator fragments.

Table 7.7 lists the common names and the comonomers for several addition copolymers that are widely used as elastomers, fibers, or films.

Table 7.7 A Few Common Copolymers and Their Constituents

Common name or acronym for copolymer	Comonomers
ABS	Acrylonitrile, butadiene, styrene
Acrylan	Acrylonitrile, vinyl acetate
Buna N	Butadiene, acrylonitrile
Buna S (SBR)	Styrene, butadiene
Butyl rubber	Isoprene, isobutylene
SAN	Styrene, acrylonitrile
Saran	Vinyl chloride, vinylidene chloride
Vinoflax	Vinyl chloride, vinyl isobutyl ether
Vinylite	Vinyl chloride, vinyl acetate
Vinyon	Vinyl chloride, acrylonitrile

In any application of a copolymer the rate of formation of the product, its molecular weight, and the uniformity of its composition during manufacture are also important considerations. While the composition of a copolymer depends only on the relative rates of the various propagation steps, the rate of formation and the molecular weight depend on the initiation and termination rates as well. We shall not discuss these points in any detail, but merely indicate that the situation parallels the presentation of these items for homopolymers as given in Chap. 6. The following can be shown:

1. Termination steps can involve either similar or dissimilar radicals:

$$R_t = k_{t,11}[M_1\cdot]^2 + k_{t,12}[M_1\cdot][M_2\cdot] + k_{t,22}[M_2\cdot]^2 \tag{7.61}$$

2. Under stationary-state conditions $R_i = R_t$, and with the use of Eqs. (6.5), (7.10), and (7.61), the stationary-state concentration of the various radicals can be found.
3. For copolymers, $R_p \propto [M]\sqrt{[I]}$ in analogy with Eq. (6.26), and $\bar{n}_n \propto [M]/\sqrt{[I]}$ in analogy with Eq. (6.37). In the copolymer case, however, $[M] = [M_1] + [M_2]$, and the proportionality "constants" are functions of the comonomer concentration ratio $[M_1]/[M_2]$, as well as the various kinetic constants.

Throughout this chapter we have assumed low conversions or monomer replacement, so that variation of the feed composition with the reaction could be neglected. Industrially, the former is impractical and the latter may be undesirable because of the added cost it entails. Figure 7.8 illustrates how the average composition of the copolymer drifts with the extent of reaction for the styrene-methyl methacrylate system. Although the instantaneous value of F follows f to either zero or unity, the average composition is seen to hold up better. For this system the reactivity ratios are very similar, so this is not a very stringent test of variability. In the context of applications, however, it raises the question as to just how much variability can be tolerated in a copolymer without deleterious effects on the properties of the product. Such considerations may reveal that the replacement of monomer through continuous addition is worth the added cost.

There are numerous other aspects of copolymer chemistry that might be taken up which we pass over because of space limitations. These include the following:

1. Systems of more than two components.
2. Complications arising from other types of chain isomerism, such as those mentioned in Sec. 1.6.
3. Copolymerization by ionic mechanisms.
4. Divinyl monomers and crosslinking.
5. Copolymers by step-growth processes.

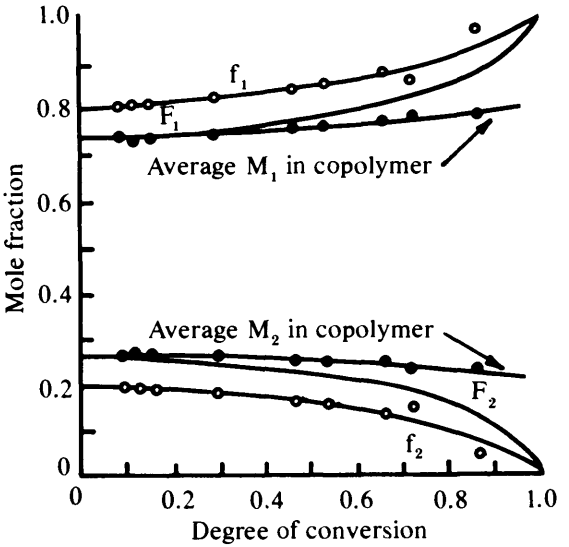

Figure 7.8 Mole fractions styrene (M_1) and methyl methacrylate (M_2) in feedstock (f) and copolymers (F) as a function of the extent of polymerization. Average copolymer compositions are also shown. [From V. E. Meyer and R. K. S. Chan, *Polym. Prepr.* 8:209(1967), used with permission.]

Instead of devoting more space to copolymers, we turn next to stereoregular polymers, in which many of the descriptions of microstructure developed in Sec. 7.6 can also find application.

7.9 Stereoregular Polymers

We introduced the concept of stereoregularity in Sec. 1.6. Figure 1.2 illustrates isotactic, syndiotactic, and atactic structures of a vinyl polymer in which successive repeat units along the fully extended chain lie, respectively, on the same side, alternating sides, or at random with respect to the backbone. It is important to appreciate the fact that these different structures—different configurations—have their origin in the bonding of the polymer, and no amount of rotation around bonds—changes in conformation—will convert one structure into another.

Our discussion of stereoregularity in this chapter is primarily concerned with polymers of monosubstituted ethylene repeat units. We shall represent these by

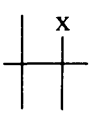

In this representation the X indicates the substituent; other bonds involve only hydrogens. This formalism also applies to 1,1-disubstituted ethylenes in which the substituents are different. With these symbols, the isotactic, syndiotactic, and atactic structures shown in Fig. 1.2 are represented by structures [VI]-[VIII], respectively:

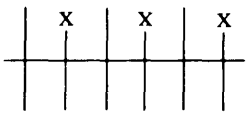

[VI]

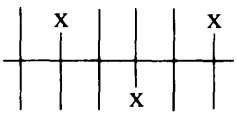

[VII]

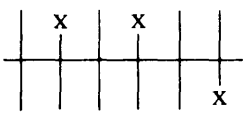

[VIII]

The carbon atoms carrying the substituents are not truly asymmetric, since the two chain sections–while generally of different length–are locally the same on either side of any carbon atom, except near the ends of the chain. As usual, we ignore any uniqueness associated with chain ends.

There are several topics pertaining to stereoregularity which we shall not cover to simplify the presentation:

1. Stereoregular copolymers. We shall restrict our discussion to stereoregular homopolymers.
2. Complications arising from other types of isomerism. Positional and geometrical isomerism, also described in Sec. 1.6, will be excluded for simplicity. In actual polymers these are not always so easily ignored.
3. Polymerization of 1,2-disubstituted ethylenes. Since these introduce two different "asymmetric" carbons into the polymer backbone (second substituent Y), they have the potential to display ditacticity. Our attention to these is limited to the illustration of some terminology which is derived from carbohydrate nomenclature (structures [IX]-[XII]):

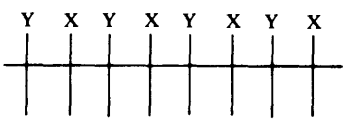

Erythro-di-isotactic

[IX]

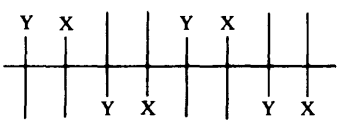

Erythro-di-syndiotactic

[X]

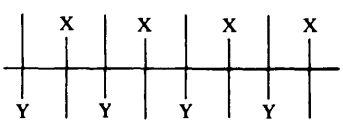

Threo-di-isotactic

[XI]

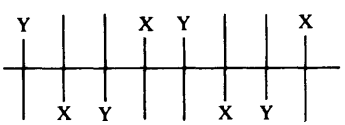

Threo-di-syndiotactic

[XII]

The successive repeat units in strucutres [VI]-[VIII] are of two different kinds. If they were labeled M_1 and M_2, we would find that, as far as microstructure is concerned, isotactic polymers are formally the same as homopolymers, syndiotactic polymers are formally the same as alternating copolymers, and atactic polymers are formally the same as random copolymers. The analog of block copolymers, stereoblock polymers, also exist. Instead of using M_1 and M_2 to differentiate between the two kinds of repeat units, we shall use the letters D and L as we did in Chap. 1.

The statistical nature of polymers and polymerization reactions has been illustrated at many points throughout this volume. It continues to be important in the discussion of stereoregularity. Thus it is generally more accurate to describe a polymer as, say, predominately isotactic rather than perfectly isotactic. More quantitatively, we need to be able to describe a polymer in terms of the percentages of isotactic, syndiotactic, and atactic sequences.

Certain bulk properties of polymers also reflect differences in stereoregularity. We saw in Chap. 4 that crystallinity is virtually impossible unless a high degree of stereoregularity is present in a polymer. Since crystallinity plays such an important part in determining the mechanical properties of polymers, stereoregularity manifests itself in these other behaviors also. These gross, bulk properties provide qualitative evidence for differences in stereoregularity, but, as with copolymers, it is the microstructural detail that quantitatively characterizes the tacticity of a polymer. We shall examine the statistics of this situation in the next section, and the application of NMR to the problem in Sec. 7.11.

The comparison between stereoregular polymers and copolymers can be extended still further. We can write chemical equations for propagation reactions leading to products which differ in configuration along with the associated rate laws. We do this without specifying anything—at least for now—about the mechanism. There are several things that need to be defined to do this:

1. These are addition polymerizations in which chain growth is propagated through an active center. The latter could be a free radical or an ion; we shall see that coordinate intermediates is the more usual case.
2. The active-center chain end is open to front or rear attack in general; hence the configuration of a repeat unit is not fixed until the next unit attaches to the growing chain.
3. The reactivity of a growing chain is assumed to be independent of chain length. In representing this schematically, we shall designate active species, of whatever chain length, as either DM* or LM*. The M* indicates the terminal active center, and the D or L, the penultimate units of fixed configuration. From a kinetic point of view, we ignore what lies further back along the chain.
4. As in Chap. 6, the monomer is represented by M.

With these definitions in mind, we can write

$$-DM^* + M \begin{cases} \nearrow DDM^* \\ \searrow DLM^* \end{cases}$$

or (7.0

$$-LM^* + M \begin{cases} \nearrow LLM^* \\ \searrow LDM^* \end{cases}$$

What is significant about these reactions is that only two possibilities exist addition with the same configuration (D → DD or L → LL) or addition with the opposite configuration (D → DL or L → LD). We shall designate these isotactic (subscript i) or syndiotactic (subscript s) additions, respectively, and shall define the rate constants for the two steps k_i and k_s. Therefore the rates of isotactic and syndiotactic propagation become

$$R_{p,i} = k_i[M^*][M] \tag{7.62}$$

and

$$R_{p,s} = k_s[M^*][M] \tag{7.63}$$

and, since the concentration dependencies are identical, the relative rates of the two processes is given by the ratio of the rate constants. This same ratio also gives the relative number of dyads having the same or different configurations

$$\frac{R_{p,i}}{R_{p,s}} = \frac{k_i}{k_s} = \frac{\text{number dyads with same configuration}}{\text{number dyads with different configurations}} \tag{7.64}$$

The Arrhenius equation enables us to expand on this still further:

$$\frac{\text{iso dyads}}{\text{syndio dyads}} = \frac{A_i}{A_s} e^{-(E_i^* - E_s^*)/RT} \tag{7.65}$$

The main conclusion we wish to draw from this line of development is that the difference between E_i^* and E_s^* could vary widely, depending on the nature of the active center.

If the active center in a polymerization is a free radical unencumbered by interaction with any surrounding species, we would expect $E_i^* - E_s^*$ to be small

Experiment confirms this expectation; for vinyl chloride it is on the order of 1.3 kJ mol^{-1}. (This is actually $\Delta H_i^* - \Delta H_s^*$ derived from an analysis based on the Eyring method: $k_i/k_s = e^{(\Delta S_i^* - \Delta S_s^*)/R}\ e^{-(\Delta H_i^* - \Delta H_s^*)/RT}$.) Thus at the temperatures usually encountered in free-radical polymerizations (~60°C), the exponential in Eq. (7.65) is small and the proportions of isotactic and syndiotactic dyads are roughly equal. This is the case for polyvinyl chloride, for which $k_i/k_s = 0.63$ at 60°C. The preference for syndiotactic additions is greater than this (that is, $E_i^* - E_s^*$ is larger) in some systems, apparently because there is less repulsion between substituents when they are staggered in the transition state. In all cases, whatever difference in activation energies exists manifests itself in product composition to a greater extent at low temperatures. At high temperatures small differences in E* value are leveled out by the high average thermal energy available.

The foregoing remarks refer explicitly to free-radical polymerization. If the active center is some kind of associated species—an ion pair or a coordination complex—then predictions based on unencumbered intermediates are irrelevant. It turns out that the Ziegler-Natta catalysts—which won their discoverers the Nobel Prize—apparently operate in this way. The active center of the chain coordinates with the catalyst in such a way as to block one mode of addition. High levels of stereoregularity are achieved in this case. Although these substances also initiate the polymerization, the term *catalyst* is especially appropriate in the present context, since the activation energy for one mode of addition is dramatically altered relative to the other by these materials. We shall discuss the chemical makeup of Ziegler-Natta catalysts and some ideas about how they work in Sec. 7.12. For now it is sufficient to recognize that these catalysts introduce a real bias into Eq. (7.65) and thereby favor one pattern of addition.

In the next section we shall take up the statistical description of various possible sequences.

7.10 A Statistical Description of Stereoregularity

Since it is unlikely that a polymer will possess perfect stereoregularity, it is desirable to quantitatively assess this property both to describe the polymer and to evaluate the effectiveness of various catalysts in this regard. In discussing tacticity in terms of microstructure, it has become conventional to designate a dyad as meso if the repeat units have the same configuration, and as racemic if the configuration is reversed. This terminology is derived from the stereochemistry of small molecules; its basis is seen by focusing attention on the methylene group in the backbone of the vinyl polymer. This methylene lies in a plane of symmetry in the isotactic molecule [XIII],

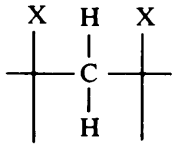

[XIII]

and thereby defines a meso (subscript m) structure as far as the dyad is concerned. Considering only the dyad, we see that these two methylene protons are in different environments. Therefore each will show a different chemical shift in an NMR spectrum. In addition, each proton splits the resonance of the other into a doublet, so a quartet of peaks appears in the spectrum. Still considering only the dyad, we see that the methylene is a syndiotactic grouping [XIV] contains two protons in identical environments:

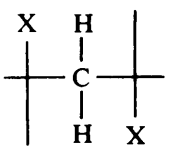

[XIV]

These protons show a single chemical shift in the NMR spectrum. This is called a racemic (subscript r) structure, since it contains equal amounts of D and L character. In the next section we shall discuss the NMR spectra of stereoregular polymers in more detail.

If we define p_m and p_r as the probability of addition occurring in the meso and racemic modes, respectively, then $p_m + p_r = 1$, since there are only two possibilities. The probability p_m is the analog of p_{ij} for copolymers; hence, by analogy with Eq. (7.30), this equals the fraction of isotactic dyads among all dyads. In terms of the kinetic approach of the last section, p_m is equal to the rate of an iso addition divided by the combined rates of iso and syndio additions:

$$p_m = \frac{k_i}{k_i + k_s} \tag{7.66}$$

This expression is the equivalent of Eq. (7.31) for copolymers.

The system of notation we have defined can readily be extended to sequences of greater length. Table 7.8 illustrates how either m or r dyads can be bracketed

Table 7.8 The Splitting of Meso and Racemic Dyads into Six Tetrads

Dyad	Triad
m	mmm
	mmr
	rmr
r	mrm
	mrr
	rrr

by two additional repeat units to form a tetrad. Each of the outer units is either m or r with respect to the unit it is attached to, so the meso dyad generates three tetrads. Note that the tetrads mmr and rmm are equivalent and are not distinguished. A similar set of tetrads is generated from the r dyad.

The same system of notation can be extended further by focusing attention on the backbone substituents rather than on the methylenes. Consider bracketing a center *substituent* with a pair of monomers in which the substituents have either the same or opposite configurations as the central substituent. Thus the two bracketing units are either m or r with respect to the central unit and the probabilities of the resulting triads are obtained from the probabilities of the respective m or r additions. The following possibilities exist:

1. An isotactic triad [XV] is generated by two successive meso additions:

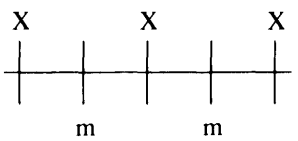

[XV]

The probability of the isotactic triad is

$$p_i = p_m^2 \tag{7.67}$$

2. A syndiotactic triad [XVI] is generated by two successive racemic additions:

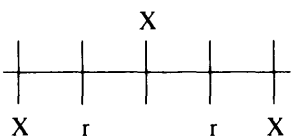

[XVI]

The probability of the syndiotactic triad is given by p_r^2, which becomes

$$p_s = (1 - p_m)^2 \tag{7.68}$$

since $p_r = 1 - p_m$.

3. A heterotactic traid [XVII] is generated by mr and rm sequences of additions:

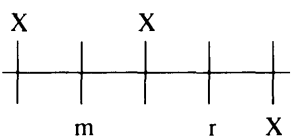

[XVII]

The probability of a heterotactic (subscript h) triad is

$$p_h = 2p_m(1 - p_m) \tag{7.69}$$

The factor 2 comes about because this particular sequence can be generated in two different orders.

These triads can also be bracketed by two more units to generate 10 different pentads following the pattern established in Table 7.8. It is left for the reader to verify this number by generating the various structures.

The probabilities of the various dyad, triad, and other sequences that we have examined have all been described by a single probability parameter p_m. When we used the same kind of statistics for copolymers, we called the situation one of terminal control. We are considering similar statistics here, but the idea that the stereochemistry is controlled by the terminal unit is inappropriate. The active center of the chain end governs the *chemistry* of the addition, but not the *stereochemistry*. Neither the terminal unit nor any other repeat unit considered alone has any stereochemistry. Equations (7.62) and (7.63) merely state that an addition must be of one kind or another, but that the rates are not necessarily identical.

A mechanism in which the stereochemistry of the growing chain does exert an influence on the addition might exist, but at least two repeat units in the chain are required to define any such stereochemistry. Therefore this possibility is equivalent to the penultimate mechanism in copolymers. In this case the addition would be described in terms of conditional probabilities, just as Eq. (7.49) does for copolymers. Thus the probability of an isotactic triad controlled by the stereochemistry of the growing chain would be represented by the reaction

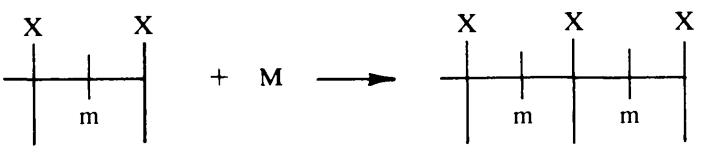

(7.P)

and described by the probability

$$p_{control} = p_m p_{m/m} \tag{7.70}$$

where $p_{m/m}$, a conditional probability, is the probability of an m addition, given the fact of a prior m addition. As with copolymers, triads must be considered in order to *test* whether the simple statistics apply. Still longer sequences need to be examined to test whether stereochemical contol is exerted by the chain. Although such situations are known, we shall limit our discussion to the simple case where the single probability p_m is sufficient to describe the various additions. The latter, incidentally, may be called zero-order Markov (or Bernoulli) statistics to avoid the vocabulary of terminal control. The case where the addition is influenced by whether the last linkage in the chain is m or r is said to follow a first-order Markov process.

The number of m or r linkages in an "n-ad" is n - 1. Thus dyads are characterized by a single linkage (either m or r), triads by two linkages (either mm,

mr, or rr), and so forth. The m and r notation thus reduces by 1 the order of the description from what is obtained when the repeat units themselves are described. For this reason the terminal control mechanism for copolymers is a first-order Markov process and the penultimate model is a second-order Markov process. Note that the compound probabilities which describe the probability of an n-ad in terms of p_m are also of order n - 1. In the following example we calculate the probability of various triads on the basis of zero-order Markov statistics.

Example 7.7

Use zero-order Markov statistics to evaluate the probability of isotactic, syndiotactic, and heterotactic triads for the series of p_m values spaced at intervals of 0.1. Plot and comment on the results.

Solution

Evaluate Eqs. (7.67)-(7.69) for p_m between zero and unity:

p_m	p_m^2	$(1 - p_m)^2$	$2p_m(1 - p_m)$
0	0	1	0
0.1	0.01	0.81	0.18
0.2	0.04	0.64	0.32
0.3	0.09	0.49	0.42
0.4	0.16	0.36	0.48
0.5	0.25	0.25	0.50
0.6	0.36	0.16	0.48
0.7	0.49	0.09	0.42
0.8	0.64	0.04	0.32
0.9	0.81	0.01	0.18
1.0	1.0	0	0

These results are plotted in Fig. 7.9. The following observations can be made from these calculations:

1. The probabilities give the fractions of the three different types of triads in the polymer.
2. If the fractions of triads could be measured, they either would or would not lie on a single vertical line in Fig. 7.9. If they did occur at a single value of p_m, this would not only give the value of p_m (which could be obtained from the fraction of one kind of triad), but would also prove the statistics assumed. If the fractions were not consistent with a single p_m value, higher-order Markov statistics are indicated.

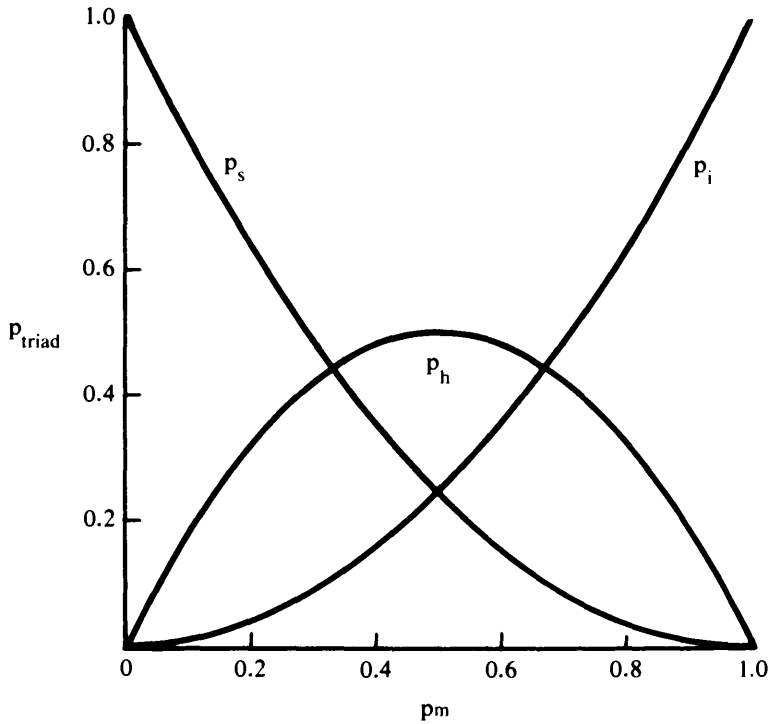

Figure 7.9 Fractions of iso, syndio, and hetero triads as a function of p_m, calculated assuming zero-order Markov (Bernoulli) statistics in Example 7.7.

3. The fraction of isotactic sequences increases as p_m increases, as required by the definition of these quantities.
4. The fraction of syndiotactic sequences increases as $p_m \rightarrow 0$, which corresponds to $p_r \rightarrow 1$.
5. The fraction of heterotactic triads is a maximum at $p_m = p_r = 0.5$ and drops to zero at either extreme.
6. For an atactic polymer the proportions of isotactic, syndiotactic, and heterotactic traids are 0.25:0.25:0.50.

To investigate the triads by NMR, the resonances associated with the chain substituent are examined, since structures [XV]-[XVII] show that it is these that experience different environments in the various triads. If dyad information is sufficient, the resonances of the methylenes in the chain backbone are measured. Structures [XIII] and [XIV] show that these serve as probes of the environment in dyads.

In the next section we shall examine in more detail how this type of NMR data is interpreted.

7.11 Measuring Stereoregularity by Nuclear Magnetic Resonance

It is not the purpose of this book to discuss in detail the contributions of NMR spectroscopy to the determination of molecular structure. This is a specialized field in itself and a great deal has been written on the subject. In this section we shall consider only the application of NMR to the elucidation of stereoregularity in polymers. Numerous other applications of this powerful technique have also been made in polymer chemistry, including the study of positional and geometrical isomerism (Sec. 1.6), copolymers (Sec. 7.7), and helix-coil transitions (Sec. 1.11). We shall also make no attempt to compare the NMR spectra of various different polymers; instead, we shall examine only the NMR spectra of different poly(methyl methacrylate) preparations to illustrate the capabilities of the method, using the first system that was investigated by this technique as the example.

Figure 7.10 shows the 60-MHz spectra of poly(methyl methacrylate) prepared with different catalysts so that predominately isotactic, syndiotactic, and atactic products are formed. The three spectra in Fig. 7.10 are identified in terms of this predominant character. It is apparent that the spectra are quite different, especially in the range of δ values between about 1 and 2 ppm. Since the atactic polymer has the least regular structure, we concentrate on the other two to make the assignment of the spectral features to the various protons.

Several observations from the last section provide the basis of interpreting these spectra:

1. The hydrogens of the methylene group in the backbone of the poly(methyl methacrylate) produce a single peak in a racemic dyad, as illustrated by structure [XVI].
2. The same group of hydrogens in a meso dyad [XIII] produce a quartet of peaks: two different chemical shifts, each split into two by the two hydrogens in the methylene.
3. The peaks centered at δ = 1.84 ppm—a singlet in the syndiotactic and a quartet in the isotactic polymers—are thus identified with these protons. This provides an unambiguous identification of the predominant stereoregularity of these samples.
4. The features that occur near δ = 1.0 ppm are associated with the protons of the α-methyl group. The location of this peak depends on the configurations of the nearest neighbors.
5. Working from the methylene assignments, we see that the peak at δ = 1.22 ppm in the isotactic polymer arises from the methyl in the center of an

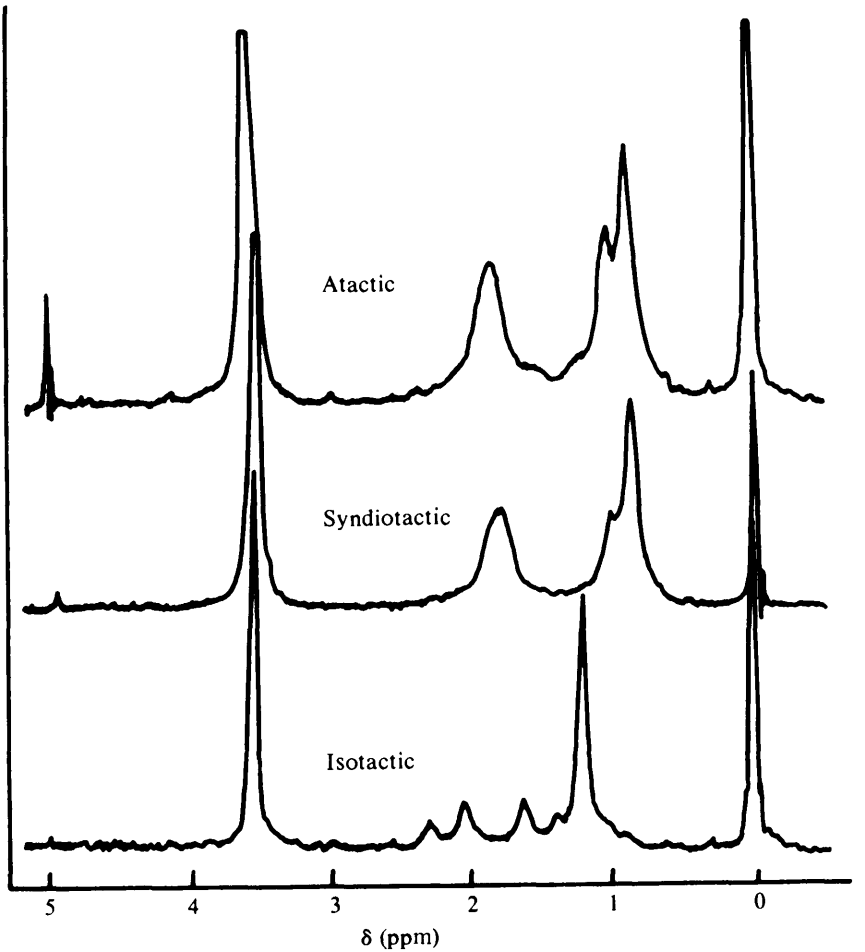

Figure 7.10 Nuclear magnetic resonance spectra of three poly(methyl methacrylate samples. Curves are labeled according to the preominant tacticity of samples. [From D. W. McCall and W. P. Slichter, in *Newer Methods of Polymer Characterization*, B. Ke (Ed.), Interscience, New York, 1964, used with permission.]

isotactic triad, the peak at $\delta = 0.87$ ppm from a syndiotactic triad, and the peak at $\delta = 1.02$ ppm from a homotactic triad.

6. The peak at $\delta = 3.5$ ppm is due to the ester methoxy group.

Once these assignments are made, the areas under the various peaks can be measured to determine the various fractions:

1. The area under the methylene peaks is proportional to the dyad concentration: The singlet gives the racemic dyads and the quartet gives the meso dyads.
2. The area under one of the methyl peaks is proportional to the concentration of the corresponding triad.
3. It is apparent that it is not particularly easy to determine the exact areas of these features when the various contributions occur together to any significant extent. This is clear from the atactic spectrum, in which slight shoulders on both the methylene and methyl peaks are the only evidence of meso methylenes and iso methyls.

The spectra shown in Fig. 7.10 were early attempts at this kind of experiment, and the measurement of peak areas in this case was a rather subjective affair. We shall continue with an analysis of these spectra—subjectivity and all—even though improved instrumentation has resulted in much improved spectra. One development that has produced better resolution in spectra is the use of higher magnetic fields. As the magnetic field increases, the chemical shifts for the various features are displaced proportionately. The splitting caused by spin–spin coupling, on the other hand, is unaffected. This can produce a considerable sharpening of the NMR spectrum. Figure 7.11 demonstrates this with the methylene portion of the spectra of predominately isotactic and predominately syndiotactic poly(methyl methacrylate) measured at 220 MHz. The contrast of these 220-MHz spectra with those measured at 60 MHz (see Fig. 7.10) reveals greatly improved resolution. In fact, additional fine structure is revealed which is more confusing than helpful at this point. We shall return to this additional fine structure below. Other procedures such as spin decoupling, isotopic substitution, computerized stripping of superimposed spectra, and ^{13}C-NMR also offer methods for identifying and quantifying NMR spectra.

Table 7.9 lists the estimated fractions of dyads of types m and r and the fractions of triads of types i, s, and h. These fractions represent the area under a specific peak (or four peaks in the case of the meso dyads) divided by the total area under all of the peaks in either the dyad or triad category. As expected for the sample labeled isotactic, 89% of the triads are of type i and 87% of the dyads are of type m. Likewise, in the sample labeled syndiotactic, 68% of the triads are s and 83% of the dyads are r.

The sample labeled atactic in Fig. 7.10 was prepared by a free-radical mechanism and, hence, is expected to follow zero-order Markov statistics. As a test of this, we examine Fig. 7.9 to see whether the values of p_i, p_s, and p_h, which are given by the fractions in Table 7.9, agree with a single set of p_m values. When this is done, it is apparent that these proportions are consistent with this type

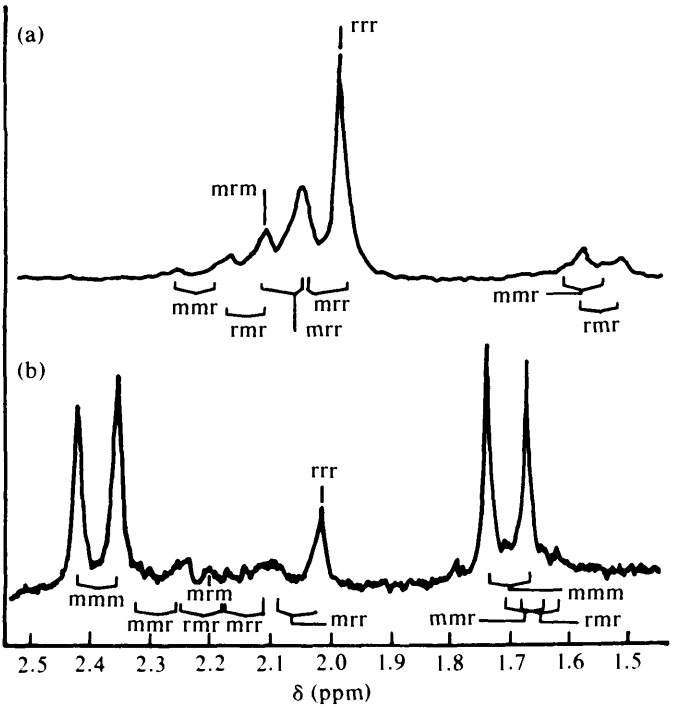

Figure 7.11 Methylene proton portion of the 220-MHz NMR spectrum of poly(methyl methacrylate): (a) predominately syndiotactic and (b) predominately isotactic. [From F. A. Bovey, *High Resolution NMR of Macromolecules*, Academic, New York, 1972, used with permission.]

Table 7.9 The Fractions of Meso and Racemic Dyads and Iso, Syndio, and Hetero Triads for the Data in Fig. 7.10

	Dyads		Triads		
Sample	Meso	Racemic	Iso	Syndio	Hetero
Atactic	0.22	0.78	0.07	0.55	0.38
Syndiotactic	0.17	0.83	0.04	0.68	0.28
Isotactic	0.87	0.13	0.89	0.04	0.07

Source: D. W. McCall and W. P. Slichter, in *Newer Methods of Polymer Characterization*, B. Ke (Ed.), Interscience, New York, 1964.

of statistics within experimental error and that $p_m \cong 0.25$ for poly(methyl methacrylate). Under the conditions of this polymerization, the free-radical mechanism is biased in favor of syndiotactic additions over isotactic additions by about 3:1, according to Eq. (6.66). Presumably this is due to steric effects involving the two substituents on the α-carbon.

With this kind of information it is not difficult to evaluate the average lengths of isotactic and syndiotactic sequences in a polymer. As a step toward this objective, we define the following:

1. The number of isotactic sequences containing n_i iso repeat units is N_{n_i}.
2. The number of syndiotactic sequences containing n_s syndio repeat units is N_{n_s}.
3. Since isotactic and syndiotactic sequences must alternate, it follows that

$$N_{n_i} = N_{n_s} \tag{7.71}$$

4. The number of iso triads in a sequence of n_i iso repeat units is $n_i - 1$, and the number of syndio triads in a sequence of n_s syndio repeat units is $n_s - 1$. We can verify these relationships by examining a specific chain segment [XVIII]:

   -DDLDLDLDLD*DDDDDDDDL-

   [XVIII]

   In this example both the iso and syndio sequences consist of eight repeat units, with seven triads in each. The repeat unit marked * is counted as part of each type of triad, but is itself the center of a hetero triad.
5. The number of racemic dyads in a sequence is the same as the number of syndiotactic units n_s. The number of meso dyads in a sequence is the same as the number of iso units n_i. These can also be verified from structure [XVIII] above.

With these definitions in mind, we can immediately write expressions for the ratio of the total number ν of iso triads to the total number of syndio triads:

$$\frac{\nu_i}{\nu_s} = \frac{\Sigma N_{n_i}(n_i - 1)}{\Sigma N_{n_s}(n_s - 1)} = \frac{\Sigma N_{n_i}(n_i) - \Sigma N_{n_i}}{\Sigma N_{n_s}(n_s) - \Sigma N_{n_s}} \tag{7.72}$$

In this equation the summations are over all values of n of the specified type. Also remember that the ν's and n's in this discussion (with subscript i or s) are defined differently from the ν's and n's defined earlier in the chapter for copolymers (where they had subscript 1 or 2). Using Eq. (7.71) and remembering

the definition of an average provided by Eq. (1.9), we see that Eq. (7.72) becomes

$$\frac{\nu_i}{\nu_s} = \frac{\bar{n}_i - 1}{\bar{n}_s - 1} \tag{7.73}$$

where the overbar indicates the average length of the indicated sequence.

A similar result can be written for the ratio of the total number (ν) of dyads of the two types (m and r), using item (5) above:

$$\frac{\nu_m}{\nu_r} = \frac{\Sigma N_{n_i}(n_i)}{\Sigma N_{n_s}(n_s)} = \frac{\bar{n}_i}{\bar{n}_s} \tag{7.74}$$

Equations (7.73) and (7.74) can be solved simultaneously for $\bar{n}_i$ and $\bar{n}_s$ in terms of the total number of dyads and triads:

$$\bar{n}_i = \frac{1 - \nu_i/\nu_s}{1 - (\nu_i/\nu_s)(\nu_r/\nu_m)} \tag{7.75}$$

and

$$\bar{n}_s = \frac{1 - \nu_i/\nu_s}{(\nu_m/\nu_t) - (\nu_i/\nu_s)} \tag{7.76}$$

Use of these relationships is illustrated in the following example:

Example 7.8

Use the dyad and triad fractions in Table 7.9 to calculate the average lengths of isotactic and syndiotactic sequences for the polymers of Fig. 7.10. Comment on the results.

Solution

Since the total numbers of dyads and triads always occur as ratios in Eqs. (7.73) and (7.74), both the numerators and denominators of these ratios can be divided by the total number of dyads or triads to convert these total numbers into fractions: That is, $\nu_i/\nu_s = (\nu_i/\nu_{tot})/\nu_s/\nu_{tot} = p_i/p_s$. Thus the fractions in Table 7.9 can be substituted for the ν's in Eqs. (7.73) and (7.74). The values of $\bar{n}_i$ and $\bar{n}_s$ so calculated for the three polymers are the following:

	$\bar{n}_i$	$\bar{n}_s$
Atactic	1.59	5.64
Syndiotactic	1.32	6.45
Isotactic	9.14	1.37

This type of analysis adds nothing new to the picture already presented by the dyad and triad probabilities. It is somewhat easier to visualize an average sequence, however, although it must be remembered that the latter implies nothing about the distribution of sequence lengths.

•

We conclude this section by returning to Fig. 7.11 for a closer look at the fine structure revealed at higher magnetic fields. What we are observing in these spectra are the methylene resonances as influenced by tetrad sequences. Table 7.8 shows that the meso dyad can be the center of three possible tetrads. Each of these is split into two, giving six spectral features. Likewise, the racemic dyad can be the center of three tetrads, one of which is further split into a doublet while the other two produce singlets in the spectrum. We need not be concerned with the various splitting patterns or with the assignment of the possible tetrads to the different features of the spectrum. It is sufficient to note that once identified, the fraction of the possible tetrads in a polymer can be evaluated by the same procedure used above. The analysis of these longer sequences is particularly important for systems following higher-order Markov statistics. The resonances of the α-methyl protons as influenced by pentad sequences can also be measured at high magnetic fields.

In the next section we shall examine the catalysts which are able to introduce this kind of regularity into polymers.

7.12 Ziegler-Natta Catalysts

For the purposes of this discussion, stereoregulating catalysts will be taken to mean Ziegler-Natta catalysts. This is a somewhat restrictive view of the situation, since there are other catalysts—phenyl magnesium bromide is a Grignard reagent—which can produce stereoregularity; the Ziegler-Natta catalysts are also used to produce polymers—unbranched polyethylene to name one—which lack stereoregularity. Ziegler-Natta catalysts are the most widely used and best-understood stereoregulating systems, so the loss of generality in this approach is not of great consequence.

The fundamental Ziegler-Natta recipe consists of two components: the halide or some other compound of a transition metal from among the group IVB to VIIIB elements and an organometallic compound of a representative metal from groups IA to IIIA. Some of the transition metal compounds that have been

studied include $TiCl_4$, $TiCl_3$, VCl_4, VCl_3, $ZrCl_4$, $CrCl_3$, $MoCl_5$, and CuCl. Some of the representative element organometallics include $(C_2H_5)_3Al$, $(C_2H_5)_2Mg$, C_4H_9Li and $(C_2H_5)_2Zn$. These are only a few of the possible compounds, so the number of *combinations* is very large.

The individual components of the Ziegler-Natta system can separately account for the initiation of some form of polymerization reaction, but not for the fact of stereoregularity. For example, butyl lithium can initiate anionic polymerization (see Sec. 6.10) and $TiCl_4$ can initiate cationic polymerization (see Sec. 6.11). In combination, still another mechanism for polymerization, coordination polymerization, is indicated. When the two components of the Ziegler-Natta system are present together, complicated exchange reactions are possible. Often the catalyst must age to attain maximum effectiveness; presumably this allows these exchange reactions to occur. Some possible exchange equilibria are

$$2\,Al(C_2H_5)_3 \rightleftarrows Al_2(C_2H_5)_6 \rightleftarrows [Al(C_2H_5)_2]^+ [Al(C_2H_5)_4]^- \qquad (7.Q)$$

$$TiCl_4 + [Al(C_2H_5)_2]^+ \rightleftarrows C_2H_5TiCl_3 + [Al(C_2H_5)Cl]^+$$

The organotitanium halide can then reduce to $TiCl_3$:

$$C_2H_5TiCl_3 \rightarrow TiCl_3 + C_2H_5\cdot \qquad (7.R)$$

Among other possible reactions, these free radicals can initiate ordinary free-radical polymerization. The Ziegler-Natta systems are thus seen to encompass several mechanisms for the initiation of polymerization. Neither ionic nor free-radical mechanisms account for stereoregularity, however, so we must look further for the mechanism whereby the Ziegler-Natta systems produce this interesting effect.

The stereoregulating capability of Ziegler-Natta catalysts is believed to depend on a coordination mechanism in which both the growing polymer chain and the monomer coordinate with the catalyst. The addition then occurs by insertion of the monomer between the growing chain and the catalyst by a concerted mechanism [XIX]:

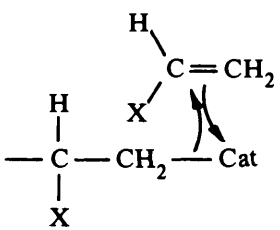

[XIX]

Since the coordination almost certainly involves the transition metal atom, there is a resemblance here to anionic polymerization. The coordination is an important aspect of the present picture, since it is this feature which allows the catalyst to serve as a template for stereoregulation.

The assortment of combinations of components is not the only variable to consider in describing Ziegler-Natta catalysts. Some other variables include the following:

1. Catalyst solubility. Polymerization systems may consist of one or two phases. Titanium-based catalysts are the most common of the heterogeneous systems; vanadium-based catalysts are the most common homogeneous systems. Since the catalyst functions as a template for the formation of a stereoregular product, it follows that the more extreme orienting effect of a solid surface (i.e., heterogeneous catalysts) are required for those monomers which interact only weakly with the catalyst. The latter are nonpolar monomers. Polar monomers interact more strongly with catalysts, and dissolved catalysts are able to exert sufficient control for stereoregularity.
2. Crystal structure of solids. The α-crystal form of $TiCl_3$ is an excellent catalyst and has been investigated extensively. In this particular crystal form of $TiCl_3$, the titanium ions are located in an octahedral environment of chloride ions. It is believed that the stereoactive titanium ions in this crystal are located at the edges of the crystal, where chloride ion vacancies in the coordination sphere allow coordination with the monomer molecules.
3. Tacticity of products. Most solid catalysts produce isotactic products. This is probably because of the highly orienting effect of the solid surface, as noted in item (1). The preferred isotactic configuration produced at these surfaces is largely governed by steric and electrostatic interactions between the monomer and the ligands of the transition metal. Syndiotacticity is mostly produced by soluble catalysts. Syndiotactic polymerizations are carried out at low temperatures, and even the catalyst must be prepared at low temperatures; otherwise specificity is lost. With polar monomers syndiotacticity is also promoted by polar reaction media. Apparently the polar solvent molecules compete with monomer for coordination sites, and thus indicate more loosely coordinated reactive species.
4. Rate of polymerization. The rate of polymerization for homogeneous systems closely resembles anionic polymerization. For heterogeneous systems the concentration of alkylated transition metal sites on the surface appears in the rate law. The latter depends on the particle size of the solid catalyst and may be complicated by sites of various degrees of activity. There is sometimes an inverse relationship between the degree of stereoregularity produced by a catalyst and the rate at which polymerization occurs.

The catalysts under consideration both initiate the polymerization and regulate the polymer formed. There is general agreement that the mechanism by which these materials exert their regulatory role involves coordination of monomer with the transition metal atom, but proposed details beyond this are almost as numerous and specific as the catalysts themselves. We shall return to a description of two specific mechanisms below. The general picture postulates an interaction between monomer and catalyst such that a complex is formed between the π electrons of the olefin and the d orbitals of the transition metal. Figure 7.12 shows that the overlap between the filled orbitals of the monomer can overlap with vacant $d_{x^2-y^2}$ orbitals of the metal. Alternatively, hybrid orbitals may be involved on the metal. There is a precedent for such bonding in simple model compounds. It is known, for example, that Pt^{2+} complexes with ethylene by forming a dsp^2 hybrid-π sigma bond and a dp hybrid-π^* pi bond. A crucial consideration in this coordination is maximizing the overlap of the orbitals involved. Titanium III ions seem ideally suited for this function; higher effective nuclear charge on the metal results in less spatial extension of d orbitals and diminished overlap.

Many mechanisms have been proposed that develop this picture more specifically. These are often so specific that they cannot be generalized beyond the systems for which they are proposed. Two schemes that do allow some generalization are presented here. Although they share certain common features, these mechanisms are distinguished by the fact that one—the monometallic model—does not include any participation by the representative metal in the mechanism. The second—the bimetallic model—does assume the involvement of both metals in the mechanism.

The monometallic mechanism is illustrated in Fig. 7.13a. It involves the monomer coordinating with an alkylated titanium atom. The insertion of the monomer into the titanium-carbon bond propagates the chain. As shown in

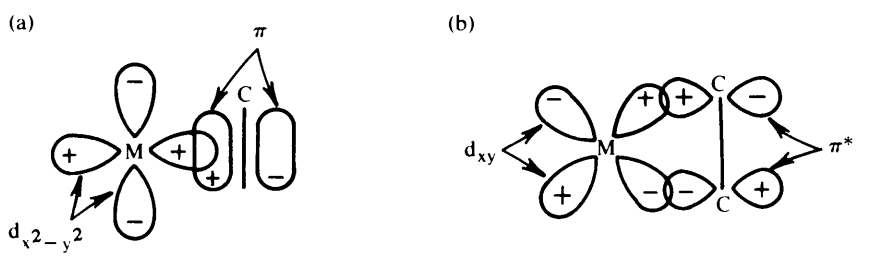

Figure 7.12 Orbital overlap between transition metal and olefin: (a) $d_{x^2-y^2}$ and π and (b) d_{xy} and π^*.

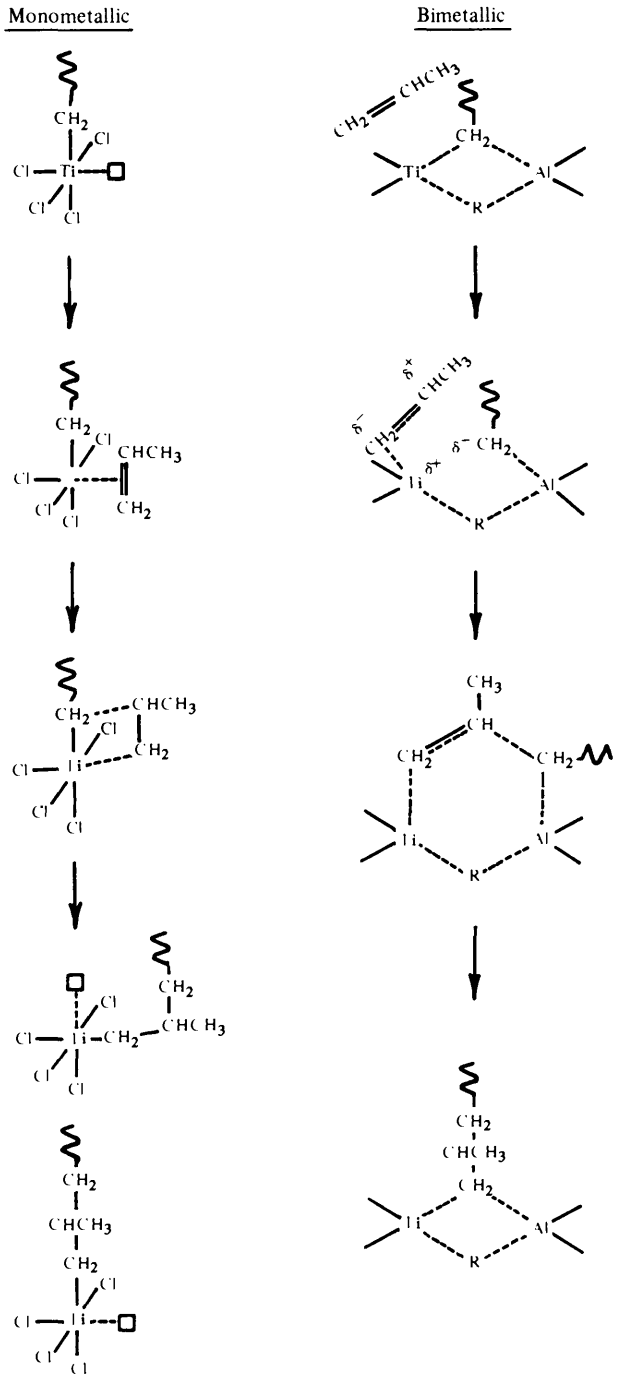

Figure 7.13 (a) The monometallic mechanism. The square indicates a vacant ligand site. (b) The bimetallic mechanism.

Fig. 7.13, this shifts the vacancy—represented by the square—in the coordination sphere of the titanium to a different site. Syndiotactic regulation occurs if the next addition takes place via this newly created vacancy. In this case the monomer and the growing chain occupy alternating coordination sites in successive steps. For the more common isotactic growth the polymer chain must migrate back to its original position.

Figure 7.14a illustrates the insertion of a propylene monomer into an edge vacancy in a crystal adjacent to an alkylated titanium atom. In Fig. 7.14b a cross-sectional view of the same site shows how the preferential orientation of the coordinated monomer is dictated by constraints imposed by the protuberances on the crystal surface.

The bimetallic mechanism is illustrated in Fig. 7.13b; the bimetallic active center is the distinguishing feature of this mechanism. The precise distribution of halides and alkyls is not spelled out because of the exchanges described by reaction (7.Q). An alkyl bridge is assumed based on observations of other organometallic compounds. The pi coordination of the olefin with the titanium is followed by insertion of the monomer into the bridge to propagate the reaction.

At present it is not possible to determine which of these mechanisms or their variations most accurately represents the behavior of Ziegler-Natta catalysts. In view of the number of variables in these catalyzed polymerizations, both mechanisms may be valid, each for different specific systems. In the following example the termination step of coordination polymerizations is considered.

Example 7.9

Polypropylene polymerized with triethyl aluminum and titanium trichloride has been found to contain various kinds of chain ends. Both terminal vinylidene unsaturation and aluminum-bound chain ends have been identified. Propose two termination reactions which can account for these observations. Do the termination reactions allow any discrimination between the monometallic and bimetallic propagation mechanisms?

Solution

A reaction analogous to the alkylation step of reaction (7.Q) can account for the association of an aluminum species with chain ends:

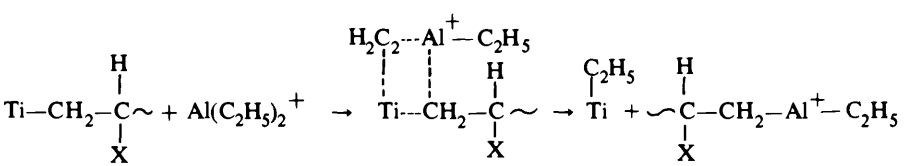

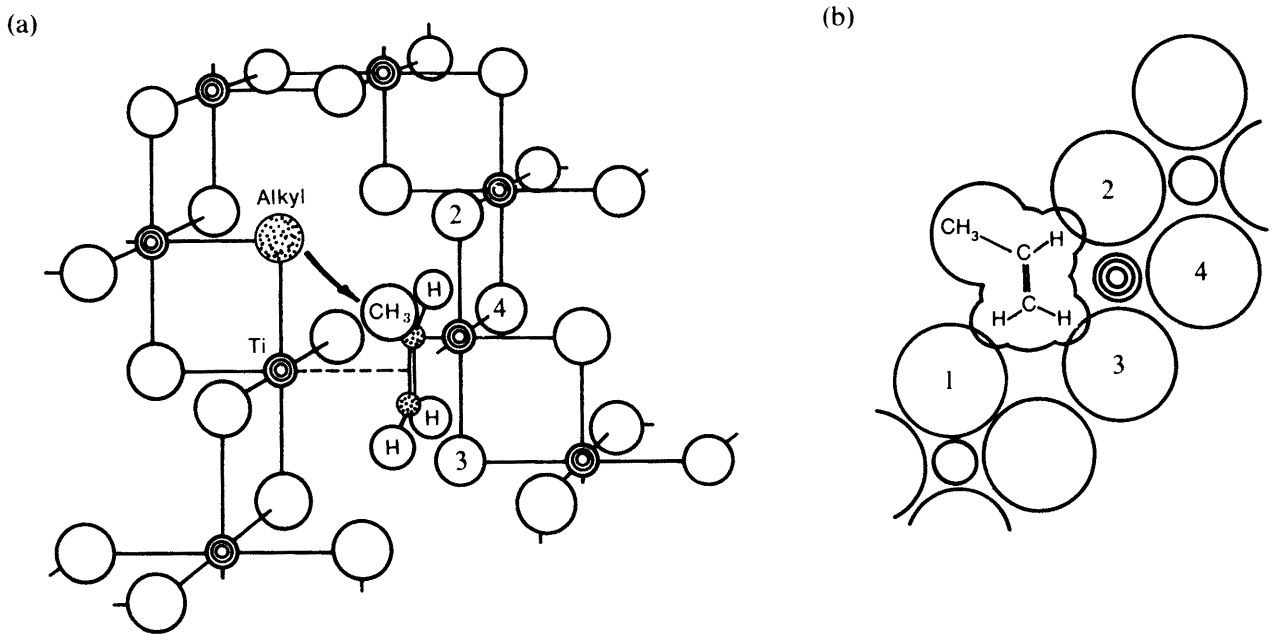

Figure 7.14 (a) The insertion of a propylene molecule into a site vacancy in the Ziegler–Natta catalyst. (b) The cross section shows the origin of stereoregulation. [From P. Cosee, *Tetrahedron Lett.* 17:17 (1960).]

The transfer of a tertiary hydrogen between the polymer chain and a monomer can account for the vinylidene group in the polymer:

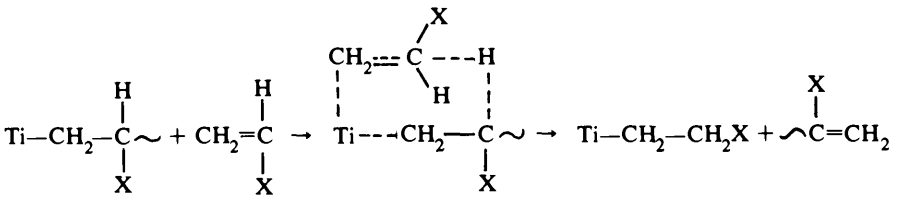

These reactions appear equally feasible for titanium in either the monometallic or bimetallic intermediate. Thus they account for the different types of end groups in the polymer, but do not differentiate between propagation intermediates.

•

In the commercial process for the production of polypropylene by Ziegler-Natta catalysts, hydrogen is added to terminate the reaction, so neither of these reactions is pertinent to this process.

7.13 Preview of Things to Come

In part 2 of this book we have focused attention on some classes of reactions which produce polymers and on some properties of the resulting products. In the final three chapters we shall consider some of the methods that are used to characterize the polymeric products of these syntheses.

In the concluding chapters we again consider assemblies of molecules–this time, polymers surrounded by solvent molecules which are comparable in size to the repeat units of the polymer. Generally speaking, our efforts are directed toward solutions which are relatively dilute with respect to the polymeric solute. The reason for this is the same reason that dilute solutions are widely considered in discussions of ionic or low molecular weight solutes, namely, solute-solute interactions are either negligible or at least minimal under these conditions.

We shall discuss three types of phenomena for polymer solutions: thermodynamic properties in Chap. 8, frictional properties in Chap. 9, and light-scattering properties in Chap. 10. A common feature of virtually all phenomena in these areas is that they all depend on the molecular weight of the solute. Thus observations of these properties can be interpreted to yield values for M; we shall use this capability as a unifying theme throughout these chapters.

In Chap. 8 we discuss the thermodynamics of polymer solutions, specifically with respect to phase separation and osmotic pressure. We shall devote considerable attention to statistical models to describe both the entropy and the enthalpy of mixtures. Of particular interest is the idea that the thermodynamic

nonideality of polymer solutions can be used as a quantitative measure of either the volume of polymer molecules or the strength of solute-solvent interactions. We shall also briefly consider charged polymers in Chap. 8; this is the only place where polymeric electrolytes are discussed in this text.

At first glance, the contents of Chap. 9 read like a catchall for unrelated topics. In it we examine the intrinsic viscosity of polymer solutions, the diffusion coefficient, the sedimentation coefficient, sedimentation equilibrium, and gel permeation chromatography. While all of these techniques can be related in one way or another to the molecular weight of the polymer, the more fundamental unifying principle which connects these topics is their common dependence on the spatial extension of the molecules. The radius of gyration is the parameter of interest in this context, and the intrinsic viscosity in particular can be interpreted to give a value for this important quantity. The experimental techniques discussed in Chap. 9 have been used extensively in the study of biopolymers.

Chemistry students are generally more familiar with the absorption of light by molecules than with more classical optical phenomena such as refraction and scattering. In Chap. 10 we attempt to remedy this situation by detailed development of those aspects of light scattering that are especially pertinent to the study of polymers. The discussion of this topic brings together certain basic ideas from electromagnetism, optics, and solution thermodynamics. Even though it is explicitly through an expression for osmotic pressure that the molecular weight enters the light-scattering equations, these two techniques give different averages for M. This makes these two methods complementary rather than redundant, and, in combination, they provide information concerning the width of the molecular weight distribution.

Although the emphasis in these last chapters is certainly on the polymeric solute, the experimental methods described herein also measure the interactions of these solutes with various solvents. Such interactions include the hydration of proteins at one extreme and the exclusion of poor solvents from random coils at the other. In between, good solvents are imbibed into the polymer domain to various degrees to expand coil dimensions. Such quantities as the Flory-Huggins interaction parameter, the Θ temperature, and the coil expansion factor are among the ways such interactions are quantified in the following chapters.

Problems

1. Write structural formulas for maleic anhydride (M_1) and stilbene (M_2). Neither of these monomers homopolymerize to any significant extent, presumably owing to steric effects. These monomers form a copolymer,

however, with $r_1 = r_2 = 0.03$.† Criticize or defend the following proposition: The strong tendency toward alternation in this copolymer suggests that polarity effects offset the steric hindrance and permit copolymerization of these monomers.

2. Styrene and methyl methacylate have been used as comonomers in many investigations of copolymerization. Use the following list‡ of r_1 values for each of these copolymerizing with the monomers listed below to rank the latter with respect to reactivity:

M_2	Styrene as M_1	Methyl methacrylate as M_1
Acrylonitrile	0.41	1.35
Allyl acetate	90	23
1,2-Dichloropropene-2	5	5.5
Methacrylonitrile	0.30	0.67
Vinyl chloride	17	12.5
Vinylidene chloride	1.85	2.53
2-Vinyl pyridine	0.55	0.395

To the extent that the data allow, suggest where these substituents might be positioned in Table 7.3.

3. The following reactivity ratios§ describe the polymerization of acrylonitrile (M_1) with the monomers listed:

M_2	r_1	r_2
Butadiene	0.02	0.3
Methyl methacrylate	0.15	1.22
Styrene	0.04	0.40
Vinyl acetate	4.2	0.05
Vinyl chloride	2.7	0.04

Use the Q and e values listed in Table 7.4 for each of the comonomers to give five independent estimates of Q and e for acrylonitrile. Compare the average of these four with the values given for acrylonitrile in Table 7.4.

† F. M. Lewis and F. R. Mayo, *J. Am. Chem. Soc.* 70:1533 (1948).
‡ Ref. 4.
§ Ref. 4.

4. As part of the research described in Fig. 7.5, Winston and Wichacheewa† measured the percentages of carbon and chlorine in copolymers of styrene (molecule 1) and 1-chloro-1,3-butadiene (molecule 2) prepared from various feedstocks. A portion of their data is given below:

f_1	Percent C	Percent Cl
0.892	81.80	10.88
0.649	71.34	20.14
0.324	64.95	27.92
0.153	58.69	34.79

Use these data to calculate F_1, the mole fraction of styrene in these copolymers.

5. Additional data from the research of the last problem‡ yield the following pairs of f_1, F_1 values (remember that styrene is component 1 in the styrene-1-chloro-1,3-butadiene system):

f_1	F_1	f_1	F_1
0.947	0.829	0.448	0.362
0.861	0.688	0.247	0.207
0.698	0.515	0.221	0.200
0.602	0.452		

Use the form suggested by Eq. (7.54) to prepare a graph based on these data and evaluate r_1 and r_2.

6. The reactivity ratios for the styrene (M_1)-1-chloro-1,3-butadiene (M_2) system were found to be $r_1 = 0.26$ and $r_2 = 1.02$ by the authors of the research described in the last two problems§ using the results of all their measurements. Use these r values and the feed compositions listed below to calculate the fraction expected in the copolymer of 1-chlorobutadiene sequences of lengths $\nu = 2$, 3, or 4. From these calculated results, evaluate the ratios N_{222}/N_{22} and N_{2222}/N_{222}. Copolymers prepared from these feedstocks were dehydrohalogenated to yield the polyenes like that whose spectrum is shown in Fig. 7.5. The specific absorbance at the indicated wavelengths was measured for 1% solutions of the products after HCl elimination:

† A. Winston and P. Wichacheewa, *Macromolecules* 6:200 (1973).
‡ Ibid.
§ Ibid.

	Specific absorbance		
f_1	$\lambda = 312$ nm	$\lambda = 367$ nm	$\lambda = 412$ nm
0.829	74	13	–
0.734	71	19	–
0.551	154	77	20
0.490	151	78	42

As noted in Sec. 7.7, these different wavelengths correspond to absorbance by sequences of different lengths. Compare the appropriate absorbance ratios with the theoretical sequence length ratios calculated above and comment briefly on the results.

7. Use the values determined in Example 7.6 for the vinylidene chloride (M_1)–isobutylene (M_2) system† to calculate F_1 for various values of f_1 according to the terminal mechanism. Prepare a plot of the results. On the same graph, plot the following experimentally measured values of f_1 and F_1:

f_1	F_1	f_1	F_1
0.548	0.83	0.225	0.66
0.471	0.79	0.206	0.64
0.391	0.74	0.159	0.61
0.318	0.71	0.126	0.58
0.288	0.70	0.083	0.52

Comment on the quality of the fit.

8. Some additional dyad fractions from the research cited in the last problem‡ are reported at intermediate feedstock concentrations (M_1 = vinylidene chloride; M_2 = isobutylene):

	Mole fraction of dyads		
f_1	11	12	22
0.418	0.55	0.43	0.03
0.353	0.48	0.49	0.04
0.317	0.44	0.52	0.04
0.247	0.38	0.58	0.04
0.213	0.34	0.62	0.04
0.198	0.32	0.64	0.05

Still assuming terminal control, evaluate r_1 and r_2 from these data. Criticize or defend the following proposition: The copolymer composition equation does not provide a very sensitive test for the terminal control mechanism.

†J. B. Kinsinger, T. Fischer, and C. W. Wilson, *Polym. Lett.* 5:285 (1967).
‡Ibid.

Dyad fractions are more sensitive, but must be examined over a wide range of compositions to provide a valid test.

9. Fox and Schnecko† carried out the free-radical polymerization of methyl methacrylate between −40 and 250°C. By analysis of the α-methyl peaks in the NMR spectra of the products, they determined the following values of α, the probability of an isotactic placement in the products prepared at the different temperatures:

T(°C)	α	T(°C)	α
250	0.36	0	0.20
150	0.33	−20	0.18
100	0.27	−40	0.14
95	0.27		
60	0.24		
30	0.22		

Evaluate $E_i^* - E_s^*$ by means of an Arrhenius plot of these data using $\alpha/(1-\alpha)$ as a measure of k_i/k_s. Briefly justify this last relationship.

10. As apparent from structure [XVIII], a hetero triad occurs at each interface between iso and syndio triads. The total number of hetero triads, therefore, equals the total number of sequences of all other types: $\nu_h = \Sigma N_{n_i} + \Sigma N_{n_s}$. Use this relationship and Eq. (7.71) to derive the expression $p_h = \nu_h/(\nu_h + \nu_i + \nu_s) = 2/\bar{n}_i + \bar{n}_s$. Criticize or defend the following proposition: The sequence DL_ is already two-thirds of the way to becoming a hetero triad, while the sequence DD_ is two-thirds of the way toward an iso triad. This means that the fraction of heterotactic triads is larger when the average length of syndio sequences is greater than the average length of iso sequences.
11. Randall‡ used ^{13}C-NMR to study the methylene spectrum of polystyrene. In 1,2,4-trichlorobenzene at 120°C, nine resonances were observed. These were assumed to arise from a combination of tetrads and hexads. Using m and r notation, extend Table 7.8 to include all 20 possible hexads. Criticize or defend the following proposition: Assuming that none of the resonances are obscured by overlap, there is only one way that nine methylene resonances can be produced, namely, by one of the tetrads to be split into hexads while the remaining tetrads remain unsplit.
12. In the research described in the preceding problem, Randall‡ was able to assign the five peaks associated with tetrads in the ^{13}C-NMR spectrum on the basis of their relative intensities, assuming zero-order Markov (or Bernoulli) statistics with $p_m = 0.575$. The five tetrad intensities and their chemical shifts from TMS are as follows:

† T. G. Fox and H. W. Schnecko, *Polymer* 3:575 (1962).

‡ J. C. Randall, *J. Polym. Sci. Polym. Phys. Ed.* 13:889 (1975).

$^{13}C\ \delta_{TMS}$ (ppm)	Relative area under peak
45.38	0.10
44.94	0.28
44.25	0.13
43.77	0.19
42.84	0.09

The remaining 21% of the peak area is distributed among the remaining hexad features. Use the value of p_m given to calculate the probabilities of the unsplit tetrads (see Problem 11) and on this basis assign the features listed above to the appropriate tetrads. Which of the tetrads appears to be split into hexads?

13. The fraction of sequences of the length indicated below have been measured† for a copolymer system at different feed ratios:

$[M_1]/[M_2]$	$P(M_1)$	$P(M_1M_1)$	$P(M_1M_1M_1)$
3	0.168	0.0643	0.0149
4	0.189	0.0563	0.0161
9	0.388	0.225	0.107
19	0.592	0.425	0.278

From appropriate ratios of these sequence lengths, what conclusions can be drawn concerning terminal versus penultimate control of addition?

14. The following are experimental tacticity fractions of polymers prepared from different monomers and with various catalysts. On the basis of Fig. 7.9, decide whether these preparations are adequately described (remember to make some allowance for experimental error) by a single parameter p_m or whether some other type of statistical description is required:

Catalyst	Solvent	Temperature (°C)	Fraction of polymer		
			Iso	Hetero	Syndio
	Methyl methacrylate‡				
Thermal	Toluene	60	8	33	59
n-Butyl lithium	Toluene	−78	78	16	6
n-Butyl lithium	Methyl isobutyrate	−78	21	31	48
	α-Methyl styrene§				
$TiCl_4$	Toluene	−78	–	19	81
$Et_3Al/TiCl_4$	Benzene	25	3	35	62
n-Butyl lithium	Cyclohexane	4	–	31	69

† K. Ito and Y. Yamashita, *J. Polym. Sci.* 3A:2165 (1965).

‡ K. Hatada, K. Ota, and H. Yuki, *Polym. Lett.* 5:225 (1967).

§ S. Brownstein, S. Bywater, and O. J. Worsfold, *Makromol. Chem.* 48:127 (1961).

On the basis of these observations, criticize or defend the following proposition: Regardless of the monomer used, zero-order Markov (Bernoulli) statistics apply to all free radical, anionic, and cationic polymerizations, but not to Ziegler–Natta catalyzed systems.

15. Replacing one of the alkyl groups in R_3Al with a halogen increases the stereospecificity of the Ziegler–Natta catalyst in the order $I > Br > Cl > R$. Replacement of a second alkyl by halogen decreases specificity. Criticize or defend the following proposition on the basis of these observations: The observed result of halogen substitution is consistent with the effect on the ease of alkylation produced by substituents of different electronegativity. This evidence thus adds credence to the monometallic mechanism, even though the observation involves the organometallic.
16. The weight percent propylene in ethylene-propylene copolymers for different Ziegler-Natta catalysts was measured† for the initial polymer produced from identical feedstocks. The following results were obtained:

Catalyst components	Weight percent propylene	Catalyst components	Weight percent propylene
VCl_4 plus		$Al(i\text{-}Bu)_3$ plus	
$Al(i\text{-}Bu)_3$	4.5	$HfCl_4$	0.7
CH_3TiCl_3	4.5	$ZrCl_4$	0.8
$Zn(C_2H_5)_2$	4.5	$VOCl_3$	2.4
$Zn(n\text{-}Bu)_2$	4.5		

Interpret these results in terms of the relative influence of the two components of the catalyst on the product found.

Bibliography

1. Alfrey, T., Jr., Bohrer, J. J., and Mark, H., *Copolymerization*, Interscience, New York, 1952.
2. Bovey, F. A., *High Resolution NMR of Macromolecules*, Academic, New York, 1972.
3. Bovey, F. A., and Winslow, F. H., *Macromolecules: An Introduction to Polymer Science*, Academic, New York, 1979.
4. Brandup, J., Immergut, E. H., and McDowell, W. (Eds.), *Polymer Handbook*, 2nd ed., Wiley, New York, 1975.
5. Ham, G. E. (Ed.), *Copolymerization*, Interscience, New York, 1964.
6. Koenig, J. L., *Chemical Microstructure of Polymer Chains*, Wiley, New York, 1980.
7. Odian, G., *Principles of Polymerization*, 2nd ed., Wiley, New York, 1981.

† F. J. Karol and W. L. Carrick, *J. Am. Chem. Soc.* 83:585 (1960).

SOME PROPERTIES OF POLYMER SOLUTIONS AND THEIR RELATION TO POLYMER CHARACTERIZATION

8

The Thermodynamics of Polymer Solutions

See plastic nature working to this end
The single atoms each to other tend
Attract, attracted to, the next in place
Formed and impelled its neighbor to embrace.

An Essay On Man, Alexander Pope

8.1 Introduction

The title of this chapter is somewhat misleading. In one sense it is too broad, in another sense too restrictive. We shall really discuss in detail only the phase separation and osmostic pressure of polymer solutions; a variety of other thermodynamic phenomena are ignored. In this regard the chapter title would better read "Some aspects of . . . ." Throughout this volume only a small part of what might be said about any topic is actually presented, so this modifying phrase is taken to be understood and is omitted.

In another sense the title is too restrictive, implying that only pure, phenomenological thermodynamics are discussed herein. Actually, this is far from true. Both thermodynamics and statistical thermodynamics comprise the contents of the chapter, with the second making the larger contribution. But the term *statistical* is omitted from the title, as it is too intimidating.

The phenomena we discuss, phase separation and osmotic pressure, are developed with particular attention to their applications in polymer characterization. Phase separation can be used to fractionate polydisperse polymer specimens into samples in which the molecular weight distribution is more narrow. Osmostic pressure experiments can be used to provide absolute values for the number average molecular weight of a polymer. Alternative methods for both fractionation and molecular weight determination exist, but the methods discussed in this chapter occupy a place of prominence among the alternatives, both historically and in contemporary practice.

Throughout this book we have emphasized fundamental concepts, and looking at the statistical basis for the phenomena we consider is the way this point of view is maintained in this chapter. All theories are based on models which only approximate the physical reality. To the extent that a model is successful, however, it represents at least some features of the actual system in a manageable way. This makes the study of such models valuable, even if the fully developed theory falls short of perfect success in quantitatively describing nature.

We shall devote a considerable portion of this chapter to discussing the thermodynamics of mixing according to the Flory-Huggins theory. Other important concepts we discuss in less detail include the cohesive energy density, the Flory-Krigbaum theory, and a brief look at charged polymers.

This is really the first time in this text that we have explicitly considered charged polymers as such. Even in the case of polymers prepared by ionic mechanisms, we tend to ignore the charge associated with the chain end as an insignificant end effect. Polymers in which ionizable functional groups occur throughout the molecule also exist, and these may carry quite high charges. Many biopolymers fall into this category. Even though we consider only a single aspect of charged polymers in this chapter, a number of pertinent considerations are clearly revealed.

8.2 Classical and Statistical Thermodynamics

In this chapter we shall consider some thermodynamic properties of solutions in which a polymer is the solute and some low molecular weight species is the solvent. Our special interest is in the application of solution thermodynamics to problems of phase equilibrium.

An important fact to remember about the field of thermodynamics is that it is blind to details concerning the structure of matter. Thermodynamics are concerned with observable, measurable quantities and the relationships between them, although there is a danger of losing sight of this fact in the somewhat abstract mathematical formalism of the subject. In discussing elasticity in Chap. 3, we took the position that entropy is often more intelligible from a statistical, atomistic point of view than from a purely phenomenological perspective. It is the latter that is *pure* thermodynamics; the former is the approach of statistical thermodynamics. In this chapter, too, we shall make extensive use of the statistical point of view to understand the molecular origin of certain phenomena.

The treatment of heat capacity in physical chemistry provides an excellent and familiar example of the relationship between pure and statistical thermodynamics. Heat capacity is defined experimentally and is measured by determining the heat required to change the temperature of a sample in, say,

a constant-pressure experiment. Numerous thermodynamic equations exist which relate the heat capacity to other thermodynamic quantities such as ΔH and ΔS. An alternative approach to heat capacity is to account for the storage of energy in molecules in terms of the various translational, rotational, and vibrational storage modes. *Doing* thermodynamics does not require so much as a knowledge that molecules exist, and much less how they store energy; *understanding* thermodynamics benefits considerably from the molecular point of view.

The drawback of the statistical approach is that it depends on a model, and models are bound to oversimplify. Nevertheless, we can learn a great deal from the attempt to evaluate thermodynamic properties from molecular models, even if the effort falls short of quantitative success.

There is probably no area of science that is as rich in mathematical relationships as thermodynamics. This makes thermodynamics very powerful, but such an abundance of riches can also be intimidating to the beginner. This chapter assumes that the reader is familiar with basic chemical and statistical thermodynamics at the level that these topics are treated in physical chemistry textbooks. In spite of this premise, a brief review of some pertinent relationships will be a useful way to get started.

Notation frequently poses problems in science, and this chapter is an example of such a situation. Our problem at present is that we have too many things to count: They cannot all be designated n. We have consistently used n to designate the degree of polymerization and shall continue with this notation. In thermodynamics n is widely used to designate the number of moles. Since we deal with (at least) two-component systems in this chapter, any count of the number of moles will always carry a subscript to indicate the component under consideration. We shall use the subscript 1 to designate the solvent, and 2 to designate the solute. The degree of polymerization is represented by n without a subscript.

To describe the state of a two-component system at equilibrium, we must specify the number of moles n_1 and n_2 of each component, as well as—ordinarily— the pressure p and the absolute temperature T. It is the Gibbs free energy that provides the most familiar access to a discussion of equilibrium. The increment in G associated with increments in the independent variables mentioned above is given by the equation

$$dG = V\,dp - S\,dT + \sum_{i=1,2} \mu_i\,dn_i \tag{8.1}$$

where μ_i is the chemical potential of component i. An important aspect of thermodynamics is the fact that the state variables (in the present context, this applies especially to the internal energy U, the enthalpy H, and the Gibbs

free energy G) can be expanded as partial derivatives of fundamental variables. Hence we can also write

$$dG = \left(\frac{\partial G}{\partial p}\right)_{T,n_1,n_2} dp + \left(\frac{\partial G}{\partial T}\right)_{p,n_1,n_2} dT + \left(\frac{\partial G}{\partial n_1}\right)_{p,T,n_2} dn_1 + \left(\frac{\partial G}{\partial n_2}\right)_{p,T,n_1} dn_2 \tag{8.2}$$

Comparing Eqs. (8.1) and (8.2) gives

$$V = \left(\frac{\partial G}{\partial p}\right)_{T,n_1,n_2} \tag{8.3}$$

$$S = -\left(\frac{\partial G}{\partial T}\right)_{p,n_1,n_2} \tag{8.4}$$

and

$$\mu_i = \left(\frac{\partial G}{\partial n_i}\right)_{p,T,n_{j\neq i}} \tag{8.5}$$

The chemical potential is an example of a partial molar quantity: μ_i is the partial molar Gibbs free energy with respect to component i. Other partial molar quantities exist and share the following features:

1. We may define, say, partial molar volume, enthalpy, or entropy by analogy with Eq. (8.5):

$$\bar{Y}_i = \left(\frac{\partial Y}{\partial n_i}\right)_{p,T,n_{j\neq i}} \tag{8.6}$$

   where Y = V, H, or S, respectively. Except for the partial molar Gibbs free energy, we shall use the notation $\bar{Y}_i$ to signify a partial molar quantity, where Y stands for the symbol of the appropriate variable.
2. Partial molar quantities have "per mole" units, and for Y_i this is understood to mean "per mole of component i." The value of this coefficient depends on the overall composition of the mixture. Thus $\bar{V}_{H_2O}$ is not the same for a water-alcohol mixture that is 10% water as for one that is 90% water.

3. For a pure component the partial molar quantity is identical to the molar (superscript °) value of the pure substance. Thus for pure component i

$$\mu_i = G_i^\circ \tag{8.7}$$

4. A useful feature of the partial molar properties is that the property of a mixture (subscript mix) can be written as the sum of the mole-weighted contributions of the partial molar properties of the components:

$$Y_{mix} = n_1\bar{Y}_1 + n_2\bar{Y}_2 \tag{8.8}$$

In this expression n_1 and n_2 are the numbers of moles of components 1 and 2 in the mixture under consideration.

5. To express the value of property Y_{mix} on a per mole basis, it is necessary to divide Eq. (8.8) by the total number of moles, $n_1 + n_2$. The mole fraction x_i of component i is written

$$x_i = \frac{n_i}{\Sigma_{i=1,2}\, n_i} \tag{8.9}$$

therefore

$$\frac{Y_{mix}}{n_1 + n_2} = x_1\bar{Y}_1 + x_2\bar{Y}_2 \tag{8.10}$$

6. Relationships which exist between ordinary thermodynamic variables also apply to the corresponding partial molar quantities. Two such relationships are

$$\mu_i = \bar{H}_i - T\bar{S}_i \tag{8.11}$$

and

$$\bar{V}_i = \left(\frac{\partial \mu_i}{\partial p}\right)_{T,\, n_{j\neq i}} \tag{8.12}$$

As noted above, all of the partial molar quantities are concentration dependent. It is convenient to define a thermodynamic concentration called the activity a_i in terms of which the chemical potential is correctly given by the relationship

$$\mu_i = \mu_i^\theta + RT \ln a_i \tag{8.13}$$

The quantity μ_i^θ is called the standard state (superscript θ) value of μ_i; it is the value of μ_i when $a_i = 1$. Neither μ_i nor G (nor U, H, etc.) can be measured

absolutely; we deal with differences in these quantities and the standard state value disappears when differences are taken. Although the standard state is defined differently in various situations, we shall generally take the pure component (superscript °) as the standard state, so $\mu_1^{\theta} = \mu_1^{\circ} = G_1^{\circ}$. Equation (8.13) defines activity in terms of the difference $\mu_i - \mu_i^{\circ}$; an obvious question is how a_i relates to the concentration of the solution as prepared or as determined by analytical chemistry.

There are two ways to arrive at the relationship between a_i and the concentration expressed as, say, a mole fraction. One is purely thermodynamic and involves experimental observations; the other involves a model and is based on a statistical approach. We shall examine both.

The first point in developing the thermodynamic method is the observation that for equilbrium between two phases—say, α and β—the chemical potential must be equal in both phases for all components:

$$\mu_i^{\alpha} = \mu_i^{\beta} \tag{8.14}$$

This becomes apparent if we consider the increment in G associated with transferring a small number of moles of component i from phase α to phase β at constant pressure and temperature. For equilibrium, $dG = 0 = dG^{\alpha} + dG^{\beta}$, and for each phase $dG = \Sigma_i \mu_i \, dn_i$. Since $dn_i^{\alpha} = -dn_i^{\beta}$, it follows that

$$dG = 0 = dG^{\alpha} + dG^{\beta} = \sum_i \mu_i^{\alpha} \, dn_i^{\alpha} + \sum_i \mu_i^{\beta} \, dn_i^{\beta} = \sum_i (\mu_i^{\alpha} - \mu_i^{\beta}) \, dn_i^{\alpha} \tag{8.15}$$

from which Eq. (8.14) is obtained.

Next we apply this result to liquid-vapor equilibrium. The following steps outline the argument:

1. Equation (8.14) applies to both components in the liquid and the vapor:

$$\mu_i^{l} = \mu_i^{v} \tag{8.16}$$

   The equality also holds if we take the partial derivative of both sides of Eq. (8.16) with respect to p.

2. We use Eq. (8.13) to take the partial with respect to p of μ_i^{l}:

$$\left(\frac{\partial \mu_i^{l}}{\partial p}\right)_{T,n_1,n_2} = RT \frac{\partial \ln a_i}{\partial p} \tag{8.17}$$

3. We use Eq. (8.12) to evaluate the partial with respect to p of μ_i^{v}:

$$\left(\frac{\partial \mu_i^{v}}{\partial p}\right)_{T,n_1,n_2} = \bar{V}_1^{v} = \frac{RT}{p_i} \tag{8.18}$$

where the second version treats the vapor as an ideal gas, an assumption we can make without loss of generality concerning the solution.

4. Equations (8.16)-(8.18) can be combined to give

$$\partial \ln a_i = \frac{\partial p_i}{p_i} = \partial \ln p_i \tag{8.19}$$

5. Equation (8.19) can be integrated using the convention that $a_i = 1$ for the pure component, which has the vapor pressure p_i°:

$$a_i = \frac{p_i}{p_i^\circ} \tag{8.20}$$

6. Finally, we note that Raoult's law (see Example 7.1) is a limiting law that is observed to apply in all solutions in the limit $x_i \to 1$:

$$\frac{p_i}{p_i^\circ} = x_i \tag{8.21}$$

7. Thus it is always observed in the limit of the pure component that

$$x_i = a_i \tag{8.22}$$

A solution which obeys Raoult's law over the full range of compositions is called an ideal solution (see Example 7.1). Equation (8.22) describes the relationship between activity and mole fraction for ideal solutions. In the case of nonideal solutions, the nonideality may be taken into account by introducing an activity coefficient as a factor of proportionality into Eq. (8.22).

A second way of dealing with the relationship between a_i and the experimental concentration requires the use of a statistical model. We assume that the system consists of N_1 molecules of type 1 and N_2 molecules of type 2. In addition, it is assumed that the molecules, while distinguishable, are identical to one another in size and interaction energy. That is, we can replace a molecule of type 1 in the mixture by one of type 2 and both ΔV and ΔH are zero for the process. Now we consider the placement of these molecules in the $N_1 + N_2 = N$ sites of a three-dimensional lattice. The total number of arrangements of the N molecules is given by N!, but since interchanging any of the 1's or 2's makes no difference, we divide by the number of ways of doing the latter—$N_1!$ and $N_2!$, respectively—to obtain the total number of different ways the system can come about. This is called the thermodynamic probabilty Ω of the system, and we saw in Sec. 3.3 that Ω is the basis for the statistical calculation of entropy. For this specific model

$$\Omega = \frac{N!}{N_1!N_2!} \tag{8.23}$$

The thermodynamic probability is converted to an entropy through the Boltzmann equation [Eq. (3.20)] so we can write for the entropy of the mixture (subscript mix)

$$S_{mix} = k \ln \Omega = k(\ln N! - \ln N_1! - \ln N_2!) \tag{8.24}$$

For large y's, we can use Sterling's approximation

$$\ln y! \cong y \ln y - y \tag{8.25}$$

in terms of which Eq. (8.24) becomes

$$S_{mix} = -k\left[N_1 \ln\left(\frac{N_1}{N}\right) + N_2 \ln\left(\frac{N_2}{N}\right)\right] \tag{8.26}$$

Multiplying and dividing the right-hand side of this expression by N converts the N_i's to mole fractions, and, if N is taken to be N_A, Avogadro's number, kN_A becomes R. Accordingly, we write for 1 mol of mixture

$$S_{mix} = -R(x_1 \ln x_1 + x_2 \ln x_2) \tag{8.27}$$

If either one of the mole fractions in Eq. (8.27) is unity, that is, for a pure component, S_{mix} becomes either S_1 or S_2. For the mixing *process* $1 + 2 \rightarrow$ mix,

$$\Delta S_m = S_{mix} - S_1 - S_2 = -R \sum_{i=1,2} (x_i \ln x_i) \tag{8.28}$$

Although the right-hand sides of Eqs. (8.27) and (8.28) are the same, the former applies to the mixture (subscript mix), while the latter applies to the mixing process (subscript m). The fact that these are identical emphasizes that in Eq. (8.27) we have calculated only that part of the total entropy of the mixture which arises from the mixing process itself. This is called the configurational entropy and is our only concern in mixing problems. The possibility that this mixing may involve other entropy effects—such as an entropy of solvation—is postponed until Sec. 8.12.

The model system for which this value of ΔS_m has been calculated is one for which ΔH_m has been specified to equal zero. Therefore, since $\Delta G = \Delta H - T\Delta S$, it follows that

$$\Delta G_m = RT \sum_{i=1,2} (x_i \ln x_i) \tag{8.29}$$

for this system. We can also use Eqs. (8.7), (8.10), and (8.13) to write ΔG_m in terms of chemical potentials:

$$\Delta G_m = G_{mix} - G_1^\circ - G_2^\circ = RT \sum_{i=1,2} (x_i \ln a_i) \tag{8.30}$$

Comparing Eqs. (8.29) and (8.30) also leads to the conclusion expressed by Eq. (8.22): $a_i = x_i$. Again we emphasize that this result applies only to ideal solutions, but the statistical approach gives us additional insights into the molecular properties associated with ideality in solutions:

1. The energy of interaction between a pair of solvent molecules, a pair of solute molecules, and a solvent-solute pair must be the same so that the criterion that $\Delta H_m = 0$ is met. Such a mixing process is said to be athermal.
2. The solvent and solute molecules must be the same size so that the criterion $\Delta V_m = 0$ is met.
3. Solutions can deviate from ideality because they fail to meet either one or both of these criteria. In reference to polymers in solutions of low molecular weight solvents, it is apparent that nonideality is present because of a failure to meet criterion (2), whether the mixing is athermal or not.

In the next section we shall examine the mixing process for molecules which differ greatly in size, building on the principles reviewed in this section. The reader who desires additional review of these ideas will find this material discussed in detail in textbooks of physical chemistry.

8.3 The Flory-Huggins Theory: The Entropy of Mixing

We concluded the last section with the observation that a polymer solution is expected to be nonideal on the grounds of entropy considerations alone. A nonzero value for ΔH_m would exacerbate the situation even further. We therefore begin our discussion of this problem by assuming a polymer-solvent system which shows athermal mixing. In the next section we shall extend the theory to include systems for which $\Delta H_m \neq 0$. The theory we shall examine in the next few sections was developed independently by Flory and Huggins and is known as the Flory-Huggins theory.

We assume that the mixture contains N_1 solvent molecules, each of which occupies a single site in the lattice we propose to fill. The system also contains N_2 polymer molecules, each of which occupies n lattice sites. The polymer molecule is thus defined to occupy a volume n times larger than the solvent molecules. Strictly speaking, this is the definition of n in the derivation which follows. We shall adopt the attitude that the repeat units in the polymer are equal to solvent molecules in volume, however, so a polymer of degree of

polymerization n will be larger than a solvent molecule by the factor n. In the event that the repeat unit and the solvent are not identical in volume, the chain can be hypothetically divided into n segments which *are* equal in volume to the solvent, and this n will be proportional to the degree of polymerization. The total number of sites in the lattice is $N_1 + nN_2 = N$.

We assign an index number to each of the polymer molecules and pick up the analysis of the problem after i polymer molecules have already been placed on an otherwise empty lattice. Our first question, then, concerns the number of ways the (i + 1)th polymer molecule can be placed in the lattice. The polymer is to be positioned one repeat unit at a time, so it is an easy matter to count the number of available positions for the first segment of the (i + 1)th molecule. Since the total lattice consists of N sites and ni of these are already occupied, the first segment of the (i + 1)th molecule can be placed on any one of the N - ni remaining sites.

There is nothing unique about the placement of this isolated segment to distinguish it from the placement of a small molecule on a lattice filled to the same extent. The polymeric nature of the solute shows up in the placement of the second segment: This must be positioned in a site adjacent to the first, since the units are covalently bonded together. No such limitation exists for independent small molecules. To handle this development we assume that each site on the lattice has z neighboring sites and we call z the coordination number of the lattice. It might appear that the need for this parameter introduces into the model a quantity which would be difficult to evaluate in any eventual test of the model. It turns out, however, that the z's cancel out of the final result for ΔS_m, so we need not worry about this eventuality.

If the molecule under consideration were being placed on an empty lattice, the second segment could go into any one of the z sites adjacent to the first. However, ni of the sites are already filled, so there is a chance that one of the z sites in the coordination sphere of the first segment is already occupied. To deal with this possibility, we assume that the fraction of vacant sites on the lattice *as a whole* also applies in the immediate vicinity of the segment positioned above. This fraction is (N - ni)/N, so the number of possible locations for segment 2 of the (i + 1)th molecule is z(N - ni)/N.

The logic that leads us to this last result also limits the applicability of the ensuing derivation. Applying the fraction of total lattice sites vacant to the immediate vicinity of the first segment makes the model descriptive of a relatively concentrated solution. This is somewhat novel in itself, since theories of solutions more commonly assume dilute conditions. More to the point, the model is unrealistic for dilute solutions where the site occupancy within the domain of a dissolved polymer coil is greater than that for the solution as a whole. We shall return to a model more appropriate for dilute solutions below. For now we continue with the case of the more concentrated solution, realizing

that with a significant fraction of the lattice sites already filled, we can treat the fraction of available sites as constant during the placement of a specific polymer molecule.

The third segment of molecule i + 1 would have z - 1 available sites on an otherwise empty lattice: The first segment, after all, already occupies a site adjacent to segment 2. For a lattice which already contains ni segments—if we consider those from molecule i + 1 as insignificant—the number of sites available for segment 3 is (z - 1)(N - ni)/N. This same number also applies to all subsequent segments. Therefore the number of ways ω_{i+1} that the (i + 1)th molecule can be placed on a lattice already containing i molecules is given by

$$\omega_{i+1} = (N - ni)\, z \left(\frac{N - ni}{N}\right) \left[(z - 1)\left(\frac{N - ni}{N}\right)\right]^{n-2}$$

$$= z(z - 1)^{n-2}\, N \left(\frac{N - ni}{N}\right)^{n} \tag{8.31}$$

or for the ith molecule

$$\omega_i = z(z - 1)^{n-2}\, N \left(\frac{N - n(i - 1)}{N}\right)^{n} \tag{8.32}$$

The total number of ways of placing N polymer molecules in the lattice is given by the product of factors like these, one for each molecule:

$$\Omega = \frac{\omega_1 \omega_2 \cdots \omega_i \cdots \omega_{N_2}}{N_2!} = \frac{1}{N_2!} \prod_{i=1}^{N_2} \omega_i \tag{8.33}$$

In writing Eq. (8.33), we have divided by $N_2!$, since the polymer molecules are interchangeable. Equation (8.33) gives the thermodynamic probabilty for the system according to this model, since there is only one way to place the solvent molecules once the polymer molecules have been positioned on the lattice.

Application of the Boltzmann equation to Eq. (8.33) gives the entropy of the mixture according to this model for concentrated solutions:

$$S_{mix} = k \ln \left(\frac{1}{N_2!}\right) \prod_{i=1}^{N_2} \omega_i \tag{8.34}$$

Substitution of Eq. (8.32) for ω_i in the above expression yields the desired result. A fair amount of algebra is required to convert this result into a usable form. We outline the tidying up in the following steps; the reader can supply the intervening steps:

1. Substitute Eq. (8.32) for ω in Ω:

$$\Omega = \frac{z^{N_2}(z-1)^{N_2(n-2)}}{N_2!\, N^{N_2(n-1)}} \prod_{i=1}^{N_2} [N - n(i-1)]^n$$

2. Examine the product of terms in this expression, replacing N by nN/n:

$$\prod_{i=1}^{N_2} [N - n(i-1)]^n = n^{nN_2} \prod_{i=1}^{N_2} \left(\frac{N}{n} + 1 - i\right)^n$$

3. Write out a few terms of the product:

$$\Pi = \left(\frac{N}{n} + 1 - 1\right)^n \left(\frac{N}{n} + 1 - 2\right)^n \left(\frac{N}{n} + 1 - 3\right)^n \cdots \left(\frac{N}{n} + 1 - N_2\right)^n$$

4. This is the same as

$$\Pi = \left(\frac{(N/n)!}{(N/n - N_2)!}\right)^n$$

5. Substitute items (2) and (3) into item (1):

$$\Omega = \frac{z^{N_2}(z-1)^{N_2(n-2)}\, n^{nN_2}}{N_2!\, N^{N_2(n-1)}} \left(\frac{(N/n)!}{(N/n - N_2)!}\right)^n$$

6. Apply Sterling's approximation to the logarithm of Ω and simplify:

$$\frac{S_{mix}}{k} = -N_2 \ln\left(\frac{nN_2}{N}\right) - N_1 \ln\left(\frac{N_1}{N}\right)$$

$$+ N_2 [\ln z + (n-2)\ln(z-1) + (1-n) + \ln n]$$

7. Consider the above result for the case of $N_2 = 0$, that is, for pure solvent: The expression in item (6) is proportional to the entropy of the pure solvent: $S_1 = 0$.
8. If $N_1 = 0$, that is, for pure polymer, the expression in item (6) gives

$$S_2 = kN_2 [\ln z + (n-2)\ln(z-1) + (1-n) + \ln n]$$

This is the entropy of the disordered polymer when the latter entirely fills the lattice.

The entropy of the mixture minus the entropy of the pure components–that is, item (6) minus items (7) and (8)–gives ΔS_m according to this model:

$$\Delta S_m = -k\left[N_1 \ln\left(\frac{N_1}{N}\right) + N_2 \ln\left(\frac{nN_2}{N}\right)\right] \tag{8.35}$$

Multiplying and dividing the right-hand side by $N_1 + N_2$ and letting this sum equal Avogadro's number of molecules gives ΔS_m per mole of solution:

$$\Delta S_m = -R\left[x_1 \ln\left(\frac{N_1}{N}\right) + x_2 \ln\left(\frac{nN_2}{N}\right)\right] \tag{8.36}$$

This result should be compared with Eq. (8.28) for the case of the ideal mixture. It is reassuring to note that for n = 1, Eq. (8.36) reduces to Eq. (8.28). Next let us consider whether a change of notation will clarify Eq. (8.36) still more. Recognizing that the solvent, the repeat unit, and the lattice site all have the same volume, we see that N_1/N is the volume fraction occupied by the solvent in the mixture and nN_2/N is the volume fraction of the polymer. Letting ϕ_i be the volume fraction of component i, we see that Eq. (8.36) becomes

$$\Delta S_m = -R(x_1 \ln \phi_1 + x_2 \ln \phi_2) \tag{8.37}$$

This model then leads us through a thicket of statistical and algebraic detail to the satisfying conclusion that going from small solute molecules to polymeric solutes only requires the replacement of mole fractions with volume fractions within the logarithms. Note that the mole fraction weighting factors are unaffected.

Since the system was defined to be athermal, $\Delta G_m = -T\,\Delta S_m$, so

$$\Delta G_m = RT(x_1 \ln \phi_1 + x_2 \ln \phi_2) \tag{8.38}$$

Since the ϕ's are fractions, the logarithms in Eq. (8.38) are less than unity and ΔG_m is negative for all concentrations. In the case of athermal mixtures entropy considerations alone are sufficient to account for polymer-solvent miscibility at all concentrations. Exactly the same is true for ideal solutions. As a matter of fact, it is possible to regard the expressions for ΔS_m and ΔG_m for ideal solutions as special cases of Eqs. (8.37) and (8.38) for the situation where n happens to equal unity. The following example compares values for ΔS_m for ideal and Flory-Huggins solutions to examine quantitatively the effect of variations in n on the entropy of mixing.

Example 8.1

Evaluate ΔS_m for ideal solutions and for athermal solutions of polymers having n values of 50, 100, and 500 by solving Eqs. (8.28) and (8.38) at regular intervals of mole fraction. Compare these calculated quantities by preparing a suitable plot of the results.

Solution

We express the calculated entropies of mixing in units of R. For ideal solutions the values of ΔS_m are evaluated directly from Eq. (8.28):

x_2	0.1	0.2	0.3	0.4	0.5	0.6	0.7	0.8	0.9
x_2	0.9	0.8	0.7	0.6	0.5	0.4	0.3	0.2	0.1
$\Delta S_m/R$	0.325	0.500	0.611	0.673	0.693	0.673	0.611	0.500	0.325

For polymer solutions we seek the relationship between mole fraction and volume fraction. Since $\phi_2/\phi_1 = nN_2/N_1$, $N_2/N_1 = (1/n)(\phi_2/\phi_1)$. Also,

$$x_2 = \frac{N_2}{N_1 + N_2} = \frac{N_2/N_1}{1 + N_2/N_1} = \frac{(1/n)\,\phi_2/\phi_1}{1 + (1/n)\,\phi_2/\phi_1}$$

Remember that both x and ϕ are fractional concentrations, so $x_1 + x_2 = 1$ and $\phi_1 + \phi_2 = 1$. Therefore

$$x_2 = \frac{(1/n)\,\phi_2/(1 - \phi_2)}{1 + (1/n)\,\phi_2/(1 - \phi_2)}$$

from which we find

$$\phi_2 = \frac{x_2}{(1/n) + x_2(1 - 1/n)}$$

This result enables us to convert mole fractions to volume fractions. Table 8.1 lists the corresponding values of ϕ_i and x_i for n = 50, 100, and 500 as needed for the evaluation of ΔS_m. With x_i's and the corresponding ϕ_i's available, the required values of $\Delta S_{mix}/R$ are calculated by Eq. (8.38):

n = 50	1.71	2.10	2.19	2.14	1.97	1.75	1.49	1.06	0.62
n = 100	2.25	2.62	2.65	2.53	2.31	1.99	1.66	1.25	0.69
n = 500	3.63	3.87	3.77	3.49	3.11	2.66	2.11	1.52	0.85

Table 8.1 Values of ϕ Corresponding to the Indicated Mole Fractions for Values of n = 50, 100, and 500 (These Quantities are Used in Example 8.1.)

	x_2	0.1	0.2	0.3	0.4	0.5	0.6	0.7	0.8	0.9
	x_1	0.9	0.8	0.7	0.6	0.5	0.4	0.3	0.2	0.1
For n = 50	ϕ_2	0.847	0.926	0.955	0.971	0.980	0.987	0.992	0.995	0.998
	ϕ_1	0.153	0.074	0.045	0.029	0.020	0.013	0.008	0.005	0.002
For n = 100	ϕ_2	0.917	0.962	0.977	0.985	0.990	0.993	0.996	0.998	0.999
	ϕ_1	0.083	0.038	0.023	0.015	0.010	0.007	0.004	0.002	0.001
For n = 500	ϕ_2	0.982	0.992	0.995	0.997	0.998	0.9987	0.9991	0.9995	0.9998
	ϕ_1	0.018	0.008	0.005	0.003	0.002	0.0013	0.0009	0.0005	0.0002

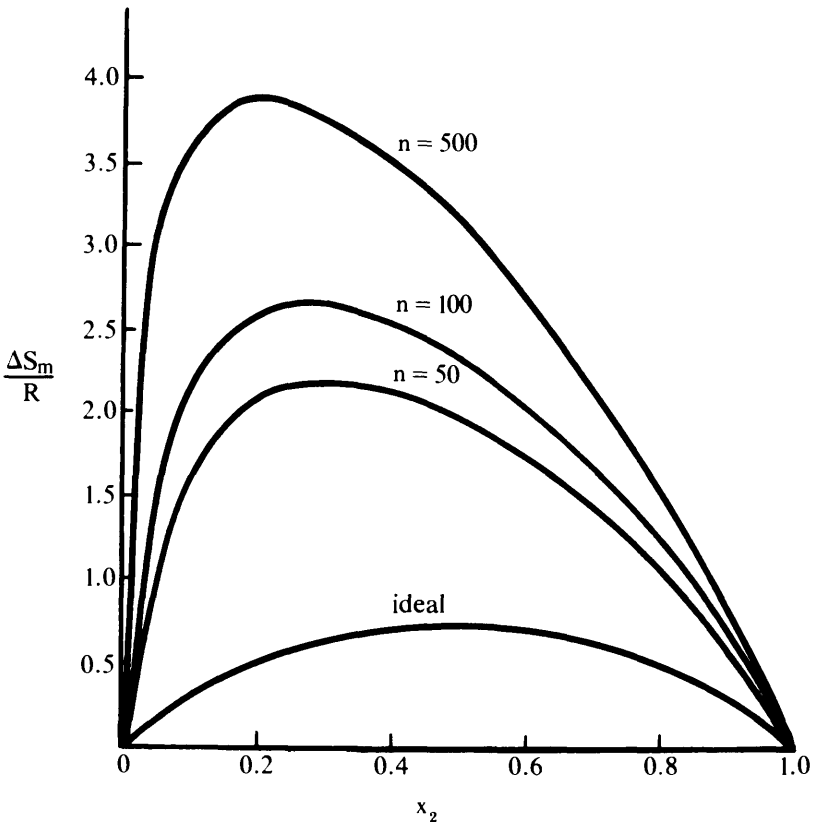

Figure 8.1 The entropy of mixing (in units of R) as a function of mole fraction solute for ideal mixing and for the Flory-Huggins lattice model with n = 50, 100, and 500. Values are calculated in Example 8.1.

A plot of these values is shown in Fig. 8.1. Note the increase in the entropy of mixing over the ideal value with increasing n value. Also note that the maximum occurs at decreasing mole fractions of polymer with increasing degree of polymerization.

•

Our ultimate goal is to develop expressions for the free energy of mixing according to the lattice model of the Flory-Huggins theory. The next step toward realization of this goal is to relax the restriction which limits the result to athermal solutions. In the next section we shall develop the theory for the enthalpy of mixing. Then we combine the equations for entropy and enthalpy to obtain an expression for ΔG_m according to the Flory-Huggins model.

8.4 The Flory-Huggins Theory: The Enthalpy of Mixing

In the liquid state molecules are in intimate contact, so the energetics of molecular interactions generally make a contribution to the overall picture of the mixing process. There are several aspects of the situation that we should be aware of before attempting to formulate a theory for ΔH_m:

1. Our immediate goal is an expression for ΔH_m and we must remember that this is the *difference* in the enthalpies of the solution and the pure components. We need not worry about the absolute values of the enthalpies of the individual states.
2. Enthalpies of mixing have their origin in the forces that operate between individual molecules. Intermolecular forces drop off rapidly with increasing distance of separation between molecules. This means that only nearest neighbors need be considered in the model.
3. Until surface contact, the force between molecules is always one of attraction, although this attraction has different origins in different systems. London forces, dipole-dipole attractions, acid-base interactions, and hydrogen bonds are some of the types of attraction we have in mind. In the foregoing list, London forces are universal and also the weakest of the attractions listed. The interactions increase in strength and also in specificity in the order listed.
4. Since London forces are universal and nonspecific, we shall eventually emphasize these, realizing that stronger forces may outweigh the London contribution in some systems. We anticipate the best results in nonpolar systems where London forces account for the interactions.

The lattice model that served as the basis for calculating ΔS_m in the last section continues to characterize the Flory-Huggins theory in the development of an expression for ΔH_m. Specifically, we are concerned with the change in enthalpy which occurs when one species is replaced by another in adjacent lattice sites. The situation can be represented in the notation of a chemical reaction:

$$(1,1) + (2,2) \rightarrow 2(1,2) \tag{8.A}$$

where 1 and 2 refer to solvent molecules and polymer *repeat units*, respectively, and the parentheses enclose the particular pair under consideration. Suppose we indicate the pairwise interaction energy between species i and j as w_{ij}; then for reaction (8.A),

$$\Delta w = 2w_{12} - w_{11} - w_{22} \tag{8.39}$$

The change in interaction energy per 1,2 pair is thus ½ Δw. Next we must consider how this scales up for a large array of molecules, and particularly how to describe the concentration dependence of the result.

Each lattice site is defined to have z nearest neighbors, and ϕ_1 and ϕ_2, respectively, can be used to describe the fraction of sites which are occupied by solvent molecules and polymer segments. The following inventory of interactions can now be made for the mixture:

1. Each polymer segment (subscript 2) is surrounded, on the average, by $z\phi_2$ polymer segments and $z\phi_1$ solvent molecules.
2. The contribution to the energy of this polymer segment interacting with its neighbors is $z\phi_2 w_{22} + z\phi_1 w_{12}$.
3. Since the lattice consists of N sites of which $\phi_2 N$ are occupied by polymer segments, the contribution to the energy of all interactions of the sort described in item (2) is $(\frac{1}{2})\, z\phi_2 N[(1 - \phi_1)w_{22} + \phi_1 w_{12}]$. The factor ½ has been introduced, since all pairs are counted twice in calculating this total.
4. Each solvent molecule (subscript 1) is surrounded, on the average, by $z\phi_2$ polymer segments and $z\phi_1$ solvent molecules.
5. The contribution to the energy of this molecule interacting with its neighbors is $z\phi_2 w_{12} + z\phi_1 w_{11}$.
6. In parallel with item (3), the contribution of all solvent interactions to the total energy is $(\frac{1}{2})\, z\phi_1 N[\phi_2 w_{12} + (1 - \phi_2)w_{11}]$.
7. When either pure component is considered, all w_{12} terms are zero, as well as the terms containing the volume fraction of the other component. Thus, for pure polymer, item (3) becomes $(\frac{1}{2})z\phi_2 N w_{22}$, and for the pure solvent item (6) becomes $(\frac{1}{2})z\phi_1 N w_{11}$.

The value of ΔH_m can be assembled from the foregoing by adding the energy contributions of items (3) and (6) and subtracting the contributions of the pure components given by item (7):

$$\Delta H_m = (\tfrac{1}{2})zN(2\phi_1\phi_2 w_{12} - \phi_1\phi_2 w_{11} - \phi_1\phi_2 w_{22}) \tag{8.40}$$

or, substituting Eq. (8.39),

$$\Delta H_m = (\tfrac{1}{2})zN\phi_1\phi_2\, \Delta w \tag{8.41}$$

Since ½ Δw is the change in interaction energy per 1,2 pair, it can be expressed as some multiple χ' of kT per pair or of RT per mole of pairs. It is also conventional to consolidate the lattice coordination number and χ' into a single parameter χ, since z and χ' are not measured separately. With this change of notation ½z Δw is replaced by its equivalent χRT, and Eq. (8.41) becomes

$$\Delta H_m = N\phi_1\phi_2\chi RT = N_1\phi_2\chi RT \tag{8.42}$$

The quantity χ is called the Flory-Huggins interaction parameter: It is zero for athermal mixtures, positive for endothermic mixing, and negative for exothermic mixing. These differences in sign originate from Eq. (8.39) and reaction (8.A).

Until now we have been purposely vague about the quantity Δw. Since we shall use the notation of Eq. (8.42) from now on, it is convenient to say a few more things about Δw before we lose sight of it entirely. Reaction (8.A) is clear enough; what is unspecific are the conditions under which this "reaction" takes place. Several possibilities come to mind, and each imparts a slightly different meaning to the "energy" w:

1. Since the solvent molecules, the polymer segments, and the lattice sites are all assumed to be equal in volume, reaction (8.A) implies constant volume conditions. Under these conditions, ΔU is needed and what we have called Δw might be better viewed as the contribution to the internal energy of a pairwise interaction ΔU_{pair}, where the subscript reminds us that this is the contribution of a single pair formation by reaction A.
2. Especially for large values of Δw, there could be an additional entropy effect beyond that calculated in the last section which arises from the interaction of nearest neighbors. That is, reaction (8.A) might be characterized by both a ΔH_{pair} *and* a ΔS_{pair}. In this case Δw might be viewed as the pairwise contribution to a free energy ΔG_{pair} with

$$\Delta G_{pair} = \Delta H_{pair} - T\,\Delta S_{pair} \tag{8.43}$$

3. In writing Eq. (8.41), we have clearly treated Δw as a contribution to enthalpy. This means we neglect volume changes (ΔH_{pair} versus ΔU_{pair}) and entropy changes beyond the configurational changes discussed in the last section (ΔG_{pair} versus ΔH_{pair}). In a subsequent development it is convenient to allow an additional entropy effect, and we shall return to Eq. (8.43) at that point.

The equations we have written until now in this section impose no restrictions on the species they describe or on the origin of the interaction energy. Volume and entropy effects associated with reaction (8.A) will be less if χ is not too large. Aside from this consideration, any of the intermolecular forces listed above could be responsible for the specific value of χ. The relationships for ΔS_m in the last section are based on a specific model and are subject to whatever limitations that imposes. There is nothing in the formalism for ΔH_m that we have developed until now that is obviously inapplicable to certain specific systems. In the next section we shall introduce another approximation

which will impose such a limitation, so it is important to recognize the point to which the generality extends.

In this section and the last, we have examined the lattice model of the Flory-Huggins theory for general expressions relating ΔH_m and ΔS_m to the composition of the mixture. The separate components can therefore be put together to give an expression for ΔG_m as a function of temperature and composition:

$$\Delta G_m = \Delta H_m - T\Delta S_m = RT[N\phi_1\phi_2\chi - (x_1 \ln \phi_1 + x_2 \ln \phi_2)] \tag{8.44}$$

The contribution of ΔS_m to this expression is given by Eq. (8.37) and is always positive; hence it contributes to a negative value of ΔG_m. The ΔH_m contribution, on the other hand, can be either positive or negative. If ΔH_m, as given by Eq. (8.41), is negative, this also contributes to a negative value for ΔG_m. If ΔH_m is positive, however, ΔS_m and ΔH_m make opposing contributions to ΔG_m, and the net effect depends on the magnitudes of the quantities involved. We shall return to an examination of this possibility in Sec. 8.6.

There are several reasons for devoting so much attention to the foregoing derivation of ΔG_m. For one thing, a theory like this gives the reader a "feel" for the origin of the various effects, which is valuable even if the theory is somewhat oversimplified. This feature is of considerable value in a textbook such as this. In addition, theories help us both in the interpretation and the prediction of experimental observations. We shall apply the ideas of the Flory-Huggins theory to the interpretation of experiments in later sections. For the present let us consider the predictive aspect. Suppose, for example, that a researcher is seeking a solvent for a particular polymer such that the two would show athermal mixing. The foregoing theory suggests that the search should focus on solvents for which the interaction with polymer molecules and among its own molecules are similar to polymer-polymer interactions. In this sense, Eq. (8.40) quantifies the rule of thumb "like dissolves like"; with no opposition from enthalpy, entropy considerations guarantee mixing. In the next section we shall develop this idea still further, although for a more limited range of systems.

8.5 Cohesive Energy Density

It is not particularly difficult to find macroscopic measures of interactions between small molecules of the same type, that is, quantities which are proportional to w_{11} and w_{22} in Eq. (8.40). Among the possibilities, we consider the change in internal energy ΔU_v for the vaporization process for component i. This can be related to w_{ii} in terms of the lattice model by the expression

$$\Delta U_{v,i} = \tfrac{1}{2}zNw_{ii} \tag{8.45}$$

where N equals Avogadro's number when ΔU_v is written per mole.

A more troublesome quantity is the interaction w_{12} between different species. It seems reasonable to expect this quantity to be some sort of hybrid of the w's for the separate components, at least provided that the mixing does not open the possibility for some specific interactions that is nonexistent among molecules of the pure components. We therefore postulate that no such possibility exists and consider for the remainder of this section only nonspecific interactions. In terms of the types of intermolecular forces enumerated in the last section, London and dipole-dipole attractions are certainly less specific than either acid-base or hydrogen bond interactions. The first two types are essentially physical interactions, depending on the distribution of charge in the interacting species. London forces are proportional to the polarizability of the molecules; dipole-dipole forces are proportional to their permanent dipole moments. These molecular parameters are also discussed in Sec. 10.3. While different molecules differ in the specific values of their polarizability and dipole moment, the notion that some sort of average value of these properties applies to the mixed interaction seems quite plausible. By contrast, the acidity or basicity of a molecule is the consequence of either empty or filled orbitals, and describing their interaction in terms of an "average orbital occupancy" is meaningless.

The application of these ideas to the mixing of low molecular weight liquids has been the object of extensive research. As a result of these investigations, the appropriate kind of "hybridization" of individual molecular properties in w_{12} is found to be the geometrical mean:

$$w_{12} \cong \sqrt{w_{11} w_{22}} \tag{8.46}$$

As argued above, this result is found to work best for substances in which both the 1,1 and 2,2 forces are either London or dipole-dipole. Even the case of one molecule with a permanent dipole moment interacting with a molecule which has only polarizability and no permanent dipole moment—such species interact by permanent dipole-induced dipole attraction—is not satisfactorily approximated by Eq. (8.46). In this context the "like dissolves like" rule means "like" with respect to the origin of intermolecular forces.

An advantage of expressing w_{12} as a geometrical mean is that Eq. (8.39) can now be written in an especially simple form. Combining Eqs. (8.39) and (8.46) gives

$$-\Delta w = w_{11} + w_{22} - 2\sqrt{w_{11} w_{22}} = (\sqrt{w_{11}} - \sqrt{w_{22}})^2 \tag{8.47}$$

As noted above, these homogeneous interaction energies can be represented by Eq. (8.45); therefore combining (8.45) and (8.47) yields

$$\Delta w \propto [(\Delta U_{v,1})^{1/2} - (\Delta U_{v,2})^{1/2}]^2 \tag{8.48}$$

where we have changed the sign in keeping with the convention that attractive energies such as w are negative while ΔU_v is positive.

Since we are explicitly interested in the difference in the sizes of solvent and solute molecules, it is more appropriate to express the values of ΔU_v on a "per unit volume" basis rather than on a molar basis. Accordingly, in Eq. (8.41) we replace the total number of sites N by the total volume of the mixture V and write

$$\Delta H_m = zV\phi_1\phi_2 \left[\left(\frac{\Delta U_{v,1}}{V_1^\circ} \right)^{1/2} - \left(\frac{\Delta U_{v,2}}{V_2^\circ} \right)^{1/2} \right]^2 \tag{8.49}$$

The quantity $\Delta U_{v,i}/V_i^\circ$ is the internal energy of vaporization per unit volume and is called the cohesive energy density (CED) of component i. The square root of the CED is generally given the symbol δ_i for component i.

The special appeal of this approach is that it allows the heat of mixing to be estimated in terms of a single parameter assigned to each component. This considerably simplifies the characterization of mixing, since m components (with m δ values) can be combined into m(m - 1)/2 binary mixtures, so a considerable data reduction follows from tabulating δ's instead of ΔH_m's. Table 8.2 is a list of CED and δ values for several common solvents, as well as estimated δ values for several common polymers.

Table 8.2 Values of the Cohesive Energy Density (CED) for Some Common Solvents and the Solubility Parameter δ for These Solvents and Some Common Polymers

Solvents	CED (cal cm^{-3})	δ [(cal $cm^{-3})^{1/2}$]	Polymers	δ [(cal $cm^{-3})^{1/2}$]
Cyclohexane	67.2	8.2	Polyisobutylene	7.5–8.0
CCl_4	74.0	8.6	Polyethylene	7.7–8.2
Toluene	79.2	8.9	Natural rubber	8.1–8.5
Benzene	84.6	9.2	Polystyrene	9.1–9.4
Methyl acetate	92.2	9.6	Poly(ethylene phthalate)	9.3–9.9
Acetone	98.0	9.9	Polyacrylonitrile	12.0–14.0
Cyclohexanone	98.0	9.9	Nylon-6,6	13.5–15.0
Acetic acid	102.0	10.1		
Furfural	125.4	11.2		
Cyclohexanol	130.0	11.4		
Methanol	210.3	14.5		
Water	547.6	23.4		

Source: H. Burrell, in J. Brandrup and E. H. Immergut (Eds.), *Polymer Handbook*, 2nd ed., Wiley, New York, 1975.

There are several additional comments regarding Eq. (8.49) which should be noted:

1. The development of Eq. (8.49) is based on the approximation given by Eq. (8.46), and the latter is applicable only under the special circumstances cited above.
2. Athermal mixing is expected in the case of $\delta_1 = \delta_2$. Since polymers generally decompose before evaporating, the definition $\delta = (\Delta U_v/V^\circ)$ is not useful for polymers. There are noncalorimetric methods for identifying athermal solutions, however, so the δ value of a polymer is equated to that of the solvent for such a system to estimate the CED for the polymer. The fact that a range of δ values is shown for the polymers in Table 8.2 indicates the margin of uncertainty associated with this approach.
3. In addition to thermodynamic applications, δ_2 values have also been related to the glass transition temperature of a polymer, and the difference $\delta_2 - \delta_1$ to the viscosity of polymer solutions. The "best" values of δ have been analyzed into group contributions, the sum of which can be used to estimate δ_2 for polymers which have not been characterized experimentally.
4. Equation (8.49) accounts only for endothermic mixing. It is not too surprising that we are thus led to associate exothermic ΔH_m values with more specifically chemical interactions between solvent and solute as opposed to the purely physical interactions we have been describing in this approximation.
5. It is only the contribution of ΔH_m to ΔG_m that we are discussing here, but we see the effect of this contribution—in the systems for which the approximation is valid—is that a solvent becomes less suitable to dissolve a polymer the greater the difference is between their δ values. At best, when $\delta_1 = \delta_2$, the solvent effect is neutral. Cases for which a favorable specific interaction between solvent and polymer actually promotes solution are characterized by negative values of ΔH_m and are therefore beyond the capabilities of this model.

Note that the development of ΔH_m in terms of the cohesive energy density is an optional extension of the Flory-Huggins theory in which χ can be either positive or negative. As a matter of fact, the principles outlined in this section were first developed and have been extensively tested for solutions of low molecular weight compounds. As might be expected, a number of variations on these basic ideas have been examined; the interested reader will find additional details in references on the theory of solutions. As far as polymers are concerned, the greatest value of this approach is that it offers useful predictive guidelines for pairing solvents and polymers to give athermal mixing. This extends to such considerations as the compatibility of plasticizers with bulk polymers and the swelling of cross-linked polymers in contact with solvents, as well as the formation of polymer solutions.

We conclude this section with a numerical example illustrating the evaluation of δ for a low molecular weight solvent.

Example 8.2

For benzene $\Delta H_v = 33.90$ kJ mol^{-1} and $\rho = 0.879$ g cm^{-3} at 25°C. Use these data to evaluate the cohesive energy density and δ for benzene at 25°C. Why is the cohesive energy density defined in terms of ΔU_v rather than ΔH_v?

Solution

The vaporization process describes the phase change liquid (l) → gas (g), so from the definition of ΔH we can write

$$\Delta U_v = \Delta H_v - P\Delta V_v = \Delta H_v - P(V_g - V_l) \cong \Delta H_v - PV_g \cong \Delta H_v - RT$$

For benzene at 25°C this becomes $\Delta U_v = 33{,}900 - 8.314\ (298) = 31{,}400$ J mol^{-1}. The molar volume of a compound is given by V° = (molecular weight)/(density). For benzene at 25°C, this becomes $V^\circ = 78.0/0.879 = 88.7$ cm^3 mol^{-1}. The cohesive energy density is simply the ratio $\Delta U_v/V^\circ$, but in evaluating this numerically, the question of units arises. By convention, these are usually expressed in calories per cubic centimeter, so we write

$$\text{CED} = \frac{31{,}400\ \text{J}}{\text{mol}} \times \frac{1\ \text{cal}}{4.184\ \text{J}} \times \frac{1\ \text{mol}}{88.7\ \text{cm}^3} = 84.6\ \text{cal cm}^{-3}$$

Therefore $\delta = (84.6)^{1/2} = 9.2(\text{cal cm}^{-3})^{1/2}$. The unit $(\text{cal cm}^{-3})^{1/2}$ is often called the Hildebrand (symbol H) in honor of Hildebrand, who made extensive contributions to the theory of solutions.

The vaporization process requires energy both to overcome intermolecular attractions and to push back the surroundings to make room for the vapor. The quantity ΔU_v measures the former, while ΔH_v takes both into account. In connection with the mixing process, it is the contribution of intermolecular forces which we seek to evaluate, so ΔU_v is a more suitable measure of this quantity.

•

8.6 Phase Separation

The criterion for phase equilibrium is given by Eq. (8.14) to be the equality of chemical potential in the phases in question for each of the components in the mixture. In Sec. 8.8 we shall use this idea to discuss the osmotic pressure of a

polymer solution. First, however, let us consider the separation of a polymer-solvent mixture into two immiscible solutions. We shall begin this discussion by examining the general thermodynamics of such a situation. Next we shall use the Flory-Huggins model as the basis for a theoretical approach to the topic. Finally, we shall consider the application of these ideas to the practical problem of polymer fractionation with respect to molecular weight.

Let us suppose that both ΔS_m and ΔH_m, and therefore ΔG_m, are known as functions of concentration for a particular mixture. We shall eventually assume the latter is given by Eq. (8.44), but the following general remarks are independent of any model. When ΔS_m is positive and ΔH_m is negative, then ΔG_m is negative and the solution process occurs spontaneously. Such a situation is seen to apply over the full range of concentrations in Fig. 8.2a. Now let us consider the significance of the tangent to the curve drawn in Fig. 8.2a. From Eqs. (8.7) and (8.10), it follows that

$$\Delta G_m = x_1 \Delta\mu_1 + x_2 \Delta\mu_2 = (1 - x_2)\Delta\mu_1 + x_2 \Delta\mu_2 \tag{8.50}$$

where $\Delta\mu_i = \mu_i - \mu_i^\circ$. Rearranging, we obtain

$$\Delta G_m = \Delta\mu_1 + x_2(\Delta\mu_2 - \Delta\mu_1) \tag{8.51}$$

This is the expression of a straight line having a slope equal to $\Delta\mu_2 - \Delta\mu_1$ and an intercept at $x_2 = 0$ equal to $\Delta\mu_1$. By rewriting Eq. (8.50) in terms of x_1, we get the equation

$$\Delta G_m = \Delta\mu_2 + x_1(\Delta\mu_1 - \Delta\mu_2) = \Delta\mu_2 - x_1(\Delta\mu_2 - \Delta\mu_1) \tag{8.52}$$

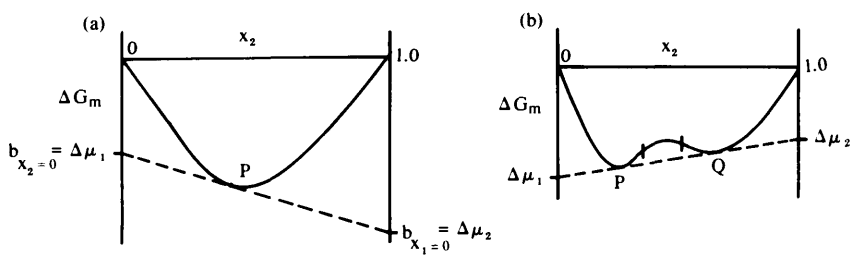

Figure 8.2 Schematic illustrations of ΔG_m versus x_2 showing how $\mu_i - \mu_i^\circ$ may be determined by the tangent drawn at any point. (a) The polymer-solvent system forms a single solution at all compositions. (b) Compositions between the two minima separate into equilibrium phases P and Q.

Both Eqs. (8.51) and (8.52) are seen to describe the line drawn tangent to the curve at point P in Fig. 8.2a, and they give the value of $\Delta\mu_i$ for each component for any mixture at which the tangent is drawn.

Next suppose ΔS_m and ΔH_m are both positive. In this case these two partially offset one another, and a plot of ΔG_m resembling that shown in Fig. 8.2b may result. We are particularly interested in the two minima in this curve and the hump between them. A common tangent can always be drawn to two such minima so the above discussion shows that the minima at points P and Q in Fig. 8.2b each have the same values of $\Delta\mu_1$ and $\Delta\mu_2$. Since $\Delta\mu_i$ is simply the difference between μ_i and its value for the pure component, the chemical potential for each component is seen to have the same value for both solution P and solution Q in Fig. 8.2b.

Now we turn our attention to the hump that separates these two minima. Between points P and Q, the plot of ΔG_m versus x_2 goes through a maximum and the values of ΔG_m along that portion of the curve are larger than the corresponding values on the line which is tangent to the two minima. This means that the mixtures whose compositions lie between points P and Q can achieve a lower free energy by separating into the two solutions at which the minima are located. Since these phases have the same chemical potential for both components, the phases at P and Q are in equilibrium, and any mixture which would otherwise fall between P and Q in composition will separate into phases with compositions $x_{2,P}$ and $x_{2,Q}$.

Remember that the hump which causes the instability with respect to phase separation arises from an unfavorable ΔH_m; considerations of configurational entropy alone favor mixing. Since ΔS_m is multiplied by T in the evaluation of ΔG_m, we anticipate that as the temperature increases, curves like that shown in Fig. 8.2b will gradually smooth out and eventually pass over to the form shown in Fig. 8.2a. The temperature at which the wiggles in the curve finally vanish will be a critical temperature for this particular phase separation. We shall presently turn to the Flory-Huggins theory for some mathematical descriptions of this critical point. The following example reminds us of a similar problem encountered elsewhere in physical chemistry.

Example 8.3

The van der Waals equation of state for 1 mol of a nonideal gas contains two constants a and b which are characteristic of a particular gas:

$$\left(p + \frac{a}{V^2}\right)(V - b) = RT$$

These constants can be related to the coordinates of the critical point of the gas: p_c, V_c, and T_c. Outline the strategy by which the van der Waals a and b

constants are related to p_c, V_c, and T_c. Point out the parallel between the van der Waals problem and the problem of separation into immiscible solutions, and suggest how the van der Waals strategy might be applied to the problem at hand.

Solution

Multiplied out, the van der Waals equation is cubic in volume,

$$pV^3 - (pb + RT)V^2 + aV - ab = 0$$

and, in general, there are three values of V which satisfy the equation for a given pressure and temperature. Of course, this contradicts the behavior of actual gases. Above a certain temperature, however, two of the roots of the van der Waals equation become imaginary, and above this temperature only one real solution to the equation exists. This mathematically unique temperature and the physically unique critical temperature are taken to be the same.

To identify this crossover point in the mathematical behavior, we recognize that the maximum and minimum that occur in the three-root region and the inflection point between them merge into a common point at the transition in behavior. The maximum and minimum are identified by the criterion $(\partial V/\partial p)_T = 0$, and the inflection point by the criterion $(\partial^2 V/\partial p^2)_T = 0$. Carrying out these two differentiations and identifying the volume and temperature that appear in the results as V_c and T_c gives two equations which are functions of a and b and the critical coordinates. These simultaneous equations can be solved for a and b to give $a = 27(RT_c)^2/64p_c$ and $b = RT_c/8p_c$.

For the phase separation problem, the maximum and minima in Fig. 8.2b and the inflection points between them must also merge into a common point at the critical temperature for the two-phase region. This is the mathematical criterion for the "smoothing out of wiggles," as the critical point was described above.

•

The procedure outlined in this example needs only one modification to be applicable to the critical point for solution miscibility. In Fig. 8.2b we observe that there are two inflection points in the two-phase region between P and Q. There is only one such inflection point in the "two-phase" region of the van der Waals equation. The presence of the extra inflection point means that still another criterion must be added to describe the critical point: The two inflection points must also merge with each other as well as with the maximum and the minima.

Before turning to the actual implementation of this strategy for characterizing the critical point, it seems worthwhile to summarize the procedure, since

the necessary steps have been described for an analogous problem above, and not for the specific problem of interest. In summary, we can state the following:

1. Figure 8.2b is a schematic representation of ΔG_m versus x_2 for a system which shows a miscibility gap. Any attempt to prepare a mixture between P and Q in composition will result in separation into the two phases P and Q at equilibrium.
2. There exists a critical temperature for this behavior above which Fig. 8.2b changes over to Fig. 8.2a, which describes miscibility in all proportions.
3. The mathematical behavior of the critical point is characterized by the two minima, the maximum, and the two inflection points all merging into a common point so that the entire function displays the smooth features seen *outside* the PQ region.
4. In Fig. 8.2b the minima and the maximum are described by $(\partial \Delta G_m/\partial x_2)_T = 0$ and the inflection points by $(\partial^2 \Delta G_m/\partial x_2^2)_T = 0$. If the second derivative describes the inflection point, the third derivative describes the *displacement* of the inflection point. Hence at the point where the two inflection points merge, $(\partial^3 \Delta G_m/\partial x^3)_T = 0$.

Since the Flory-Huggins theory provides us with an analytical expression for ΔG_m in Eq. (8.44), it is not difficult to carry out the differentiations indicated above to consider the critical point for miscibility in terms of the Flory-Huggins model. While not difficult, the mathematical manipulations do take up too much space to include them in detail. Accordingly, we indicate only some intermediate points in the derivation. We begin by recalling that $(\partial \Delta G_m/\partial n_i)_{p,T} = \Delta \mu_i$, so by differentiating Eq. (8.44) with respect to either N_1 or N_2, we obtain

$$\mu_1 - \mu_1^\circ = RT\left[\ln(1 - \phi_2) + \phi_2\left(1 - \frac{1}{n}\right) + \chi\phi_2^2\right] \tag{8.53}$$

and

$$\mu_2 - \mu_2^\circ = RT\left[\ln \phi_2 + (1 - \phi_2)(1 - n) + \chi n (1 - \phi_2)^2\right] \tag{8.54}$$

These differentiations are easily accomplished by noting that $N_1 = V\phi_1$ and recalling that $\phi_2 = nN_2/(N_1 + nN_2)$. Of course, n, χ, and RT are constant in the differentiation.

Since $\Delta \mu_1$ and $\Delta \mu_2$ are both obtained from differentiating the same expression for ΔG_m, it makes no difference which of these we work with further. In addition, it makes no difference whether we differentiate with respect to x_2 or x_1, since $dx_1 = -dx_2$ and we are setting the results equal to zero. Furthermore, since higher derivatives will be set equal to zero, we can differentiate with respect to volume fraction instead of mole fraction. This is because $\partial/\partial x =$

$(\partial\phi/\partial x)(\partial/\partial\phi)$ and the factor arising from the $\partial\phi/\partial x$ operation will cancel when the result is set equal to zero. With these considerations in mind, the criterion for the critical point can be written as

$$\frac{\partial^2 \Delta G_m}{\partial x_2^{\,2}} = 0 = \frac{\partial \Delta\mu_1}{\partial\phi_2} = -\frac{1}{1-\phi_{2,c}} + 1 - \frac{1}{n} + 2\chi_c\phi_{2,c} \tag{8.55}$$

and

$$\frac{\partial^3 \Delta G_m}{\partial x_2^{\,3}} = 0 = \frac{\partial^2 \Delta\mu_1}{\partial\phi_2^{\,2}} = -\frac{1}{(1-\phi_{2,c})^2} + 2\chi_c \tag{8.56}$$

In these expressions χ_c is the critical (subscript c) value of χ which marks the threshold at which immiscibility sets in, and $1 - \phi_{2,c}$ or $\phi_{1,c}$ is the volume fraction of the solvent in the solution at this point. Rearranging Eq. (8.56), we obtain

$$\chi_c = \frac{1}{2\phi_{1,c}^{\,2}} \tag{8.57}$$

which, on substitution back into Eq. (8.55), gives

$$-\frac{1}{\phi_{1,c}} + 1 - \frac{1}{n} + \frac{1-\phi_{1,c}}{\phi_{1,c}^{\,2}} = 0 \tag{8.58}$$

Solving Eq. (8.58) for $\phi_{1,c}$ yields

$$\phi_{1,c} = \frac{1}{1+n^{-1/2}} \tag{8.59}$$

which shows that the critical solution is almost pure solvent for polymers of very large n. Combining Eqs. (8.57) and (8.59) gives

$$\chi_c = \tfrac{1}{2}(1+n^{-1/2})^2 \tag{8.60}$$

For a polymer of infinite chain length, $\chi_c = 0.500$, and for n values of 10^4, 10^3, and 10^2 respectively, χ_c equals 0.510, 0.532, and 0.605.

Experimental results describing limited mutual solubility are usually presented as phase diagrams in which the compositions of the phases in equilibrium with each other at a given temperature are mapped for various temperatures. As noted above, the chemical potentials are the same in the equilibrium phases, so Eqs. (8.53) and (8.54) offer a method for calculating such

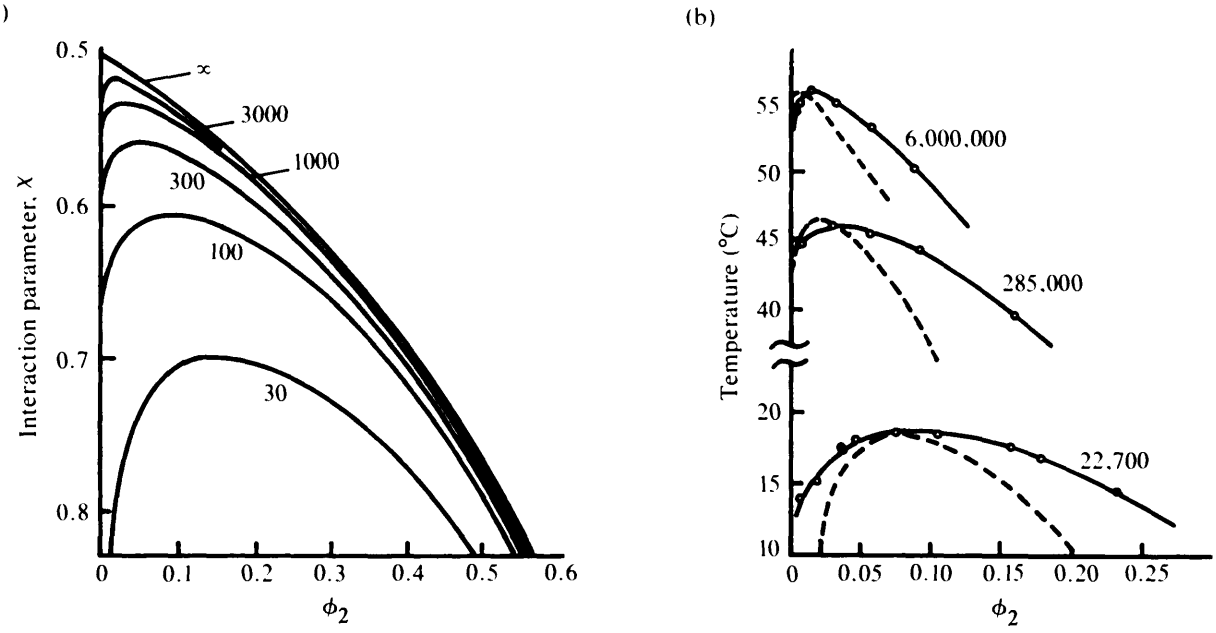

Figure 8.3 Volume fraction polymer in equilibrium phases for chains of different length. (a) Theoretical curves drawn for the indicated value of n, with the interaction parameter as the ordinate. Note that χ increases downward. (Redrawn from Ref. 6.) (b) Experimental curves for the molecular weights indicated, with temperature as the ordinate. [Reprinted with permission from A. R. Shultz and P. J. Flory, *J. Am. Chem. Soc.* 74:4760 (1952), copyright 1952 by the American Chemical Society.]

a phase diagram. The procedure is somewhat involved, so we dispense with the details and merely show the results of such calculations. Figure 8.3a shows the fraction of polymer in the equilibrium phases plotted against χ for polymers with the indicated values of n. Increasing values of χ are toward the bottom of Fig. 8.3a, so the curves have the same shape as would be obtained if temperature were the ordinate. Several features of these theoretical phase diagrams are noteworthy:

1. The miscibility gap becomes progressively more lopsided as n increases. This means that $\phi_{2,c}$ occurs at lower concentrations and that the tie line coordinates—particularly for the more dilute phase—are lower for large n.
2. For the case of $n \to \infty$, the limiting values of $\phi_{2,c}$ and χ_c are shown to be 0 and 0.5, as required by Eqs. (8.59) and (8.60), respectively.
3. Increasing positive values of χ—moving downward in Fig. 8.3—correspond to more endothermic values of ΔH_m. Interpreting the latter in terms of Eq. (8.49) means that systems for which $\delta_2 - \delta_1$ is large might show a miscibility gap for a given n, while complete miscibility is obtained for the same polymer in a solvent for which $\delta_2 - \delta_1$ is smaller. Decreasing the solvent "goodness" by the addition of a less suitable solvent may induce phase separation, at least for those molecules of large n.
4. If the poorer solvent is added incrementally to a system which is polydisperse with respect to molecular weight, the phase separation affects molecules of larger n, while shorter chains are more uniformly distributed. These ideas constitute the basis for one method of polymer fractionation. We shall develop this topic in more detail in the next section.

The curves shown in Fig. 8.3a are theoretical phase diagrams based on the Flory-Huggins model. Comparing theoretical predictions with experimental data thus provides our first opportunity to test the model. Figure 8.3b shows phase diagrams for polyisobutylene samples with the molecular weights indicated in diisobutyl ketone. Temperature variation is used to change the solvent "goodness." The broken lines in Fig. 8.3b are theoretical. We observe that the theory is qualitatively accurate, but that there is considerable discrepancy in quantitative detail. In particular, the experimental curves are considerably broader than predicted by theory. Generally speaking, the theory is more successful in accounting for χ_c than for $\phi_{2,c}$. It should be noted, however, that critical phenomena are extremely sensitive to small variations in a model—remember that at a critical point it only takes an infinitesimal variation to push the system into different regions of phase behavior—so Fig. 8.3b is not the best way to test the Flory-Huggins theory.

A far more satisfactory test of the Flory-Huggins theory is based on the chemical potential. According to Eqs. (8.13) and (8.20),

$$\mu_1 - \mu_1^{\theta} = RT \ln\left(\frac{p_1}{p_1^{\circ}}\right) \tag{8.61}$$

in which the vapor pressures are measurable quantities. According to the Flory-Huggins theory $\mu_1 - \mu_1^{\circ}$ is given by Eq. (8.53). Combining these two results gives

$$RT \ln\left(\frac{p_1}{p_1^{\circ}}\right) = RT\left[\ln \phi_1 + \left(1 - \frac{1}{n}\right)\phi_2 + \chi\phi_2^2\right] \tag{8.62}$$

which suggests that a plot of $\ln (p_1/p_1^{\circ}) - \ln \phi_1 - (1 - 1/n)\phi_2$ versus ϕ_2^2 should give a straight line of slope χ. Figure 8.4 is such a plot for several different polymer-solvent systems. In view of the complexity of the phenomena

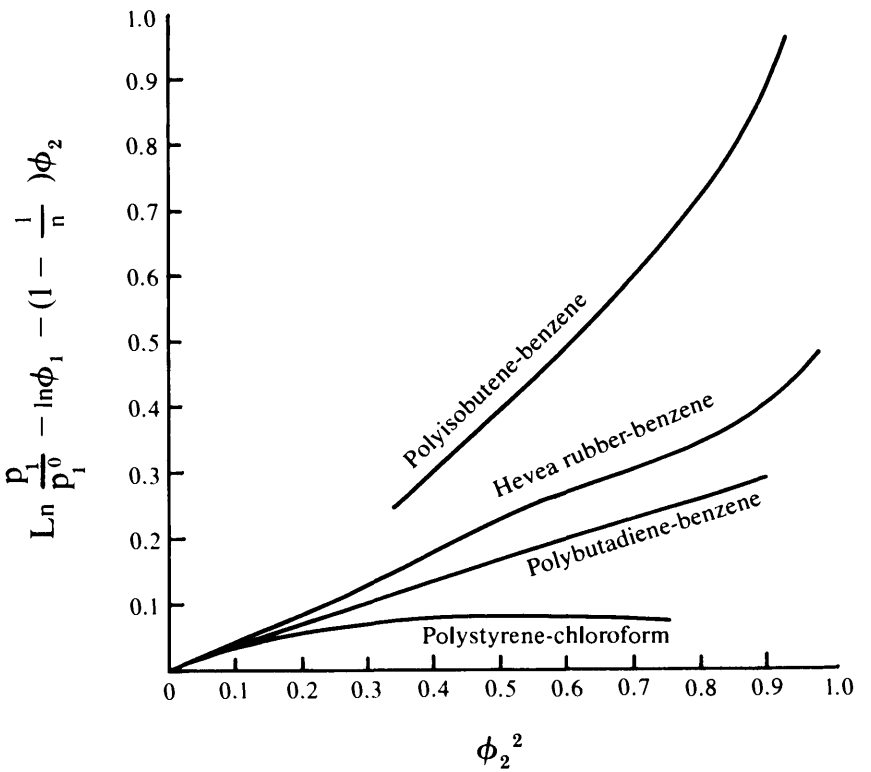

Figure 8.4 Experimental test of Flory-Huggins theory by Eq. (8.62) for the systems indicated. (From Ref. 3, used with permission.)

involved, the ability of the theoretical function to describe experimental results is remarkably good. It is interesting to note that the system for which the poorest agreement is observed—polystyrene in chloroform—is one in which it is easy to rationalize an acid-base-type of interaction between the hydrogen in $CHCl_3$ and the electrons in the phenyl groups. A chemical type interaction such as this is expected to show more complicated concentration effects than the Flory-Huggins model predicts. In the discussion of osmotic pressure in Sec. 8.8 we shall see that the latter experiment can also be used to measure $\Delta\mu_1$ and thereby test the Flory-Huggins theory.

8.7 Polymer Fractionation

Except for the living polymers described in Sec. 6.10, a high degree of polydispersity is expected in synthetic polymers. In most scientific research a narrow distribution of chain lengths must be present in the samples used to test theories. Similar though generally less stringent requirements also apply in applications technology. In both situations fractionation of the polymer sample into cuts of narrower molecular weight distribution is indicated. A variety of techniques exist for doing this, and the method of choice depends in part on the motive for doing the fractionation in the first place. If the objective of a fractionation experiment is the analysis of a molecular weight distribution, then it is not necessary to obtain large quantities of the separated product. For this type of application gel permeation chromatography has become the standard approach. We shall discuss this analytical method in Chap. 9.

For preparative purposes batch fractionation is often employed. Although fractional crystallization may be included in a list of batch fractionation methods, we shall consider only those methods based on the phase separation of polymer solutions: fractional precipitation and coacervate extraction. The general principles for these methods were presented in the last section. In this section we shall develop these ideas more fully with the objective of obtaining a more narrow distribution of molecular weights from a polydisperse system. Note that the final product of fractionation still contains a distribution of chain lengths; however, the ratio $\bar{M}_w/\bar{M}_n$ is smaller than for the unfractionated sample.

Figure 8.3b shows that phase separation in polymer mixtures results in two solution phases which are both dilute with respect to solute. Even the relatively more concentrated phase is only 10–20% by volume in polymer, while the more dilute phase is nearly pure solvent. The important thing to remember from both the theoretical and experimental curves of Fig. 8.3 is that both of the phases which separate contain some polymer. If it is the polymer-rich or precipitated phase that is subjected to further work-up, the method is called fractional precipitation. If the polymer-poor phase is the focus of attention, the method

is called coacervate extraction, since coacervation is the general term for this sort of phase separation.

The general procedure consists of first dissolving the polymer in a good solvent and then incrementally decreasing the solvent goodness by either lowering the temperature or adding a poor solvent as a precipitant. The high molecular weight polymers in a distribution are most affected by this reduction in solvent goodness; therefore it is this portion of the polymer that is most unevenly distributed between the two phases. We can use the Flory-Huggins theory to estimate the magnitude of this effect.

We shall identify the equilibrium phases by the labels P and Q in keeping with the notation established in Fig. 8.2b. The criterion for equilibrium is that for any n-mer, $\mu_{2,n}^{P} = \mu_{2,n}^{Q}$; using Eq. (8.54), we write

$$\ln \phi_{n,P} + \phi_{1,P}(1 - n) + n\chi\phi_{1,P}^2 = \ln \phi_{n,Q} + \phi_{1,Q}(1 - n) + n\chi\phi_{1,Q}^2 \tag{8.63}$$

Rearranging, we obtain

$$\ln \frac{\phi_{n,P}}{\phi_{n,Q}} = n\left[\left(\frac{1}{n} - 1\right)(\phi_{1,Q} - \phi_{1,P}) + \chi(\phi_{1,Q}^2 - \phi_{1,P}^2)\right] = nA \tag{8.64}$$

where the quantity inside the brackets is represented by A. If the (small) term $1/n$ inside the bracketed factor is treated as $1/\bar{n}$ for a polydisperse system and is independent of n, then A is constant. Strictly speaking, $\bar{n}_P \neq \bar{n}_Q$, and the first term in the brackets should not be factored as shown in Eq. (8.64), but this complication does not alter the essential conclusion that the bracketed term is constant. Therefore Eq. (8.64) can be written as

$$\frac{\phi_{n,P}}{\phi_{n,Q}} = e^{An} \tag{8.65}$$

which shows that the greater n becomes, the greater is the dissimilarity in the concentration of n-mer in the two equilibrium phases. This qualitative conclusion is certainly correct and independent of any model used to derive it.

Next we consider the fraction of n-mer in a specific phase. The volume of n-mer in each of the phases is given by $\phi_{n,P}V_P$ and $\phi_{n,Q}V_Q$; therefore the fraction of polymer in the two phases is

$$f_{n,P} = \frac{\phi_{n,P}V_P}{\phi_{n,P}V_P + \phi_{n,Q}V_Q} = \frac{V_P e^{An}}{V_P e^{An} + V_Q} = \frac{Re^{An}}{1 + Re^{An}} \tag{8.66}$$

and

$$f_{n,Q} = \frac{\phi_{n,Q}V_Q}{\phi_{n,P}V_p + \phi_{n,Q}V_Q} = \frac{V_Q}{V_P e^{An} + V_Q} = \frac{1}{1 + Re^{An}} \tag{8.67}$$

where Eq. (8.65) was used to eliminate $\phi_{n,P}/\phi_{n,Q}$ and $R = V_P/V_Q$. Now consider the case for which n is large and R is small. In this situation Re^{An} is large and $f_{n,P} > f_{n,Q}$. This indicates that the concentration of n-mer in phase P, for large values of n, will be maximized if the volume of the P phase is kept to a minimum compared to phase Q. Stated simply, the longer chains are concentrated in one of the phases, while the shorter chains are relatively unaffected by the phase separation and distribute themselves evenly and in proportion to the volume of the phases. As a practical matter, then, keeping the volume of the dilute phase as large as possible allows the optimum partitioning of the largest molecules into the smaller but more discriminating concentrated phase.

The relative amounts of various n-mers in a fractionated sample is examined numerically in the following example.

Example 8.4

Evaluate A in Eq. (8.64), assuming the polymer with n = 200 is divided equally between the two phases and taking the ratio of phase volumes R to be 10^{-1}, 10^{-2}, and 10^{-3}. Use these A values to evaluate the relative amounts of n-mer in the two phases for polymers with n = 100, 400, 600, and 800. Comment on the significance of the numerical results.

Solution

The ratio of Eq. (8.66) to Eq. (8.67) gives the ratio of the concentrations of n-mers in phases P and Q: $f_{n,P}/f_{n,Q} = Re^{An}$. Taking this ratio to be unity for n = 200 gives $Re^{A(200)} = 1$, which is readily solved for A using the R values given. Once these A values are obtained, $f_{n,P}/f_{n,Q}$ can be evaluated for the required n values. For the phase volume ratios under consideration, the corresponding values of A are listed below; also tabulated are the ratios $f_{n,P}/f_{n,Q}$ for the various n's:

	$R = V_P/V_Q$:	10^{-1}	10^{-2}	10^{-3}
	$A_{n=200}$:	1.15×10^{-2}	2.30×10^{-2}	3.45×10^{-2}
$\frac{f_{n,P}}{f_{n,Q}}$ for n =	100	0.32	0.099	0.032
	400	9.95	99.0	985
	600	99.9	9850	9.77×10^5
	800	990	9.80×10^5	9.69×10^8

Note that phase P is more concentrated in polymer, although smaller in volume than phase Q. It is apparent from these values that the combination of large n's

and large differences in the volumes of the separated phases gives rise to the most efficient segregation of polymer between phases. Also note that the requirement that 200-mers be evenly distributed between the phases creates the situation in which 100-mers are present in higher proportion in the more dilute phase.

•

Figure 8.5 illustrates the sort of separation this approach predicts. Curve A in Fig. 8.5 shows the weight fraction of various n-mers plotted as a function of n. Comparison with Fig. 6.7 shows that the distribution is typical of those obtained in random polymerization. Curve B shows the distribution of molecular weights in the more dilute phase—the coacervate extract—calculated for the volumes of the two phases in the proportion 100:1. The distribution in the concentrated phase is shown as curve C; it is given by the difference between curves A and B.

In practice, such a fractionation experiment could be carried out by either lowering the temperature or adding a poor solvent. In either case good temperature control during the experiment is important. Note that the addition of a poor solvent converts the system to one containing three components, so it is apparent that the two-component Flory-Huggins model is at best only qualitatively descriptive of the situation. A more accurate description would require a

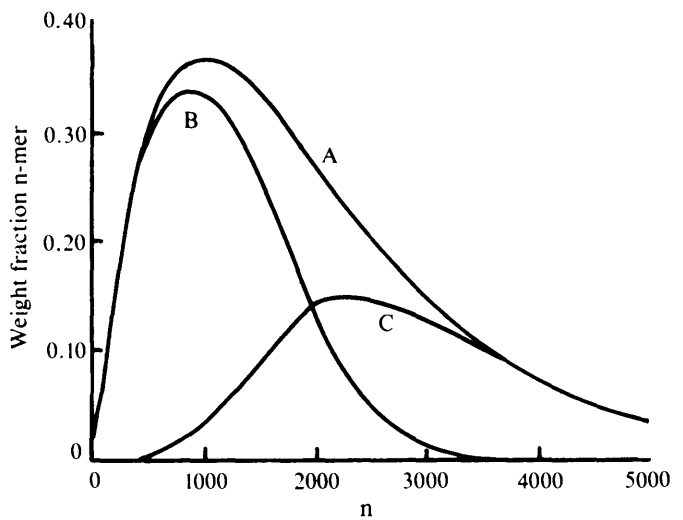

Figure 8.5 Theoretical plots of weight fraction n-mers versus n for unfractionated polymer (A), the dilute phase (B), and the concentrated phase (C) (drawn with $R = 10^{-2}$). (Adapted from Ref. 1.)

triangular phase diagram. The onset of precipitation is marked by the appearance of turbidity. In keeping with the principle outlined above, only a small volume of the precipitated phase is allowed to form. Then the sample is allowed to stand undisturbed until the two phases can be physically separated. This step can require quite a long wait.

This procedure is then repeated by decreasing the solvent goodness even further by another decrease in temperature or addition of precipitant. In this manner a set of fractions such as those shown in Fig. 8.6 are obtained from the initial distribution. In Fig. 8.6 curve A again represents the initial distribution. Eight fractions are obtained by precipitating successive portions of the polymer of progressively lower molecular weights as shown, until the dilute phase contains only the lowest molecular weight fraction as a residue. The curves in Fig. 8.6 are calculated for a phase volume ratio of 1000:1.

Figure 8.6 shows that the individual fractions still contain a considerable range of chain lengths, with this effect becoming less pronounced in the later cuts. In addition, there is a definite overlap among the fractions. Nevertheless, the approach results in a sharpening of the distribution of molecular weights in a sample. The method is time-consuming and involves large quantities of solvent, which must be subsequently removed to obtain pure polymer.

With these remarks, we conclude our discussion of phase separation. In the remainder of the chapter we consider another thermodynamic property of

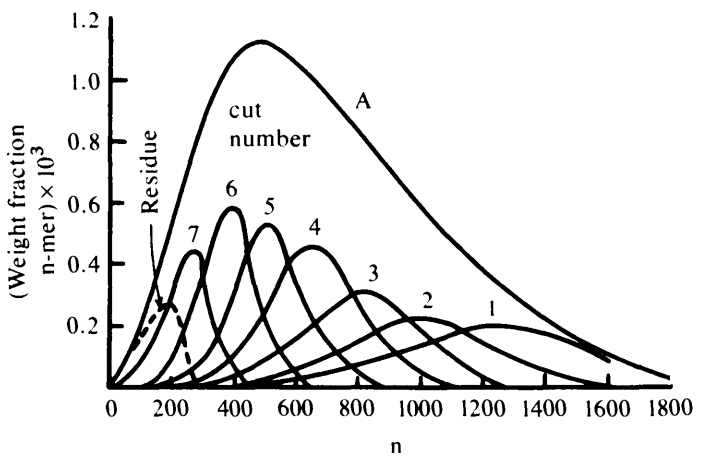

Figure 8.6 Effect of successive fractionations: weight fraction n-mer versus n for seven successive precipitates and final residue (calculated for $R = 10^{-3}$). [Adapted from G. V. Schulz, *Z. Phys. Chem.* B46:137 (1940); B47:155 (1940).]

polymer solutions, namely the osmotic pressure. As in the previous sections, we shall combine pure thermodynamics as well as statistical models to understand osmostic pressure more fully and to maximize our ability to interpret experimental osmometry.

8.8 Osmotic Pressure

Osmotic pressure is one of four closely related properties of solutions that are collectively known as colligative properties. In all four, a difference in the behavior of the solution and the pure solvent is related to the thermodynamic activity of the solvent in the solution. In ideal solutions the activity equals the mole fraction, and the mole fractions of the solvent (subscript 1) and the solute (subscript 2) add up to unity in two-component systems. Therefore the colligative properties can easily be related to the mole fraction of the solute in an ideal solution. The following review of the other three colligative properties indicates the similarity which underlies the analysis of all the colligative properties:

1. Vapor pressure lowering. Equation (8.20) shows that for any component in a binary liquid solution $a_i = p_i/p_i^\circ$. For an ideal solution, this becomes

$$p_1 = x_1 p_1^\circ = (1 - x_2) p_1^\circ \tag{8.68}$$

or

$$p_1^\circ - p_1 = \Delta p = x_2 p_1^\circ \tag{8.69}$$

This is an expression of Raoult's law which we have used previously.

2. Freezing point depression. A solute which does not form solid solutions with the solvent and is therefore excluded from the solid phase lowers the freezing point of the solvent. It is the chemical potential of the solvent which is lowered by the solute, so the pure solvent reaches the same (lower) value at a lower temperature. At equilibrium

$$\ln a_1 = -\frac{\Delta H_f^\circ}{R}\left(\frac{1}{T_f} - \frac{1}{T_f^\circ}\right) \tag{8.70}$$

where ΔH_f° is the heat of fusion of the solvent, T_f is the freezing point of the solution, and T_f° is the freezing point of the pure solvent. For an ideal solution the following relationships apply:

$$\ln a_1 = \ln x_1 = \ln (1 - x_2) \cong -x_2 \tag{8.71}$$

where the last approximation requires dilute conditions as well.

3. Boiling point elevation. A solute which does not enter the vapor phase to any significant extent raises the boiling point of the solvent. As above, the solute lowers the activity of the solvent, which, in turn, lowers the vapor pressure. Therefore the solution must be raised to a higher temperature before its vapor pressure reaches 1.0 atm. At equilibrium

$$\ln a_1 = \frac{\Delta H_v^\circ}{R}\left(\frac{1}{T_b} - \frac{1}{T_b^\circ}\right) \tag{8.72}$$

where ΔH_v° is the heat of vaporization of the solvent, T_b is the boiling point of the solution, and T_b° is the boiling point of the pure solvent. For ideal or ideal and dilute solutions, the approximations of Eq. (8.71) can be applied here as well.

For each of these phenomena in the limit of dilute solutions, some difference in the behavior of the solvent—Δp_1, ΔT_f, or ΔT_b—is proportional to the mole fraction of the solute. Since the solutions are already assumed to be dilute, we note that

$$x_2 = \frac{n_2}{n_1 + n_2} \cong \frac{n_2}{n_1} \tag{8.73}$$

under these conditions. The number of moles of solvent in a solution is generally known from its mass and molecular weight. Therefore measuring the colligative properties Δp_1, ΔT_f, and ΔT_b and using the dilute, ideal solution approximation provides a means for evaluating n_2, the number of moles of solute in the sample. If the solute is unknown with respect to molecular weight but its mass in the solution is known, then the colligative properties can be used to determine the molecular weight of the solute: $M_2 = m_2/n_2$.

One way to describe this situation is to say that the colligative properties provide a method for counting the number of solute molecules in a solution. In these ideal solutions this is done without regard to the chemical identity of the species. Therefore if the solute consists of several different components which we index i, then $n_2 = \Sigma_i n_{2,i}$ is the number of moles counted. Of course, the total mass of solute in this case is given by $m_2 = \Sigma_i n_{2,i} M_{2,i}$, so the molecular weight obtained for such a mixture is given by

$$\bar{M}_2 = \frac{\Sigma_i n_i M_i}{\Sigma_i n_i} \tag{8.74}$$

which is the definition of the number average molecular weight [Eq. (1.3)]. Measurements of the colligative properties are often used to evaluate the molecular weight of an unknown solute. The foregoing remarks show that the

molecular weight thus obtained is subject to whatever approximation arises from the assumption of ideality and is an average value over all species present. For something like NaCl in water, for example, $\bar{M} \cong 58/2 = 29$, since two moles of ions are counted for every mole of solute weighed into solution.

As noted above, all of the colligative properties are very similar in their thermodynamics if not their experimental behavior. This similarity also extends to an application like molecular weight determination and the kind of average obtained for nonhomogeneous samples. All of these statements are also true of osmotic pressure. In the remainder of this section we describe osmotic pressure experiments in general and examine the thermodynamic origin of this behavior.

In an osmotic pressure experiment two phases are brought to isothermal equilibrium: a solution and a pure solvent. Note that this statement also applies to the freezing and boiling equilibria described above. In an osmotic experiment the partitioning of the two phases is accomplished by means of a semipermeable membrane which, by definition, allows the solvent to pass but not the solute. Figure 8.7 is a schematic representation of this state of affairs. In order for the solvent to be in equilibrium on both sides of the membrane, the solution must be under a greater pressure than the pure solvent and it is this pressure difference that is designated as the osmotic pressure Π. If the solvent and solution are brought together at the same pressure in a suitable apparatus, an osmometer, then a hydrostatic pressure will develop on the solution side by the solvent diffusing through the membrane until the equilibrium criterion is satisfied.

Thermodynamics provide a straightforward method for quantifying this situation. The criterion for equilibrium is the equality of chemical potential in

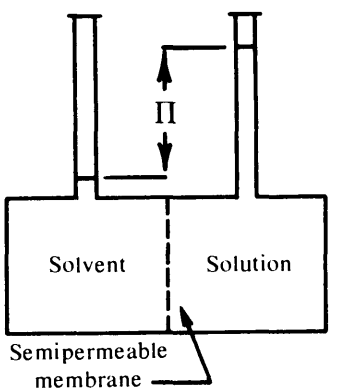

Figure 8.7 Schematic representation of an osmotic pressure experiment.

the equilibrium phases. Since one of the phases is pure solvent, the standard state, this means

$$\mu_1^\circ = \mu_1^{soln} = \mu_1^\circ + (\text{concentration effect}) + (\text{pressure effect}) \tag{8.75}$$

At equilibrium, these concentration and pressure effects must be equal and opposite for Eq. (8.75) to apply. Equation (8.13) describes the concentration dependence of μ_1, and Eq. (8.12) describes the pressure effect. Assembling these results, we write

$$\mu_1^\circ = \mu_1^\circ + RT \ln a_1 + \int_p^{p+\Pi} \bar{V}_1 \, dp \tag{8.76}$$

Remember that $\bar{V}_1$ is the partial molar volume of the solvent. Therefore a completely general relationship between Π and the solvent activity is given by

$$RT \ln a_1 = - \int_p^{p+\Pi} \bar{V}_1 \, dp \tag{8.77}$$

Next we seek a method for evaluating this integral. Since condensed phases show little volume change with changing pressure, $\bar{V}_1$ can be regarded as a constant and taken out of the integral. Then Eq. (8.77) is readily integrated to give

$$\ln a_1 = - \frac{\Pi \bar{V}_1}{RT} \tag{8.78}$$

Combining this result with Eq. (8.13) gives

$$\mu_1 = \mu_1^\circ - \Pi \bar{V}_1 \tag{8.79}$$

which could be used as the basis for testing the Flory-Huggins expression for μ_1.

Precisely the same substitutions and approximations that we wrote in Eq. (8.71) can be applied again to $\ln a_1$. Thus for the case of dilute, ideal solutions, Eq. (8.78) becomes

$$- \ln a_1 \cong x_2 \cong \frac{n_2}{n_1} = \frac{\Pi \bar{V}_1}{RT} \tag{8.80}$$

or

$$\Pi (n_1 \bar{V}_1) \cong \Pi V_1 \cong \Pi V = n_2 RT \tag{8.81}$$

where we use $\bar{V}_1 \cong V_1^\circ$ and $V_1 \cong V$ for dilute solutions. This solution-analog of the ideal gas law is called the van't Hoff equation and, like its counterpart, is a limiting law which applies perfectly in the limits of $\Pi \to 0$ or $n_2/V \to 0$. This relationship shows how the measurement of Π for solutions which are quantitatively characterized with respect to other pertinent factors can be used to measure n_2 and M_2. As with the other colligative properties, this latter value is a number average for nonhomogeneous samples. In the next section we shall examine osmometry as a method for molecular weight determination in more detail.

The approximations involved in going from Eq. (8.78) to Eq. (8.81) can be divided into three categories:

1. Those involving volume approximations. We replace $n_1\bar{V}_1$ by V_1 and identify the latter as the total volume of the solution. For dilute solutions these do not introduce serious errors and do simplify the notation somewhat.
2. Those involving series truncation. The quantity $\ln(1 - x_2)$ can be represented by the infinite series $-[x_2 + (1/2)x^2 + (1/3)x^3 + \cdots]$. Truncating this series after the first term is a valid approximation for dilute solutions and also simplifies the form of the equation. It is an optional step, however, and can be avoided or mitigated by simply retaining more terms in the series.
3. Those involving solution nonideality. This is the most serious approximation in polymer applications. As we have already seen, the large differences in molecular volume between polymeric solutes and low molecular weight solvents is a source of nonideality even for athermal mixtures.

In thermodynamics the formal way of dealing with nonideality is to introduce an activity coefficient γ into the relationship between activity and mole fraction:

$$a_i = \gamma_i x_i \tag{8.82}$$

such that γ_i is an empirical parameter which describes the nonideality. In view of the approximation mentioned in item (2) above, we introduce coefficients to deal with nonideality in the form

$$\frac{\Pi\bar{V}_1}{RT} = -\ln a_1 = x_2 + \frac{1}{2}B'x_2^2 + \frac{1}{3}C'x_2^3 + \cdots \tag{8.83}$$

where B' and C' are called the second and third virial coefficients. The first virial coefficient is unity, since the van't Hoff equation must be obtained in the limit $x_2 \to 0$.

In the next section we shall describe the use of Eq. (8.83) to determine the number average molecular weight of a polymer, and in subsequent sections we shall examine models which offer interpretations of the second virial coefficient.

Before doing this, however, it is informative to compare the sensitivity of the four colligative properties in the determination of molecular weight. In the following example this is done by making the appropriate numerical calculations.

Example 8.5

Calculate Δp_1, ΔT_f, ΔT_b, and Π for solutions which are 1% by weight in benzene of solutes for which $M = 10^2$ and 10^5. Assume that these solutions are adequately described by dilute ideal solution expressions. Consult a handbook for the physical properties of benzene. Comment on the significance of the results with respect to the feasibility of these various methods for the determination of M for solutes of high and low molecular weight.

Solution

We use the approximation $-\ln a_1 \cong x_2 \cong n_2/n_1$ as the basis for all of these calculations. Since a 1% solution contains 1.0 g solute per 99 g solvent,

$$\frac{n_2}{n_1} = \frac{1 \text{ g solute} \times (1 \text{ mol solute})/(M_2 \text{ g})}{99 \text{ g solvent} \times (1 \text{ mol benzene})/(78 \text{ g})} = \frac{0.788}{M_2}$$

This becomes 7.88×10^{-3} for $M_2 = 10^2$ and 7.88×10^{-6} for $M_2 = 10^5$. By Eq. (8.68), $p_1 = (n_2/n_1)\, p_1^\circ$. For benzene at 25°C, $p_1^\circ = 95.9$ Torr; therefore

$$\Delta p_1 = 95.9 \left(\frac{n_2}{n_1}\right) \text{ Torr}$$

By Eqs. (8.70) and (8.71), $-x_2 = -(\Delta H_f^\circ/R)(1/T_f - 1/T_f^\circ)$; therefore $T_f^\circ - T_f \cong (n_2/n_1)(RT_f^{\circ 2}/\Delta H_f^\circ)$.

For benzene $\Delta H_f^\circ = 10.6$ kJ mol^{-1} and $T_f^\circ = 5.5$°C = 278.7 K; hence

$$T_f^\circ - T_f = \left(\frac{n_2}{n_1}\right) (60.9) \text{ K}$$

By Eqs. (8.71) and (8.72), $-x_2 = (\Delta H_v^\circ/R)(1/T_b - 1/T_b^\circ)$; therefore $T_b^\circ - T_b \cong (n_2/n_1)(RT_b^{\circ 2}/\Delta H_v^\circ)$.

For benezene $\Delta H_v^\circ = 30.8$ kJ mol^{-1} and $T_b^\circ = 80.1$°C = 353.3 K; hence

$$T_b^\circ - T_b = -33.7 \left(\frac{n_2}{n_1}\right) \text{ K}$$

By Eq. (8.80), $\Pi = (n_2 RT/n_1 \bar{V}_1) \cong (n_2/n_1)(RT/V_1^\circ)$. For benzene $\rho = 0.879$ g cm^{-3} and $V_1^\circ = 88.7$ cm^3 mol^{-1} at 25°C; hence

$$\Pi = \frac{(82.1 \text{ cm}^3 \text{ atm mol}^{-1} \text{ K}^{-1})(298 \text{ K})}{88.7 \text{ cm}^3 \text{ mol}^{-1}} \frac{n_2}{n_1} = 276 \left(\frac{n_2}{n_1} \right) \text{ atm}$$

	$M_2 = 10^2$	$M_2 = 10^5$
n_2/n_1	7.88×10^{-3}	7.88×10^{-6}
Δp_1 at 25°C (Torr)	0.756	7.56×10^{-4}
$T_f^\circ - T_f$ (K)	0.480	4.80×10^{-4}
$T_b - T_b^\circ$ (K)	0.266	2.66×10^{-4}
Π (atm)	2.17	2.17×10^{-3}
Π (Torr)	1.65×10^3	1.65
Π (mm soln)	2.52×10^4	25.2

In these unit conversions on Π, we have used the facts that 1 atm = 760 Torr and the ratio of densities $\rho_{Hg}/\rho_{soln} = 13.5/\rho_{soln}$ converts from Torr to millimeters of solution. These numerical examples show that experiments in which Δp_1, ΔT_f, or ΔT_b are measured are perfectly feasible for solutes of molecular weight 100, but call for unattainable sensitivity for polymeric solutes of M = 10^5. By contrast, osmometry produces so much larger an effect that this method is awkward (at least for 1% concentration) for a low molecular weight solute, but is entirely feasible with the polymer.

•

8.9 Molecular Weight by Osmometry

Our primary objective in this section is the discussion of practical osmometry, particularly with the goal of determining the molecular weight of a polymeric solute. We shall be concerned, therefore, with the design and operation of osmometers, with the question of units, and with circumventing the problem of nonideality. The key to these points is contained in the last section, but the details deserve additional comment.

First, we consider the experimental aspects of osmometry. The semipermeable membrane is the basis for an osmotic pressure experiment and is probably its most troublesome feature in practice. The membrane material must display the required selectivity in permeability—passing solvent and retaining solute—but a membrane that works for one system may not work for another. A wide variety of materials have been used as membranes, with cellophane, poly(vinyl alcohol), polyurethanes, and various animal membranes as typical examples. The membrane must be thin enough for the solvent to pass at a reasonable rate, yet sturdy enough to withstand the pressure difference which can be

considerable. Above all, the membrane must be free from imperfections which allow solute to leak across the barrier and thus invalidate the experiment.

Osmometers are designed to allow maximum contact of the two liquids with the membrane and to provide sufficient support for the fragile membrane at the same time. Since the experiments are conducted under isothermal conditions, good temperature control is also required. Finally, it must be possible to accurately determine the difference in liquid column heights, since this is the quantity which is actually measured. Both of the osmometers shown in Fig. 8.8 meet these requirements, although they are but two of many designs that have been employed. In the osmometer of Fig. 8.8a the inner compartment contains the solution, while the solvent is placed in the outer vessel. The membrane is clamped across the wide opening at the bottom of the solution chamber and the pressure is measured in the capillary neck of the latter. The entire apparatus can be submerged in a constant-temperature bath for equilibration. In the apparatus shown in Fig. 8.8b, the solvent and solution are placed in the grooves–shown in Fig. 8.8c–of opposing faces of the central block and the membrane is sandwiched between them. The assembly is sealed and placed in a thermostat. The osmotic pressure is measured by the difference in liquid levels in the vertical capillaries.

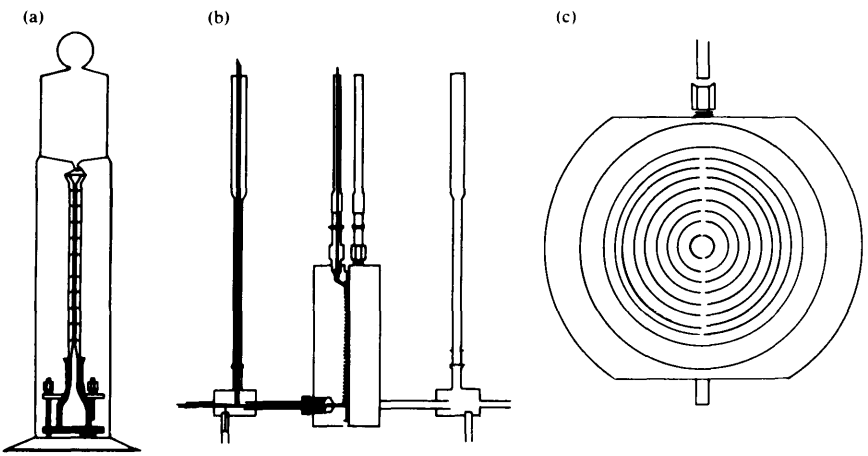

Figure 8.8 Two osmometer designs: (a) solution (inner chamber) separated from solvent by clamped membrane. [Reprinted with permission from D. M. French and R. H. Ewert, *Anal. Chem.* 19:165 (1947), copyright 1947 by the American Chemical Society.] (b) Solution and solvent in grooved faces shown in detail in (c). [Reprinted with permission from R. M. Fuoss and D. J. Mead, *J. Phys. Chem.* 47:59 (1943), copyright 1943 by the American Chemical Society.]

In both of these pieces of apparatus, isothermal operation and optimum membrane area are obtained. Good temperature control is essential not only to provide a value for T in the equations, but also because the capillary attached to a larger reservoir behaves like a thermometer, with the column height varying with temperature fluctuations. The contact area must be maximized to speed up an otherwise slow equilibration process. Various practical strategies for "presetting" the osmometer to an approximate Π value have been developed, and these also accelerate the equilibration process.

Since capillary tubing is involved in osmotic experiments, there are several points pertaining to this feature that should be noted. First, tubes that are carefully matched in diameter should be used so that no correction for surface tension effects need be considered. Next it should be appreciated that an equilibrium osmotic pressure can develop in a capillary tube with a minimum flow of solvent, and therefore the measured value of Π applies to the solution as prepared. The pressure, of course, is independent of the cross-sectional area of the liquid column, but if too much solvent transfer were involved, then the effects of dilution would also have to be considered. Now let us examine the practical units that are used to express the concentration of solutions in these experiments.

In molecular weight determinations it is conventional to dissolve a measured mass of polymer m_2 into a volumetric flask and dilute to the mark with an appropriate solvent. We shall use the symbol c_2 to designate concentrations in mass per volume units. In practice, 100-ml volumetric flasks are often used, in which case c_2 is expressed in grams per 100 ml or grams per deciliter. Even though these are not SI units, they are encountered often enough in the literature to be regarded as conventional solution units in polymer chemistry.

These mass per volume concentration units can be written as

$$c_2 = \frac{n_2 M}{n_1 \bar{V}_1 + n_2 \bar{V}_2} \tag{8.84}$$

where the $\bar{V}_i$'s are the partial molar volumes and may be expressed in whatever volumes unit is desired. We continue to use M (no subscript) for the (average) molecular weight of the polymer.

We are most often concerned with solutions which are dilute with respect to polymer. This means that $n_2 \bar{V}_2 \ll n_1 \bar{V}_1$ and that $n_2 \ll n_1$. Because the volume of the polymer molecule is so much greater than that of the solvent, the disparity in the number of moles is even more extreme than for the same approximation applied to compounds of comparably sized molecules. Since the approximation $x_2 = n_2/(n_1 + n_2) \cong n_2/n_1$ applies to dilute solutions, we can write

$$c_2 \cong \frac{n_2}{n_1} \frac{M}{\bar{V}_1} \cong x_2 \frac{M}{\bar{V}_1} \cong x_2 \frac{M}{V_1^\circ} \tag{8.85}$$

where the last relationship is justified because partial molar quantities approach molar quantities in the limit of the pure components.

Equation (8.85) can be solved for x_2 and the latter substituted into Eq. (8.83) to give an expression for Π which applies to dilute—but not necessarily ideal—solutions:

$$\Pi = RT\left(\frac{c_2}{M} + \frac{B'V_1^\circ}{2M^2}c_2^2 + \cdots\right) \tag{8.86}$$

Upon rearrangement, this becomes

$$\frac{\Pi}{RTc_2} = \frac{1}{M} + \frac{B'V_1^\circ}{2M^2}c_2 + \cdots = \frac{1}{M} + Bc_2 + \cdots \tag{8.87}$$

where the cluster of parameters $B'V_1^\circ/2M^2$ has been replaced by B, which is the second virial coefficient in these units. In writing Eq. (8.87), we have truncated the series in Eq. (8.83) after the second term. This restricts Eq. (8.87) to solutions which are sufficiently dilute that the term which is third order in c_2 is insignificant but at the same time does make allowance for the first manifestation of nonideality. The second virial coefficient embodies the latter.

What makes Eq. (8.87) especially important is that it is the equation of a straight line. It predicts that a plot of Π/RTc_2 versus c_2 will be linear for dilute solutions and that the slope and intercept of the plot will have the following significance:

$$\text{Intercept} = \left(\frac{\Pi}{RTc_2}\right)_0 = \frac{1}{M} \tag{8.88}$$

$$\text{Slope} = B \tag{8.89}$$

Figure 8.9 is a plot of osmotic pressure data for a nitrocellulose sample in three different solvents analyzed according to Eq. (8.87). As required by Eq. (8.88), all show a common intercept corresponding to a molecular weight of 1.11×10^5; the various systems show different deviations from ideality, however, as evidenced by the range of slopes in Fig. 8.9.

In the next sections we shall discuss the second virial coefficient in terms of several different models. Before turning to these models, however, it is important to summarize the foregoing conclusions:

1. The molecular weight analysis presented above is a purely thermodynamic result and is independent of any model. The procedure requires dilute solutions, but is not based on the assumption of ideality, even though Eq. (8.88) is a variation of the van't Hoff equation.

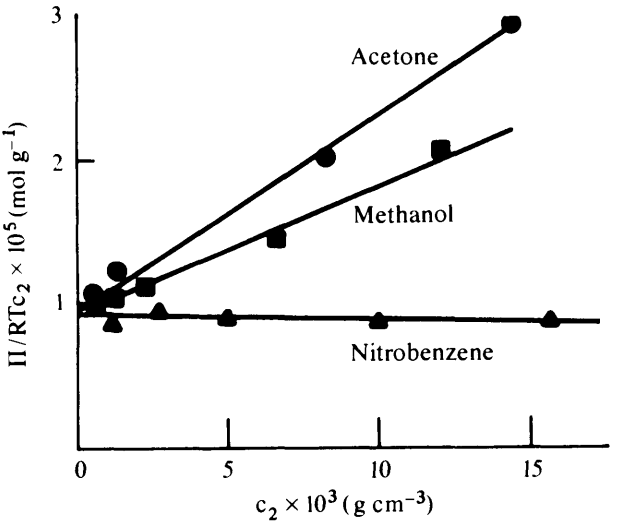

Figure 8.9 Osmotic pressure data plotted as Π/RTc_2 versus concentration for nitrocellulose in three different solvents. [Data from A. Dobry, *J. Chem. Phys.* 32:50 (1935).]

2. The solute molecular weight enters the van't Hoff equation as the factor of proportionality between the number of solute particles that the osmotic pressure counts and the mass of solute which is known from the preparation of the solution. The molecular weight that is obtained from measurements on polydisperse systems is a number average quantity.
3. Osmotic pressure experiments provide absolute values for $\bar{M}_n$: Neither a model nor independent calibration is required to use this method. Experimental errors can arise, of course, and we note particularly the effect of impurities. Polymers which dissociate into ions can also be confusing. We shall return to this topic in Sec. 8.13; for now we assume that the polymers under consideration are nonelectrolytes.
4. The ratio Π/c_2 is called the reduced osmotic pressure—and can be plotted with or without the RT—and the zero-intercept value (subscript 0) is the limiting value of the reduced osmotic pressure. Quite an assortment of different pressure units are used in the literature in reporting Π values, and the units of R in Eq. (8.88) must be reconciled with these pressure (as well as concentration) units.

The following example illustrates the sort of deciphering that is associated with the use of diverse units.

Example 8.6

The limiting reduced osmotic pressure for a sample of polystyrene in chlorobenzene at 25°C is reported† to be 257 cm. Account for these units for $(\Pi/c_2)_0$ and evaluate $\bar{M}_n$ for the polymer.

Solution

The authors of this research selected units which could be written with maximum simplification to report their results. We must replace the factors which have canceled out. Assuming that the cgs system of units was used throughout, we note that possible units for Π are grams per square centimeter and possible unts for c_2 are grams per cubic centimeter, which yield the required units for Π/c_2: Note that these units of Π must be multiplied by the gravitational constant to give Π in dynes per square centimeter:

$$257 \text{ cm} \times \frac{980 \text{ cm}}{\text{sec}^2} = 2.52 \times 10^5 \frac{\text{dyne cm}^{-2}}{\text{g cm}^{-3}} = 2.52 \times 10^5 \frac{\text{erg}}{\text{g}}$$

$\bar{M}_n$ may be evaluated from Eq. (8.88) by using $R = 8.314 \times 10^7$ erg K^{-1} mol^{-1}:

$$\bar{M}_n = \frac{RT}{(\Pi/c_2)_0} = \frac{(8.314 \times 10^7 \text{ erg K}^{-1} \text{ mol}^{-1})(298 \text{ K})}{2.52 \times 10^5 \text{ erg g}^{-1}}$$

$$= 9.84 \times 10^4 \text{ g mol}^{-1}$$

•

The matter of units also complicates the second virial coefficient, which we consider next.

8.10 Excluded Volume

Considering our approach to the topic, we might be tempted to believe that the second virial coefficient is small for a polymer, depending as it does in Eq. (8.87) on $\bar{M}^{-2}$. Experimental results such as those shown in Fig. 8.9, however, reveal that plots of Π/c_2 versus c_2 have slopes quite different from zero. In fact, any inquiry into the significance of the second virial coefficient must seek to explain both positive and negative slopes in such plots. The form of the virial expansion suggests that the molecular origin of the second virial coefficient is the pairwise interaction of solute particles—B' is the coefficient of the x_2^2 term in Eq. (8.83)—with the higher coefficients arising from the third- or higher-order

† J. Leonard and H. Daoust, *J. Phys. Chem.* 69:1174 (1965).

interactions. We shall restrict our discussion to the second virial coefficient: Things are complicated enough at this level of nonideality without looking for still more complex interactions!

It is convenient to begin by backtracking to a discussion of ΔS_m for an athermal mixture. We shall consider a *dilute* solution containing N_2 solute molecules, each of which has an excluded volume u. The excluded volume of a particle is that volume for which the center of mass of a second particle is excluded from entering. Although we assume no specific geometry for the molecules at this time, Fig. 8.10 shows how the excluded volume is defined for two spheres of radius a. The two spheres are in surface contact when their centers are separated by a distance 2a. The excluded volume for the pair has the volume $(4/3)\pi(2a)^3$, or eight times the volume of one sphere. This volume is indicated by the broken line in Fig. 8.10. Since this volume is associated with the interaction of two spheres, the excluded volume per sphere is

$$u_{sphere} = 4(\text{volume of sphere}) \tag{8.90}$$

Regardless of the particle geometry, the excluded volume exceeds the actual volume of the molecules by a factor which depends on the shape of the particles.

To arrive at an expression for ΔS_m, we follow a series of steps which parallel—for a different model—the development of the Flory-Huggins model for ΔS_m:

1. The number of ways of placing the first solute molecule ω_1 is proportional to the total volume of the solution V:

   $$\omega_1 = KV$$

   In this model we start with pure solvent so an undiminished value of V can be used for the first solute molecule.

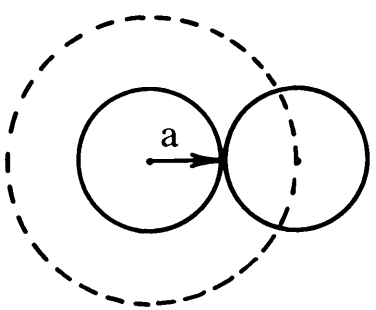

Figure 8.10 Excluded volume for two spheres (dotted surface) as determined by the distance of closest approach.

2. The number of ways of placing the second molecule is proportional to the volume remaining unoccupied after the first solute molecule is placed:

$$\omega_2 = K(V - u)$$

3. The number of ways of placing the ith molecule is therefore

$$\omega_i = K[V - (i - 1)u]$$

4. The total number of ways Ω of placing N_2 solute molecules is

$$\Omega = \frac{1}{N_2!} \prod_{i=1}^{N_2} K[V - (i - 1)u]$$

where the factor $N_2!$ enters because of the interchangeability of the particles.

5. By changing the limits of the product, the latter can be written as

$$\prod_{i=1}^{N_2} K[V - (i - 1)u] = \prod_{i=0}^{N_2-1} K(V - iu) = \prod_{i=0}^{N_2-1} KV\left(1 - \frac{iu}{V}\right)$$

6. Since the entropy of the mixture S_{mix} is proportional to $\ln \Omega$ by the Boltzmann equation, we write

$$\frac{S_{mix}}{k} = N_2 \ln (KV) - \ln N_2! + \sum_{i=0}^{N_2-1} \ln \left(1 - \frac{iu}{V}\right)$$

The summation in the last term results from taking the logarithm of the product.

7. The ratio iu/V is small for all values of i; hence the last term can be approximated by the series expansion of the logarithm [$\ln (1 - y) \cong -y$]:

$$\frac{S_{mix}}{k} = N_2 \ln KV - \ln N_2! - \frac{u}{V} \sum_{i=0}^{N_2-1} i$$

8. Since the sum of integers from 0 to y is $y(y + 1)/2$, the summation in the last expression can be written as

$$\sum_{i=0}^{N_2-1} i = \frac{(N_2 - 1)(N_2)}{2} \cong \frac{1}{2} N_2^2$$

where the approximation applies since N_2 is large.

9. We can shift from numbers of molecules to numbers of moles of solute by dividing by Avogadro's number N_A and changing k to R. Also, recalling that $V = \Sigma_i n_i \bar{V}_i$, we write

$$\frac{S_{mix}}{R} = n_2 \ln K + n_2 \ln (n_1 \bar{V}_1 + n_2 \bar{V}_2) - \frac{1}{N_A} \ln N_2 ! - \frac{1}{2} u N_A \frac{n_2^2}{n_1 \bar{V}_1 + n_2 \bar{V}_2}$$

10. By separately letting n_2 and n_1 equal zero, we obtain the configurational entropy for the pure solvent ($S_1 = 0$) and the pure solute ($S_2 = n_2 \ln K + n_2 \ln n_2 \bar{V}_2 - (1/N_A) \ln N_2 ! - u N_A n_2 / 2 \bar{V}_2$).

Subtracting the entropy contributions of the pure components from S_{mix} gives the entropy of mixing according to the present model:

$$\frac{\Delta S_m}{R} = n_2 \ln \left(\frac{n_1 \bar{V}_1 + n_2 \bar{V}_2}{n_2 \bar{V}_2} \right) - \frac{1}{2} u N_A \frac{n_2^2}{n_1 \bar{V}_1 + n_2 \bar{V}_2} + \frac{1}{2} u \frac{N_A n_2}{\bar{V}_2} \tag{8.91}$$

This is converted to a partial molar quantity by differentiation:

$$\bar{S}_1 - S_1^\circ = \frac{\partial}{\partial n_1} (\Delta S_m) = R \left[\frac{n_2 \bar{V}_1}{n_1 \bar{V}_1 + n_2 \bar{V}_2} + \frac{1}{2} N_A \bar{V}_1 u + \frac{1}{2} N_A \bar{V}_1 u \left(\frac{n_2}{n_1 \bar{V}_1 + n_2 \bar{V}_2} \right)^2 \right] \tag{8.92}$$

Since the solution is athermal by hypothesis, $\Delta \mu_1 = -T \Delta \bar{S}_1$, or

$$\Delta \mu_1 = - RT \left[\frac{n_2 \bar{V}_1}{V} + \frac{1}{2} N_A \bar{V}_1 u \left(\frac{n_2}{V} \right)^2 \right] \tag{8.93}$$

Upon incorporation of Eq. (8.85), this becomes

$$\Delta \mu_1 = - RT \bar{V}_1 \left(\frac{c_2}{M} + \frac{1}{2} \frac{N_A u}{M^2} c_2^2 \right) \tag{8.94}$$

Equation (8.79) permits this result to be directly converted to an expression for osmotic pressure:

$$\Pi = RT\left(\frac{c_2}{M} + \frac{1}{2}\frac{N_A u}{M^2}c_2^2\right) \tag{8.95}$$

or

$$\frac{\Pi}{RTc_2} = \frac{1}{M} + \frac{1}{2}\frac{N_A u}{M^2}c_2 \tag{8.96}$$

Comparing Eqs. (8.87) and (8.96) shows that

$$B = \frac{1}{2}\frac{N_A u}{M^2} \tag{8.97}$$

according to this model.

Equation (8.97) shows that the second virial coefficient is a measure of the excluded volume of the solute according to the model we have considered. From the assumption that solute molecules come into surface contact in defining the excluded volume, it is apparent that this concept is easier to apply to, say, compact protein molecules in which hydrogen bonding and disulfide bridges maintain the tertiary structure (see Sec. 1.4) than to random coils. We shall return to the latter presently, but for now let us consider the application of Eq. (8.97) to a globular protein. This is the objective of the following example.

Example 8.7

The bovine serum albumin molecule is known to be nearly spherical and uncharged in a solution of pH 5.37. A plot of Π/c_2 versus c_2 for this polymer at 25°C is linear and has an intercept corresponding to M = 69,000. The slope of the line is 1.37×10^{-3} Torr liter^2 g^{-2}. Use this slope to estimate the radius of this spherical molecule.

Solution

We convert the units to SI units; then we use Eqs. (8.97) and (8.90) to calculate the volume of the sphere:

$$\text{Slope} = \frac{1.37 \times 10^{-3}\ \text{Torr liter}^2}{\text{g}^2} \times \frac{1.01 \times 10^5\ \text{N m}^{-2}}{760\ \text{Torr}}$$

$$\times \left(\frac{(10^{-1}\ \text{m})^3}{1\ \text{liter}}\right)^2 \times \left(\frac{10^3\ \text{g}}{1\ \text{kg}}\right)^2 = 0.182\ \text{N m}^4\ \text{kg}^{-2}$$

Since the plot is one of Π/c_2, not Π/RTc_2, versus c_2, we must divide the slope by RT to get B:

$$B = \frac{0.182 \text{ N m}^4 \text{ kg}^{-2}}{(8.314 \text{ J K}^{-1} \text{ mol}^{-1})(298 \text{ K})} = 7.35 \times 10^{-5} \text{ m}^3 \text{ kg}^{-2} \text{ mol}$$

From Eq. (8.97),

$$u = \frac{2BM^2}{N_A} = \frac{2(7.35 \times 10^{-5} \text{ m}^3 \text{ kg}^{-2} \text{ mol})(69 \text{ kg mol}^{-1})^2}{6.02 \times 10^{23} \text{ mol}^{-1}}$$

$$= 1.16 \times 10^{-24} \text{ m}^3$$

From Eq. (8.90), $V_{sphere} = (1/4)\, u = 2.90 \times 10^{-25}$ m^3. Since $V_{sphere} = (4/3)\pi r^3$, we can readily convert this to the radius of the sphere: $r = 4.11 \times 10^{-9}$ m = 4.11 nm = 41 Å.

•

We saw in Chap. 1 that the random coil is characterized by a spherical domain for which the radius of gyration is a convenient size measure. As a tentative approach to extending the excluded volume concept to random coils, therefore, we write for the volume of the coil domain (subscript d) $V_d = (4/3)\pi r_g^3$, and combining this result with Eq. (8.90), we obtain

$$u_{coil} = 4\left(\frac{4}{3}\pi r_g^3\right) \tag{8.98}$$

from which B can be calculated via Eq. (8.97). As noted above, the excluded volume concept appears to be more applicable to particles with a molecular structure which is more compact than the random coil. The following argument however, shows how the excluded volume model can be extended to random coils as well.

Equations (1.48) and (1.59) show that r_g varies as $n^{1/2}$ for the random coil. This means that the volume of the spherical domain of the coil varies with the degree of polymerization as $n^{3/2}$. We shall disregard all other numerical coefficients in the remainder of this paragraph to argue that a spherical excluded volume of radius r_g is at least plausible for chains of large n. That portion of the domain which is actually occupied by chain segments is proportional to n so the volume fraction of segments in the domain ϕ^* is proportional to $n/n^{3/2}$ or $n^{-1/2}$. For large n this is very small. The fraction of the coil domain which is not occupied by chain segments is $1 - \phi^*$ and is proportional to $1 - n^{-1/2}$. The number of sites into which segments of a *second* chain might be placed within the domain of the first is proportional to this "empty" volume. If the

second chain also consists of n segments, the number of ways of placing the second varies with n as $(1 - n^{-1/2})^n$. This is approximately equal to $e^{-n^{1/2}}$, which shows that the probability of a second coil overlapping the domain of the first decreases as n increases.

The above argument shows that complete overlap of coil domains is improbable for large n and hence gives plausibility to the excluded volume concept as applied to random coils. More importantly, however, it introduces the notion that coil interpenetration must be discussed in terms of probability. For hard spheres the probability of interpenetration is zero, but for random coils the boundaries of the domain are "softer" and the probability for interpenetration must be analyzed in more detail. One method for doing this will be discussed in the next section. Before turning to this, however, we note that the Flory-Huggins theory can also be used to yield a value for the second virial coefficient.

To use the Flory-Huggins theory as a source for understanding the second virial coefficient, we return to Eq. (8.53), which gives an expression for $\mu_1 - \mu_1^\circ$. Combining this result with Eq. (8.79) gives

$$-\Pi\bar{V}_1 = RT\left[\ln(1 - \phi_2) + \phi_2\left(1 - \frac{1}{n}\right) + \chi\phi_2^2\right] \tag{8.99}$$

At the same level of approximation as produced Eq. (8.85), we note

$$\phi_2 = \frac{n_2\bar{V}_2}{n_1\bar{V}_1 + n_2\bar{V}_2} \cong \frac{n_2}{n_1}\frac{\bar{V}_2}{\bar{V}_1}$$

so

$$\phi_2 \cong x_2\frac{\bar{V}_2}{\bar{V}_1} \cong c_2\frac{\bar{V}_2}{M} \tag{8.100}$$

Expanding the logarithm in Eq. (8.99) as $-\phi_2 - (1/2)\phi_2^2$ and combining with Eq. (8.100) yields

$$\frac{\Pi\bar{V}_1}{RT} = \left[\frac{\bar{V}_2}{M} - \left(1 - \frac{1}{n}\right)\frac{\bar{V}_2}{M}\right]c_2 + \left(\frac{1}{2} - \chi\right)\left(\frac{\bar{V}_2}{M}\right)^2 c_2^2 + \cdots \tag{8.101}$$

In terms of the reduced osmostic pressure, this becomes

$$\frac{\Pi}{RTc_2} = \frac{\bar{V}_2}{nM\bar{V}_1} + \frac{(1/2 - \chi)}{\bar{V}_1}\left(\frac{\bar{V}_2}{M}\right)^2 c_2 = \frac{1}{M} + \frac{(1/2 - \chi)}{\bar{V}_1}\left(\frac{\bar{V}_2}{M}\right)^2 c_2 \tag{8.102}$$

where the last simplification recalls the definition of n as $\bar{V}_2/\bar{V}_1$. Comparing this result with Eq. (8.87) shows that, according to the Flory-Huggins theory,

$$B = \left(\frac{1}{2} - \chi\right)\frac{\bar{V}_2^2}{\bar{V}_1 M^2} \tag{8.103}$$

If we further compare this result with Eq. (8.97), we can write

$$u_{coil} = \frac{2(1/2 - \chi)\bar{V}_2^2}{N_A \bar{V}_1} \tag{8.104}$$

which gives us two totally different expressions for the excluded volume of the random coil: Eqs. (8.98) and (8.104). In the next section we shall consider the reconciliation of these divergent relationships.

8.11 The Flory-Krigbaum Theory

We begin our attempt to reconcile these two expressions for the excluded volume of the random coil by reviewing some ideas about random coils from Chap. 1:

1. We saw in Sec. 1.11 that coil dimensions are affected by interactions between chain segments and solvent. Both the coil expansion factor α defined by Eq. (1.63) and the interaction parameter χ are pertinent to describing this situation.
2. Use of random flight statistics to derive r_g for the coil assumes the individual segments exclude no volume from one another. While physically unrealistic, this assumption makes the derivation mathematically manageable. Neglecting this volume exclusion means that coil dimensions are underestimated by the random fight model, but this effect can be offset by applying the result to a solvent in which polymer-polymer contacts are somewhat favored over polymer-solvent contacts.
3. Conditions in which the effects of item (2) exactly compensate are called Θ conditions. The expansion factor α gives the ratio of coil dimensions under non-Θ conditions to those under Θ conditions.

To apply these ideas to solution nonideality, we consider a theory developed by Flory and Krigbaum. This is only one of several approaches to the problem, but it is one which can be readily outlined in terms of material we have already developed. We shall only sketch the highlights of the Flory-Krigbaum theory, since the details are complicated and might actually obscure the principal ideas.

We consider the approach of two polymer coils in dilute solution until the two coil domains overlap to some extent, as shown in Fig. 8.11. According to

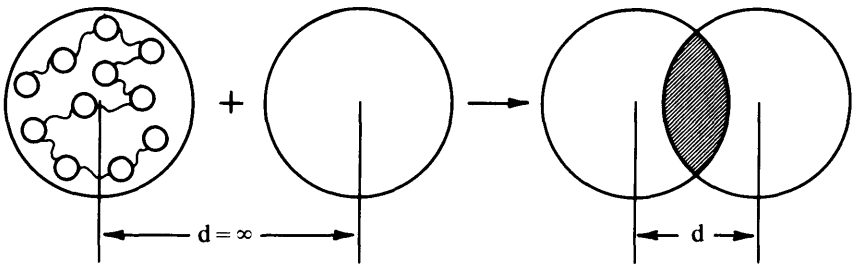

Figure 8.11 The coil domains of two polymer molecules. The schematic shows by shading how the region of overlap increases as the distance between centers decreases.

this theory, we shall consider the coil domain as a solution of chain segments in which the volume fraction is uniformly ϕ^*. Within the shaded area in Fig. 8.11, therefore, the segment volume fraction is $2\phi^*$. It is apparent that the volume of the lens-shaped overlap region V_{lens} is a function of the distance of separation of the coil centers.

The objective of the Flory-Krigbaum theory is to find a quantitative expression for the placement probability $\Omega(d)$ of the two coils as a function of their separation d. There are three stages to the derivation:

1. The statistical problem. The relative probability associated with the placement of the two coils such that $d = \infty$ is unity: The solution is so dilute that we can place the polymer molecules anywhere. It is at smaller d's that the placement probability drops off because of a generally unfavorable ΔG associated with the overlap. We assume that the decrease in probability is described by the Boltzmann factor and write

$$\Omega(d) = \Omega(d = \infty)\, e^{-\Delta G/kT} = e^{-\Delta G/kT} \tag{8.105}$$

2. The thermodynamic problem. There is a ΔG associated with the change in ϕ^* in the overlap region. This, in turn, is the product of two factors:

$$\Delta G = (\text{concentration effect})(\text{geometrical effect}) \tag{8.106}$$

The concentration effect involves the ΔG's of mixing for the solutions of concentrations ϕ^* and $2\phi^*$. We shall return to this presently.

3. The geometrical problem. This involves evaluating the "geometrical effect" in item (2). It requires calculation of the volume of the overlapping regions as a function of d and the coil dimensions, say, r_g. The mathematics of this step are tedious and add little to the polymer aspects of the theory.

Of the three stages outlined above, only the calculation of ΔG for the process in Fig. 8.11 warrants further discussion. Recalling that the volume of the shaded region is V_{lens}, we write

$$\Delta G = V_{lens}\,\Delta G_{m,2\phi^*} - 2V_{lens}\,\Delta G_{m,\phi^*} \tag{8.107}$$

where the ΔG_m's are the free energies of mixing per unit volume of the segment solutions of the indicated concentrations. Factoring out V_{lens} and identifying it as the geometrical effect in Eq. (8.106), we describe the concentration effect in the lens-shaped volume when the coils interpenetrate:

$$\Delta G_{lens} = \Delta G_{m,2\phi^*} - 2\,\Delta G_{m,\phi^*} \tag{8.108}$$

Next we use the Flory-Huggins theory to evalute ΔG_m by Eq. (8.44). As noted above, the volume fraction occupied by polymer segments within the coil domain is small, so the logarithms in Eq. (8.44) can be approximated by the leading terms of a series expansion. Within the coil $N_2 = 1$ and $N_1 = (1 - \phi^*)V_d N_A/\bar{V}_1$, where V_d is the volume of the coil domain. When all of these considertions are taken into account, Eq. (8.108) becomes

$$\Delta G_{lens} = 2kT\left(\frac{1}{2} - \chi\right)\frac{\bar{V}_2^{\,2}}{\bar{V}_1 V_d} \tag{8.109}$$

The volume of the coil domain which appears in Eq. (8.109) can also be grouped with related quantities as a factor in the geometrical part of the problem. Our primary interest is in the appearance of the factor $1/2 - \chi$ in the expression for ΔG_{lens} and—via Eqs. (8.105) and (8.106)—the idea that

$$\ln\left(\frac{\Omega(d)}{\Omega(d=\infty)}\right) \propto \left(\frac{1}{2} - \chi\right) \times f(d, r_g) \tag{8.110}$$

where the geometrical aspect of the problem is described by some function of the separation and the radii of gyration of the coils. While the precise details of such a function depend on the specific parameters used in the theory, it is sufficient to note that the probability undergoes a relatively rapid decrease from unity (for unhindered placement) to zero (for the excluded volume effect) as d decreases. This is sketched qualitatively in Fig. 8.12. For comparison, the broken line in Fig. 8.12 shows how the hard-sphere model would appear in the same representation. The more gradual transition in probability according to the Flory-Krigbaum model means the polymer coil is a relatively "soft" sphere but has a definite excluded volume nevertheless. Furthermore, the value of d at which the probability drops off is in the neighborhood of $2r_g$.

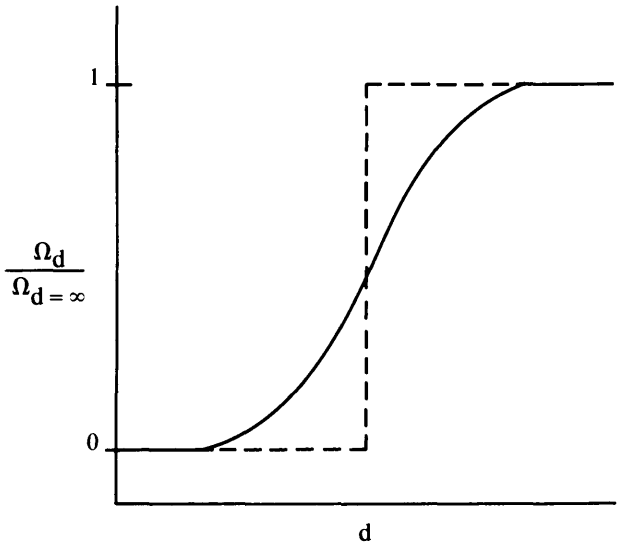

Figure 8.12 Schematic illustration showing with the solid line how the probability of placement varies with the distance of separation between the centers of the coils. The broken line is the equivalent result for hard spheres.

Converting the probability function described above into an excluded volume is accomplished by integrating the probability $1 - \Omega(d)$ of exclusion over a spherical volume encompassing all values of d:

$$u = \int_0^\infty [1 - \Omega(d)]\, 4\pi d^2\, d(d) \tag{8.111}$$

The full Flory-Krigbaum theory results in the following expression for the excluded volume:

$$u = \frac{2\bar{V}_2^2}{\bar{V}_1 N_A}\left(\frac{1}{2} - \chi\right)\left(1 - \frac{y}{2!2^{3/2}} + \frac{y^2}{3!3^{3/2}} + \cdots\right) \tag{8.112}$$

where

$$y = \frac{2\bar{V}_2^2}{\bar{V}_1 N_A}\left(\frac{1}{2} - \chi\right)\left(\frac{3}{4\pi r_g}\right)^{3/2} \tag{8.113}$$

The complicated form of the final result makes it clear why we have skipped over the details of the Flory-Krigbaum derivation!

If we disregard the term in brackets in Eq. (8.112)—which we shall call f(y) and which is close to unity for values of χ that are not too different from 1/2—this expression gives the same result for the excluded volume of the coil as given by Eq. (8.104) from a comparison of Eqs. (8.97) and (8.103). We may regard f(y) as a correction factor which is required for Eq. (8.104) to be valid as the difference $1/2 - \chi$ increases. In the next section we shall discuss the implications of Eq. (8.112) in greater detail.

Our primary interest in the Flory-Krigbaum theory is in the conclusion that the second virial coefficient and the excluded volume depend on solvent-solute interactions and not exclusively on the size of the polymer molecule itself. It is entirely reasonable that this should be the case in light of the discussion in Sec. 1.11 on the expansion or contraction of the coil depending on the solvent. The present discussion incorporates these ideas into a consideration of solution nonideality.

The parameter α which we introduced in Sec. 1.11 to measure the expansion which arises from solvent being imbibed into the coil domain can also be used to describe the second virial coefficient and excluded volume. We shall see in Sec. 9.7 that the difference $1/2 - \chi$ is proportional to $\alpha^5 - \alpha^3$. When the fully developed function of α is used to replace $1/2 - \chi$ in Eq. (8.112), the excluded volume according to the Flory-Krigbaum theory becomes

$$u = \left(\frac{4}{3}\pi r_g^3\right) 2\left(\frac{4}{3}\pi\right)^{1/2} (\alpha^2 - 1)\left(1 - \frac{z}{2!2^{3/2}} + \frac{z^2}{3!3^{3/2}} + \cdots\right) \tag{8.114}$$

where $z = 2(\alpha^2 - 1)$. What is noteworthy about this form of the theory is that the excluded volume is proportional to the volume of a sphere whose radius is r_g, as proposed in Eq. (8.98). Depending, then, on the particular algebraic form we examine, the Flory-Krigbaum theory ties together several ideas that have been in apparent opposition until now.

8.12 Theta Conditions

So far we have avoided mentioning one of the most interesting features of Eq. (8.112): the fact that u and therefore B equal zero when $\chi = 1/2$. From an examination of Eq. (8.114), it is also apparent that this corresponds to the condition $\alpha = 1$. We shall presently introduce still another way of describing the condition $B = u = 0$, but first we summarize the information we have accumulated until now pertaining to this condition:

1. When $B = 0$, the solution behaves ideally, at least through second-order effects. This means that deviations from ideality might be observed at still higher concentrations, but that the van't Hoff equation applies at least in dilute solutions for systems with $B = 0$.

2. B = 0 when $\chi = 1/2$, a condition we have already seen [Eq. (8.60)], corresponds to a critical value of χ for a copolymer of infinite molecular weight. For finite molecular weights this condition is not quite a threshold for precipitation, but is close to it. Polymer-polymer contacts are sufficiently favored over polymer-solvent contacts that a chain of infinite length would undergo phase separation.
3. We can imagine the coil tightening up as this point is approached from "better" conditions. This is not a shrinking to the vanishing point as suggested by the u = 0 criterion, but a contraction to the point where intramolecular exclusion effects are offset by shrinkage.
4. This was precisely the point where α was defined to equal unity, so it is entirely appropriate that inter- and intramolecular exclusion volumes are effectively zero under the same conditions.
5. In Chap. 1 we referred to these as Θ conditions, and we shall examine the significance of this term presently. Note that Θ conditions for a polymer solution are analogous to the Boyle temperature of a gas: Each behaves ideally under its respective conditions.
6. It is interesting to note that for a van der Waals gas, the second virial coefficient equals b - a/RT, and this equals zero at the Boyle temperature. This shows that the excluded volume (the van der Waals b term) and the intermolecular attractions (the a term) cancel out at the Boyle temperature. This kind of compensation is also typical of Θ conditions.

Many presentations of the second virial coefficient of polymer solutions contain different expressions for the quantities we have discussed. The difference lies in the fact that the factor $\psi(1 - \Theta/T)$ appears in place of $1/2 - \chi$. There are several attitudes we can take toward this difference. For one thing, we can regard the discrepancy as nothing more than different notation:

$$\frac{1}{2} - \chi \equiv \psi\left(1 - \frac{\Theta}{T}\right) \tag{8.115}$$

Based on this point of view, we can draw several conclusions:

1. ψ must be dimensionless.
2. Θ must have the units of temperature.
3. The conditions $\chi < 1/2$ and $\chi > 1/2$ correspond to positive and negative B values, respectively.
4. The same positive and negative B values must result from $T > \Theta$ and $T < \Theta$, respectively.
5. This alternative notation is especially suited to describe changes in solvent goodness which arise from temperature variations for a fixed system. By contrast, the χ notation is more descriptive of different solvents at a single temperature.

As a device for describing the effect of temperature on solution nonideality, it is entirely suitable to think of Eq. (8.115) as offering an alternate notation which accomplishes the desired effect with ψ and Θ as adjustable parameters. We note, however, that the left-hand side of Eq. (8.115) contains only one such parameter, χ, while the right-hand side contains two: ψ and Θ. Does this additional parameter have any physical significance?

To answer this question, we recall that χ is defined in Sec. 8.4 as a measure of the "energy" change associated with reaction (8.A), the solution process. In this context we acknowledged that there could very well be an entropy effect also associated with that process: a ΔS arising from some sort of "bonding" between solvent and polymer which is not included in the configurational entropy. If such an entropy effect is operative, then the quantity Δw on which the definition of χ is based would be better viewed as a free-energy change, as in Eq. (8.43). Although we discussed this possibility earlier, we have not acted upon it until now. Some manipulations on $1/2 - \chi$ provide a strategy for introducing this effect, which we shall call a solvation entropy ΔS_s:

1. We multiply $1/2 - \chi$ by RT to obtain

$$\left(\frac{1}{2} - \chi\right) RT = -\left(\chi RT - \frac{1}{2} RT\right)$$

2. With the absorbed coordination number, χRT is taken to be the value of ΔH for reaction (8.A); therefore we write

$$\left(\frac{1}{2} - \chi\right) RT = -\left(\Delta H - \frac{1}{2} RT\right)$$

3. The quantity in parentheses on the right-hand side is reminiscent of the expression $\Delta H - T\,\Delta S$, with the quantity $1/2R$ a contribution from the configurational entropy of the Flory-Huggins theory. Since our objective is to incorporate a solvation entropy into the discussion, we add the latter – in units of R for convenience – to $1/2R$:

$$\left(\frac{1}{2} - \chi\right) RT = -\left[\Delta H - \left(\frac{1}{2} + \Delta S_s\right) RT\right]$$

4. We define $1/2 + \Delta S_s$ by the parameter ψ and factor:

$$\left(\frac{1}{2} - \chi\right) RT = -\psi RT \left(\frac{\Delta H}{(1/2 + \Delta S_s) RT} - 1\right)$$

5. We define Θ to be $\Delta H/(1/2 + \Delta S_s)R$. Since the numerator of this definition is an enthalpy and the denominator an entropy, Θ must have the units of a temperature:

$$\left(\frac{1}{2} - \chi\right)RT = -\psi RT\left(\frac{\Theta}{T} - 1\right) = \psi RT\left(1 - \frac{\Theta}{T}\right)$$

6. By reversing step (1), we obtain Eq. (8.115), which we had set out to interpret.

The "new" parameter ψ, then, is a measure of the solvation entropy—except for the term 1/2—which we can regard as a measure of ΔS of reaction (8.A), just as χ or $\psi\Theta R$ measures ΔH for that reaction.

We can therefore include ψ and Θ along with χ and α as parameters which are measured by the second virial coefficient. The usefulness of having these alternative formulations for the second virial coefficient lies in the flexibility they give us for describing the chemical potential of a polymer solution. Thus we can say that the chemical potential behaves ideally in a solvent for which $\chi = 1/2$ or at a temperature equal to Θ. From a practical point of view, this means that the slope of a Π/c_2-versus-c_2 plot is horizontal under Θ conditions. Therefore a correct value of M can be evaluated from the van't Hoff equation using data measured at a single concentration in the dilute range without any need to extrapolate to $c_2 = 0$. Of course, it may take extensive preliminary experimentation to establish what the Θ conditions are, as well as to determine the range of acceptable concentrations within which this ideality is observed.

Figure 8.13 shows the reduced osmotic pressure for solutions of polyisobutylene in benzene plotted against c_2 at several different temperatures. The

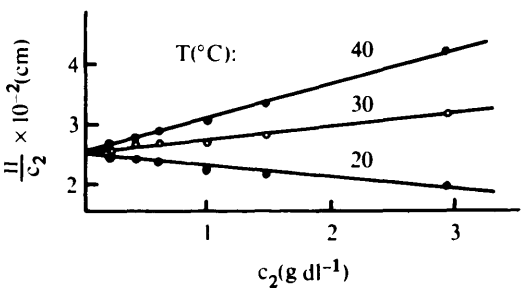

Figure 8.13 Π/c_2 versus c_2 for polyiosbutylene in benzene at the temperatures shown. [Reprinted with permission from W. R. Krigbaum and P. J. Flory, *J. Am. Chem. Soc.* 75:5254 (1953), copyright 1953 by the American Chemical Society.]

Table 8.3 Theta Temperatures for a Few Polymer–Solvent Systems

Polymer	Solvent	Θ (°C)
Poly(dimethyl siloxane)	Cyclohexane	-81
Poly(methyl methacrylate)	Toluene	-65
Polyisobutene	Toluene	-13
Poly(dimethyl siloxane)	2-Butanone	20
Poly(methyl methacrylate)	2-Ethylbutyraldehyde	22
Polyisobutene	Benzene	24
Polystyrene	Decalin	31
Poly(methyl methacrylate)	Amyl acetate	41
Polystyrene	Ethyl cyclohexane	70

Source: H. G. Elias et al., in J. Bandrup and E. H. Immergut (Eds.), *Polymer Handbook*, 2nd ed., Wiley, New York, 1975.

Θ temperature for this system is identified as the temperature at which this plot shows a horizontal slope. For the system shown in Fig. 8.13, Θ lies between 20 and 30°C; additional measurements in this range indicate this temperature to be about 24°C. Table 8.3 lists, in increasing order, the Θ temperatures for a few polymer-solvent systems. The following observations are pertinent to the entries in Table 8.3:

1. Although the systems listed were chosen arbitrarily, it is apparent that Θ values span a wide range.
2. A variety of systems exist for which Θ is in the vicinity of room temperature.
3. The nature of the solvent is as important as the polymer in determining Θ, as is apparent from the wide range of Θ values for poly(dimethyl siloxane) in different solvents.

We shall have occasion to refer to Θ conditions in the next two chapters as well, so the ideas of the past few sections have applications beyond merely describing the nonideality of osmostic pressure experiments.

In this chapter, and throughout this entire book for that matter, we have been concerned with uncharged polymers. We shall conclude this chapter with a brief discussion of the osmostic pressure of charged polymer molecules.

8.13 Osmotic Pressure of Charged Polymers

In this section we briefly consider the osmotic pressure of polymers which carry an electric charge in solution. These include synthetic polymers with ionizable functional groups such as $-NH_2$ and $-COOH$, as well as biopolymers such as proteins and nucleic acids. In this discussion we shall restrict our consideration

to solutions which are relatively dilute in polymer, thereby focusing attention on only the first or van't Hoff term of the concentration dependence of Π. This emphasis is strictly a matter of convenience; theories which deal with solution nonideality in charged systems are also available.

We shall be interested in determining the effect of electrolytes of low molecular weight on the osmotic properties of these polymer solutions. To further simplify the discussion, we shall not attempt to formulate the relationships of this section in general terms for electrolytes of different charge types–2:1, 2:2, 3:1, 3:2, and so on–but shall consider the added electrolyte to be of the 1:1 type. We also assume that these electrolytes have no effect on the state of charge of the polymer itself; that is, for a polymer such as, say, poly(vinyl pyridine) in aqueous HCl or NaOH, the state of charge would depend on the pH through the water equilibrium and the reaction

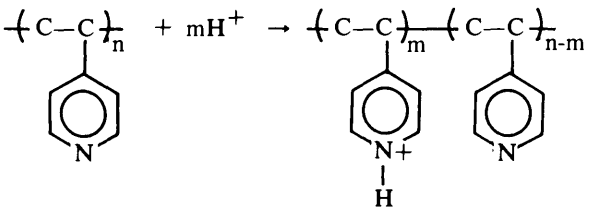

(8.B)

We shall refer to electrolytes which do not affect the charge of the polymer as indifferent electrolytes. In the situation illustrated by reaction (8.B), the HCl and NaOH are clearly not indifferent. We shall also assume that the indifferent electrolytes are 100% ionized in the polymer solution.

We continue to designate the solvent (usually water) as component 1, the polymer as component 2, and the indifferent electrolyte MX as component 3. We arbitrarily designate the polymer to be a cation with a relative charge of +z, having associated with it the same anion as is present in MX. Accordingly, we designate the polymer PX_z and represent its dissociation by

$$PX_z \rightarrow P^{+z} + zX^- \tag{8.C}$$

We consider this system in an osmotic pressure experiment based on a membrane which is permeable to all components except the polymeric ion P^{+z}; that is, solvent molecules, M^+, and X^- can pass through the membrane freely to establish the osmotic equilibrium, and only the polymer is restrained. It does not matter whether pure solvent or a salt solution is introduced across the membrane from the polymer solution or whether the latter initially contains salt or not. At equilibrium both sides of the osmometer contain solvent, M^+, and X^- in such proportions as to satisfy the constaints imposed by electroneutrality and equilibrium conditions.

It is conventional to use molality—moles of solute per kilogram of solvent (symbol m)—as the concentration unit in electrolyte thermodynamics. Accordingly, we shall represent the concentrations of both the indifferent electrolyte and the polymer in these units in this section: m_3 and m_2, respectively. In the same dilute (with respect to polymer) approximation that we have used elsewhere in this chapter, m_2 is related to the mass volume^{-1} system of units c_2 by

$$m_2 = \frac{1000\bar{V}_1}{M_1 M} c_2 \tag{8.116}$$

Neglecting the higher-order terms, we can write the osmotic pressure for this three-component system in terms of the van't Hoff equation:

$$\Pi \frac{1000\bar{V}_1}{M_1} = mRT \tag{8.117}$$

where m (no subscript) is the number of moles of pressure-producing solute per kilogram of solvent and $1000\bar{V}_1/M_1$ is the volume of that amount of solvent. Next we examine the molal concentration of "pressure-producing solute." Considering the definition of the system, this appears, at first thought, to describe only the polymer. We shall see presently, however, that the indifferent electrolyte is generally not uniformly distributed on both sides of the membrane, so any asymmetry in its concentration will also contribute to m in Eq. (8.117). If we designate the phase containing the polyelectrolyte as the α phase. and that from which the polymer is excluded as the β phase, we can write

$$m = m_{2,\alpha} + m_{M^+,\alpha} + m_{X^-,\alpha} - m_{M^+,\beta} - m_{X^-,\beta} \tag{8.118}$$

If the concentrations of M^+ and X^- were both the same in the α and β phases, $m = m_2$; this formalism allows for the more general case where the α and β concentrations are not equal.

There are two additional concepts which we can invoke to simplify Eq. (8.118): electroneutrality and a less familiar principle called Donnan equilibrium. Some relationships pertaining to these are developed below:

1. Electroneutrality requires simply that the same amounts of positive and negative charge be present in a solution. Applying this separately to both the α and β phases, we obtain

$$zm_{P,\alpha} + m_{M^+,\alpha} = m_{X^-,\alpha} \tag{8.119}$$

and

$$m_{M^+,\beta} = m_{X^-,\beta} \tag{8.120}$$

2. Donnan equilibrium arises from applying the phase equilibrium criterion to the indifferent electrolyte: $\mu_3^{\alpha} = \mu_3^{\beta}$. From Eq. (8.13) this is $\mu_3 = \mu_3^{\theta} + RT \ln a_{3,\beta}$ for the side under normal pressure. From Eq. (8.76), $\mu_3 = \mu_3^{\theta} + RT \ln a_{3,\alpha} + \Pi \bar{V}_3$ for the side containing the polymer. If the polymer concentration is low, the term $\Pi \bar{V}_3$ is insignificant compared to the terms arising from the electrolyte itself; therefore

$$a_{3,\alpha} = a_{3,\beta} \tag{8.121}$$

3. The activity of an electrolyte is given by the product of the activities of the individual ions. Applied to MX, this means that Eq. (8.121) becomes

$$a_{M^+,\alpha}\, a_{X^-,\alpha} = a_{M^+,\beta}\, a_{X^-,\beta} \tag{8.122}$$

4. The activity of an ion is related to its molality through the mean activity coefficient $\gamma_{\pm}$; therefore

$$(m_{M^+,\alpha})(m_{X^-,\alpha})\,\gamma_{\pm}^{\,2} = (m_{M^+,\beta})(m_{X^-,\beta})\,\gamma_{\pm}^{\,2} \tag{8.123}$$

   For low concentrations of electrolyte, $\gamma_{\pm} \to 1$. Since we are not concerned with electrolyte nonideality per se, we shall assume this last condition and write

$$m_{M^+,\alpha}\, m_{X^-,\alpha} = m_{M^+,\beta}\, m_{X^-,\beta} \tag{8.124}$$

5. This last result describes the Donnan equilibrium condition as it applies to the system under consideration. Like other ionic equilibrium expressions, it requires the equality of *ion products* in equilibrium solutions.

Equations (8.119), (8.120), and (8.124) provide some additional relationships which can be substituted into Eq. (8.118). When all of these results are combined, we obtain

$$m = m_{2,\alpha}(1 + z) + 2m_{M^+,\alpha} - 2\left[m_{M^+,\alpha}(zm_{2,\alpha} + m_{M^+,\alpha})\right]^{1/2} \tag{8.125}$$

Since all of the concentrations now apply to the phase containing the polymer, the α subscript has become redundant and will be dropped. Combining Eqs. (8.117) and (8.125) yields the desired result:

$$\Pi = \frac{M_1 RT}{1000\bar{V}_1}\left[(1 + z)\,m_2 + 2m_{M^+} - 2m_{M^+}\left(1 + \frac{zm_2}{m_{M^+}}\right)^{1/2}\right] \tag{8.126}$$

Note that if $z = 0$, the entire quantity in the brackets would equal m_2, and Eq. (8.126) would be the van't Hoff equation applied to an ordinary polymer.

The effect of the charge as well as that of the indifferent electrolyte, then, is contained in the term in brackets. A numerical calculation is probably the easiest way to examine this effect. This is illustrated in the following example.

Example 8.8

Evaluate the bracketed quantity in Eq. (8.126) for m_{M^+} between 10^{-6} and 10^{-1} mol kg^{-1} at intervals differing by powers of 10. Do this for polyelectrolytes with the following charge-concentration ($z\text{-}m_2$) combinations: $50\text{-}10^{-6}$, $50\text{-}10^{-5}$, $100\text{-}10^{-5}$, and $100\text{-}10^{-4}$. Comment on the results.

Solution

The factors zm_2 and $(z + 1)m_2$ in combination with the different values for m_{M^+} determine the magnitude of this term. We begin by tabulating these:

z	m_2 (mol kg^{-1})	zm_2 (mol kg^{-1})	$(z + 1)m_2$ (mol kg^{-1})
50	10^{-6}	5.0×10^{-5}	5.1×10^{-5}
50	10^{-5}	5.0×10^{-4}	5.1×10^{-4}
100	10^{-5}	1.00×10^{-3}	1.01×10^{-3}
100	10^{-4}	1.00×10^{-2}	1.01×10^{-2}

This particular combination of parameters enables us to do the following:

1. Vary m_2 at constant z.
2. Vary z at constant m_2.
3. Span a 200-fold variation in zm_2, the charge concentration contributed by polymer.
4. Use approximations developed for dilute polymer solutions. Note that the values for m_{M^+} satisfy the requirement for dilution at 10^{-6} m but not at 10^{-1} m.

Table 8.4 lists numerical values for the quantity in brackets for the required ranges of parameters.

The trends that we note in these calculations are the following:

1. The bracketed term approaches the value of m_2 as the concentration of indifferent electrolyte increases.
2. This is true in all cases, but is most evident in the first column of calculated quantities in Table 8.4.
3. The bracketed term approaches the value of $(z + 1)m_2$ as the concentration of indifferent electrolyte decreases.

Table 8.4 Numerical Values for the Bracketed Term in Eq. (8.126) for the Parameters m_2, z, and m_{M^+} Shown (Values Discussed in Example 8.8)

m_2 (mol kg^{-1}):	10^{-6}	10^{-5}	10^{-5}	10^{-4}
$(z+1)\,m_2$ (mol kg^{-1}):	5.1×10^{-5}	5.1×10^{-4}	1.01×10^{-3}	1.01×10^{-2}
m_{M^+} (mol kg^{-1}):	Bracketed term in Eq. (8.126) (mol kg^{-1})			
10^{-6}	3.87×10^{-5}	4.67×10^{-4}	9.49×10^{-4}	9.90×10^{-3}
10^{-5}	2.20×10^{-5}	3.87×10^{-4}	8.29×10^{-4}	9.49×10^{-3}
10^{-4}	6.05×10^{-6}	2.20×10^{-4}	5.47×10^{-4}	8.29×10^{-3}
10^{-3}	1.61×10^{-6}	6.05×10^{-5}	1.82×10^{-4}	5.47×10^{-3}
10^{-2}	1.06×10^{-6}	1.61×10^{-5}	3.38×10^{-5}	1.82×10^{-3}
10^{-1}	1.01×10^{-6}	1.06×10^{-5}	1.25×10^{-5}	3.38×10^{-4}

4. This is true in all cases, but is most evident in the last column of Table 8.4. Of course, for large values of z, $z \cong z + 1$, and it is not readily apparent that it is $(z + 1)m_2$ rather than zm_2 that is the correct limit. The value given is correct, however.

•

The generalizations demonstrated in the preceding example can be proved without resorting to numbers, but we have looked at enough algebra in this chapter already without adding these manipulations as well!

Combining Eqs. (8.116) and (8.126) with the conclusions from the example, we obtain the following:

1. For the case of $m_{M^+} \to 0$,

$$\frac{\Pi}{RTc_2} = \frac{z + 1}{M} \tag{8.127}$$

2. For the other extreme in which the concentration of the indifferent electolyte is high,

$$\frac{\Pi}{RTc_2} = \frac{1}{M} \tag{8.128}$$

3. These results show more clearly than Eq. (8.126)—of which they are special cases—the effect of charge and indifferent electrolyte concentration on the osmotic pressure of the solution. In terms of the determination of molecular weight of a polyelectrolyte by osmometry . . . .
4. A correct value of the molecular weight is obtained for the charged polymer by the van't Hoff equation, provided that a large excess of indifferent electrolyte is present. These high concentrations are described as swamping electrolyte conditions.
5. A value for the molecular weight which is low by a factor z + 1 is obtained for salt-free solutions if the experimental results are analyzed as if the polymer were uncharged.
6. Again, Eq. (8.126) describes the situation for known values of z and intermediate concentrations of electrolyte.

What makes the latter items particularly important is the fact that the charge and electrolyte content of an unknown polymer may not be known; hence it is important to design an osmotic pressure experiment correctly for such a system. It is often easier to add swamping amounts of electrolyte than to totally eliminate all traces of electrolyte. Under the former conditions a true molecular weight is obtained. Trouble arises only when the experimenter is indifferent toward indifferent electrolyte; this sort of carelessness can be the source of much confusion.

The algebra and arithmetic of this section have led us to the correct conclusions, but the underlying physical reality may be obscured by all these manipulations. The situation is simply this: In the complete absence of indifferent electrolyte, the polymer ion *and* its counterions are restricted to the same phase. The polymer is held back by the membrane, the counterions are held back by electroneutrality. The polymer side of the membrane, therefore, contains z + 1 mol of solute particles for every molar mass of polymer introduced. Since osmotic pressure gives a number average molecular weight, Eq. (8.127) is the logical result. With a sufficiently large excess of indifferent electrolyte, the small ions effectively "swamp out" the charge contributed by the polymer, and the latter behaves as if it were uncharged.

Problems

1. In the derivation of Eq. (8.40) it is assumed that each polymer segment is surrounded by z sites which are occupied at random by either solvent molecules or polymer segments. Actually, this is true of only z - 2 of the sites in the coordination sphere—z - 1 for chain ends—since two of the sites are occupied by polymer segments which are covalently bound to other polymer segments. Criticize or defend the following proposition concerning this effect: The kinds of physical interactions that we identify as London or dipole-dipole attractions can also operate between segments which are covalently bonded together, so the w_{22} contribution continues to be valid. A slight error in counting is made—to allow for simplification of the resulting function—but this is a tolerable approximation in concentrated solutions. In dilute solutions the approximation introduces more error, but the model is in trouble in such solutions anyhow, so another approximation makes little difference.
2. By combining Eqs. (8.42), (8.49), and (8.60), show that $V_1^\circ(\delta_2 - \delta_1)^2 = (1/2)RT_c$, where T_c is the critical temperature for phase separation. For polystyrene with $M \cong 3 \times 10^6$, Shultz and Flory† observed T_c values of 68 and 84°C, respectively, for cyclohexanone and cyclohexanol. Values of V_1° for these solvents are abut 108 and 106 $cm^3\ mol^{-1}$, respectively, and δ_1 values are listed in Table 8.2. Use each of these T_c values to form separate estimates of δ_2 for polystyrene and compare the calculated values with each other and with the value for δ_2 from Table 8.2. Briefly comment on the agreement or lack thereof for the calculated and accepted δ's in terms of the assumptions inherent in this method. Criticize or defend the following proposition for systems where use of the above relationship is justified: Polymer will be miscible in all proportions in low molecular weight solvents from which they differ in δ value by about 3 or less.

† A. R. Shultz and P. J. Flory, *J. Am. Chem. Soc.* 75:5681 (1953).

3. The accompanying sketch qualitatively describes the phase diagram for the system nylon-6,6, water, phenol for $T \geqslant 70^{\circ}C$.† In this figure the broken lines are the lines whose terminals indicate the concentrations of the three components in the two equilibrium phases. Consult a physical chemistry textbook for the information as to how such concentrations are read. In the two-phase region, both phases contain nylon, but the water-rich phase contains the nylon at a lower concentration. On this phase diagram or a facsimile, draw arrows which trace the following procedure:

   a. Water is added to solution A until the system separates into solutions B and C.
   b. Solution C is removed and water is added to solution B until the system separates into D and E.
   c. Phenol is added to solution C until a solution A′ results which is close to A in concentration.

   Would you expect solutions C and E or B and D to contain the higher molecular weight polymer? Briefly explain. Outline a strategy for nylon fractionation based on steps (a)–(c). Some steps may be repeated as needed.

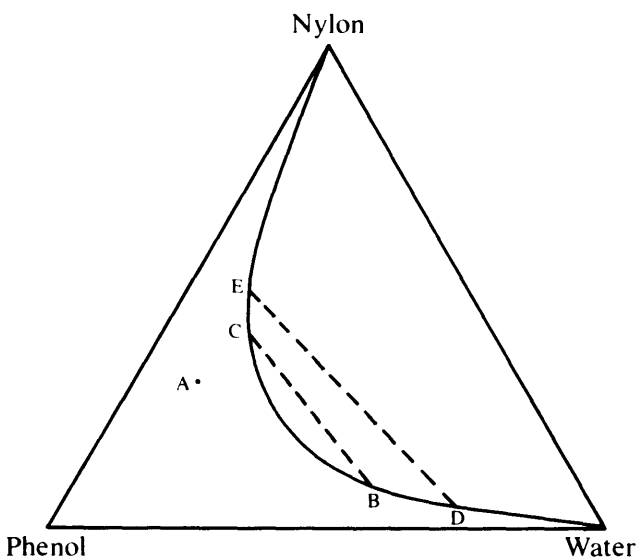

† G. B. Taylor, *J. Am. Chem. Soc.* 69:638 (1947).

4. Following the procedure described in the last problem, Taylor† fractionated nylon-6,6 into a series of cuts which he characterized by viscosity. These cuts were then refractionated. The following is a list of the intrinsic viscosities $[\eta]$ —which increase as $M^{0.72}$ in this system—of the various fractions:

$[\eta]$ for the concentrated phase				$[\eta]$ for the dilute phase			
Cut number	First fraction	Cut number	Second fraction	Cut number	First fraction	Cut number	Second fraction
1	1.40	1.1	2.02	1	0.97	1.1	1.37
		1.2	1.80			1.2	1.24
		1.3	1.55			1.3	1.04
		1.4	1.17			1.4	0.65
		1.5	0.71			1.5	0.15
		1.6	0.30				
2	1.27	2.1	1.67	2	0.88	2.1	1.11
		2.2	1.61			2.2	0.93
		2.3	1.45			2.3	0.58
		2.4	1.30			2.4	0.37
		2.5	0.85				
		2.6	0.38				
3	1.01	3.1	1.28	3	0.74	3.1	0.94
		3.2	1.06			3.2	0.81
		3.3	0.68			3.3	0.58
		3.4	0.58			3.4	0.36
4	0.75	4.1	0.90	4	0.59	4.1	0.71
		4.2	0.75			4.2	0.62
		4.3	0.54			4.3	0.46
		4.4	0.46			4.4	0.36
5	0.57			5	0.44		
6	0.38			6	0.30		
7	0.23			7	0.18		

On the basis of these observations, criticize or defend the following proposition: In the first fractionation, the average molecular weight of the polymer in the concentrated phase is about 50% higher than that in the dilute phase, and between the first and last cut of either phase there is more than a 10-fold range in M. In the second fractionation the lower cut numbers fractionate into a narrower range of M's because they are more nearly pure samples of the high molecular weight polymer.

† G. B. Taylor, *J. Am. Chem. Soc.* 69:638 (1947).

5. In some IUPAC-sponsored research†, samples of the same polystyrene preparation were distributed among different laboratories for characterization. The following molecular weights were obtained for one particular sample by osmotic pressure experiments using the solvents, membranes, and temperatures listed below:

Laboratory	T (°C)	Solvent[a]	Membrane	$M \times 10^{-3}$ (g mol^{-1})
I	27.5	T	Gel cellophane	79
I	27.5	MEK	Gel cellophane	78
H	25	MEK	Gel cellophane	98
M	25	B	Denitrated collodion	77.5
M	25	MEK	Denitrated collodion	77.5
U	28	B	Denitrated collodion	83
U	28	MEK	Denitrated collodion	100
O	25	B	Regenerated cellulose	75
T	26	MEK	Bacterial cellulose	78

[a] T = toluene, B = benzene, and MEK = methyl ethyl ketone.

Based on these observations, criticize or defend the following proposition: Except for two of the values in MEK, the reproducibility of M determinations is quite acceptable. MEK consistently gives erroneous values, probably because the solutions are highly nonideal for this solvent, which is more polar than either benzene or toluene.

6. The osmotic pressure of polystyrene fractions in toluene and methyl ethyl ketone was measured‡ at 25°C and the following results were obtained:

	Toluene		Methyl ethyl ketone	
Fraction number	$c_2 \times 10^3$ (g cm^{-3})	Π (g cm^{-2})	$c_2 \times 10^3$ (g cm^{-3})	Π (g cm^{-2})
I	4.27	0.22	2.67	0.04
	6.97	0.58	6.12	0.14
	9.00	1.00	8.91	0.31
	10.96	1.53		

† The International Union of Pure and Applied Chemistry, *J. Polym. Sci.* 10:129 (1953).
‡ C. Bawn, R. Freeman, and A. Kamaliddin, *Trans. Faraday Soc.* 46:862 (1950).

Fraction number	Toluene		Methyl ethyl ketone	
	$c_2 \times 10^3$ (g cm^{-3})	Π (g cm^{-2})	$c_2 \times 10^3$ (g cm^{-3})	Π (g cm^{-2})
II	1.55	0.16	3.93	0.40
	2.56	0.28	8.08	0.95
	2.93	0.32	10.13	1.30
	3.80	0.47		
	5.38	0.77		
	7.80	1.36		
	8.68	1.60		
III	1.75	0.31	1.41	0.23
	2.85	0.53	2.90	0.48
	4.35	0.88	6.24	1.11
	6.50	1.49	8.57	1.63
	8.85	2.36		
V	1.65	0.61	2.49	0.87
	2.97	1.16	4.21	1.53
	4.80	2.00	5.56	2.03
	7.66	3.52	7.76	2.96

From plots of Π/c_2 versus c_2, evaluate M for each of the four polymer fractions. Do the data collected from the two different solvents conform to expectations with respect to slope and intercept values?

7. The osmotic pressure of solutions of polystyrene in cyclohexane was measured† at several different temperatures, and the following results were obtained:

Fraction	T = 24°C	
	c_2 (g cm^{-3})	$\Pi/RTc_2 \times 10^6$ (mol g^{-1})
II	0.0976	8.0
	0.182	6.0
	0.259	8.7

† W. R. Krigbaum and D. O. Geymer, *J. Am. Chem. Soc.* 81: 1859 (1959).

	T = 34°C	
Fraction	c_2 (g cm^{-3})	$\Pi/RTc_2 \times 10^6$ (mol g^{-1})
II	0.0081	13.3
	0.0201	14.2
	0.0964	14.2
	0.180	18.7
	0.257	26.2
III	0.0156	2.46
	0.0482	2.24
	0.0911	3.42
	0.126	4.96
	0.139	6.05
	T = 44°C	
Fraction	c_2 (g cm^{-3})	$\Pi/RTc_2 \times 10^6$ (mol g^{-1})
II	0.0959	18.6
	0.178	28.1
	0.255	40.0
III	0.0478	5.50
	0.125	11.0
	0.138	13.2

Plot all of these data on a single graph as Π/RTc_2 versus c_2, connecting the points so as to present as coherent a display of the results as possible. Evaluate the molecular weights of the two polystyrene fractions. Criticize or defend the following propostion: These data show that the Θ temperature for this system is about 34°C. As expected, the range of concentrations which are adequately described by the first two terms of the virial equation is less for sample III than for sample II. Above this range other contributions to nonideality contribute positive deviations from the two-term osmotic pressure equation. It would be interesting to see how this last effect appears for sample III at 24°C, but this measurement was probably impossible to carry out owing to phase separation.

8. Krigbaum† measured the second virial coefficient of polystyrene in cyclohexane at several different temperatures. The observed values of B as well as some pertinent volumes at those temperatures are listed below:

† W. R. Krigbaum, *J. Am. Chem. Soc.* 76:3758 (1954).

T (K)	303	313	323
$B \times 10^5$ (cm^3 mol g^{-2})	-4.55	4.45	9.01
$\bar{V}_1$ (cm^3 mol^{-1})	109.5	110.9	112.3
$\bar{V}_2/M$ (cm^3 g^{-1})	0.930	0.935	0.940

Use these data to estimate the Θ temperature for this system by graphical interpolation. By combining Eqs. (8.97), (8.112), and (8.115), the product $\psi f(y)$ can be evaluated at each temperature once Θ has been determined. Since $f(y) = 1.00$ at $T = \Theta$, ψ can be evaluated by a graphical interpolation of $\psi f(y)$ versus T. Use this procedure to estimate ψ from these data. Based on these values of Θ and ψ, estimate χ at 25°C for polystyrene in cyclohexane.

9. By combining Eqs. (8.60) and (8.115), the following relationship is obtained between the critical temperature T_c for phase separation and the degree of polymerization:

$$\frac{1}{T_c} = \frac{1}{\Theta} - \frac{1}{\Theta\psi}\left(\frac{1}{n^{1/2}} + \frac{1}{2n}\right)$$

Derive this relationship and explain the graphical method it suggests for evaluating Θ and ψ. The critical temperatures for precipitation for the data shown in Fig. 8.3b are the following:

M (g mol^{-1})	22,700	285,000	6,000,000
T_c (°C)	18.2	45.9	56.2

Use the graphical method outlined above to evaluate Θ and ψ and, from these, χ for polyisobutylene in diisobutylketone.

10. Shultz and Flory† measured the critical temperature for precipitation for polystyrene fractions of different molecular weight in cyclohexane. The following results were obtained:

	A	B	C	D
T_c (°C)	19.4	23.6	27.5	31.1
$\bar{n}$	419	856	2,404	12,210

Use the method described in Problem 9 to obtain values of Θ and ψ from these data. How do the values of these parameters compare with the values obtained for the same system from osmotic pressure data in Problem 8?

† A. R. Shultz and P. J. Flory, *J. Am. Chem. Soc.* 74:4760 (1952).

Compare the two methods in terms of the assumptions involved, the supplementary information required, and the sensitivity to experimental error.

11. The following values of Π/c_2 versus c_2 were measured† at 25°C in 0.15 m NaCl solutions for bovine serum albumin:

At pH 5.37				
c_2 (g liter^{-1})	8.8	17.5	27.5	56.3
Π/c_2 (Torr liter g^{-1})	0.280	0.284	0.308	0.348
At pH 7.00				
c_2 (g liter^{-1})	16.9	29.4	50.6	56.9
Π/c_2 (Torr liter g^{-1})	0.312	0.336	0.384	0.399

At pH 5.37 this molecule is known to possess no net charge. The data under these conditions is the basis for Example 8.7. Verify the values of M and the slope given in that example. At pH 7.00 this polymer is known to have a charge of about −12. Based on a comparison of the above data at pH 5.37 and 7.00, what conclusion can be drawn about the swamping electrolyte concentration relative to 0.15 m NaCl? Criticize or defend the following proposition: The excluded volume of the bovine serum albumin molecule is larger at pH 7.00 than at pH 5.37 because the atmosphere of counterions contributes to the excluded volume for a charged polymer. If this is the case, the slope at pH 7.00 is expected to show a smaller intercept and a slope closer to that at pH 5.37 if the salt concentration is lowered significantly. (Hint: Consult a physical chemistry textbook for the concentration dependence of the thickness of the ion atmosphere according to the Debye-Huckel theory.)

Bibliography

1. Flory, P. J., *Principles of Polymer Chemistry*, Cornell Univesity Press, Ithaca, N.Y., 1953.
2. Hiemenz, P. C., *Principles of Colloid and Surface Chemistry*, Marcel Dekker, New York, 1977.
3. Morawitz, H., *Macromolecules in Solution*, Interscience, New York, 1965.
4. Richards, E. G., *An Introduction to the Physical Properties of Large Molecules in Solution*, Cambridge University Press, Cambridge, 1980.
5. Tanford, C., *Physical Chemistry of Macromolecules*, Wiley, New York, 1961.
6. Tompa, H., *Polymer Solutions*, Butterworths, London, 1956.

† G. Scatchard, A. C. Batchelder, and A. Brown, *J. Am. Chem. Soc.* 68:2320 (1946).

9

Frictional Properties of Polymers in Solution

I give you the end of a golden string,
Only wind it into a ball
It will lead you in at Heaven's gate,
Built in Jerusalem's wall.

Jerusalem, William Blake

9.1 Introduction

This chapter contains one of the more diverse assortments of topics of any chapter in the volume. In it we discuss the viscosity of polymer solutions, especially the intrinsic viscosity; the diffusion and sedimentation behavior of polymers, including the equilibrium between the two; and the analysis of polymers by gel permeation chromatography (GPC). At first glance these seem to be rather unrelated topics, but features they all share are a dependence on the spatial extension of the molecules in solution and applicability to molecular weight determination.

In addition to an array of experimental methods, we also consider a more diverse assortment of polymeric systems than has been true in other chapters. Besides synthetic polymer solutions, we also consider aqueous protein solutions. The former polymers are well represented by the random coil model; the latter are approximated by rigid ellipsoids or spheres. For random coils changes in the goodness of the solvent affects coil dimensions. For aqueous proteins the solvent-solute interaction results in various degrees of hydration, which also changes the size of the molecules. Hence the methods we discuss are all potential sources of information about these interactions between polymers and their solvent environments.

Both the intrinsic viscosity and GPC behavior of random coils are related to the radius of gyration as the appropriate size parameter. We shall see how the radius of gyration can be determined from solution viscosity data for these

systems, and how changes in the coil dimensions with changing conditions can be measured. We emphasize biopolymers in discussing diffusion-sedimentation behavior and discover that the axial ratio of the ellipsoidal particles is the kind of size information we obtain from these studies.

Another parameter that plays an important role in unifying viscosity, diffusion, and sedimentation is the friction factor. This proportionality factor between velocity and the force of frictional resistance was introduced in Chap. 2, and its role in interrelating the topics of this chapter is reflected in the title of the chapter.

Some exceptionally gifted researchers have made contributions to the topics we discuss here, and their impact on these and other areas of inquiry have earned them special recognition. Specifically, we note that Einstein, Svedberg, Staudinger, and Flory have all been awarded the Nobel Prize, and Stokes and Poiseuille have been honored by having units named after them. These are but a few of the "superstars" whose work we encounter in this chapter.

9.2 Viscous Forces on Rigid Spheres

In Sec. 2.2 we saw that the coefficient of viscosity is defined as the factor of proportionality between the shearing force per unit area $\sigma_s = F_s/A$ and the velocity gradient dv/dy within a liquid [Eq. (2.2)]:

$$\frac{F_s}{A} = \eta \frac{dv}{dy} \tag{9.1}$$

This definition is general; it applies equally to pure liquids and to solutions, to situations in which η is constant and those in which it is a function of the velocity gradient or rate of shear. Our interest in this chapter is the application of this concept to polymer solutions—dilute solutions at that—and we shall limit our attention to cases in which the rate of shear is low enough that the Newtonian limiting behavior applies and η is independent of dv/dy. In the next section we shall consider the measurement and interpretation of viscosity under these conditions, but, rather than turning to this immediately, we begin by considering the frictional force arising from viscosity as it affects rigid spheres submerged in a flowing liquid. The purpose of starting this way is twofold. First, it will review some of the general ideas about viscosity from Chap. 2, and, second, it will introduce two important relationships, due to Stokes and Einstein, respectively, which will recur often in this chapter.

The shearing force that is part of the definition of viscosity can also be analyzed in terms of Newton's second law and written as

$$F = ma = m \frac{dv}{dt} \tag{9.2}$$

When Eqs. (9.1) and (9.2) are combined, we obtain

$$\frac{m}{A}\frac{dv}{dt} = \eta \frac{dv}{dy} \tag{9.3}$$

If it were complete, Eq. (9.3) would be a differential equation whose solution would give v, the velocity of the flowing liquid, as a function of time and position within the sample. Equation (9.3) does not tell the whole story, however. Other forces are also operative: External forces of, say, gravitational or mechanical origin are responsible for the motion in the first place, and pressure forces are associated with the velocity gradient. In general, things are not limited to one direction in space, but the forces, gradients, and velocities have x, y, and z components. It is possible to bring these considerations together in a very general form by adding together all of the forces acting on a volume element of liquid, including the viscous force defined by Eq. (9.1), and using the net force and the mass of the volume element in Eq. (9.2). The resulting expression is called the equation of motion and is the cornerstone of fluid mechanics. The equation of motion is generally written in terms of vector operators and takes on a variety of forms, depending on the system of coordinates and the vector identities that have been employed. If the equation of motion is complicated even in the writing, things are even worse in the solving! Accordingly, we defer solutions to the experts in this area and merely note that a full-fledged hydrodynamic analysis of a flow problem begins with the equation of motion, which, in turn, is F = ma applied to a volume element subject to complex forces.

As with any differential equation, an important part of solving the equation of motion is defining the boundary conditions. For the purpose of our discussion, an important boundary condition is that no slippage occur at the boundary between a moving fluid and a rigid wall. This is best understood by imagining the liquid to consist of an array of thin slices which follow the contours of the wall. The nonslip condition means that the layer which is adjacent to a stationary wall has a velocity of zero also, with successive layers away from the wall possessing larger increments of velocity. At a sufficiently large distance from the wall, a net velocity is attained which is unperturbed by the presence of the surface. In Sec. 9.4, we shall apply this idea to the flow of a liquid through a capillary tube. For now we qualitatively consider two classic problems involving the effect of rigid spheres on the flow behavior of a liquid.

The first of these problems involves relative motion between a rigid sphere and a liquid as analyzed by Stokes in 1850. The results apply equally to liquid flowing past a stationary sphere with a steady-state (subscript s) velocity v_s or to a sphere moving through a stationary liquid with a velocity $-v_s$; the relative motion is the same in both cases. If the relative motion is in the vertical direction, we may visualize the slices of liquid described above as consisting of

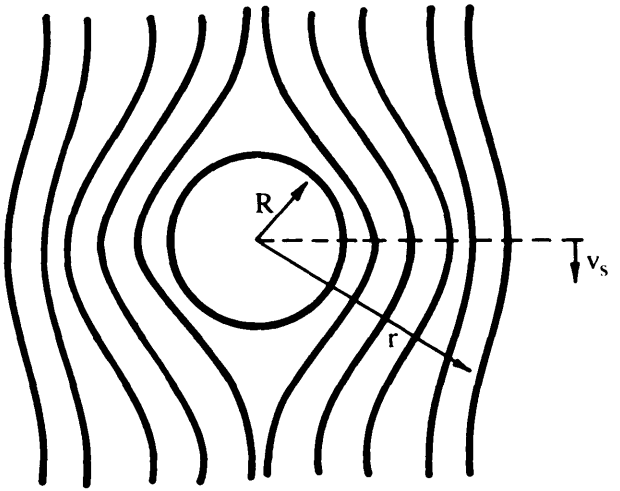

Figure 9.1 Distortion of flow streamlines around a spherical particle of radius R. The relative velocity in the plane containing the center of the sphere equals v_s as $r \to \infty$.

a bundle of layers, some of which are shown schematically in Fig. 9.1. In the plane containing the center of the sphere a limiting velocity v_s is reached as the distance r from the center of the sphere becomes large. This would be the observable settling velocity of such a spherical particle, for example. In an infinitesimally thin layer adjacent to the surface, the tangential component of velocity would be that of the solid sphere. This is the nonslip condition as it applies to this problem. This means that a velocity gradient exists that is described in terms of the distance from the center of the sphere and the component of velocity which is perpendicular to r. By considering the units of the velocity gradient and the units of some physically pertinent variables, it seems plausible that dv/dr is proportional to v_s/R, where R is the radius of the sphere. (In this chapter our problem is too many r's; be attentive to the specific radius this symbol represents in different contexts.) Formal analysis of the problem via the equation of motion verifies this argument from dimension and provides the necessary proportionality factors as well.

From Eq. (9.1) we see that the viscous force associated with this motion equals $[\eta(dv/dr)]$ (area), where the pertinent area is proportional to the surface of the sphere and varies as R^2. This qualitative argument suggests that the viscous force opposing the relative motion of the liquid and the sphere is proportional to $[\eta(v_s/R)](R^2)$. The complete solution to this problem reveals that both pressure and shear forces arising from the motion are proportional to $\eta R v_s$, and the total force of viscous resistance is given by

$$F_{vis} = 6\pi\eta R v_s \tag{9.4}$$

which is Stokes' law for rigid spheres. In Chap. 2 we found it convenient to call the factor of proportionality between the force of resistance and the steady-state velocity the friction factor f. We emphasize that the viscosity in Eq. (9.4) is that of the medium surrounding the sphere by labeling it with the subscript 0, and write

$$f = 6\pi\eta_0 R \tag{9.5}$$

for spherical particles of radius R.

A somewhat similar problem arises in describing the viscosity of a suspension of spherical particles. This problem was analyzed by Einstein in 1906, with some corrections appearing in 1911. As we did with Stokes' law, we shall only present qualitative arguments which give plausibility to the final form. The fact that it took Einstein 5 years to work out the "bugs" in this theory is an indication of the complexity of the formal analysis. Derivations of both the Stokes and Einstein equations which do not require vector calculus have been presented by Lauffer [Ref. 3]. The latter derivations are at about the same level of difficulty as most of the mathematics in this book. We shall only hint at the direction of Lauffer's derivation, however, since our interest in rigid spheres is marginal, at best.

Figure 2.1 served as the basis for our initial analysis of viscosity, and we return to this representation now with the stipulation that the volume of fluid sandwiched between the two plates is a unit of volume. This unit is defined by a unit of contact area with the walls and a unit of separation between the two walls. Next we consider a shearing force acting on this cube of fluid to induce a unit velocity gradient. According to Eq. (2.6), the rate of energy dissipation per unit volume from viscous forces dW/dt is proportional to the square of the velocity gradient, with η_0 (pure liquid, subscript 0) the factor of proportionality:

$$\frac{dW}{dt} = \eta_0 \left(\frac{dv}{dy}\right)^2 \tag{9.6}$$

Thus, to maintain a unit gradient, a volume rate of energy dissipation equal to η_0 is required.

Next we consider replacing the sandwiched fluid with the same liquid in which solid spheres are suspended at a volume fraction ϕ. Since we are examining a unit volume of liquid—a suspension of spheres in this case—the total volume of the spheres is also ϕ. We begin by considering the velocity gradient if the velocity of the top surface is to have the same value as in the case of the

pure liquid. Being solid, the suspended spheres contribute nothing to the velocity gradient. As far as the gradient is concerned, the spheres might as well be allowed to settle to the bottom and then be fused to the lower, stationary wall. The equivalency of the suspended spheres and a uniform layer of the same volume are illustrated schematicaly in Figs. 9.2a and b, respectively. Since the unit volume has a unit cross-sectional area, a volume ϕ fused to the base will raise the stationary surface by a distance ϕ and leave a liquid of thickness $1 - \phi$ to develop the gradient. These dimensions are also shown in Fig. 9.2b. If the velocity of the top layer is required to be the same in this case as for the pure solvent, then the gradient *in the liquid* need only be the fraction $1/(1 - \phi)$ of that for the pure liquid. Of course, since ϕ is less than unity, this "fraction" is grater than unity.

Now we return to consider the energy that must be dissipated in a unit volume *of suspension* to produce a unit gradient, as we did above with the pure solvent. The same "fraction" applied to the shearing force will produce the unit gradient, and the same "fraction" also describes the volume rate of energy dissipation compared to the situation described above for pure solvent. Since the latter was η_0, we write for the suspension, in the case of $dv/dy = 1$,

$$\frac{dW}{dt} = \eta = \frac{1}{1 - \phi}\,\eta_0 \tag{9.7}$$

Again, since $\phi < 1$, $\eta > \eta_0$.

This is only one of the contributions to the total volume rate of energy dissipation; a second term which arises from explicit consideration of the individual spheres must also be taken into account. This second effect can be shown to equal $1.5\,\phi\eta_0/(1 - \phi)^2$; therefore the fully theory gives a value for η, the viscosity of the suspension:

$$\eta = \frac{\eta_0}{1 - \phi} + \frac{1.5\,\phi\eta_0}{(1 - \phi)^2} = \eta_0\,\frac{1 + 0.5\,\phi}{(1 - \phi)^2} \tag{9.8}$$

One additional assumption which underlies the derivation of the second term in Eq. (9.8) is that ϕ is small. This being the case, $1/(1 - \phi)^2$ can be replaced by the leading terms of the series expansion $(1 + \phi + \phi^2 + \cdots)^2$ to give

$$\eta = \eta_0\left(1 + \frac{1}{2}\,\phi\right)(1 + \phi + \cdots)^2 = \eta_0(1 + 2.5\,\phi + 4\,\phi^2 + \cdots) \tag{9.9}$$

This is Einstein's famous viscosity equation:

1. η is the viscosity of the suspension as a whole; η_0 is the viscosity of the solvent, and ϕ is the volume fraction occupied by the spheres.

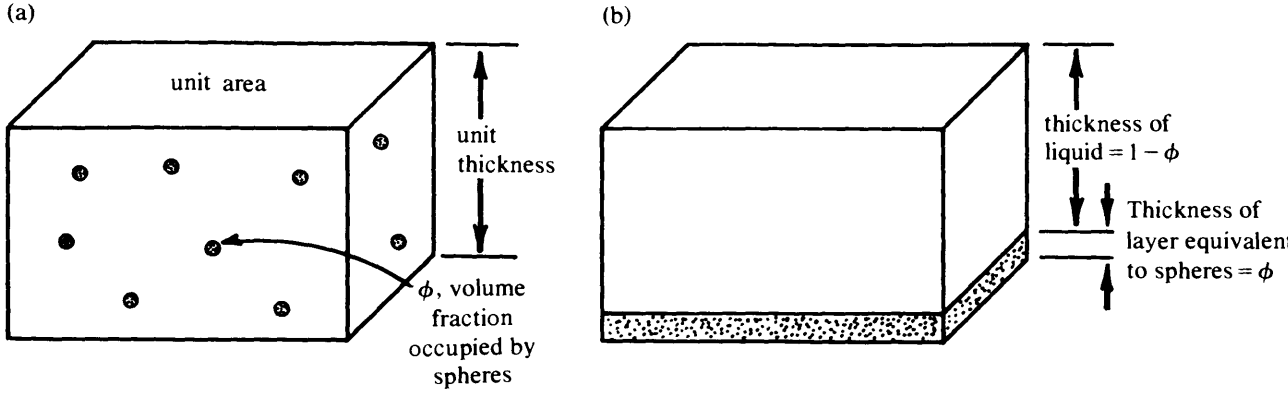

Figure 9.2 (a) Schematic representation of a unit cube containing a suspension of spherical particles at volume fraction ϕ. (b) The volume equivalent to the spheres in (a) is fused to the base, leaving $1 - \phi$ as the thickness of liquid.

2. The validity is limited to small values of ϕ, so Eq. (9.9) is generally truncated after the first two terms on the right-hand side.
3. By describing the concentration dependence of an observable property as a power series, Eq. (9.9) plays a comparable role for viscosity as Eq. (8.83) does for osmotic pressure.
4. The volume fraction emerges from the Einstein derivation at the natural concentration unit to describe viscosity. This parallels the way volume fraction arises as a natural thermodynamic concentration unit in the Flory–Huggins theory as seen in Sec. 8.3.

Both the Stokes and Einstein equations have certain features in common which arise from the hydrodynamic origins they share:

1. The liquid medium is assumed to be continuous. This makes the results suspect when applied to spheres which are so small that the molecular nature of the solvent cannot be ignored.
2. Both relationships have been repeatedly verified for a variety of systems and for spheres with a wide range of diameters. Despite item (1), both Eqs. (9.4) and (9.9) have often been applied to individual molecules, for which they work surprisingly well.
3. The spherical geometry assumed in the Stokes and Einstein derivations gives the highly symmetrical boundary conditions favored by theoreticians. For ellipsoids of revolution having an axial ratio a/b, friction factors have been derived by F. Perrin, and the coefficient of the first-order term in Eq. (9.9) has been derived by Simha. In both cases the calculated quantities increase as the axial ratio increases above unity. For spheres, $a/b = 1$.
4. In the derivation of both Eqs. (9.4) and (9.9), the disturbance of the flow streamlines is assumed to be produced by a single particle. This is the origin of the limitation to dilute solutions in the Einstein theory, where the net effect of an array of spheres is treated as the sum of the individual nonoverlapping disturbances. When more than one sphere is involved, the same limitation applies to Stokes' law also. In both cases contributions from the walls of the container are also assumed to be absent.

We shall make further use of the Stokes' equation later in this chapter; for the present, viscosity is our primary concern, and the Einstein equation is our point of departure.

9.3 The Intrinsic Viscosity of Rigid Molecules

One thing that is apparent at the outset is that polymer molecules in solution are very different species from the rigid spheres upon which the Einstein theory is based. On the other hand, we saw in the last chapter that the random coil contributes an excluded volume to the second virial coefficient that is at least

proportional to the volume of a sphere of radius r_g [see Eq. (8.114)]. Whether this thermodynamic conclusion applies to hydrodynamic behavior or not, and, if so, under what conditions, will be discussed in Sec. 9.6. By contrast, a compact protein molecule held in a spherical tertiary structure by hydrogen bonds and disulfide linkages may be reasonably approximated as a rigid sphere. Accordingly, we begin this section by considering the applicability of the Einstein equation to the latter systems. Then we shall consider the extension of these ideas to other rigid particles of nonspherical geometry. Again we emphasize that proteins, because of the intramolecular crosslinking they possess, are the kind of polymers that are best approximated by models of rigid bodies.

As in osmotic pressure experiments, polymer concentations are usually expressed in mass volume^{-1} units rather than in the volume fraction units indicated by the Einstein equation. For dilute solutions, however, Eq. (8.100) shows that ϕ can be approximated as $c_2\bar{V}_2/M$, where c_2 is the mass of polymer per volume of solution, $\bar{V}_2$ is the partial molar volume of the polymer in solution, and M is the molecular weight of the polymer. Substituting this relationship for ϕ in Eq. (9.9) gives

$$\eta = \eta_0 \left[1 + 2.5 \frac{\bar{V}_2}{M} c_2 + 4\left(\frac{\bar{V}_2}{M}\right)^2 c_2^2 + \cdots \right] \tag{9.10}$$

a form which is reminiscent of Eq. (8.86) for osmotic pressure. A comparison of these results may momentarily suggest that Eq. (9.10) can also be used to evaluate the molecular weight of a polymer—at least for rigid-sphere molecules. Further reflection, however, shows that the first-order term in the osmotic pressure expression is proportional to M^{-1}, while the corresponding term in Eq. (9.10) involves $\bar{V}_2/M$, which is simply the reciprocal of the density of the polymer *as it exists in solution*. While this density is not as fundamental as the molecular weight in the characterization of a polymer, it turns out that the ability to measure this quantity through viscosity is an important application of viscosity studies. As indicated above, the most plausible systems on which to apply Eq. (9.10) are solutions of those proteins which are known to possess spherical molecules. Such molecules are often extensively hydrated in aqueous solutions, and the degree of solvation is reflected in $\bar{V}_2$. We shall presently consider an example which illustrates how the extent of protein hydration can be extracted from viscosity data.

Before turning to this, however, it is useful to introduce some additional vocabulary that is often employed in discussing solution viscosity. Equation (9.10) is a special case of the general function

$$\eta = A + Bc_2 + Cc_2^2 + \cdots \tag{9.11}$$

in which the coefficients A, B, and so on, are determined simply by fitting experimental data. Since the viscosity of the solution must approach that of

the solvent as the solute concentration goes to zero, it is apparent that $A = \eta_0$; the Einstein equation tells what the coefficient B must be for spherical particles. Working with the more general form for the moment, we can define the following quantities and symbols in terms of Eq. (9.11):

1. The relative viscosity η/η_0. This is obtained from Eq. (9.11) simply by dividing both sides of the equation through by the viscosity of the solvent ($B' = B/\eta_0$, etc.):

$$\eta_r = \frac{\eta}{\eta_0} = 1 + B'c_2 + C'c_2^2 + \cdots \tag{9.12}$$

2. The specific viscosity, $\eta/\eta_0 - 1$. This is obtained by subtracting unity from both sides of Eq. (9.12):

$$\eta_{sp} = \frac{\eta}{\eta_0} - 1 = B'c_2 + C'c_2^2 + \cdots \tag{9.13}$$

Since $\eta/\eta_0 - 1 = (\eta - \eta_0)/\eta_0$, the specific viscosity describes the excess viscosity of the solution above the viscosity of the solvent relative to the latter.

3. The reduced viscosity $(1/c_2)(\eta/\eta_0 - 1)$. This is obtained by dividing both sides of Eq. (9.13) by c_2; in this sense it is analogous to the reduced osmotic pressure:

$$\eta_{red} = \frac{1}{c_2}\left(\frac{\eta}{\eta_0} - 1\right) = B' + C'c_2 + \cdots \tag{9.14}$$

The reduced viscosity expresses the specific viscosity per unit of solute concentration.

4. The intrinsic viscosity $\lim_{c_2 \to 0} \eta_{red}$. Equation (9.14) shows that η_{red} varies linearly with c_2, at least for dilute solutions. In graphical terms, the intrinsic viscosity—B' in Eq. (9.14)—is the intercept in a plot of η_{red} versus c_2. Since the intrinsic viscosity is a limiting value at infinite dilution, it is a parameter which directly reflects the molecular properties of the solute. For this last reason intrinsic viscosity is the form of greatest usefulness in discussing solution viscosity. Intrinsic viscosity is given the symbol $[\eta]$ and has units of concentration^{-1}.

5. The inherent viscosity $(1/c_2) \ln (\eta/\eta_0)$. A plot of inherent viscosity versus concentration also extrapolates to $[\eta]$ in the limit of $c_2 \to 0$. That this is the case is readily seen by combining Eq. (9.12) with the definition of the inherent viscosity and then expanding the logarithm:

$$\eta_{inh} = \frac{1}{c_2} \ln (1 + B'c_2 + C'c_2^2 + \cdots) \cong \frac{B'c_2 + C'c_2^2 + \cdots}{c_2} \tag{9.15}$$

In the polymer literature each of the five quantities listed above is encountered frequently. Complicating things still further is the fact that a variety of concentration units are used in actual practice. In addition, IUPAC terminology is different from the common names listed above. By way of summary, Table 9.1 lists the common and IUPAC names for these quantities and their definitions. Note that when ϕ is used as the unit of concentration, $[\eta] = 2.5$ for spheres according to the Einstein equation.

With this terminology in mind, we can restate the objective of this section as the interpretation of the intrinsic viscosities of solutions of rigid molecules. If the solute molecules are known to be spherical, comparison of Eqs. (9.10) and (9.14) shows that the intrinsic viscosity for such systems is given by

$$[\eta] = 2.5 \frac{\bar{V}_2}{M} \tag{9.16}$$

Table 9.1 Summary of Names and Definitions of the Various Functions of η, η_0, and c_2 in Which Solution Viscosities are Frequently Discussed

Symbol	Definition	Common name	IUPAC name
η_r	$\frac{\eta}{\eta_0}$	Relative viscosity	Viscosity ratio
η_{sp}	$\frac{\eta}{\eta_0} - 1$	Specific viscosity	–
η_{red}	$\frac{1}{c_2}\left(\frac{\eta}{\eta_0} - 1\right)$	Reduced viscosity	Viscosity number
$[\eta]$	$\lim_{c_2 \to 0} \frac{1}{c_2}\left(\frac{\eta}{\eta_0} - 1\right)$	Intrinsic viscosity	Limiting viscosity number
η_{inh}	$\frac{1}{c_2} \ln\left(\frac{\eta}{\eta_0}\right)$	Inherent viscosity	Logarithmic viscosity number
	$\left(\lim_{c_2 \to 0} \eta_{inh} = [\eta] \text{ also}\right)$		

We take the position that $[\eta]$ is known from experiment and assume that M is also known from some other type of experiment, say, osmostic pressure. Assuming that these data are available enables us to evaluate $\bar{V}_2$, and we consider next what this quantity tells us about the state of solvation of the polymer.

If the solute molecule is solvated, then any bound (subscript b) solvent (subscript 1) must be added to the volume of the unsolvated solute (subscript 2): that is,

$$\text{Volume of solvated particle} = V_{2,\text{dry}} + V_{1,\text{b}} \tag{9.17}$$

where $V_{2,\text{dry}}$ is the volume of the unsolvated solute molecule. If we further define $m_{1,\text{b}}/m_2$ as the mass of solvent bound per mass of solute and represent the densities of the solvent and solute as ρ_1 and ρ_2, respectively, then Eq. (9.17) becomes

$$\begin{aligned}\text{Volume of solvated particle} &= V_{2,\text{dry}}\left(1 + \frac{V_{1,\text{b}}}{V_{2,\text{dry}}}\right) \\ &= V_{2,\text{dry}}\left(1 + \frac{m_{1,\text{b}}}{m_2}\frac{\rho_2}{\rho_1}\right)\end{aligned} \tag{9.18}$$

An alternative in writing this last result would be to use $\rho_{1,\text{b}}$, since the density of the bound solvent is expected to be different from that in bulk. Rather than pursue this, however, we shall assume instead that $\rho_{1,\text{b}} = \rho_1$ and, on this basis, seek to evaluate $m_{1,\text{b}}/m_2$ from intrinsic viscosity data. The factor in parentheses in Eq. (9.18) corrects the volume of any amount of solute for the effects of solvation. Applied to the volume of 1 mol of dry polymer, we obtain for Eq (9.16)

$$[\eta] = 2.5\left(1 + \frac{m_{1,\text{b}}}{m_2}\frac{\rho_2}{\rho_1}\right)\Big/\rho_2 \tag{9.19}$$

where $1/\rho_2 = (V_2^\circ/M)_{\text{dry}}$. In the following example we see how this result can be applied to data collected from solutions of spherical protein molecules.

Example 9.1

The serum albumin molecule is known to have an approximately spherical shape (see Example 8.7) and is found† to have an intrinsic viscosity in aqueous buffer solutions of 3.7 $\text{cm}^3\ \text{g}^{-1}$. Using $\rho_2 = 1.34\ \text{g cm}^{-3}$ as the density of the

† C. Tanford, *Adv. Protein Chem.* 23:121 (1968).

unsolvated polymer, estimate the quantity of water bound by this protein under the conditions of the experiment.

Solution

The units of $[\eta]$ reveal the concentration units in this experiment to be grams of protein per cubic centimer of solution. Dividing this concentration unit by the density of the unsolvated protein converts these concentration units to volume fractions:

$$\frac{\text{g protein}}{\text{cm}^3 \text{ solution}} \times \frac{\text{cm}^3 \text{ protein}}{\text{g protein}} = \frac{\text{cm}^3 \text{ protein}}{\text{cm}^3 \text{ solution}}$$

Since c_2 rather than ϕ is used in the determination of $[\eta]$, the factor $1/\rho_2$ as well as any contribution of solvation increases $[\eta]$ above the value 2.5; thus we can use Eq. (9.19) directly to interpret this data:

$$\left(1 + \frac{m_{1,b}}{m_2}\frac{\rho_2}{\rho_1}\right) = \frac{[\eta]\,\rho_2}{2.5} = \frac{3.7(1.34)}{2.5} = 1.98$$

Therefore

$$\frac{m_{1,b}}{m_2} = 0.98\,\frac{\rho_1}{\rho_2} = \frac{0.98(1.00)}{1.34} = 0.73 \text{ g water (g protein)}^{-1}$$

•

In the last section we noted that Simha and others have derived theoretical expressions for η_{sp}/ϕ for rigid ellipsoids of revolution. Solving the equation of motion for this case is even more involved than for spherical particles, so we simply present the final result. Several comments are necessary to appreciate these results:

1. The totally symmetrical sphere is characterized by a single size parameter: its radius. Ellipsoids of revolution are used to approximate the shape of unsymmetrical bodies. Ellipsoids of revolution are characterized by two size parameters.
2. The ellipsoid of revolution is swept out by rotating an ellipse along its major or minor axis. When the major axis is the axis of rotation, the resulting rodlike figure is said to be prolate; when the minor axis is the axis of rotation, the disklike figure is said to be oblate.
3. We designate the length of the ellipsoid along the axis of rotation as 2a and the equatorial diameter as 2b to define the axial ratio a/b which characterizes the ellipticity of the particle. By this definition, $a/b > 1$ corresponds to prolate ellipsoids, and $a/b < 1$ to oblate ellipsoids.

4. The viscosity of a suspension of ellipsoids depends on the orientation of the particle with respect to the flow streamlines. The ellipsoidal particle causes more disruption of the flow when it is perpendicular to the streamlines than when it is aligned with them; the viscosity in the former case is greater than in the latter. For small particles the randomizing effect of Brownian motion is assumed to override any tendency to assume a preferred orientation in the flow.

Based on these ideas, the intrinsic viscosity (in ϕ concentration units) has been evaluated for ellipsoids of revolution. Figure 9.3 shows $[\eta]$ versus a/b for oblate and prolate ellipsoids according to the Simha theory. Note that the intrinsic viscosity of serum albumin from Example 9.1–3.7(1.34) = 4.96 in volume fraction units—is also consistent with, say, a nonsolvated oblate ellipsoid of axial ratio about 5.

For solutions of rigid particles, then, the intrinsic viscosity exceeds 2.5 as a result of some combination of the following effects:

$$\frac{[\eta]}{2.5} = (\text{effect of concentration units})(\text{effect of solvation})(\text{effect of ellipticity}) \tag{9.20}$$

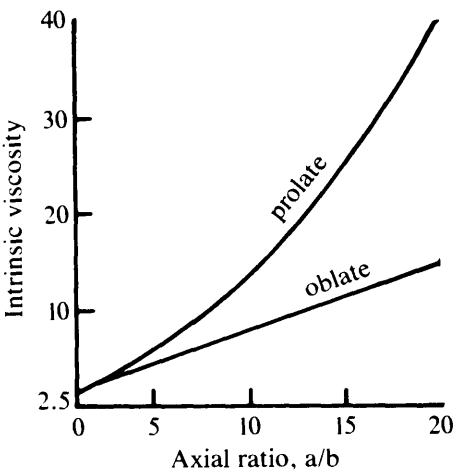

Figure 9.3 Intrinsic viscosity according to the Simha theory in terms of the axial ratio for prolate and oblate ellipsoids of revolution.

These factors having the following significance:

1. The first term reflects the fact that, in practice, volume fraction is not the concentration unit ordinarily used. Even for nonsolvated spheres, some factors will modify the Einstein 2.5 term merely as a result of reconciling practical concentration units with ϕ [Eq. (9.16)]. We assume that this factor poses no particular problem in evaluation.
2. The second term allows for solvation, which effectively increases the volume fraction of the particles to a larger value than that calculated on the basis of dry solute. Equation (9.18) shows how this can be quantified.
3. The effect of ellipticity also increases $[\eta]$ above the 2.5 value obtained for spheres. Analytical functions as well as graphical representations like Fig. 9.3 are available to describe this effect in terms of the axial ratios of the particles. In principle, therefore, a/b values for nonsolvated, rigid particles can be estimated from experimental $[\eta]$ values.
4. It is a frustrating aspect of Eq. (9.20) that the observed intrinsic viscosities contain the effects of ellipticity and solvation such that the two cannot be resolved by viscosity experiments alone. That is, for any value of $[\eta]$, there is a whole array of solvation-ellipticity values which are consistent with the observed intrinsic viscosity.

This state of affairs is summarized in Fig. 9.4a, which plots contours for different values of $[\eta]$ in terms of compatible combinations of $m_{1,b}/m_2$ and a/b. For the aqueous serum albumin described in Example 9.1 as an illustration, any solvation-ellipticity combination which corresponds roughly to $[\eta] = 5$ is possible for this system. Data from some other source are needed to pin down a more specific characterization.

We shall see in Sec. 9.10 that sedimentation and diffusion data yield experimental friction factors which may also be described–by the ratio of the experimental f to f_0, the friction factor of a sphere of the same mass–as contours in solvation-ellipticity plots. The two different kinds of contours differ in detailed shape, as illustrated in Fig. 9.4b, so the location at which they cross provides the desired characterization. For the hypothetical system shown in Fig. 9.4b, the axial ratio is about 2.5 and the protein is hydrated to the extent of about 1.0 g water (g polymer)$^{-1}$.

In all of these derivations concerning rigid bodies, no other walls are considered except the particle surfaces. Before we turn to the question of the intrinsic viscosity of flexible polymers, let us consider the relationship between the viscosity of a fluid and the geometry and dimensions of the container in which it is measured.

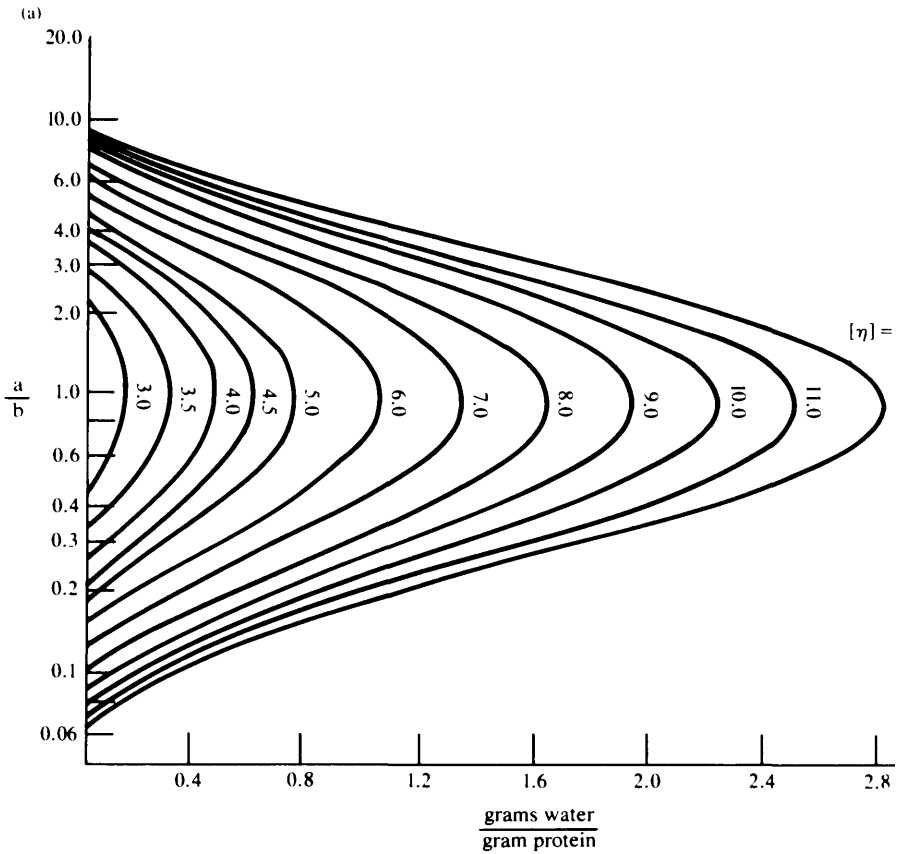

Figure 9.4 (a) For aqueous protein solutions, variation of $[\eta]$ with the axial ratio and extent of hydration. [Redrawn with permission from J. L. Oncley, *Ann. N.Y. Acad. Sci.* 41:121 (1941).] (b) Intrinsic viscosity and friction factor contours in terms of the axial ratio and extent of hydration. The crossover gives unambiguous characterization. (From Ref. 2, p. 106.)

9.4 The Poiseuille Equation and Capillary Viscometers

We defined the equation of motion as a general expression of Newton's second law applied to a volume element of fluid subject to forces arising from pressure, viscosity, and external mechanical sources. Although we shall not attempt to use this result in its most general sense, it is informative to consider the equation of motion as it applies to a specific problem: the flow of liquid through a capillary. This consideration provides not only a better appreciation of the equation of

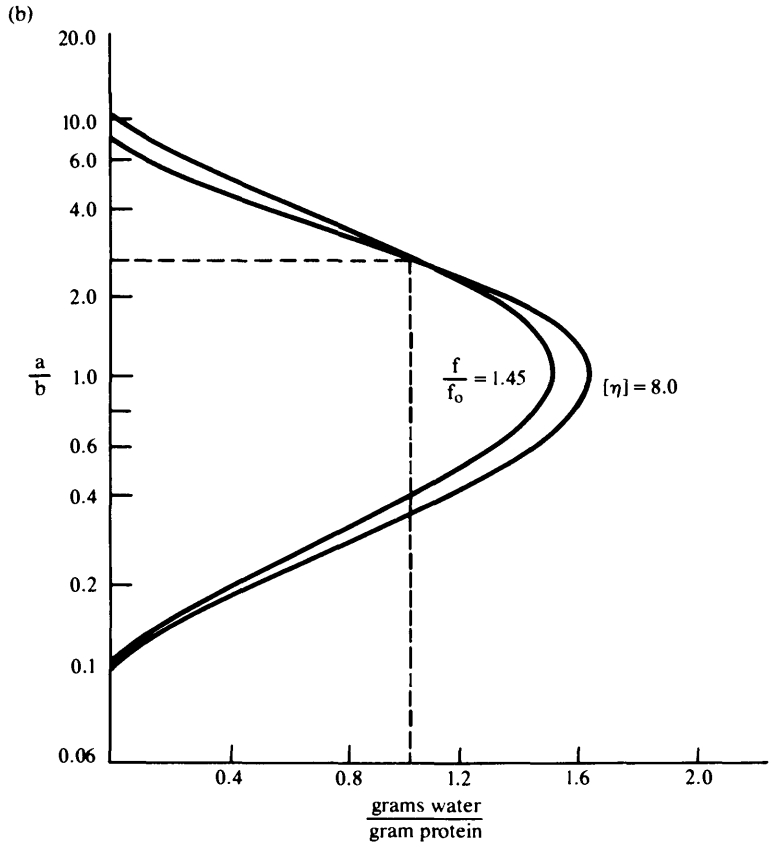

Figure 9.4 *(continued)*

motion, but also serves as the basis for an important technique for measuring solution viscosity. We shall examine the derivation first and then discuss its application to experiment.

Figure 9.5a shows a portion of a cylindrical capillary of radius R and length l. We measure the general distance from the center axis of the liquid in the capillary in terms of the variable r and consider specifically the cylindrical shell of thickness dr designated by the broken line in Fig. 9.5a. In general, gravitational, pressure, and viscous forces act on such a volume element, with the viscous forces depending on the velocity gradient in the liquid. Our first task, then, is to examine how the velocity of flow in a cylindrical shell such as this varies with the radius of the shell.

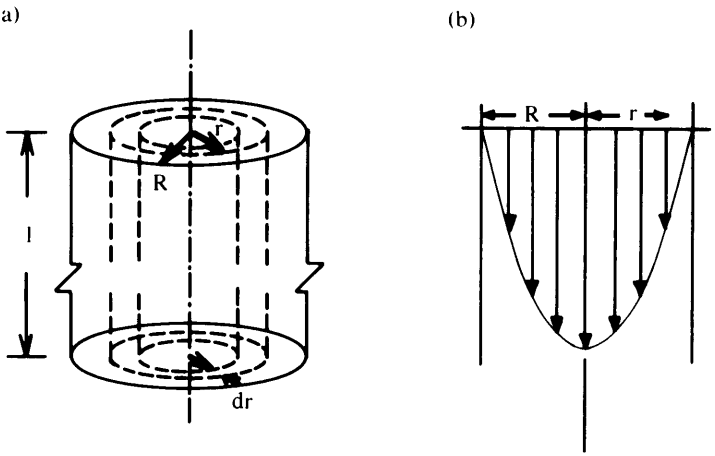

Figure 9.5 (a) Portion of a cylinder of radius R and length l showing (by broken lines) section of thickness dr. (b) Profile of flow velocity in the cylinder. (From Ref. 2, pp. 52 and 54.)

The net viscous force acting on this volume element is given by the difference between the frictional forces acting on the outer and inner surfaces of the shell:

$$F_{vis,net} = (F_{vis})_{out} - (F_{vis})_{in} = 2\pi(r + dr)\,l\eta\left(\frac{dv}{dr}\right)_{r+dr} - 2\pi r\,l\eta\left(\frac{dv}{dr}\right)_{r} \tag{9.21}$$

where the length times the circumference of the surface describes the appropriate area in Eq. (9.1). The relationship between the velocity gradient at the two locations is given by

$$\left(\frac{dv}{dr}\right)_{r+dr} = \left(\frac{dv}{dr}\right)_{r} + \left(\frac{d^2v}{dr^2}\right) dr \tag{9.22}$$

provided that dr is small. Combining Eqs. (9.21) and (9.22) and retaining only those terms which are first order in dr gives

$$F_{vis,net} = 2\pi\eta l\left[r\left(\frac{d^2v}{dr^2}\right)dr + \left(\frac{dv}{dr}\right)dr\right] = 2\pi\eta l\,\frac{d}{dr}\left(r\,\frac{dv}{dr}\right) \tag{9.23}$$

Under stationary-state conditions of flow, that is, when no further acceleration occurs, this force is balanced by gravitational and pressure forces. For

simplicity, we assume that the capillary is oriented vertically so that gravity operates downward and, for generality, we assume that an additional mechanical pressure Δp exists between the two ends of the capillary. Under these conditions the net gravitational and mechanical forces acting on the volume element equal

$$F_{grav,mech,net} = (2\pi\, l\, r\, dr)\rho g + (2\pi r\, dr)\,\Delta p \tag{9.24}$$

where $2\pi l r\, dr$ is the volume of the element and $2\pi r\, dr$ is its cross-sectional area. Under the stationary-state conditions we seek to describe, Eqs. (9.24) and (9.23) are equal and the following relationship applies to the volume element:

$$\eta \frac{d}{dr}\left(r \frac{dv}{dr}\right) = \left(\rho g + \frac{\Delta p}{l}\right) r\, dr \tag{9.25}$$

Integration converts this to

$$\eta r \frac{dv}{dr} = \frac{1}{2}\left(\rho g + \frac{\Delta p}{l}\right) r^2 \tag{9.26}$$

where the fact that $r(dv/dr) = 0$ at $r = 0$ is used to eliminate the integration constant. Note that the velocity gradient is directly proportional to the radial position in the fluid: It is zero at the axis and has a maximum value at $r = R$.

Equation (9.26) can be integrated again to give v as a function of r:

$$\int dv = \frac{\rho g + \Delta p/l}{2\eta} \int r\, dr \tag{9.27}$$

Because of the nonslip condition at the wall, $v = 0$ when $r = R$, and the constant of integration can be evaluated to give

$$v = \frac{\rho g + \Delta p/l}{4\eta}(r^2 - R^2) \tag{9.28}$$

This result describes a parabolic velocity profile, as sketched in Fig. 9.5b.

Equation (9.28) describes the velocity with which a cylindrical shell of liquid moves through a capillary under stationary-state conditions. This velocity times the cross-sectional area of the shell gives the incremental volume of liquid dV which is delivered from the capillary in an interval of time Δt. The total volume delivered in this interval ΔV is obtained by integrating this product over all values of r:

$$\frac{\Delta V}{\Delta t} = \frac{2\pi(\rho g + \Delta p/l)}{4\eta} \int_0^R (r^2 - R^2)\, r\, dr = \frac{(\rho g l + \Delta p)\pi R^4}{8\eta l} \tag{9.29}$$

This result is called the Poiseuille equation, after Poiseuille, who discovered this fourth-power dependence of flow rate on radius in 1844. The poise unit of viscosity is also named after this researcher. The following example illustrates the use of the Poiseuille equation in the area where it was first applied.

Example 9.2

Poiseuille was a physician-physiologist interested in the flow of blood through blood vessels in the body. Estimate the viscosity of blood from the fact that blood passes through the aorta of a healthy adult at rest at a rate of about 84 $cm^3\ sec^{-1}$, with a pressure drop of about 0.98 mmHg m^{-1}. Use 9 mm as the radius of the aorta for a typical human.

Solution

The pumping action of the heart rather than gravity is responsible for blood flow; hence the term ρgl can be set equal to zero in Eq. (9.29) and the result solved for η:

$$\eta = \frac{\Delta p \pi R^4}{8 l \Delta V/\Delta t}$$

The units must be expressed in a common system, with the pressure gradient requiring the most modification:

$$\frac{\Delta P}{l} = \frac{0.98\ \text{mmHg}}{\text{m}} \times \frac{133.3\ \text{N m}^{-2}}{1\ \text{mmHg}} = 131\ \text{kg m}^{-2}\ \text{sec}^{-2}$$

Therefore

$$\eta = \frac{(131\ \text{kg m}^{-2}\ \text{sec}^{-2})\pi(9 \times 10^{-3}\ \text{m})^4}{8(84 \times 10^{-6}\ \text{m}^3\ \text{sec}^{-1})} = 4.0 \times 10^{-3}\ \text{kg m}^{-1}\ \text{sec}^{-1}$$

At 37°C the viscosity of water is about 0.69×10^{-3} kg m^{-1} sec^{-1}; the difference between this figure and the viscosity of blood is due to the dissolved solutes in the serum and the suspended cells in the blood. The latter are roughly oblate ellipsoids of revolution in shape.

•

The Poiseuille equation provides a method for measuring η by observing the time required for a liquid to flow through a capillary. The apparatus shown in Fig. 9.6 is an example of one of many different instruments designed to use this relationship. In such an experiment the time required for the meniscus to drop

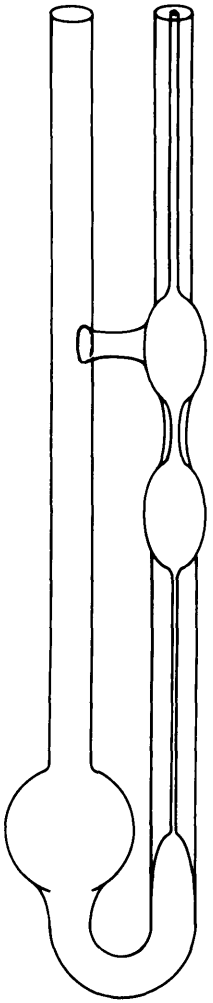

Figure 9.6 A typical capillary viscometer. (From Ref. 2, p. 55.)

the distance between the lines etched at opposite ends of the top bulb is measured. This corresponds to the drainage of a fixed volume of liquid through a capillary of constant R and l. The weight of the liquid is the driving force for the flow in this case, so the Δp term in Eq. (9.29) is zero and the observed flow time equals

$$\Delta t = \left(\frac{8\,\Delta V}{\pi g R^4}\right) \frac{\eta}{\rho} \tag{9.30}$$

or

$$\eta = A\rho\,\Delta t \tag{9.31}$$

where A represents a cluster of factors which are constant for a particular apparatus. The constant A need not be evaluated in terms of the geometry of the apparatus, but can be eliminated from Eq. (9.31) by measuring both a known (subscript 2) and an unknown (subscript 1) liquid in the same instrument:

$$\eta_1 = \frac{\rho_1}{\rho_2}\,\frac{\Delta t_1}{\Delta t_2}\,\eta_2 \tag{9.32}$$

In more precise work an additional term is added to Eq. (9.31) which corrects for effects arising at the ends of the tube. This correction—which is often negligible can be incorporated by writing

$$\eta = A\rho\,\Delta t - B\,\frac{\rho}{\Delta t} \tag{9.33}$$

where $B = \Delta V/8\pi$. As above, both A and B can be treated as instrument constants and evaluated by measuring *two* liquids which are known with respect to η and ρ, and then solving a pair of simultaneous equations for A and B.

The concentric cylinder viscometer described in Sec. 2.3, as well as numerous other possible instruments, can also be used to measure solution viscosity. The apparatus shown in Fig. 9.6 and its variations are the most widely used for this purpose, however. One limitation of this method is the fact that the velocity gradient is not constant, but varies with r in this type of instrument, as noted in connection with Eq. (9.26). Since we are not considering shear-dependent viscosity in this chapter, we shall ignore this limitation.

Experiments based on the Poiseuille equation make intrinsic viscosity an easily measured parameter to characterize a polymer. In the next section we consider how this property can be related to the molecular weight of a polymer.

9.5 The Mark-Houwink Equation

The viscosity of a polymer solution is one of its most distinctive properties. Only a minimum amount of research is needed to establish the fact that $[\eta]$ increases with M for those polymers which interact with the solvent to form a random coil in solution. In the next section we shall consider the theoretical foundations for the molecular weight dependence of $[\eta]$, but for now we approach this topic from a purely empirical point of view.

We saw in Sec. 2.9 that the viscosity of a bulk polymer is proportional to M^a, where a is either 1.0 or 3.4, depending on whether the polymer is below or above, respectively, the critical chain length for entanglement. For solutions, a similar result is obtained, only it is $[\eta]$ rather than η itself which is proportional to M^a:

$$[\eta] = kM^a \tag{9.34}$$

This relationship with a = 1 was first proposed by Staudinger, but in this more general form it is known as the Mark-Houwink equation. The constants k and a are called the Mark-Houwink coefficients for a system. The numerical values of these constants depend on both the nature of the polymer and the nature of the solvent, as well as the temperature. Extensive tabulations of k and a are available; Table 9.2 shows a few examples. Note that the units of k are the same as those of $[\eta]$, and hence literature values of k can show the same diversity of units as c_2, the polymer concentration.

Table 9.3 lists the intrinsic viscosity for a number of poly(caprolactam) samples of different molecular weight. The M values listed are number average figures based on both end group analysis and osmotic pressure experiments. The values of $[\eta]$ were measured in *m*-cresol at 25°C. In the following example we consider the evaluation of the Mark-Houwink coefficients from these data.

Table 9.2 Values for the Mark-Houwink Coefficients for a Selection of Polymer-Solvent Systems at the Temperatures Noted

Polymer	Solvent	T (°C)	k × 10^5 (dl/g)	a
Polyisobutene	Benzene	40	43	0.60
Polystyrene	Toluene	25	17	0.69
Poly(vinyl alcohol)	Water	25	20	0.76
Poly(vinyl chloride)	Chlorobenzene	30	71.2	0.59
Polyacrylonitrile	Dimethyl formamide	50	30	0.752
Poly(methyl methacrylate)	Chloroform	25	4.8	0.80
Poly(ethylene terephthalate)	*m*-Cresol	25	0.77	0.95
Poly(ϵ-caprolactam)	*m*-Cresol	25	320	0.62

Source: M. Kurata, M. Iwama, and K. Kamada, in J. Bandrup and E. H. Immergut (Eds.), *Polymer Handbook*, 2nd ed., Wiley, New York, 1975.

Table 9.3 Intrinsic Viscosity as a Function of Molecular Weight for Samples of Poly(caprolactam)[a]

$[\eta]$ (dl g^{-1})	$M \times 10^{-3}$	$[\eta]/M^{0.69} \times 10^3$
0.34	3.24	1.29
0.36	3.50	1.29
0.43	4.46	1.30
0.48	5.52	1.26
0.54	6.11	1.32
0.61	7.69	1.27
0.69	8.6	1.33
0.71	8.8	1.35
0.74	9.63	1.32
0.79	10.3	1.35
0.88	12.2	1.33
0.87	13.0	1.26
0.89	13.92	1.23
0.95	14.1	1.30
0.94	15.8	1.19
0.98	17.4	1.16
1.06	17.5	1.25
1.10	17.6	1.29
1.17	19.5	1.28
1.25	21.6	1.28
1.11	22.2	1.11
1.40	25.0	1.29
1.59	30.8	1.27

[a]These data are used to evaluate k and a in Example 9.3 and Fig. 9.7. Values of k are calculated for each measurement by the relationship $k = [\eta]/M^{0.69}$.
Source: Data from H. K. Reimschussel and G. J. Dege, *J. Polym. Sci.* 9:2343 (1971).

Example 9.3

Evaluate the Mark-Houwink coefficients for poly(caprolactam) in *m*-cresol at 25°C from the data in Table 9.3.

Solution

By taking the logarithm of both sides of Eq. (9.34), the Mark-Houwink equation is transformed into the equation of a straight line:

$$\ln [\eta] = \ln k + a \ln M$$

This form suggests that a plot of $\ln [\eta]$ versus $\ln M$ is a straight line whose slope equals a and whose intercept equals $\ln k$. The data in Table 9.3 are plotted

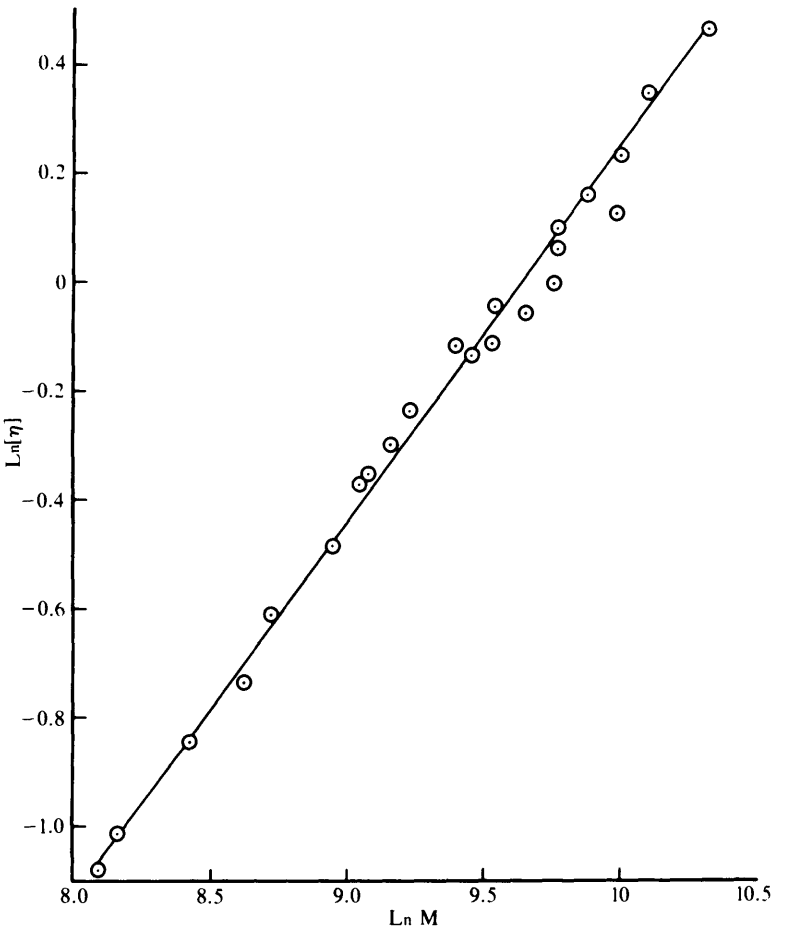

Figure 9.7 Plot of ln $[\eta]$ versus ln M for the data in Table 9.3. An analysis of the Mark-Houwink coefficients from these data is presented in Example 9.3.

according to this representation in Fig. 9.7. The points† are observed to define a straight line over the 20-fold range of M values studied. The slope of this line is 0.69, which gives the Mark-Houwink a coefficient. Because of the high values of M, evaluation of the intercept at ln M = 0 would involve an extrapolation over too great a range. Accordingly, the graphically determined a value is used to evaluate k analytically for each measurement. The individual k values so

† H. K. Reimschuessel and G. J. Dege, *J. Polym. Sci.* 9:2343 (1971).

determined are shown in Table 9.3; the average value is 1.27×10^{-3} g dl^{-1} For these data the Mark-Houwink equation becomes

$$[\eta] = 1.27 \times 10^{-3} M^{0.69}$$

Note that this can be rearranged to give M directly in terms of the observed value of $[\eta]$:

$$M = \left\{(1.27 \times 10^{-3})^{-1} [\eta]\right\}^{1/0.69} = 1.58 \times 10^{4} [\eta]^{1.45}$$

Since viscometer drainage times are typically on the order of a few hundred seconds, intrinsic viscosity experiments provide a rapid method for evaluating the molecular weight of a polymer. A limitation of the method is that the Mark-Houwink coefficients must be established for the particular system under consideration by calibration with samples of known molecular weight. The speed with which intrinsic viscosity determinations can be made offsets the need for prior calibration, especially when a particular polymer is going to be characterized routinely by this method.

Even fractionated polymer samples are generally polydisperse, which means that the molecular weight determined from intrinsic viscosity experiments is an average value. The average obtained is the viscosity average as defined by Eqs. (1.20) and (2.40) as seen by the following argument:

1. The experimental (subscript ex) intrinsic viscosity is proportional to some average - the nature of which we seek to verify - value of M raised to the power a, according to Eq. (9.34),

$$[\eta]_{ex} = k\bar{M}^{a} \tag{9.35}$$

2. Since $[\eta]_{ex}$ is a limiting value as $c_2 \to 0$, the concentration effect it contains can be written as

$$[\eta]_{ex} = \frac{(\eta_{sp})_{ex}}{c_{ex}} \tag{9.36}$$

3. For a polydisperse system containing molecules in different molecular weight categories which we index i, we can write $(\eta_{sp})_{ex} = \Sigma_i \eta_{sp,i}$ and $c_{ex} = \Sigma_i c_i$, with

$$\eta_{sp,i} = c_i [\eta]_i = c_i k M_i^{a} \tag{9.37}$$

4. Combining the results in items (1)-(3), we obtain

$$\bar{M}^{a} = \frac{\Sigma_i c_i M_i^{a}}{\Sigma_i c_i} = \frac{\Sigma_i w_i M_i^{a}}{\Sigma_i w_i} \tag{9.38}$$

since $c_i = w_i/V$.

5. Since $w_i = n_i M_i$, Eq. (9.38) can be written as

$$\bar{M}_v = \left(\frac{\Sigma_i N_i M_i^{1+a}}{\Sigma_i N_i M_i} \right)^{1/a} \tag{9.39}$$

which is the viscosity (subscript v) average molecular weight as defined in Chap. 2.

In general, $\bar{M}_n < \bar{M}_v < \bar{M}_w$, and $\bar{M}_v = \bar{M}_w$ if $a = 1$. On the basis of this last observation, it can be argued that the Mark-Houwink coefficients should be evaluated using weight average rather than number average molecular weights as calibration standards. We shall see in Chap. 10 how $\bar{M}_w$ values can be obtained from light-scattering experiments.

It is apparent from an examination of Table 9.2 that the Mark-Houwink a coefficients fall roughly in the range 0.5-1.0. We conclude this section with some qualitative ideas about the origin of these two limiting values for a. We consider a polymer molecule consisting of n repeat units, and two different representations of its interaction with solvent.

According to one point of view, the entire domain of the coil is unperturbed by the flow. The coil in this case behaves effectively like a rigid body whose volume is proportional to r_g^3, where r_g is the radius of gyration of the coil. Such a coil is said to be nondraining, since the interior of its domain is unaffected by the flow. We anticipate using Eq. (1.58) to describe the molecular weight dependence of r_g. In view of this, we replace r_g^3 by $(\overline{r_g^2})^{3/2}$ and attach a subscript 0 to the latter as a reminder that, under Θ conditions, solvent and excluded-volume effects cancel to give a true value. With these ideas in mind, the volume fraction of the nondraining coil is written

$$\phi \propto (\overline{r_{g,0}^2})^{3/2} \frac{c_2}{M} \tag{9.40}$$

since the number of these spheres is proportional to c_2/M. Applying the Einstein equation and the idea that $\overline{r_{g,0}^2} \propto n$, we obtain

$$\left(\frac{\eta}{\eta_0} - 1 \right) \propto n^{3/2} \left(\frac{c_2}{n} \right) \tag{9.41}$$

or

$$[\eta] = \frac{1}{c_2} \left(\frac{\eta}{\eta_0} - 1 \right) \propto M^{1/2} \tag{9.42}$$

An alternative point of view assumes that each repeat unit of the polymer chain offers hydrodynamic resistance to the flow such that ζ—the friction factor per repeat unit—is applicable to each of the n units. This situation is called the free-draining coil. The free-draining coil is the model upon which the Debye viscosity equation is based in Chap. 2. Accordingly, we use Eq. (2.53) to give the contribution of a single polymer chain to the rate of energy dissipation:

$$\frac{dW}{dt} \propto (n\zeta \overline{r_{g,0}^2}) \left(\frac{dv}{dy}\right)^2 \tag{9.43}$$

Once again the subscript 0 is attached to $\overline{r_g^2}$ in anticipation of using Eq. (1.58) to give the molecular weight dependence of the latter. Since $dW/dt = \eta(dv/dy)^2$ by Eq. (2.6), this result gives the contribution to viscosity of a single molecule in the absence of interactions with other molecules. A solution containing $N_A c_2/M$ molecules per volume will therefore display an excess viscosity given by

$$\frac{\eta - \eta_0}{\eta_0} \propto \left(\frac{n\zeta \overline{r_{g,0}^2}}{\eta_0}\right) \left(\frac{N_A c_2}{M}\right) \tag{9.44}$$

Recalling that $M \propto n$ and $\overline{r_{g,0}^2} \propto n$, we obtain

$$\frac{\eta - \eta_0}{\eta_0} \propto nc_2 \tag{9.45}$$

or

$$[\eta] \propto M^1 \tag{9.46}$$

Equations (9.42) and (9.46) reveal that the range of a values in the Mark-Houwink equation is traceable to differences in the permeability of the coil to the flow streamlines. It is apparent that the extremes of the nondraining and free-draining polymer molecule bracket the range of intermediate permeabilities for the coil. In the next section we examine how these ideas can be refined still further.

9.6 To Drain or Not to Drain?

The emphasis in the foregoing analysis was explaining the range of exponents which describe the dependence of $[\eta]$ on M. In this section we retreat a bit from this objective and reexamine Eqs. (9.40) and (9.44) without regard to the molecular weight dependence of the individual factors:

1. In writing Eqs. (9.40) and (9.44) we did not worry about numerical coefficients and we continue to disregard these.

2. Equation (9.40) treats the nondraining coil as a rigid sphere and shows that in this limit $[\eta] \propto (\overline{r_{g,0}^2})^{3/2}/n$.
3. Equation (9.44) treats the free-draining molecule as an assembly of independent hydrodynamic units and shows that in this limit $[\eta] \propto (n\zeta/\eta_0)(\overline{r_{g,0}^2}/n)$.
4. These results arise from considering the same polymer molecule under different conditions of permeability to the streamlines of solvent flow.
5. As special cases, both Eqs. (9.40) and (9.44) must be limits of a *single* function which also describes the intermediate situations in which the interior of the coil domain is partially penetrated by the pattern of flow.

Taking the attitude described in item (5) toward the previously developed equations for $[\eta]$ is an important step. What this enables us to do is write a *general* expression for $[\eta]$ in solutions of flexible polymers:

$$[\eta] \propto \frac{(\overline{r_{g,0}^2})^{3/2}}{n} \times f\left(\frac{n\zeta}{\eta_0 (\overline{r_{g,0}^2})^{1/2}}\right) \tag{9.47}$$

where $f[n\zeta/\eta_0 (\overline{r_{g,0}^2})^{1/2}]$ is some function – as yet unknown – of the indicated variables. Of this function, the following observations can be made:

1. The cluster of variables – which we designate X for simplicity – is dimensionless. Since ζ is the friction factor per repeat unit, it can at least be approximated by Eq. (9.5): $\zeta = 6\pi\eta_0 b$, where b is the radius of a repeat unit and η_0 is the viscosity of the medium. Thus ζ/η_0 has the units of length, as does $(\overline{r_{g,0}^2})^{1/2}$, making this particular cluster dimensionless.
2. The function f(X) approaches a constant value for nondraining coils to generate Eq. (9.40), and approaches some constant times $n\zeta/\eta_0 (\overline{r_{g,0}^2})^{1/2}$ for free-draining coils to generate Eq. (9.44).
3. A detailed hydrodynamic theory has been developed by Kirkwood and Riseman which indeed reduces to the limits predicted above.
4. The details of the Kirkwood-Riseman theory are sufficiently involved that we shall not consider the derivation of this theory. We shall, however, examine in somewhat greater detail the cluster of variables we have designated by X as a measure of the permeability of the molecule to the flowing solvent.

Rather than discuss the penetration of the flow streamlines into the molecular domain of a polymer in terms of viscosity, we shall do this for the overall friction factor of the molecule instead. The latter is a similar but somewhat simpler situation to examine. For a free-draining polymer molecule, the net friction factor f is related to the segmental friction factor ζ by

$$f = n\zeta = n6\pi\eta_0 b \tag{9.48}$$

The premise which underlies Eq. (9.48) is that all segments experience the flow as if it were undisturbed by other segments in the chain. This is the free-draining limit for the friction factor and, of course, assumes no interference from neighboring polymer molecules either. This result can be criticized on two grounds: applying Stokes' law to individual polymer segments and ignoring that there is ordinarily overlap of the hydrodynamic effect caused by neighboring units. The latter is the more serious of the two. The Kirkwood method of dealing with this overlap effect is to modify Eq. (9.48) as follows:

$$f = \frac{n 6\pi\eta_0 b}{1 + (b/n) \sum_{i=1}^{n} \sum_{j=1}^{n} \overline{r_{ij}^{-1}}} \tag{9.49}$$

where $\overline{r_{ij}^{-1}}$ is the average value of the reciprocal distance between units i and j in the chain. As the value of this distance becomes larger, its reciprocal becomes smaller and the interference between units i and j decreases. The summations in Eq. (9.49) are to be carried out for each pair of i-j units, excluding i = j.

To evaluate r_{ij}^{-1} we return to the concepts of Sec. 1.10 and, using Eq. (1.44) for P(n, r), write

$$\overline{r^{-1}} = \int_0^\infty r^{-1} P(n, r)\, dr = \left(\frac{6}{\pi \overline{r_0^2}}\right)^{1/2} \tag{9.50}$$

This integral is a gamma function and is readily solved using a table of integrals. In writing the last result nl_0^2 has been replaced by $\overline{r_0^2}$, the mean-square coil dimensions under Θ conditions. Equation (9.49) involves $\overline{r_{ij}^{-1}}$, not $\overline{r^{-1}}$, so we note that $\overline{r_0^2} = nl_0^2$ and replace n by $|i - j|$, the number of units separating units i and j, to obtain

$$\overline{r_{ij}^{-1}} = \left(\frac{6}{\pi |i - j| l_0^2}\right)^{1/2} \tag{9.51}$$

Substituting this value into Eq. (9.49), replacing the sums by integrals, and performing the indicated operations eventually yields

$$f = \frac{n 6\pi\eta_0 b}{1 + (8/3)(6/\pi)^{1/2} (b/l_0) n^{1/2}} \tag{9.52}$$

This expression can be cast into a more useful form by making the following modifications on the second term in the denominator:

1. We begin by ignoring all purely numerical coefficients. In the final result we shall represent all such factors by the numerical constant K.

2. Multiply the numerator and denominator by $n^{1/2}$ and replace $n^{1/2}l_0$ by $(6\overline{r_{g,0}^2})^{1/2}$:

$$\frac{b}{l_0} n^{1/2} \propto \frac{bn}{(\overline{r_{g,0}^2})^{1/2}}$$

3. Replace b, the radius of the repeat unit, by $\zeta/6\pi\eta_0$:

$$\frac{bn}{(\overline{r_{g,0}^2})^{1/2}} \propto \frac{\zeta n}{\eta_0 (\overline{r_{g,0}^2})^{1/2}} \propto X$$

where X again represents the same cluster of constants used to describe $[\eta]$.

Substituting back into Eq. (9.52) gives

$$f = \frac{n6\pi\eta_0 b}{1 + K n\zeta/[\eta_0 (\overline{r_{g,0}^2})^{1/2}]} = \frac{n\zeta}{1 + KX} \tag{9.53}$$

This result shows that the friction factor of the coil equals $n\zeta$ when $KX \ll 1$, and equals a numerical factor times $\eta_0 (\overline{r_{g,0}^2})^{1/2}$ when $KX \gg 1$. The first of these limits is the free-draining case; the second is Stokes' law for a nondraining sphere. The denominator in Eq. (9.53) can be regarded as a function $f'(X)$ which corrects the friction factor for variable coil permeability just as $f(X)$ in Eq. (9.47) corrects $[\eta]$ for this effect. The two correction functions $f(X)$ and $f'(X)$ are different, but the point we wish to illustrate is that the cluster of constants represented by X does describe the perturbation of the coil interior by the flow and illustrates that the condition $X \to 0$ corresponds to free-draining coils, and $X \to \infty$ to nondraining coils. Both of these conclusions are consistent with the anticipated interpretation of Eq. (9.47) for $[\eta]$.

From the definition of this permeability parameter [Eq. (9.47)], we see that X depends on $n/(\overline{r_{g,0}^2})^{1/2}$ or $n^{1/2}$, since $(\overline{r_{g,0}^2})^{1/2} \propto n^{1/2}$. Remember that the subscript 0 in all the preceding relationships specifies Θ conditions where the intramolecular volume exclusion effects and solvent effects on the random coil dimensions cancel. Since $X \to 0$ corresponds to the free-draining limit, and $X \to \infty$ to the nondraining limit, we see that the transition between these two extremes is predicted to occur with increasing n. Thus for short chains each segment experiences the flow of the solvent as if it were an isolated unit. For chains of intermediate length those segments near the perimeter of the coil partially shield those near the center from the flow. Finally, for very long chains the shielding is so effective that the solvent in the core of the molecular domain is immobilized.

We now have two entirely different contexts in which we speak of a coil as "unperturbed," with the term having a different meaning in each case:

1. In this section an unperturbed coil refers to the condition of immobilized solvent in the interior of the molecular domain. This is a hydrodynamic criterion and leads to Eq. (9.42).
2. In earlier chapters an unperturbed coil referred to molecular dimensions as predicted by random flight statistics. We saw in the last chapter that this thermodynamic criterion is met under Θ conditions.
3. To use the proportionality between $\overline{r_{g,0}^2}$ and n in this section, we have stipulated unperturbed dimensions—in the sense of item (2)—as indicated by the subscript 0 on the various size parameters.

In the nondraining limit of Eq. (9.47), the coils are unperturbed in both senses of the word: nondraining *and* Θ conditions. To emphasize the latter we attach the subscript Θ to $[\eta]$ when these conditions are met. Thus for high polymers under Θ conditions

$$[\eta]_\Theta = \frac{\Phi(\overline{r_{g,0}^2})^{3/2}}{M} = \Phi\left(\frac{\overline{r_{g,0}^2}}{M}\right)^{3/2} M^{1/2} \tag{9.54}$$

where Φ is the proportionality constant. Since $\overline{r_0^2}/n$ is a constant according to Eq. (1.61), this result predicts the value of 1/2 for the Mark-Houwink a coefficient under Θ conditions. Figure 9.8 shows the experimental intrinsic viscosities of four different polymer-solvent-temperature combinations corresponding to Θ conditions plotted against molecular weight on log-log coordinates. All of the data display lines of slope 1/2 in this representation in accord with Eq. (9.54).

The fully developed Kirkwood-Riseman theory predicts that in the limit of molecular weights above about 10^4 the function f(X) in Eq. (9.47) reaches a limiting value of 5.32×10^{24} for $[\eta]$ expressed in cubic centimeters per gram and r_g in centimeters. A somewhat revised version of this theory gives 4.22×10^{24} for this limit. Because of the relationship between $\overline{r_{g,0}^2}$ and $\overline{r_0^2}$ [Eq. (1.59)], these values are decreased by $6^{3/2} = 14.7$ when written in terms of the end-to-end distance instead of the radius of gyration. We shall see in Chap. 10 that the radius of gyration of a polymer can be independently evaluated from light-scattering experiments. When $(\overline{r_{g,0}^2})$ values so determined are combined with measured M and $[\eta]$ values, an empirical value for Φ is found to be about 3.1×10^{24}—in the same units cited above—for a variety of systems under Θ conditions. Although there is some uncertainty as to its exact value, it is important to note that Φ is a universal parameter which permits the ratio $(\overline{r_{g,0}^2})^{3/2}/M$ to be evaluated from $[\eta]$ or—if the molecular weight is also known—allows the evaluation of $\overline{r_{g,0}^2}$ itself. Note that the precise numerical

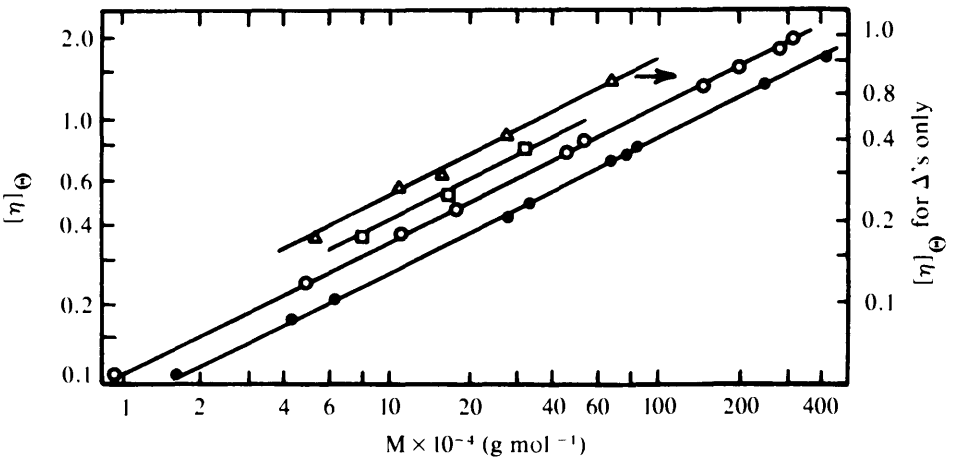

Figure 9.8 Log-log plot of $[\eta]_\Theta$ versus M for four different polymer-solvent-temperature combinations corresponding to Θ conditions. All lines have a slope of 1/2 as required by Eq. (9.54). (Reprinted with permission from Ref. 1.)

value used for Φ depends on the system of units used, the choice of size parameters, and whether theoretical or empirical values are selected. The application of Eq. (9.54) is illustrated in the following example.

Example 9.4

Under Θ conditions occurring near room temperature, $[\eta] = 0.83$ dl g^{-1} for a polystyrene sample of molecular weight 10^6.† Use this information to evaluate $\overline{r_{g,0}^2}$ and $\overline{r_0^2}$ for polystyrene under these conditions. For polystyrene in ethylcyclohexane, Θ = 70°C and the corresponding calculation shows that $(\overline{r_0^2}/M)^{1/2} = 0.071$ nm. Based on these two calculated results, criticize or defend the following proposition: The discrepancy in calculated $(\overline{r_0^2}/M)^{1/2}$ values must arise from the uncertainty in Φ, since this ratio should be a constant for polystyrene, independent of the nature of the solvent.

Solution

Since these are Θ conditions, use Eq. (9.54) and the empirical value of Φ to evaluate $\overline{r_{g,0}^2}/M$:

† See Fig. 9.8.

$$(\overline{r_{g,0}^2}/M)^{3/2} = \frac{[\eta]}{\Phi M^{1/2}} = \frac{0.83 \text{ dl/g} \times 100 \text{ cm}^3/\text{dl}}{(3.1 \times 10^{24})(10^6)^{1/2}} = 2.68 \times 10^{-26} \text{ cm}^3$$

and

$$(\overline{r_{g,0}^2}/M)^{1/2} = (2.68 \times 10^{-26})^{1/3} = 3.0 \times 10^{-9} \text{ cm}$$

Since $M = 10^6$, $(\overline{r_{g,0}^2})^{1/2} = 30 \times 10^{-9}$ m = 30 nm. Since $\overline{r_0^2} = 6\overline{r_{g,0}^2}$, $(\overline{r_0^2})^{1/2} = 6^{1/2}(30) = 73.5$ nm. This figure was given in Example 1.6 as the rms end-to-end distance of an unperturbed polystyrene molecule of $M = 10^6$. Therefore for $\Theta \cong 25°C$, $(\overline{r_0^2}/M)^{1/2} = 73.5/(10^6)^{1/2} = 0.074$ nm, while for $\Theta = 70°C$, $(\overline{r_0^2}/M)^{1/2} = 0.071$ nm. As stated in the proposition, these values should be independent of the nature of the solvent. In both cases the ratios were evaluated using the empirical value of Φ, which, in turn, is based on a range of solvents. The above discrepancy in $(\overline{r_0^2}/M)^{1/2}$ is comparable to the range of empirical Φ values calculated from different solvents under Θ conditions. However, the calculated ratios are typical of a *systematic* trend to show slightly lower values of $(\overline{r_0^2}/M)^{1/2}$ at higher values of Θ. Therefore, before simply attributing this to the uncertainty in an empirical constant, let us examine the significance of this ratio in terms of Eq. (1.16). According to the latter,

$$\frac{\overline{r_0^2}}{n} \propto (\text{bond length})(\text{effect of bond angle})(\text{effect of hindered rotation})$$

The first two of these factors are constant for a given polymer, as are the absolute heights of the barriers to free rotation. The absolute barrier heights, however, are not as important as these heights *relative to RT*, since it is the relative height that determines the probability of overcoming the barrier. Therefore at higher temperatures the barriers to rotation are less effective and the coil can snuggle into a tighter coil. The slight decrease in $(\overline{r_0^2}/M)^{1/2}$ with increasing Θ is apparently a real effect.

•

Next we consider the situation of a coil which is unperturbed in the hydrodynamic sense of being effectively nondraining, yet having dimensions which are perturbed away from those under Θ conditions. As far as the hydrodynamics are concerned, a polymer coil can be expanded above its random flight dimensions and still be nondraining. In this case, what is needed is to correct the coil dimension parameters by multiplying with the coil expansion factor α, defined by Eq. (1.63). Under non-Θ conditions (no subscript), $r_g = \alpha(r_g)_0$; therefore under these conditions we write

$$[\eta] = \Phi\alpha^3 \frac{(\overline{r_{g,0}^2})^{3/2}}{M} = \frac{\Phi r_g^3}{M} = \Phi\alpha^3 \left(\frac{\overline{r_{g,0}^2}}{M}\right)^{3/2} M^{1/2} \qquad (9.55)$$

Comparing this result with Eq. (9.54) shows that

$$\alpha^3 = \frac{[\eta]}{[\eta]_\Theta} \tag{9.56}$$

for nondraining polymers. This provides a method for evaluating the coil expansion factor for a specific system.

In addition to the thermodynamic interpretation of Θ conditions that we discussed in Chap. 8, we have now established the hydrodynamic significance of these conditions as the point at which $[\eta] \propto M^{0.5}$. Summarizing in terms of the Mark-Houwink a coefficient we have the following:

1. For nondraining coils, a = 0.5 identifies the Θ condition.
2. As discussed in connection with Eq. (9.47), the Kirkwood-Riseman theory predicts that a = 1 in the free-draining limit. This limit is expected for small values of n, however, and does not explain a > 0.5 for high molecular weight polymers.
3. Under better-than-Θ conditions, $[\eta] > [\eta]_\Theta$, according to Eq. (9.56). Experimental a values are greater than 0.5 under these conditions also.

Next we shall examine the molecular weight dependence of the coil expansion factor α to see if the latter can explain the observations of a's greater than 0.5.

9.7 The Coil Expansion Factor

The coil expansion factor α has been examined by Flory and other workers, and is discussed in detail in Ref. 1. We shall not consider the full details of this topic, but shall be content with examining the dependence of α on the molecular weight of the polymer and on the energetics of the interaction between the polymer and the solvent. Figure 1.9 shows how a coil expands from its dimensions under Θ conditions as a result of imbibing a good solvent. Although coil shrinkage is also possible owing to solvent exclusion, we recognize that the range of the effect in this direction is limited. Before a solvent gets too poor, high molecular weight polymers will begin to precipitate out of solution; therefore we concentrate on the expansion aspect of the factor α.

The key to understanding α is the realization that two opposing forces operate on the coil to establish its equilibrium dimensions:

1. The molecule tends to imbibe a good solvent to dilute the chain segments within the coil domain. This is analogous to the solvent passing through the membrane in an osmotic pressure experiment, with the hypothetical boundary of the coil functioning as an imaginary membrane.

2. The expansion of the coil domain produces an elastic restoring force which opposes the expansion by tending to restore the molecule to its most probable conformation.
3. Since these forces work in opposition, the actual coil dimensions describe the point of balance between the two.

Our strategy in proceeding, therefore, is to write separate expressions for the forces cited in items (1) and (2), and then set them equal to each other as required by item (3). Since we have discussed osmotic effects in Chap. 8 and elastic forces in Chap. 3, we shall invoke certain concepts and relationships from these chapters in this discussion. In this derivation we continue to omit numerical coefficients and some of the less pertinent parameters (although we retain $\bar{V}_1$ for the sake of Problem 5 at the end of the chapter), and focus attention on the relationship between α, M, and the interaction parameter χ.

We begin by writing the volume of the spherical coil domain as $V_d = (4/3)\pi r^3$, where $r = \alpha(\overline{r_0^2})^{1/2}$. For simplicity we temporarily write this as $r = \alpha r_0$; we return to $(\overline{r_0^2})^{1/2}$ below to introduce the molecular weight dependence of the latter. Accordingly, $V_d = (4/3)\pi\alpha^3 r_0^3$, and the increment in domain volume associated with an incremental increase in r_0 is

$$dV_d \propto \alpha^3 r_0^2 \, dr_0 \tag{9.57}$$

Only a fraction of the chain segments will be present in this spherical shell, but whatever their number is, it will increase with the degree of polymerization n. Therefore, in the volume element associated with the expansion of the coil, the volume fraction of chain segments ϕ^* is proportional to n/dV_d, or $\phi^* \propto n/\alpha^3 r_0^2 \, dr_0$.

The change in free energy for the imbibed solvent is given by $\Delta G = (\mu_1 - \mu_1^\circ) \, dn_1$, where $dn_1 \propto dV_d(1 - \phi^*)/\bar{V}_1$, or $\alpha^3(1 - \phi^*) r_0^2 \, dr_0/\bar{V}_1$. Remembering that a force times the distance through which it operates gives an energy—in this case $F_{os} \, d\alpha = \Delta G$—we write the following for the osmotic force (subscript os) associated with the imbibed solvent:

$$F_{os} = \frac{\partial}{\partial \alpha} [(\mu_1 - \mu_1^\circ) \, dn_1] \propto \frac{\partial}{\partial \alpha} \left(\frac{(\mu_1 - \mu_1^\circ) \alpha^3 (1 - \phi^*) r_0^2 \, dr_0}{\bar{V}_1} \right) \tag{9.58}$$

Expanding the logarithm in Eq. (8.53) [$\ln(1 - \phi^*) \cong - \phi^* - 1/2 \, \phi^{*2}$] and considering the limit as $n \to \infty$ gives $\mu_1 - \mu_1^\circ \propto (1/2 - \chi) \phi^{*2}$ for this situation. Substituting into Eq. (9.58) and retaining no terms higher than second order in ϕ^*, we obtain

$$F_{os} \propto \frac{\partial}{\partial \alpha} \left[\frac{1/2 - \chi}{\bar{V}_1} \left(\frac{n}{\alpha^3 r_0^2 \, dr_0} \right)^2 \alpha^3 r_0^2 \, dr_0 \right] \tag{9.59}$$

Carrying out the indicated differentiation and reintroducing $(\overline{r_0^2})^{1/2}$ for r_0, this becomes

$$F_{os} \propto \frac{(1/2 - \chi)\, n^2}{\alpha^4 \bar{V}_1 (\overline{r_0^2})\, d(\overline{r_0^2})^{1/2}} \tag{9.60}$$

Since $\overline{r_0^2} \propto n$, we obtain for the molecular weight dependence of F_{os}

$$F_{os} \propto \frac{(1/2 - \chi)\, n^2}{\bar{V}_1 \alpha^4 n^{3/2}} \propto \frac{(1/2 - \chi)\, n^{1/2}}{\bar{V}_1 \alpha^4} \tag{9.61}$$

As noted above, this force is counterbalanced by an entropy-based, elastic force which prevents the molecule from uncoiling. Entropy elasticity was discussed in Sec. 3.4, where the elastic (subscript el) force between crosslinks is given by Eq. (3.19) to be

$$F_{el} \propto \frac{\partial\, \Delta S}{\partial L} \propto \frac{1}{L_0} \frac{\partial\, \Delta S}{\partial \alpha} \tag{9.62}$$

where ΔS is the entropy of stretching, L is the stretched length of the sample, and L_0 the unstretched length. The ratio L/L_0 is close enough to the definition of α in the present context to allow this expression from Chap. 3 to be used here.

We might be tempted to equate the forces given by Eqs. (9.61) and (3.38) and solve for α from the resulting expression. However, Eq. (3.38) is not suitable for the present problem, since it was derived for a cross-linked polymer stretched in one direction with no volume change. We are concerned with a single, un-cross-linked molecule whose volume changes in a spherically symmetrical way. The precursor to Eq. (3.36) in a more general derivation than that presented in Chap. 3 is

$$\Delta S \propto \frac{1}{2} \left[\alpha_x^2 + \alpha_y^2 + \alpha_z^2 - 3 - \ln (\alpha_x \alpha_y \alpha_z)\right] \tag{9.63}$$

where the α's are the relative elongations in the x, y, and z directions. Equation (3.36) is obtained from Eq. (9.63) by letting $\alpha_x = \alpha_y = \alpha_z^{-1/2} = \alpha^{-1/2}$. If we allow each of the components of α to be identical, as appropriate for symmetrical expansion, we obtain from Eq. (9.63)

$$\Delta S \propto \frac{3}{2} \left[(\alpha^2 - 1) - \ln \alpha\right] \tag{9.64}$$

From this expression we obtain

$$F_{el} \propto \frac{\partial \Delta S}{\partial \alpha} \propto \alpha - \frac{1}{\alpha} \tag{9.65}$$

instead of Eq. (3.38).

Equating Eqs. (9.61) and (9.65) yields the desired result:

$$\frac{(1/2 - \chi) n^{1/2}}{\bar{V}_1 \alpha^4} \propto \alpha - \frac{1}{\alpha} \tag{9.66}$$

or

$$\alpha^5 - \alpha^3 \propto \frac{(1/2 - \chi) n^{1/2}}{\bar{V}_1} \tag{9.67}$$

This expression was anticipated in the last chapter in writing Eq. (8.114). Equation (8.115) can also be substituted into this expression to eliminate $1/2 - \chi$ and give

$$\alpha^5 - \alpha^3 \propto \psi \left(1 - \frac{\Theta}{T}\right) M^{1/2} \tag{9.68}$$

In the fully developed theory, the proportionality factors in Eqs. (9.67) and (9.68) are also evaluated.

Our primary objective in undertaking this examination of the coil expansion factor was to see whether the molecular weight dependence of α could account for the fact that the Mark-Houwink a coefficient is generally greater than 0.5 for $T \neq \Theta$. More precisely, it is generally observed that $0.5 \leqslant a \leqslant 0.8$. This objective is met by combining Eqs. (9.55) and (9.68):

1. At $T = \Theta$ (or $\chi = 1/2$), $\alpha = 1$ and $[\eta] \propto M^{1/2}$, as required by Eq. (9.54).
2. For good solvents where $\alpha > 1$, $\alpha^5 > \alpha^3$, so $\alpha^5 \propto M^{1/2}$ or $\alpha \propto M^{0.1}$. Because of the factor α^3 in Eq. (9.55), an additional factor $M^{0.3}$ enters the latter to give an overall proportionality between $[\eta]$ and $M^{0.8}$.
3. For conditions of intermediate solvent goodness, α shows a dependence on M which is intermediate between the limits described in items (1) and (2) with the corresponding intermediate values for the Mark-Houwink a coefficient.

What is especially significant about Eq. (9.68) is the observation that the coil expansion factor α definitely increases with M for good solvents, meaning that—all other things being equal—longer polymer chains expand above their Θ dimensions more than shorter chains. Even though the dependence of α on

M is a small fractional order, this can amount to a considerable effect over a wide range of M values. For example, in the limit described in item (2), where $\alpha \propto M^{0.1}$, two samples of the same polymer showing a 1000-fold range of M will differ in α—as well as $(\overline{r^2}/M)^{1/2}$ and $(\overline{r_g^2}/M)^{1/2}$—by a factor of 2. This result assumes the same (favorable) interaction between polymer and solvent and is a consequence of the difference in chain length alone.

Equation (9.68) requires that $(\alpha^5 - \alpha^3)/M^{1/2}$ be a constant for a particular system if the molecular weight dependence of α has been correctly assessed. While not absolutely constant, experimental values of such a ratio show only a slight variation over a 1000-fold change in M. This indicates that the functional dependence of α on M predicted above is correct, at least to a first approximation. Additional efforts have been directed toward refining this prediction still further, but we shall not pursue these.

This concludes our discussion of the viscosity of polymer solutions per se, although various aspects of the viscous resistance to particle motion continue to appear in the remainder of the chapter. We began this chapter by discussing the intrinsic viscosity and the friction factor for rigid spheres. Now that we have developed the intrinsic viscosity well beyond that first introduction, we shall do the same (more or less) for the friction factor. We turn to this in the next section, considering the relationship between the friction factor and diffusion.

9.8 The Diffusion Coefficient and the Friction Factor

We begin our discussion of diffusion by assuming that a gradient of solute concentration exists in a solution. We designate this dc/dx, without specifying the units of concentration. The second law of thermodynamics generalizes the familiar experience that such a gradient is unstable in the absence of some sustaining force: The molecules will diffuse throughout the space available to them until a uniform concentration is reached. We imagine a cross section of area A perpendicular to the concentration gradient, and consider the flow of material across that surface. The rate per unit area at which matter diffuses through this cross section is called the flux J and is directly proportional to the concentration gradient:

$$J = -D\frac{dc}{dx} \tag{9.69}$$

In this expression, called Fick's first law, the proportionality constant D is the diffusion coefficient of the solute. Since $J = (1/A)(dQ/dt)$ and $c = Q/V$, where Q signifies the quantity of solute in unspecified units, it follows that D has the units length^2 time^{-1}, or m^2 sec^{-1} in the SI system. The minus sign in Eq. (9.69)

is introduced in recognition of the fact that the direction of the flow is that of decreasing concentration. Rewriting Eq. (9.69) in terms of Q, we obtain

$$\frac{1}{A}\frac{dQ}{dt} = -\frac{D}{V}\frac{dQ}{dx} \tag{9.70}$$

which is formally the same sort of differential equation as the corresponding expression for viscosity, Eq. (9.3). The solution to Eq. (9.70) gives the amount of solute as a function of location and time so as to satisfy the boundary conditions of the problem. In general, both the gradient and the flux have x, y, and z components, and solving the three-dimensional analog of Eq. (9.70) for various boundary conditions can become quite complicated. For our purposes it suffices to consider only the one-dimensional case. The formal similarity of the defining equations for D and η makes the study of both of these–along with charge and heat transport–part of the general topic of transport phenomena. In Eq. (9.3) it is momentum, not matter per se, that is transported across the reference surface in response to a gradient.

As with viscosity, we must consider a volume element and the flux of solute in and out of that element. Figure 9.9a schematically represents three regions of an apparatus containing a concentration gradient. The end compartments contain the solute at two different concentrations c_1 and c_2, with $c_2 > c_1$. The center region, which in practice could be something like a porous plug, is the volume element of cross section A and thickness dx, along which the gradient exists. The arrows in Fig. 9.9a represent the flux of solute from the more concentrated solution to the less concentrated one. The change in the amount of material dQ in the center volume element can be developed in two different ways:

1. In terms of fluxes,

$$dQ = Q_{in} - Q_{out} = (J_{in} - J_{out})\,A\,dt \tag{9.71}$$

2. In terms of a concentration change dc in the element of volume A dx,

$$dQ = dc\,(A\,dx) \tag{9.72}$$

3. The expressions for dQ in items (1) and (2) can be equated and the difference in fluxes in Eq. (9.71) eliminated by substituting Eq. (9.69):

$$-D\left[\left(\frac{dc}{dx}\right)_x - \left(\frac{dc}{dx}\right)_{x+dx}\right] A\,dt = A\,dx\,dc \tag{9.73}$$

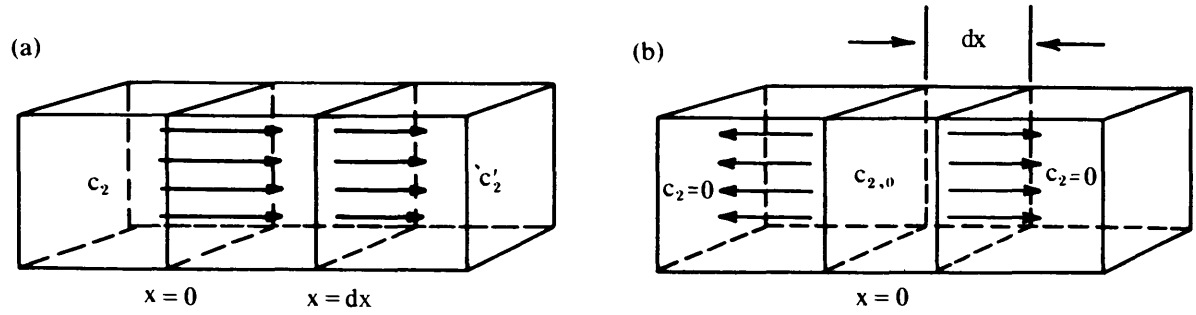

Figure 9.9 Schematic of diffusion with respect to a volume element of thickness dx located at x = 0: (a) $c_2 > c_1$ and (b) $c = c_0$ in volume element. The flux is shown by arrows.

4. Since

$$\left[\left(\frac{dc}{dx}\right)_{x+dx} - \left(\frac{dc}{dx}\right)_x\right] = \frac{d^2c}{dx^2}\ dx$$

this last result can be written as

$$\frac{dc}{dt} = D\frac{d^2c}{dx^2} \tag{9.74}$$

Equation (9.74) is a one-dimensional version of Fick's second law. We shall presently consider a statistical approach to solving this equation. If c is measured as a function of x and t in an experiment which corresponds to the boundary conditions of the mathematical solution to Eq. (9.74), then D can be evaluated for the solute. We shall consider this below also.

Before pursuing the diffusion process any further, let us examine the diffusion coefficient itself in greater detail. Specifically, we seek a relationship between D and the friction factor of the solute. In general, an increment of energy is associated with a force and an increment of distance. In the present context the driving force behind diffusion (subscript diff) is associated with an increment in the chemical potential of the solute and an increment in distance dx:

$$F_{diff} = -\frac{1}{N_A}\frac{d\mu_2}{dx} \tag{9.75}$$

We divide by Avogadro's number to convert the partial molar Gibbs free energy to a molecular quantity, and the minus sign enters because the force and the gradient are in opposing directions. Recalling the definition of chemical potential [Eq. (8.13)], we write $\mu_2 = \mu_2^{\theta} + RT \ln a_2 = \mu_2^{\theta} + RT \ln \gamma_2 c$, where a_2 and γ_2 are the activity and activity coefficient, respectively, of the solute. In dilute solutions $\gamma_2 \to 1$ and $d\mu_2/dx = RT(d \ln c/dx)$; therefore

$$F_{diff} = -\frac{RT}{N_A}\frac{d \ln c}{dx} = -\frac{kT}{c}\frac{dc}{dx} \tag{9.76}$$

Under stationary-state flow conditions, F_{diff} equals the force of viscous resistance experienced by the particle. The latter, in turn, equals the friction factor times the stationary velocity v_s; therefore

$$-\frac{kT}{c}\frac{dc}{dx} = fv_s \tag{9.77}$$

The product cv_s can be written

$$\frac{Q}{V}\frac{dx}{dt} = \frac{Q}{A\,dx}\frac{dx}{dt} = \frac{1}{A}\frac{dQ}{dt}$$

which defines the flux. Accordingly, Eq. (9.77) becomes

$$J = -\frac{kT}{f}\frac{dc}{dx} \tag{9.78}$$

Comparing Eqs. (9.69) and (9.78) gives

$$D = \frac{kT}{f} \tag{9.79}$$

We shall see in Sec. 9.9 that D is a measurable quantity; hence Eq. (9.79) provides a method for the determination of an experimental friction factor as well. Note that no assumptions are made regarding the shape of the solute particles in deriving Eq. (9.79), and the assumption of ideality can be satisfied by extrapolating experimental results to $c = 0$, where $\gamma = 1$.

In contrast with Eq. (9.79), prior theoretical discussions of the friction factor for various particles were based on some assumed structure or geometry for the molecule:

1. Random coils. Equation (9.53) gives the Kirkwood-Riseman expression for the friction factor of a random coil. In the free-draining limit, the segmental friction factor can, in turn, be evaluated from f. In the nondraining limit the radius of gyration can be determined. We have already discussed ζ in Chap. 2 and $(\overline{r_g^2})^{1/2}$ in this chapter and again in Chapter 10, so we shall not examine the information provided by D for the random coil any further.
2. Rigid, unsolvated spheres. Stokes' law, Eq. (9.5), provides a relationship between f and the radius of the particle. Since this structure is a reasonable model for some protein molecules, experimental D values can be interpreted, via f, to yield values of R for such systems. Note that this application can also yield a value for M, since $M = N_A \rho_2 [(4/3)\pi R^3]$, where ρ_2 is the density of the unsolvated material.
3. Rigid particles other than unsolvated spheres. It is easy to conclude qualitatively that either solvation or ellipticity (or both) produces a friction factor which is larger than that obtained for a nonsolvated sphere of the same mass. This conclusion is illustrated in Fig. 9.10, which shows the swelling of a sphere due to solvation and also the spherical excluded volume that an ellipsoidal particle requires to rotate through all possible orientations.

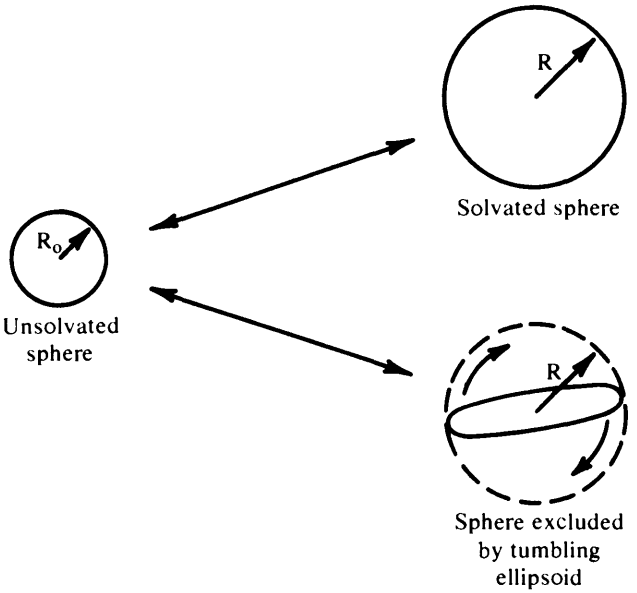

Figure 9.10 Schematic relationship between the radius R_0 of an unsolvated sphere and the effective radius R of a solvated sphere or of a spherical volume excluded by an ellipsoidal particle rotating through all directions.

Since f is a measurable quantity for, say, a protein, and since the latter can be considered to fall into category (3) in general, the friction factor provides some information regarding the ellipticity and/or solvation of the molecule. In the following discussion we attach the subscript 0 to both the friction factor and the associated radius of a nonsolvated spherical particle and use f and R without subscripts to signify these quantities in the general case. Because of Stokes' law, we write

$$\frac{f}{f_0} = \frac{R}{R_0} \tag{9.80}$$

where $R/R_0 > 1$. It is evident from Fig. 9.10 that the amount by which R/R_0 or f/f_0 exceeds unity increases with increasing solvation, ellipticity, or both.

The dependence of f/f_0 on solvation and ellipticity has been worked out in detail. Since the situation parallels the way $[\eta]$ exceeds its value for nonsolvated spheres, we shall not elaborate on the details, but merely summarize the conclusions:

1. The quantitative analysis of this problem results in a set of contours in terms of the axial ratio a/b and the solvation $m_{1,b}/m_2$ for constant values of f/f_0.
2. The general shape of the contours resembles the corresponding curves for $[\eta]$, which are shown in Fig. 9.4a. The contours for f/f_0 and $[\eta]$ differ in quantitative detail, however.
3. Figure 9.4b shows a theoretical f/f_0 contour for a value of this ratio equal to 1.45. As noted in the discussion of this figure in Sec. 9.3, the intersection of the f/f_0 and $[\eta]$ contours permits the state of solvation and ellipticity of such a protein molecule to be characterized uniquely.

The foregoing discussion is incomplete, since it offers an interpretation of f/f_0 while presenting, through Eq. (9.79), a method for evaluating f alone. What is needed to be able to take advantage of this approach is a value for the friction factor of a nonsolvated spherical particle having the same mass as the species under consideration. Fortunately, this reference value f_0 can be calculated if the molecular weight of the solute is known, since we are comparing f and f_0 for particles of the same mass. The mass of a molecule divided by its (unsolvated) density gives the volume of an equivalent spherical particle. From this volume R_0 can be evaluated, and this, in turn, allows f_0 to be calculated from Stokes' law. The following example illustrates this computational procedure.

Example 9.5

The hemoglobin molecule has a molecular weight of 62,300 and is observed to have a diffusion coefficient of 6.9×10^{-11} m^2 sec^{-1} in water at 20°C. Calculate the ratio f/f_0 which is consistent with these data, using 1.34 g cm^{-3} as the density of the dry polymer and 10^{-3} kg m^{-1} sec^{-1} as the viscosity of water at 20°C.

Solution

The friction factor of the actual particle is given by Eq. (9.79):

$$f = \frac{kT}{D} = \frac{(1.38 \times 10^{-23}\ \text{J K}^{-1})(293\ \text{K})}{6.9 \times 10^{-11}\ \text{m}^2\ \text{sec}^{-1}} = 5.89 \times 10^{-11}\ \text{kg sec}^{-1}$$

If the hemoglobin molecule were a nonsolvated sphere, we could write for its volume

$$\left(\frac{62{,}300\text{ g}}{\text{mol}} \times \frac{\text{cm}^3}{1.34\text{ g}}\right)\left(\frac{1\text{ mol}}{6.02 \times 10^{23}\text{ molecules}}\right) = \frac{4}{3}\pi R_0^3$$

from which $R_0 = 2.64 \times 10^{-7}$ cm $= 2.64 \times 10^{-9}$ m. By Stokes' law, $f_0 = 6\pi\eta R_0 = 6\pi(10^{-3}\text{ kg m}^{-1}\text{ sec}^{-1})(2.64 \times 10^{-9}\text{ m}) = 4.98 \times 10^{-11}$ kg sec^{-1}. Therefore $f/f_0 = 5.89 \times 10^{-11}/4.98 \times 10^{-11} = 1.18$. If this value had equaled unity, the particle would be proved to be a nonsolvated sphere.

•

All that can be concluded from the data given in the preceding example is that the particle is not an unsolvated sphere. However, when an appropriate display of contours is examined for f/f_0 (e.g., Ref. 2), the latter is found to be consistent with an unsolvated particle of axial ratio about 4:1 or with a spherical particle hydrated to the extent of about 0.48 g water (g polymer)$^{-1}$. Of course, there are a number of combinations of these variables which are also possible, and some additional experimental data—such as the intrinsic viscosity—are needed to select that combination which is consistent with all experimental observations.

In the next section we return to Eq. (9.74) and a consideration of the experimental determination of D.

9.9 The Diffusion Coefficient: Experimental Aspects

There is an intimate connection at the molecular level between diffusion and random flight statistics. The diffusing particle, after all, is displaced by random collisions with the surrounding solvent molecules, travels a short distance, experiences another collision which changes its direction, and so on. Such a zigzagged path is called Brownian motion when observed microscopically, describes diffusion when considered in terms of net displacement, and defines a three-dimensional random walk in statistical language. Accordingly, we propose to describe the net displacement of the solute in, say, the x direction as the result of a ν-step random walk, in which the number of steps is directly proportional to time:

$$\nu = Kt \tag{9.81}$$

When we discussed random walk statistics in Chap. 1, we used n to represent the number of steps in the process and then identified this quantity as the number of repeat units in the polymer chain. We continue to reserve n as the symbol for the degree of polymerization, so the number of diffusion steps is represented by ν in this section.

Next suppose we apply this idea to describe the spreading by diffusion of an infinitesimally thin solution layer sandwiched between two portions of pure solvent. Figure 9.9b represents this situation. In Fig. 9.9b the two end compartments contain solvent, with the central portion containing solution at some concentration c_0. The practical implementation of such an experiment is not our primary concern, although we can imagine successive portions of the various liquids being carefully layered in a tube, or the solution filling the pores of a plug between two portions of solvent. Of concern to us is the description of the process by which the solute diffuses from a narrow band at $x = 0$ to a condition where it exists at uniform concentration throughout the vessel. Any other factors which might disturb the solute concentration are assumed to be absent. In practice, this implies excellent temperature control, since convection currents would totally invalidate experimental results. The mathematics developed in Chap. 1 in reference to the one-dimensional random walk is what we propose to use to describe this diffusion process.

Equation (1.34) gives the probability that a molecule will be displaced a distance x after ν steps of length l. Adapting this to the present problem, we use Eq. (9.81) to replace ν and write

$$P(x, t)\,dx = (2\pi K t l^2)^{-1/2} \exp\left(-\frac{x^2}{2Ktl^2}\right) dx \tag{9.82}$$

The ratio $c(x, t)/c_0$ would, in practice, be the logical measure of $P(x, t)$, so we write

$$c(x, t)\,dx = c_0\,P(x, t)\,dx = c_0\,(2\pi K t l^2)^{-1/2} \exp\left(-\frac{x^2}{2Ktl^2}\right) dx \tag{9.83}$$

The proposal we wish to examine is that Eq. (9.83) is a solution to Eq. (9.74) for the case of material initially present at $x = 0$ at a concentration c_0.

Several features of Eq. (9.83) assure us that this expression has the correct form:

1. $P(x, t)\,dx$ has the familiar bell shape of a normal distribution function [Eq. (1.39)], the width of which is measured by the standard deviation σ. In Eq. (9.83), t takes the place of σ. It makes sense that the distribution of matter depends in this way on time, with the width increasing with t.
2. Equation (1.34) is a normalized expression which means that, integrated over all values of x, it equals unity. Accordingly, adding together the

concentration of solute in a series of slices through the apparatus—that is, $\int c\,dx = \int c_0 P(x, t)\,dx$—always accounts for all of the solute, whatever its distribution.

3. The combined consideration of items (1) and (2) indicates that the profile of c throughout the apparatus gets flatter as it gets broader. At $t = 0$ the initial concentration is sharply peaked at c_0 at $x = 0$; at $t = \infty$, c is uniform from one end of the apparatus to the other.

All of these points are entirely reasonable. What is confusing about Eq. (9.83) is the step length and the undetermined constant K. Fortunately, they can both be eliminated in a single step. If Eq. (9.83) is a solution to Eq. (9.74), then both sides of the latter must be equal when the indicated operations are performed on Eq. (9.83). Carrying out these operations yields the following:

1. The first derivative of c with respect to t is

$$\left(\frac{\partial c}{\partial t}\right)_x = c_0 (2\pi K t l^2)^{-1/2}\ e^{-x^2/2Ktl^2} \left[\frac{x^2}{2Kt^2 l^2} - \frac{1}{2t}\right]$$

2. The second derivative of c with respect to x is obtained from

$$\left(\frac{\partial c}{\partial x}\right)_t = c_0 (2\pi K t l^2)^{-1/2}\ e^{-x^2/2Ktl^2} \left(-\frac{x}{Kt l^2}\right)$$

followed by

$$\left(\frac{\partial^2 c}{\partial x^2}\right)_t = c_0 (2\pi K t l^2)^{-1/2}\ e^{-x^2/2Ktl^2} \left[\left(-\frac{x}{Kt l^2}\right)^2 - \frac{1}{Kt l^2}\right]$$

3. Combining items (1) and (2) as required by Fick's second law yields

$$D = \frac{(\partial c/\partial t)_x}{(\partial^2 c/\partial x^2)_t} = \frac{x^2/2Kt^2 l^2 - 1/2t}{x^2/K^2 t^2 l^4 - 1/Ktl^2} = \frac{K^2 t^2 l^4}{2Kt^2 l^2} = \frac{Kl^2}{2}$$

These manipulations show that Eq. (9.83) satisfies Fick's second law with

$$K = \frac{2D}{l^2} \tag{9.84}$$

so the solution becomes

$$c(x, t)\,dx = c_0(4\pi Dt)^{-1/2} \exp\left(-\frac{x^2}{4Dt}\right) dx \tag{9.85}$$

Figure 9.11 is a plot of this function at two different times for a solute with a diffusion coefficient arbitrarily selected to be 5×10^{-11} m^2 sec^{-1}.

We can imagine measuring experimental curves equivalent to those in Fig. 9.11 by, say, scanning the length of the diffusion apparatus by some optical method for analysis after a known diffusion time. Such results are then interpreted by rewriting Eq. (9.85) in the form of the normal distribution function, $\mathbf{P}(z)\,dz$. This is accomplished by defining a parameter z such that

$$z = \frac{x}{(2Dt)^{1/2}} \tag{9.86}$$

in terms of which Eq. (9.85) becomes

$$\frac{c}{c_0} dx = \frac{1}{(2\pi)^{1/2}} \exp\left(-\frac{z^2}{2}\right) dz = P(z)\,dz \tag{9.87}$$

The inflection point of this function—where the second derivative changes sign—occurs at $z = 1$; hence the experimental analogs of Fig. 9.11 are examined for the location of their inflection points (subscript infl). The distance through which the material has diffused at this point is therefore given by

$$x_{infl} = (2Dt)^{1/2} \tag{9.88}$$

from which D can be evaluated if t is known. If Fig. 9.11 had been determined experimentally, such a procedure would be used by observing that $x_{infl} \cong 10^{-2}$ m for the curve at $t = 10^6$ sec. From this information, $D = (10^{-2}\ \text{m})^2/2(10^6\ \text{sec}) = 5 \times 10^{-11}$ m^2 sec^{-1}.

The experiment we have just described is not very satisfactory from a practical point of view, since it is very difficult to deposit a thin layer of solution between two bulk portions of solvent without some mixing. An experimentally more convenient method consists of layering equal volumes of solvent and solution so that a sharp boundary exists between them at $x = 0$, with $c = c_0$ for

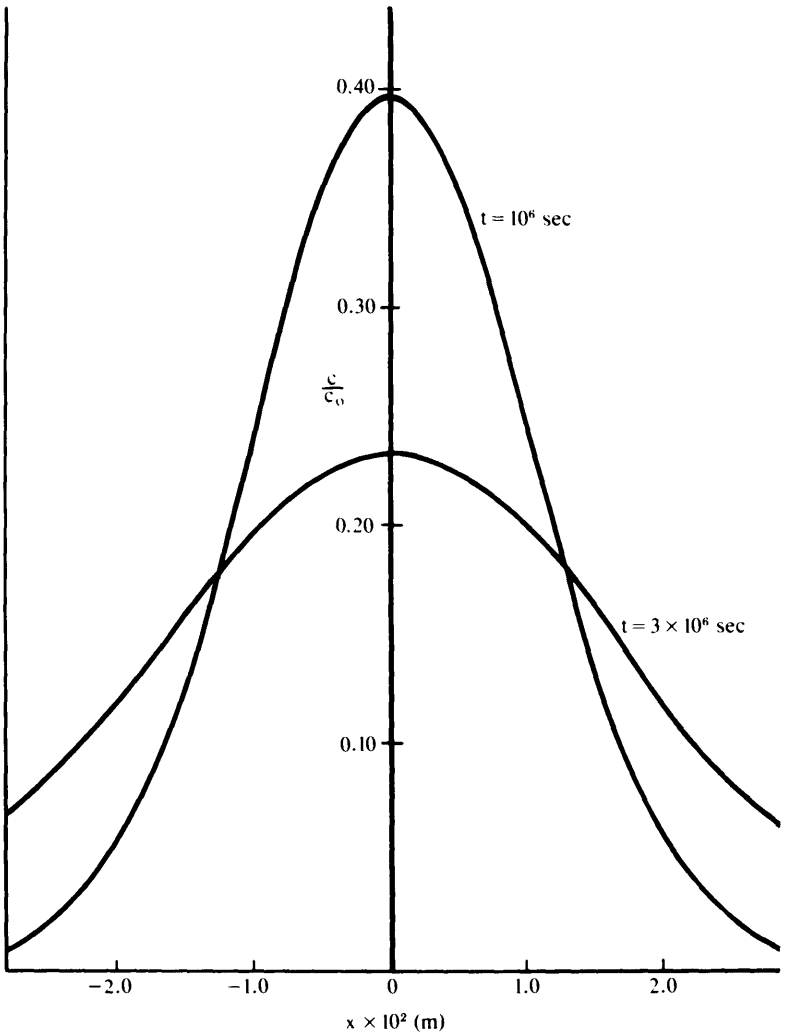

Figure 9.11 Variation of c/c_0 with x for one-dimensional diffusion [calculated from Eq. (9.85) with $D = 5 \times 10^{-11}$ m^2 sec^{-1}].

$x < 0$ and $c = 0$ for $x > 0$. This procedure also depends on layering liquids, but it is easier to do this with bulk quantities of material than to sandwich a thin layer between two bulk portions of solvent as required above.

At the outset of such an experiment, the gradient of concentration is zero on either side of the boundary and sharply peaked near $x = 0$. As diffusion occurs, the boundary becomes progressively less sharp. For $x < 0$, $c < c_0$, and for $x > 0$, $c > 0$, with both the magnitude and spatial extension of the effect increasing with time. Figure 9.12a shows how the overall concentration profile varies with time, and Fig. 9.12b shows the gradient dc/dx at corresponding times. Formal solution of Fick's second law with these boundary conditions proves that the shape of the gradient curves in this situation are identical to the curves in Fig. 9.11. Measuring the concentration gradient poses no serious experimental difficulty, so this method can also be analyzed by Eq. (9.87).

We are aware of the bending of a light ray when light passes from a medium of one refractive index to another. If light passes through a layer of optically homogeneous material and then reenters the original medium, then the emerging ray is bent back to the original direction. On the other hand, if there is a gradient of refractive index perpendicular to the direction of the light beam, the ray continues to experience additional bending as it passes through the medium with the gradient. Thus, when it reenters the surrounding medium, the emerging ray will make an angle with the incident beam. The size of this angle depends on

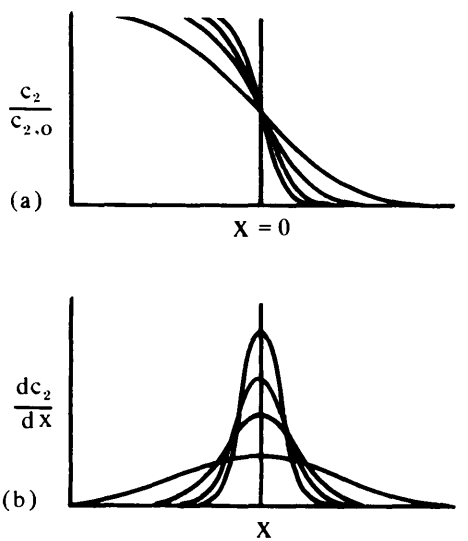

Figure 9.12 Progress of diffusion with time in an experiment like that shown in Fig. 9.9a, with the initial conditions given by $c = c_0$ for $x < 0$ and $c = 0$ for $x > 0$: (a) c/c_0 versus x and (b) dc/dx versus x.

the thickness of the sample and on the magnitude of the refractive index gradient. With the use of a diaphragm, the bent portion of the light beam can be excluded from a photographic plate or a photoelectric device. The magnitude of the resulting light attenuation is directly proportional to the refractive index gradient in the specimen. Such measurements can be made along the length of an apparatus to record the profile of the refractive index gradient. Procedures based on this concept are said to employ Schlieren optics.

The refractive indices of a solvent and a dilute solution, $\tilde{n}_0$ and $\tilde{n}$, respectively, can be related through

$$\tilde{n} = \tilde{n}_0 + \frac{d\tilde{n}}{dc} c \tag{9.89}$$

Over a reasonable range of c values, $d\tilde{n}/dc$ is constant; hence

$$\frac{d\tilde{n}}{dx} = \left(\frac{d\tilde{n}}{dc}\right)\frac{dc}{dx} = (\text{constant})\frac{dc}{dx}$$

This shows that Schlieren optics provide a means for directly monitoring concentration gradients. The value of the diffusion coefficient which is consistent with the variation of $d\tilde{n}/dx$ with x and t can be determined from the normal distribution function. Methods that avoid the difficulty associated with locating the inflection point have been developed, and it can be shown that the area under a Schlieren peak divided by its maximum height equals $(4\pi Dt)^{1/2}$. Since there are no unknown proportionality factors in this expression, D can be determined from Schlieren spectra measured at known times.

The standard procedure is to measure D at several different initial concentrations, using the procedure just described, and then extrapolating the results to $c = 0$. We symbolize the resulting limiting value D°. This value can be interpreted in terms of Eq. (9.79), which is derived by assuming $\gamma \to 1$ and therefore requires extreme dilution. It is apparent from Eqs. (9.79) and (9.5) that D° depends on the ratio T/η_0, as well as on the properties of the solute itself. In order to reduce experimental (subscript ex) values of D° to some standard condition (subscript s), it is conventional to write

$$D_s^\circ = \frac{T_s}{T_{ex}} \frac{\eta_{0,ex}}{\eta_{0,s}} D_{ex}^\circ \tag{9.90}$$

Note that this method of standardizing D values makes no allowance for the possibility that a molecule may change size, shape, or solvation with changes in temperature. In the next section we shall survey the behavior of polymeric materials in an ultracentrifuge. We shall see that diffusion coefficients can be

estimated from such experiments also and provide a valuable adjunct to the rate at which molecules settle in the ultracentrifuge.

9.10 Sedimentation Velocity and Sedimentation Equilibrium

In discussing diffusion in the last section we explicitly assumed the absence of forces which would complicate the boundary broadening in a diffusion experiment. Even though the force of gravity is always present in earthbound experiments, this is of negligible importance on a molecular scale, except over very large distances, such as in the earth's atmosphere. The equivalent to this force is not negligible in an ultracentrifuge, however, where accelerations, say, 10^5 times larger than gravity are readily achieved.

In ultracentrifugation a solution is placed in the cavity of a rotor which is spun at very high speeds in an instrument which allows vibration-free, constant-temperature operation. Two sidewalls of the sample compartment follow the radial lines of the rotor to prevent gradients of concentration from developing perpendicular to the radial direction of the acceleration. The sides of the sample space which are perpendicular to the axis of rotation are transparent, and an important part of the instrument is the optical system which allows a beam of light to pass through the rotating sample. The light which passes through the system can be analyzed by spectrophotometry or, most commonly, by Schlieren optics to monitor the progress of the molecules as they migrate in response to the radial acceleration.

Since the radial acceleration functions simply as an amplified gravitational acceleration, the particles settle toward the "bottom"—that is, toward the circumference of the rotor—if the particle density is greater than that of the supporting medium. A distance r from the axis of rotation, the radial acceleration is given by $\omega^2 r$, where ω is the angular velocity in radians per second. The midpoint of an ultracentrifuge cell is typically about 6.5 cm from the axis of rotation, so at 10,000, 20,000, and 40,000 rpm, respectively, the accelerations are 7.13×10^4, 2.85×10^5, and 1.14×10^6 m sec^{-2} or 7.27×10^3, 2.91×10^4, and 1.16×10^5 times the acceleration of gravity (g's).

The ultracentrifuge has been used extensively, especially for the study of biopolymers, and can be used in several different experimental modes to yield information about polymeric solutes. Of the possible procedures, we shall consider only sedimentation velocity and sedimentation equilibrium. We shall discuss these in turn, beginning with an examination of the forces which operate on a particle setting under stationary-state conditions.

Three kinds of forces must be considered:

1. The force of a molecule subject to radial acceleration is given by Newton's second law:

$$F_{accel} = \frac{M}{N_A} \omega^2 r \tag{9.91}$$

2. A buoyant force is given by the product of the volume V of the particle, the density ρ of the solution, and the radial acceleration:

$$F_{buoy} = V\rho\omega^2 r = \frac{M}{N_A \rho_2} \rho\omega^2 r \tag{9.92}$$

3. A force of viscous resistance is proportional to the stationary-stage velocity v_s according to Stokes' law:

$$F_{vis} = fv_s \tag{9.93}$$

4. The stationary-state velocity is rapidly achieved, and v_s corresponds to the force in item (1) equalling the opposing forces in items (2) and (3):

$$\frac{M}{N_A} \omega^2 r = \frac{M}{N_A} \frac{\rho}{\rho_2} \omega^2 r + fv_s \tag{9.94}$$

Since the velocity is dr/dt, Eq. (9.94) can also be written as

$$\frac{M}{fN_A} \left(1 - \frac{\rho}{\rho_2}\right) \omega^2 r = \frac{dr}{dt} \tag{9.95}$$

The stationary-state velocity per unit acceleration is a parameter which characterizes the settling particle and is called the sedimentation coefficient s:

$$s = \frac{dr/dt}{\omega^2 r} = \frac{M}{fN_A} \left(1 - \frac{\rho}{\rho_2}\right) \tag{9.96}$$

As a velocity divided by an accleration, s has units of time, and 10^{-13} sec—the order of magnitude for a typical solute—is called a svedberg (symbol S) in honor of Svedberg, a pioneer worker in this field.

Equation (9.95) can be integrated to give

$$\ln r = \frac{M}{fN_A} \left(1 + \frac{\rho}{\rho_2}\right) \omega^2 t + \text{const.} = s\omega^2 t + \text{const.} \tag{9.97}$$

which shows that the radial location of a species at various times is described by a straight line in a plot of ln r versus t. The slope of this line equals $\omega^2 s$. Many biopolymers are simply identified in terms of their sedimentation coefficient if

insufficient information is available to further resolve the cluster of constants which define s.

In a solution of molecules of uniform molecular weight, all particles settle with the same value of v_s. If diffusion is ignored, a sharp boundary forms between the "top" portion of the cell, which has been swept free of solute, and the "bottom," which still contains solute. Figure 9.13a shows schematically how the concentration profile varies with time under these conditions. It is apparent that the Schlieren optical system described in the last section is ideally suited for measuring the displacement of this boundary with time. Since the velocity of the boundary and that of the particles are the same, the sedimentation coefficient is readily measured.

As with the diffusion coefficient, sedimentation coefficients are frequently corrected for concentration dependence and reduced to standard conditions:

1. The concentration dependence of s is eliminated by making measurements at several different concentrations and then extrapolating to zero concentration. The limiting value is given by the symbol s°. This is the sedimentation analog of D°.

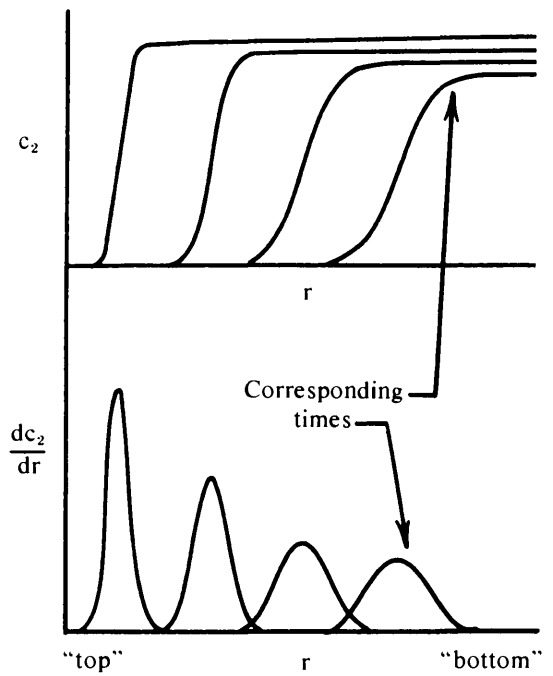

Figure 9.13 Location of sedimentation boundary after various times in an ultracentrifuge: (a) c versus r and (b) dc/dr versus r.

2. The temperature of an experiment affects s° through Eqs. (9.5) and (9.96), from which it is evident that s° is proportional to $(1 - \rho/\rho_2)/\eta_0$, all of which are temperature dependent.
3. In view of item (2), experimental (subscript ex) values of s° are reduced to standard (subscript s) temperature conditions by the expression

$$s_s^\circ = \frac{(1 - \rho/\rho_2)_s}{(1 - \rho/\rho_2)_{ex}} \frac{\eta_{0,ex}}{\eta_{0,s}} s_{ex}^\circ \tag{9.98}$$

This is the sedimentation analog of Eq. (9.90) for D°.

Diffusion effects are not absent during a sedimentation experiment as assumed above. As a matter of fact, the longer the experiment proceeds, the more diffuse the boundary between solvent and solution becomes owing to this effect. Figure 9.13b schematically illustrates the effect of this broadening in the Schlieren traces of the concentration profiles shown in Fig. 9.13a. The widths of these peaks depend on D, although correction must be made for the acceleration, which distorts the shape of the peaks from the ideal form indicated in Fig. 9.13b. Nevertheless, in principle, a study of sedimentation velocity permits the sedimentation coefficient to be evaluated unambiguously and the diffusion coefficient to be at least estimated. The proviso "in principle" is added, since s and D vary differently with M, and it may be only for an optimum range of M's that both s and D can be determined from a single experiment with sufficient accuracy.

Once a sedimentation coefficient has been measured, there are several ways in which it can be used:

1. As noted above, s_s° can be used directly to characterize a solute. This practice is widely followed with biopolymers.
2. The particle can be assumed to be spherical, in which case M/N_A can be replaced by $(4/3)\pi R^3 \rho_2$, and f by $6\pi\eta_0 R$. In this case the radius can be evaluated from the sedimentation coefficient: $s = 2R^2(\rho_2 - \rho)/9\eta_0$. Then, working in reverse, we can evaluate M and f from R. These quantities are called, respectively, the mass, friction factor, and radius of an equivalent sphere, a hypothetical spherical particle which settles at the same rate as the actual molecule.
3. If we assume that the densities of the solute and solution are known from separate experiments, the ratio M/f can be evaluated: $M/f = N_A s/(1 - \rho/\rho_2)$. By Eq. (9.79), f can be replaced by kT/D, with no assumptions regarding the shape of the particle. Therefore, if D is measured from the Schlieren traces of the sedimentation or in an independent experiment, s can be interpreted to give a value for M:

$$M = \frac{N_A kT}{(1 - \rho/\rho_2)} \frac{s}{D}$$

4. For polydisperse systems the value of M obtained from the values of s° and D°—or, better yet, the value of the s/D ratio extrapolated to c = 0—is an average value. Different kinds of average are obtained, depending on the method used to define the "average" location of the boundary. The weight average is the type obtained in the usual analysis.

If a sedimentation experiment is carried out long enough, a state of equilibrium is eventually reached between sedimentation and diffusion. Under these conditions material will pass through a cross section perpendicular to the radius in both directions at equal rates: "downward" owing to the centrifugal field, and "upward" owing to the concentration gradient. It is easy to write expressions for the two fluxes which describe this situation:

1. The flux due to sedimentation is equal to the concentration of solute times v_s as given by Eq. (9.96):

$$J_{sed} = cv_s = c\omega^2 rs \tag{9.99}$$

2. The flux due to diffusion is given by Fick's first law:

$$J_{diff} = -D\frac{dc}{dr} \tag{9.100}$$

3. Under conditions of sedimentation equilibrium, the sum of these two fluxes equals zero, or

$$D\frac{dc}{dr} = c\omega^2 sr \tag{9.101}$$

which can be integrated to give

$$\ln c = \frac{s}{2D}\omega^2 r^2 + \text{const.} \tag{9.102}$$

Using Eqs. (9.96) and (9.79) to replace s and f, respectively, we obtain

$$\ln c = \frac{M(1 - \rho/\rho_2)}{2N_A kT}\omega^2 r^2 + \text{const.} \tag{9.103}$$

Note that this expression is equivalent to the barometric formula which gives the variation of atmospheric pressure ($\propto$ c) with elevation ($\propto$ r). A first-order dependence on the distance variable holds in the barometric equation, since the acceleration is constant in this case.

If the solute concentration is measured at different values of r in a sedimentation equilibrium experiment, Eq. (9.103) predicts that a plot of ln c versus r^2 is linear with a slope equal to $M(1 - \rho/\rho_2)\omega^2/2RT$. This type of experiment, therefore, allows M to be determined without either measuring D or assuming anything about the shape of the particle. For a polydisperse sample with a continuous distribution of molecular weights, several different kinds of average values of M—starting with $\bar{M}_w$ and including $\bar{M}_z$ [Eq. (1.19)] and still higher averages—can be extracted from this kind of data, particularly under Θ conditions. Protein preparations which are more commonly studied by this method are likely to contain several distinctly different molecular weight species rather than a broad distribution of molecular weights. In the case of discrete molecular weights it may be possible to resolve the data in such a way as to obtain M values for the individual components. The following example considers such a case.

Example 9.6

A preparation of reduced and carboxymethylated protein particles in water reached sedimentation equilibrium after 40 hr at 12,590 rpm. When the data are plotted as suggested by Eq. (9.103), two distinctly linear portions are observed in the graph. The following pairs of points are taken from these two regions:

	Region I		Region II	
Recorder displacement ($\propto$ c)	2.51	3.09	3.89	6.61
r (cm)	6.58	6.65	6.69	6.79

Calculate the molecular weight of the two fractions indicated to be present in this preparation, taking the density of each to be 1.37 g cm^{-3} and the density of the medium to be unity.

Solution

With only two points to work with in each region, it is preferable to integrate Eq. (9.101) between definite limits c_1 at r_1 and c_2 at r_2, thereby evaluating the integration constant in Eq. (9.103):

$$\ln\left(\frac{c_1}{c_2}\right) = \frac{M(1 - \rho/\rho_2)\omega^2}{2RT}(r_1^2 - r_2^2)$$

Since the factor $(1 - \rho/\rho_2)\omega^2/2RT$ is common to both fractions, it can be evaluated separately:

$$\frac{\left(1 - \frac{1}{1.37}\right)\left(\frac{12{,}590 \text{ rev}}{\text{min}} \times \frac{2\pi \text{ rad}}{1 \text{ rev}} \times \frac{1 \text{ min}}{60 \text{ sec}}\right)^2}{2(8.314 \text{ J K}^{-1})(298 \text{ K})} = 94.7 \text{ mol kg}^{-1} \text{ m}^{-2}$$

Then for region I,

$$M = \frac{\ln\left(\frac{3.09}{2.51}\right)}{94.7 \frac{\text{mol}}{\text{kg m}^2} [(6.65)^2 - (6.58)^2] \, 10^{-4} \text{ m}^2} = 23.7 \text{ kg mol}^{-1}$$

$$= 23{,}700 \text{ g mol}^{-1}$$

For region II,

$$M = \frac{\ln\left(\frac{6.61}{3.89}\right)}{94.7 [(6.79)^2 - (6.69)^2] \, 10^{-4}} = 41.5 \text{ kg mol}^{-1} = 41{,}500 \text{ g mol}^{-1}$$

These values are in agreement with the values obtained from the slopes of the two linear portions of the appropriate graph which includes many more points.

•

We have emphasized biopolymers in this discussion of the ultracentrifuge and in the discussion of diffusion in the preceding sections, because these two complementary experimental approaches have been most widely applied to this type of polymer. Remember that from the combination of the two phenomena, it is possible to evaluate M, f, and the ratio f/f_0. From the latter, various possible combinations of ellipticity and solvation can be deduced. Although these methods can also be applied to synthetic polymers to determine M, they are less widely used, because the following complications are more severe with the synthetic polymers:

1. Nonideality requires that especially dilute solutions be used.
2. Polydispersity obscures the nature of the average obtained, although the possibility of extracting more than one kind of average from the same data under optimum conditions partially offsets this.
3. The factor $1 - \rho/\rho_2$ cannot be too close to zero, nor can the refractive index of the polymer and the solvent be too similar. These additional considerations limit the choice of solvents for a synthetic polymer, while their values are optimal for aqueous protein solutions.

All of the experimental procedures we have discussed in this chapter yield, among other things, information concerning the average molecular weight of a

polymer sample. We conclude this chapter with still another technique for characterizing a polymer in this regard: gel permeation chromatography.

9.11 Gel Permeation Chromatography

Gel permeation chromatography (GPC) is one of several different types of liquid chromatography which separate a mixture of solutes by passing a solution through an appropriate column. As the mobile phase passes through the column packing, different solute species are retained to various degrees by their interaction with the stationary phase. Surface adsorption, liquid partitioning, and ion exchange describe the interactions which serve as the basis for other types of liquid chromatography. In GPC the columns are packed with porous particles, and the separation occurs because molecules of different size penetrate the pores of the stationary phase to various degrees. The method is somewhat like a reverse sieving operation at the molecular level. The largest molecules are excluded from the pores to the greatest extent and, hence, are the first to emerge from the column. Progressively smaller molecules permeate the porous stationary phase to increasing extents and are eluted sequentially. The eluted material is monitored for solute by a suitable detector, and an instrumental trace of the detector output provides distinct peaks for well-resolved mixtures and broad peaks for a continuous distribution of molecular sizes. With suitable calibration, this can be translated into a quantitative characterization of the sample. In our discussion of this material we shall consider the "safe" empirical approach to this calibration, partially successful approaches to theoretical calibration, and briefly some aspects of the instrumentation and technique associated with GPC.

What is essentially the same method is known by several different names—and their acronyms—by workers in different fields who are interested in this technique. As a matter of vocabulary, we review some alternatives in terminology:

1. The term *size exclusion chromatography* (SEC) is the general name for this method of separation, emphasizing—as it does—the mechanism for the separation (size exclusion) rather than directing attention to one of several column packing materials (the gels). This is the name of preference among analytical chemists who are concerned with both the theory and practice of the method in its broadest sense.
2. Gel filtration chromatography (GFC) is the name used to describe this method of separation in the biochemical literature. Under this heading, the method is primarily applied to aqueous solutions of solutes of biological origin.
3. Gel permeation chromatography (GPC) is the term found most widely in the polymer literature. In this context it is used most widely as an analytical

technique for determining the molecular weight and molecular weight distribution of a synthetic polymer sample.

4. All three of these names are also modified by the term *high-performance*, or its acronym, to give HPSEC, HPGFC, and HPGPC. The additional feature implied by this terminology is the increased speed of efficient separations due to rapid flow through the column under the influence of relatively high applied pressures.

To use GPC for molecular weight determination, we must measure the volume of solvent that passes through the column before a polymer of particular molecular weight is eluted. This quantity is called the retention volume V_R. Figure 9.14 shows schematically the relationship between M and V_R; it is an

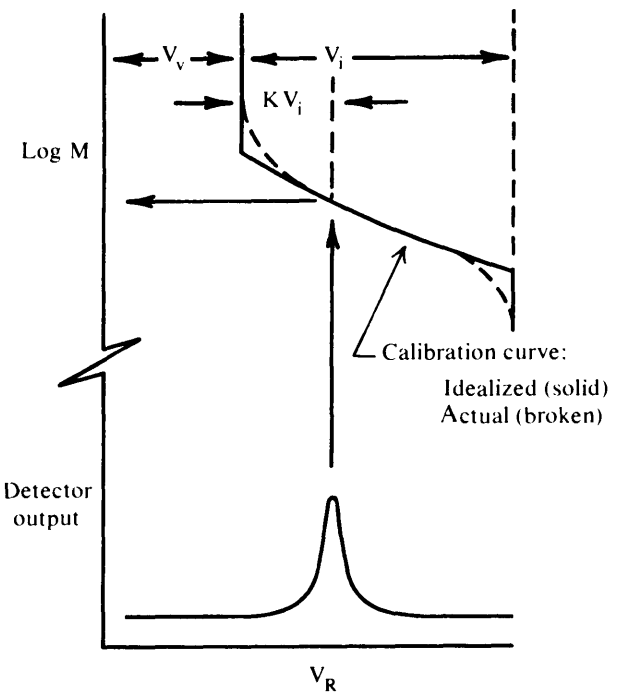

Figure 9.14 Calibration curve for GPC as log M versus the retention volume V_R, showing how the location of the detector signal can be used to evaluate M. Also shown are the void volume V_v and the internal volume V_i in relation to V_R, and KV_i as a fraction of V_i.

experimental fact that such calibration curves are approximately linear over about two orders of magnitude in M. In practice, the column is calibrated by constructing such a curve with standards of known molecular weight. We shall see presently that the "size" dependence of V_R is more a matter of spatial extension than molecular weight; hence the calibration should be carried out with standards of the same type as the unknown sample and under conditions which duplicate the treatment of the unknown. This sort of individual calibration is tedious and costly and thereby detracts from one of the principal advantages of GPC: speed.

To circumvent this need for calibration as well as to better understand the separation process itself, considerable effort has been directed toward developing the theoretical basis for the separation of molecules in terms of their size. Although partially successful, there are enough complications in the theoretical approach that calibration is still the safest procedure. If a calibration plot such as Fig. 9.14 is available and a detector output indicates a polymer emerging from the column at a particular value of V_R, then the molecular weight of that polymer is readily determined from the calibration, as indicated in Fig. 9.14.

Polydisperse polymers do not yield sharp peaks in the detector output as indicated in Fig. 9.14. Instead, broad bands are produced which reflect the polydispersity of synthetic polymers. Assuming that suitable calibration data are available, we can construct molecular weight distributions from this kind of experimental data. An indication of how this is done is provided in the following example.

Example 9.7

A broad chromatogram is subdivided into 20 slices, each 1 mm wide, and these are indexed from i = 1 to 20. The height h of the curve above a horizontal base line is carefully measured for each slice. The molecular weight of the ith slice is assigned from independent calibration via the retention volume. Columns 2-4 in Table 9.4 list h_i, $V_{R,i}$, and M_i values, respectively, for a particular chromatogram. Explain the significance and/or use of the remaining columns in Table 9.4 for the determination of a molecular weight distribution from this data.

Solution

The basic premise of this method is that the magnitude of the detector output, as measured by h_i for a particular fraction, is proportional to the weight of that component in the sample. In this sense the chromatogram itself presents a kind of picture of the molecular weight distribution. The following column entries provide additional quantification of this distribution, however.

Table 9.4 Data for the Analysis of the Gel Permeation Chromatogram of a Polydisperse Polymer Used in Example 9.7

(1) i	(2) h_i (mm)	(3) $V_{R,i}$ (ml)	(4) $M_i \times 10^{-6}$ (g mol^{-1})	(5) $\Sigma_{i=1}^{N} h_i$ (mm)	(6) $h_i/M_i \times 10^6$	(7) $h_i M_i \times 10^{-6}$	(8) A_i (mm^2)	(9) A_i/A_{tot}
21	0.0	20	4.709	545.0	0.0	0.0	545.0	1.0
20	0.0	21	3.302	545.0	0.0	0.0	545.0	1.0
19	0.8	22	2.327	545.0	0.34	1.86	544.6	0.999
18	3.5	23	1.640	544.2	2.13	5.74	542.5	0.995
17	16.8	24	1.1555	540.7	14.54	19.40	532.3	0.977
16	42.4	25	0.8142	523.9	52.08	34.52	502.7	0.922
15	67.9	26	0.5738	481.5	118.2	38.90	447.6	0.821
14	81.5	27	0.4003	413.7	203.6	32.62	373.0	0.684
13	81.4	28	0.2821	322.2	288.6	22.96	291.5	0.535
12	71.0	29	0.1988	250.8	357.1	14.12	215.3	0.395
11	57.0	30	0.1401	179.8	406.8	7.98	151.3	0.278
10	43.0	31	0.09872	122.8	435.6	4.24	101.3	0.186
9	30.0	32	0.06887	79.8	435.6	2.07	64.8	0.119
8	19.0	33	0.04853	49.8	391.5	0.92	40.3	0.074
7	12.2	34	0.03420	30.8	356.7	0.42	24.7	0.045
6	9.0	35	0.02410	18.6	373.4	0.22	14.1	0.026
5	4.0	36	0.01698	9.6	235.6	0.07	7.6	0.014
4	2.6	37	0.01197	5.6	217.2	0.03	4.3	0.008
3	2.0	38	0.00843	3.0	237.1	0.02	2.0	0.004
2	1.0	39	0.00588	1.0	170.0	0.01	0.5	0.001
1	0.0	40	0.00414	0.0	0.0	0.0	0.0	0.0

Source: Reprinted with permission from Ref. 6.

Column 5. $\Sigma_{i=1}^{N} h_i$ is proportional to the cumulative weight of all polymers in all categories up to the Nth.

Column 6. h_i/M_i is proportional to the weight of material in the ith class w_i divided by M_i, that is, to the number of moles in that class n_i. Therefore $\bar{M}_n$ can be evaluated as follows:

$$\bar{M}_n = \frac{\Sigma_i n_i M_i}{\Sigma_i n_i} = \frac{\Sigma_i (h_i/M_i)(M_i)}{\Sigma_i (h_i/M_i)} = \frac{\Sigma_i h_i}{\Sigma_i (h_i/M_i)} = \frac{545}{4.29 \times 10^{-3}}$$

$$= 127{,}000 \text{ g mol}^{-1}$$

Column 7. $h_i \times M_i$ is proportional to $w_i M_i$, and $\bar{M}_w$ is evaluated as follows:

$$\bar{M}_w = \frac{\Sigma_i w_i M_i}{\Sigma_i w_i} = \frac{\Sigma_i h_i M_i}{\Sigma_i h_i} = \frac{1.86 \times 10^6}{545} = 341{,}000 \text{ g mol}^{-1}$$

Column 8. $A_i = \Sigma_{i=1}^{N} [h_i + 1/2 (h_{i+1} - h_i)]$. Adding $1/2 (h_{i+1} - h_i)$ to h_i gives the height of the midpoint of each slice, and, since each slice is 1 mm wide, the summation gives the area under the curve up to the Nth class.

Column 9. A_i/A_{tot} gives that fraction of the area under the entire curve which has accumulated up to the Nth class. Since the curve is a weight distribution, this is equal to the weight fraction of material in the sample having $M < M_i$.

A plot of the last entry versus M gives the integrated form of the distribution function. The more familiar distribution function in terms of weight fraction versus M is given by the derivative of this cumulative curve. It can be obtained from the digitized data by some additional manipulations, as discussed in Ref. 6.

•

A detailed examination of the correlation between V_R and M is discussed in references on analytical chemistry such as Ref. 6. We shall only outline the problem, with particular emphasis on those aspects which overlap other topics in this book. To consider the origin of the calibration curve, we begin by picturing a narrow band of polymer solution being introduced at the top of a solvent-filled column. The volume of this solvent can be subdivided into two categories: the stagnant solvent in the pores (subscript i for internal) and the interstitial liquid in the voids (subscript v) between the packing particles:

$$V_{solvent} = V_v + V_i \tag{9.104}$$

The entire interstitial volume must pass through the column before any polymer emerges. Then the first polymer that does appear is the one with the highest

molecular weight. This solute has spent all its time in the voids—not the pores—of the packing and passes through the column with the velocity of the solvent.

Progressively smaller molecules have access to successively larger fractions of the internal volume. Therefore, as V_i emerges, consecutive fractions of the polymer come with it. Thus we can write the retention volume for a particular molecule weight fraction as

$$V_R = V_v + KV_i \tag{9.105}$$

where K is a function of both the pore size and the molecular size and indicates what fraction of the internal volume is accessible to that particular solute. The relationships between V_R, V_v, V_i, and KV_i are also shown in Fig. 9.14. When K = 0, the solute is totally excluded from the pores; when K = 1, it totally penetrates the pores.

It is instructive to consider a simple model for the significance of the constant K in Eq. (9.105). For simplicity, we assume a spherical solute molecule of radius R and a cylindrical pore of radius a and length l. As seen in Fig. 9.15a, an excluded volume effect prevents the center of the spherical solute molecule from approaching any closer than a distance R from the walls of the pore. This effectively decreases the volume accessible to the solute to a smaller cylinder of radius a - R. In this accessible cylinder the concentration of the solute is the same as in the interstitial fluid outside the pore. The excluded volume—that shell of thickness R around the walls of the pore—is devoid of solute. Hence the average concentration of solute in the pore *as a whole* is less than that outside the pore. The fraction of the external concentration in the pore is given by the ratio of the accessible volume to the actual volume of the cylindrical pore: $\pi(a - R)^2 l/\pi a^2 l$. This fraction gives K for the case of spherical solute molecules in cylindrical cavities. If we assume that the pore is long enough to neglect end effects, we have

$$K = \frac{(a - R)^2}{a^2} = \left(1 - \frac{R}{a}\right)^2 \tag{9.106}$$

Note that the fraction is zero when R = a, and unity when R = 0.

This simple model illustrates how the fraction K and, through it, V_R are influenced by the dimensions of both the solute molecules and the pores. For solute particles of other shapes in pores of different geometry, theoretical expressions for K are quantitatively different, but typically involve the ratio of solute to pore dimensions.

The extension of these ideas to random coils can proceed along two lines. In one analysis the coil domain is visualized as a sphere, as in the case above, with r_g taking the place of R. Alternatively, statistical methods can be employed

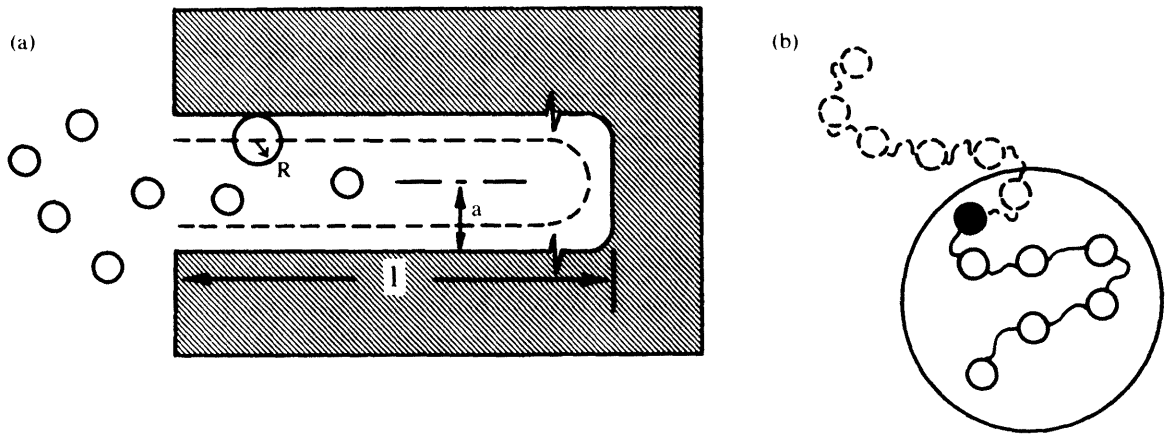

Figure 9.15 Schematic illustration of size exclusion in a cylindrical pore: (a) for spherical particles of radius R and (b) for a flexible chain, showing allowed (solid) and forbidden (broken) conformations of polymer.

to consider those conformations of a random chain which are excluded for a coil confined to a pore. This latter situation is illustrated in Fig. 9.15b. Figure 9.15b represents by solid and broken lines two conformations of the same chain, with the filled-in repeat unit being held in a fixed position. If the molecule were in bulk solution, both conformations would be possible. In a pore, represented by the enclosing circle in Fig. 9.15b, the broken line conformation is impossible. This is equivalent to a decrease in entropy for the coil in the pore, and the effect can be translated into an equilibrium constant between the solute in the pore and in the bulk solution. The factor K in Eq. (9.105) is just such a constant—the distribution coefficient—and can be evaluated by this approach for pores of different shape.

Figure 9.16 shows the theoretical predictions for K versus r_g/a compared with experimental findings. The solid line is drawn according to the statistical theory. The experimental points correspond to the same porous beads used as the stationary phase with their pore size analyzed by two different experimental procedures: mercury penetration (circles in Fig. 9.16, $\bar{a}$ = 21 nm) and gas adsorption (squares in Fig. 9.16, $\bar{a}$ = 41 nm). We can draw several conclusions from an examination of Fig. 9.16:

1. The characterization of the solid is also a source of discrepancy: The polymers are not the only source of difficulty!
2. Despite item (1), the fact that one set of experimental points agrees reasonably well with theory verifies the basic soundness of this approach.
3. Since K represents the fraction of V_i at which a particular molecular weight fraction emerges from the column, and since $\ln M \propto \ln r_g$, we see that this model correctly accounts for the form of the calibration curve shown in Fig. 9.14.

An interesting outgrowth of these considerations is the idea that $\ln r_g$ versus K or V_R should describe a universal calibration curve in a particular column for random coil polymers. This conclusion is justified by examining Eq. (9.55), in which the product $[\eta]M$ is seen to be proportional to $(\overline{r_g^2})^{3/2}$, with $r_g = \alpha(\overline{r_{g,0}^2})^{1/2}$. This suggests that $\ln r_g$ in the theoretical calibration curve can be replaced by $\ln[\eta]M$. The product $[\eta]M$ is called the hydrodynamic volume, and Fig. 9.17 shows that the calibration curves for a variety of polymer types merge into a single curve when the product $[\eta]M$, rather than M alone, is used as the basis for the calibration.

Although theoretical considerations still fall short of the goal of giving absolute values of M from V_R, they do suggest ways in which empirical calibrations can be extended beyond the stringent requirement of identical polymers under identical conditions being the only acceptable calibrations.

We conclude this section with a few remarks about GPC instrumentation. As with other areas of chromatography, this field is served by a variety of

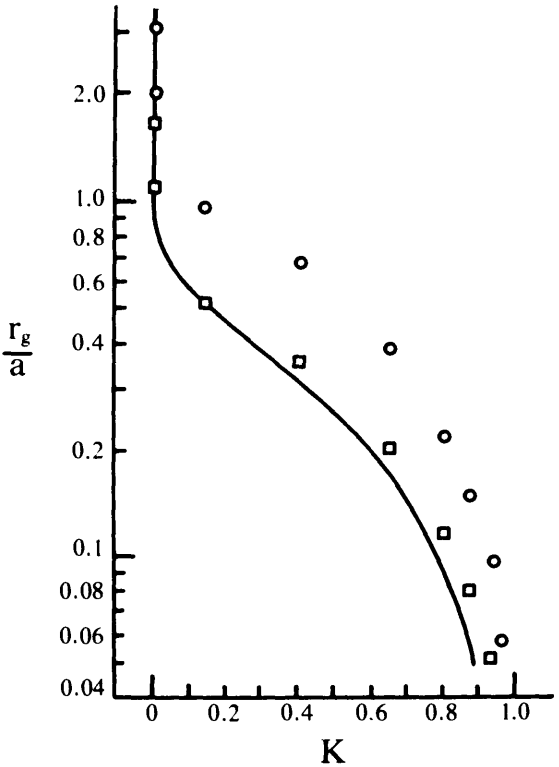

Figure 9.16 Comparison of theory with experiment for r_g/a versus K. The solid line is drawn according to the theory for flexible chains in a cylindrical pore. Experimental points show some data, with pore dimensions determined by mercury penetration (circles, $\bar{a}$ = 21 nm) and gas adsorption (squares, $\bar{a}$ = 41 nm). [From W. W. Yau and C. P. Malone, *Polym. Prepr.* 12:797 (1971), used with permission.]

commercial instruments, with "new and improved" models appearing regularly. It is therefore inappropriate to attempt to summarize the state of the art in a general discussion such as this. We can, however, consider some of the components of a GPC apparatus. While these have already and will continue to evolve through successive generations of instruments, we may reasonably expect that their basic functions will continue to be pertinent. Some key features of any GPC instrument are high-pressure liquid pumps, precise sample injection, sensitve detectors, and efficient columns.

A constant, reproducible flow rate on the order of 3-10 ml min^{-1} at a pressure of several thousand pounds per square inch makes the pump the most

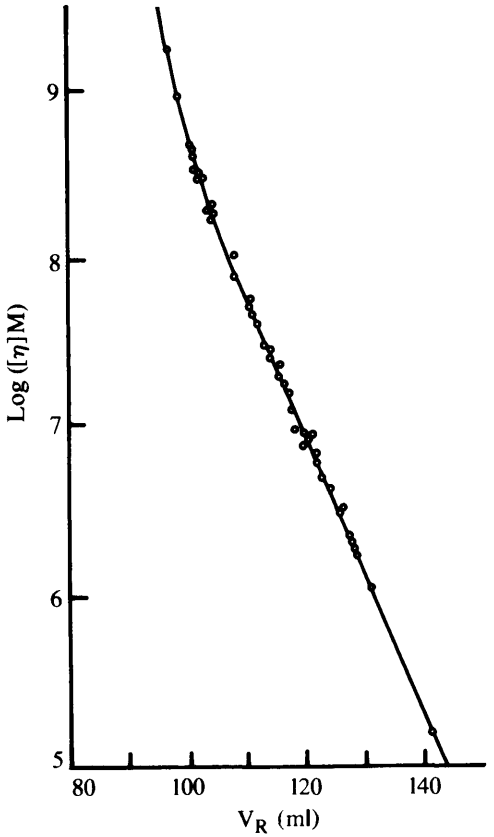

Figure 9.17 Plot of log $[\eta]M$ versus retention volume for various polymers, showing how different systems are represented by a single calibration curve when data are represented in this manner. The polymers used include linear and branched polystyrene, poly(methyl methacrylate), poly(vinyl chloride), poly(phenyl siloxane), polybutadiene, and branched, block, and graft copolymers of styrene and methyl methacrylate. [From Z. Grubisec, P. Rempp, and H. Benoit, *Polym. Lett.* 5:753 (1967), used with permission of Wiley.]

important part of the solvent-monitoring system. Good sample injection capability is crucial because of the desirability of maintaining as narrow a band of solute as possible in the column. A certain amount of band broadening inevitably occurs during passage through the column, but the sample injection procedure should not aggravate this. The detector output is proportional to the solute concentration in the column effluent. Therefore versatility, sensitivity, and accuracy are all important requirements in the detection system. The

difference in refractive index between the solvent and the solution is probably the most widely used method of detection. Various spectrophotometric methods are also employed.

The column is the site of actual separation, and, of the variables involved in its preparation, the packing material is the most important. Historically, cross-linked polystyrene gel particles were used as the stationary phase. Being only semirigid, these are of limited utility in modern high-performance, high-pressure equipment. These and other cross-linked polymers in the form of spheres with diameters in the range 10-100 μm are commercially available with a range of pore sizes, and are still widely used when pressures less than about 3000 psi are sufficient. More recently, silica particles with dimensions in the 5-10 μm range have also become available with a range of pore dimensions. Being rigid, these can withstand higher pressures. Silica particles are also available with various organic functional groups chemically bonded to their surface to minimize adsorption. If adsorption occurs, then both size exclusion and adsorption mechanisms are involved and the experiment is no longer governed by size exclusion principles alone.

Finally, we note that the size and shape of the particles of the packing, the packing technique, and column dimensions and configuration are additional factors which influence a GPC experiment. In addition, the flow rate, the sample size, the sample concentration, the solvent, and the temperature must all be optimized. Details concerning these considerations are found in analytical chemistry references, as well as in the technical literature of instrument manufacturers.

Problems

1. The intrinsic viscosity of poly(γ-benzyl-L-glutamate) (M_0 = 219) shows such a strong molecular weight dependence in dimethyl formamide that the polymer was suspected to exist as a helix which approximates a prolate ellipsoid of revolution in its hydrodynamic behavior†:

$M \times 10^{-3}$ (g mol^{-1})	21.4	66.5	130	208	347
$[\eta]$ (dl g^{-1})	0.107	0.451	1.32	3.27	7.20

Using 1.32 g cm^{-3} as the density of the polymer, estimate the axial ratio for these molecules, using Simha's equation:

$$\frac{\eta_{sp}}{\phi} = \frac{p^2}{15[\ln(2p) - 3/2]} + \frac{p^2}{5[\ln(2p) - 1/2]} + \frac{14}{15} \cong 175\left(\frac{p}{50}\right)^{1.8}$$

(for large p = a/b)

† P. Doty, J. H. Bradbury, and A. M. Holtzer, *J. Am. Chem. Soc.* 78:947 (1956).

For the α-helix, the length per residue is about 1.5 Å. Use this figure with the molecular weight to estimate the length 2a of the particle. Use the estimated a/b ratios to calculate the diameter 2b of the helix, which should be approximately constant if this interpretation is correct. Comment on the results.

2. Fox and Flory† used experimental molecular weights, intrinsic viscosities, and rms end-to-end distances from light scattering to evaluate the constant Φ in Eq. (9.55). For polystyrene in the solvents and at the temperatures noted, the following results were assembled:

Solvent	T (°C)	$M \times 10^{-3}$ (g mol^{-1})	$[\eta]$ (dl g^{-1})	r_{rms} (Å)
Methyl ethyl ketone	22	1760	1.65	1070
	22	1620	1.61	1015
	67	1620	1.50	980
	22	1320	1.40	900
	25	980	1.21	840
	22	940	1.17	750
	22	520	0.77	545
	25	318	0.60	475
	22	230	0.53	400
Dichloroethane	22	1780	2.60	1410
	22	1620	2.78	1335
	67	1620	2.83	1295
	22	562	1.42	760
	22	520	1.38	680
Toluene	22	1620	3.45	1290
	67	1620	3.42	1280

Evaluate Φ for each set of data and compare the average with the value given in the text.

3. Under Θ conditions for the polystyrene–cyclohexane system, intrinsic viscosities were measures‡ for polymers of different molecular weights:

M (g mol^{-1})	320,000	16,000	10,400	8,370	3,990
$[\eta]$ (dl g^{-1})	0.473	0.107	0.089	0.078	0.056

Use these data to evaluate $(\overline{r_{g,0}^2})^{1/2}$ for these polymers. To what step length l_0 in Eq. (1.62) do these values of $r_{g,0}$ correspond?

† T. G. Fox, Jr., and P. J. Flory, *J. Am. Chem. Soc.* 73:1915 (1951).

‡ W. R. Krigbaum, L. Mandelkern, and P. J. Flory, *J. Polym. Sci.* 9:381 (1952).

4. The intrinsic viscosity of polystyrene in benzene at 25°C was measured† for polymers with the following molecular weights:

M (g mol^{-1})	$[\eta]$ (dl g^{-1})	M (g mol^{-1})	$[\eta]$ (dl g^{-1})
6,970,000	11.75	277,000	1.07
4,240,000	8.15	63,800	0.358
2,530,000	5.54	63,100	0.356
838,000	2.43	43,200	0.268
784,000	2.32	16,050	0.136
676,000	2.07	10,430	0.106
335,000	1.23	8,370	0.0932
		3,990	0.0608

Evaluate $(\overline{r_g^2})^{1/2}$ for these polymers from these data. Use the value of l_0 determined in the last problem to calculate $(\overline{r_{g,0}^2})^{1/2}$ and, from the ratio of the two radii, evaluate α for each fraction.

5. According to Eq. (8.42), the parameter χ is proportional to the energy of interaction per 1-2 pair of molecules. To allow for solvent molecules of various sizes, we can write this as $\chi \propto n_1^* \Delta w$, where n_1^* is the number of segments *in the solvent molecule* and equals $\bar{V}_1/V_1^*$, with V_1^* the volume per mole of solvent segments. Use this concept to criticize or defend the following proposition: According to Eq. (9.67), $\alpha^5 - \alpha^3$ is proportional to $(1/2 - \chi)/\bar{V}_1$ or to $(2\bar{V}_1)^{-1} - (z\,\Delta w/2RTV_1^*)$. For a particular polymer in a homologous series of solvent molecules of different sizes, the second of these terms should be constant, while the first term decreases with increasing $\bar{V}_1$. This shows that $\alpha = 1$ for a polymer molecule dissolved in a "solvent" of other polymer molecules identical to itself. That is, that unperturbed coil dimensions apply to bulk polymer.

6. Mandelkern and Flory‡ have assembled the sedimentation coefficients and intrinsic viscosities for polymers of various molecular weights. As shown by the following data, the quantity $s_0[\eta]^{1/3}/M^{2/3}$ is constant for a particular system:

† W. R. Krigbaum and P. J. Flory, *J. Polym. Sci.* 11:37 (1953).
‡ L. Mandelkern and P. J. Flory, *J. Chem. Phys.* 20:212 (1952).

Polystyrene molecular weight	$s_0[\eta]^{1/3}/M^{2/3} \times 10^{17}$ In methyl ethyl ketone	$s_0[\eta]^{1/3}/M^{2/3} \times 10^{17}$ In toluene	Cellulose acetate molecular weight	$s_0[\eta]^{1/3}/M^{2/3} \times 10^{17}$ In acetone
1,240,000	25.3	13.6	194,000	54.0
830,000	25.0	13.4	130,000	59.5
519,000	26.6	13.4	53,000	59.0
254,000	25.6	13.9	11,000	50.3

Propose a brief explanation why this should be the case.

7. Protein molecules extracted from *Escherichia coli* ribosomes were examined by viscosity, sedimentation, and diffusion experiments for characterization with respect to molecular weight, hydration, and ellipticity. These data† are examined in this and the following problem. Use Fig. 9.4a to estimate the axial ratio of the molecules, assuming a solvation of 0.26 g water (g protein)$^{-1}$. At 20°C, $[\eta]$ = 27.7 cm^3 g^{-1} and ρ_2 = 1.36 for aqueous solutions of this polymer.

8. For the protein described in the last problem‡, M = 24,000 and D° = 5.59 × 10^{-11} m^2 sec^{-1}. Estimate f/f_0 from these data, taking ρ = 1.00 and η_0 = 0.01 P for the medium. The experimental ratio f/f_0 is the product of contributions from solvation and ellipticity: $(f/f_0)_{ex} = (f/f_0)_{solv}(f/f_0)_{ellip} = (R/R_0)_{solv}(f/f_0)_{ellip} = [1 + (m_{1,b}/m_2)(\rho_2/\rho_1)]^{1/3}(f/f_0)_{ellip}$. Briefly justify this expansion of the $(f/f_0)_{solv}$ factor. Assuming these particles were solvated to the extent of 0.26 g water (g protein)$^{-1}$, calculate $(f/f_0)_{ellip}$. For prolate ellipsoids of revolution (b/a < 1), Perrin has derived the following expression:

$$\left(\frac{f}{f_0}\right)_{ellip} = \left[1 - \left(\frac{b}{a}\right)^2\right]^{1/2} \Big/ \left(\frac{b}{a}\right)^{2/3} \ln\left(\frac{1 + [1 - (b/a)^2]^{1/2}}{b/a}\right)$$

Verify—or revise, if necessary—the axial ratio estimated in the last problem for this protein.

9. The sedimentation boundary of an enzyme preparation in an aqueous buffer at 20.6°C was measured after various times in an ultracentrifuge at 56,050 rpm. The following results were obtained§:

† K-P. Wong and H. H. Paradies, *Biochem. Biophys. Res. Commun.* 61:178 (1974).

‡ Ibid.

§ Data of P. Modrich, quoted by I. Tinoco, Jr., K. Sauer, and J. C. Wang, *Physical Chemistry*, Prentice-Hall, Englewood Cliffs, N.J. (1978).

Time (min)	r (cm)
0	5.9110
20	6.0217
40	6.1141
60	6.2068
80	6.3040
100	6.4047
120	6.5133
140	6.6141

Determine the sedimentation coefficient of this enzyme and, from this, its molecuar weight, assuming that $f = 8.24 \times 10^{-11}$ kg sec^{-1} and taking the factor $1 - \rho/\rho_2$ to be 0.256.

10. The sedimentation and diffusion coefficients for three different preparations of poly(methyl methacrylate) were measured† in *n*-butyl chloride at 35.6°C (= Θ) and in acetone at 20°C (> Θ) and the following results were obtained:

Solvent	Preparation	s° (S)	$D^\circ \times 10^7$ (cm^2 sec^{-1})	M
n-Butyl chloride	1	15.7	7.18	1.97×10^5
	2	39.1	2.91	–
	3	86.0	1.15	–
Acetone	1	20.3	6.80	–
	2	46.1	2.20	–
	3	88.5	0.92	6.35×10^6

Use the molecular weights given to evaluate the factor $1 - \rho/\rho_2$ for each of the systems; then use these factors to evaluate M for the other fractions. Compare the molecular weights obtained in the two solvents.

11. Both preparative and analytical GPC were employed to analyze a standard (NBS 706) polystyrene sample. Fractions were collected from the preparative column, the solvent was evaporated away, and the weight of each polymer fraction was obtained. The molecular weights of each fraction were obtained using an analytical gel permeation chromatograph calibrated in terms of both $\bar{M}_n$ and $\bar{M}_w$. The following data were obtained‡:

† H. Lütje and G. Meyerhoff, *Makromol. Chem.* 68:180 (1963).

‡ Y. Kato, T. Kametani, K. Furukawa, and T. Hashimoto, *J. Polym. Sci. Polym. Phys. Ed.* 13:1695 (1975).

Fraction number	Mass polymer (mg)	$M_n \times 10^{-4}$ (g mol^{-1})	$M_w \times 10^{-4}$ (g mol^{-1})
6	2	109	111
7	8	90.8	92.5
8	20	76.7	78.0
9	42	62.3	63.5
10	64	51.5	52.5
11	84	41.7	42.5
12	102	34.7	35.4
13	110	28.7	29.3
14	110	23.3	23.8
15	96	18.9	19.4
16	86	15.9	16.3
17	68	13.0	13.3
18	54	11.0	11.2
19	42	9.14	9.35
20	30	7.52	7.68
21	28	6.16	6.28
22	18	5.12	5.22
23	12	4.09	4.18
24	8	3.33	3.40
25	6	2.63	2.69
26	5	2.01	2.06
27	4	1.52	1.56
28	3	1.13	1.16
29	2	0.83	0.85
30	1	0.59	0.61

Calculate $\bar{M}_n$ and $\bar{M}_w$ and the ratio $\bar{M}_w/\bar{M}_n$ for the original polymer. Also evaluate the ratio $\bar{M}_w/\bar{M}_n$ for the individual fractions. Comment on the significance of $\bar{M}_w/\bar{M}_n$ for both the fractionated and unfractionated polymer.

12. Use the model for the size exclusion of a spherical solute molecule in a cylindrical capillary to calculate K_{GPC} for a selection of R/a values which are compatible with Fig. 9.16. Plot your values on a photocopy or tracing of Fig. 9.16. On the basis of the comparison between these calculated points and the line in Fig. 9.16 drawn on the basis of a statistical consideration of chain exclusion, criticize or defend the following proposition: There is not much difference between the K values calculated by the equivalent sphere and statistical models. The discrepancy between various experimental methods for evaluating $\bar{a}$ is much greater than the differences arising from different models. Even for random coil molecules the simple equivalent sphere model is acceptable for qualitative discussions of V_R.

13. Three polystyrene samples of narrow molecular weight distribution were investigated† for their retention in GPC columns in which the average particle size of the packing was varied. In all instances the peaks were well resolved. The following results were obtained:

Mean dimension of particles in packing (μm)		Molecular weight of polystyrene		
		411,000	51,000	2,030
120	t_R (min)	160	200	230
	V_R (ml)	160	200	230
44	t_R (min)	9	12	15
	V_R (ml)	4.5	6.0	7.5
6	t_R (sec)	20	2.7	32
	V_R (ml)	0.33	0.43	0.53

It is also known that smaller particles in the packing material are more difficult to pack homogeneously, and that higher pressures are required to pump liquid through them. On the basis of these observations, criticize or defend the following proposition: Between the largest and smallest particle sizes in these packing materials there is a 7.5-fold decrease in retention time. This increase in rate with undiminished resolution shows that still smaller packing particles should be developed, perhaps using something like emulsion polymerization to prepare small, cross-linked polymer gels.

Bibliography

1. Flory, P. J., *Principles of Polymer Chemistry*, Cornell University Press, Ithaca, N.Y., 1953.
2. Hiemenz, P. C., *Principles of Colloid and Surface Chemistry*, Marcel Dekker, New York, 1977.
3. Lauffer, M. A., *J. Chem. Educ.* 58:250 (1981).
4. Richards, E. G., *An Introduction to the Physical Properties of Large Molecules in Solution*, Cambridge University Press, Cambridge, 1980.
5. Tanford, C., *Physical Chemistry of Macromolecules*, Wiley, New York, 1961.
6. Yau, W. W., Kirkland, J. J., and Bly, D. D., *Modern Size Exclusion Liquid Chromatography*, Wiley, New York, 1979.

† E. P. Otocka, *Acc. Chem. Res.* 6:348 (1973).

10
Light Scattering by Polymer Solutions

Nature, and Nature's Laws lay hid in Night.
God said, *Let Newton be!* and All was Light.

Epitaph for Isaac Newton, Alexander Pope

10.1 Introduction

This chapter is the narrowest in scope of any chapter in this book. In it we discuss a single experimental procedure and its interpretation. It is appropriate to examine light scattering in considerable detail, since the theory underlying this method is relatively unfamiliar to students and the interpretation yields information concerning a variety of polymer parameters.

There are really only two major conclusions presented in the chapter, and even these can be consolidated into a single analysis when applied to experimental data. First, we shall develop the Rayleigh theory for the scattering of light by molecules whose linear dimensions are small compared to the wavelength of the light. For visible light Rayleigh scattering applies to gases and low molecular weight liquids, and we discuss these applications as part of the process for gaining understanding of this powerful technique. Next we derive the Debye theory for scattering by particles whose dimensions are no longer insignificant compared to the wavelength of light. This theory corrects Rayleigh scattering for interference effects and therefore includes the assumptions and limitations of Rayleigh scattering, plus some added features of its own.

Although we take a while before eventually casting these theories in forms which are directly applicable to polymers, the final results are highly practical. Throughout the chapter the presentation is aimed toward these eventual applications. We begin by comparing and contrasting the turbidity of solutions which scatter light with the absorbance of solutions which absorb light. We describe the experiments whereby scattering data are collected, and discuss the extrapolation procedures that must be followed to match experimental results with

theoretical models. Although we develop the various stages stepwise, we conclude by describing the Zimm method for combining all extrapolations in a single graphical method. Through these manipulations of light-scattering data, absolute values of the molecular weight, the second virial coefficient, and the radius of gyration can all be determined. Thus a single procedure can be used to evaluate several different parameters which would otherwise entail more than one kind of experiment. In contrast with osmometry, light scattering is rapid and free from complications associated with finding a suitable membrane. In contrast with viscometry and GPC, light scattering is absolute and does not require prior calibration. In spite of these advantages, light scattering has some limitations of its own which we shall discover as the theory unfolds. Leaving their respective limitations aside, we see that light scattering and osmometry complement each other, since each gives a different kind of molecular weight average; therefore, taken together, they provide information about the width of the molecular weight distribution.

This chapter is the only place in this volume that we encounter electrical units. Certain equations in electrostatics differ by the factor 4π, depending on whether they are written for SI or cgs units. To help clarify this situation, the chapter contains an appendix on electrical units which may be helpful, particularly when references based on other units are consulted.

10.2 The Intensity of Scattered Light and Turbidity

Chemistry students are familiar with spectrophotometry, the qualitative and quantitative uses of which are widespread in contemporary chemistry. The various features of absorption spectra are due to the absorption of radiation to promote a particle from one quantized energy state to another. The scattering phenomena we discuss in this chapter are of totally different origin: classical not quantum physics. However, because of the relatively greater familiarity of absorption spectra, a comparison between absorption and scattering is an appropriate place to begin our discussion.

We begin with a consideration of notation, defining I_0 as the intensity of light incident (subscript 0) upon a sample and I_t as the intensity of the light transmitted (subscript t) through a sample of thickness x. There are two different mechanisms that can account for the fact that $I_t < I_0$:

1. When the energy of the light matches the spacing of quantum states, some light is absorbed. In this case $I_0 - I_t = I_{abs}$.
2. When light interacts with the electrons in molecules in a nonquantized fashion, some of the incident light is redistributed in all directions, that is, scattered. As a result of this redistribution, $I_t < I_0$, with $I_0 - I_t = I_{sca}$.
3. It items (1) and (2), the effects are considered separately, although they may both occur together. When absorption is the primary interest, it is

rarely necessary to consider the accompanying scattering, since the latter contributes far less than absorption to the attenuation of intensity. When scattering is the primary interest, it is generally investigated in a portion of the spectrum which is free from absorption peaks. We shall always assume the latter situation, although scattering theories for absorbing particles are also available.

Figure 10.1 schematically illustrates the relationship between I_0, I_t, and I_s.

In spectrophotometry the absorbance per unit length of path through the sample ϵ is defined as

$$\epsilon = - \ln\left(\frac{I_t}{I_0}\right) \tag{10.1}$$

In the absence of absorption, scattering alone is responsible for any attenuation; therefore

$$\epsilon = - \ln\left(\frac{I_0 - I_s}{I_0}\right) = - \ln\left(1 - \frac{I_s}{I_0}\right) \cong \frac{I_s}{I_0} \tag{10.2}$$

where the last approximation is justified since the scattering intensity is ordinarily quite small. It does not make much sense to call this quantity "absorbance" when no absorption is involved; the scattering equivalent is called turbidity and given the symbol τ. These ideas enable us to write $(I_t/I_0)_{abs} = \exp(-\epsilon x)$,

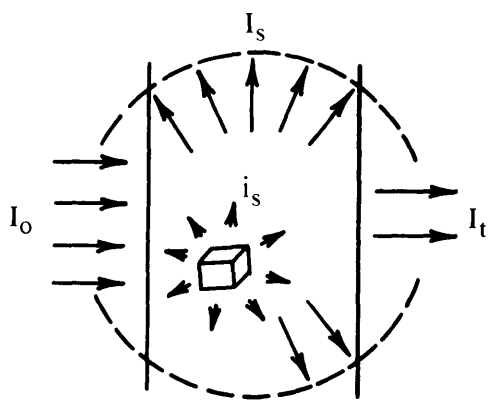

Figure 10.1 Relationships between I_0, I_t, and I_s. The light scattered per unit volume i_s is also shown.

$(I_t/I_0)_{sca} = \exp(-\tau x)$ and $(I_t/I_0)_{net} = \exp[-(\epsilon + \tau)x]$ for the situations itemized above. The turbidity of a specimen, then, is experimentally equivalent to absorption, except it is a small ($\tau \ll \epsilon$), classical effect which is generally ignored in absorption studies. To prevent it from being overshadowed by absorption, we consider nonabsorbing systems for which $\epsilon = 0$.

Like ϵ, τ is the product of two contributions: the concentration N/V of the centers responsible for the effect and the contribution per particle to the attenuation. It may help us to become oriented with the latter to think of the scattering centers as opaque spheres of radius R. These project opaque cross sections of area πR^2 in the light path. The actual cross section is then multiplied by the scattering efficiency factor Q_{sca}, so that $\pi R^2 Q_{sca}$ gives the *optical* cross section of the particle. The fact that the actual particle may not be opaque or spherical is taken into account by Q_{sca}. Thus we can think of the turbidity as the product of three factors:

$$\tau = (\pi R^2)\, Q_{sca} \left(\frac{N}{V}\right) \tag{10.3}$$

At this point it is instructive to examine the units of each of the terms in Eq. (10.3):

1. τ has units of length^{-1}. By analogy with Eq. (10.1), it is the "absorbance" per unit path length.
2. πR^2 has the units of length^2, since it is an area. This is the case regardless of the geometry of the actual particle.
3. N/V has units of length^{-3}, since it is a concentration.

It is apparent from these considerations that Q_{sca} is dimensionless. It is also clear that neither πR^2 nor N/V have anything to do with the wavelength λ of the light used in the experiment. In spite of this, τ is wavelength dependent, showing a broad, smooth variation with λ—as opposed to sharp peaks—for nonabsorbing particles. What this means is that the wavelength dependence of τ enters Eq. (10.3) through Q_{sca}. Furthermore, since Q_{sca} is dimensionless, λ must enter Q_{sca} in the form of a ratio, with some other variable having units of length. A fairly obvious choice for the latter is R, since Q_{sca} is a property of the scattering center.

An important aspect of the realization that Q_{sca} can be represented by $f(R/\lambda)$ is the fact that the function has the same value for any particles with the same R/λ ratio. Thus x rays interacting with atoms and microwaves interacting with fog drops have about the same R/λ ratio as polymer molecules interacting with visible light. As far as the size dependence of Q_{sca} is concerned, all of these systems are described by the same value of Q_{sca}, provided that the wavelength of the illumination is scaled to make the R/λ ratio the same in all cases.

The purpose of these qualitative remarks is to show that turbidity experiments are potential sources of information concerning both the spatial extension ($\propto$ R) of the scatterers and their molecular weight (since $N/V \propto c_2/M$). We anticipated these conclusions earlier in this volume by noting elsewhere that light scattering provides absolute values for the radius of gyration and the weight average molecular weight of a polymer.

In developing these ideas quantitatively, we shall derive expressions for the light scattered by a volume element in the scattering medium. The symbol i_s is used to represent this quantity; its physical significance is also shown in Fig. 10.1. [Our problem with notation in this chapter is too many i's!] Before actually deriving this, let us examine the relationship between i_s and I_s or, more exactly, between i_s/I_0 and I_s/I_0.

In order to do this, we anticipate the form of the expression for i_s/I_0. Equation (10.31) will show that i_s/I_0 can be written as the product of two terms: an optical-molecular factor we symbolize as R_ϕ and a geometrical factor $1 + \cos^2 \phi_x/r^2$, where r is the distance from the scattering molecule and ϕ_x is the angle between the x axis and a specific line of sight. The unscattered—that is, incident and transmitted—light beam in Fig. 10.1 is assumed to travel in the x direction. Accordingly, the total scattered intensity I_s is equal to the summation *over all angles* of the scattering per unit volume, i_s. The factor R_ϕ does not affect this summation and can be factored out. For the present we are only concerned with the summation:

$$\frac{I_s}{I_0} = \sum_{\substack{\text{all} \\ \text{angles}}} \frac{i_s}{I_0} = \int_0^\pi \frac{i_s}{I_0} 2\pi r \sin \phi_x \, (r \, d\phi_x) \tag{10.4}$$

The justification for replacing the summation with this integral is seen by examining Fig. 10.2. An element of area on the surface of a sphere of radius r has a circumference $2\pi r \sin \phi_x$ and a thickness $r \, d\phi_x$. Integration of these increments of area gives the light scattered at all angles. As noted above, $i_s/I_0 = R_\phi (1 + \cos^2 \phi_x)/r^2$. Substituting this into Eq. (10.4) and canceling the r^2's gives

$$\frac{I_s}{I_0} = 2\pi R_\phi \int_0^\pi (1 + \cos^2 \phi_x) \sin \phi_x \, d\phi_x \tag{10.5}$$

This standard integral is readily evaluated to give the numerical factor 8/3; therefore

$$\tau = \frac{I_s}{I_0} = \frac{16\pi}{3} R_\phi \tag{10.6}$$

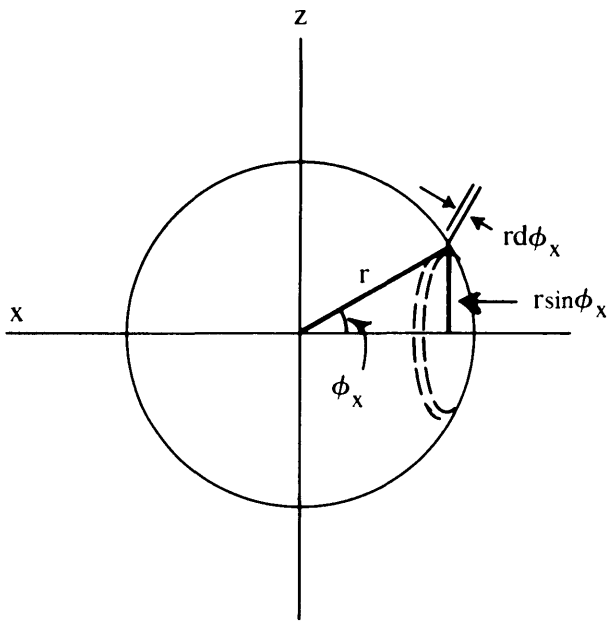

Figure 10.2 Definition of an element of area for the purpose of integrating $i_s(r, \phi_x)$ over all angles to evalute I_s. (Reprinted from Ref. 2, p. 178.)

In Sec. 10.5 we shall consider the derivation of i_s/I_0 and the factor R_ϕ which appears in Eq. (10.6). First, however, it is worthwhile to review some basic ideas about light itself.

10.3 Electric Fields and Their Interaction with Matter

The scattering of visible light by polymer solutions is our primary interest in this chapter. However, since Q_{sca} is a function of the ratio R/λ, as we saw in the last section, the phenomena we discuss are applicable to the entire range of the electromagnetic spectrum. Accordingly, a general review of the properties of this radiation and its interactions with matter is worthwhile before a specific consideration of scattering.

In this discussion we define the x direction to be the direction of propagation of the light waves. This means that the yz plane contains the oscillating electrical and magnetic fields which carry the energy of the radiation. Only the electric field concerns us in scattering. Since the oscillation is periodic in both time t and location x, the electric field can be represented by the equation

$$E = E_0 \cos\left[2\pi\left(\nu t + \frac{x}{\lambda}\right)\right] \tag{10.7}$$

in which the following applies:

1. ν is the frequency and at a fixed location—say, $x = 0$—one full wave is traced out in a time $1/\nu$.
2. λ is the wavelength and at a fixed time—say, $t = 0$—one full wave is traced out over a distance λ.
3. E_0 is the maximum amplitude of the field, since the cosine factor which modifies it oscillates between -1 and +1.
4. E oscillates in sign, as described by Eq. (10.7), yet the wave manifests itself with an intensity which is always positive. This suggests that E^2 rather than E itself be used as a measure of light intensity.
5. E causes a particle of charge q to experience a force and hence a displacement. Both the force and the displacement are proportional to E; therefore the energy of the field-charge interaction—the product of the force and the displacement—is proportional to E^2.
6. The combination of items (4) and (5) leads to the important conclusion that light intensity is the measure of the flux of energy through a surface perpendicular to the direction of propagation—the yz plane in our convention—and this is proportional to E^2.

Under vacuum, the velocity of propagation c of an electromagnetic wave is 3.0×10^8 m sec^{-1}, and this is related to the frequency and wavelength by

$$c = \nu\lambda_0 \tag{10.8}$$

In a medium of refractive index $\tilde{n}$, both c and λ_0 are decreased to $1/\tilde{n}$ of their value under vacuum: $v = c/\tilde{n}$ and $\lambda = \lambda_0/\tilde{n}$:

$$v = \nu\lambda \tag{10.9}$$

Note that c and λ_0 are used as symbols for velocity and wavelength, respectively, under vacuum, and that v and λ signify their counterparts in some medium. In addition, we observe that the frequency ν is not affected by the passage from one medium to another. As the light passes through a substance, its electric field interacts with the electrons of that substance, inducing oscillations in them at the same frequency as the frequency of the original field. Since no change in frequency is involved in going from vacuum into matter, it is the wavelength that must also adjust along with velocity. Figure 10.3 illustrates this by showing successive crests of electromagnetic waves traveling in the direction of the arrow as they pass from vacuum into a substance of refractive index $\tilde{n}$. At the surface

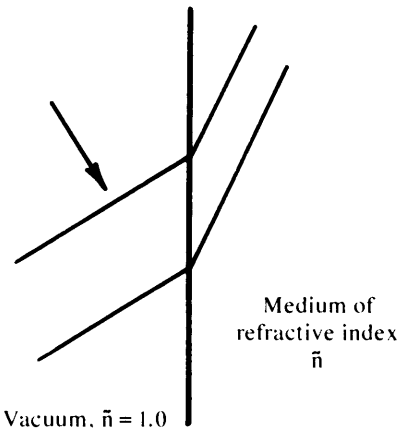

Figure 10.3 Schematic illustration showing the bending of light and the decrease in wavelength as the radiation passes from a vacuum to a medium of refractive index ñ.

between the two media, there is a continuity in E with respect to frequency. That is, from whichever side of the surface it is viewed, the trace of E on the boundary is the same. To achieve this "fit," the wave front bends, as shown in Fig. 10.3, and the spacing between the wave crests, the wavelength, decreases. Both the bending of light and the change in wavelength are required by the continuity of E at the interface.

As our discussion of scattering proceeds, we shall examine the coupling between the oscillating electrical field of light and the electrons of the scatterer in detail. First, it is useful to consider the interaction of an electric field with matter, as this manifests itself in the dielectric behavior of a substance. This will not only introduce us to the field-matter interaction, but will also provide some relationships which will be useful later.

For this purpose we compare a parallel plate capacitor under vacuum and one containing a dielectric, as shown in Figs. 10.4a and b, respectively. The plates of the capacitor carry equal but opposite charges ±Q which can be described as $\pm\sigma A$, where σ is the surface charge density and A is the area of the plates. In this case, the field between the plates is given by

$$E_0 = \frac{\sigma}{\epsilon_0} \tag{10.10}$$

where ϵ_0 is the permittivity of vacuum, 8.85×10^{-12} C^2 J^{-1} m^{-1}. If the space between the plates is filled with a dielectric as shown in Fig. 10.4b, the field is decreased to a value

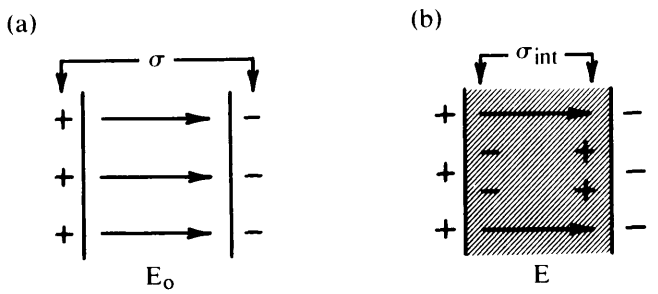

Figure 10.4 Parallel-plate capacitor with surface charge density σ. (a) The field is E_0 with no dielectric present. (b) The field is reduced to E by a dielectric which acquires a surface charge of its own, σ_{int}.

$$E = \frac{\sigma}{\epsilon} \tag{10.11}$$

where the ratio $\epsilon/\epsilon_0 = \epsilon_r$ is called the relative dielectric constant of the medium and is measured as the ratio of the capacitances of the apparatus with and without the substance. Sometimes the term *relative permittivity* and the symbol K_r are used instead of ϵ_r to describe this ratio.

Since $\epsilon > \epsilon_0$, we seek to explain the smaller field in the presence of the dielectric in terms of molecular properties and the way in which they are affected by the electric field. An easy way to visualize the effect is to picture an opposing surface charge—indicated as σ_{int} in Fig. 10.4b—accumulating on the dielectric. This partially offsets the charge on the capacitor plates to a net charge density $\sigma - \sigma_{int}$ so that E_0 becomes E and is given by

$$E = \frac{\sigma - \sigma_{int}}{\epsilon_0} \tag{10.12}$$

Next we can eliminate σ from Eqs. (10.11) and (10.12) to obtain

$$\sigma_{int} = \epsilon_0 (\epsilon_r - 1) E \tag{10.13}$$

Now let us examine the molecular origin of σ_{int}. Molecular polarity may be the result of either a permanent dipole moment μ or an induced dipole moment μ_{ind}, where the latter arises from the distortion of the charge distribution in a molecule due to an electric field. We saw in Chap. 8 that each of these types of polarity are sources of intermolecular attraction. In the present discussion we assume that no permanent dipoles are present and note that the induced dipole moment is proportional to the net field strength at the molecule:

$$\mu_{ind} = \alpha E_{net} \tag{10.14}$$

where α is called the polarizability of the molecule. It is apparent from this definition that the larger α is, the greater is the induced dipole moment per unit field. Thus α is aptly named, since it measures the ability of a molecule to undergo polarization.

Next we consider the net field at the molecule. This turns out to be the sum of two effects: the macroscopic field given by Eq. (10.12) plus a local field that is associated with the charge on the surface of the cavity surrounding the molecule of interest. The latter may be shown to equal $(1/3)(\sigma_{int}/\epsilon_0)$. Hence the net field at the molecule is

$$E_{net} = E + \frac{1}{3}\frac{\sigma_{int}}{\epsilon_0} = \frac{\sigma_{int}}{\epsilon_0(\epsilon_r - 1)} + \frac{1}{3}\frac{\sigma_{int}}{\epsilon_0} = \frac{\sigma_{int}}{3\epsilon_0}\left(\frac{\epsilon_r + 2}{\epsilon_r - 1}\right) \tag{10.15}$$

All that remains to be done is to connect σ_{int} with μ_{ind}. This is done by the observation that $\sigma_{int} = Q_{int}/A$, where Q_{int} is the charge on the surface of the dielectric. Next, Q_{int}/A can be written $(Q_{int}/V)d$, where V and d are the volume and the thickness of the dielectric, respectively. The product of a charge and the distance that separates it from its opposite charge defines a dipole moment. This means that σ_{int} has the significance of a net dipole moment per unit volume for the sample. If only induced dipole moments operate, as we have specified, this net dipole per unit volume is simply the product of the number of molecules per unit volume $\rho N_A/M$ and the induced dipole moment of each: $\sigma_{int} = (\rho N_A/M)\mu_{ind}$. Combining this idea with Eqs. (10.14) and (10.15) gives

$$\sigma_{int} = \frac{\rho N_A \alpha}{M}\left[\frac{\sigma_{int}}{3\epsilon_0}\left(\frac{\epsilon_r + 2}{\epsilon_r - 1}\right)\right] \tag{10.16}$$

or

$$\frac{1}{3}\frac{\rho N_A \alpha}{M\epsilon_0} = \frac{\epsilon_r - 1}{\epsilon_r + 2} \tag{10.17}$$

This result, called the Clausius-Mosotti equation, gives the relationship between the relative dielectric constant of a substance and its polarizability, and thus enables us to express the latter in terms of measurable quantities. The following additional comments will connect these ideas with the electric field associated with electromagnetic radiation:

1. If molecules have permanent dipole moments and can orient themselves with respect to the field, then Eq. (10.17) must be modified by inclusion of a term associated with μ.

2. In discussing capacitance, we implied nothing about the frequency of the field. The results given are general, applying equally to the frequencies of alternating current and of the electric field in electromagnetic radiation.
3. At the high frequencies of visible light, any permanent dipoles present cannot respond rapidly enough to contribute to the dielectric behavior; hence Eq. (10.17) applies to polar molecules also under the influence of light.
4. Under the same conditions, Maxwell's theory of radiation shows that the refractive index and the relative dielectric constant are simply related by

$$\epsilon_r = \bar{n}^2 \tag{10.18}$$

Both ϵ_r and $\bar{n}$ are clearly frequency dependent, since the foregoing argument shows that various effects contribute to the polarity of a molecule at different frequencies.

Equations (10.17) and (10.18) show that both the relative dielectric constant and the refractive index of a substance are measurable properties of matter that quantify the interaction between matter and electric fields of whatever origin. The polarizability is the molecular parameter which is pertinent to this interaction. We shall see in the next section that α also plays an important role in the theory of light scattering. The following example illustrates the use of Eq. (10.17) to evaluate α and considers one aspect of the applicability of this quantity to light scattering.

Example 10.1

The refractive index of CCl_4 at 20°C and 589 nm, the D line of the sodium spectrum, is 1.4607. At this temperature the density of this compound is 1.59 g cm^{-3}. Use this information to calculate α for CCl_4. Criticize or defend the following proposition: The prediction that $Q_{sca} = f(R/\lambda)$ may have been premature. The consideration of Eq. (10.3) which led to this conclusion could just as well predict $Q_{sca} = f(\alpha^{1/3}/\lambda)$.

Solution

According to Eq. (10.18), $\epsilon_r = \bar{n}^2 = (1.4607)^2 = 2.1336$ at $\nu = 5.09 \times 10^{14}$ Hz (589 nm). The number of CCl_4 molecules at 20°C is given by

$$\frac{\rho N_A}{M} = \frac{(1.59 \text{ g cm}^{-3})(6.02 \times 10^{23} \text{ molecules mol}^{-1})}{153.8 \text{ g mol}^{-1}}$$

$$= 6.245 \times 10^{21} \text{ molecules cm}^{-3}$$

Therefore, by Eq. (10.17),

$$\alpha = \frac{3\epsilon_0(\epsilon_r - 1)/(\epsilon_r + 2)}{\rho N_A/M} = \frac{3(8.85 \times 10^{-12}\ \mathrm{J^{-2}\ C^{-2}\ m^{-1}})(0.2742)}{6.245 \times 10^{21}\ \mathrm{molecules\ cm^{-3}}}$$

$$= 1.166 \times 10^{-39}\ \mathrm{C^2\ J^{-1}\ m^2\ molecule^{-1}}$$

This is the correct value for α in SI units, as can be verified by examining the units in Eq. (10.14): αE_{net} has units $(\mathrm{C^2\ J^{-1}\ m^2})(\mathrm{V\ m^{-1}}) = \mathrm{C\ m}$, which is correct for μ_{ind}. In this instance cgs units are also informative: to effect the transformation we divide by $4\pi\epsilon_0$ as described in the appendix, Sec. 10.12:

$$\alpha_{cgs} = \frac{\alpha}{4\pi\epsilon_0} = \frac{1.166 \times 10^{-39}\ \mathrm{C^2\ J^{-1}\ m^2\ molecule^{-1}}}{1.113 \times 10^{-10}\ \mathrm{C^2\ J^{-1}\ m^{-1}}}$$

$$= 1.05 \times 10^{-29}\ \mathrm{m^3\ molecule^{-1}} = 10.5\ \mathrm{\AA^3\ molecule^{-1}}$$

Expressed in these units, α resembles a molecular volume; hence $\alpha^{1/3}$ has units of length and is thus a length which characterizes the interaction between a molecule and the field. In view of this, it may be true that $Q_{sca} = f(\alpha^{1/3}/\lambda)$, since all we can say about Q_{sca} is that it is dimensionless.

•

With this as background, we are finally in a good position to look at the scattering process itself.

10.4 Light Scattering by an Isolated Molecule

Ordinarily, light-scattering experiments are conducted with unpolarized light, but the following discussion is more easily visualized in terms of light which is linearly polarized. For light propagating in the x direction, the electric field lies in the yz plane and may be resolved into y and z components. Polarizing filters have different absorption coefficients in perpendicular directions, and hence absorb light in which the field oscillates in one direction and pass the perpendicular component. For convenience, we speak of vertically and horizontally polarized light when the oscillations are parallel to the z and y axes, respectively.

To quantify the interaction between a molecule and an incident ray of light, we imagine the molecule situated at the origin of a coordinate system as shown in Fig. 10.5 and consider its interaction with vertically polarized light traveling in the x direction. Since it is the mobile charge in the molecule that couples with the light, we represent the molecule as a quantity of charge q. As discussed in the last section, the oscillating field induces an oscillation in the charge q,

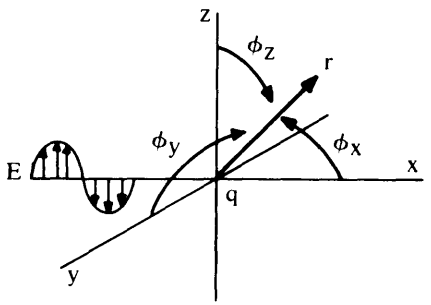

Figure 10.5 Definition of the variables used to describe the electric field produced by the oscillation of the charge q under the influence of vertically polarized light. (Reprinted from Ref. 2, p. 164.)

and it is a basic fact of electromagnetism that this situation is a source of radiation. On a molecular scale this molecule behaves like an antenna, sending out a signal along a line of sight represented by the arrow in Fig. 10.5. The radial distance from the radiating dipole is r and the angles between the line of sight and the coordinate axes are designated ϕ_x, ϕ_y, and ϕ_z, respectively.

Since the charge becomes coupled with the oscillating field, q undergoes a periodic acceleration which we represent by a_p. Next we borrow a relationship from electromagnetic theory to describe the field produced by an oscillating dipole such as the molecule we have described:

$$E = \frac{q a_p \sin \phi_z}{4\pi\epsilon_0 c^2 r} \tag{10.19}$$

Since we have introduced this relationship without proof, it will be helpful to consider its components with respect to their plausibility:

1. It is reasonable that the field produced by the accelerating charge should be proportional to the magnitude of both the charge and the acceleration.
2. The energy that is radiated spreads out over a solid angle and is therefore proportional to r^{-2}. We saw in Sec. 10.2 that this energy is proportional to E^2; hence E varies with r^{-1}.
3. The factor $4\pi\epsilon_0$ arises from the choice of SI units. Since a_p has units time^{-2}, the acceleration is divided by c^2 to convert the units of the denominator to length^2, as required by the definition of the field.
4. The $\sin \phi_z$ factor shows that the field produced by the oscillator is maximum in the xy plane, zero along the z axis, and symmetrical with respect to the z axis. This geometry is consistent with the vertical polarization of the field which is driving the dipole and producing the field described by Eq. (10.19).

Next we look for a substitution for a_p, the acceleration experienced by the charge. A convenient device for doing this originates from considering the oscillating dipole produced by the driving field. Since $\mu = \alpha E$,we can describe the periodic (subscript p) dipole moment of a molecule by

$$\mu_p = \alpha E_0 \cos(2\pi\nu t) \tag{10.20}$$

where we have used Eq. (10.7) with x = 0 to describe the incident field. Since the dipole moment also equals the charge times the distance of charge separation and it is the latter that is periodic, we identify the displaced charge q as αE_0 and $\xi = \cos(2\pi\nu t)$ as the separation. Therefore the acceleration is

$$a_p = \frac{d^2\xi}{dt^2} = -4\pi^2\nu^2 \cos(2\pi\nu t) \tag{10.21}$$

Substituting these results into Eq. (10.19) gives

$$E = \frac{(\alpha E_0)[-4\pi^2\nu^2 \cos(2\pi\nu t)] \sin\phi_z}{4\pi\epsilon_0 c^2 r} \tag{10.22}$$

for the field produced by the oscillating dipole.

As noted previously, the intensity of light is proportional to the square of the field; hence the intensity of the light radiated by the dipole is given by

$$i_v \propto \frac{\pi^2\nu^4\alpha^2 E_0^2 \cos^2(2\pi\nu t) \sin^2\phi_z}{\epsilon_0^2 c^4 r^2} \tag{10.23}$$

while the intensity of the driving radiation incident (subscript 0) on the molecule is given by squaring Eq. (10.7):

$$I_{0,v} \propto E_0^2 \cos^2(2\pi\nu t) \tag{10.24}$$

The subscript v is attached to both of these intensities as a reminder that the foregoing analysis is based on the assumption of vertical polarization for the incident light beam. The ratio of these intensities gives the fraction of light scattered per molecule by vertically polarized light:

$$\frac{i_v}{I_{0,v}} = \frac{\pi^2\nu^4\alpha^2 \sin^2\phi_z}{\epsilon_0^2 c^4 r^2} = \frac{\pi^2\alpha^2 \sin^2\phi_z}{\epsilon_0^2 \lambda_0^4 r^2} \tag{10.25}$$

Since the vertically polarized light postulated in the derivation of Eq. (10.25) involves both the z component of the electric field and the angle ϕ_z, it is

apparent that the corresponding expression for horizontally (subscript h) polarized light—which involves the y component of the field—is identical to Eq. (10.25), except for the $\sin^2 \phi$ term:

$$\frac{i_h}{I_{0,h}} = \frac{\pi^2 \alpha^2 \sin^2 \phi_y}{\epsilon_0^2 \lambda_0^4 r^2} \tag{10.26}$$

Note that this also involves the assumption of isotropic molecules, which have the same polarizability in all directions. Unpolarized light consists of equal amounts of vertical and horizontal polarization, so the fraction of light scattered in the unpolarized (subscript u) case is given by

$$\frac{i_u}{I_{0,u}} = \frac{1/2\,(i_v + i_h)}{I_{0,u}} = \frac{1}{2} \frac{\pi^2 \alpha^2 (\sin^2 \phi_z + \sin^2 \phi_y)}{\epsilon_0^2 \lambda_0^4 r^2} \tag{10.27}$$

It is awkward to use two different angles to describe the intensity of light scattered along a particular line of sight, but this situation is easily remedied by referring back to Fig. 10.5. It is apparent from Fig. 10.5 that r cos ϕ is the projection of r along either the x, y, or z axis, depending on the choice of ϕ. We therefore see that

$$r^2 (\cos^2 \phi_x + \cos^2 \phi_y + \cos^2 \phi_z) = r^2 \tag{10.28}$$

Replacing $\cos^2 \phi_y$ by $1 - \sin^2 \phi_y$ and $\cos^2 \phi_z$ by $1 - \sin^2 \phi_z$ leads to the relationship

$$\sin^2 \phi_y + \sin^2 \phi_z = 1 + \cos^2 \phi_x \tag{10.29}$$

in terms of which Eq. (10.27) becomes

$$\frac{i_u}{I_{0,u}} = \frac{1}{2} \frac{\pi^2 \alpha^2}{\epsilon_0^2 \lambda_0^4 r^2} (1 + \cos^2 \phi_x) \tag{10.30}$$

The $\sin^2 \phi$ terms in Eqs. (10.25) and (10.26) arise from the consideration of polarized light. The light scattered by polarized incident light is also polarized in the same direction, so the term $1 + \cos^2 \phi_x$ in Eq. (10.30) describes the overall polarization of the scattered light. Before we lose sight of the individual contributions to this, it will be helpful to consider this polarization somewhat further. This is done in the following example.

Example 10.2

Describe the angular dependence of the vertically and horizontally polarized light scattered by a molecule and their resultant by considering the intensity as a vector anchored at the origin whose length in various directions is given by the trigonometric terms in Eqs. (10.25), (10.26), and (10.30).

Solution

The intensity of the vertically polarized scattered light is proportional to $\sin^2 \phi_z$ which, in polar coordinates, is described by a figure 8-shaped curve centered at the origin and having maximum values of ± 1 at $\phi_z = 90°$. Because ϕ_z is symmetrical with respect to the z axis, this component of scattered light is described in three dimensions by a doughnut-shaped surface in which the hole has shrunk to a point - centered symmetrically in the xy plane.

The horizontal component is identical except for its orientation in space. In the horizontal case the "doughnut" lies in the xz plane.

Since the intensities are additive, we can make the following statements about their resultant:

1. Along the z axis, $\sin^2 \phi_z$ contributes nothing but $\sin^2 \phi_y = 1$, so the net scattered light is horizontally polarized.
2. Along the y axis, $\sin^2 \phi_y$ contributes nothing but $\sin^2 \phi_z = 1$, so the net scattered light is vertically polarized.
3. Along the x axis, both $\sin^2 \phi_y$ and $\sin^2 \phi_z$ equal unity. The light consists of equal amounts of horizontally and vertically polarized components, that is, it is unpolarized, and has twice the intensity observed in the perpendicular directions.

This situation is summarized by the term $1 + \cos^2 \phi_x$ in Eq. (10.30), which we now consider. The following table lists some values for this factor for various values of ϕ_x:

ϕ_x (°)	0	15	30	45	60	75	90
$1 + \cos^2 \phi_x$	2.00	1.93	1.75	1.50	1.25	1.07	1.00

These are plotted in Fig. 10.6, which shows the net intensity envelope in the xy plane as a solid line and represents the horizontally and vertically polarized contributions to the resultant by the broken lines. Since ϕ_x is symmetrical with respect to the x axis, the three-dimensional scattering pattern is generated by rotating the solid contour around the x axis.

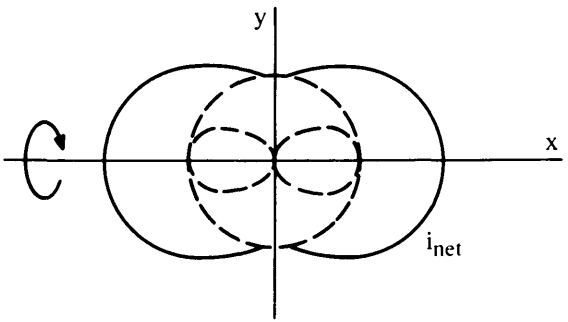

Figure 10.6 Two-dimensional representation of i_v and i_h (broken lines) and their resultant i_{total} (solid line) for scattering by a molecule situated at the origin and illuminated by unpolarized light along the x axis. The intensity in any direction is proportional to the length of the radius vector at that angle. (Reprinted from Ref. 2, p. 168.)

From now on we shall describe the scattered light by Eq. (10.30) exclusively, rather than considering the separate components. We shall also consider ϕ_x only in the xy plane, in which case we use the symbol θ to describe this angle. By convention, the incident light approaches the scattering dipole from $\theta = 180°$, and the transmitted light leaves the sample at $\theta = 0°$.

The equations we have developed in this section describe scattering originating from a point charge located at the origin. Since the charge is, in fact, the electron cloud of a molecule, we must consider the implications of treating a molecule as if it had no spatial extension. The way this consideration explicitly enters the relationships of this section is through the assumption that the dipole "sees" the same field throughout [see Eq. (10.20)]. In visible light, the wavelength is on the order of 500 nm. If the linear dimension of a molecule is small compared to this—as is the case for low molecular weight compounds—then the field is approximately uniform over the dimensions of the molecule and the assumption is valid. For polymer molecules, on the other hand, the dimensions of the molecule may not be insignificant compared to the wavelength of the radiation. In larger particles different parts of the molecule experience significantly different fields, oscillate independently, and produce light which interferes with itself. One way to circumvent this complication appears to be in working with radiation of longer wavelength, but the latter (e.g., infrared) can be absorbed in more ways, so this approach simply trades one source of difficulty for another. It turns out, however, that extrapolating i_s measured at different angles to $\theta = 0°$ also eliminates this interference effect. In Sec. 10.10 we shall discover how the additional complexity of interference can

be interpreted to yield additional information about the scattering source. Before considering this, however, let us further examine the implications of Eq. (10.30) for molecules which are small compared to the wavelength of light.

10.5 Rayleigh Scattering

The scattering formula we have derived in Eq. (10.30) applies to an isolated molecule whose dimensions are small compared to λ. A gas molecule satisfies this description, so we expect that this relationship applies to gases. Since the molecules are far apart in that case, each molecule behaves as an independent scattering center. Therefore the light scattered per unit volume of gas is given simply by the number of molecules per unit volume $\rho N_A/M$ times $i_u/I_{0,u}$. Using the symbol i_s/I_0 for the light scattered per unit volume (unpolarized light is assumed, and the subscript u is dropped), we obtain

$$\frac{i_s}{I_0} = \frac{\rho N_A}{M} \frac{1}{2} \frac{\pi^2 \alpha^2}{\epsilon_0^2 \lambda_0^4} \frac{1 + \cos^2 \theta}{r^2} . \tag{10.31}$$

This is precisely the same quantity we discussed in Sec. 10.2 and illustrated in Fig. 10.1. As anticipated in that section, i_s/I_0 can be written as the product $R_\phi(1 + \cos^2 \theta)/r^2$. In the xy plane, R_ϕ becomes R_θ:

$$R_\theta = \frac{1}{2} \frac{\pi^2 \alpha^2 \rho N_A}{\epsilon_0^2 \lambda_0^4 M} \tag{10.32}$$

which is called the Rayleigh ratio and is given for a gas by Eq. (10.32). By combining Eqs. (10.6) and (10.32), we obtain

$$\tau = \frac{8\pi^3 \alpha^2 \rho N_A}{3M\epsilon_0^2 \lambda_0^4} \tag{10.33}$$

as the turbidity of a gas. Recall from Sec. 10.2 that the turbidity is the analog of absorbance, the light attentuation per unit path through a substance, in the absence of absorption. Equation (10.33) shows that this quantity does the following:

1. It increases with the concentration of scattering centers, which is equivalent to Beer's law.
2. It depends on the nature of the molecules through the factor α^2, where α measures the ability of the molecules to be polarized by an electric field.
3. It varies with the wavelength of the incident radiation as λ_0^{-4}.

The application of this last result to light scattered by the earth's atmosphere is especially interesting. The wavelengths of light at the red and blue ends of the

visible spectrum differ in λ_0 by about a factor of 2, which means that bluish light is scattered about 16 times as much as reddish light. If there were no atmosphere around the earth, the sky would look black, except along direct lines of sight toward the sun or other stars. Instead, we see blue sky overhead where the earth's atmosphere scatters light toward an earthbound observer. This situation is illustrated in Fig. 10.7. Figure 10.7 also shows why sunsets have a reddish hue. In that case the light we see is essentially transmitted light from which the blues have been more effectively removed by scattering. Several additional comments about the color of the sky are pertinent to this discussion:

1. We are explicitly excluding absorption effects: Light-absorbing pollutants modify this description.
2. Skylight is polarized to an extent that depends on the angle between I_0 and I_s in Figs. 10.6 and 10.7.
3. Water drops condensed in the atmosphere have much larger dimensions than gas molecules; hence they are subject to the interference phenomena mentioned at the end of the last section. This alters the color of the scattered light. Smoke and dust particles are also larger and may absorb as well.

The scattering relationships we have considered in this section were published by Lord Rayleigh in 1871 as an explanation for the color and polarization of skylight. Light scattering by small, nonabsorbing particles is known as Rayleigh scattering and is characterized by the λ^{-4} dependence on wavelength. The factor R_θ is known as the Rayleigh ratio of a substance; additional expressions for this quantity in terms of other variables will be developed below.

Before attempting further development of Eq. (10.33), it is useful to examine the dimensions of the various terms in that expression in SI units:

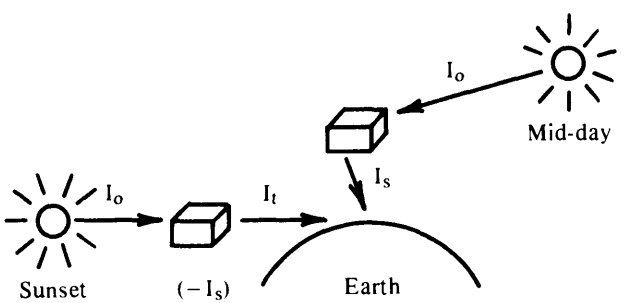

Figure 10.7 Schematic of light reaching an earthbound observer from different regions of the sky.

1. τ is expressed per length of path and has units of meter^{-1}.
2. $\rho N_A/M$ is a concentration and has units of meter^{-3}.
3. λ_0 is the wavelength, so λ_0^{-4} has units of meter^{-4}.
4. The equation is dimensionally consistent if α^2/ϵ_0^2 has units of meter^6. Example 10.2 shows that $\alpha/4\pi\epsilon_0$ has units of meter^3, so the relationship has the proper dimensions.

For the moment, let us define $\alpha/4\pi\epsilon_0$ as α_V, where the subscript V reminds us that the polarizability is being expressed in volume units. Multiplying the numerator and denominator of Eq. (10.33) by $(4\pi)^2$ gives

$$\tau = \frac{128\pi^5}{3} \frac{\alpha_V^2}{\lambda_0^4} \frac{\rho N_A}{M} \tag{10.34}$$

If we think of α_V as a parameter which is proportional to the cube of some kind of molecular "radius" R, then $\alpha_V^2 \propto R^6$ and $\alpha_V^2/\lambda_0^4 \propto R^2(R/\lambda)^4$, which is the form predicted by Eq. (10.3).

The Clausius-Mosotti equation with $\tilde{n}^2$ written for ϵ_r can be used to eliminate α from Eq. (10.33). For gases the refractive index is close to unity, so the factor $\tilde{n}^2 - 1/\tilde{n}^2 + 2$ is approximately

$$\frac{(\tilde{n}+1)(\tilde{n}-1)}{\tilde{n}^2+2} \cong \frac{2}{3}(\tilde{n}-1)$$

Therefore Eq. (10.17) becomes

$$\alpha \cong \frac{2\epsilon_0 M}{\rho N_A}(\tilde{n}-1) \tag{10.35}$$

and Eq. (10.33) is given by

$$\tau = \frac{8\pi^3}{3\lambda_0^4\epsilon_0^2}\left(\frac{2M\epsilon_0}{\rho N_A}(\tilde{n}-1)\right)^2 \frac{\rho N_A}{M} = \frac{32\pi^3}{3\lambda_0^4}(\tilde{n}-1)^2 \frac{M}{\rho N_A} \tag{10.36}$$

An important historic application of this relationship was the determination of Avogadro's number from measurements of light scattered by the atmosphere (see Problem 3).

Next let us consider the light scattered by liquids of low molecular weight compounds. We are actually not directly interested in this quantity per se, but in scattering by solutions–polymer solutions eventually, but for now solutions of small solute molecules. The solvent in such a solution does scatter, but, in practice, the intensity of light scattered by pure solvent is measured and subtracted as a "blank" correction from the scattering by the solution.

Therefore we do not need a theory for scattering by pure liquids to be able to deal with solutions experimentally. The theory for scattering by homogeneous liquids is somewhat simpler to visualize than that for solutions, and the same principles are involved for each. Accordingly, we shall develop the results for pure liquids up to a point and then apply the result to solutions by drawing the appropriate analogy.

The first thing to realize about scattering by liquids is that individual molecules can no longer be viewed as independent scatterers. If a liquid were perfectly uniform in density at the molecular level, its molecules could always be paired in such a way that the light scattered by each member of a pair would be exactly out of phase with the other, resulting in destructive interference. No net scattering results in this case. The second thing to realize, however, is that density is *not* perfectly uniform at the molecular level.

Molecules are in continuous random motion, and as a result of this, small volume elements within the liquid continuously experience compression or rarefaction such that the local density deviates from the macroscopic average value. If we represent by $\delta\rho$ the difference in density between one such domain and the average, then it is apparent that, averaged over all such fluctuations, $\overline{\delta\rho} = 0$: Equal contributions of positive and negative δ's occur. However, if we consider the average value of $\delta\rho^2$, this quantity has a nonzero value. Of these domains of density fluctuation, the following statements can be made:

1. The domain has slightly different properties than its surroundings and can be considered a scattering center itself.
2. Their random, fluctuating nature prevents these domains from destructively interfering with each other's scattered light.
3. The domain is small compared to the wavelength of visible light, so Eq. (10.33) describes the scattering, provided that we can find appropriate values for the concentration and polarizability of these domains.

In the next section we shall pursue the scattering by fluctuations in density. In the case of solutions of small molecules, it is the fluctuations in the solute concentration that plays the equivalent role, so we shall eventually replace $\delta\rho$ by δc_2. First, however, we must describe the polarizability of a density fluctuation and evaluate $\delta\rho$ itself.

10.6 Fluctuations and Rayleigh Scattering

We define the concentration of fluctuation domains at any instant by the symbol N*. In addition, we assume that the polarizability associated with one of these domains differs from the macroscopic average value for the substance

by $\delta\alpha$. As with $\delta\rho$, we expect $\overline{\delta\alpha}$ to equal zero, but $\overline{\delta\alpha^2}$ to have a nonzero value. Accordingly, we can write an expression which is equivalent to Eq. (10.33) for the fluctuations:

$$\tau = \frac{8\pi^3}{3\epsilon_0{}^2\lambda^4}\,\overline{\delta\alpha^2}\,N^* \tag{10.37}$$

Note that the wavelength in vacuum has been replaced by the wavelength in the medium, since it is the latter that drives the oscillations in the fluctuation domain. Now what can we say about $\overline{\delta\alpha^2}$?

The Clausius-Mosotti equation relates the polarizability of a substance to

$$\frac{\epsilon_r - 1}{\epsilon_r + 2} = \frac{\epsilon - \epsilon_0}{\epsilon + 2\epsilon_0}$$

where ϵ is the permittivity of the substance and ϵ_0 is the permittivity of the vacuum that surrounds it. Applied to a fluctuation, we replace ϵ by $\epsilon + \delta\epsilon$ and use ϵ itself rather than ϵ_0 to describe the surroundings. Therefore $(\epsilon - \epsilon_0)/(\epsilon + 2\epsilon_0)$ becomes $\delta\epsilon/(3\epsilon + \delta\epsilon)$, and if we assume that $\delta\epsilon$ is small compared to 3ϵ, Eq. (10.17) becomes

$$\delta\alpha = \frac{\epsilon_0}{N^*}\,\frac{\delta\epsilon}{\epsilon} \tag{10.38}$$

In addition, we can treat the δ's as differential quantities and write

$$\delta\epsilon = \frac{d\epsilon}{d\rho}\,\delta\rho \tag{10.39}$$

Since $\epsilon = \epsilon_r\epsilon_0$ and $\epsilon_r = \tilde{n}^2$ for optical frequencies, Eq. (10.39) becomes

$$\delta\epsilon = \epsilon_0 2\tilde{n}\,\frac{d\tilde{n}}{d\rho}\,\delta\rho \tag{10.40}$$

Combining Eqs. (10.38) and (10.40) gives

$$\overline{\delta\alpha^2} = \frac{\epsilon_0{}^2}{N^{*2}}\left(\frac{\epsilon_0 2\tilde{n}\,d\tilde{n}/d\rho}{\epsilon}\right)^2 \overline{\delta\rho^2} \tag{10.41}$$

where the method of averaging is based on the considerations presented above. Recognizing that $\lambda^{-4}(\epsilon_0/\epsilon)^2 = \lambda^{-4}\,n^{-4} = \lambda_0{}^{-4}$, Eq. (10.41) can be substituted into Eq. (10.37) to yield

$$\tau = \frac{8\pi^3}{3\lambda_0^4} \frac{1}{N^*} \left(2\bar{n} \frac{d\bar{n}}{d\rho}\right)^2 \overline{\delta\rho^2} \tag{10.42}$$

Next we consider how to evaluate the factor $\overline{\delta\rho^2}$. We recognize that there is a local variation in the Gibbs free energy associated with a fluctuation in density, and examine how this value of G can be related to the value at equilibrium, G_0. We shall use the subscript 0 to indicate the equilibrium value of free energy and other thermodynamic quantities. For small deviations from the equilibrium value, G can be expanded about G_0 in terms of a Taylor series:

$$G = G_0 + \left(\frac{\partial G}{\partial \rho}\right)_0 \delta\rho + \frac{1}{2!} \left(\frac{\partial^2 G}{\partial \rho^2}\right)_0 \delta\rho^2 + \cdots \tag{10.43}$$

The quantity $G - G_0 = \delta G$ is the change in G associated with the fluctuation, and the term $(\partial G/\partial\rho)_0\ \delta\rho = 0$ because of the cancellation of positive and negative density fluctuations. Therefore we obtain

$$\delta G \cong \frac{1}{2} \left(\frac{\partial^2 G}{\partial \rho^2}\right)_0 \delta\rho^2 \tag{10.44}$$

Now we evaluate the probability of a fluctuation $\delta\rho$ in terms of a Boltzmann factor:

$$P(\delta\rho) = A \exp\left(-\frac{\delta G}{kT}\right) \tag{10.45}$$

where normalization requires that the constant A be given by

$$\left[\int \exp\left(-\frac{\delta G}{kT}\right) d\,\delta\rho\right]^{-1}$$

integrated over all fluctuations, that is, from $\delta\rho = 0$ to ∞. Using the definition of an average provided by Eq. (1.9), we write

$$\overline{\delta\rho^2} = \frac{\int_0^\infty \delta\rho^2\, e^{-\delta G/kT}\, d\,\delta\rho}{\int_0^\infty e^{-\delta G/kT}\, d\delta\rho}$$

$$= \frac{\int_0^\infty \delta\rho^2 \exp\left[-(1/2)(\partial^2 G/\partial\rho^2)_0\, \delta\rho^2/kT\right] d\delta\rho}{\int_0^\infty \exp\left[-(1/2)(\partial^2 G/\partial\rho^2)_0\, \delta\rho^2/kT\right] d\delta\rho} \tag{10.46}$$

By letting $y = \delta\rho$ and $a = (\partial^2 G/\partial\rho^2)_0/2kT$, these rather formidable-looking integrals are recognized as gamma functions: $\int y^m e^{-ay^2}\, dy$. Using tabulated values for these integrals for $m = 0$ and $m = 2$, we obtain

$$\overline{\delta\rho^2} = \frac{kT}{(\partial^2 G/\partial\rho^2)_0} \tag{10.47}$$

Substitution of this result into Eq. (10.42) yields

$$\tau = \frac{32\pi^3}{3\lambda_0^4} \frac{1}{N^*} \left(\tilde{n} \frac{d\tilde{n}}{d\rho}\right)^2 \frac{kT}{(\partial^2 G/\partial\rho^2)_0} \tag{10.48}$$

As it stands, Eq. (10.48) is not an encouraging-looking result, but it is actually very close to a highly useful form.

Rather than continuing to discuss the scattering of pure liquids at the theoretical level, let us consider an example to illustrate the application of these ideas.

Example 10.3

By an assortment of thermodynamic manipulations, the quantities $d\tilde{n}/d\rho$ and $[N^*(\partial^2 G/\partial\rho^2)_0]^{-1}$ can be eliminated from Eq. (10.48) and replaced by the measurable quantities α, β, and $d\tilde{n}/dT$: the coefficients of thermal expansion, isothermal compressibility, and the temperature coefficient of refractive index, respectively. With these substitutions, Eq. (10.48) becomes

$$\tau = \frac{32\pi^3}{3\lambda_0^4} \frac{kT\beta}{\alpha^2} \tilde{n} \frac{d\tilde{n}}{dT}^2$$

For benzene†, $\alpha = 1.21 \times 10^{-3}\ \text{deg}^{-1}$, $\beta = 9.5 \times 10^{-10}\ \text{m}^2\ \text{N}^{-1}$, and $d\tilde{n}/dT = 6.38 \times 10^{-4}\ \text{deg}^{-1}$. At 23°C, $\tilde{n} = 1.503$ for benzene at $\lambda_0 = 546$ nm. Use these data to evaluate τ for benzene under these conditions.

Solution

Direct substitution into the equation given provides the required value for τ:

$$\tau = \frac{32\pi^3(1.38 \times 10^{-23}\ \text{J K}^{-1})(296\ \text{K})(9.5 \times 10^{-10}\ \text{m}^2\ \text{N}^{-1})}{3(546 \times 10^{-9}\ \text{m})^4(1.21 \times 10^{-3}\ \text{deg}^{-1})^2}$$

$$= 9.07 \times 10^{-3}\ \text{m}^{-1} \qquad (\text{since J} = \text{N m})$$

●

† M. Kerker, *The Scattering of Light and Other Electromagnetic Radition*, Academic, New York, 1969.

Experimentally the Rayleigh ratio for benzene at 90° has been observed to equal about 1.58×10^{-3} m^{-1} under the conditions described in this example. By Eq. (10.6), $\tau = (16\pi/3)\, R_\theta$ so the value of R_θ corresponding to this calculated turbidity is $R_{\theta,calc} = 5.41 \times 10^{-4}$ m^{-1}. The ratio between the observed value of R_θ and that calculated in the example is called the Cabannes factor and equals about 2.9 in this case.

The origin of this enhanced scattering is understood to originate from the anisotropy of the scattering centers. In terms of the analysis we have presented, this amounts to some scrambling of horizontally and vertically polarized components of light. This means that the light scattered at 90° is not totally polarized as suggested by Fig. 10.6. By using polarizing filters with the detection system, the intensities of the horizontally and vertically polarized components of the scattered light can be measured. The ratio of $i_{s,h}(\theta)$ to $i_{s,v}(\theta)$ is called the depolarization ratio and is given the symbol $\rho_u(\theta)$ (u unpolarized incident light; θ, angle at which measured). The Cabannes factor which corrects for this effect can be evaluated from the measured depolarization ratio. Applied to turbidity, the Cabannes factor C as a function of $\rho_u(90)$ is $C_\tau = [6 + 3\rho_u(90)]/[6 - 7\rho_u(90)]$ and applied to the Rayleigh ratio at 90°, $C_{R_{90}} = [6 + 6\rho_u(90)]/[6 - 7\rho_u(90)]$. Note that for the isotropic scatterers we have assumed, $\rho_u(90) = 0$, so the Cabannes factor equals unity. Corrections of this sort are also required for scattering by solutions. When the turbidity value calculated in Example 10.3 is multiplied by the appropriate Cabannes factor, the calculated and experimental results agree very well. We shall not pursue this correction any further, but shall continue to assume isotropic scatterers; additional details concerning the measurement and use of the Cabannes factor will be found in Ref. 3.

As noted at the end of the last section, it is fluctuations in concentration δc_2 rather than density which act as the scattering centers of interest for solutions of small molecules. There is nothing in the forgoing theory that prevents us from placing $\delta\rho$ by δc_2, the solute concentration in mass volume^{-1} units. Therefore we write for a solution of small molecules

$$\tau = \frac{32\pi^3}{3\lambda_0^4} \frac{1}{N^*} \left(\tilde{n} \frac{d\tilde{n}}{dc_2} \right)^2 \frac{kT}{(\partial^2 G/\partial c_2^2)_0} \tag{10.49}$$

In the next section, we consider the application of Eq. (10.49) to scattering from fluctuations in concentration.

10.7 Light Scattering by Solutions

We saw in Example 10.3 that Eq. (10.48) for the turbidity of pure liquids could be converted to a usable expression by suitable thermodynamic manipulations. The corresponding relationship for solutions can also be transformed into the following useful form:

$$\tau = \frac{32\pi^3}{3\lambda_0^4} \, kT \left(\tilde{n} \frac{d\tilde{n}}{dc_2} \right)^2 \frac{c_2}{(\partial \Pi / \partial c_2)_0} \tag{10.50}$$

where $(\partial \Pi / \partial c_2)_0$ describes the concentration dependence of the equilibrium (subscript 0) osmotic pressure. The following outline summarizes the steps involved in this transformation:

1. From the definition of the partial molar quantities [Eq. (8.8)] we write $\delta G = \mu_1 \delta n_1 + \mu_2 \delta n_2$ and $\delta V = \bar{V}_1 \delta n_1 + \bar{V}_2 \delta n_2$, where the δ's refer to an individual fluctuation. The changes in concentration in a fluctuation arise from changes in the number of moles of solvent (subscript 1) and solute (subscript 2), not because of volume changes. Hence $\delta V = 0$; therefore $\delta n_1 = -(\bar{V}_2/\bar{V}_1)\delta n_2$ and $\delta G = [\mu_2 - (\bar{V}_2/\bar{V}_1)\mu_1]\delta n_2$.
2. Since c_2 is expressed as mass volume^{-1}, N^* can be related to the δc_2 by the relationship $\delta c_2/M = N^* \delta n_2$. Therefore $\delta G = [\mu_2 - (\bar{V}_2/\bar{V}_1)\mu_1](\delta c_2/MN^*)$ or $\partial G/\partial c_2 = [\mu_2 - (\bar{V}_1/\bar{V}_2)\mu_1]/MN^*$.
3. Differentiating item (2) again with respect to c_2 gives

$$\frac{\partial^2 G}{\partial c_2^2} = \left(\frac{d\mu_2}{dc_2} - \frac{\bar{V}_2}{\bar{V}_1} \frac{d\mu_1}{dc_2} \right) \Big/ MN^*$$

The Gibbs-Duhem equation also follows from the definition of partial molar quantities: $n_1 d\mu_1 + n_2 d\mu_2 = 0$. With the Gibbs-Duhem equation, $\partial^2 G/\partial c_2^2$ becomes

$$-\left(\frac{n_1}{n_2} + \frac{\bar{V}_2}{\bar{V}_1} \right) \frac{(\partial \mu_1/\partial c_2)_0}{MN^*}$$

4. The factor $[N^*(\partial^2 G/\partial c_2^2)_0]^{-1}$ in Eq. (10.49) can therefore be written

$$\left[-\left(\frac{n_1}{n_2} + \frac{\bar{V}_2}{\bar{V}_1} \right) \frac{(\partial \mu_1/\partial c_2)_0}{M} \right]^{-1} \quad \text{or} \quad \left(-\frac{n_1 \bar{V}_1 + n_2 \bar{V}_2}{n_2 M} \frac{(\partial \mu_1/\partial c_2)_0}{\bar{V}_1} \right)^{-1}$$

Since $c_2 = n_2 M/(n_1 \bar{V}_1 + n_2 \bar{V}_2)$, this is more concisely written as

$$\left(-\frac{1}{c_2} \frac{(\partial \mu_1/\partial c_2)_0}{\bar{V}_1} \right)^{-1}$$

5. Equation (8.79) gives $\mu_1 = \mu_1^0 - \Pi \bar{V}_1$ at equilibrium, so $(\partial \mu_1/\partial c_2)_0 = -\bar{V}_1 (\partial \Pi/\partial c_2)_0$, and the factor in item (4) becomes

$$\left[\frac{1}{c_2} \left(\frac{\partial \Pi}{\partial c_2} \right)_0 \right]^{-1}$$

Substituting this result into Eq. (10.49) gives Eq. (10.50).

Although Eq. (10.50) is still plagued by remnants of the Taylor series expansion about the equilibrium point in the form of the factor $(\partial\Pi/\partial c_2)_0$, we are now in a position to evaluate the latter quantity explicitly. Equation (8.87) gives an expression for the equilibrium osmotic pressure as a function of concentration: $\Pi = RT(c_2/M + Bc_2^2 + \cdots)$. Therefore

$$\left(\frac{\partial \Pi}{\partial c_2}\right)_0 = RT\left(\frac{1}{M} + 2Bc_2 + \cdots\right) \tag{10.51}$$

in terms of which Eq. (10.50) becomes

$$\tau = \frac{32\pi^3}{3\lambda_0^4 N_A} \frac{(\tilde{n}\, d\tilde{n}/dc_2)^2\, c_2}{(1/M + 2Bc_2)} \tag{10.52}$$

This is the result toward which we have been working. Representing the following cluster of constants by the symbol H, we have

$$H = \frac{32\pi^3 (\tilde{n}\, d\tilde{n}/dc_2)^2}{3\lambda_0^4 N_A} \tag{10.53}$$

Eq. (10.52) can be written

$$\frac{Hc_2}{\tau} = \frac{1}{M} + 2Bc_2 \tag{10.54}$$

This is the equation of a straight line and indicates that a plot of Hc_2/τ versus c_2 has the following properties:

$$\text{slope} = 2B \tag{10.55}$$

and

$$\text{intercept} = \frac{1}{M} \tag{10.56}$$

Thus we have finally established how light scattering can be used to measure the molecular weight of a solute. The concentration dependence of τ enters Eq. (10.54) through an expression for osmotic pressure, and this surprising connection deserves some additional comments:

1. In Chap. 8 we saw how the equilibrium osmotic pressure of a solution is related to ΔG for the mixing process whereby the solution is formed. Any difference in the concentration of the solution involves a change in ΔG_{mix}

and would be reflected by a change in Π. Since the occurrence of a fluctuation in concentration depends on the value of the associated δG, the fluctuation can also be expressed in terms of an equivalent $\delta\Pi$.

2. The value of B given by Eq. (10.55) has exactly the same significance that we discussed for the second virial coefficient in Chap. 8.
3. The limiting value of Hc_2/τ is proportional to $1/M$, which shows that τ/c_2 increases with increasing M, at least if interference effects are ignored. This is just the opposite of the molecular weight dependence of the colligative properties and makes light-scattering experiments ideally suited for polymeric solutes. We shall discuss in Sec. 10.10 the implications of interference effects for solute particles whose dimensions are comparable to λ.
4. For polydisperse systems the molecular weight obtained from light scattering is a weight average value, rather than the number average value obtained from an osmotic pressure experiment. This is an unexpected result in view of the role of Eq. (10.51) in relating τ to M.

It is easy to show that a light-scattering experiment "sees" a polydisperse system in such a way as to average the different molecular weights in terms of their mass rather than their number. We only need to consider the leading term of Eq. (10.54) to see the origin of this effect. For a polydisperse system we write $Hc_{ex}/\tau_{ex} = 1/M$, with $c_{ex} = \Sigma c_i$ and $\tau_{ex} = \Sigma\tau_i$, where the summations extend over all molecular weight categories. For any one molecular weight category it is also true that $Hc_i/\tau_i = 1/M_i$. Combining these various results gives

$$\bar{M} = \frac{\tau_{ex}}{Hc_{ex}} = \frac{\Sigma\tau_i}{H\Sigma c_i} = \frac{H\Sigma c_i M_i}{H\Sigma c_i} = \frac{\Sigma m_i M_i}{\Sigma m_i} \tag{10.57}$$

which is the weight average as defined by Eq. (1.12).

Since the development of a method for polymer characterization has been spread over several sections and since the literature contains several variations in the manner data is displayed, a summary of some pertinent definitions and relationships will be helpful at this point:

1. The relative intensity of light scattered per unit volume i_s/I_0 is a function of factors of three different origins: geometrical (r and θ), optical (λ, $\tilde{n}$, and $d\tilde{n}/dc_2$), and thermodynamic (c_2, M, and B).
2. The Rayleigh ratio combines the intensity factors with those associated with the geometry of the experiment:

$$R_\theta = \frac{i_s}{I_0} \frac{r^2}{1 + \cos^2\theta} \tag{10.58}$$

Thus R_θ is a constant in any particular experiment where Rayleigh scattering is obtained, since the entire angular dependence of the light intensity is correctly contained in the $1 + \cos^2 \theta$ term.

3. As the attenuation of the incident beam per unit path through the solution, the turbidity is larger than the Rayleigh ratio by the factor $16\pi/3$, since τ is obtained by integrating R_θ over a spherical surface. Thus, if Eq. (10.54) is written in terms of R_θ rather than τ, the proportionality constant H must also be decreased by $16\pi/3$, in which case the constant is represented by the symbol K:

$$K = \frac{2\pi^2 (\tilde{n}\, d\tilde{n}/dc_2)^2}{\lambda_0^4 N_A} \tag{10.59}$$

and

$$\frac{Kc_2}{R_\theta} = \frac{1}{M} + 2Bc_2 \tag{10.60}$$

4. If turbidity itself is the quantity which is used to characterize a polymer solution, then Eqs. (10.53) and (10.54) are used as derived above:

$$H = \frac{32\pi^3 (\tilde{n}\, d\tilde{n}/dc_2)^2}{3\lambda_0^4 N_A} \tag{10.53}$$

and

$$\frac{Hc_2}{\tau} = \frac{1}{M} + 2Bc_2 \tag{10.54}$$

Figure 10.8 shows two sets of data plotted according to these conventions, after correction for the effect of interference. In Fig. 10.8a, Hc_2/τ is plotted against c_2 for three different fractions of polystyrene in methyl ethyl ketone. Figure 10.8b shows Kc_2/R_θ versus c_2 for solutions of polystyrene in cyclohexane at five different temperatures. These results are discussed further in the following example.

Example 10.4

In both parts of Fig. 10.8, c_2 is expressed in grams per cubic centimeter, with H (or K) and τ (or R_θ) in cgs units also. Verify that the units of the intercept are appropriate units for M^{-1}. Evaluate $\bar{M}_w$ and B for the data in Fig. 10.8a, and $\bar{M}_w$ and Θ from the data in Fig. 10.8b. (K is independent of temperature over the range of T's studied in Fig. 10.8b.)

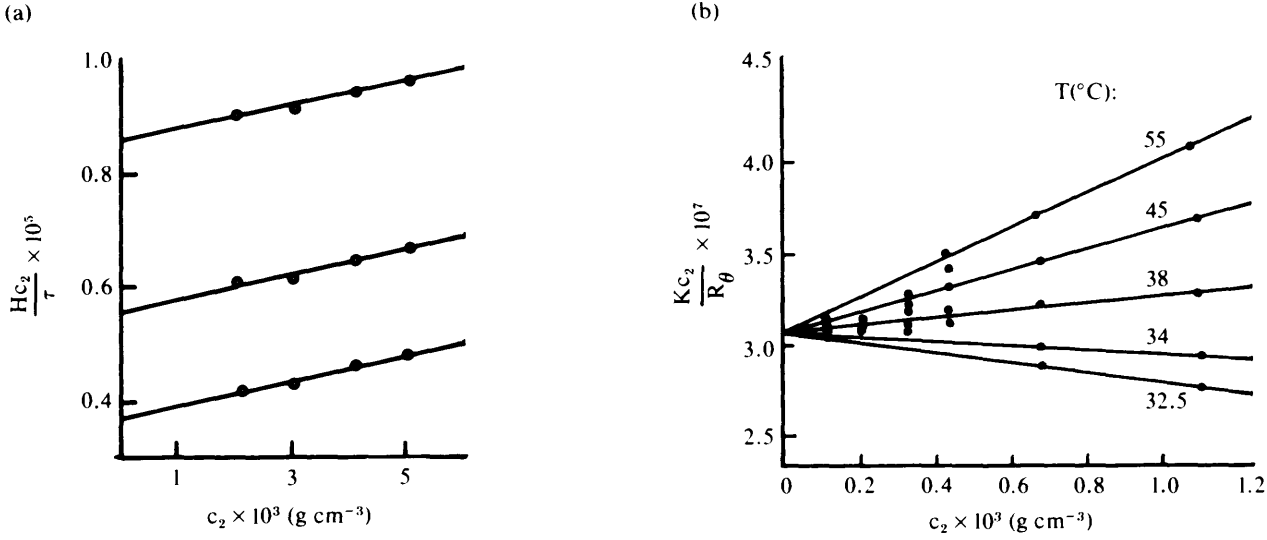

Figure 10.8 Light-scattering data plotted to give slope–intercept values which can be interpreted in terms of M and B. (a) Polystyrene in methyl ethyl ketone. [From B. A. Brice, M. Halwer, and R. Speiser, *J. Opt. Soc. Am.* 40:768 (1950), used with permission.] (b) Polystyrene in cyclohexane at temperatures indicated. Units of ordinates are given in Example 10.4. [Reprinted with permission from W. R. Krigbaum and D. K. Carpenter, *J. Phys. Chem.* 59:1166 (1955), copyright 1955 by the American Chemical Society.]

Solution

Since c_2 has units of grams per cubic centimeter, $\tilde{n}\, d\tilde{n}/dc_2$ has units of cubic centimeters per gram, because $\tilde{n}$ is dimensionless. This means that H (and K) has the cgs units centimeter^2 mole gram^{-2}. τ (and R_θ) has units of centimeter^{-1}, hence Hc_2/τ (and Kc_2/R_θ) has the units moles per gram, which are appropriate for the interpretation of this quantity given by Eq. (10.56). The three lines in Fig. 10.8a have the following intercepts, and the corresponding molecular weights are simply the reciprocals of these values:

$(Hc_2/\tau)_{c=0} \times 10^5$ (mol g^{-1})	0.862	0.556	0.370
$\bar{M}_w$ (g mol^{-1})	116,000	180,000	270,000

Each fraction in Fig. 10.8a has the same slope, and therefore the same value of B is expected. The slope of the lines is approximately $(13 \times 10^{-7}$ mol g$^{-1})/(6 \times 10^{-3}$ g cm$^{-3}) = 2.2 \times 10^{-4}$ cm^3 g^{-2} mol and B = 1.1×10^{-4} cm^3 g^{-2} mol. These are also the correct cgs units for B, as seen by comparison with, say, Eq. (8.97). In Fig. 10.8b the lines for the different temperatures meet at a common intercept of about 3.1×10^{-7} mol g^{-1}, which means that $\bar{M}_w = 3.2 \times 10^6$ g mol^{-1} for the polystyrene sample under investigation. The slopes and B values for the various temperatures are tabulated below:

T (°C)	55	45	38	34	32.5
T (K)	328.2	318.2	311.2	307.2	305.7
Slope $\times 10^5$ (cm^3 g^{-2} mol)	10.76	6.24	2.26	-1.68	-3.06
B $\times 10^5$ (cm^3 g^{-2} mol)	5.38	3.12	1.13	-0.84	-1.53

The Θ temperature is that value of T for which B = 0; therefore Θ can be determined from the results above by graphical interpolation. Although there is some scatter in such a graph, the best value for the temperature at which B = 0 appears to be 308.4 K, which agrees well with values determined for this system by other methods.

Figure 10.8 and Example 10.4 show that light-scattering experiments can be interpreted to yield much the same information as obtained from an osmotic pressure experiment. The fact that the latter yields $\bar{M}_n$ while light scattering gives $\bar{M}_w$ prevents the two methods from being redundant, however. When we discuss interference phenomena in Sec. 10.10, we shall see that the radius of gyration can also be obtained from scattering experiments. Now that the utility of light-scattering experiments in polymer chemistry is well established, let us consider the experimental aspects of this topic.

10.8 Experimental Aspects of Light Scattering

We initiated our discussion of light scattering at the beginning of this chapter by comparing turbidity with the (more familiar) absorbance of a solution. The comparison of these two quantities is also a useful place to begin a consideration of the experimental aspects of light scattering. The components of a spectrophotometer and a light-scattering photometer are largely identical, the primary difference being that absorbance is always measured at $\theta = 0°$, while it is advantageous to measure scattering at various different angles. There are several reasons for using the Rayleigh ratio evaluated at various angles in reporting scattering results:

1. Since i_s is a small quantity, it is better to measure it directly and report it as R_θ rather than by difference, as in the case when turbidity is reported.
2. If experimental values of R_θ are observed to be independent of θ, then Rayleigh scattering is established and Eq. (10.60) can be applied to the data with confidence.
3. If the experimental values of R_θ vary with θ, then the effects of interference are demonstrated. We shall see later in this section that these effects can be eliminated by extrapolating R_θ values to $\theta = 0°$, at which limit Eq. (10.60) also applies.
4. We shall see in subsequent sections that measuring R_θ as a function of θ can be used to evaluate the radius of gyration of the scattering molecules, thereby providing more information about the polymer in addition to M and B.

As a result of these considerations, the primary difference between a spectrophotometer and a light-scattering photometer is the fact that the photodetector is mounted on an arm which pivots at the sample so that intensity measurements can be made at various angles.

Figure 10.9a is a schematic top view of such a photometer, and Fig. 10.9b is a cutaway view of a commercially available instrument which operates on the principles we describe here. The apparatus shown is the Brice-Phoenix universal scattering photometer. Like spectrophotometers, these light-scattering photometers consist of a light source, a sample cell, and a detector, as well as filtering and collimating systems for both the incident and scattered light. The interior of the photometer is painted black and the transmitted beam is absorbed in a light trap to prevent stray light from reaching the detector.

In contrast to spectrophotometry, light-scattering experiments are generally conducted at constant wavelength. Mercury vapor lamps are the most widely used light sources, since the strong lines at 436 and 546 nm are readily isolated by filters to allow monochromatic illumination. Polarizing filters are also included for both the incident and scattered beams so that depolarization can

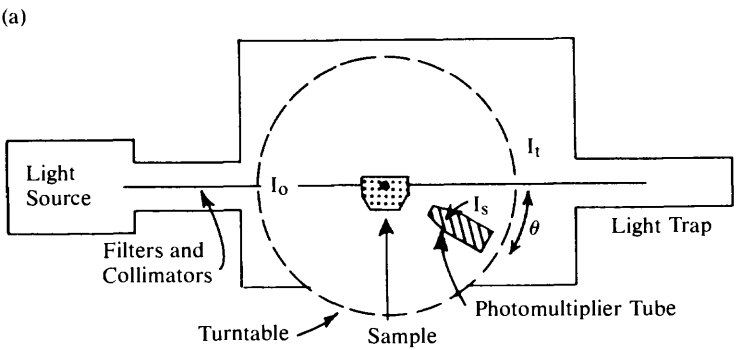

Figure 10.9 Light-scattering photometers. (a) Schematic top view showing movable photodetector. (Reprinted from Ref. 2, p. 176.) (b) Cutaway photograph of commercial light-scattering instrument, the Brice-Phoenix Universal Scattering Photometer. (Photo courtesy of the Virtis Co., Gardiner, New York.)

be studied. The usual assortment of lenses and slits assures that the beams are properly collimated, but these details need not concern us here.

The scattering of laser light is also of considerable importance in contemporary light-scattering practice. As a source of high-intensity monochromatic light, the laser source makes it possible to carry out light-scattering experiments on samples of greatly reduced volume. This means that laser light scattering can be used as a detection system in GPC and also aids in minimizing the scatter produced by dust particles, gas bubbles, and so on, which can invalidate measurements made on larger volumes of solution. Incidentally, as a detection system in GPC, light scattering offers sensitivity to both concentration changes and differences in molecular weight. Combined with refractive index measurements—to supply values for $d\tilde{n}/dc_2$—laser light-scattering detectors provide data which allow for calibration with respect to molecular weight, as well as measure the relative concentrations of the various components.

A variety of cell designs have been successfully employed in light-scattering experiments. Cylindrical cells offer symmetry with respect to viewing angle, but care must be exercised in their use because of reflection from cell walls. This difficulty is not encountered when intensity measurements are made normal to planar cell windows. Cells of octagonal cross section have planar viewing surfaces at $\theta = 0$, 45, 90, 135, and 180°; these are especially convenient for light-scattering experiments.

The solutions must be carefully prepared so as to be free of dust particles and other extraneous scatterers. Filtration through sintered glass or centrifugation is widely used to clarify solutions of particles which would compete with polymeric solutes. This concern for cleanliness also extends to glassware, especially scattering cells. A fingerprint on the viewing window is disastrous!

Photomultipliers are used to measure the intensity of the scattered light. The output is compared to that of a second photocell located in the light trap which measures the intensity of the incident beam. In this way the ratio i_s/I_0 is measured directly with built-in compensation for any variations in the source. When filters are used for measuring depolarization, their effect on the sensitivity of the photomultiplier and its output must also be considered. Instrument calibration can be accomplished using well-characterized polymer solutions, dispersions of colloidal silica, or opalescent glass as standards.

The Rayleigh ratio is not the only optical measurement that must be made in order to interpret light-scattering experiments. In addition, the factor $\tilde{n}\, d\tilde{n}/dc_2$ must also be accurately measured. The refractive index itself is easily determined at the temperature and wavelength of the experiment and requires no further comment. The refractive index gradient $d\tilde{n}/dc_2$, by contrast, presents more of a challenge. Although nominally the slope of a plot of the solution refractive index versus c_2, the gradient is not determined in this manner, since acceptable precision could not be achieved by differences: The solutions

involved are too dilute and the solvent and solute are often not too different in their respective refractive indices.

Instead, the difference between the refractive index of the solvent and that of a solution can be measured directly by one of several designs of differential refractometer. It is apparent that solute and solvent must differ in refractive index, otherwise the solute and its concentration fluctuations are effectively "invisible" in the solvent. The intrinsic difference in the $\tilde{n}$ values of the constituents as well as the concentration of the solution, therefore, determine the small differences in refractive index that must be accurately measured. What is sought is an optical measurement that compares the light interacting with both the solvent and the solution to produce an effect which is sensitive to the refractive index difference. One instrument design for a differential refractometer passes light through a divided cell, the two halves of which contain solvent and solution, respectively. The amount by which the light beam deviates in passing through such a cell is measured by a position-sensitive photodetector. Alternatively, another design uses a split beam to reflect light off the surface of another divided cell, so that part of the beam is reflected by the solvent and part by the solution. The two reflected beams are compared by a dual-element photodetector, and the difference in intensity is related to the difference in $\tilde{n}$. By amplification of the small signals involved, each of these methods is capable of measuring down to 10^{-7} refractive index units under optimum conditions. The usefulness of $d\tilde{n}/dc_2$ as the basis for a detection system in liquid chromatography has contributed to the development of instrumentation in this area.

As noted at the beginning of this section, extrapolation of R_θ to $\theta = 0^\circ$ is one way to correct light-scattering data for interference effects. Interference becomes troublesome for particles whose dimensions are larger than about $\lambda/20$, because light scattered from one portion of the molecule interferes with that scattered by another portion. This situation is shown schematically in Fig. 10.10, which shows the incident light in phase as it passes the surface AA′, but shows different phase relationships in the scattered light at the (distant) surface BB′. It is typical of interference phenomena (think of the colors displayed by a soap film) to show different intensities depending on the angle of observation. Thus in Fig. 10.10 the light scattered at the smaller value of θ remains more nearly in phase than that scattered at the larger angle, where significant destructive interference occurs. This situation is generally true and constitutes the basis for extrapolating to $\theta = 0^\circ$ to eliminate interference effects. The data in Fig. 10.8b were "corrected" in this way.

In the last sentence the word *corrected* is in quotation marks to emphasize the point that the observation *is* corrct: Rather, we are not in a position to deal with the information it tells us, namely, that these particles do not have negligible dimensions compared to λ. Until now we have lacked theory for dealing with this fact. It should be recognized that, by circumventing the

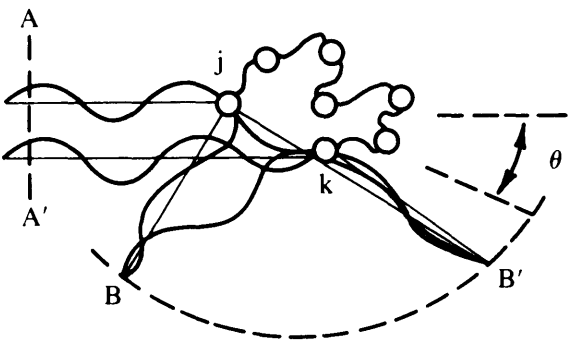

Figure 10.10 Interference of light rays scattered by segments j and k in a polymer chain. Destructive interference increases with increasing θ.

interference effect by extrapolation, we are wasting potentially usable information. Interference occurs in Fig. 10.10 because the light scattered at site j and that scattered at k travel different distances between AA′ and BB′. The wavelength of the light is the "yardstick" that measures this difference in distance traveled. Of course, the latter difference is somehow related to the dimensions of the scattering molecule taken as a whole. Therefore, to bypass this effect by extrapolation is to ignore light as a probe of molecular dimensions. In the next section we shall examine the theory of interference per se, and in Sec. 10.10 we apply the resulting theory to the interpretation of light-scattering data.

10.9 Optical Interference

The Rayleigh scattering theory which culminates in Eq. (10.60) as its most pertinent form for our purposes is based on the explicit assumption that interference effects are absent. The objective of the present section is to correct the Rayleigh theory to allow for interference effects. There are several assumptions-limitations that are implied by our approach:

1. We assume that the Rayleigh theory can be corrected by subdividing the actual solute particle into an array of scattering sites which, considered individually, obey the Rayleigh theory. It can be shown that this approach is a valid approximation so long as $(4\pi R/\lambda)(\tilde{n}_2/\tilde{n}_1 - 1) \ll 1$, where R is the radius of the overall molecule and $\tilde{n}_2$ and $\tilde{n}_1$ are the refractive indices of the solute and solvent, respectively. This shows that the validity of the model involves a trade-off: To apply to progressively larger molecules, the difference in refractive index between solute and solvent must decrease. This particular limitation is not especially severe in polymer applications

of light scattering, but can be a real problem in applications to still larger colloidal particles.

2. We assume that the observed interference is the cumulative effect of the contributions of the individual polymer molecules and that solute-solute interactions do not enter the picture. This effectively limits the model to dilute solutions. This restriction is not particularly troublesome, since our development of the Rayleigh theory also assumes dilute solutions.
3. We assume that there exists a function which we represent by $P(\theta)$—in recognition of the fact that it is angle dependent—which can be multiplied by the scattered intensity as predicted by the Rayleigh theory to give the correct value for i_s, even in the presence of interference. That is,

$$P(\theta) = \frac{i_{s,\text{actual}}}{i_{s,\text{Rayleigh}}} \tag{10.61}$$

4. Based on considerations we have encountered earlier in this chapter, we can anticipate two limiting cases of this function: $P(\theta)$ approaches unity both in the limit of small particles and in the limit of small angles of observation. Interference is absent in both of these cases.

Equation (10.61) suggests how Eq. (10.60), which is valid in the absence of interference, should be corrected. Using Eq. (10.58) for $R_{\theta,\text{Rayleigh}}$, Eq. (10.60) is corrected for interference by dividing both sides of the equation by $P(\theta)$:

$$\frac{Kc_2\,(1+\cos^2\theta)\,I_0}{i_{s,\text{Rayleigh}}\,P(\theta)\,r^2} = \frac{1}{P(\theta)}\left(\frac{1}{M} + 2Bc_2\right) \tag{10.62}$$

Since $P(\theta)\,i_{s,\text{Rayleigh}}$ gives the *observed* scattering intensity at θ—the value that is actually used in the evaluation of R_θ—Eq. (10.62) can be simply written as

$$\frac{Kc_2}{R_\theta} = \frac{1}{P(\theta)}\left(\frac{1}{M} + 2Bc_2\right) \tag{10.63}$$

Our objective now becomes finding an expression for $P(\theta)$.

The theory for $P(\theta)$ proceeds through three stages:

1. We must describe the light scattered with interference in terms of phase differences that develop as the waves pass through a molecule consisting of multiple scattering sites.
2. We must find a way to describe these phase differences in terms of the distances traveled through the array of scattering sites, since this is how the size of the molecule enters the theory.

3. We must average the effect described in item (2) so that no assumed orientation of the scattering sites remains in the final result.

We shall take up these various steps in the following paragraphs.

Figure 10.10 shows that interference is the result of phase differences which arise as the incident light—initially in phase—is scattered by different sites in the molecule. In principle, any particle can be subdivided into a number of hypothetical sites whose isolated behavior is described by the Rayleigh theory. For polymers it is convenient to use the repeat unit of the polymer as the individual scattering site. Thus a polymer whose degree of polymerization is n consists of n independent scattering sites. We can describe each of these by an index number and describe the electric field scattered by the jth using Eq. (10.7), including a phase angle δ_j which is characteristic of the jth repeat unit:

$$E_j = E_0 \cos(2\pi\nu t + \delta_j) \tag{10.64}$$

The net field produced by n such sites is given by

$$E_{net} = \sum_{j=1}^{n} E_j = \sum_{j=1}^{n} E_0 \cos(2\pi\nu t + \delta_j) \tag{10.65}$$

A very useful way to simplify Eq. (10.65) involves the complex number e^{iy} in which $i = \sqrt{-1}$; e^{iy} equals cos y + i sin y. Therefore cos y is given by the real part of e^{iy}. Since exponential numbers are easy to manipulate, we can gain useful insight into the nature of the cosine term in Eq. (10.65) by working with this identity. Remembering that only the real part of the expression concerns us, we can write Eq. (10.65) as

$$E_{0,net}\, e^{i(2\pi\nu t + \delta_{net})} = \sum_{j=1}^{n} E_0\, e^{i(2\pi\nu t + \delta_j)} \tag{10.66}$$

Dividing both sides by $e^{i2\pi\nu t}$ gives

$$E_{0,net}\, e^{i\delta_{net}} = \sum_{j=1}^{n} E_0\, e^{i\delta_j} \tag{10.67}$$

It is the net intensity, not the electric field, which concerns us. We previously used the fact that intensity is proportional to E^2 to evaluate i_s. Using complex numbers to represent E requires one slight modification of this procedure. In the present case we must multiply E by its complex conjugate—obtained by replacing $\sqrt{-1}$ by $-\sqrt{-1}$—to evaluate intensity:

$$i_s \propto \left(\sum_{j=1}^{n} E_0 e^{i\delta j}\right)\left(\sum_{k=1}^{n} E_0 e^{-i\delta k}\right) \tag{10.68}$$

where we have introduced k as the index simply to distinguish between the two summations. Equation (10.68) can be written

$$i_s \propto E_0^2 \sum_{j=1}^{n} \sum_{k=1}^{n} e^{i(\delta j - \delta k)} \tag{10.69}$$

For every term $\delta_j - \delta_k$ in this double summation, there is a term $\delta_k - \delta_j$ which equals $-(\delta_j - \delta_k)$; therefore Eq. (10.69) is equivalent to

$$i_s \propto \frac{1}{2} E_0^2 \sum_{j=1}^{n} \sum_{k=1}^{n} (e^{i(\delta j - \delta k)} + e^{-i(\delta j - \delta k)}) \tag{10.70}$$

By using this form, we can take advantage of the identity that $\cos y = 1/2(e^{iy} + e^{-iy})$, from which it follows that

$$i_s \propto E_0^2 \sum_{j=1}^{n} \sum_{k=1}^{n} \cos(\delta_j - \delta_k) \tag{10.71}$$

For Rayleigh scattering, $\delta_j - \delta_k = 0$—there are no phase differences—and each of the cosine terms in Eq. (10.71) equals unity. In this case, which corresponds to $i_{s,\,Rayleigh}$, the right-hand side of Eq. (10.71) equals $E_0^2 n^2$, and we can write

$$\frac{i_s}{i_{s,\,Rayleigh}} = P(\theta) = \frac{1}{n^2} \sum_j \sum_k \cos(\delta_j - \delta_k) \tag{10.72}$$

This expression formalizes the anticipated conclusion that it is the *difference* in phase between light scattered by different segments that is responsible for the interference effect we seek to analyze. Equation (10.72) completes the first of the three stages in the development of $P(\theta)$.

In the next stage of the derivation we replace the difference in phase angles by the difference in the distance traveled by the light in reaching the observer via site j compared with site k. We shall develop this connection for the specific geometry of Fig. 10.11, but in the third stage of the derivation an average for all possible geometries is performed. Hence we need not worry about the specific model for which the second stage is obtained.

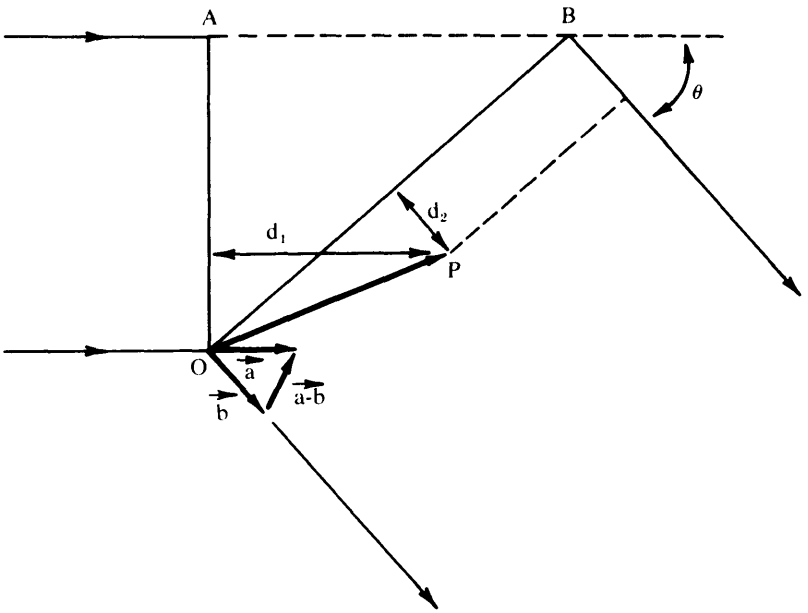

Figure 10.11 Definition of variables required to describe interference of light scattered from points O and P.

Equation (10.72) shows that it is the difference in phase between light scattered by two sites that determines the interference. Hence in Fig. 10.11 we construct two surfaces OA and OB which are perpendicular to the incident and scattered light, respectively. These lines might represent wave crests and, since they meet at O, any segment situated at O is defined to have a phase angle of zero. Suppose we consider a second segment situated at P. To reach a distant observer in the scattering direction, light scattered by a segment located at P must travel a distance d_1 farther in the incident direction compared to a scatterer located at O. In addition, light scattered by a segment at P would have to travel a distance d_2 *less* than light scattered from O to reach the observer. The difference in the distance traveled by light scattered from this pair of sites is therefore given by $d_1 - d_2$. These distances are illustrated in Fig. 10.11. Since there is no phase angle for a scattering segment located at O, the difference in phase angles between O and P can be written

$$\delta_O - \delta_P = \frac{2\pi(d_1 - d_2)}{\lambda} \tag{10.73}$$

Next we look for a relationship between $d_1 - d_2$ and the geometry of the experiment.

The easiest way to proceed is to use vectors to describe this part of the problem. We represent the distance between the pair of scattering sites by the vector $\overrightarrow{OP}$ the length of which is simply r. To express d_1 and d_2 in terms of $\overrightarrow{OP}$ we construct the unit vectors $\vec{a}$ and $\vec{b}$ which are parallel to the incident and scattered directions, respectively. The projection of $\overrightarrow{OP}$ into direction $\vec{a}$, given by the dot product of these two vectors, equals d_1. Likewise, the projection of $\overrightarrow{OP}$ into direction $\vec{b}$ gives d_2. Therefore we can write

$$d_1 - d_2 = \overrightarrow{OP} \cdot \vec{a} - \overrightarrow{OP} \cdot \vec{b} = \overrightarrow{OP} \cdot (\vec{a} - \vec{b}) \tag{10.74}$$

The vector $\vec{a} - \vec{b}$ is also shown in Fig. 10.11 and may be described as the product of a unit vector $\vec{c}$ in the direction $\vec{a} - \vec{b}$ times the scalar length of $\vec{a} - \vec{b}$. This length is easily evaluated, since $\vec{a}$ and $\vec{b}$ are both of unit length and are separated by the angle θ. Therefore a perpendicular to $\vec{a} - \vec{b}$ through O bisects both the angle θ and the length of $\vec{a} - \vec{b}$. The length of $\vec{a} - \vec{b}$ is therefore $2 \sin(\theta/2)$ and we can describe $\vec{a} - \vec{b}$ as

$$\vec{a} - \vec{b} = 2 \sin\left(\frac{\theta}{2}\right) \vec{c} \tag{10.75}$$

Combining Eqs. (10.73)-(10.75) gives

$$\delta_O - \delta_P = \frac{4\pi}{\lambda} \sin\left(\frac{\theta}{2}\right) (\overrightarrow{OP} \cdot \vec{c}) = s(\overrightarrow{OP} \cdot \vec{c}) \tag{10.76}$$

where the scalar quantity s is defined by

$$s = \frac{4\pi}{\lambda} \sin\left(\frac{\theta}{2}\right) \tag{10.77}$$

The phase difference $\delta_O - \delta_P$ given by Eq. (10.76) describes a particular geometrical arrangement between scatterers. This difference can be substituted for the phase difference $\delta_j - \delta_k$ between an arbitrary pair of segments in Eq. (10.72), provided that a suitable averaging is carried out to allow for all possible orientations between segments j and k. We shall take up this averaging in the final stage of the derivation. For now we simply anticipate the average by using an overbar and substitute Eq. (10.76) for $\delta_j - \delta_k$ in Eq. (10.72):

$$P(\theta) = \frac{1}{n^2} \sum_j \sum_k \overline{\cos(s[\vec{r}_{jk} \cdot \vec{c}])} \tag{10.78}$$

In writing this last result, we have replaced $\overrightarrow{OP}$ by the vector $\overrightarrow{r_{jk}}$ between the generalized pair of segments j and k.

In the final stage of this involved derivation, we have to free Eq. (10.78) from the dependence it contains on the geometry of Fig. 10.11. The problem lies in the dot product of the vector $\overrightarrow{r_{jk}}$—which replaces $\overrightarrow{OP}$ in Fig. 10.11—and $\vec{c}$, the unit vector in the direction $\vec{a} - \vec{b}$ in Fig. 10.11. In Fig. 10.11 these two vectors have a specific orientation with respect to each other, but between an arbitrary pair of segments the vectors are separated by a general angle we call γ. The dot product $\overrightarrow{r_{jk}} \cdot \vec{c}$ then becomes $r_{jk} \cos \gamma$, where r_{jk} is the (scalar) distance between j and k, since the vector $\vec{c}$ has unit length. With this substitution, Eq. (10.78) becomes

$$P(\theta) = \frac{1}{n^2} \sum_j \sum_k \overline{\cos(sr_{jk} \cos \gamma)} \tag{10.79}$$

Now we consider how the averaging implied by the overbar is carried out. What this involves is multiplying $\cos(sr_{jk} \cos \gamma)$ by $P(\gamma)\, d\gamma$—the probability that a particular angle is between γ and $\gamma + d\gamma$—and then integrating the result over all values of γ in keeping with the customary definition of an average quantity.

We can describe the function $P(\gamma)\, d\gamma$ in terms of the same geometrical arrangement shown in Fig. 10.2, with γ replacing ϕ_x. That is, $P(\gamma)\, d\gamma$ is proportional to the area traced on the surface of a sphere by angles in the range γ to $\gamma + d\gamma$:

$$P(\gamma)\, d\gamma = A r \sin \gamma\, (r\, d\gamma) \tag{10.80}$$

where $A = \left(\int_0^\pi r^2 \sin \gamma\, d\gamma\right)^{-1}$ satisfies the normalization criterion. Using this as the expression for $P(\gamma)\, d\gamma$ gives

$$P(\theta) = \frac{1}{n^2} \frac{\int_0^\pi \Sigma_j \Sigma_k \cos(sr_{jk} \cos \gamma) \sin \gamma\, d\gamma}{\int_0^\pi \sin \gamma\, d\gamma} \tag{10.81}$$

This unattractive integral is readily solved by introducing a change of variable in the numerator. If we let $y = sr_{jk} \cos \gamma$, then $dy = -sr_{jk} \sin \gamma\, d\gamma$. The corresponding limits for y—after dividing the range of integration in half and multiplying the integral by 2—are $y = sr_{jk}$ for $\gamma = 0$ and $y = 0$ for $\gamma = \pi/2$. With this change of variable, Eq. (10.81) becomes

$$P(\theta) = \frac{(-2/sr_{jk}) \int_{y=sr_{jk}}^{0} \Sigma_j \Sigma_k \cos y \, dy}{n^2 \, 2 \int_{\gamma=0}^{\pi/2} \sin \gamma \, d\gamma} = \frac{(2/sr_{jk}) \Sigma_j \Sigma_k \sin (sr_{jk})}{2}$$

$$= \sum_j \sum_k \frac{\sin (sr_{jk})}{sr_{jk}} \tag{10.82}$$

This is the result we have sought, although it needs a bit of additional manipulation to make its usefulness evident. The derivation we have followed in this section was developed by Debye in the context of x-ray scattering by the individual atoms of small molecules. Since $s \propto \lambda^{-1}$, this function again emphasizes the idea that R/λ ratios rather than absolute distances themselves are the pertinent quantities in the discussion of optical phenomena. We shall call this theory and its subsequent developments the Debye scattering theory. (Remember that Chap. 2 contains the Debye viscosity theory.) In the next section we examine how Eq. (10.82) can be converted into a practical form.

10.10 The Radius of Gyration

Equation (10.82) is a correct but unwieldy form of the Debye scattering theory. The result benefits considerably from some additional manipulation which converts it into a useful form. Toward this end we assume that the quantity sr_{jk} is not too large, in which case $\sin (sr_{jk})$ can be expanded as a power series. Retaining only the first two terms of the series, we obtain

$$P(\theta) = \frac{1}{n^2} \sum_j \sum_k \frac{\sin (sr_{jk})}{sr_{jk}} = \frac{1}{n^2} \sum_j \sum_k \frac{sr_{jk} - (sr_{jk})^3/3!}{sr_{jk}}$$

$$= \frac{1}{n^2} \sum_j \sum_k \left(1 - \frac{(sr_{jk})^2}{6}\right) \tag{10.83}$$

Since $\Sigma_j \Sigma_k 1 = n^2$, this becomes

$$P(\theta) = 1 - \frac{s^2}{6n^2} \sum_j \sum_k r_{jk}^2 \tag{10.84}$$

At this point it is useful to compare the result we have obtained with the expected behavior of $P(\theta)$ that we anticipated from the definition of this quantity:

1. The smaller the overall dimensions of a molecule, the smaller will be the r_{jk} value for any pair of sites in the molecule. As the values of r_{jk} approach zero, $P(\theta) \to 1$, as required.
2. Equation (10.77) shows that $s \propto \sin(\theta/2)$; therefore $\sin(\theta/2)$ and s approach zero as $\theta \to 0$. This means that $P(\theta) \to 1$ in this limit also, as required.
3. Since the product sr_{jk} appears in Eq. (10.84), there is a trade-off possibility between particle size and the angle of observation. That is, the Debye scattering theory applies with the same level of accuracy to larger molecules at smaller angles and to smaller molecules at larger angles.

Since Eq. (10.63) contains $1/P(\theta)$, since we have already assumed sr_{jk} to be small, and since $1/(1 - y) \cong 1 + y$, Eq. (10.84) can be rewritten as

$$\frac{1}{P(\theta)} = 1 + \frac{s^2}{6n^2} \sum_j \sum_k r_{jk}^2 \tag{10.85}$$

At this point we return to Chap. 1 to connect Eq. (10.85) with the radius of gyration. Although we have not encountered the form $\Sigma_j \Sigma_k r_{jk}^2$ explicitly before, a moment's reflection will convince us that it is identical to the bracketed quantity in Eq. (1.54):

$$\sum_{j=1}^{n} \sum_{k=1}^{n} r_{jk}^2 = \sum_{j=1}^{n} \left(\sum_{k=1}^{j} P(r)\, r^2 + \sum_{k=1}^{n-j} P(r)\, r^2 \right) \tag{10.86}$$

To clarify this identification we note the following:

1. The bracketed summations span the full range of k values from 1 to n and hence can be combined into a single summation.
2. The probability P(r) times r^2 gives a particular value of r^2 which, in the context of Eq. (10.86), is equivalent to r_{jk}^2.
3. Therefore it follows from Eq. (1.54) that

$$\overline{r_g^2} = \frac{1}{2n^2} \sum_j \sum_k r_{jk}^2 \tag{10.87}$$

in the present notation.

Combining Eqs. (10.84) and (10.87) gives

$$\frac{1}{P(\theta)} = 1 + \frac{s^2}{3} \overline{r_g^2} = 1 + \frac{16\pi^2}{3\lambda^2} \overline{r_g^2} \sin^2\left(\frac{\theta}{2}\right) \tag{10.88}$$

Finally, we can incorporate this result into Eq. (10.63) to obtain

$$\left(\frac{Kc_2}{R_\theta}\right)_{c=0} = \frac{1}{M}\left[1 + \frac{16\pi^2}{3\lambda^2}\,\overline{r_g^2}\sin^2\left(\frac{\theta}{2}\right)\right] \tag{10.89}$$

where the concentration term on the right-hand side of Eq. (10.63) has been omitted, since the Debye scattering theory applies in the limit of $c_2 \to 0$. We see that there is a certain analogy in the way the Rayleigh and the Debye theories must be "corrected":

1. In applying the Rayleigh theory to large polymer molecules, we had to extrapolate results measured at different θ's to $\theta = 0$ to eliminate the interference effect.
2. In applying the Debye theory to concentrated solutions, we must extrapolate the results measured at different concentrations to $c_2 = 0$ to eliminate the effects of solute-solute interactions.
3. Experimentally, R_θ is measured at a series of different c_2's and θ's, which makes the extrapolations of Kc_2/R_θ at constant θ to $c_2 = 0$ and of Kc_2/R_θ at constant c_2 to $\theta = 0$ equally feasible. In the next section we shall examine a specific graphical technique which combines these two extrapolations in a single procedure.

Assuming that concentration effects have been eliminated by extrapolating Kc_2/R_θ to $c_2 = 0$ (subscript $c = 0$), we see that Eq. (10.89) is the equation of a straight line if $(Kc_2/R_\theta)_{c=0}$ is plotted against $\sin^2(\theta/2)$. The characteristic parameters of the line have the following significance:

$$\text{Slope} = \frac{16\pi^2}{3\lambda^2 M}\,\overline{r_g^2} \tag{10.90}$$

$$\text{Intercept} = \frac{1}{M} \tag{10.91}$$

or

$$\overline{r_g^2} = \frac{3\lambda^2}{16\pi^2}\left(\frac{\text{slope}}{\text{intercept}}\right)_{c=0} \tag{10.92}$$

Figure 10.12 shows data for cellulose nitrate in acetone measured at $\lambda_0 = 436$ nm, and plotted in the manner suggested in Eq. (10.89). The following example completes the analysis of these data.

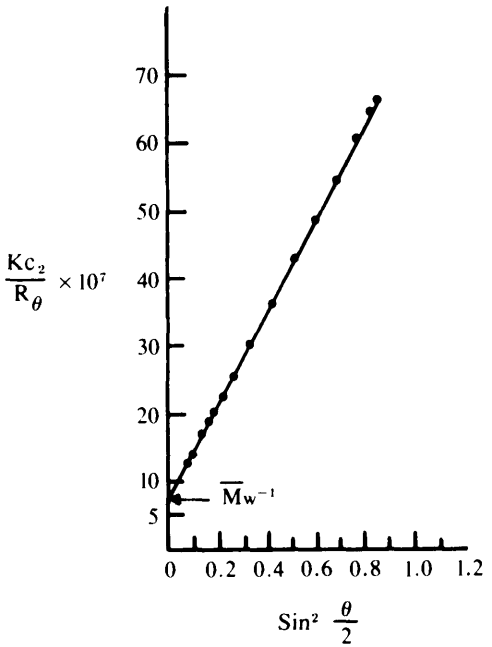

Figure 10.12 Light-scattering data in the limit of $c_2 = 0$ plotted according to Eq. (10.89) for cellulose nitrate in acetone. [Data from H. Benoit, A. M. Holtzer, and P. Doty, *J. Phys. Chem.* 58:635 (1954).]

Example 10.5

Interpret the slope and intercept values of the line in Fig. 10.12 in terms of the molecular weight and radius of gyration of cellulose nitrate in this solution. At 436 nm the refractive index of acetone is 1.359.

Solution

Examination of the graph shows that the line is characterized by the following parameters:

$$\text{Slope} = 6.78 \times 10^{-6} \text{ mol g}^{-1}$$

$$\text{Intercept} = 7.87 \times 10^{-7} \text{ mol g}^{-1}$$

The units of these quantities are determined solely by the ordinate, since the abscissa is dimensionless. Example 10.4 verifies that moles per gram are the units for Kc_2/R_θ. The molecular weight is given by the inverse of the intercept:

$$\bar{M}_w = 1.27 \times 10^6 \text{ g mol}^{-1}$$

Since the intercept corresponds to the Rayleigh limit also (i.e., $\theta = 0°$), Eq. (10.57) demonstrates this to be the weight average value of M.

In acetone $\lambda = \lambda_0/\tilde{n} = 436/1.359 = 321$ nm; therefore

$$\overline{r_g^2} = \frac{3\lambda^2 M\,(\text{slope})_{c=0}}{16\pi^2}$$

$$= \frac{3(321 \text{ nm})^2 (1.27 \times 10^6 \text{ g mol}^{-1})(6.78 \times 10^{-6} \text{ mol g}^{-1})}{16\pi^2}$$

$$\overline{r_g^2} = 1.69 \times 10^4 \text{ nm}^2 \qquad \text{or} \qquad (\overline{r_g^2})^{1/2} = r_{g,\text{rms}} = 130 \text{ nm}$$

This distance parameter which characterizes the polymer is about 40% of λ at $\lambda_0 = 436$ nm.

For a polydisperse system not only M but also the radius of gyration will be an average value. Let us next consider the type of average that is obtained for this quantity from light scattering. For this purpose it is sufficient to consider the kind of average obtained for $P(\theta)$: Eq. (10.84) shows that the weighting factor used to average $P(\theta)$ is also that for r_g^2. We proceed as in Sec. 10.7, where we considered the same question for M:

1. We begin with Eq. (10.89)–that is, we neglect solute-solute interactions–and write

$$\frac{Kc_2}{R_\theta} = \frac{1}{\bar{M}_w}\,\frac{1}{\bar{P}(\theta)} \tag{10.93}$$

   This result uses the already established fact that $M = \bar{M}_w$ when the molecular weight is determined by light scattering for a polydisperse system.
2. Equation (10.93) can be written for both the individual components and the mixture as a whole, yielding $Kc_iM_iP_i(\theta) = R_{\theta,i}$ and $Kc_{ex}\bar{M}_w\bar{P}(\theta) = R_{\theta,ex}$, respectively.
3. Since $c_{ex} = \Sigma_i c_i$ and $R_{\theta,ex} = \Sigma_i R_{\theta,i}$, these results can be combined to give

$$\bar{M}_w\,\bar{P}(\theta) = \frac{R_{\theta,ex}}{Kc_{ex}} = \frac{K\Sigma_i M_i c_i P_i(\theta)}{K\Sigma_i c_i} \tag{10.94}$$

4. Because $c_i \propto m_i$, $\bar{M}_w = \Sigma_i c_i M_i / \Sigma_i c_i$; therefore $(\Sigma_i c_i M_i / \Sigma_i c_i)\bar{P}(\theta) = \Sigma_i c_i M_i P_i(\theta)/\Sigma_i c_i$ or

$$\bar{P}(\theta) = \frac{\Sigma_i c_i M_i P_i(\theta)}{\Sigma_i c_i M_i} = \frac{\Sigma_i m_i M_i P_i(\theta)}{\Sigma_i m_i M_i} \tag{10.95}$$

5. Finally, $m_i = n_i M_i$; therefore

$$\bar{P}(\theta) = \frac{\Sigma_i n_i M_i^2 P_i(\theta)}{\Sigma_i n_i M_i^2} \tag{10.96}$$

which shows that the weighting factor for each of the categories averaged is $m_i M_i = n_i M_i^2$. This kind of average is known as a z average. The similarly defined z-average molecular weight, $\bar{M}_z = \Sigma_i n_i M_i^3 / \Sigma_i n_i M_i^2$, is given as Eq. (1.19) in Chap. 1.

Although we presented the derivation for $P(\theta)$ in terms of a random coil, the result is applicable to particles of other geometries–for example, rigid spheres or ellipsoids–provided that the particles fall in the size range where the Debye theory is applicable. The radius of gyration thus obtained is an exact measure of this parameter for the particle in question, regardless of its shape, although its relationship to the physical dimensions of the scatterer does depend on the geometry of the particle. Relationships between the radius of gyration and the dimensions of bodies of various geometries are derived in elementary physics textbooks. Several of these are listed in Table 10.1 for some geometries that are encountered among polymeric solutes. Thus if a particle is known to possess some specific geometry, the radius of gyration can be translated into a geometrical particle dimension through these relationships. It should be emphasized, however, that this type of conversion merely helps us picture the molecule; r_g itself is an equally valid way to describe its dimensions.

In Example 10.5 we extracted both the molecular weight and the radius of gyration from light-scattering data. There may be circumstances, however, when nothing more than the dimensions of the molecule are sought. In this case a simple alternative to the analysis discussed above can be followed. This technique is called the dissymmetry method and involves measuring the ratio of intensities scattered at 45° and 135°. The ratio of these intensities is called the dissymmetry ratio z:

$$z = \frac{i_{s,45°}}{i_{s,135°}} \tag{10.97}$$

This parameter should also be extrapolated to $c_2 = 0$, so the amount of experimental data required in this approach is not significantly less than in the method

Table 10.1 Relationships Between the Radius of Gyration and Geometrical Dimensions for Some Bodies Having Shapes Pertinent to Polymers

Geometry	Definition of parameters	Radius of gyration through the center of gravity
Random coil	$\overline{r^2}$: mean-square end-to-end distance ($\propto n$)	$r_g^2 = \frac{\overline{r^2}}{6}$
Sphere	R: radius of sphere	$r_g^2 = \frac{2}{5} R^2$
Thin rod	L: length of rod (approximation for prolate ellipsoids for which $a/b \gg 1$)	$r_g^2 = \frac{L^2}{12}$
Cylindrical disk	R: radius of disk (approximation for oblate ellipsoids for which $a/b \ll 1$)	$r_g^2 = \frac{1}{2} R^2$

described above. The advantage of working with this quantity, however, is that it can yield a particle dimension with very little calculation through the use of published tables and graphs. To see how this is possible, consider the following points:

1. The factor $1 + \cos^2 \theta$ in R_θ has the same value at $\theta = 45°$ and $135°$; hence the ratio $i_{s,45°}/i_{s,135°}$ is the same as $R_{45°}/R_{135°}$ [Eq. (10.58)].
2. Equation (10.63) shows that in the limit of $c_2 = 0$ this ratio also equals the ratio $P(45°)/P(135°)$.
3. By Eq. (10.88), this becomes

$$z = \frac{P(45°)}{P(135°)} = \frac{1 + (16\pi^2/3)(r_g/\lambda)^2 \sin^2 67.5}{1 + (16\pi^2/3)(r_g/\lambda)^2 \sin^2 22.5} \tag{10.98}$$

   and a master curve can be drawn which shows z for different ratios r_g/λ. Of course, this result is subject to the limitations of Eq. (10.88). Especially pertinent is the idea that the particles should not be too large if Eq. (10.98) is used, since large angles are involved.
4. Taking the concept of a master curve a step further, the relationships in Table 10.1 can also be incorporated into such curves so that graphs of z versus a characteristic dimension relative to λ are plotted for various geometries.

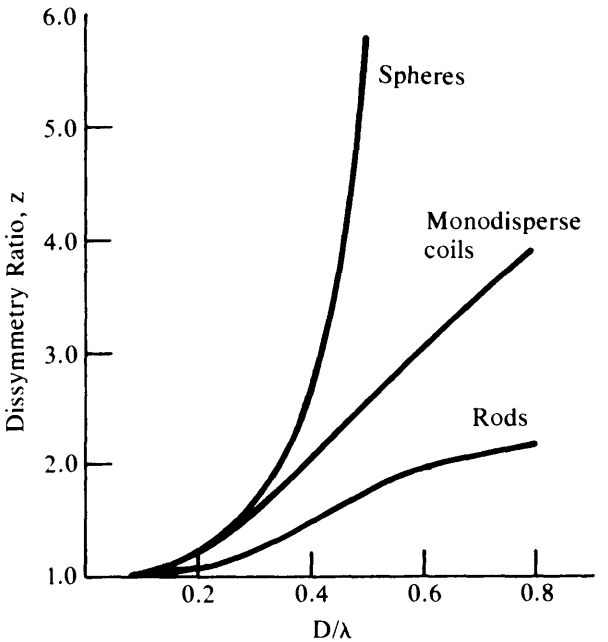

Figure 10.13 Variation of the dissymmetry ratio z with a characteristic dimension D (relative to λ) for spheres, random coils, and rods. (Data from Ref. 4.)

Figure 10.13 shows such plots of z versus D/λ, where D is r_{rms} for random coils, R for spheres and disks, and L for rods. More detailed theories permit these curves to be extended to larger values of r_g/λ than is justified by consideration of Eq. (10.97) alone. In the following example we illustrate an application of this simple method for estimating particle dimensions.

Example 10.6

Poly(γ-benzyl-L-glutamate) is known to possess a helical structure in certain solvents. As part of an investigation† of this molecule, a fractionated sample was examined in chloroform ($CHCl_3$) and chloroform saturated (~0.5%) with dimethyl formamide (DMF). The following results were obtained:

† P. Doty, J. H. Bradbury, and A. M. Holtzer, *J. Am. Chem. Soc.* 78:947 (1956).

	$CHCl_3$	$CHCl_3$ + DMF
$\bar{M}_w$ (g mol^{-1})	144,000	73,000
$(z)_{c=0}$ at 436 nm	1.30	1.11

Taking $\tilde{n} = 1.446$ as the refractive index in both media, estimate the length of the helix in these two situations. Propose a possible interpretation of the results.

Solution

The helix can be approximated as a rod; therefore values of L/λ which are consistent with the observed dissymmetries can be read from Fig. 10.13 or equivalent sources. Also, $\lambda = \lambda_0/\tilde{n} = 436/1.446 = 302$ nm in each of these systems. In view of these considerations, the following results are obtained:

	$CHCl_3$	$CHCl_3$ + DMF
L/λ	0.31	0.19
L (nm)	94	57

The observed molecular weight suggests that this polymer associates into a "dimer" in $CHCl_3$, but that this aggregation is effectively blocked by small amounts of DMF. The particle lengths are not quite in the 2:1 ratio indicative of end-to-end association, but the increase in length is sufficiently large to make such a mechanism worthy of additional study.

•

Until now we have looked at various aspects of light scattering under several limiting conditions, specifically, $c_2 = 0$, $\theta = 0$, or both. Actual measurements, however, are made at finite values of both c_2 and θ. In the next section we shall consider a method of treating experimental data that consolidates all of the various extrapolations into one graphical procedure.

10.11 Zimm Plots

If we substitute Eq. (10.88) into Eq. (10.63) we obtain

$$\frac{Kc_2}{R_\theta} = \left(\frac{1}{M} + 2Bc_2\right)\left[1 + \frac{16\pi^2\overline{r_g^2}}{3\lambda^2}\sin^2\left(\frac{\theta}{2}\right)\right] \tag{10.99}$$

and, since R_θ is measured as a function of both c_2 and θ, this relationship brings together all of the experimental variables and molecular parameters that are

related through light scattering. In the development of this chapter we have looked at special cases of this general function:

1. In the limit of $c_2 = 0$ *and* $\theta = 0°$, $(Kc_2/R_\theta)_{\theta=c=0} = 1/\bar{M}_w$.
2. In the limit of $\theta = 0°$, $(Kc_2/R_\theta)_{\theta=0} = 1/\bar{M}_w + 2Bc_2$.
3. In the limit of $c_2 = 0$, $(Kc_2/R_\theta)_{c=0} = (1/\bar{M}_w)\,[1 + (16\pi^2/3)\,(r_g/\lambda)^2 \sin^2(\theta/2)]$.

The assumptions made in deriving the two factors in Eq. (10.99) restrict the validity of the respective parts of the general expression to these limiting cases. A method for extrapolating experimental data to the limits itemized above has been devloped by Zimm, and the resulting graph—called a Zimm plot—has become a standard way of representing light-scattering data.

There is really nothing in this method that we have not already considered, one aspect at a time, in this chapter. The Zimm plot simply brings it all together in a single analysis.

We shall presently construct a Zimm plot in detail in an example. In anticipation of this, we label each of the paragraphs describing Zimm's procedure for ease of cross-referencing in the example.

1. The method consists of plotting Kc_2/R_θ as the ordinate and $\sin^2(\theta/2) + kc_2$ as the abscissa, where k is a number which is chosen to give a good distribution of data points in the graph. We assign to this constant reciprocal concentration units so that kc_2 can be added to the dimensionless $\sin^2(\theta/2)$. When a suitable scale has been selected, the experimental points are spread over a large area in the graph.
2. Next the points at constant values of c_2 are connected. Likewise, points at constant values of θ are also connected. This produces a grid of intersecting lines that may be straight but which are not necessarily so.
3. On each of the lines that has been drawn, a mark is made at the value of the abscissa corresponding to one of the limiting cases above. Specifically, along the line where $c_2 = c^*$, a mark is placed where the abscissa has the value kc^*. Since the abscissa is $\sin^2(\theta/2) + kc_2$, this mark corresponds to $\theta = 0°$ for this concentration. Similarly, along a line for which $\theta = \theta^*$, a mark is placed where the abscissa equals $\sin^2(\theta^*/2)$. This corresponds to the $c_2 = 0$ limit at this angle.
4. When each of the constant c_2 and constant θ lines has been marked off in this way, the various derived points can be connected. One of these groups of points gives values of Kc_2/R_θ for a range of c's at $\theta = 0°$. The other group of points gives Kc_2/R_θ for a range of θ's at $c_2 = 0$. The two lines thus derived should meet at a common intercept which equals $1/\bar{M}_w$, and their slopes are given by Eqs. (10.55) and (10.90), respectively.

Table 10.2 Values for Kc_2/R_θ at the Indicated Values of θ and c_2 for Solutions of Polystyrene in Benzene at 546 nm

$c_2 \times 10^3$ ($g\ cm^{-3}$)	θ (deg)							
	30	37.5	45	60	75	90	105	120
2.00	3.18	3.26	3.25	3.45	3.56	3.72	3.78	4.01
1.50	2.73	2.76	2.81	2.94	3.08	3.27	3.40	3.57
1.00	2.29	2.33	2.37	2.53	2.66	2.85	2.96	3.12
0.75	2.10	2.14	2.17	2.32	2.47	2.64	2.79	2.93
0.50	1.92	1.95	1.98	2.16	2.33	2.51	2.66	2.79

Source: Data from D. Margerison and G. C. East, *An Introduction to Polymer Chemistry*, Pergamon, Oxford, 1967.

For a sample of polystyrene in benzene, experimental values of Kc_2/R_θ are entered in the body of Table 10.2. The values are placed at the intersection of rows and columns labeled c_2 and θ, respectively. In the following example these values are used to construct a Zimm plot.

Example 10.7

Prepare a Zimm plot using the data in Table 10.2 and evaluate M, B, and $\overline{r_g^2}$ for this solution of polystyrene in benzene. The effective wavelength in the medium is $\lambda_0/\bar{n} = 546/1.501 = 364$ nm for this experiment.

Solution

We follow the procedure outlined above, cross-referencing the individual steps with the labels introduced above.

1. The abscissa values for the Zimm plot are given by $\sin^2(\theta/2) + kc_2$. For these data, $k = 100\ cm^3\ g^{-1}$ gives a good array of points. Table 10.3 shows the values of the abscissa in the same format used in Table 10.2.
2. Figure 10.14a shows a plot of these data with the lines drawn between points of constant c_2. Likewise, Fig. 10.14b shows the same data with lines drawn between points of constant θ.
3. When $\theta = 0°$, $\sin^2(\theta/2) = 0$ and the abscissa in Fig. 10.14a is simply kc_2. For the solution with $c_2 = 0.5 \times 10^{-3}\ g\ cm^{-3}$, $kc_2 = 0.05$, and this point is marked by an x on the line through the points at this concentration. The x's on other lines in Fig. 10.14a correspond to the $\theta = 0°$ limit for each concentration. When $c_2 = 0$, the abscissa in Fig. 10.14b becomes $\sin^2(\theta/2)$. For the measurements at $\theta = 30°$, $\sin^2 15 = 0.067$, and this

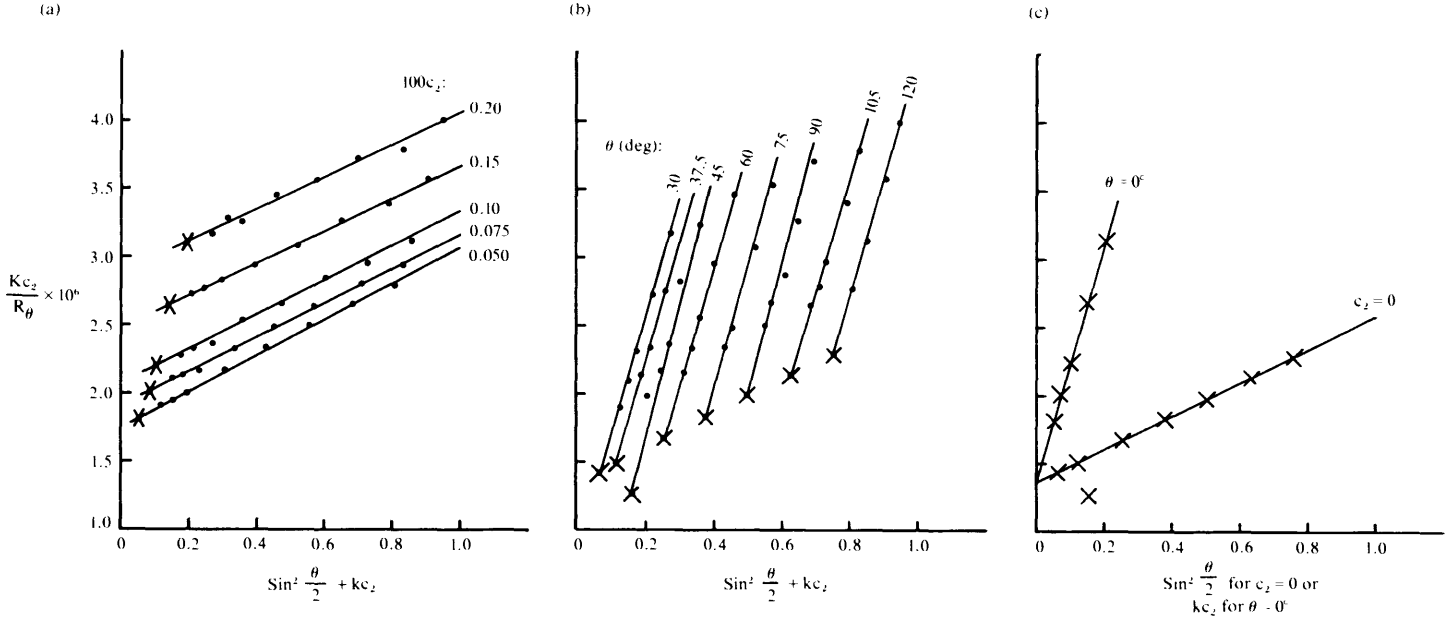

Figure 10.14 Construction of a Zimm plot from the data of Tables 10.2 and 10.3: (a) extrapolation to $\theta = 0^\circ$, (b) extrapolation to $c_2 = 0$, and (c) derived lines.

Table 10.3 Values of $\sin^2(\theta/2) + 100\, c_2$ for the Data in Table 10.2 (used as Abscissa Coordinates in the Construction of Fig. 10.14)

$c_2 \times 10^3$ ($g\ cm^{-3}$)	θ (deg)							
	30	37.5	45	60	75	90	105	120
2.00	0.267	0.303	0.346	0.450	0.571	0.700	0.829	0.950
1.50	0.217	0.253	0.296	0.400	0.521	0.650	0.779	0.900
1.00	0.167	0.203	0.246	0.350	0.471	0.600	0.729	0.850
0.75	0.142	0.178	0.221	0.325	0.446	0.575	0.704	0.825
0.50	0.117	0.153	0.196	0.300	0.421	0.550	0.679	0.800

point is marked by an x on the line through the points at 30°. The x's on the other lines in Fig. 10.14b correspond to the $c_2 = 0$ limit for each angle.

4. Figure 10.14c shows the two limiting lines defined in Figs. 10.14a and b. The derived lines in Fig. 10.14c have the following properties: common intercept = 1.35×10^{-6} mol g^{-1}, slope $c_2 = 0$ line = 1.25×10^{-6} mol g^{-1}, slope $\theta = 0°$ line = 9.0×10^{-6} mol g^{-1} (as drawn), slope $\theta = 0°$ line = 9.0×10^{-4} cm^3 mol g^{-2} (corrected for k). Using Eqs. (10.56) and (10.91), we have

$$\bar{M}_w = \text{intercept}^{-1} = 7.41 \times 10^5 \text{ g mol}^{-1}$$

Using Eq. (10.55), we have

$$B = \frac{(\text{slope})_{\theta=0}}{2} = \frac{9.0 \times 10^{-4}}{2} = 4.5 \times 10^{-4} \text{ cm}^3 \text{ mol g}^{-2}$$

Using Eq. (10.92), we have

$$\overline{r_g^2} = \frac{3\lambda^2}{16\pi^2} \left(\frac{\text{slope}}{\text{intercept}} \right)_{c=0} = \frac{3(364)^2}{16\pi^2} \frac{1.25 \times 10^{-6}}{1.35 \times 10^{-6}} = 2330 \text{ nm}^2$$

$$(\overline{r_g^2})^{1/2} = r_{g,\text{rms}} = 48.2 \text{ nm}$$

•

The objective of the Zimm plot is to conduct all extrapolations on a single graph. The three-stage development of Fig. 10.14 is not typical, but it is intended to clarify the discussion.

Not all Zimm plots show the same grid of essentially parallel straight lines found in Fig. 10.14. In some cases there is considerable curvature, and quite a bit of "interpretation" is required to extract the molecular parameters from the data. In this connection we note that the reciprocal of Eq. (10.83)

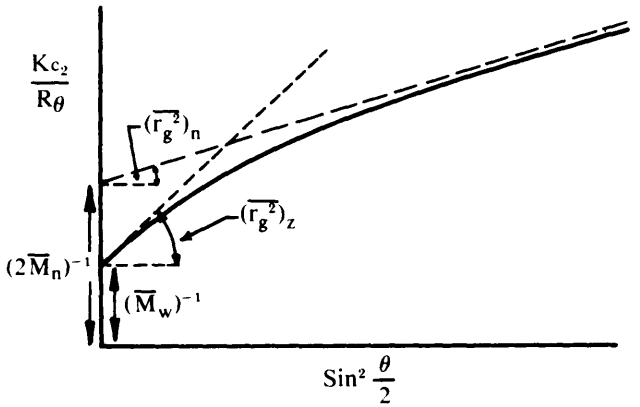

Figure 10.15 Schematic showing alternative limits in the plot of Kc_2/R_θ versus $\sin^2(\theta/2)$ and their interpretation. [Reprinted with permission from H. Benoit, A. M. Holtzer, and P. Doty, *J. Phys. Chem.* 58:635 (1954), copyright 1954 by the American Chemical Society.]

approaches an asymptotic value for large values of sr_{jk}. Instead of Eq. (10.88), the reciprocal of $P(\theta)$ for *large* values of s, r_{jk}, or both (indicated by a prime) is given by

$$\frac{1}{P'(\theta)} = \frac{8\pi^2}{\lambda^2}(\overline{r_g^2})_n \sin^2\left(\frac{\theta}{2}\right) \tag{10.100}$$

In addition, the intercept obtained by extrapolating this asymptote back to $\sin^2(\theta/2) = 0$ equals $(2\overline{M}_n)^{-1}$. Note that both $\overline{M}$ and r_g^2 are *number* averages when this asymptotic limit is used. This is illustrated schematically in Fig. 10.15 and indicates that even more information pertaining to polymer characterization can be extracted from an analysis of the curvature in Zimm plots.

10.12 Appendix: Electrical Units

At one time or another, all of us have tangled with problems of units, but generally these decrease in severity and frequency with experience. Advanced students juggle kilograms and grams, centimeters and angstroms, joules and calories, and rarely fumble in the process. Electrical units are sometimes more troublesome.

In 1785 Coulomb showed that the force between two charges q_1 and q_2 separated by a distance r is proportional to q_1q_2/r^2, a result we know as

Coulomb's law. This relationship poses no particular difficulties as a qualitative statement; the problem arises when we attempt to calculate something with it, since the proportionality constant depends on the choice of units. In the cgs system of units, the electrostatic unit of charge is defined to produce a force of 1 dyne when two such charges are separated by a distance of 1 cm. In the cgs system the proportionality factor in Coulomb's law is unity and is dimensionless. For charges under vacuum we write

$$F_{cgs} = \frac{q_1 q_2}{r^2} \tag{10.101}$$

By contrast, in SI units, the coulomb (C) is the unit of charge and is defined as an ampere second (A sec). To reconcile this with newtons and meters, the units of F and r, respectively, a proportionality constant that is numerically different from unity and which has definite units is required. For charges under vacuum we write

$$F_{SI} = \frac{1}{4\pi\epsilon_0} \frac{q_1 q_2}{r^2} \tag{10.102}$$

where ϵ_0, the permittivity of vacuum, is 8.854×10^{-12} C^2 N^{-1} m^{-2} (or C^2 J^{-1} m^{-1} or kg^{-1} m^{-3} sec^2) and $1/4\pi\epsilon_0$ is 8.988×10^9 N m^2 C^{-2}.

In a medium where the relative dielectric constant is ϵ_r, the force between fixed chages at a definite separation is decreased by the dimensionless factor ϵ_r. This is true regardless of the system of units and is incorporated into Eqs. (10.101) and (10.102) by dividing the right-hand side of each by ϵ_r.

So far, so good. The situation is really no different, say, than the ideal gas law, in which the gas constant is numerically different and has different units depending on the units chosen for p and V. The unit change in Example 10.1 is analogous to changing the gas constant from liter-atmospheres to calories; it is apparent that one system is physically more meaningful than another in specific problems. Several considerations interfere with this straightforward parallel, however, and cause confusion:

1. The fact that the proportionality factor in Eq. (10.101) is numerically equal to unity and is dimensionless makes us tend to forget that any such factor is needed.
2. The fact that the proportionality constant in Eq. (10.102) is not written as, say, k but also includes the factor $(4\pi)^{-1}$ is a recognition of the fact that 4π arises frequently in equations from geometrical considerations and can be conveniently eliminated by this device.

3. In media other than vacuum, the product $\epsilon_0\epsilon_r$ is sometimes written ϵ (no subscript), where ϵ is the permittivity of the medium. Thus in a specific substance, $F_{cgs} \propto 1/\epsilon_r$ and $F_{SI} \propto 1/4\pi\epsilon_r\epsilon_0 = 1/4\pi\epsilon$.
4. In calculation, however, ϵ_r and ϵ are quite different. We must remember that ϵ_r is dimensionless, while ϵ is the product of ϵ_r and ϵ_0, with the latter having definite units.
5. Since the factor 4π is introduced into Eq. (10.102) to encourage cancellation, we frequently find expressions for the same quantity differing by this factor, depending on the system of units used by the author. For example, the Clausius-Mosotti equation [Eq. (10.17)] is written $(4\pi/3)(\rho N_A\alpha/M) = (\epsilon_r - 1)/(\epsilon_r + 2)$ in the cgs system.

Since an electric field E in space is defined as the force experienced by a unit test charge q_t (strictly, in the limit of $q_t \to 0$), it follows that the field produced by q_1 is obtained by letting $q_2 = q_t = 1$ in Coulomb's law:

$$E_{cgs} = \frac{q_1}{\epsilon_r r^2} \tag{10.103}$$

and

$$E_{SI} = \frac{q_1}{4\pi\epsilon_0\epsilon_r r^2} = \frac{q_1}{4\pi\epsilon r^2} \tag{10.104}$$

Even when we discuss the electric field of light without reference to any particular charge, we must be aware of these differences. When that field interacts with a charge, as in light scattering, we will be in trouble unless a self-consistent set of units has been employed.

Problems

1. The geometry of Fig. 10.3 leads to a result known as Snell's law, which relates the refractive index of the medium to the angles formed by two wave fronts with the interface. Defining θ_0 and θ, respectively, as the angles between the phase boundary and the wave front under vacuum and in the medium of refractive index $\tilde{n}$, show that Snell's law requires $\tilde{n} = \sin\theta_0/\sin\theta$.
2. Use the expression given in Example 10.3 to evaluate the compressibility of CCl_4 from the fact† that $R_{90} = 5.38 \times 10^{-4}$ m^{-1} at room temperature for $\lambda_0 = 546$ nm. The depolarization ratio $\rho_u(90)$ is 0.042 for this liquid and $\tilde{n} = 1.460$, $\alpha = 1.21 \times 10^{-3}$ deg^{-1}, and $d\tilde{n}/dT = 58.6 \times 10^{-5}$ deg^{-1}. Compare the light-scattering value with a literature value for β_{CCl_4}; be sure to cite the reference consulted.

† Data from Ref. 3.

3. Fowle† measured the turbidity of air at Mt. Wilson, California, on a clear day in 1913. Values of τx for dry air at different wavelengths are tabulated below, where x is essentially the thickness of the atmosphere corrected to standard temperature and pressure (STP) conditions:

λ (μm)	τx	λ (μm)	τx
0.3504	0.459	0.5026	0.122
0.3600	0.423	0.5348	0.108
0.3709	0.377	0.5742	0.100
0.3838	0.338	0.5980	0.091
0.3974	0.285	0.6238	0.074
0.4127	0.245	0.6530	0.064
0.4307	0.213	0.6858	0.0419
0.4516	0.174	0.7222	0.0304
0.4753	0.147	0.7644	0.0212

Prepare a log-log plot of τx versus λ and evaluate the slope as a test of the Rayleigh theory applied to air. The factor $M/\rho N_A$ in Eq. (10.36) becomes $6.55 \times 10^5/N_0$, where N_0 is the number of gas molecules per cubic centimeter at STP and the numerical factor is the thickness of the atmosphere corrected to STP conditions. Use a selection of the above data to determine several estimates of N_0, and from the average, calculate Avogadro's number. The average value of $\tilde{n} - 1$ is 2.97×10^{-4} over the range of wavelengths which are most useful for the evaluation of N_A.

4. Bhatnagar and Biswas‡ measured the turbidity at 436 nm of a *single* sample of poly(methyl methacrylate) in several solvents, including acetone and methyl ethyl ketone (MEK):

	$d\tilde{n}/dc_2$	$(Hc_2/\tau)_{c=0}$	M
In acetone	0.13914	1.75×10^{-6}	571,000
In MEK	0.01385	2.60×10^{-8}	38,400,000

Working with different samples of the same polymer, other researchers have published conflicting values for the refractive index gradient in these solvents:

	$d\tilde{n}/dc_2$ in acetone	$d\tilde{n}/dc_2$ in MEK
Cohn and Schuele §	0.137	0.113
Tremblay et al.#	0.107	0.093

† F. E. Fowle, *Astrophys. J.* 40:435 (1914).
‡ H. L. Bhatnagar and A. B. Biswas, *J. Polym. Sci.* 13:461 (1954).
§ E. S. Cohn and E. M. Schuele, *J. Polym. Sci.* 14:309 (1954).
# R. Tremblay, Y. Sicotte, and M. Rinfret, *J. Polym. Sci.* 14:310 (1954).

Using the original Hc_2/τ values, recalculate M using the various refractive index gradients. On the basis of self-consistency, estimate the molecular weight of this polymer and select the best value of $d\bar{n}/dc_2$ in each solvent. Criticize or defend the following proposition: Since the extension of the Debye theory to large particles requires that the difference between $\bar{n}$ for solute and solvent be small, this difference should routinely be minimized for best results.

5. Various amounts of either ethanol or hexane were added to polystyrene solutions in benzene and τ was measured for several concentrations of polymer. The following results were obtained† (c_2 in g liter^{-1}; Hc_2/τ in mol g^{-1}):

Pure benezene	
c_2	$Hc_2/\tau \times 10^6$
0.73	1.47
1.21	1.82
2.00	2.38

Benzene + percent ethanol			
20%		28.5%	
c_2	$Hc_2/\tau \times 10^6$	c_2	$Hc_2/\tau \times 10^6$
0.52	0.75	0.52	0.51
1.06	0.87	1.00	0.56
1.60	1.00	–	–

Benzene + percent hexane			
50%		58%	
c_2	$Hc_2/\tau \times 10^6$	c_2	$Hc_2/\tau \times 10^6$
0.28	0.95	0.28	0.89
0.66	1.00	0.66	0.89
0.88	1.06	0.88	0.91

Evaluate M and B for each of the five runs on this polymer sample and comment on the following points:

a. What is the significance of the runs for which $B \cong 0$?
b. What is the significance of the difference in the amount of the two diluents needed to produce the B = 0 condition?
c. What is the significance of the different behavior with respect to M for the two diluents?

† E. D. Kunst, *Rec. Trav. Chim. Pays Bas* 69:125 (1950).

6. Zimm† has reported the intensity of scattered light at various angles of observation for polystyrene in toluene at a concentration of 2×10^{-4} g cm^{-3}. The following results were obtained (values marked * were estimated and not measured):

θ (deg)	i_s (arbitrary units)
0	4.29*
25.8	3.49
36.9	2.89
53.0	2.18
66.4	1.74
90.0	1.22
113.6	0.952
143.1	0.763
180	0.70*

Draw a plot in polar coordinates of the scattering envelope in the xy plane. How would the envelope of a Rayleigh scatterer compare with this plot? By interpolation, evaluate i_{45}, i_{135}, and z. Use Fig. 10.13 to estimate the value of r_{rms} to which this dissymmetry ratio corresponds if λ (in toluene) is 364 nm. What are some practical and theoretical objections to this procedure for estimating r_{rms}?

7. The effect of adenosine triphosphate (ATP) on the muscle protein myosin was studied by light scattering in an attempt to resolve conflicting interpretations of viscosity and ultracentrifuge data. The controversy hinged on whether the myosin dissociated or changed molecular shape by interaction with ATP. Blum and Morales‡ reported the following values of $(Kc_2/R_\theta)_{c=0}$ versus $\sin^2(\theta/2)$ for myosin in 0.6 M KCl at pH 7.0:

$\sin^2(\theta/2)$	0.15	0.21	0.29	0.37	0.50	0.85
$Hc_2/\tau \times 10^7$						
(Before ATP)	0.9	1.1	1.5	1.8	2.2	2.7
(During ATP)	1.9	2.8	3.7	4.6	6.0	6.8

Which of the two models for the mode of ATP interaction with myosin do these data support? Explain your answer by quantitative interpretation of the light-scattering data.

† B. H. Zimm, *J. Chem. Phys.* 16:1093 (1948).

‡ J. J. Blum and M. F. Morales, *Arch. Biochem. Biophys.* 43:208 (1953).

8. Aggregation of fibrinogen molecules is involved in the clotting of blood. To learn something about the mechanism of this process, Steiner and Laki† used light scattering to evaluate M and the length of these rod-shaped molecules as a function of time after a change from stable conditions. The stable molecule has a molecular weight of 540,000 g mol^{-1} and a length of 840 Å. The following table shows the average molecular weight and average length at several times for two different conditions of pH and ionic strength μ:

pH = 8.40 and μ = 0.35 M			pH = 6.35 and μ = 0.48 M		
t (sec)	M × 10^{-6} (g mol^{-1})	length (Å)	t (sec)	M × 10^{-6} (g mol^{-1})	length (Å)
650	1.10	1300	900	1.10	1100
1150	1.65	1600	1000	2.0	1200
1670	2.20	1900			
2350	3.30	2200			

Criticize or defend the following proposition: The apparent degree of aggregation x at various times can be obtained in terms of either the molecular weight *or* the length. The ratio of the values of x based on M to that based on length equals unity for exclusively end-to-end aggregation and increases from unity as the proportion of edge-to-edge aggregation increases. In the higher pH-lower μ experiment there is considerably less end-to-end aggregation in the early stages of the process than in the lower pH-higher μ experiment.

9. Zimm plots at 546 nm were prepared for a particular polystyrene at two temperatures and in three solvents. The following summarizes the various slopes and intercepts obtained‡:

	T = 22°C		
Solvent	Intercept	$\left(\frac{\text{slope}}{\text{intercept}}\right)_{c=0}$	$\left(\frac{\text{slope}}{\text{intercept}}\right)_{\theta=0}$
Methyl ethyl ketone	0.896	0.608	260
Dichloroethane	1.61	1.16	900
Toluene	3.22	1.14	1060

† R. F. Steiner and K. Laki, *Arch. Biochem. Biophys.* 34:24 (1951).
‡ P. Outer, C. I. Carr, and B. H. Zimm, *J. Chem. Phys.* 18:830 (1950).

Solvent	T = 67°C		
	Intercept	$\left(\frac{\text{slope}}{\text{intercept}}\right)_{c=0}$	$\left(\frac{\text{slope}}{\text{intercept}}\right)_{\theta=0}$
Methyl ethyl ketone	0.840	0.551	230
Dichlorethane	1.50	1.05	870
Toluene	2.80	1.09	800

The slope–intercept ratios have units of cubic centimeters per gram, and the intercepts are $c/R_{\theta,v}$, where the subscript v indicates vertically polarized light. In this case $K_v = 4\pi^2 (\tilde{n}d\tilde{n}/dc_2)^2/\lambda_0{}^4 N_A$. The following values of $\tilde{n}$ and $d\tilde{n}/dc_2$ can be used to evaluate K_v:

	T = 20° C ≅ 22°C		T = 67°C	
	$\tilde{n}$	$d\tilde{n}/dc_2$	$\tilde{n}$	$d\tilde{n}/dc_2$
Methyl ethyl ketone	1.378	0.221	1.359	0.230
Dichloroethane	1.444	0.158	1.423	0.167
Toluene	1.496	0.108	1.472	0.118

Evaluate M, $(\overline{r_g^2})^{1/2}$, and B from each piece of pertinent data and comment on the following points:

a. Agreement between M values.
b. Correlation of $(\overline{r_g^2})^{1/2}$ and B with solvent "goodness."

10. For polystyrene in butanone at 67°C the following values of $Kc_2/R_\theta \times 10^6$ were measured† at the indicated concentrations and angles. Construct a Zimm plot from the data below using k = 100 $cm^3\ g^{-1}$ for the graphing constant. Evaluate M, B, and $(\overline{r_g^2})^{1/2}$ from the results. In this experiment λ_0 = 546 nm and $\tilde{n}$ = 1.359 for butanone at this temperature.

θ (deg)	c_2 (g cm^{-3})	
	1.9×10^{-3}	3.8×10^{-4}
25.8	–	1.48
36.9	1.84	1.50
53.0	1.93	1.58
66.4	1.98	1.62
90.0	2.10	1.74
113.6	2.23	1.87
143.1	2.34	1.98

† B. H. Zimm, *J. Chem. Phys.* 16:1093 (1948).

11. Benoit et al.† prepared a mixture of two different fractions of cellulose nitrate and determined the molecular weight of the mixture by light scattering. The mixture was 25.8% by weight fraction A and 74.2% fraction B, where the individual fractions have the following properties:

Fraction	$\bar{M}_n$	$\bar{M}_w$
A	635,000	1,270,000
B	199,000	400,000

Calculate $\bar{M}_n$ and $\bar{M}_w$ for the mixture on the basis of this information concerning the components and their proportions. The following light-scattering data for the mixture allow $\bar{M}_n$ and $\bar{M}_w$ to be evaluated by the procedure shown in Fig. 10.15:

θ (deg)	$(Kc_2/R_\theta) \times 10^7$ (mol g^{-1})	θ (deg)	$(Kc_2/R_\theta) \times 10^7$ (mol g^{-1})
30	19.6	80	42.2
35	21.7	90	48.7
40	24.4	100	53.0
45	26.4	110	57.0
50	28.3	120	61.3
55	31.0	130	64.9
60	33.0	140	67.4
70	37.4		

Evaluate $\bar{M}_n$ and $\bar{M}_w$ from the light-scattering data and compare the values with those calculated from the preparation of the mixture.

Bibliography

1. Dover, S. D., in *An Introduction to the Physical Properties of Large Molecules in Solution*, by E. G. Richards, Cambridge University Press, Cambridge, 1980.
2. Hiemenz, P. C., *Principles of Colloid and Surface Chemistry*, Marcel Dekker, New York, 1977.
3. Kerker, M., *The Scattering of Light and Other Electromagnetic Radiation*, Academic, New York, 1969.
4. Stacey, K. A., *Light Scattering in Physical Chemistry*, Butterworths, London, 1956.
5. Tanford, C., *The Physical Chemistry of Macromolecules*, Wiley, New York, 1961.

† H. Benoit, A. M. Holtzer, and P. Doty, *J. Phys. Chem.* 58:635 (1954).